

Award Number:
W81XWH-05-1-€330

TITLE:
A Biophysical-Computational Perspective of Breast Cancer
Pathogenesis and Treatment Response

PRINCIPAL INVESTIGATOR:
Valerie M. Weaver Ph.D.

CONTRACTING ORGANIZATION:
University of California San Francisco
San Francisco, CA 94143-0456

REPORT DATE:
March 2009

TYPE OF REPORT:
Annual

PREPARED FOR: U.S. Army Medical Research and Materiel Command
Fort Detrick, Maryland 21702-5012

DISTRIBUTION STATEMENT:

Approved for public release; distribution unlimited

The views, opinions and/or findings contained in this report are those of the author(s) and should not be construed as an official Department of the Army position, policy or decision unless so designated by other documentation.

Table of Contents

Introduction.....	4
Body.....	5-24
Key Research Accomplishments.....	6-7, 9-10, 12-19
Reportable Outcomes.....	19-22
Conclusions.....	22-23
References.....	24
Appendices.....	25 onwards

INTRODUCTION:

Apoptosis resistance regulates the pathogenesis, and treatment response of breast tumors. Despite concerted effort towards understanding the molecular basis for apoptosis resistance in breast tumors, progress in this area has been frustratingly slow. Lack of advancement may be attributed in part to the current cell autonomous view of breast cancer etiology and treatment responsiveness. What we now know is that the organ microenvironment can and does regulate the therapeutic responsiveness of metastatic tumors (Taylor et al., 2000, Zahir et al., 2004), and that stromal-epithelial interactions influence mammary gland development, tissue homeostasis and breast tumor progression (Unger and Weaver, 2003). Alterations in the mammary gland ECM correlate with changes in mammary differentiation, involution (apoptosis) and tumor progression, and culture experiments clearly show that the stromal ECM can modulate mammary epithelial cell (MEC) growth, differentiation and survival and alter apoptotic responsiveness (Zahir et al., 2004, Truong et al., 2003, Lewis, Truong and Schwartz, 2002). **How the stroma promotes apoptosis-resistant breast tumors remains unclear.**

We have been studying the role of integrin ECM receptors as key regulators of mammary tissue behavior as well as malignant transformation and metastasis. We have been exploring the molecular mechanisms whereby the ECM can regulate mammary tissue homeostasis, invasion and apoptosis responsiveness. We found that integrin expression, organization and activity are consistently altered in breast tumors and that perturbing integrin expression and activity can drive malignant behavior of non-malignant and pre-malignant MECs, and that normalizing integrin activity represses expression of the malignant breast phenotype in culture and in vivo (Unger et al., 2003; White et al., 2004). We also determined that integrins regulate cell survival and modulate the apoptotic responsiveness of mammary tissues to a diverse array of exogenous stimuli including various chemotherapies and immune receptor activators (Weaver et al., 2002, Zahir et al., 2004). We found that integrin-dependent apoptosis resistance and survival are intimately linked to many of the biochemical pathways and mechanisms that regulate tissue organization and specifically tissue polarity. For example, we found that $\alpha 6\beta 4$ integrin directs mammary epithelial cells to assemble polarized mammary tissue structures that display apoptosis resistance to a wide spectrum of apoptotic insults. We are now exploring the underlying mechanisms whereby integrin expression and/or function becomes altered in breast tumors, how integrin modulate the survival of nonmalignant and transformed mammary epithelial cells, what the molecular link could be between integrin-dependent survival and tissue polarity and the clinical relevance of these findings.

We found that prior to malignant transformation the mammary gland exhibits a 'desmoplastic' response that is associated with an incremental and significant increase in global elastic modulus (stiffness) of the gland and elevated/altered expression of integrins and integrin adhesions (Krouskop et al., 1998; Paszek and Weaver 2004; Paszek et al., 2005; unpublished data). Consistent with results from other laboratories we determined that externally-applied mechanical force regulates the behavior and phenotype of multiple cell types including endothelial, fibroblasts, neurons, and MECs (Grinnell, F. 2003, Bershadsky, Balaban and Geiger, 2003, Geiger, B. et al., 2001). Although the mammary gland is not traditionally viewed as a mechanically-regulated tissue, MECs within the ductal tree and alveolus experience passive (isometric) and active mechanical force throughout the lifetime of the mammary gland most notably during development, lactation and involution (Paszek and Weaver, 2004; Samani et al., 2003, Plewes et al., 2000). Similar to other solid tumors, the mammary gland also becomes appreciably stiffer in association with its malignant transformation and mammary epithelial cells within the tumorigenic mammary gland experience an array of additional compression and stress and interstitial associated forces (REF). During the process of metastasis and once at the metastatic site breast tumor cells also encounter an array of external mechanical forces that could conceivably influence their behavior and alter their response to treatment. For example, many of the common metastatic sites for breast cancer differ appreciably with respect to their stiffness and biochemical compositions than a normal mammary gland such as bone (very stiff, high vitronectin), in the vasculature (high pulsatile

pressures, high fibronectin and fibrin), pleural cavity (very compliant with high fibrin composition but also adjacent fibrotic lung could be quite stiff with a high amount of elastin).

Because physical forces so profoundly influence cell proliferation, survival and differentiation of multiple cell types, we maintain that it is critical to understand how mechanical cues could influence mammary tissue behavior and apoptosis responsiveness.

Accordingly, we predict that the physical organization of the ECM (which contributes to its mechanical properties) constitutes an independent regulator of mammary epithelial behavior and apoptosis resistance. Delineating the molecular basis for this phenotype will likely have important consequences for tumor therapy. To rigorously test this idea we are in the process of achieving the following specific aims:

Specific Aim 1. Engineer tractable 3D organo-typic model systems that recapitulate the biophysical properties of primary and metastatic breast tumor tissues, and then use these models to dissect candidate molecular stress-response mechanisms whereby ECM stiffness could regulate apoptosis resistance in culture and in vivo.

Specific Aim 2. Develop xenograft and transgenic mouse models to test whether ECM stiffness regulates apoptotic responsiveness of mammary epithelia in vivo.

Specific Aim 3. Build a computational model that can predict how changes in ECM compliance could influence integrin-dependent apoptosis responsiveness of mammary epithelia and query this model with clinical data.

Specific Aim 4. Develop non-invasive imaging tools that could be used to monitor changes in ECM stiffness or stiffness-induced changes in mammary tissue phenotype.

Summary of Achievements - Proposal Body:

Task 1: *Engineer tractable 3D organo-typic model systems that recapitulate the biophysical properties of primary and metastatic breast tumor tissues, and then use these models to dissect candidate molecular stress-response mechanisms whereby ECM stiffness could regulate apoptosis resistance in culture and in vivo.*

PART A Development of natural 3D model systems that recapitulate the biophysical properties of primary normal and malignant breast tissue and metastatic breast tissues.

In the first 3 grant cycles which covered the first 3 years of funding for this project (with a delay due to the grant being placed on hold for an 8 month time period to accommodate the move of my group from the University of Pennsylvania to the University of California, San Francisco) we reported excellent progress in all of the initial work goals outlined in the grant. These findings have been reported in prior progress reports and have also been published in peer reviewed articles (Johnson et al., 2007; Paszek et al., 2005, Butcher et al., 2009; see attached list and attachments). Furthermore, these experimental findings will be the subject of at least 2 additional publications and will be summarized in more detail in the next years progress report.

In this 4th year of funding we have moved towards completing and following up the last part of the work objectives outlined in Task 1. This includes the setting up and that analysis of a method to apply acute and chronic forces to nonmalignant and malignant MECs embedded within 3D gels. The

rationale for this approach is that we will be able to identify a cause and effect relationship between mechanical force and mammary cell behavior through direct, acute force application. To achieve this goal we have set up and validated a bioreactor system in which we have been able to apply acute cyclic compression forces and we can also apply chronic compression and then assess effects on the behavior of MECs and colonies. While we originally had anticipated applying these forces to MECs embedded within 3D collagen/rBM gels - we have since discovered that these gels are not amenable to these manipulations as application of these types of forces will cause irreversible modification to natural gels such as collagen that lead to major and irreversible alterations in their pore size and architecture. In the case of reconstituted basement membrane gels - these gels are far too soft to sustain application of a compression force. Therefore to address this we have instead begun to work with HA gels in which we can add reconstituted basement membrane or purified laminin-1. We have thus far established the conditions to apply both cyclic acute and chronic compression forces to these gels and using scanning EM demonstrated that these gels retain their pore size, shape and resiliency under these conditions. We first established conditions that would support the growth and survival of nonmalignant and malignant MECs in these gels. Thereafter, using these HA gels in which we incorporated limiting quantities of reconstituted basement membrane we were able to establish that we can drive the morphogenesis of nonmalignant MECs such that these structures are fully polarized, growth arrested and viable, even after 21 days in culture. We have also calibrated the bioreactor system which will permit the accurate, directed and temporal application of compression force. We have been able to methodically demonstrate that we can apply direct compression forces that are transmitted through the gel to the MECs to modify their behavior. We have now begun in earnest a rigorous characterization of the effect of force application on nonmalignant MEC behavior including morphogenesis, gene expression and treatment resistance. Thus far we have been able to demonstrate that application of compression force to pre formed, polarized, growth arrested nonmalignant MEC colonies induces the expression of fibronectin, disrupts tissue polarity and increases colony size consistent with what appears to be a concomitant induction of cellular growth. We have also observed a filling of the lumens of these structures which is consistent with a force-induced effect on cell survival. In this next fiscal year we intend to continue with these studies which will include a more detailed analysis of the effect of acute force application on mammary colony behavior. The intention is to extend the work to combine with susceptibility to chemotherapy treatment and assay for death inducibility. We believe that these findings will bear relevance to treatment responsiveness and force-induced modification of breast tissue behavior that promote tumor progression in vivo because human tumors experience very profound increases in mechanical force linked to ECM remodeling, cellular compression due to increased cell mass and altered vascular and lymphatic behavior. In addition, it is well established that the treatment responsiveness of breast tumors varies significantly between metastatic sites - and while genetic selection/variation could contribute to this phenotype...we also maintain that the tissue microenvironment, of which mechanical cues are key, will also contribute substantially to this differential responsiveness.

- a. Manipulate natural ECM gel stiffness - keeping BM and collagen concentration constant through an increase in relative stiffness mediated by application of an exogenous force. The increase in stiffness will be deduced through calculations based upon the known magnitude of the force and the materials properties of the ECM gel. **Partially completed. Completed initial characterization of compression force system, completed manipulation and characterization of MEC morphogenesis and behavior in HA gels.**
- b. We will assess effects of application of an exogenous stress force on mammary morphology and behavior when embedded within a HA gel. **Partially completed. Completed initial characterization of effect of force on MEC behavior. In this next fiscal year we will complete these studies and summarize our findings in a publication.**

- c. Analyze the growth behavior of normal and malignant MECs in HA gels following application of an exogenous stress force. **Partially completed. In this next fiscal year we will continue to work on these studies and to explore additional bio mimetic matrices that could be amenable to these types of manipulations.**
- d. Analyze the survival behavior of normal and malignant MECs in HA gels following application of an exogenous stress force. **Not yet initiated. In this next fiscal year we hope to begin these studies.**
- e. Analyze the apoptosis sensitivity of normal and malignant MECs to chemotherapeutic agents (taxol, doxorubicin, etoposide), immune receptor apoptotic agents (trails, TNFalpha) and gamma radiation following application of an exogenous stress force. **Not yet initiated. In this next fiscal year we hope to initiate these studies and anticipate that the work will be done in the next few years.**

PART B Development of synthetic 3D model systems that recapitulate the biophysical and biochemical properties of primary and metastatic breast tumor tissues.

In the first 3 years of funding we completed much of the studies outlined in this section and this work has already been published in peer reviewed journals or is about to be published. The list of achieved work aims was summarized in earlier reports and therefore will not be duplicated in this report. However, we have also extended these experiments to also include further analysis of one of the synthetic systems we developed with our colleague at Boston University - self assembling peptide polymer gels because this system has the unique property of not changing pore size when the concentration is increased to enhance gel stiffness. Moreover, these self assembling peptide polymer gels retain an architecture that recapitulates native extracellular matrix found in the human breast, thereby differing from other synthetic systems including PEG and HA gels. This work is now nearing completion and with the inclusion of some scanning EM experimental data as well as further cell biological details we hope to be in a position to write up and submit our findings to a peer reviewed journal (Leight, Levental and Weaver, In preparation; Miroshinova et al., In Preparation). We will include our findings on this work in our progress report for 2009-2010.

PART B Development of synthetic 3D model systems that recapitulate the biophysical and biochemical properties of primary and metastatic breast tumor tissues. (NOTE: These studies have been conducted in collaboration with Dr. Joyce Wong who is a Bioengineer and materials scientist at Boston University. Initial studies also involved Drs. Shuguang and Cam who are on faculty in the Biomedical Engineering group at MIT. Funds were subcontracted to Dr. Wong at Boston University from years 1 through 4 to cover materials costs and efforts of one graduate student to be able to achieve the goals set out in this S.O.W. including effective technology transfer to the Weaver laboratory).

In the first few years of funding we worked collaboratively with the Wong, Shuguang and Cam laboratories to establish methodologies to generate and measure the materials properties of synthetic matrices - including PVC gels and self assembling peptide polymers. Feasibility studies were all completed and established so that we were able to achieve a good range of stiffness through either concentration modification or else via cross linking of the synthetic gels/biomaterials. We were also able to show that mammary cells and fibroblasts were biocompatible in these synthetic gels. In this past year we have extended two aspects of these studies in preparation for in vivo manipulations which we hope to conduct in this next upcoming fiscal year. Nevertheless as time progressed and we became more familiar with working with these materials we came to recognize the limitations of these materials for reconstructing normal and tumorigenic breast microenvironment. Consequently we have begun to

exploit the new range of biomaterials and tools now available in the engineering community. In particular throughout this past year we have focused on developing novel substrata that will enable the study of breast cancer cell behavior in different microenvironments. The substrata properties increase in complexity, with the ultimate goal of developing 3-dimensional substrata with defined material properties. These studies have focused primarily on self assembling peptide polymer gels, creating durotactic substrata to study directed cell migration and invasion and oriented silk biopolymers with "tuned" diameters, orientations and stiffness.

A. Gradient mechanically compliant substrata to investigate durotaxis:

1. Background and Rationale:

A critical aspect of breast cancer (and other cancers) is the ability of cancer cells to spread from the primary tumor to form metastases in distant locations in the body. An early step in this metastatic process involves cell migration. While growth factors are often considered to be 'chemotactic' agents that drive cell migration, substrata with gradients in substrate compliance have revealed the 'durotactic' potential of cells, i.e. tendency to migrate in response to changes or gradients in substrate stiffness.

2. Approach:

In collaboration with the Wong laboratory we developed gradient substrata that ranged in stiffness from 1, 2, 4, and 6 kPa / 100 μm . We validated the stiffness gradients using atomic force microscopy. We are now conducting cellular migration studies on these gradient substrata and dissecting the molecular pathways driving this unique durotactic behavior.

B. Silk microfibers with tunable diameter and mechanical properties:

1. Background and Rationale:

Probably however, the most exciting discovery/application we have made this past year is adoption of biopolymer silk. The biopolymer silk is an attractive biomaterial scaffold because it can be manipulated at the nano and microscales to provide a unique range of morphologies, chemistries, and mechanical properties. These features are particularly critical for reconstructing the physical and biochemical environment of breast tissue and the tissue of metastatic sites that breast tumor cells migrate to. Indeed, through either genetic engineering or chemical functionalization, silk can be tuned for desired surface chemistry and can be further processed into controlled fiber architectures for desired stiffness and surface geometry to faithfully recreate the in vivo stroma "ex vivo".

2. Silk microfibers with tunable diameter and mechanical properties:

In collaboration with the Wong laboratory we developed a microfluidics technique to generate silk microfibers with tunable fiber diameters. These fibers can be further processed through a drawing process, which also enhances their mechanical properties. These fibers can be formed with diameters at the micron scale. Using these fibers, one can examine single-cell interactions on the fibers. The fibers can also be formed from genetic variants of silk that contain specific adhesion moieties.

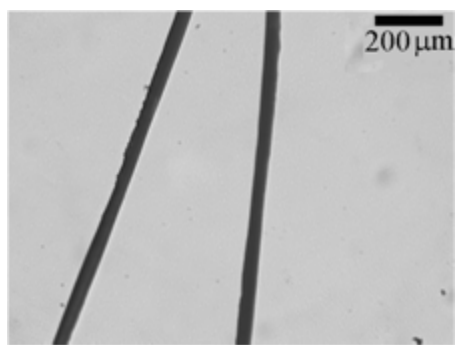


Fig 1. Silk fiber formed using a microfluidic channel with a pH gradient. The fibers are very reproducible, and the diameter can be tuned by controlling the flow rates of the silk and polymer solutions.

3. Electrospun silk nanofibers with specific alignment in layered films:

In collaboration with Julie Chen, PhD (University of Massachusetts, Lowell) and David Kaplan, PhD (Tufts University) together with Joyce Wong, Ph.D. (Boston University) we have also developed nanofibrous substrata with defined alignment. Specifically, we used the electrospinning technique to form silk into nanofibers (**Fig 2**). These fibers can be aligned into specific orientations and layered to form three-dimensional structures. Ongoing work is being carried out to characterize the mechanical properties of these substrata. Briefly, the fiber diameter, porosity of the network, and the orientation of the fibers can be modulated to generate silk films with different mechanical properties. In addition, silk-based electrospun nanofibers modified via peptide chemistry offer a versatile system that can be sterilized, fabricated in an aqueous environment, and easily scaled for commercialization.

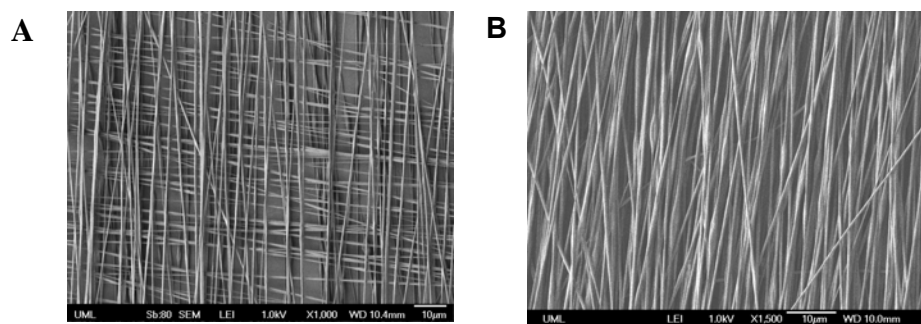


Fig 2. Field-emission scanning electron micrograph of electrospun silk nanofibers. Fibers are aligned perpendicular to each other ($0^\circ/90^\circ$) (A) or in the same direction (B). Scale bar is 10 μm .

In this next fiscal year we will be exploiting these substrata to study the migratory, invasive and treatment responsiveness of normal and transformed breast tissue.

Weaver laboratory with advice from **Cam and Shuguang** and **Wong laboratories** will attempt to incorporate methods to cross-link laminin, RGD and collagenase sensitive collagen peptides into self-assembling peptide lattices for 3D studies. **Completed. This past year we have completed this task.**

Weaver laboratory will analyze the morphogenesis behavior of normal and malignant MECs in self-assembling peptide lattices for 3D studies with increasing stiffness with defined ECM (laminin) binding properties. **Completed. This objective has now been completed.**

Weaver laboratory will analyze the growth behavior of normal and malignant MECs in self-assembling peptide lattices of increasing stiffness with defined ECM laminin binding properties. **Partially Completed. We have completed the first sets of studies to address this issue. In the next few years we will work diligently to complete this analysis.**

Weaver laboratory will analyze the survival behavior of normal and malignant MECs in self-assembling peptide lattices of increasing stiffness with defined ECM laminin binding properties. **Partially Completed. We have completed the first sets of studies aimed at addressing this issue. In the next fiscal year we hope to complete this work.**

Weaver laboratory will analyze the apoptosis sensitivity of normal and malignant MECs to three commonly used chemotherapeutic agents (taxol, doxorubicin, etoposide), and two immune receptor apoptotic agents (trails, TNFalpha) and gamma radiation grown within self-assembling peptides lattices of increasing stiffness with defined ECM laminin binding properties. **We have yet to initiate these**

studies. In this next two fiscal years we will be conducting these studies in anticipation of thereafter conducting in vivo manipulations with these self assembling polymer gels.

Wong laboratory to expand methodology to incorporate cross-linking chemistry to laminin and collagen and collagenase sensitive collagen peptides with the PVD synthetic gels. Partially Completed. We have decided to abandon these PVD gels and instead are now using HA gels since these PVD gels do not represent the optimal biocompatible system to use with breast epithelial cells. What we have opted to do in lieu of this work is to develop novel approaches to build ECMs using newer technological approaches now on hand. This has included the development/validation and testing of novel durotactic gradient gels using nonmalignant and transformed mammary epithelial cells. This has also included the development of a novel silk biopolymers that will permit us to recreate the architectural three dimensional fibril size, orientation and physical properties of normal and transformed human breast.

PART C Characterization of tumor associated changes in ECM composition and processing.

We have made substantial progress on this aim this past fiscal year. We have set up and completed analysis of shear and nonconfined compression to assess tumor physical stiffness changes during breast tumor progression using 2 different genetic models of breast cancer progression - the MMTV-Neu model which models ErbB2 human breast cancer progression and the MMTV-PyMT model which is a rapid well characterized model that is frequently used to assay for effects on tumor metastasis. The work on the MMTV-Neu model is the subject of an article that has received strong positive feedback when the work has been presented at national and international meetings. This work was summarized in an article that is currently being reviewed by CELL journal. The editors have stated that they are quite optimistic that the article will eventually be accepted and that they are quite interested in publishing this work in their high profile journal. Based upon initial positive feedback from the initial set of reviewers we are now in the midst of completing the experiments suggested by the third reviewer and anticipate re submitting the article for publication by the summer of 2009. Please see the attached manuscript Levental et al., Cell which is now in revision.

The Levental et al. manuscript shows that both shear rheology and nonconfined compression increase significantly in the MMTV-Neu model of breast tumor progression well before the epithelium invades to become a tumor. Moreover, while the tumor itself once formed is significantly stiffer than normal tissue - the adjacent nontransformed tissue which is composed of extracellular matrix and fibroblasts and adipocytes is also significantly stiffer than normal tissue (see Figure 1; Levental et al; attached). Upon further analysis we could show that the pre malignant and transformed mammary glands in these mice exhibit profound and striking modifications in their collagen extracellular matrix as revealed by picroserius red staining and polarized light imaging (see Figure 1C; Levental et al). Furthermore, second generation harmonics imaging revealed that the collagen in the mammary glands becomes progressively linearized as the gland transforms implying that the collagen is either under high tension or else it is cross linked (see Figure 1E; Levental et al). Upon further investigation we noted that there was a significant increase in collagen cross linking (see Figure 1G; Levental et al), consistent with our observation that there was a detectable increase in levels and expression of the collagen cross linking enzyme lysyl oxidase (see Figure 1H; Levental et al.).

To determine the significance of the lysyl oxidase induced cross linking and the importance of gland stiffening to breast tumor progression we treated a cohort of MMTV-Neu animals with a pharmacological inhibitor of lysyl oxidase. To be sure that we were not observing any off target effects we also treated in parallel a small group of animals with a lysyl oxidase function blocking antibody inhibitor through twice weekly injection. These studies have been repeated several times and each study entails extensive animal breeding and treatment over an extended period of time (i.e. 8-9 months per

experiment). Importantly, we could show that inhibiting the activity of an abundant collagen cross-linking enzyme lysyl oxidase (which is significantly upregulated PRIOR to breast tumor invasion) inhibits collagen crosslinking, reduced gland stiffness, normalized the extracellular stroma surrounding breast lesions, enhanced tumor latency significantly and significantly decreased tumor incidence (see Figures 3 and 4; Levental et al). Upon further exploration we noted that even though some of the treated animals eventually did begin to develop tumors - these tumors were not very aggressive, and often were very low grade and could be classified as non invasive or premalignant in many cases. Indeed, we noted that when collagen cross-linking was reduced and stiffness was lower there was a marked reduction in the proliferation rate of the lesions found in these animal breasts and they were also smaller and appeared more differentiated. Obviously, we are keen to further explore the relationship between extracellular matrix tension/stiffness and breast tumor progression. Therefore, in the next few years we will be examining the relevance of mechanical force and ECM remodeling and tension to additional genetic models of breast tumorigenesis including PyMT. In this respect early studies confirm our observations with the less aggressive Her2/Neu mouse model in that we do appear to see a reduced tumor incidence and heightened latency. We will now be looking into effects on tumor metastasis.

To address the likelihood that the elevated lysyl oxidase could be promoting mammary gland stiffness and collagen remodeling and linearization to promote tumor progression we induced remodeling of the mammary gland stroma in nude mice by transplanting fibroblasts that expressed elevated levels of activated lysyl oxidase. When we compared the effect of lysyl oxidase remodeling to that induced by control fibroblasts we noted that the glands with the elevated lysyl oxidase were significantly different in that they had a detectable fibrotic response. We could see a significant stiffening of the glands, an increase in the linearization of the collagen and more deposition and assembly of fibrillar collagen as revealed by picrosirius red and polarized light imaging (see Figures 2B-F; Levental et al). More importantly, when we injected pre malignant mammary organoids into these pre treated mammary glands - only the mammary epithelial cells injected into the lysyl oxidase stiffened, fibrotic glands underwent full transformation as can be observed by the huge increase in tumor size, the invasive behavior of the epithelial cells as revealed by H&E staining and the obvious induction of angiogenesis (see Figures 2G-I; Levental et al.). Importantly, we also noted that increasing breast stroma stiffening and crosslinking promoted the invasiveness of these pre malignant breast lesions.

To rule out the possibility that we might have observed these phenotypes merely because of the elevated lysyl oxidase and not due to mechanical changes we conducted a series of experiments using organotypic culture models. We used ribose to cross link and stiffen the matrix surrounding nonmalignant mammary organoids and assayed for changes in cellular behavior. We also induced expression and activation of ErbB2 to determine whether the physical properties of the ECM could modify the transformation effect of a well known/characterized oncogene very frequently elevated/amplified in human breast cancer. We noted that increasing matrix stiffness destabilized the architecture of these pre assembled mammary acini although there was not noticeable effect on cellular invasion (see Figure 5; Levental et al.). Likewise when we turned on the activity of the ErbB2 oncogene we also observed a destabilization of the tissue phenotype that included elevated cell proliferation and filling of the lumens similar to what has been observed in the premalignant breast in association with high grade DCIS lesions with amplified ErbB2 oncogene. Nevertheless, once again we did not observe any invasive behavior. However, when we turned on the ErbB2 oncogene in the structures that were embedded in the cross-linked stiffened extracellular matrix we now observed marked and robust invasion. Upon investigation we could show that there was an elevation in focal adhesion activity (see Figure 5D; Levental et al). We further implicated force-dependent integrin clustering and focal adhesion assembly in this phenotype by co expressing a cluster mutant beta 1 integrin that recapitulates the stiffness behavior of integrins in soft matrices. Again and consistent with a central role for mechanotransduction through integrins we noted that forced clustering of integrins not only elevated cellular signaling but promoted the invasive behavior of oncogenically pre transformed mammary

epithelial cells into a soft gels and drove their tumorigenic behavior in vivo in nude mice (Figure 6; Levental et al). Finally, to understand HOW force dependent integrin signaling could exert such a profound effect on breast tumor behavior we explored functional links to PI3Kinase signaling. PI3Kinase is induced by growth factors (EGFR, Her2/Neu etc) and elevated by ras signaling both of which are frequently elevated in human breast cancers. Upon investigation we noted that extracellular matrix stiffness enhanced PI3kinase activity, promoted EGFR and ErbB2 dependent PI3Kinase activation and regulated the invasive phenotype of the breast cells in response to elevated matrix cross-linking and stiffening. Indeed, we could show that inhibiting PI3kinase activity prevented force-dependent invasion of breast tumor cells and that inhibiting collagen cross-linking and stiffening in vivo reduced integrin focal adhesions and tempered PI3kinase signaling/activity while coincidentally reducing tumor incidence and aggressiveness (see Figure 7; Levental et al).

In addition to these studies over the past year we have also set up and calibrated a novel nano indenter method with our collaborator Dr. Hansma (Hansma et al., 2009, see attached PDF). We have used this micro indenter to show that breast tumorigenesis in the MMTV-PyMT model is associated with significant changes in matrix remodeling that induce a stiffening of the tissue. The work is now being continued and will comprise another manuscript that we hope to submit for publication later on this fiscal year. We anticipate that this work will be reported in the next progress report for 2009-2010.

- a. Immunostaining to characterize changes in ECM composition, deposition, and modification during mammary gland malignant transformation. **This task is now completed using the MMTV-Neu mouse breast tumor model and the work has been summarized in a manuscript that we believe will be accepted for publication at Cell Journal. In this next fiscal year we will be completing the analysis of ECM modifications and stiffening during breast tumor progression in an independent mouse model the MMTV-PyMT model for validation of our findings and also to explore potential relevance of our findings to tumor metastasis.**
- b. Analysis of changes in ECM composition, deposition, and modification during mammary gland transformation. **This task has now been completed. See above for details with regards to publication of findings and extension to a different mouse model to explore relationship to breast tumor metastasis.**
- c. Analysis of elastin and collagen cross-linking. **This task has now been completed. See above for details with regards to publication of findings and extension to a different mouse model to explore relationship to breast tumor metastasis.**

PART D Correlation of effects with malignancy-dependent changes in epithelium and fibroblasts.

- a. Morphological and histological analysis of primary murine tissue to establish stage, fibroblast number, transdifferentiation, proliferation, and apoptosis. **This task has now been completed see above for details with regards to publication of findings and extension to a different mouse model to explore relationship to breast tumor metastasis. In the next year we also plan on exploring in depth the relationship of matrix remodeling and stiffening to fibroblast phenotype since it has come to light that there are several different types of fibroblasts in the breast epithelium that each could contribute unique aspects of breast tumorigenesis - including those derived from the resident pool of mammary gland fibroblasts, those recruited from the mesenchymal stem like pool, those induced to transdifferentiate from adipocytes and those induced to transdifferentiate from pluropotent breast stem cells. This will be achieved through two**

initiatives - the first being via application of a panel of immuno markers that will be applied in situ to tissue sections and the second through the isolation of fibroblasts and their subsequent analysis through FACS manipulations.

Task 2: Develop xenograft and transgenic mouse models to test whether ECM stiffness regulates apoptotic responsiveness of mammary epithelia in vivo.

We have not made significant progress on this aim this past fiscal year. However in the next funding cycles and over the next few years we hope to execute studies to assess apoptotic treatment response assays in nude mice to assess effects of matrix physical properties on epithelial cell behavior in response to radiation treatment in vivo. Due to the delayed transfer of funds from the University of Pennsylvania to UCSF we anticipate carry over funds will exist and we will therefore be requesting a no cost extension to complete this set of studies.

Task 2: Develop xenograft and transgenic mouse models to test whether ECM stiffness regulates apoptotic responsiveness of mammary epithelia in vivo.

PART A. Xenograft studies to test whether ECM stiffness could regulate apoptotic responsiveness of a mammary epithelium in vivo. NOTE: These studies were to be conducted in collaboration with Dr. Bernhard from the Radiation Biology Department at the University of Pennsylvania. However Dr. Bernhard relocated to Oxford University at the beginning of the second year of funding of this proposal. Thereafter, Dr. Weaver relocated to UCSF towards the end of the second year of funding of this proposal. After having relocating to UCSF, Dr. Weaver established collaborators in the area of radiation biology for breast cancer - she has recruited Dr. Zena Werb to participate as a collaborator on these studies as well as Dr. Mary Helen Barcellos-Hoff at LBNL in Berkeley California. Drs. Werb and Barcellos-Hoff have more than 20 years of experience conducting radiation studies in culture and in vivo. While this has certainly delayed the initiation of these experiments somewhat - we anticipate making good progress in this aim in the forthcoming years of funding.

- a. Based upon doses of established short-term and long-term re-growth assays Weaver laboratory in collaboration with Werb laboratory will conduct xenograft assays of radiation sensitivity of tumorigenic MECs in vivo following their injection and establishment of viable, palpable tumors sub-cutaneously in nude mice based upon short-term viability effects as the end point. (Months 6-36). These studies have yet to be initiated.**
- f. Based upon doses of established short term and long term re-growth assays Weaver laboratory in collaboration with Werb laboratory will conduct xenograft assays of radiation sensitivity of tumorigenic MECs in vivo following their injection and establishment of viable, palpable tumors sub-cutaneously in nude mice based upon long-term re-growth assays as an end point. (Months 12-36) These studies have yet to be initiated.**
- g. Weaver laboratory will assess biocompatibility of PEG gels injected sub-cutaneously into nude mice. (Months 24-36) **These studies have yet to be initiated.****
- i. Weaver laboratory in collaboration with Werb laboratory will assess effect of radiation responsiveness of tumorigenic MECs embedded within soft versus stiff PEG gels and/or cross-linked collagen gels or collagen gels co injected with LOX expressing fibroblasts to induce collagen cross linking in vivo, injected sub-cutaneously into nude mice and assessed for short term viability as the end point. (Months 24-36) We have completed studies aimed at exploring**

the effect of collagen crosslinking on MEC behavior in vivo. We have yet to assess collaborative effects of collagen crosslinking on radiation responsiveness.

- j. Weaver laboratory in collaboration with Werb laboratory will assess effect of radiation responsiveness of tumorigenic MECs embedded within soft versus stiff self-assembling peptides and/or cross-linked collagen gels in vivo, injected sub-cutaneously into nude mice, and **assessed for long term re-growth as the end point.** (*Months 24-36*) **These studies have yet to be initiated.****
- k. Weaver laboratory in collaboration with Werb laboratory will assess effect of radiation responsiveness of tumorigenic MECs embedded within soft versus stiff PEG gels and/or cross-linked collagen gels in vivo, injected sub-cutaneously into nude mice, and assessed for long term effects on tissue morphology as the end point. (*Months 24-36*). **These studies have yet to be initiated.****
- l. Weaver laboratory in collaboration with Werb laboratory will assess effect of radiation responsiveness of tumorigenic MECs embedded within soft versus stiff PEG gels in vivo, injected sub-cutaneously into nude mice, and assessed for long term effects on gene expression markers as the end point. (*Months 24-36*). **These studies have yet to be initiated.****
- m. Weaver laboratory in collaboration with Werb laboratory will assess effect of radiation responsiveness of tumorigenic MECs embedded within soft versus stiff PEG gels and/or cross-linked collagen gels in vivo, injected sub-cutaneously into nude mice, and assessed for long term effects on apoptosis resistance/stress response protein expression as the end point. (*Months 24-36*). **These studies have yet to be initiated.****

PART B. Transgenic animal studies designed to test whether ECM stiffness could influence apoptosis regulation in vivo. These studies are being conducted in collaboration with Dr. Zena Werb.

- a. Validation of beta 1 integrin cluster mutant ES cell generation (*Months 0-4*). **We have generated the targeting vector and have completed the first rounds of ES cell screening. These ES cells have now been expanded and we are in the process of rescreening these lines. We anticipate that this will be completed and we will then arrange to have transgenic mouse injections initiated during the next funding cycle.****
- b. Generation of transgenic beta 1 integrin mouse model through the UCSF Cancer Center Sponsored cell center transgenic mouse resource. (*Months 4-12*) **No progress this year see above.****
- c. Breeding and line generation of beta 1 integrin cluster mutant mouse model (*Months 12-24*) **No Progress this year see above****
- d. Initial analysis of behavior of isolated mammospheres in 2D and 3D culture from beta 1 integrin cluster mutant transgenic mouse model (*Months 24-36*). **We have analyzed the behavior of the beta 1 integrin cluster mutant in mammary epithelial cell lines that co express various oncogenes including ras, EGFR and ErbB2. The isolation and analysis of the mouse lines has yet to be conducted but we hope will begin in the next few years.****

- e. Assessment of the effect of beta 1 integrin clustering on breast tissue behavior in vivo using xenograft manipulations and immortalized human mammary epithelial cells. (*Months 0-24*). **We have completed these studies.**
- f. Characterization of the cross linking of mouse breast tissue before and during malignant transformation using biochemical analysis. (*Months 0-36*). **We have completed these studies in the Her2/Neu mouse model.**
- g. Assessment of the status and effect of lysyl oxidase during breast tumorigenesis (*Months 0-18*). **We have completed these studies using the Her2/Neu mouse model and are in the process of examining effects using the PyMT mouse model which is a much more aggressive genetic model and therefore is more rigorous proof.**
- h. Assessment of the effect of increasing lysyl oxidase activity on breast transformation in vivo. (*Months 0-18*). **These studies have been completed.**
- i. Assessment of the effect of decreasing lysyl oxidase activity on breast transformation in vivo using pharmacological inhibitors. (*Months 6-18*). **These studies have been completed although we are continuing with work to assess effects on more aggressive models including the PyMT which is highly penetrant AND very metastatic.**
- j. Assessment of the effect of decreasing lysyl oxidase activity on breast transformation in vivo using antibody inhibition. (*Months 8-18*). **These studies have been completed in the Her2/Neu mouse model although we are in the process of conducting studies using antibody inhibition in the PyMT mouse model and intend to also assess effects in other transgenic models.**
- k. Assessment of the effect of circulating lysyl oxidase on breast tumor metastasis in vivo (*Months 12-36*). **These studies have just been initiated.**
- l. Assessment of the biophysical properties of COLA mutant mice which fails to turn over collagen I due to a mutation in its MMP9 recognition site using shear rheology (*Months 24-36*). **These studies have been completed..**
- m. Assessment of the biophysical properties of the OS mouse which fails to assemble proper collagen bundles. (*Months 24-36*) **These studies have been completed.**
- n. Assessment of the effect of increasing collagen stiffness on breast tissue behavior and response to therapy ex vivo using collagen generated from the COLA mouse (*Months 24-36*). **These studies have yet to be started.**
- o. Assessment of the effect of decreasing collagen stiffness on breast tissue behavior and response to therapy ex vivo using collagen generated from the OS mouse. (*Months 24-36*). **These studies have yet to be started.**

Task 3: *Build a computational model that can predict how changes in ECM compliance could influence integrin-dependent apoptosis responsiveness of mammary epithelia and query this model with clinical data.*

PART A. To assemble and generate cell biology and published data required for basic computational model. These studies are to be conducted in collaboration with Dr. Hammer from the Department of Bioengineering at the University of Pennsylvania.

PART B. Generate a simple cell adhesion computational model based upon published values from the literature and data generated using culture models. These studies are to be conducted in collaboration with Dr. Hammer from the University of Pennsylvania Bioengineering Department.

- a. Using published data and our experimental data initiate calculations and assumptions required for the basic cell adhesion model without incorporating force parameters. (*Months 12-24*). **This work has now been completed**
- b. Pilot testing of basic computational model and comparison with experimental data obtained using cell culture model without incorporating force parameters. (*Months 24-28*) **This work has now been completed.**
- c. Adjust basic cell adhesion model to incorporate experimental data. (*Months 28-36*). **This work has now been completed.**

PART C. Incorporate mechanical force values and assumptions into the basic adhesion model. These studies are to be conducted in collaboration with Dr. Hammer from the University of Pennsylvania Bioengineering Department.

- a. Amend basic cell adhesion model to incorporate force parameters. (*Months 28-36*). **This work has been completed and has been written for peer reviewed publication submission.**
- b. Test mechano-adhesion model and compare theoretical values with experimental data obtained using cell culture model. (*Months 24-36*). **These studies are now in progress.**
- c. Adjust mechano-adhesion model to incorporate experimental data. (*Months 24-36*). **Model adaptation has yet to be initiated.**

PART D. Initiate modeling studies using micro array data sets from the cell culture models.

- a. Isolate RNA from MECs within a 3D matrix with varying matrix compliances. (*Months 0-12*). **We have not yet initiated these studies.**
- b. Purify and prepare samples for micro array analysis. (*Months 0-12*). **We have not yet initiated these studies.**
- c. Generate micro array data sets from samples of MECs in 3D matrices of varying compliances. (*Months 12-18*). **We have not yet initiated these studies.**
- d. Conduct statistical analysis of micro array data sets generated from MECs in 3D matrices of varying compliances. (*Months 18-24*). **We have not yet initiated these studies.**
- e. Conduct bioinformatics analysis of micro array data sets generated from MECs in 3D matrices of varying compliances. (*Months 18-24*). **We have not yet initiated these studies.**
- f. Verify validity of micro array analysis by RT-PCR or real time PCR of 10 target genes. (*Months 24-36*). **We have not yet initiated these studies.**

PART E. Initiate pilot studies to analyze micro array data sets and clinical samples from neoadjuvant breast cancer clinical trial data using a simple model generated using gene data from

culture systems. These studies are to be conducted in collaboration with Dr. Esserman from the University of California San Francisco and with Drs. Hammer from the Department of Bioengineering at the University of Pennsylvania.

- a. Select clinical samples to be examined in collaboration with Dr. Esserman. (Months 6-18). **We have yet to begin the work.**
- b. Obtain micro array data sets from clinical samples. (Months 12-18). **We have yet to begin this work.**
- c. Conduct statistical analysis of clinical micro array data sets. (Months 12-24). **We have yet to begin this work.**
- d. Conduct bioinformatics analysis of clinical micro array data sets. (Months 12-36). **We have yet to begin this work.**
- e. Test predictability of identified force regulated targets in micro array data sets. (Months 24-36). **We have yet to begin this work.**
- f. Secure clinical biopsy specimens for experimental validation. (Months 24-36) **We have yet to begin this work.**
- g. Begin to examine targets identified using virtual model analysis of micro array data sets using either immunohistochemistry or in situ analysis. (Months -30-36). **We have yet to begin this work.**

Task 4: *Develop non-invasive imaging tools that could be used to monitor changes in ECM stiffness or stiffness-induced changes in mammary tissue phenotype.*

PART A. Proof of principal studies for imaging sensitivity using 3D culture models and imaging analysis of excised mouse breast tissue. These experiments are to be done in collaboration with Dr. Wong at Boston University with input from Dr. Hammer at University of Pennsylvania and with Dr. Paul Barbone at Boston University.

In the first two funding cycles of this grant we worked in collaboration with colleagues both at University of Pennsylvania and also at Boston University to develop non-invasive imaging tools to monitor changes in ECM stiffness or stiffness-induced changes in mammary tissue phenotype. We attempted to set up sonoelastography imaging. While we made good progress and we able to assess stiffness modifications in our animal models - the difficulty in any of these current imaging techniques is their lack of resolution. Thus, both sono elastography and MR elastography are inherently nonsensitive and their length scale of detection does not even approach 1 mm. This is not then useful for many of the issues we aim to address. We had also outlined a strategy to develop novel quantum dot imaging tools - and while this work is slowly progressing identifying high stringency targets that reflect specific modifications in collagen or extracellular matrix remodeling is more challenging than we had initially anticipated. Instead, what we have done is to work in collaboration with Dr. Paul Hansma to assess the efficacy of an insitu indenter probe which could be used to assess mammary gland stiffness in situ in the clinic. We have conducted feasibility studies using this probe on experimental breast tumor models (MMTV-PyMT) (see Hansma et al In Press 2009). We are the process of acquiring an IRB to permit us to apply this probe to human tissue in the clinic. Prior to commencing with these studies we will obtain DOD IRB approval status. Moreover, given the limited time remaining on this DOD Scholar Award it is

not clear if we will be able to complete these studies and secure their publication rapidly. Nevertheless we do hope to be able to report some progress in this area in next years 2010 progress report.

- b. **Weaver laboratory to obtain scanning electron microscopy imaging** analysis of organization of 3D hydrogels with differing stiffness and correlate these measurements with those obtained using shear rheology and indenter. (*Months 8-18*). **These studies are still in progress.**
- c. **Weaver laboratory to obtain scanning electron microscopy images** of organization of stromal matrix surrounding normal and malignantly transformed breast tissue from mice and correlate these measurements with those obtained using shear rheology and indenter. (*Months 8-18*) **These studies are still in progress.**
- f. **Weaver laboratory in collaboration with Wong laboratory and Dr. Paul Barbone at Boston University** to conduct measurements of imaging elastography of progressively malignantly transformed mouse breast tissue. (*Months 16-36*) **As discussed above - we have opted to use a novel micro indenter device to conduct these studies. Therefore these studies are completed but using a different approach.**
- g. **Weaver laboratory in collaboration with Wong laboratory and Dr. Paul Barbone at Boston University** to conduct measurements of imaging elastography of transgenic mouse models with breast tumors treated with a pharmacological cross linker inhibitor. (*Months 16-36*) **These studies have been completed using our new micro indenter device.**
- h. **Weaver laboratory in collaboration with Wong laboratory and Dr. Paul Barbone at Boston University** to conduct measurements of imaging elastography of transgenic mouse models with breast tumors treated with a lox inhibitory antibody. (*Months 18-36*) **These studies have been completed using our new micro indenter device.**
- i. **Wong laboratory to conduct trial studies using quantum dots** to image single well characterized abundant cell surface molecules in MEC colonies in 3D cultures. (*Months 24-30*). **These studies have not been initiated yet.**
- j. **Wong laboratory to conduct trial studies using quantum dots** to image two different well characterized abundant cell surface molecules in MECs in 3D cultures. (*Months 28-32*). **These studies have not been initiated yet.**
- k. **Wong laboratory to work jointly with Weaver laboratory** to conduct studies to assess the sensitivity of quantum dot technology against low abundance cell surface molecules in MECs in 3D cultures. (*Months 32-36*). **These studies have not been initiated yet.**

PART B. Set up and initial screening trials with peptide library for identification of novel stiffness markers in the ECM.

- b. **Weaver laboratory to conduct a thorough analysis of the collagen cross linking** induced in developing breast tumors initially through a consultancy fee and thereafter through establishment of technology in the Weaver laboratory. (*Months 0-24*) **These studies have not been initiated.**
- c. **Weaver laboratory to test and conduct proof of principal experiments using the phage display library with appropriately cross linked collagen hydro gels.** (*Months 6-30*). **These studies have not been initiated yet.**

- d. **Weaver laboratory to conduct pilot studies** aimed at identifying novel conformational changes in collagen cross linked gels with differing stiffness properties. (*Months 24-36*). **These studies have not been initiated yet.**
- e. **Weaver laboratory to conduct initial analysis of peptide antibody efficacy** against human breast tumor tissues to determine whether antibodies will detect changes in matrix cross linking in these samples. (*Months 24-36*). **These studies have not been initiated yet.**

Reportable Outcomes:

A. Manuscripts

1. Lopez, J.I, Mouw, J.K., Weaver V.M. Biomechanical regulation of cell orientation and fate, *Oncogene* 27:6981-6993, 2008. (see attached)
2. Mouw, J., Desai, S., and Weaver V.M. Forcing transformation: biophysical regulation of mammary epithelial cell transformation, *The Pathomechanics of Tissue Injury and Disease, and the Mechanophysiology of Healing*", 2008. (see attached - NOTE last years report had an earlier version of this manuscript - version included in this progress report is now the final version that published).
3. Kang, I., and Weaver, V.M. Tensional Homeostasis, *Encyclopedia of Cancer* Springer-Verlag Berlin Heidelberg, New York 2008. (see attached)
4. Erler, J., and Weaver V.M. Tissue Context and Tumor Metastasis, *Clin Exp Met*, 1:35-49, 2009. (see attached)
5. Butcher, D., Alliston, T., Weaver, V.M. A tense situation: forcing tumor progression. *Nat Rev Cancer*, 2:108-122, 2009. (see attached)
6. Kumar, S., and Weaver, V.M. Mechanics, malignancy, and metastasis: The force journey of a tumor cell, *Cancer and Metastasis Reviews*, 2009 (Epub Ahead of print). (see attached)
7. Engler, A., Humbert, P., Wehltre-Haller, B., and Weaver V.M. Multi-Scale modeling of form and function. *Science*, 324:208-212, 2009. (see attached)
8. Paul Hansma, Hongmei Yu, David Schultz, Azucena Rodriguez, Eugene Yurtsev, Jessica Orr, Simon Tang, Jon Miller, Joseph Wallace, Frank Zok, Chen Li, Richard Souza, Alexander Proctor, Davis Brimer, Xavier Nogues-Solan, Leonardo Mellbovsky, M. Jesus Peña, Oriol Diez-Ferrer, Phillip Mathews, Connor Randall, Alfred Kuo, Carol Chen, Mathilde Peters, David Kohn, Jenni Buckley, Xiaojuan Li, Lisa Pruitt, Adolfo Diez-Perez, Tamara Alliston, Valerie Weaver, Jeffrey Lotz, *The tissue diagnostic instrument. Review of Scientific Instruments*, In Press, 2009 (see attached revised article: note we attached an earlier version in last years progress report - this attached version in this report is now the final accepted version).
9. Levental, K.R., Yu, H., Kass, L., Lakins, J.N., Erler, J.T., Egeblad, M., Fong, S.F.T., Csiszar, K., Giaccia, A., Yamauchi, M., Well, R., Gasser, D.L., Weaver V.M., *Matrix Cross-linking Forces Tumor Progression by Enhancing Integrin-dependent signaling*. In *Revision Cell*. This manuscript is being modified as per reviewers suggestions to that it is acceptable for publication (see attached submitted article that is now being revised - i.e. we are performing experiments requested by reviewers and will amend the manuscript and hope to re submit by end of June 2009)

10. Tsai K.K.C. Chatterjee, C., Werner, M.E., Jonathan N. Lakins, Nuth, M., Tobias, J, Mian, S. and Weaver V.M. The Third Dimension Drives N-CoR2-dependent Death Resistance. Under Revision Nature Medicine. This manuscript is being modified so that it will be acceptable to the editors for publication (see Weaver Progress report attachments 2007-2008 - once the final article has been accepted and in press we will send in this version - in next years progress report).
11. Gilbert, P., Mouw, J., Unger, M., Lakins, J.N., Gbengnon, M.K., Nuth, M., Clemmer, V., Colligon, T., Naylor, T., Licht, J., Boudreau, N., Weber, B., and Weaver, V.M. Global expression profiling reveals a novel role for HoxA9 in breast cancer and BRCA1 regulation. ReSubmitted J Clin Invest. This manuscript is currently under review (see attached submitted article version).
12. Paszek, M.J., Boettiger, D., Weaver, V.M., and Daniel A. Hammer, D.A. Mechanical Mechanisms of Integrin Binding Cooperativity and Clustering elucidated with Adhesive Dynamics Simulation. Submitted PLOS Computational (NOTE: In last years progress report we attached a copy of the proposed manuscript - therefore we have not re attached the manuscript here - it has been somewhat modified - instead we will attach the final accepted and published version with next years progress report.)

B. Abstracts

1. C. Frantz, J. Friedland, J. Lakins, W. Liu, J. Chernoff, M. Schwartz, C. Chen, D. Boettiger, V.M. Weaver. Deconstructing the 3rd Dimension: How matrix dimensionality promotes survival. Dec 17 2008, ASCB 48th Annual Meeting, San Francisco, CA (see attached)
2. Lopez J., Weaver V. Evidence of Durotaxis in Transformed Mammary Epithelial Cells. Dec 15 2008, ASCB 48th Annual Meeting, San Francisco, CA. (see attached)
3. Miroshnikova, Y.A., Frantz, C., Leight J.L., Johnson, K.R., Jorgens, D.M., Auer, M., Spirio, L., Sieminski, A.L., Weaver V.M. Analysis of MCF10A mammary epithelial cell acinar morphogenesis within a well-defined 3-dimensional system, the self assembling peptides. Dec 15 2008, ASCB 48th Annual Meeting, San Francisco, CA. (see attached)
4. J. Mouw, P. Gilbert, M. Unger, J. Lakins, M. Gbengnon, M. Nuth, V. Clemmer, T. Colligan, M. Benezra, J. Licht, M. Feldman, N. Boudreau, B. Weber, V. Weaver. HoxA9 Regulates Stromal-Mammary Epithelial Interactions through Modulation of BRCA1 Expression. Dec 16 2008, ASCB 48th Annual Meeting, San Francisco, CA. (see attached)
5. M. J. Paszek, D. Boettiger, D. A. Hammer, V. Weaver. An Integrated Response Mechanism That Encompasses Cell and Extracellular Matrix Mechanics Regulates Integrin Binding Cooperativity, Clustering, and Adhesion Function. Dec 14 2008, ASCB 48th Annual Meeting, San Francisco, CA. (see attached)
6. K. M. Stewart, N. Cohet, D. Reisman, J. Lakins, G. I. Rozenberg, A. N. Imbalzano, J. A. Nickerson, V. M. Weaver. Loss of BRM Expression Contributes to a Tumor-Like Phenotype via Enhanced $\alpha 5 \beta 1$ Integrin Expression and Activity. Dec 15 2008, ASCB 48th Annual Meeting, San Francisco, CA. (see attached)
7. H. Yu, K. Levantal, L. Kass, J. Erler, M. Yamauchi, R. Wells, D. Gasser, V. Weaver. Roles of Collagen Crosslinking and ECM Remodeling in Mammary Tumor Malignant Transformation. Dec 17 2008, ASCB 48th Annual Meeting, San Francisco, CA. (see attached)

8. Kelvin K.C. Tsai , Patrick Chu , Jonathan N. Lakins , Valerie M. Weaver, Pleiotropic Effects of Nuclear Corepressor-2 on Breast Cancer Progression, Dec 17 2008, ASCB 48th Annual Meeting, San Francisco, CA. (see attached)
9. Kandice Levantal, Hongmei Yu., Inkyung Kang, David Gasser, Rebecca Wells and Valerie M. Weaver. Collagen remodeling affects mammary tumor progression through PI3K mediated signaling. Oct 4th 2008, BMES Annual Meeting, Chicago, IL. (see attached)
10. Paszek, Matthew, David Boettiger, David, Valerie Weaver, Valerie and Hammer, Daniel. The integrated mechanics of the cell and ECM regulate integrin binding cooperativity and clustering, 4th 2008, BMES Annual Meeting, Chicago, IL. (see attached).

C. Oral Meetings Presentations:

1. Weaver, V.M., Plenary Speaker, “Forcing form and function”, Growth/Signaling/Adhesion II, in the Physics and Biology of Morphogenesis Workshop at Kalvi Institute for Theoretical Physics, UCSB, Santa Barbara, California, 03/07/08
2. Weaver, V.M., Symposium speaker, “Forcing Tumor Progression,” Tissue Microenvironment session, for the EMT meeting, Cold Spring Harbor Laboratories, in Cold Spring Harbor, New York, 03/19/08.
3. Weaver, V.M., Symposium speaker, “Forcing Transformation”, Canceropôle PACA Mechanisms of Invasion Innovative Targeted Therapies in Head and Neck Cancer, Nice, France, 04/04/08
4. Weaver, V.M., Symposium speaker , “Tumor Microenvironment”, Era of Hope DOD Breast Cancer Meeting, Baltimore, Maryland, 06/27/08
5. Weaver, V.M., Symposium speaker, “Matrix Topology and Cell Fate”, Gordon Conference on Signaling by Adhesion Receptors, Mount Holyoke College, South Hadley, Massachusetts, 07/30/08
6. Weaver, V.M., Keynote Speaker, “Forcing Tumor Progression” NCI Tumor Microenvironment Conference, Seattle, Washington, 07/07/08
7. Weaver, V.M., Symposium speaker, “Forcing Transformation” for Cell Interactions Microenvironment session at the International Metastasis Research Society & American Association for Cancer Research meeting, Vancouver, British Columbia, Canada, 08/04/08
8. Weaver, V.M., Plenary Presentation “Matrix Topology and Durotaxis in Tumors”, Regulation of Cell Shape and Form Plenary Session, ELSO 2008 Frontiers of Cellular, Developmental and Molecular Biology Conference, in Nice, France, 09/02/08
9. Weaver, V.M., Keynote speaker, “Stromal Factors in Tumorigenesis”, How Critical are Stromal Factors in Tumourigenesis session at the Cancer Research UK Cambridge Research Institute (RCI) Inaugural Annual Symposium in Cambridge, United Kingdom, 09/13/08
10. Weaver, V.M., Invited Symposia Speaker, “Context-dependent Migration,” Frontiers in Cell Migration: from Mechanism to Disease meeting, National Institute of General Medical Sciences, and Cell Migration Consortium, Natcher Conference Center, Bethesda, Maryland, 09/16/08.

11. Weaver, V.M. Symposium speaker, "Matrix Topology", Extracellular and Membrane Proteases in Cell Signaling symposium, Iowa State University, Ames, Iowa, 09/19/08
12. Weaver, V.M. Symposium speaker, "Matrix Architecture and Cell Fate", 2008 Biennial Meeting of the Society of Matrix Biology, (ASMB), San Diego, California, 12/08/08.
13. Weaver, V.M., Symposium speaker, "Forcing form and Function", Keystone Meeting on Mechanotransduction, Taos, New Mexico, 01/23/09.

D. Invited Institutional Presentations:

1. Weaver, V.M., Invited Seminar, "Forcing form and function," Department of Microbiology and Immunology, ReMS Seminar series Stanford School of Medicine, Palo Alto, California, 05/01/08.
2. Weaver, V.M., Invited Seminar, "Transformation – a force to resist", Basic Reproductive Sciences Seminar, University of Colorado, Denver, Colorado, 05/13/08
3. Weaver, V.M. Invited Seminar, "Matrix architecture and breast tumor progression," Harvard Medical School June 2008, Boston, Massachusetts, 06/17/08
4. Weaver, V.M. Invited Seminar, "Matrix architecture and force dependent breast transformation," Tufts University, Boston, Massachusetts, 06/19/08
5. Weaver, V.M., Invited Seminar, "Dimensionality and treatment resistance" Life Science Group ICBP Meeting, LBNL, Berkeley, CA, 10/22/08
6. Weaver, V.M. Invited Seminar, "Forcing Transformation", University of San Francisco, Berkeley, Department of Bioengineering, Berkeley, CA, 11/120/08

E. Student Matriculation/Ph.D. Degrees

1. Kandice Levental, Ph.D. Bioengineering, Department of Bioengineering, University of Pennsylvania, May 2008
2. Matthew Paszek, Ph.D. Bioengineering, Department of Bioengineering, University of Pennsylvania, January 2009

Progress Summary and Conclusions

In this past fiscal year we have made encouraging progress in the development of novel biomaterials and approaches to measure, manipulate and modify native and synthetic biomaterials to recreate the natural extracellular matrix milieu found in the normal human breast and in breast tumors. We have also made significant advancements to be able to specifically manipulate isolated parameters associated with extracellular matrix remodeling including validation and analysis of novel self assembling peptide polymer gels and HA gels as well as the use of a compression device to apply mechanical force to 3D mammary organoids. While these synthetic matrices do NOT faithfully recapitulate all aspects of the human breast microenvironment they are/will be critical for elaboration of molecular mechanisms. These materials are also a critical step towards the development of high throughput screening approaches needed for drug discovery. In this past year we have also completed a series of animal manipulations using transgenic mice as well as xenografts and 3D organotypic culture studies to explore the relevance of collagen remodeling, cross linking and stiffening on breast tumor progression. This work has taken several years to complete and has now been written up and submitted for publication at

CELL Journal. We are confident that the manuscript will be accepted for publication this coming year. The work is highly significant because it is the FIRST ever demonstration that mechanical force regulates breast tumorigenesis and identifies a new therapeutic approach to treat and restrict tumor progression. We hope to be able to explore the relevance of these parameters on breast tumor treatment response. This past year we have also completed our studies with Dr. Hansma to calibrate his novel micro indenter device as a novel mechanosensory probe that might be useful in the clinic. Finally and importantly we have also made very good progress on completing the generation of a novel in silico model of cell adhesion/mechanotransduction that has yielded novel insight with regards to how mechanical force could modulate breast tumor progression and treatment. In addition to these research milestones my group has made dozens of presentations throughout the world at National and International conferences in cancer biology, breast cancer, bioengineering and the tumor microenvironment. I have in addition matriculated two Bioengineering graduate students who are continuing their cancer research studies in research labs that focus on breast cancer and have assisted two of my senior postdoctoral fellows to establish their own breast cancer research laboratories.

References:

- Bershadsky, A. D., Balaban, N. Q. and Geiger, B.** (2003). Adhesion-dependent cell mechanosensitivity. *Annu Rev Cell Dev Biol* **19**, 677-95.
- Geiger, B., Bershadsky, A., Pankov, R. and Yamada, K. M.** (2001). Transmembrane crosstalk between the extracellular matrix--cytoskeleton crosstalk. *Nat Rev Mol Cell Biol* **2**, 793-805.
- Grinnell, F.** (2003). Fibroblast biology in three-dimensional collagen matrices. *Trends Cell Biol* **13**, 264-9.
- Kass, L., Erler, J. T., Dembo, M. and Weaver, V. M.** (In progress). Matrix form and function regulate mammary tissue behavior. In Progress. *The International Journal of Biochemistry and Cell Biology/Cells in Focus*.
- Krouskop, T. A., Wheeler, T. M., Kallel, F., Garra, B. S. and Hall, T.** (1998). Elastic moduli of breast and prostate tissues under compression. *Ultrason Imaging* **20**, 260-74.
- Lewis, J. M., Truong, T. N. and Schwartz, M. A.** (2002). Integrins regulate the apoptotic response to DNA damage through modulation of p53. *Proc Natl Acad Sci U S A* **99**, 3627-32.
- Lo, C.M., H.B. Wang, M. Dembo, and Wang, Y.L.** (2000) Cell movement is guided by the rigidity of the substrate. *Biophys J* **79**, 144-52.
- Paszek, M. J. and Weaver, V. M.** (2004). The tension mounts: mechanics meets morphogenesis and malignancy. *J Mammary Gland Biol Neoplasia* **9**, 325-42.
- Paszek, M. J., Zahir, N., Johnson, K. R., Lakins, J. N., Rozenberg, G. I., Gefen, A., Reinhart-King, C. A., Margulies, S. S., Dembo, M., Boettiger, D. et al.** (2005). Tensional homeostasis and the malignant phenotype. *Cancer Cell* **8**, 241-54.
- Plewes, D. B., Bishop, J., Samani, A. and Sciarretta, J.** (2000). Visualization and quantification of breast cancer biomechanical properties with magnetic resonance elastography. *Phys Med Biol* **45**, 1591-610.
- Samani, A., Bishop, J., Luginbuhl, C. and Plewes, D. B.** (2003). Measuring the elastic modulus of ex vivo small tissue samples. *Phys Med Biol* **48**, 2183-98.
- Taylor, S. T., Hickman, J. A. and Dive, C.** (2000). Epigenetic determinants of resistance to etoposide regulation of Bcl-X(L) and Bax by tumor microenvironmental factors. *J Natl Cancer Inst* **92**, 18-23.
- Truong, T., Sun, G., Doorly, M., Wang, J. Y. and Schwartz, M. A.** (2003). Modulation of DNA damage-induced apoptosis by cell adhesion is independently mediated by p53 and c-Abl. *Proc Natl Acad Sci U S A* **100**, 10281-6.
- Unger, M. and Weaver, V. M.** (2003). The tissue microenvironment as an epigenetic tumor modifier. *Methods Mol Biol* **223**, 315-47.
- Weaver, V. M., Lelievre, S., Lakins, J. N., Chrenek, M. A., Jones, J. C., Giancotti, F., Werb, Z. and Bissell, M. J.** (2002). beta4 integrin-dependent formation of polarized three-dimensional architecture confers resistance to apoptosis in normal and malignant mammary epithelium. *Cancer Cell* **2**, 205-16.
- White, D.E., Kurpios, N.A., Zuo, D., J.A. Hassell, Blaess, S., Mueller, U., Muller, W.J.** (2004) Targeted disruption of beta-1-integrin in a transgenic mouse model of human breast cancer reveals an essential role in mammary tumor induction. **6**, 159-70.
- Wong, J.Y., Velasco, A., Rajagopalan, P., and Pham, Q.** (2003) Directed movement of vascular smooth muscle cells on gradient compliant hydrogels. *Langmuir*, **19**, 1908-13.
- Zaari, N., Rajagopalan, P., Kim, S.K., Engler, A., and Wong, J.Y.** (2004) Photopolymerization in microfluidic gradient generators: Microscale control of substrate compliance to manipulate cell response. *Advanced Materials*, **16**, 2133-37.
- Zahir, N. and Weaver, V. M.** (2004). Death in the third dimension: apoptosis regulation and tissue architecture. *Curr Opin Genet Dev* **14**, 71-80.



Published in final edited form as:

Oncogene. 2008 November 24; 27(55): 6981–6993. doi:10.1038/onc.2008.348.

Biomechanical regulation of cell orientation and fate

JI Lopez¹, JK Mouw¹, and VM Weaver^{1,2,3,4,5}

¹ Department of Surgery and Center for Bioengineering and Tissue Regeneration, University of California at San Francisco, San Francisco, CA, USA; ² Institute for Regeneration Medicine, University of California at San Francisco, San Francisco, CA, USA; ³ Department of Bioengineering and Therapeutic Sciences, University of California at San Francisco, San Francisco, CA, USA; ⁴ Department of Anatomy, University of California at San Francisco, San Francisco, CA, USA and ⁵ Department of Bioengineering, University of Pennsylvania, Philadelphia, PA, USA

Abstract

Biomechanical regulation of tumor phenotypes have been noted for several decades, yet the function of mechanics in the co-evolution of the tumor epithelium and altered cancer extracellular matrix has not been appreciated until fairly recently. In this review, we examine the dynamic interaction between the developing epithelia and the extracellular matrix, and discuss how similar interactions are exploited by the genetically modified epithelium during tumor progression. We emphasize the process of mechanoreciprocity, which is a phenomenon observed during epithelial transformation, in which tension generated within the extracellular microenvironment induce and cooperate with opposing reactive forces within transformed epithelium to drive tumor progression and metastasis. We highlight the importance of matrix remodeling, and present a new, emerging paradigm that underscores the importance of tissue morphology as a key regulator of epithelial cell invasion and metastasis.

Keywords

tension; integrins; migration; extracellular matrix; epithelial cell; force

Introduction

The majority of adult human cancers originate from the epithelial cells that line the surfaces of our bodies. Recent work has highlighted the mechanical changes associated with epithelial carcinomas, including elevated extracellular matrix (ECM) stiffness and increased interstitial pressure. Despite the association between mechanical force and tumors, however, cancer research has historically focused primarily on defining the role of genetic and biochemical changes in tumor progression. Nevertheless, a novel paradigm has emerged over the past few decades that brings a three-dimensional (3D) tissue perspective to epithelial cancers and that views cancer as a dynamic organ that exploit similar biochemical and biomechanical stimuli utilized during development to drive tumor evolution (Lelievre *et al.*, 1996; Wiseman and Werb, 2002; Nelson and Bissell, 2006).

Among the greater than 200 cell types in our bodies, epithelial cells have unique interactions with their microenvironment such that they maintain three distinct types of interfaces along

their cell surfaces. The apical surface of a simple epithelium is free of adhesion contact, whereas the lateral surfaces of the cells interact with neighboring cells through adhesions such as gap and adherens junctions. The basal surface of the epithelium, on the other hand, interacts with a specialized ECM that is rich in extracellular matrix laminin protein and is called the basement membrane (BM). The entire epithelium together with the BM thereafter is embedded within a collagen rich interstitial matrix. Through these different adhesive interactions, biochemical and biomechanical cues regulate epithelial cell fate to direct the development of the tissue and contribute to disease (Helmlinger *et al.*, 1997; Farge, 2003; Keller *et al.*, 2003; Brancaccio *et al.*, 2006). At the cellular level there exist a number of molecular mechanisms through which cells sense and transduce biochemical and mechanical cues that are localized within the membrane, the cytoskeleton and at specific cell-matrix complexes (Hamill and Martinac, 2001; Tamada *et al.*, 2004; Chiquet *et al.*, 2007). Although we know much about the effect of biochemical cues on epithelial behavior, we know relatively less about how force could influence cell and tissue fate. Nevertheless, branched epithelial structures, such as the mammary gland ductal tree, present multiple opportunities for force sensing and transmission that undoubtedly modify its structure, integrity and function. For instance, epithelial ducts are often embedded within an architecturally complex extracellular microenvironment that broadly encompasses cellular (fibroblasts, adipocytes, endothelial cells and immune cells) and non-cellular (structural extracellular and soluble factors such as cytokines and growth factors) components. In the context of tissues such as the breast, lung and heart, mechanical loading can physically alter the conformation of extracellular receptor complexes present in stromal cells such as fibroblasts and in the epithelial cells. In response to force, domains within these adhesion complexes can be stretched or compressed, either directly or indirectly, and these biomechanical changes thereafter elicit alterations in the structure and function of the ECM receptor complexes to actively influence signaling. Force can also modify the activity and function of other membrane complexes such as growth factor receptors, cytokine receptors, ion channels and cell-cell junctional complexes (Silver and Siperko, 2003). During tumor progression, importantly, the relationship between the epithelium and the ECM becomes increasingly perturbed. As tissues transform and metastasize, a dynamic interaction is established wherein changes in the ECM enable cells to undergo uncontrolled cell proliferation, resist apoptosis and acquire an invasive phenotype.

Epithelial tumor cell invasion and metastasis is the leading cause of mortality amongst cancer patients. Before the tumor epithelium can move away from its site of origin and become metastatic, tumor cells must first detach from neighboring cells, remodel the ECM and attain a migratory phenotype. In this review, we examine how directed ECM remodeling conspires with genetically transformed cells to promote cancer progression and metastasis. Although changes in the makeup of the tumor microenvironment ultimately affect all stages of tumor progression, this review specifically focuses on describing how forces generated between cells and the ECM influence cell orientation at the tissue, cell and molecular level to regulate tissue homeostasis. We begin the review by examining how epithelial cell/ECM interactions evolve during development to produce the different patterns seen in tissues that undergo morphogenetic programs such as branching morphogenesis. We describe the unique function that the BM has in the establishment of cell and tissue polarity. We then outline epithelial cell transformation and detail the reciprocal changes that occur between the epithelial cells and the ECM during tumor evolution, and discuss how these affect the morphology, orientation and metastatic behavior of transformed tissues. Finally, we present various technologies that have been developed to help us understand how force could modulate cancer progression.

Dynamic reciprocity in development

The development of distinct tissues and specialized organs require precise spatial and temporal coordination of cell growth and differentiation. The heterogeneity of cell types with distinct

positioning within epithelial tissues is the result of molecular pathways that establish tissue polarity to appropriately orient epithelial cells so that the cell's apical surface faces the luminal space and the basal surface is positioned towards the basal lamina. The development of this cellular orientation within a tissue depends upon a combination of internal and external biochemical and biophysical cues. In this regard, studies examining the phenomena of branching morphogenesis have provided important insight into how microenvironmental signals direct the spatial orientation of cells within epithelial tissues such as the lungs, kidneys and the mammary gland. Thus to generate epithelial structures that bud or branch, a cell or group of cells within the epithelium must correctly interpret microenvironmental cues to proliferate or migrate with the proper orientation to the established plane of tissue growth while maintaining the growth of the neighboring cells along the established polarity plane. Clearly biochemical signals such as growth factors or hormones have a key function in dictating tissue patterning (Chrenek *et al.*, 2001; Sternlicht *et al.*, 2006; Robinson, 2007). Nevertheless, biophysical cues also induce local changes in developmental processes such as branching morphogenesis, affecting a variety of cellular processes such as the rate of proliferation, the establishment of cell and tissue polarity, determination of cell shape and even specification of cell fate (Wang *et al.*, 2001; Wong *et al.*, 2003; Paszek *et al.*, 2005).

The development of epithelial tissues is tightly coupled to the production of the BM and interstitial matrix at all stages ranging from the newly formed embryonic endoderm and ectoderm (Leivo, 1983) to the remodeled pregnant mammary gland in the adult organism (Watson, 2006). As epithelial cells proliferate and differentiate, they remodel the BM and interstitial matrix to facilitate proper development and orientation in a process termed dynamic reciprocity (Bissell *et al.*, 1982). The ECM affects the behavior of cells through a variety of biochemical and biophysical mechanisms. For example, the composition of the BM and the interstitial matrix and the topology of the ECM cooperate to determine cell phenotype by triggering biochemical responses within a cell that alter gene expression, as well as protein synthesis and function (Kleinman *et al.*, 2003; Larsen *et al.*, 2006). ECM components also modulate cell phenotype by generating tensional forces within the matrix, as well as through matrix topology cues, that is, the spatial orientation of matrix fibrils. Cells interpret and respond to physical cues in their external matrix by generating tensional forces through cytoskeletal remodeling and actomyosin contractility by a process termed mechanoreciprocity (Paszek and Weaver, 2004; Polte *et al.*, 2004; Ghosh *et al.*, 2007). In this fashion, mechanoreciprocity critically modulates branching morphogenesis of epithelial tissues by regulating cell shape, polarity, motility and proliferation.

The interplay between biochemical and biophysical cues from the ECM and their influence on developmental processes such as epithelial branching morphogenesis has been elegantly described during lung alveolar expansion and branching morphogenesis (Cardoso and Lu, 2006). During lung development, the topology of the matrix governs the formation of epithelial buds that direct the fractal arrangement of ducts found in the mature lung. Force regulates ductal development as revealed by experiments using mouse pulmonary rudiments, which require cellular tension to undergo epithelial bud formation. Studies have demonstrated that local thinning of the BM, possibly induced through mechanical force, predicts the localization of epithelial cell budding revealed by the presence of a thicker BM in the quiescent tissue regions surrounding the areas undergoing localized budding. That tensional forces generated by the epithelial cells themselves could drive branching morphogenesis was illustrated through the use of inhibitory pharmacological agents that modify the activity of Rho-associated kinase (ROCK), myosin light chain kinase, myosin ATPase and via microfilament toxins which showed that following treatment with these agents, actomyosin tension was greatly diminished and epithelial budding was tempered with minimal effects on BM integrity. In contrast, when Rho GTPase was activated using CFN-1, epithelial budding was enhanced and branching morphogenesis was stimulated, with evident localized thinning of BM that correlated with

budding and cleft formation (Moore *et al.*, 2005). Biochemical assays further revealed that branching morphogenesis is not solely due to reduced Rho activity but was more closely associated with cell contractility. Interestingly, these studies showed that the rate of epithelial or mesenchymal cell proliferation was not widely affected by these treatments, despite extensive alterations in tissue patterning.

The mammary gland is a unique and dynamic organ that undergoes a variety of different gross morphological changes during development, differentiation, and pregnancy. Mammary gland development is governed by biochemical and biophysical cues that influence all stages of branching morphogenesis, differentiation and involution. As with the lung, the mammary epithelium is subject to a dynamic interplay between epithelial cells and the ECM stroma. Thus, either accelerating or inhibiting ECM turnover by modulating the activity or levels of matrix metalloproteases (MMPs) has a profound effect on the branching phenotype of the mammary gland. For example, inhibition of MMP-dependent ECM turnover by pharmaceutical inhibition or through genetic ablation or mutation reduces the degree of epithelial branching (Reviewed in Unger and Weaver, 2003; Page-McCaw *et al.*, 2007; Butcher *et al.*, 2008), whereas the introduction of an ectopically expressed MMP enhances ECM turnover and induces precocious branching morphogenesis (Simian *et al.*, 2001). Such experimental observations imply that ECM integrity is necessary for epithelial tissue homeostasis and that localized remodeling of the BM is required for tissue patterning. Similar to the lung epithelium, the mammary epithelium generates tension to modulate MEC behavior through actin cytoskeleton remodeling and through activation of actomyosin elements (Paszek *et al.*, 2005) (reviewed in Paszek and Weaver, 2004). For instance, primary cultures of murine MECs differentiate and assemble polarized growth-arrested acini that differentiate in response to lactogenic hormones when embedded in floating type I collagen gels. In contrast, these same cells assemble non-polarized continuously growing colonies when embedded in mechanically restrained collagen I gels (Barcellos-Hoff *et al.*, 1989). Biochemical cues from the BM are also important for normal tissue behavior as emphasized by the observation that a mixed MEC cell population, isolated from pre-lactating mouse mammary glands, neither polarize nor form functionally differentiated acini, unless they retain the ability to produce and assemble their own BM (Emerman and Pitelka, 1977; Barcellos-Hoff *et al.*, 1989).

Experiments performed in our laboratory have highlighted the interplay between physical force from the ECM and MECs during epithelial morphogenesis. Human MECs form growth-arrested, polarized, acini with cleared lumens when grown within compliant collagen I + recombinant BM (Figure 1a, first two columns). Yet we could show that as the matrix is progressively stiffened, MECs assemble colonies in which cell–cell junction and tissue polarity are compromised, luminal clearance fails and growth control is perturbed (Figure 1a, latter 3 columns, 1b). Importantly, we observed that the MECs within the structures interacting with the most compliant matrices form immature nascent focal contacts that mature into focal adhesions only when the ECM is significantly stiffened or the cells are exposed to exogenously applied force. We could additionally show that this process depends upon actomyosin contractility and substantial actin remodeling through experiments illustrating that introducing active V17Rho promotes focal adhesion maturation in MECs interacting with highly compliant matrices (Paszek *et al.*, 2005).

Although the idea of mechanoreciprocity is relatively new, evidence that ECM and actomyosin tensional force could influence cell shape and behavior has been observed for decades (Rodriguez-Boulán *et al.*, 1983; Ingber *et al.*, 1986). To this end Madin–Darby Canine Kidney (MDCK) cells are a valuable resource to study the molecular mechanisms directing the establishment of tissue polarity. Using the MDCK cell system, studies examining the phenomenon of polarity reversal have illustrated how the BM provides critical cues necessary for establishing apical–basal polarity. Thus, MDCK cells grown in 3D collagen gels form

polarized cysts with appropriate apical and basal orientation. However, in the absence of an exogenous ECM, MDCK cells form cysts with reversed polarity such that the apical surface of the cell faces the periphery of the cyst whereas the basal surface is oriented towards the lumen face which contains deposited BM proteins (Chambard *et al.*, 1984; Wang *et al.*, 1990a). Yet, when these reverse polarity cysts were challenged with a second ECM cue by re-embedding the cysts within 3D collagen gels, appropriate tissue polarity could be induced, suggesting BM is a critical regulator of tissue polarity. Importantly, in these experiments epithelial re-polarization was contingent upon loss of the inappropriate apical BM cue, because inhibition of luminal BM degradation compromised acini morphogenesis and led to the generation of aberrant multiple *de novo* lumens formation (Wang *et al.*, 1990a, b). The importance of BM in polarity was directly demonstrated by studies showing how MDCK fail to polarize when BM synthesis and assembly are inhibited (O'Brien *et al.*, 2001).

Transformation

Epithelial tissue homeostasis is defined as the maintenance of a polarized cellular monolayer in which cell growth and survival are tightly regulated and differentiation is promoted. Consistently, loss of tissue integrity is a hallmark of cancer, and compromised cell and tissue polarity indicates epithelial cell dedifferentiation that often precedes malignant transformation. Given that normal tissue homeostasis depends upon appropriate stromal–epithelial interactions, it is not surprising that tumor progression is frequently associated with changes in the extracellular stroma and BM. Indeed, tumors are characterized by profound ECM remodeling that alters their composition, topology and mechanical properties.

The progression of epithelial cancers from normal to malignant disease is characterized by genetic changes in the epithelium as well as modifications within the stroma termed tissue desmoplasia. Indeed, the induction of tissue desmoplasia can drive cancer progression, and inhibiting the reactive stroma can restrict and in some instances even prevent, tumor development (Bissell *et al.*, 1999; Unger and Weaver, 2003). Thus, cancer is a disease, the behavior of which is regulated by biochemical and biophysical cues not only at the cellular level, but also at the tissue, organ and system level. For instance, uncontrolled epithelial cell proliferation that increases tumor cell mass also elevates compressive forces on the BM and the surrounding ECM that can induce growth factor and MMP secretion, enhance growth factor and cytokine signaling and reduce BM integrity to enhance cancer cell invasion (Paszek *et al.*, 2005; reviewed in Paszek and Weaver 2004). Factors released by tumor cells can also activate the fibroblasts within the stroma and stimulate inflammatory cells to induce tumor cell migration. Activated fibroblasts deposit and remodel ECM proteins including Collagens I, III and IV, fibronectin, elastin and tenascin (Bissell *et al.*, 2002; Coussens and Werb, 2002; Wiseman and Werb, 2002). Increased deposition of matrix components and tumor mass expansion coupled with global and local changes in the quality and topology of the ECM, collectively generate a microenvironment that can be up to an order of magnitude stiffer than that observed in normal tissues, and that has been correlated with high histological tumor grade (Paszek *et al.*, 2005; Rutkowski and Swartz, 2007; Samani *et al.*, 2007). Thus, fibrotic premalignant lesions are consistently 3- to 6-fold stiffer than normal tissue and high grade ductal carcinomas are up to 13-fold stiffer (Samani *et al.*, 2007). Such changes in the material properties of the tissue are likely the result of chronic ECM remodeling, increased cell mass and altered tumor cell rheology that profoundly alter tumor phenotype and pathophysiology.

Loss of polarity, epithelial-to-mesenchymal transition (EMT), resistance to apoptosis and cell proliferation are all force-dependent phenotypes. Although the overall importance of mechanical force to tissue behavior is generally acknowledged, much remains to be discovered about cell and tissue mechanotransduction and little is known about how such mechanosensory signals might guide cellular behavior. Investigators are just beginning to elucidate how

mechanical stimulation induces structural, compositional and functional changes at the cellular level and how these physical cues could alter the structural integrity and function of differentiated tissues. What is known is that compressive forces are generated by the expanding fibrotic tumor mass and reciprocal resistance to the cellular expansion by the extracellular tissue adjacent to the transformed tissue (Volokh, 2006). Mechanical loading in the form of compression force alters gene expression and modifies cell signaling and can potentially induce MMP-dependent ECM remodeling. For instance, IL-8 and NF- κ B ligand production are increased by compression (Ichimiya *et al.*, 2007; Muroi *et al.*, 2007) as is FGF-mediated ERK activation (Vincent *et al.*, 2007). Indeed, the significance of compression force as a key regulator of tumor cell behavior has been illustrated by studies on TGF β function. These TGF β studies showed how dynamic compression and contraction can lead to the activation of latent ECM bound TGF β , which thereafter stimulates a fibrotic response by the tumor-associated fibroblasts that then feeds back to induce epithelial-to-mesenchymal transition of the tumor (Leivonen and Kahari, 2007; Willis and Borok, 2007; Wipff *et al.*, 2007). TGF β activation also stimulates the production of matrix remodeling enzymes such as MMPs and lysyl-oxidase (LOX) to alter matrix topology and induce matrix stiffening that, in turn, can also alter tumor cell behavior (Heinemeier *et al.*, 2007). In this regard, studies that have examined hypertrophic scars could show that MMP-9 and MMP-28 secretion and activity is enhanced when the tissue is mechanically loaded, and emphasize how compression force can induce ECM remodeling (Reno *et al.*, 2002, 2005).

The ECM stroma adjacent to an expanding tumor mass responds to the tumor-generated compression force by exerting a reciprocal resistance force on the expanding tumor mass. This tumor-initiated resistance force increases tensional forces within the tumor cells to alter their behavior, in part by regulating the activity of various biochemical-signaling cascades, and also by actomyosin-induced cytoskeletal reorganization. For instance, tensional forces are transmitted from tumor cell to tumor cell through adhesion plaques, and within the tumor cells through the cytoskeleton to cell-ECM adhesions (Katsumi *et al.*, 2004). In addition, the expanding tumor mass and actively migrating tumor cells can each independently deliver direct forces to cell-ECM and cell-cell adhesion plaques, thereby impacting tumor cell behavior by physically distorting the ECM (Figure 2).

External tensile forces can effect changes in cellular phenotype either by altering biochemical signaling within cells to alter gene expression and protein function or by inducing cytoskeletal remodeling to change cell shape and signaling, modify tissue organization and alter cell growth, survival and motility. Thus, conformational changes in membrane cytoskeletal proteins such as vinculin, that are induced by tensional force, influence signaling within the cell by altering the activity of ion channels or by promoting integrin clustering and activation to alter cytokine and growth factor receptor signaling (Paszek *et al.*, 2005; Gupta and Grande-Allen, 2006). Examples of these effects include experiments showing how α V β 3 integrins cluster in response to the application of an extracellular tensile force that potentiate JNK signaling (Katsumi *et al.*, 2005). These data demonstrate how an elevated tensile force can induce VEGF expression to drive vascular growth (Quinn *et al.*, 2002). Indeed, cyclic strain can induce p38 SAPK2, ErbB2 and AT1 activity while simultaneously stimulating PDGF production in a PI3K-dependent manner (Nguyen *et al.*, 2000; Adam *et al.*, 2003). Wnt, β -catenin, IGF-1, CREB, c-myc and Stat1/3 are examples of other intracellular signaling molecules whose activity can be modulated by external tensional force (Avvisato *et al.*, 2007; Reichelt, 2007; Triplett *et al.*, 2007). Given space limitations, we have chosen not to delve into the details of how force could alter cell signaling and elicit biochemical changes in proteins and nucleic acids and instead refer the reader to several excellent, recent reviews (Pedersen and Swartz, 2005; Wang *et al.*, 2006; Schwartz and Desimone, 2008).

Integral membrane proteins such as integrins or dystroglycan couple extracellular tensional forces with intracellular cytoskeletal tension (Muschler *et al.*, 2002; Katsumi *et al.*, 2004). β -integrins for instance respond to extracellular force stimuli by forming intracellular interactions with cytoskeletal adaptor proteins such as talin or α -actinin and thereafter recruit a plethora of adhesion plaque proteins and cytoskeletal interactions to reciprocally transduce extracellular and intracellular forces. Force-dependent ECM-mediated integrin ligation activate and oligomerize integrins, stimulate Rho GTPases and drive cytoskeletal rearrangements that promote the maturation of focal adhesions and influence adhesion and growth factor signaling (Figure 3). Mature focal adhesions generate intrinsic cellular traction forces through actomyosin-induced contractility and through cytoskeletal remodeling (Beningo and Wang, 2002; Mogilner and Oster, 2003). The small GTPases Ras, Rho and Rac respond to tensile stimuli and can mediate focal adhesion formation by promoting contractility thereby inducing cell proliferation, survival and motility (Clark *et al.*, 1998; Cox *et al.*, 2001; del Pozo *et al.*, 2004).

Traction force microscopy is a recently developed tool that permits the visualization and quantification of actomyosin and cytoskeletal generated forces. Thus, mechanoreciprocity can be clearly observed and quantified using traction force microscopy, which demonstrates how cells generate actomyosin contractility tensional forces of increasing magnitude in response to matrices of incremental stiffness. This reciprocal relationship between the cell and its mechanical substrate can influence the behavior and phenotype of the cell by altering the degree of cell spreading, the rate of cell growth, the amount of cell survival and even the speed and direction of cell motility (Wang *et al.*, 2001; Wong *et al.*, 2003; Paszek *et al.*, 2005).

Migration and metastasis

Metastasis is the major cause of cancer fatality, underscoring the urgency of understanding the molecular mechanisms regulating this process. A key step in tumor metastasis is destabilization of tissue structure and thereafter the directed migration of tumor cells towards the vasculature or lymphatics. Both of these steps require dynamic modulation of cell and tissue polarity and are influenced by force. What we and others now appreciate is that the mechanical and topological features of the ECM influence tumor metastasis by promoting directed tumor cell invasion into the parenchyma and by fostering rapid and efficient tumor cell extravasation and colonization at distant tissue sites. Evidence to support these conclusions is given by work showing how matrix stiffness and topology can enhance cell migration speed and facilitate directed cell motility. For example, in one study fibroblasts seeded on a substrate made up of materials of two distinct stiffnesses, with similar ligand densities, durotaxed towards the stiffer substrate, regardless of matrix composition or density. The fibroblasts seeded on the compliant substrate could 'sense' the stiffer substrate, project membrane structures towards the rigid matrix, and showed persistent migration toward the stiffer substrate. In the vicinity of the stiff matrix the associated cells exhibited greater cell motility yet remained locally adherent (Lo *et al.*, 2000). Intriguingly, micro-aspiration experiments in which the substrate was deformed using a micro pipettor demonstrated how the directionality of this fibroblast movement was enhanced by tensional forces induced within the matrix (that is, a micropipettor was used to gently pull the substrate away from the cell to generate a directed tensile force (Lo *et al.*, 2000)). Similarly, vascular endothelial cells and smooth muscle cells exhibit directed and rapid cell migration termed 'durotaxis' in response to a gradient of matrix stiffness, emphasizing how this mechanically regulated process is likely highly conserved (Wong *et al.*, 2003).

Cells exhibit widely divergent responses to an exogenous force and evidence to date emphasize how mechanoresponsiveness is cell and tissue specific (Yeung *et al.*, 2005; Wells and Discher, 2008). For example, neutrophils exert a very low force and are themselves highly sensitive to an exogenous force such that they respond to even small changes in shear stress, typically in

the range of 1 Pa (Fukuda and Schmid-Schonbein, 2003). On the other hand, mechanically resistant cells such as osteoblasts require much larger exogenous force stimuli, typically in the 20 MPa range, before they will modify their behavior (Grodzinsky *et al.*, 2000). Indeed, tissue pathology is often accompanied by an altered mechanoresponsiveness of the cells within the tissue. This phenomenon has been observed most prominently during transformation in which the rheology and mechanosensitivity of the cancer cells are known to differ substantially from that of their non-transformed counterparts (compare Figures 1a–c). In this regard, we showed that transformed human MECs spread appreciably, migrate rapidly and exert significantly higher actomyosin-dependent cellular force as compared with nonmalignant MECs interacting with a similar compliant matrix (Paszek *et al.*, 2005; Kass *et al.*, 2007). These data imply that small changes in ECM composition or remodeling such as localized fibrillogenesis could theoretically induce profound changes in tumor cell behavior including altered cell polarity and directed cell migration.

Matrix topology-directed migration has been observed in MECs *in vivo* and likely facilitates tumor cell metastasis. Using two-photon intravital imaging coupled with second harmonic generation the directed, rapid epidermal growth factor-stimulated migration of MECs along prominent collagen bundles adjacent to blood vessels has been observed (Condeelis and Segall, 2003; Ingman *et al.*, 2006; Wyckoff *et al.*, 2006). Although the molecular mechanisms regulating such directed cellular migration *in vivo* have yet to be delineated, bundled, linearized collagens are characteristically stiff, while we showed that matrix stiffness enhances EGF-induced signaling (Paszek *et al.*, 2005; unpublished observations) and increases the speed of cell migration ((Wong *et al.*, 2003); unpublished observations). These and other data imply that the altered matrix material properties and changes in ECM topology associated with tumor progression could foster directed tumor cell migration towards the vasculature to facilitate tumor cell intravasation and metastasis. Although it is well known that the stroma surrounding developing breast tumors is stiffer and the collagen fibrils are highly oriented and bundled (Demou *et al.*, 2005; Paszek *et al.*, 2005; Samani *et al.*, 2007), to date no direct evidence exists to substantiate such claims. In this regard, using atomic force microscopy to probe the mechanical properties of developing transgenic tumors, we could show that matrix stiffness increases in association with tumor progression and that the stroma at the front of the invading tumor, where we and others have observed prominent linear collagen bundling, is substantially stiffer than the noninvasive edge. We also determined that the stroma adjacent to peripheral bloody vessels, in regions where rapidly migrating breast tumor cells have been observed, is also quite rigid (unpublished observations; (Condeelis and Segall, 2003; Ingman *et al.*, 2006; Wyckoff *et al.*, 2006)).

Matrix orientation and mechanical integrity influence cell migration by modifying the direction and composition of integrin adhesions. Thus, fibroblasts orient themselves on rigid collagen I fibers so that they are able to generate maximal traction forces that stabilize integrin adhesions to promote focal adhesion maturation in the direction of the collagen fiber alignment (Figures 3a and c). This phenotype is not favored if the cells are perpendicularly oriented to the fibrils or if they interact with collagen gels of low tensile strength where cellular force is neither reinforced nor greatly resisted (Figures 3a–c). Consistently, atomic force microscopy has shown that traction forces directed along parallel collagen I fibers develop in cells plated on these oriented substrates (Friedrichs *et al.*, 2007). The directed maturation of focal adhesions permit cells to adopt a shape and orientation that optimizes their migration in the direction of collagen fiber alignment.

Although tumor cells respond to matrix material properties and topology, they are not merely passive participants and themselves respond to the mechanical and topological properties of the ECM. Tumor cells actively remodel their local extracellular microenvironment either by directly releasing ECM remodeling enzymes such as MMPs, serine and cysteine proteases or

hyaluronidases (Lopez-Otin and Matrisian, 2007; Lokeshwar *et al.*, 2008; Stern, 2008), or indirectly by stimulating stromal cells to deposit, process and reorganize their ECMs. Thus, the ECM-associated remodeling observed with tumor desmoplasia is the net result of stromally-induced matrix remodeling as well as matrix deposition, degradation and cross-linking mediated by the tumor cells (Egeblad and Werb, 2002; Strongin, 2006; Payne *et al.*, 2007). Indeed, tumor progression is associated with altered expression of a number of ECM proteins including cellular fibronectin, collagens I, III and IV, tenascin and various proteoglycans produced by the cellular stroma and the tumor cells that collectively promote tumor migration, proliferation and survival (Bissell *et al.*, 2002; Coussens and Werb, 2002; Wiseman and Werb, 2002). Increased expression and activity of MMPs expressed by fibroblasts, infiltrating immune cells and the transformed cells together release growth factors trapped in the stromal matrix to stimulate invasion, and contribute significantly to ECM remodeling to facilitate cell invasion and metastasis through the vasculature. For instance, MMP2 and -14 secreted by tumors cells can cleave pro laminin-5 to expose a cryptic site within laminin-5 that promotes cell migration (Giannelli *et al.*, 1997). Both fibroblasts and tumors secrete matrix cross-linkers that alter the topology of the ECM and enhance its material properties or stiffness. In particular, TBG β and HIF-1 α induce the expression of lysyl oxidases (LOX), which in turn cross-link type I and III collagens to increase their stiffness (Erler and Giaccia, 2006). The importance of matrix cross-linking in metastatic disease is underscored by the observation that increased LOX expression is positively associated with the most advanced stage of renal cell carcinoma and highly expressed in invasive and metastatic breast cancer cell lines (Kirschmann *et al.*, 2002). In fact, ductal breast carcinomas and fibrotic tissue show elevated levels of LOX (Decitre *et al.*, 1998) and inhibiting LOX activity reduces tumor cell invasion *in vitro* (Kirschmann *et al.*, 2002), and reduces breast cancer cell metastasis *in vivo* (Erler and Giaccia, 2006). Indeed, enzymes and proteins such as transglutaminase and the proteoglycans lumican and decorin also modify tumor cell behavior and might do so by modifying the mechanical properties and topology of the ECM (Decitre *et al.*, 1998; Wiseman and Werb, 2002; Akiri *et al.*, 2003; Alowami *et al.*, 2003; Eshchenko *et al.*, 2007). Thus, a dynamic physical and biochemical dialog between the tumor cells and their microenvironment contribute to tumor progression and metastasis.

Investigating epithelial mechanotransduction

Future research in the area of cell mechanobiology will require novel experimental and theoretical methodologies to determine the type and magnitude of the forces experienced at the cellular and sub-cellular levels, and to identify the force sensors/receptors that initiate the cascade of cellular and molecular events. To investigate epithelial morphogenesis and malignant transformation, 3D culture systems have been developed to model the *in vivo* environment of epithelial cells. Original 3D culture models were designed to completely embed epithelial cells within a polymerized ECM to closely recapitulate the structure and composition of the polarized structures *in vitro*. These models have now been modified to study how mechanical properties affect morphogenesis and biochemical processes (Hebner *et al.*, 2007). We now present an overview of these 3D models and the modifications used to study mechanotransduction. In addition, we discuss engineering approaches to modulate the physical forces applied to cells.

3D culture systems

As discussed in this review, ECM composition and architecture are frequently altered in breast transformation and can influence epithelial cell growth, differentiation and migration. Methods to study these biological processes traditionally involve culturing isolated cells on a 2D surface. However, cells *in vivo* exist in a complex 3D microenvironment. To more accurately study epithelial cell morphogenesis *in vitro*, models have been developed to recapitulate the *in*

vivo 3D environment. The simplest 3D models involve embedding a single type of cell in a biocompatible scaffold. These biocompatible scaffolds provide cells with a prefabricated ECM, which is often modifiable by the embedded cells. Scaffolding materials commonly used for complete embedment of epithelial cells include rBMs produced and isolated from Engelbreth–Holm–Swarm mouse tumor matrices, collagen I and fibrin. Laminin 1, collagen IV, entactin and heparin sulfate proteoglycans are the major components of the EHS rBM. rBM has been utilized extensively to study morphogenesis and transformation in normal, non-transformed epithelial cells, such as MDCK and MCF-10A cells (Petersen *et al.*, 1992; Weaver *et al.*, 1995, 1997; Debnath *et al.*, 2003). Indeed, when various non-transformed epithelial cells (primary and cell lines) are mixed with rBM they form polarized structures, with hollow lumens, and assemble their own endogenous BM that is surrounded by the polymerized gel (Gudjonsson *et al.*, 2002; Kenny *et al.*, 2007). A modified version of this method utilizes a rBM undercoat on the tissue culture surface, with cells plated on top of the rBM, and then adds another layer of rBM on top of the plated cells, resulting in a pseudo-3D system (Debnath *et al.*, 2003; Hebner *et al.*, 2007). Although the cells are not mixed directly with the rBM, they are nevertheless surrounded by rBM and are able to form acinar structures, presumably by remodeling the rBM. Drawbacks of using rBM matrices include the fact that the matrix is not fully characterized and that it has considerable lot-to-lot variability. Another commonly used embedment scaffold, collagen I, is better defined than rBM derived from EHS. However, although certain epithelial cells polarize in collagen I, such as MDCK cells, many others either fail to undergo acinar morphogenesis, or assemble colonies with reversed polarity (Aunins, 1990). One advantage collagen I has over rBM is that the mechanical properties can be modified by titrating the collagen concentration and extent of cross-linking. Yet, collagen is also biologically derived, and therefore is subject to variability between preparations, species and processing techniques (for instance, intact- versus telopeptide-free collagen).

Synthetic materials have been developed and are being applied to manipulate substrate stiffness and matrix composition and material properties for cell preparation. For instance, bis poly acrylamide gels, traditionally used to separate biomolecules, have been manipulated in the 3D culture system and illustrate the effect of substrate stiffness on cell and tissue phenotype (Pelham and Wang, 1997). By varying the concentration of poly acrylamide to bis acrylamide cross-linker, a range of quantifiable matrix stiffnesses can be achieved onto which ligand of choice can be conjugated. The limitation of this system is that non-polymerized poly acrylamide is cytotoxic and therefore the matrix does not lend itself to a bona fide pseudo-3D embedment protocol. Thus the system is limited to 2D manipulation or pseudo 3D assays (Schmedlen *et al.*, 2002). Nevertheless, using this approach, gels have been prepared with a precisely calibrated modulus range (200–10 000 Pa) and 2D and pseudo 3D systems have been used successfully to study matrix stiffness and composition on the behavior of cells (Paszek *et al.*, 2005).

Engineered bioreactors

Knowledge of the types, magnitude and duration of forces within the cell and tissue are essential to understand the molecular mechanisms regulating mechano-transduction. The cellular response to mechanical stimulation depends upon the type of force applied, with tensile and compressive forces being applied perpendicular to the surface of the cell or 3D construct and shear forces being applied parallel to the cell or 3D construct surface. The cellular response also depends upon on the magnitude, frequency and duration of the applied stimuli. To delineate the role of physical force in cell behavior and tissue homeostasis, researchers apply physiologically relevant mechanical stimuli at the cell and tissue level using specially engineered devices which have been designed to control the temporal, spatial and intensity of the force parameter.

There are two general approaches to study cellular mechanotransduction. The first approach uses multiple cells which are collectively mechanically stimulated and which mimic the forces that the cell would typically experience within their physiological microenvironment (tissue). This first set of techniques includes the simple application of hydrostatic pressure, compression, tension and shear stress to cell monolayers, or tissue fragments (*ex vivo* explant culture or cells embedded in tissue-engineered scaffolds). For instance, flow chambers have been developed that apply shear stresses to cell monolayers, either through pressure-driven systems that apply a parabolic laminar flow profile or cone-and-plate flow chambers which apply a uniform shear stress with a linear flow profile (Davies, 1995). The role of hydrostatic pressure in cell and tissue growth and differentiation has been investigated in a 2D format by applying a transmembrane pressure to cells plated on a porous, stiff substrate. Similarly, the effect of hydrostatic pressure in 2D or 3D has been assessed by directing compressed air or a column of fluid over a culture of cells (reviewed in Paszek and Weaver, 2004). Alternatively, techniques investigating the mechanoreponse of cells to tensile stress involve the application of static or cyclic, axial or biaxial strains to monolayers of cells plated on a deformable membrane, or within a deformable 3D scaffold (Vanderploeg *et al.*, 2004; Wall *et al.*, 2007). In addition, mechanical devices have been used since the 1970s to deconstruct the role of static and dynamic compression in cell growth and metabolism (Panjabi *et al.*, 1979).

A recent approach to studying cellular mechanotransduction has been used to investigate the response of individual cells to a directed mechanostimuli. This approach uses sophisticated devices that apply pico- or nano-Newton forces to individual cell membranes, receptors or cytoskeletal elements. These methods include the use of particle attachment to apply precise forces to the surface of cells, using small microbeads coated with adhesive ligands or antibodies that bind to a specific cell surface receptor through which the force can be directly transmitted (Huang *et al.*, 2004; Gan, 2007). Different techniques for applying these types of forces include optical trapping, micropipette aspiration and the application of both linear and torsional forces by magnetic manipulation (Pommerenke *et al.*, 1996; Choquet *et al.*, 1997; Hochmuth, 2000). Similar, methods have been developed that can assess and measure cellular and material forces at the nano-scale level. This includes atomic force microscopy and traction force microscopy that can be used to determine the material properties, as well as the forces generated by single cells (Munevar *et al.*, 2001; Garcia *et al.*, 2007; Sabass *et al.*, 2008). The development of such innovative approaches and tools now permits endless approaches to obtain insight into the fundamental processes regulating mechanotransduction and for analyzing specific physical interactions between cells and their surrounding micro-environment.

Conclusions

Stromal–epithelial interactions drive developmental processes such as polarity, and maintain tissue homeostasis through a network of physical and biochemical processes that operate within the 3D epithelial tissue. Although this review focuses on the effect of micro-environmental force on cell and tissue polarity, force also influences many other aspects of normal tissue behavior and tumor biology including cancer initiation, transformation, metastasis and treatment efficacy and our understanding of these effects are just now beginning to be appreciated. For instance, force appears to exert a profound effect on apoptosis resistance and likely alters the efficacy of drug delivery to tumors (Chen *et al.*, 1997; Numaguchi *et al.*, 2003; Padera *et al.*, 2004). Furthermore, cellular and ECM interactions evolve over time, dynamically guiding and responding to development. Integral to this process is the complex interplay between soluble factors, cell–cell and cell–ECM interactions and the mechanical microenvironment, which cooperatively drive epithelial morphogenesis and differentiation, and regulate tissue homeostasis.

Mechanical force elicits a myriad of biochemical responses in a cell, altering how a cell responds to an exogenous signal, and dramatically influencing how differentiation decisions are made during development. Tumor progression is associated with pronounced changes in cell and tissue force, including increased compression, altered ECM composition, stiffness and topology that elevate extracellular tension and the elastic modulus of the tissue, modify the cytoskeleton, enhance cell rheology and tension and induce interstitial pressure to alter cellular mechanotransduction. Compromised mechanotransduction perturbs mechanohomeostasis and contributes to tumor progression. Yet, although the overall importance of mechanical force to tumor etiology is slowly becoming acknowledged, much still remains to be discovered about how mechanotransduction is regulated at the cell and tissue level. Furthermore, we know little about how mechanosensory mechanisms might guide critical processes such as cell and tissue polarity. Thus the quest to elucidate how mechanical stimulation induces structural, compositional and functional changes at the cellular and tissue levels has just begun.

Acknowledgements

We apologize to the authors whose work is not cited because of space limitations. This work was supported by NIH Grant 7R01CA078731-07, DOD Breast Cancer Research Era of Hope Grant W81XWH-05-1-330 (BC044791), CIRM Grant RS1-00449 and DOE Grant A107165 to VMW, NIH NCI Training Grant 5T32CA108462-04 to JL and DOD Breast Cancer Research Era of Hope Grant BC06262 to JM.

References

- Adam RM, Roth JA, Cheng HL, Rice DC, Khoury J, Bauer SB, et al. Signaling through PI3K/Akt mediates stretch and PDGF-BB-dependent DNA synthesis in bladder smooth muscle cells. *J Urol* 2003;169:2388–2393. [PubMed: 12771803]
- Akiri G, Sabo E, Dafni H, Vadasz Z, Kartvelishvily Y, Gan N, et al. Lysyl oxidase-related protein-1 promotes tumor fibrosis and tumor progression *in vivo*. *Cancer Res* 2003;63:1657–1666. [PubMed: 12670920]
- Alowami S, Troup S, Al-Haddad S, Kirkpatrick I, Watson PH. Mammographic density is related to stroma and stromal proteoglycan expression. *Breast Cancer Res* 2003;5:R129–R135. [PubMed: 12927043]
- Aunins JGWDIC. Experimental collision efficiencies of polymer-flocculated animal cells. *Biotechnol Prog* 1990;6:54–61. [PubMed: 1366435]
- Avvisato CL, Yang X, Shah S, Hoxter B, Li W, Gaynor R, et al. Mechanical force modulates global gene expression and beta-catenin signaling in colon cancer cells. *J Cell Sci* 2007;120:2672–2682. [PubMed: 17635998]
- Barcellos-Hoff MH, Aggeler J, Ram TG, Bissell MJ. Functional differentiation and alveolar morphogenesis of primary mammary cultures on reconstituted basement membrane. *Development* 1989;105:223–235. [PubMed: 2806122]
- Beningo KA, Wang YL. Flexible substrata for the detection of cellular traction forces. *Trends Cell Biol* 2002;12:79–84. [PubMed: 11849971]
- Bissell MJ, Hall HG, Parry G. How does the extracellular matrix direct gene expression? *J Theor Biol* 1982;99:31–68. [PubMed: 6892044]
- Bissell MJ, Radisky DC, Rizki A, Weaver VM, Petersen OW. The organizing principle: microenvironmental influences in the normal and malignant breast. *Differentiation* 2002;70:537–546. [PubMed: 12492495]
- Bissell MJ, Weaver VM, Lelievre SA, Wang F, Petersen OW, Schmeichel KL. Tissue structure, nuclear organization, and gene expression in normal and malignant breast. *Cancer Res* 1999;59:1757s–1763s.discussion 1763s–1764s
- Brancaccio M, Hirsch E, Notte A, Selvetella G, Lembo G, Tarone G. Integrin signalling: the tug-of-war in heart hypertrophy. *Cardiovasc Res* 2006;70:422–433. [PubMed: 16466704]
- Butcher DT, Alliston T, Weaver VM. A tense situation: forcing tumor progression. *Nat Rev Cancer*. 2008 (in press)

- Cardoso WV, Lu J. Regulation of early lung morphogenesis: questions, facts and controversies. *Development* 2006;133:1611–1624. [PubMed: 16613830]
- Chambard M, Verrier B, Gabrion J, Mauchamp J. Polarity reversal of inside-out thyroid follicles cultured within collagen gel: reexpression of specific functions. *Biol Cell* 1984;51:315–325. [PubMed: 6098327]
- Chen CS, Mrksich M, Huang S, Whitesides GM, Ingber DE. Geometric control of cell life and death. *Science* 1997;276:1425–1428. [PubMed: 9162012]
- Chiquet M, Tunc-Civelek V, Sarasa-Renedo A. Gene regulation by mechanotransduction in fibroblasts. *Appl Physiol Nutr Metab* 2007;32:967–973. [PubMed: 18059623]
- Choquet D, Felsenfeld DP, Sheetz MP. Extracellular matrix rigidity causes strengthening of integrin-cytoskeleton linkages. *Cell* 1997;88:39–48. [PubMed: 9019403]
- Chrenek MA, Wong P, Weaver VM. Tumour-stromal interactions. Integrins and cell adhesions as modulators of mammary cell survival and transformation. *Breast Cancer Res* 2001;3:224–229. [PubMed: 11434873]
- Clark EA, King WG, Brugge JS, Symons M, Hynes RO. Integrin-mediated signals regulated by members of the rho family of GTPases. *J Cell Biol* 1998;142:573–586. [PubMed: 9679153]
- Condeelis J, Segall JE. Intravital imaging of cell movement in tumours. *Nat Rev Cancer* 2003;3:921–930. [PubMed: 14737122]
- Coussens LM, Werb Z. Inflammation and cancer. *Nature* 2002;420:860–867. [PubMed: 12490959]
- Cox EA, Sastry SK, Huttenlocher A. Integrin-mediated adhesion regulates cell polarity and membrane protrusion through the Rho family of GTPases. *Mol Biol Cell* 2001;12:265–277. [PubMed: 11179414]
- Davies PF. Flow-mediated endothelial mechanotransduction. *Physiol Rev* 1995;75:519–560. [PubMed: 7624393]
- Debnath J, Muthuswamy SK, Brugge JS. Morphogenesis and oncogenesis of MCF-10A mammary epithelial acini grown in three-dimensional basement membrane cultures. *Methods* 2003;30:256–268. [PubMed: 12798140]
- Decitre M, Gleyzal C, Raccurt M, Peyrol S, Aubert-Foucher E, Csiszar K, et al. Lysyl oxidase-like protein localizes to sites of de novo fibrinogenesis in fibrosis and in the early stromal reaction of ductal breast carcinomas. *Lab Invest* 1998;78:143–151. [PubMed: 9484712]
- del Pozo MA, Alderson NB, Kiosses WB, Chiang HH, Anderson RG, Schwartz MA. Integrins regulate Rac targeting by internalization of membrane domains. *Science* 2004;303:839–842. [PubMed: 14764880]
- Demou ZN, Awad M, McKee T, Perentes JY, Wang X, Munn LL, et al. Lack of telopeptides in fibrillar collagen I promotes the invasion of a metastatic breast tumor cell line. *Cancer Res* 2005;65:5674–5682. [PubMed: 15994941]
- Egeblad M, Werb Z. New functions for the matrix metalloproteinases in cancer progression. *Nat Rev Cancer* 2002;2:161–174. [PubMed: 11990853]
- Emerman JT, Pitelka DR. Maintenance and induction of morphological differentiation in dissociated mammary epithelium on floating collagen membranes. *In vitro* 1977;13:316–328. [PubMed: 559643]
- Erler JT, Giaccia AJ. Lysyl oxidase mediates hypoxic control of metastasis. *Cancer Res* 2006;66:10238–10241. [PubMed: 17079439]
- Eshchenko TY, Rykova VI, Chernakov AE, Sidorov SV, Grigorieva EV. Expression of different proteoglycans in human breast tumors. *Biochemistry (Mosc)* 2007;72:1016–1020. [PubMed: 17922662]
- Farge E. Mechanical induction of Twist in the Drosophila foregut/stomodaeal primordium. *Curr Biol* 2003;13:1365–1377. [PubMed: 12932320]
- Friedrichs J, Taubenberger A, Franz CM, Muller DJ. Cellular remodelling of individual collagen fibrils visualized by time-lapse AFM. *J Mol Biol* 2007;372:594–607. [PubMed: 17686490]
- Fukuda S, Schmid-Schonbein GW. Regulation of CD18 expression on neutrophils in response to fluid shear stress. *Proc Natl Acad Sci USA* 2003;100:13152–13157. [PubMed: 14595007]

- Gan Y. Invited review article: a review of techniques for attaching micro- and nanoparticles to a probe's tip for surface force and near-field optical measurements. *Rev Sci Instrum* 2007;78:081101. [PubMed: 17764306]
- Garcia R, Magerle R, Perez R. Nanoscale compositional mapping with gentle forces. *Nat Mater* 2007;6:405–411. [PubMed: 17541439]
- Ghosh K, Pan Z, Guan E, Ge S, Liu Y, Nakamura T, et al. Cell adaptation to a physiologically relevant ECM mimic with different viscoelastic properties. *Biomaterials* 2007;28:671–679. [PubMed: 17049594]
- Giannelli G, Falk-Marzillier J, Schiraldi O, Stetler-Stevenson WG, Quaranta V. Induction of cell migration by matrix metalloprotease-2 cleavage of laminin-5. *Science* 1997;277:225–228. [PubMed: 9211848]
- Grodzinsky AJ, Levenston ME, Jin M, Frank EH. Cartilage tissue remodeling in response to mechanical forces. *Annu Rev Biomed Eng* 2000;2:691–713. [PubMed: 11701528]
- Gudjonsson T, Ronnov-Jessen L, Villadsen R, Rank F, Bissell MJ, Petersen OW. Normal and tumor-derived myoepithelial cells differ in their ability to interact with luminal breast epithelial cells for polarity and basement membrane deposition. *J Cell Sci* 2002;115:39–50. [PubMed: 11801722]
- Gupta V, Grande-Allen KJ. Effects of static and cyclic loading in regulating extracellular matrix synthesis by cardiovascular cells. *Cardiovasc Res* 2006;72:375–383. [PubMed: 17010955]
- Hamill OP, Martinac B. Molecular basis of mechanotransduction in living cells. *Physiol Rev* 2001;81:685–740. [PubMed: 11274342]
- Hebner C, Weaver VM, Debnath J. Modeling morphogenesis and oncogenesis in three-dimensional breast epithelial cultures. *Annu Rev Pathol* 2007;3:313–339. [PubMed: 18039125]
- Heinemeier KM, Olesen JL, Haddad F, Langberg H, Kjaer M, Baldwin KM, et al. Expression of collagen and related growth factors in rat tendon and skeletal muscle in response to specific contraction types. *J Physiol* 2007;582:1303–1316. [PubMed: 17540706]
- Helmlinger G, Netti PA, Lichtenbeld HC, Melder RJ, Jain RK. Solid stress inhibits the growth of multicellular tumor spheroids. *Nat Biotechnol* 1997;15:778–783. [PubMed: 9255794]
- Hochmuth RM. Micropipette aspiration of living cells. *J Biomech* 2000;33:15–22. [PubMed: 10609514]
- Huang H, Kamm RD, Lee RT. Cell mechanics and mechanotransduction: pathways, probes, and physiology. *Am J Physiol Cell Physiol* 2004;287:C1–11. [PubMed: 15189819]
- Ichimiya H, Takahashi T, Ariyoshi W, Takano H, Matayoshi T, Nishihara T. Compressive mechanical stress promotes osteoclast formation through RANKL expression on synovial cells. *Oral Surg Oral Med Oral Pathol Oral Radiol Endod* 2007;103:334–341. [PubMed: 17321443]
- Ingber DE, Madri JA, Folkman J. A possible mechanism for inhibition of angiogenesis by angiostatic steroids: induction of capillary basement membrane dissolution. *Endocrinology* 1986;119:1768–1775. [PubMed: 2428602]
- Ingman WV, Wyckoff J, Gouon-Evans V, Condeelis J, Pollard JW. Macrophages promote collagen fibrillogenesis around terminal end buds of the developing mammary gland. *Dev Dyn* 2006;235:3222–3229. [PubMed: 17029292]
- Kass L, Erler JT, Dembo M, Weaver VM. Mammary epithelial cell: influence of extracellular matrix composition and organization during development and tumorigenesis. *Int J Biochem Cell Biol* 2007;39:1987–1994. [PubMed: 17719831]
- Katsumi A, Naoe T, Matsushita T, Kaibuchi K, Schwartz MA. Integrin activation and matrix binding mediate cellular responses to mechanical stretch. *J Biol Chem* 2005;280:16546–16549. [PubMed: 15760908]
- Katsumi A, Orr AW, Tzima E, Schwartz MA. Integrins in mechanotransduction. *J Biol Chem* 2004;279:12001–12004. [PubMed: 14960578]
- Keller R, Davidson LA, Shook DR. How we are shaped: the biomechanics of gastrulation. *Differentiation* 2003;71:171–205. [PubMed: 12694202]
- Kenny PA, Lee GY, Myers CA, Neve RM, Semeiks JR, Spellman PT, et al. The morphologies of breast cancer cell lines in three-dimensional assays correlate with their profiles of gene expression. *Mol Oncol* 2007;1:84–96. [PubMed: 18516279]
- Kirschmann DA, Seftor EA, Fong SF, Nieva DR, Sullivan CM, Edwards EM, et al. A molecular role for lysyl oxidase in breast cancer invasion. *Cancer Res* 2002;62:4478–4483. [PubMed: 12154058]

- Kleinman HK, Philp D, Hoffman MP. Role of the extracellular matrix in morphogenesis. *Curr Opin Biotechnol* 2003;14:526–532. [PubMed: 14580584]
- Larsen M, Artym VV, Green JA, Yamada KM. The matrix reorganized: extracellular matrix remodeling and integrin signaling. *Curr Opin Cell Biol* 2006;18:463–471. [PubMed: 16919434]
- Leivo I. Structure and composition of early basement membranes: studies with early embryos and teratocarcinoma cells. *Med Biol* 1983;61:1–30. [PubMed: 6341722]
- Leivonen SK, Kahari VM. Transforming growth factor-beta signaling in cancer invasion and metastasis. *Int J Cancer* 2007;121:2119–2124. [PubMed: 17849476]
- Lelievre S, Weaver VM, Bissell MJ. Extracellular matrix signaling from the cellular membrane skeleton to the nuclear skeleton: a model of gene regulation. *Recent Prog Horm Res* 1996;51:417–432. [PubMed: 8701089]
- Lo CM, Wang HB, Dembo M, Wang YL. Cell movement is guided by the rigidity of the substrate. *Biophys J* 2000;79:144–152. [PubMed: 10866943]
- Lokeshwar VB, Gomez P, Kramer M, Knapp J, McCornack MA, Lopez LE, et al. Epigenetic regulation of hyal-1 hyaluronidase expression: identification of hyal-1 promoter. *J Biol Chem*. 2008(e-pub ahead of print)
- Lopez-Otin C, Matrisian LM. Emerging roles of proteases in tumour suppression. *Nat Rev Cancer* 2007;7:800–808. [PubMed: 17851543]
- Mogilner A, Oster G. Force generation by actin polymerization II: the elastic ratchet and tethered filaments. *Biophys J* 2003;84:1591–1605. [PubMed: 12609863]
- Moore KA, Polte T, Huang S, Shi B, Alsberg E, Sunday ME, et al. Control of basement membrane remodeling and epithelial branching morphogenesis in embryonic lung by Rho and cytoskeletal tension. *Dev Dyn* 2005;232:268–281. [PubMed: 15614768]
- Munavar S, Wang Y, Dembo M. Traction force microscopy of migrating normal and H-ras transformed 3T3 fibroblasts. *Biophys J* 2001;80:1744–1757. [PubMed: 11259288]
- Muroi Y, Kakudo K, Nakata K. Effects of compressive loading on human synovium-derived cells. *J Dent Res* 2007;86:786–791. [PubMed: 17652211]
- Muschler J, Levy D, Boudreau R, Henry M, Campbell K, Bissell MJ. A role for dystroglycan in epithelial polarization: loss of function in breast tumor cells. *Cancer Res* 2002;62:7102–7109. [PubMed: 12460932]
- Nelson CM, Bissell MJ. Of extracellular matrix, scaffolds, and signaling: tissue architecture regulates development, homeostasis, and cancer. *Annu Rev Cell Dev Biol* 2006;22:287–309. [PubMed: 16824016]
- Nguyen HT, Adam RM, Bride SH, Park JM, Peters CA, Freeman MR. Cyclic stretch activates p38 SAPK2-, ErbB2-, and AT1-dependent signaling in bladder smooth muscle cells. *Am J Physiol Cell Physiol* 2000;279:C1155–C1167. [PubMed: 11003596]
- Numaguchi Y, Huang S, Polte TR, Eichler GS, Wang N, Ingber DE. Caldesmon-dependent switching between capillary endothelial cell growth and apoptosis through modulation of cell shape and contractility. *Angiogenesis* 2003;6:55–64. [PubMed: 14517405]
- O'Brien LE, Jou TS, Pollack AL, Zhang Q, Hansen SH, Yurchenco P, et al. Rac1 orientates epithelial apical polarity through effects on basolateral laminin assembly. *Nat Cell Biol* 2001;3:831–838. [PubMed: 11533663]
- Padera TP, Stoll BR, Tooredman JB, Capen D, di Tomaso E, Jain RK. Pathology: cancer cells compress intratumour vessels. *Nature* 2004;427:695. [PubMed: 14973470]
- Page-McCaw A, Ewald AJ, Werb Z. Matrix metalloproteinases and the regulation of tissue remodeling. *Nat Rev Mol Cell Biol* 2007;8:221–233. [PubMed: 17318226]
- Panjabi MM, White AA III, Wolf JW Jr. A biomechanical comparison of the effects of constant and cyclic compression on fracture healing in rabbit long bones. *Acta Orthop Scand* 1979;50:653–661. [PubMed: 532593]
- Paszek MJ, Weaver VM. The tension mounts: mechanics meets morphogenesis and malignancy. *J Mammary Gland Biol Neoplasia* 2004;9:325–342. [PubMed: 15838603]
- Paszek MJ, Zahir N, Johnson KR, Lakins JN, Rozenberg GI, Gefen A, et al. Tensional homeostasis and the malignant phenotype. *Cancer Cell* 2005;8:241–254. [PubMed: 16169468]

- Payne SL, Hendrix MJ, Kirschmann DA. Paradoxical roles for lysyl oxidases in cancer—a prospect. *J Cell Biochem* 2007;101:1338–1354. [PubMed: 17471532]
- Pedersen JA, Swartz MA. Mechanobiology in the third dimension. *Ann Biomed Eng* 2005;33:1469–1490. [PubMed: 16341917]
- Pelham RJ Jr, Wang Y. Cell locomotion and focal adhesions are regulated by substrate flexibility. *Proc Natl Acad Sci USA* 1997;94:13661–13665. [PubMed: 9391082]
- Petersen OW, Ronnov-Jessen L, Howlett AR, Bissell MJ. Interaction with basement membrane serves to rapidly distinguish growth and differentiation pattern of normal and malignant human breast epithelial cells [published erratum appears in *Proc Natl Acad Sci USA* 1993 Mar 15;90(6):2556]. *Proc Natl Acad Sci USA* 1992;89:9064–9068. [PubMed: 1384042]
- Polte TR, Eichler GS, Wang N, Ingber DE. Extracellular matrix controls myosin light chain phosphorylation and cell contractility through modulation of cell shape and cytoskeletal prestress. *Am J Physiol Cell Physiol* 2004;286:C518–C528. [PubMed: 14761883]
- Pommerenke H, Schreiber E, Durr F, Nebe B, Hahnel C, Moller W, et al. Stimulation of integrin receptors using a magnetic drag force device induces an intracellular free calcium response. *Eur J Cell Biol* 1996;70:157–164. [PubMed: 8793388]
- Quinn TP, Schlueter M, Soifer SJ, Gutierrez JA. Cyclic mechanical stretch induces VEGF and FGF-2 expression in pulmonary vascular smooth muscle cells. *Am J Physiol Lung Cell Mol Physiol* 2002;282:L897–L903. [PubMed: 11943652]
- Reichelt J. Mechanotransduction of keratinocytes in culture and in the epidermis. *Eur J Cell Biol* 2007;86:807–816. [PubMed: 17655967]
- Reno F, Grazianetti P, Stella M, Magliacani G, Pezzuto C, Cannas M. Release and activation of matrix metalloproteinase-9 during *in vitro* mechanical compression in hypertrophic scars. *Arch Dermatol* 2002;138:475–478. [PubMed: 11939809]
- Reno F, Sabbatini M, Stella M, Magliacani G, Cannas M. Effect of *in vitro* mechanical compression on Epilysin (matrix metalloproteinase-28) expression in hypertrophic scars. *Wound Repair Regen* 2005;13:255–261. [PubMed: 15953044]
- Robinson GW. Cooperation of signalling pathways in embryonic mammary gland development. *Nat Rev Genet* 2007;8:963–972. [PubMed: 18007652]
- Rodriguez-Boulan E, Paskiet KT, Sabatini DD. Assembly of enveloped viruses in Madin–Darby canine kidney cells: polarized budding from single attached cells and from clusters of cells in suspension. *J Cell Biol* 1983;96:866–874. [PubMed: 6300140]
- Rutkowski JM, Swartz MA. A driving force for change: interstitial flow as a morphoregulator. *Trends Cell Biol* 2007;17:44–50. [PubMed: 17141502]
- Sabass B, Gardel ML, Waterman CM, Schwarz US. High resolution traction force microscopy based on experimental and computational advances. *Biophys J* 2008;94:207–220. [PubMed: 17827246]
- Samani A, Zubovits J, Plewes D. Elastic moduli of normal and pathological human breast tissues: an inversion-technique-based investigation of 169 samples. *Phys Med Biol* 2007;52:1565–1576. [PubMed: 17327649]
- Schmedlen RH, Masters KS, West JL. Photocrosslinkable polyvinyl alcohol hydrogels that can be modified with cell adhesion peptides for use in tissue engineering. *Biomaterials* 2002;23:4325–4332. [PubMed: 12219822]
- Schwartz MA, Desimone DW. Cell adhesion receptors in mechanotransduction. *Curr Opin Cell Biol* 2008(e-pub ahead of print)
- Silver FH, Siperko LM. Mechanosensing and mechanochemical transduction: how is mechanical energy sensed and converted into chemical energy in an extracellular matrix? *Crit Rev Biomed Eng* 2003;31:255–331. [PubMed: 15095950]
- Simian M, Hirai Y, Navre M, Werb Z, Lochter A, Bissell MJ. The interplay of matrix metalloproteinases, morphogens and growth factors is necessary for branching of mammary epithelial cells. *Development* 2001;128:3117–3131. [PubMed: 11688561]
- Stern R. Hyaluronidases in cancer biology. *Semin Cancer Biol* 2008;18:275–280. [PubMed: 18485730]
- Sternlicht MD, Kouros-Mehr H, Lu P, Werb Z. Hormonal and local control of mammary branching morphogenesis. *Differentiation* 2006;74:365–381. [PubMed: 16916375]

- Strongin AY. Mislocalization and unconventional functions of cellular MMPs in cancer. *Cancer Metastasis Rev* 2006;25:87–98. [PubMed: 16680575]
- Tamada M, Sheetz MP, Sawada Y. Activation of a signaling cascade by cytoskeleton stretch. *Dev Cell* 2004;7:709–718. [PubMed: 15525532]
- Triplet JW, O'Riley R, Tekulve K, Norvell SM, Pavalko FM. Mechanical loading by fluid shear stress enhances IGF-1 receptor signaling in osteoblasts in a PKCzeta-dependent manner. *Mol Cell Biomech* 2007;4:13–25. [PubMed: 17879768]
- Unger M, Weaver VM. The tissue microenvironment as an epigenetic tumor modifier. *Methods Mol Biol* 2003;223:315–347. [PubMed: 12777739]
- Vanderploeg EJ, Imler SM, Brodtkin KR, Garcia AJ, Levenston ME. Oscillatory tension differentially modulates matrix metabolism and cytoskeletal organization in chondrocytes and fibrochondrocytes. *J Biomech* 2004;37:1941–1952. [PubMed: 15519602]
- Vincent TL, McLean CJ, Full LE, Peston D, Saklatvala J. FGF-2 is bound to perlecan in the pericellular matrix of articular cartilage, where it acts as a chondrocyte mechanotransducer. *Osteoarthr Cartil* 2007;15:752–763. [PubMed: 17368052]
- Volokh KY. Stresses in growing soft tissues. *Acta Biomater* 2006;2:493–504. [PubMed: 16793355]
- Wall ME, Weinhold PS, Siu T, Brown TD, Banes AJ. Comparison of cellular strain with applied substrate strain *in vitro*. *J Biomech* 2007;40:173–181. [PubMed: 16403503]
- Wang AZ, Ojakian GK, Nelson WJ. Steps in the morphogenesis of a polarized epithelium. I. Uncoupling the roles of cell–cell and cell–substratum contact in establishing plasma membrane polarity in multicellular epithelial (MDCK) cysts. *J Cell Sci* 1990a;95 (Part 1):137–151. [PubMed: 2351699]
- Wang AZ, Ojakian GK, Nelson WJ. Steps in the morphogenesis of a polarized epithelium. II. Disassembly and assembly of plasma membrane domains during reversal of epithelial cell polarity in multicellular epithelial (MDCK) cysts. *J Cell Sci* 1990b;95 (Part 1):153–165. [PubMed: 2351700]
- Wang HB, Dembo M, Hanks SK, Wang Y. Focal adhesion kinase is involved in mechanosensing during fibroblast migration. *Proc Natl Acad Sci USA* 2001;98:11295–11300. [PubMed: 11572981]
- Wang JH, Thampatty BP. An introductory review of cell mechanobiology. *Biomech Model Mechanobiol* 2006;5:1–6. [PubMed: 16489478]
- Watson CJ. Involution: apoptosis and tissue remodelling that convert the mammary gland from milk factory to a quiescent organ. *Breast Cancer Res* 2006;8:203. [PubMed: 16677411]
- Weaver VM, Howlett AR, Langton-Webster B, Petersen OW, Bissell MJ. The development of a functionally relevant cell culture model of progressive human breast cancer. *Semin Cancer Biol* 1995;6:175–184. [PubMed: 7495986]
- Weaver VM, Petersen OW, Wang F, Larabell CA, Briand P, Damsky C, et al. Reversion of the malignant phenotype of human breast cells in three-dimensional culture and *in vivo* by integrin blocking antibodies. *J Cell Biol* 1997;137:231–245. [PubMed: 9105051]
- Wells RG, Discher DE. Matrix elasticity, cytoskeletal tension, and TGF-beta: the insoluble and soluble meet. *Sci Signal* 2008;1:pe13. [PubMed: 18334714]
- Willis BC, Borok Z. TGF-beta-induced EMT: mechanisms and implications for fibrotic lung disease. *Am J Physiol Lung Cell Mol Physiol* 2007;293:L525–L534. [PubMed: 17631612]
- Wipff PJ, Rifkin DB, Meister JJ, Hinz B. Myofibroblast contraction activates latent TGF-beta1 from the extracellular matrix. *J Cell Biol* 2007;179:1311–1323. [PubMed: 18086923]
- Wiseman BS, Werb Z. Stromal effects on mammary gland development and breast cancer. *Science* 2002;296:1046–1049. [PubMed: 12004111]
- Wong JY, Velasco A, Rajagopalan P, Pham Q. Directed movement of vascular smooth muscle cells on gradient-compliant hydrogels. *Langmuir* 2003;19:1908–1913.
- Wyckoff JB, Pinner SE, Gschmeissner S, Condeelis JS, Sahai E. ROCK- and myosin-dependent matrix deformation enables protease-independent tumor-cell invasion *in vivo*. *Curr Biol* 2006;16:1515–1523. [PubMed: 16890527]
- Yeung T, Georges PC, Flanagan LA, Marg B, Ortiz M, Funaki M, et al. Effects of substrate stiffness on cell morphology, cytoskeletal structure, and adhesion. *Cell Motil Cytoskeleton* 2005;60:24–34. [PubMed: 15573414]

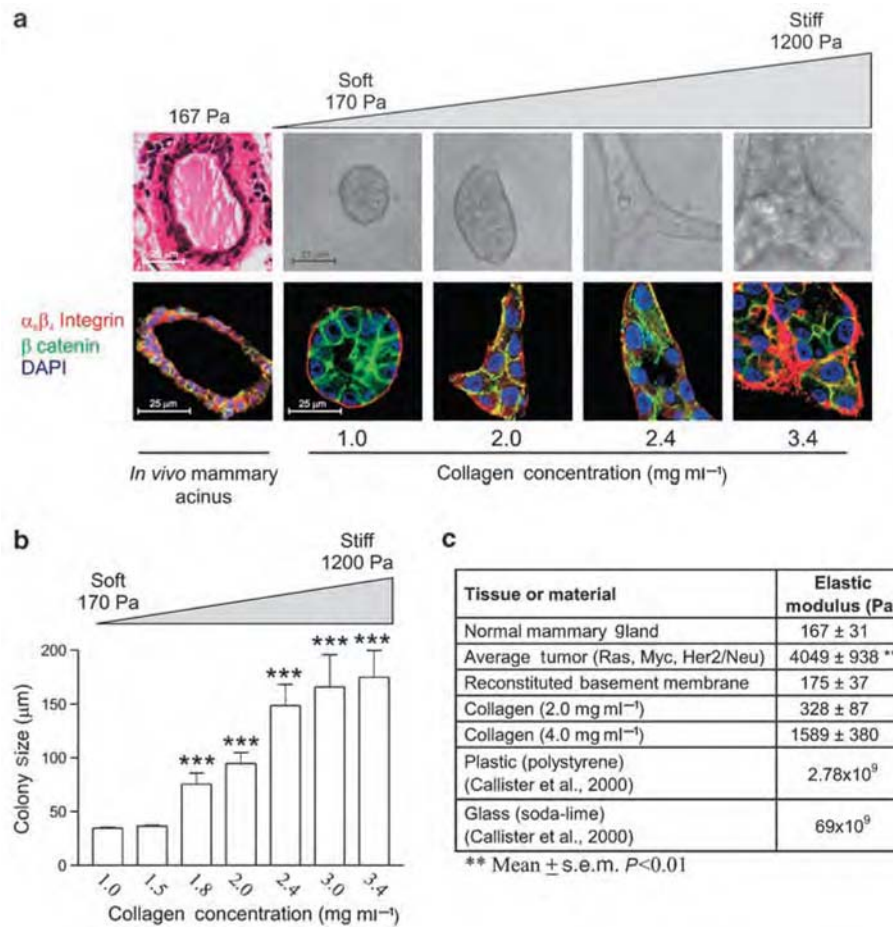


Figure 1.

MEC growth and morphogenesis reflect changes in matrix stiffness. **(a)** Confocal images of MEC grown in 3D cultures. As MECs grow in progressively stiffened matrices (170–1200 Pa), MEC morphology becomes progressively disrupted. Irregular MEC changes are characterized by disrupted cell–cell adherens junctions and tissue polarity, illustrated by a loss of β -catenin (green) and loss of β_4 integrin (red) organization (nuclei =blue). **(b)** Normal MEC acini reaches a proliferative growth-arrested phase when cultured in soft gels that is lost as they are cultured in stiffer matrices. **(c)** Measured elastic modulus for a variety of substrates. Values represent the mean \pm s.e.m. of four measurements from multiple mice and gels. ** $P \leq 0.01$, *** $P \leq 0.001$. (Reproduced with modification and proper permission obtained from Elsevier as published in Paszek *et al.*, 2005.)

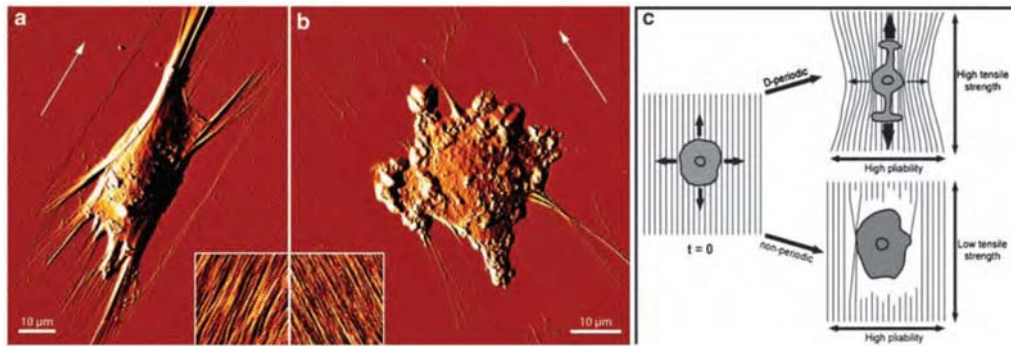


Figure 2.

SAOS-A2 cells were seeded on (a) D-periodic, or (b) non-periodic collagen matrices and allowed to spread for 45 min. Subsequently, cells were glutaraldehyde/paraformaldehyde-fixed and AFM deflection images representing the error signal were recorded while scanning the sample in contact mode. White arrows indicate the orientation of the collagen fibrils within the matrices. (a) On D-periodic collagen, cells polarize strongly and deform the D-periodic matrix perpendicular to the fibril direction, as indicated by the exposed surface. Collagen fibrils are bundled at the front and back of the cell without rupturing. The inset ($3 \mu\text{m} \times 3 \mu\text{m}$) shows an AFM contact mode topograph of $\approx 3 \text{ nm}$ thick collagen matrices assembled on freshly-cleaved mica in the presence of potassium ions. (b) Cell adhesion causes frequent rupture of non-periodic collagen fibrils, as demonstrated by the frayed appearance of the fibril ends and the widespread exposure of the mica surface in the cell periphery. The inset ($3 \mu\text{m} \times 3 \mu\text{m}$) shows an AFM contact mode topograph of $\approx 3 \text{ nm}$ thick collagen matrices assembled in the absence of potassium ions. (c) Model illustrating how differences in matrix rigidity between D-periodic and non-periodic collagen matrices affect cell polarization. Upon seeding, cells explore the mechanical properties of the surrounding D-periodic or non-periodic matrix by forming protrusions in all directions. Subsequently, cells form adhesion complexes and begin to exert pulling forces on the matrix. The high tensile strength of D-periodic collagen fibrils permits the establishment of strong cellular traction along the fibril direction. In contrast, the high pliability of the fibrils prevents traction when cells pull perpendicular to the fibril orientation. As a result of the directional traction the cells elongate. The low tensile strength of non-periodic collagen fibrils avoids traction build-up in the fibril direction, preventing cells from polarizing (Reproduced with modifications and proper permission obtained from Elsevier as published in Friedrichs *et al.*, 2007)

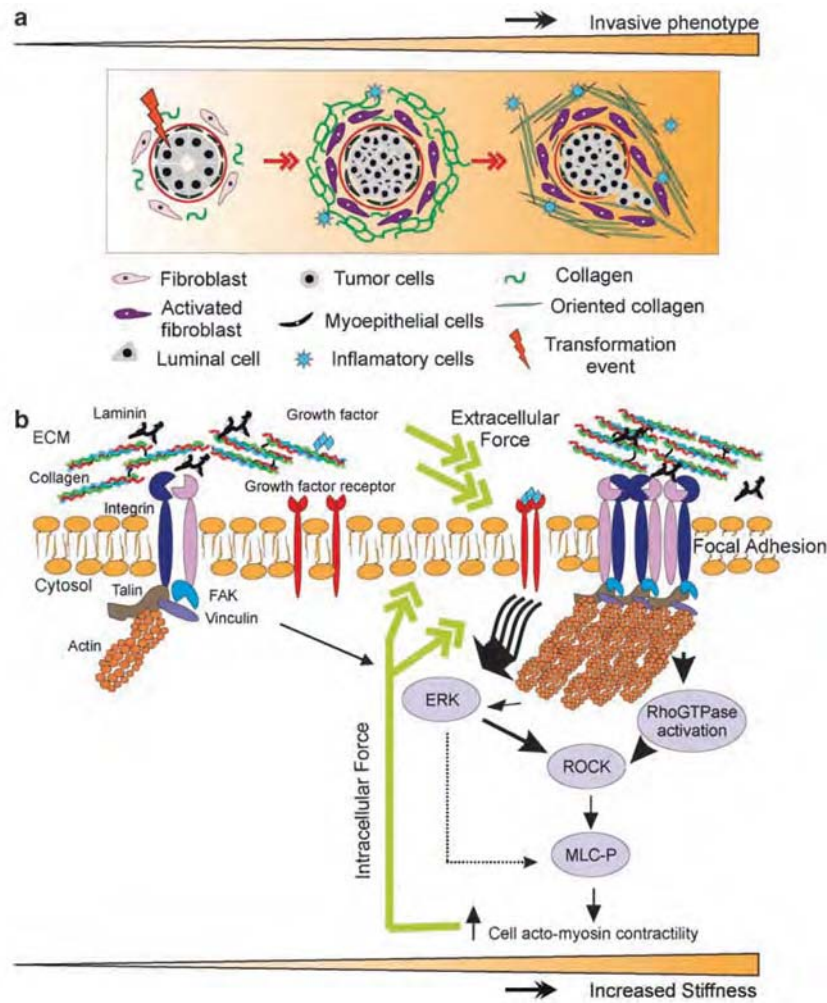


Figure 3. Malignant transformation of mammary epithelial cells is regulated by matrix stiffness. Breast transformation ensues through progressive acquisition of genetic alterations in the luminal epithelial cells residing within the mammary ducts. The tissue stroma responds to these epithelial alterations by initiating a desmoplastic response that is characterized by activation and transdifferentiation of fibroblasts, infiltration of immune cells, increased secretion of growth factors and cytokines, and elevated matrix synthesis and remodeling that manifests as matrix stiffening. **(a)** Cartoon depicting the stages of breast tumorigenesis (from left to right; normal ducts, ductal carcinoma *in situ* and invasive phenotype), highlighting key desmoplastic changes within the tissue stroma. **(b)** Force-dependent focal adhesion maturation mediated by elevated tumor matrix stiffness. Integrins are bidirectional mechanosensors that integrate biochemical and biophysical cues from the matrix and the actin cytoskeleton and transduce cell-generated force to the surrounding microenvironment. Activated integrins bind to ECM proteins via cooperative interactions between their alpha and beta extracellular domains and form nascent highly dynamic adhesion signaling complexes. In response to external mechanical force or elevated cell-generated contractility integrin clustering is enhanced and the recruitment of multiple integrin adhesion plaque proteins including talin and vinculin is favored. These, in turn, associate with the actin cytoskeleton and multiple signaling proteins including focal adhesion kinase (FAK), Src family kinases, and integrin-linked kinase, to promote cell growth, survival, migration and differentiation. Matrix stiffening, which reflects

elevated matrix deposition, linearization and cross-linking, can co-operate with oncogenic signaling to enhance cell-generated contractility to foster integrin associations and focal adhesion maturation. Maturation of focal adhesions promotes cell generated forces by enhancing Rho GTPase and ERK-mediated acto-myosin contractility—which feed forward to further promote integrin clustering and focal adhesion assembly and transmit acto-myosin-generated cellular forces to the ECM. (Reprinted with appropriate permission obtained from Elsevier as published in Kass *et al.*, 2007.)

Research Signpost
37/661 (2), Fort P.O., Trivandrum-695 023, Kerala, India



Recent Res. Devel. Immunology, 3(2001): 145-159 ISBN: 81-7736-073-6

Forcing transformation: Biophysical regulation of mammary epithelial cell transformation

Janna K. Mouw, Sonal J. Desai and Valerie M. Weaver*
Department of Surgery, Center for Bioengineering and Tissue
Regeneration, University of California, San Francisco, San Francisco
CA 94143 USA

Abstract

The mechanical microenvironment plays an important role in modulating mammary gland development, maintenance, and remodeling, and regulates the behavior of the epithelium and cellular stroma. The cellular and extracellular components which comprise the three-dimensional stroma regulate the growth, survival, migration and differentiation of the mammary epithelium. Disruption of microenvironmental cues and the loss of tissue architecture are associated with and may drive malignant progression. Malignant progression of the breast is associated with regional increases in compressive stresses and/or high tensional resistance forces, and a global stiffening of the extracellular matrix. These mechanical forces can modulate growth factor and cytokine activation and signaling within the cellular components of the tissue to alter mammary epithelial morphology and growth and promote survival and invasion. Because mammary gland development and tumorigenesis are linked to altered biomechanics, and both differentiating and transformed cells experience altered mechano-responsiveness, defining the role of biomechanics in mammary gland development and tumorigenesis is important. In this chapter, we discuss the participation of stromal-epithelial interactions in normal and malignant epithelial cell behavior, specifically focusing on how the biochemical and biomechanical properties of the extracellular matrix dramatically influence mammary gland development and homeostasis, as well as tumor progression and the malignant phenotype. We also provide a brief overview of tools and methods available for studying the extracellular matrix and biomechanics in breast carcinogenesis.

Correspondence/Reprint request: Dr. Valerie M. Weaver, Department of Surgery, UCSF, 513 Parnassus Ave. Room S-1364, San Francisco, CA 94122-0456. E-mail: weaverv@surgery.ucsf.edu

INTRODUCTION

Breast cancer is the most common cancer in Western women, with a cancer mortality rate second only to lung cancer [1]. Due to the mechanical changes associated with mammary carcinoma, including increased extracellular matrix (ECM) deposition and interstitial pressure, breast palpation is often an initial measure used to detect breast carcinoma. Despite the connection between altered ECM biophysical properties and breast cancer, cancer research has historically focused on biochemical changes [2]. Nevertheless, a novel paradigm has emerged over the past few decades, bringing a three-dimensional (3D) tissue perspective to breast cancer and breast cancer research that encompasses a dynamic feedback

loop between epithelial morphogenesis and transformation and the biochemical and biophysical properties of the breast stroma [3-5].

Biomechanical cues influence development, regulate cell fate and contribute to disease [6-9]. At the cellular level there exist a number of molecular mechanisms through which cells sense and transduce mechanical cues that are localized within the membrane, the cytoskeleton and at specific cell-matrix complexes [10-12]. In particular, branched epithelial structures, such as the mammary gland, present multiple opportunities for force sensing. The mammary ductal tree is embedded within an architecturally complex extracellular microenvironment that broadly encompasses both cellular (myofibroblasts, fibroblasts, adipocytes, endothelial cells and immune cells) and non-cellular (structural extracellular and soluble factors such as cytokines and growth factors) components. In the context of a 3D tissue, such as the breast, mechanical loading can physically alter the conformation of extracellular receptor complexes present in fibroblasts and in mammary epithelial cells (MECs). Domains within these complexes can be stretched or compressed, either directly or indirectly altering the structure and function of the ECM receptor complexes influencing their signaling. Force can also directly or indirectly modify the activity and function of other membrane complexes such as growth factor receptors, cytokine receptors, ion channels, and cell-cell junctional complexes [13].

The mammary gland is a dynamic tissue, with the cellular and ECM compositions evolving over time, guiding and responding to changes in the development of the gland by a process termed dynamic reciprocity [14]. By incorporating the interplay between soluble factors, cell-cell and cell-ECM interactions and the mechanical microenvironment in the regulation of mammary morphogenesis and differentiation and tissue homeostasis the concept can be broadened as mechano-reciprocity [15]. Perturbations in dynamic reciprocity and mechano-reciprocity have been implicated in breast tumor progression. Specifically, interactions between the ECM and adhesion receptor complexes, such as integrin focal adhesions, influence both branching morphogenesis and mammary gland involution through directed cycles of ECM remodeling of the stromal-epithelial interface [16, 17]. Alterations in the ECM ligand or receptor expression and/or activity and aberrant matrix remodeling and matrix stiffening can drive mammary tumorigenesis and metastasis [18, 19]. Consistently, inhibiting aberrant ECM remodeling, reducing stromal stiffness and normalizing integrin receptor function can revert the malignant phenotype or restrict tumor progression [19]. Interestingly, dysregulated expression and activity of growth factors that participate in embryonic and adult mammary tissue development, including members of

the transforming growth factor (TGF), epidermal growth factor (EGF), hepatocyte growth factor (HGF) and fibroblast growth factor (FGF) families, not only drive breast tumorigenesis and metastasis by increasing cell growth and survival but also alter integrin and ECM ligand expression and induce cell-generated force to modify cell-ECM interactions [20-25].

Breast cancer is characterized by a persistent increase in mammary gland stiffness and the transformed behavior of MECs [25, 26]. Transformed MECs exhibit increased mechano-sensitivity [27, 28]. In this chapter, we summarize experimental evidence that the ECM content and structure dramatically influence mammary gland development and homeostasis, as well as tumor progression and the malignant phenotype. Of the various perspectives contributing to mammary epithelial cell behavior, the roles of biomechanics in guiding mammary epithelial morphogenesis, homeostasis and transformation are discussed. Several approaches used to study the participation of mechanical forces on cell behavior are described. Methods used to elucidate the biochemical pathways associated with cell-generated forces are also provided. This chapter highlights how the critical interplay of cell and tissue mechanics within the mammary microenvironment could influence development and carcinogenesis, and reviews strategies useful for experimentally exploring this phenomenon.

Deleted: that

MAMMARY GLAND DEVELOPMENT AND MAINTENANCE

The mammary gland is a functional secretory unit and a modified sweat gland. Normal breast development begins *in utero* and continues after birth. The mammary gland is the only branching organ that becomes fully mature during adulthood. The general structure of the mature mammary gland is a network of highly organized and branched ducts made up of epithelial cells. These ducts are surrounded by myoepithelial cells and basement membrane (BM), the entirety of which is embedded in a complex stroma consisting of extracellular matrix (ECM), mesenchymal cells, connective tissue and adipose tissue. Control of mammary development is a carefully orchestrated exchange of biochemical and biophysical cues between the cells of the developing mammary gland and the surrounding microenvironment. A great deal of effort has been invested in identifying biochemical regulatory mechanisms involved in all stages of breast development and a plethora of information about the key signals and molecules involved is readily available; however, an exhaustive discussion of all such regulatory mechanisms is beyond the scope of this review. There have been excellent reviews about biochemical cues, such

as hormonal regulation and signaling mechanisms, that regulate mammary gland development and we direct the reader to those comprehensive and elegant publications for more detail [29-35]. In this section, we will first focus on the development of the mammary gland and then discuss how ECM-cell interactions and mechanical force could modulate this process.

THE DEVELOPMENT PROCESS

The mammary gland develops in four stage of a female's life: embryogenesis, puberty, pregnancy and lactation, and menopause. During embryogenesis, the mammary gland arises from cells of the ectoderm which migrate in response to signals from the mesenchyme [36]. These epithelial cells initially proliferate to form two mammary ridges, or milk lines, that then regress back to become two solid epithelial masses, called the mammary buds, which subsequently give rise to the nipples [33]. Approximately 10-15 ducts arise from the nipple. The tips of the ducts, bulbous terminal end buds, invade into the mammary fat pad as the ducts elongate and branch to form the rudimentary ductal tree [37]. The ducts terminate in clusters of alveoli called terminal ductal lobular units. The luminal epithelial layer differentiates into secretory cells while the basal epithelial layer becomes the myoepithelium. The breast remains in this state until puberty.

At the onset of puberty, the mammary gland changes in response to hormonal cues and undergoes branching morphogenesis [35]. The breast is stimulated to develop in response to estrogen signaling in mesenchymal cells and increases in size due to adipose tissue expansion during puberty. The epithelial cells proliferate and the BM is remodeled, as the rudimentary ductal tree further elongates and branches into the expanding stroma [38]. By the end of puberty, the lumens of the secretory alveoli have been established at the ends of the smaller ducts of the branched structure. At this point, the mammary gland is considered mature but inactive, and remains in this state until pregnancy. It is interesting to note that there are small cyclical changes during the menstrual cycle, such as changes in epithelial cell shape, proliferation and apoptosis, BM remodeling, luminal size and stromal density, underscoring the theory that the adult breast, although considered "inactive" outside of pregnancy, is by no means static.

In response to estrogens and progesterone, the epithelium of the mammary gland undergoes extensive and rapid proliferation during pregnancy. The terminal ductal lobular units branch further and elongate and the terminal end buds differentiate into alveoli [39]. As the glandular structure enlarges, the stromal components thin. The myoepithelial cells extend contractile processes in a network around the alveolus. In the final stages of pregnancy, the luminal epithelial cells become cuboidal as the

alveoli mature and distend. After childbirth, there is a drop in estrogen and progesterone levels, and the structure of the gland is maintained by prolactin signaling. Suckling stimulates milk production by the secretory cells, causing the alveoli to dilate until they comprise most of the mammary gland [40]. The stroma is reduced to a fibrous capsule surrounding the lobules. Suckling also stimulates the release of oxytocin which induces myoepithelial cell contraction, facilitating expulsion of the alveolar contents and milk delivery to the young. At the end of the lactation period, the ECM undergoes extensive matrix metalloproteinase (MMP)-dependent remodeling, the extraneous epithelial cells undergo apoptosis, and the remaining epithelial cells become smaller and inactive [41]. The ducts and alveoli degenerate back to a resting state while the stroma is reconstructed [42, 43], though the glandular structure and the stromal composition of the post-lactation breast is not identical to their counterparts before pregnancy. The breast remains in this state, with the ability to become fully functional again during subsequent pregnancies, until menopause. After menopause, stromal density increases, adipose density decreases and the glandular structure regresses.

BIOCHEMICAL REGULATION

Mammary gland development is a dynamic process mediated through reciprocal interactions between the epithelium and the stroma that continue throughout the life span of the female. A myriad of continuously evolving biochemical and biophysical cues are required to direct the proper formation and function of the breast. The stroma is an instructive compartment of the mammary gland which changes in composition and architecture during mammary gland development and with age. The composition of the stroma includes the non-cellular ECM which is made up primarily of laminins (1, 5 and 10), collagens (I, III and IV), proteoglycans (including lumican and decorin), entactin, tenascin and fibronectin, and the cellular constituents which include fibroblasts, endothelial cells, adipocytes and infiltrating leukocytes (e.g. macrophages and lymphocytes). The BM constitutes the part of the ECM that is directly associated with the ductal epithelium, which is embedded within the interstitial ECM. The interstitial ECM, composed primarily of type I collagen, fibronectin and proteoglycans, is particularly important since it provides structure and support for the ductal tissue and stromal cells. In addition, it is also a repository for various growth factors and chemokines. ECM-cell interactions transmit physical cues from outside of the cell, modifying cell behavior by inducing cytoskeletal remodeling and inducing biochemical signaling cascades [44].

During embryogenesis, signals from fat pad adipocytes and interstitial fibroblasts direct mammary gland development. These two cell types express distinct ECM receptors and secrete different types of ECM ligands that reciprocally regulate their differentiated function and direct the development of the gland. For instance, the cells of the fat pad express laminin receptors and secrete laminin 5 and perlecan sulfate to promote the elongation of the ductal tree, whereas fibroblasts express high levels of $\alpha 5\beta 1$ and $\alpha 2\beta 1$ integrins, and deposit fibronectin and collagen to facilitate duct maturation and branching [45, 46]. During the branching morphogenesis associated with the onset of puberty, the composition of the BM changes. The BM surrounding the ducts consists primarily of laminins 1, 5 and 10, collagen IV, entactin and various heparin sulfate proteoglycans, except at the invasive front of the ductal tree which is enriched in hyaluronic acid [38]. However, the BM is not static and is continuously being remodeled during development by multiple MMPs. For instance, MMP2 activity is important for ductal elongation, while MMP3 and MMP14 activities are important for branching [38, 47, 48]. MMP activity is tempered by tissue inhibitors of metalloproteinases (TIMPs) to tightly regulate spatial and temporal remodeling of the ECM during development [38, 49, 50].

Transmembrane receptors within the epithelium interact with the ECM to physically anchor the cell within the tissue and to relay biochemical and mechanical information into the cell. Multiple families of ECM receptors exist including the syndecans, the discoidin receptors (DDR1 and DDR2), dystroglycan, and integrins. Loss of DDR1 results in excessive collagen deposition, impeded ductal formation and incomplete lactational differentiation [51]. Integrins are the best characterized and most abundant of the ECM receptors. Integrins are composed of α and β subunits which heterodimerize to form an array of 24 different receptors that can bind to specific collagens, laminins, tenascin and fibronectin. Integrins can also associate with other ECM receptors such as syndecans, growth factor receptors and members of the tetraspanin transmembrane protein family, to cooperatively modulate cell fate and tissue processes such as branching morphogenesis, injury and fibrosis [38, 52]. For instance, $\alpha 2$ integrin but not $\alpha 3$, $\alpha 4$ or $\alpha 6$ is required for branching morphogenesis during pregnancy in gene knockout mouse models [53, 54]. During pregnancy, alveolar maturation is primarily mediated through $\beta 1$ signaling; loss of $\beta 1$ results in improper alveoli formation and lack of prolactin-induced epithelial cell differentiation and milk synthesis [55, 56].

MECHANICAL REGULATION

The mammary gland is not generally thought of as a mechanically active tissue. However, given that physical force regulates embryogenesis and tissue-specific differentiation, it is highly likely that the mammary gland is also subject to a range of forces that shape its development and homeostasis [57, 58]. For instance, MECs migrate and invade the mammary fat pad early during embryogenesis and the coordinated movement of these cells appears to be largely governed by an exchange between exerted force and the mechanical properties of the tissue, including the ECM. During development, MECs also experience variations in intracellular tension that modulate their shape and behavior and dictate the architecture of the tissue. This cellular tension arises from two sources including actomyosin contractility linked to actin cytoskeletal dynamics and an “opposing” reaction force resisting the cytoskeletal contraction (physical adhesions to another cell or the ECM) (Figure 1). Physical movement of the cells occurs early in embryogenesis when the MECs migrate and invade the mammary fat pad, and continues through adolescent- and pregnancy-associated branching morphogenesis. The coordinated movement of cells is largely determined by an exchange between exerted forces and the mechanical properties of the reactive tissue, primarily the ECM. Migration appears to be mediated by remodeling of the ECM, which is driven by tension fields and a combination of durotaxis (migration along a stiffness gradient) and chemotaxis (migration along a chemical gradient), similar to the migration of fibroblast along ECM fibers [59-61]. Interestingly, tensional force can activate β -catenin, an effector of Wnt signaling which directs embryonic mammary gland development, and FGF and HGF, which also participate in breast development and activate actomyosin contractility in MECs [20, 61-67]. While these observations suggest that ECM-directed tensional stress is important in embryogenesis and mammary development, neither definitive evidence nor molecular mechanisms have been described.

ECM remodeling influences terminal end bud invasion, modulating branching morphogenesis by activating biochemical signaling cascades within the epithelium and by releasing soluble factors that regulate epithelial cell behavior. Physical parameters exerted by fluid flow or contractility within cells in the stroma and epithelium or via cellular interactions also influence epithelial morphogenesis [38]. For instance, clefting forces and surface tension between the epithelium and the stroma have been proposed to affect the shape of the branched mammary ductal structure, using computational fluid dynamics modeling [68, 69]. External forces can alter epithelial invasion directly or cooperatively with cytokine and growth factor receptors by stimulating ERK and RhoGTPases to

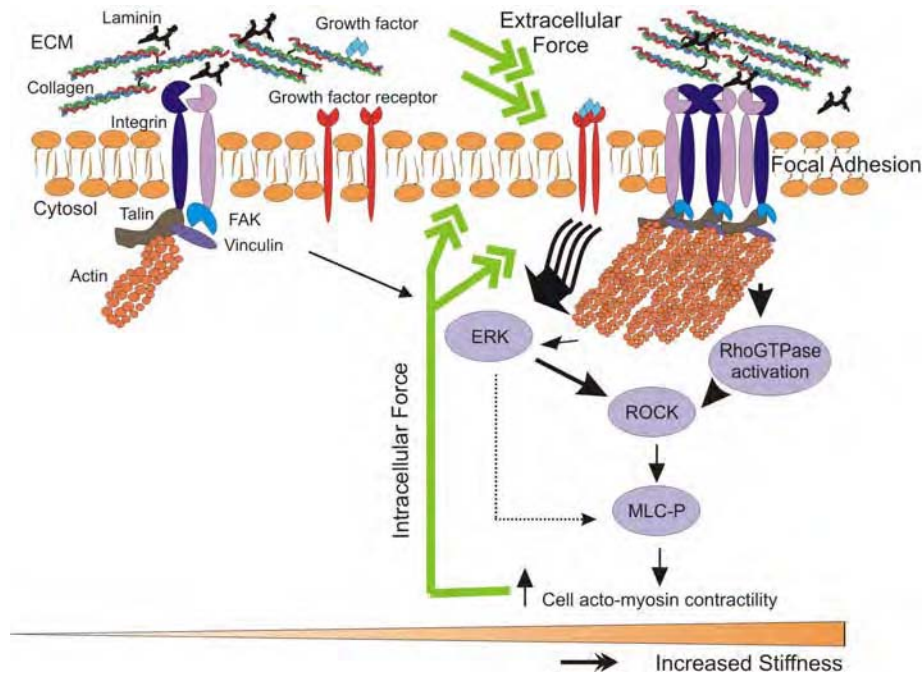


Figure 1: Force-dependent focal adhesion maturation mediated by extracellular force. Integrins are bi-directional mechanosensors that integrate biochemical and biophysical cues from the matrix and the actin cytoskeleton and transduce cell-generated force to the surrounding microenvironment. Activated integrins bind to ECM proteins via cooperative interactions between their alpha and beta extracellular domains and form nascent highly dynamic adhesion signaling complexes. In response to external mechanical force or elevated cell-generated contractility, integrin clustering is enhanced and the recruitment of multiple integrin adhesion plaque proteins including talin and vinculin is favored. These, in turn, associate with the actin cytoskeleton and multiple signaling proteins including FAK, Src family kinases, and integrin-linked kinase, to promote cell growth, survival, migration and differentiation. Matrix stiffening, which reflects elevated matrix deposition, linearization and cross-linking, can cooperate with oncogenic signaling to enhance cell-generated contractility to foster integrin associations and focal adhesion maturation. Maturation of focal adhesions promotes cell generated forces by enhancing Rho GTPase and ERK-mediated actomyosin contractility - which feed forward to further promote integrin clustering and focal adhesion assembly and transmit actomyosin-generated cellular forces to the ECM, as outlined in Paszek et al., 2005. Modified from Paszek et al., 2005. (reprinted from *Int J Biochem Cell Biol*, 39, Kass L, Ertler JT, Dembo M, Weaver VM, "Mammary epithelial cell: influence of extracellular matrix composition and organization during development and tumorigenesis", 1987-1984, 2007, with permission from Elsevier.)

induce actomyosin contractility and cytoskeletal remodeling [70] (Figure 1). In the lung and kidney, inhibiting Rho activity restricts branching morphogenesis whereas activating Rho promotes abnormal branching [71, 72]. In the breast, elevated collagen levels, elevated crosslinking of the ECM or reduced MMP-dependent remodeling modifies matrix stiffness to

reduce terminal end bud invasion (unpublished observations) and disrupt acinar morphogenesis by possibly altering RhoGTPase activity. Consistently, mammary tumor cells exert significantly more force on their surrounding microenvironment than normal mammary cells and have elevated ERK and RhoGTPase activity. Reducing actomyosin or RhoGTPase activity can revert the malignant phenotype [28].

Functional differentiation of the mammary gland following pregnancy proceeds within the context of a highly compliant interstitial matrix and a mechanically-relaxed BM. Consistent with the observation that elevated matrix stiffness compromises mammary epithelial morphogenesis, culture studies have shown that mechanically loading collagen gels inhibits the functional differentiation (β -casein expression) of MECs [73]. For instance, early studies showed that functional acinar formation occurs only when a mixed cell population isolated from pre-lactating mice are plated on floating collagen gels (conditions in which the fibrillar tension is significantly reduced as compared to gels left attached to the tissue culture plate) and are able to assemble their own endogenous BM [73, 74]. This observation is supported by recent studies demonstrating that elevated matrix stiffness compromises β -casein expression by immortalized murine MECs (personal communication with M. Bissell). Although the molecular mechanisms underlying these phenotypes remain poorly understood, data suggest that matrix stiffness promotes focal adhesion assembly, destabilizes tissue architecture and enhances integrin and growth factor-dependent signaling [75, 76]. Furthermore, data suggest that elevated substrate stiffness might also interfere with tissue differentiation by stimulating the activity of MMPs to compromise BM assembly and stability and destabilize cell-cell E cadherin junctions [77]. Our own laboratory has been able to precisely calibrate ECM stiffness using both natural and synthetic laminin-containing matrices and we have shown that BM matrix compliance regulates cell shape, tissue morphogenesis and endogenous BM assembly in part by regulating focal adhesion maturation and signaling [25].

The most profound mechanical activity in the breast occurs during breastfeeding. Oxytocin is released in response to suckling and stimulates the myoepithelial cells to contract and secrete milk from the ducts. Build up of the secreted milk within the gland produces an increase in the intra-gland pressure, causing the alveoli to distend due to elevated tensional “hoop” stress, similar to the increase in air volume when blowing up a balloon. This force is countered by a reaction force generated by the surrounding tissue and by the tensile stress of the contracting myoepithelium [78]. These counteracting forces are essential for efficient milk delivery and functional strength of the lactating gland. Once lactation

ceases, the breast undergoes involution during which hormonal changes signal the remodeling of the mammary gland [41]. The specific mechanical forces that regulate involution have yet to be fully elucidated; however compression forces have been implicated in this process [79].

MAMMARY GLAND TRANSFORMATION

THE DESMOPLASTIC RESPONSE AND TUMOR PROGRESSION

The tissue desmoplasia that accompanies breast cancer was first described by pathologists several decades ago; however its significance to tumorigenesis was only recently appreciated. The desmoplastic response is distinguished by changes in the stromal mechanical environment arising with the inappropriate activation or induction of resident fibroblasts and myofibroblasts, as well as infiltrating immune cells [80] (Figure 2). For instance, macrophages recruited to the tumor site by chemokines secrete cytokines, growth factors and proteases that stimulate remodeling of the tissue stroma and promote angiogenesis [81]. Similarly, tumor-associated fibroblasts upregulate or stimulate the activity of various growth factors to promote cancer progression, including TGF- β , insulin-like growth factor (IGF) and HGF [82, 83]. Characteristics of the tumor stroma include an increase in matrix proteins such as collagens I, III and IV, fibronectin, elastin and tenascin [4, 84-86]. There is also elevated crosslinking of these matrix proteins by lysyl oxidase (LOX) family members, transglutaminase and the proteoglycans lumican and decorin [4, 87-89]. An abnormal MMP-9/TIMP-1 balance has been shown to participate in tumor growth and overall invasiveness, while an abnormal MMP-2/TIMP-2 balance could be associated with lymph node invasion [90].

The desmoplastic response is characterized by dramatic changes in the composition of the ECM and the mechanical properties of the mammary tissue. Thus, invasive ductal breast tumors with pronounced desmoplasia are characteristically stiffer than normal tissue and this feature has permitted the detection of breast tumors by physical palpation. More recently, ultrasound imaging modalities including sonoelastography and magnetic resonance elastography have been developed to visualize the mechanical changes in the tissue surrounding the primary lesion and have been proposed as alternative detection strategies [91]. Direct measurement of the stiffnesses (as represented by the Young's moduli) of fibrocystic tissue, as well as benign and pre-malignant lesions, showed these lesions to be 3-6-fold stiffer than normal tissue, and high-grade invasive ductal carcinoma to be 13-fold stiffer, suggesting that changes in the material properties of the tissue temporally parallel and may even contribute to the malignant behavior of the tissue [26].

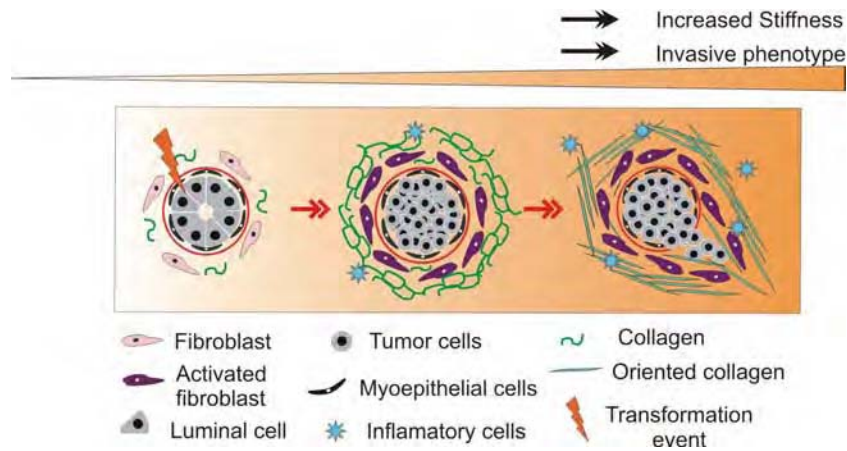


Figure 2: Malignant transformation of MECs is regulated by matrix stiffness. Breast transformation ensues through progressive acquisition of genetic alterations in the luminal epithelial cells residing within the mammary ducts. The tissue stroma responds to these epithelial alterations by initiating a desmoplastic response that is characterized by activation and trans-differentiation of fibroblasts, infiltration of immune cells, increased secretion of growth factors and cytokines, and elevated matrix synthesis and remodeling that manifests as matrix stiffening. Cartoon depicts the stages of breast tumorigenesis, (from left to right; normal ducts, ductal carcinoma in situ and invasive phenotype) highlighting key desmoplastic changes within the tissue stroma. (reprinted from *Int J Biochem Cell Biol*, 39, Kass L, Erler JT, Dembo M, Weaver VM, “Mammary epithelial cell: influence of extracellular matrix composition and organization during development and tumorigenesis”, 1987-1984, 2007, with permission from Elsevier.)

The enhanced deposition, elevated crosslinking and abnormal MMP-dependent remodeling contribute to an overall increase in stromal stiffness. Specific changes in the mechanics of the breast include zones of both increased intraductal compression and elevated intracellular and extracellular tension, as well as an overall progressive increase in ECM stiffening. When the extracellular microenvironment becomes perturbed, the mammary tissue and all of its inclusive cell types respond with alterations in their intracellular tension. Specifically, MECs within a transformed breast experience areas of increased resistance force in their stromal environment linked to elevated matrix stiffness [25, 26].

Changes in the form and function of the breast ECM can influence mammary tissue behavior not only on a mechanical level, but also biochemically through the release and activation of soluble growth factors, cytokines, matrix degrading enzymes and bioactive peptides [92]. Altered mammary mechanics, such as a dramatic increase in ECM stiffness, may promote the malignant transformation of MECs by altering growth factor responsiveness [27], increasing adhesion receptor expression and activation [93], or by enhancing motility and migration [94, 95]. Additionally,

transformed cells influenced by oncogenes such as Ras and ErbB/HER experience increased stiffness [96, 97]. Ras and ErbB/HER can also activate Rho and ERK, which drive alterations in actomyosin assembly, also altering intracellular tension.

Cell-ECM interactions actively participate in epithelial cell transformation and can modify tumor behavior and treatment responsiveness [98]. Aberrant expression of ECM receptors such as β 1-, β 4-, α 2-, α 3- and α 6-integrins have been documented in transformed MECs; *in vitro* and *in vivo* work has functionally implicated these ECM receptor alterations in breast tumor progression. Elevated levels of β 4-integrin via direct interactions with either the ErbB2 or MET receptors perturb matrix adhesion and promote tumor invasion, and reducing β 4 signaling or decreasing β 1 integrin levels or function inhibit mammary tumor progression and revert expression of the malignant phenotype in culture and *in vivo* [19, 99-103].

Metastasis of transformed MECs is associated with a high percentage of disease fatalities and, thus, restricting metastasis is a primary objective of many cancer prevention programs. During invasion, cells extend pseudopodia at the leading edge that attach to collagen fibers in the ECM, allowing cells to migrate along the fibers towards blood vessels [104]. To promote metastasis of tumor cells, the basement membrane must be compromised and transformed MECs must migrate into the surrounding stroma. MMP-2 and -14 have been shown to cleave laminin-5, exposing a cryptic site of this protein involved in epithelial migration [105]. Additionally, increased MMP activity release and activate growth factors trapped in the stroma which, in turn, leads to increased growth factor signaling, thereby stimulating further invasion. Migration is regulated by cellular adhesion, cell-generated contractility and cell haptotaxis to maximize ligand binding [106]. Durotaxis linked to enhanced cytoskeletal remodeling and increased intracellular tension might also contribute to tumor metastasis [59, 107]. Importantly, elevated matrix deposition and tension may couple with ECM degradation, modulating tumor invasion and metastasis. For instance, it has been shown that the family of Rho GTPases is linked to cell migration and MMP-mediated invasion. Consistent with this paradigm, Rho and Rac expression and activity are increased in tumors and, specifically, over-expression of RhoC and loss of the tumor growth suppressor WISP3, have been implicated in aggressive, metastatic forms of inflammatory breast cancers [108, 109]. Interestingly, inhibiting the collagen cross-linking LOX dramatically reduced metastasis in a xenograft model of breast cancer [110].

Taken together, the cellular response to both altered biochemical signaling, as well as a stiffer microenvironment, may create a

synergistically negative, tumorigenic feedback loop. These overall changes in the cell-generated forces alter the activity and function of signaling cascades that ultimately determine their growth, survival, motility and invasion. Such changes might also modulate the response of the transformed MECs to chemo- and radiation therapies.

MAMMOGRAPHIC DENSITY

Mammographic density is defined by the percentage of the breast rich in stroma and epithelium, as opposed to adipose tissue. Clinical studies suggest that mammographic density is a strong risk factor for breast cancer [111, 112]. Data indicate that risk increases 4-fold in women whose breast tissue is greater than 75% mammographically dense. In fact, some studies showed that approximately one-third of patients with breast cancer had mammographic densities that scored equal to or great than 50% [113]. Moreover, DCIS predominantly occurs in mammographically dense areas of the breast, and may be preceded by increased density [114]. One explanation for the associated risk between mammographic density and breast cancer risk is that increased breast density masks the tumor, making clinical detection difficult. Yet, mammographic density is a heterogeneous condition that is not always associated with elevated breast tumor risk. Histologically, mammographic density is associated with epithelial and stromal cell proliferation, and increased deposition of collagen [111]. While some studies suggest elevated collagen could actively promote tumor progression by promoting local invasion of tumor cells [115-117], contributing factors such as collagen remodeling and post-translational modifications complicate the paradigm. In this regard, increased levels of small leucine-rich proteoglycans, such as lumican and decorin, have also been implicated in dense breasts [89]. Additionally, elevated expression of LOXL2, a member of the LOX family of collagen crosslinking proteins, correlates with increased tumor fibrosis and progression in vivo [87]; and increased LOX and LOXL2 expressions correlate with invasive potential in many highly invasive/metastatic breast cancer cell lines [118]. Mammographically dense breasts have also been linked to increased IGF-1 and metalloproteinase-3 (TIMP-3) expression [119]. These findings suggest the mechanical changes in breast tissue associated with increased mammographic density drive tumorigenesis, most likely due to perturbations in mechanical homeostasis. Increased breast stiffness is a critical readout of altered tissue homeostasis during the early events of tumor progression.

Deleted: ,

Deleted:

TISSUE COMPRESSIVE FORCES

Compressive forces are generated by the resistance of the mammary tissue adjacent to the pool of transformed MECs actively proliferating within the ductal tree, as well as the invasive tumorigenic MECs confined within the expanding fibrotic tumor mass [120]. Additionally, dysfunctional vascular and lymphatic transport can lead to increases in interstitial fluid and pressure of the transformed tissue. These increases in intraductal compression and interstitial pressure can lead to an overall decrease in blood flow through the tumor vasculature, resulting in hypoxic areas. Hypoxia has been linked to increased tumor aggressiveness, as well as resistance to radiation and chemotherapy [121, 122].

At the molecular level, normal and transformed MEC behavior can be altered by compression through the activation and function of various soluble cytokines and growth factors, as well as through alterations in gene and protein expression. Compression-induced changes in microtubule dynamics can alter cell motility and morphology [123]. Compressive mechanical loading has been shown to upregulate inflammatory cytokines such as IL-8 [124] and receptor activator nuclear factor kappa-B ligand [125], stimulate cell growth through FGF-dependent activation of ERK [126], facilitate invasion through elevations in MMP-9 and MMP-28 release and activation [127, 128], and drive cell differentiation through upregulated TGF- β signaling [129]. Increases in TGF- β signaling in response to increase hydrostatic and dynamic compression can trigger a pro-fibrotic response of the stromal fibroblast population of the breast tumor, resulting in an increase in tumor growth and viability, an induction of angiogenesis and promotion of an epithelial-mesenchymal transition (EMT) [130, 131].

Compressive forces could regulate tumor behavior indirectly through non-molecular and more “physical” mechanisms. A decrease in interstitial space around ductal structures within a compliant environment such as the mammary gland has been shown to slow the transport of secreted ligand away from the cell surface, triggering an autocrine ligand-receptor signaling response. Tschumperlin et al. have shown that compressive stress elicits ERK phosphorylation through autocrine ligand-receptor signaling involving heparin-binding EGF (HB-EGF), leading to subsequent binding and activation of the EGFR [132]. This suggests that proliferating DCIS lesions could experience an increase in EGFR activation in response to increased compressive pressure, enhancing tumor growth without ErbB receptor amplification.

Deleted:

INTRACELLULAR TENSION & MATRIX RIGIDITY

The tissue adjacent to an expanding tumor mass responds to the tumor-generated compressive force by exerting a reaction force on the expanding tumor mass itself. These tumor-initiated resistance forces may translate to transformed cells as tensional forces. By regulating the activity of various biochemical signaling cascades, cytoskeletal-mediated tensional forces alter tumor behavior. Tensional forces can be transmitted from tumor cell to tumor cell through adhesion plaques, and within the tumor cells via the cytoskeleton to cell-ECM adhesions [133]. The expanding tumor mass and actively migrating tumor cells can each independently deliver direct forces to cell-ECM and cell-cell adhesion plaques, impacting tumor cell behavior by physically distorting the ECM. Tensional forces can incur conformational changes of proteins at the integrin adhesion plaque, such as vinculin, to activate integrin adhesion signaling either directly, by influencing receptor clustering or indirectly, inducing changes in lipid packing and thus affecting ion channel gating [134]. Tensile mechanical loading has also been shown to modulate intracellular signaling. For instance, mechanical strain increased the ligand-binding and activation of $\alpha V\beta 3$ integrin leading to the upregulation of JNK signaling through PI3 kinase [135] and promoted angiogenesis through increased vascular endothelial growth factor (VEGF) expression [136]. Cell survival is also mediated by mechanical stress through the activation of PI3 kinase, AKT, p38 SAPK2 and JNK, independent of ErbB2 and angiotensin receptor type I activation [137, 138]. Tensional forces may not only exert oriented alterations in the cytoskeleton, but could also induce changes in overall dynamic remodeling of the cytoskeleton. Therefore, a tissue-derived tensional force could additionally influence cell-cell adhesion dependent signaling to alter cell behavior.

Deleted:

Deleted:

Deleted:

Our laboratory has found that even a small increase in matrix rigidity will perturb normal MEC architecture, disrupting polarity and cell-cell junctions, and ultimately enhancing MEC growth through an increase in Rho-generated cytoskeletal tension, promotion of focal adhesions, and upregulation of growth factor-dependent ERK activation (Figure 3). Increasing ECM stiffness increased the recruitment of actin-binding proteins, such as vinculin, to $\beta 1$ integrins, thereby promoting large focal adhesion assembly and increased cell-generated traction forces. Similarly, by inhibiting Rho-generated cytoskeletal tension or ERK activity, highly contractile, EGFR-transformed MECs could be phenotypically reverted to form differentiated acini lacking focal adhesions and with reduced EGFR activity and ERK signaling [25]. These findings suggest that breast tumors react to stromal stiffening via tensional homeostasis, with maximum intracellular forces exerted at the focal adhesion through assembly by

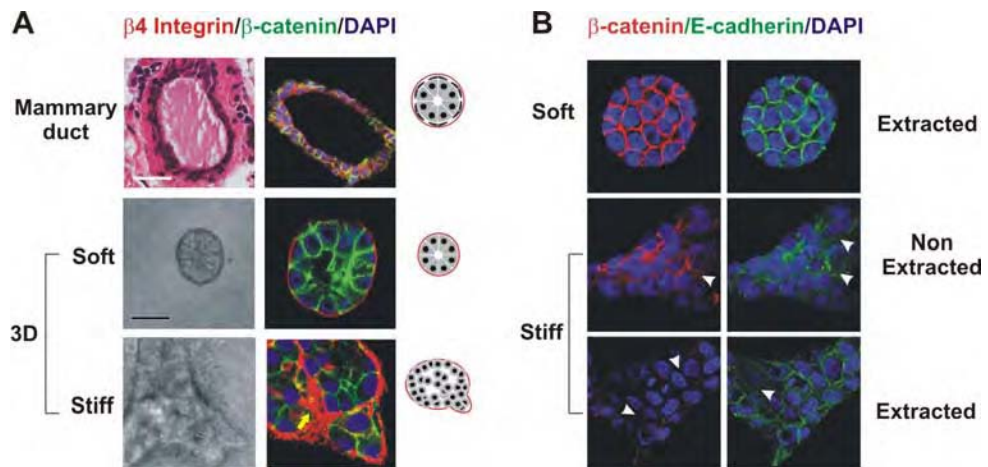


Figure 3: MEC growth and morphogenesis is regulated by matrix stiffness. **A)** 3D cultures of normal MECs within collagen gels of different concentration. Stiffening the ECM through an incremental increase in collagen concentration (soft gels: 1mg/ml Collagen I, 140Pa; stiff gels 3.6mg/ml Collagen I, 1200Pa) results in the progressive perturbation of morphogenesis, and the increased growth and modulated survival of MECs. Altered mammary acini morphology is illustrated by the destabilization of cell-cell adherens junctions and disruption of basal tissue polarity, indicated by the gradual loss of cell-cell localized β -catenin (green) and disorganized $\beta 4$ integrin (red)(visualized through immunofluorescence and confocal imaging). Column 2 illustrates mammary ductal structure (luminal and myoepithelial cells surrounded by BM), and depicts MEC morphogenesis in soft and stiff gels. Scale bars represent 25 μ m. **B)** Confocal immunofluorescence images of MEC colonies on soft and stiff gels (140 versus >5000 Pa) stained for β -catenin (red) and E-cadherin (green), and counterstained with DAPI (blue) after triton X-100 extraction. β -catenin could be extracted from the sites of cell-cell interaction in MEC colonies formed on a stiff but not on a soft gel, indicating that adherens junctions are less stable in MEC structures formed on stiff gels. White arrows indicate diffuse staining patterns of β -catenin and E-cadherin. Modified from Paszek et al., 2005. (reprinted from *Int J Biochem Cell Biol*, 39, Kass L, Erler JT, Dembo M, Weaver VM, "Mammary epithelial cell: influence of extracellular matrix composition and organization during development and tumorigenesis", 1987-1984, 2007, with permission from Elsevier.)

actomyosin cytoskeletal networks. According to this model, the resulting effect of the mechanical environment amplifies oncogene-driven ERK activation, facilitating malignant transformation through cytoskeletal contractility via the small GTPase, Rho.

In summary, tensional homeostasis may be critical for normal tissue growth and differentiation. Thus, increasing matrix rigidity through changes in ECM composition, organization and crosslinking, or by elevated Rho signaling, could induce cytoskeletal contractility to enhance integrin-dependent growth and destabilize tissue architecture [139]. Increased cell contractility through Rho could facilitate malignant transformation in conditions accompanied by the induction of tissue

fibrosis and/or the amplification of ERK signaling through oncogenic activity. In this regard, tumors that have undergone EMT have vastly reorganized cytoskeletons and altered adhesions, and, as such, respond differently to the physical forces present in the tumor microenvironment [140, 141]. Part of a potentially negative feedback ~~loop~~, induction of a tumor EMT could alter how tensional force is sensed and transduced within a transformed cell, leading to further progression of the EMT phenomena.

Deleted: look

UNDERSTANDING MAMMARY GLAND MECHANOTRANSDUCTION

While the overall importance of mechanical force to tissue behavior is generally acknowledged, much remains to be discovered about cell and tissue mechanotransduction, and how such mechanosensory signals might guide cellular behavior. Investigators are just beginning to elucidate how mechanical stimulation induces structural, compositional and functional changes at the cellular level, and how these cues could alter the structural integrity and function of differentiated tissues. What is clear is that cells must have elements that can detect and integrate different combinations of forces and magnitudes, in a multitude of contexts. Once stimulated, these “mechanosensor” elements must be able to propagate these cues by signaling a cascade of downstream events that alter cell behavior through effector mechanisms such as cytoskeletal reorganization, conformational changes in transmembrane proteins (ion channels, etc.) and alterations in gene and protein expression. As reviewed in this chapter, cellular growth, differentiation and migration have all been linked to mechanotransduction mechanisms [142].

Multiple mechano-sensitive players have emerged: the cytoskeleton, integrins, receptor tyrosine kinases, mitogen-activated protein kinases, G proteins, and stretch-activated ion channels, to name a few [143]. Currently, the best studied mechanotransduction pathway is the ECM-integrin-cytoskeletal interface [142, 144, 145]. Because the expression and activity of integrins and adhesion-plaque associated proteins differ so dramatically in breast cancer cells, mechanotransduction is likely altered in transformed MECs. This raises the intriguing possibility that mammary gland transformation may be functionally linked to perturbed mechanical-homeostasis. Future research in the area of cell mechanobiology will require novel experimental and theoretical methodologies to determine the type and magnitude of the forces experienced at the cellular and sub-cellular levels, and to identify the force sensors/receptors that initiate the cascade of cellular and molecular events.

MODELS OF MAMMARY MORPHOGENESIS AND TRANSFORMATION

To investigate mammary epithelial morphogenesis and malignant transformation, 3D culture systems have been developed to model the *in vivo* environment of MECs. The original 3D models were designed to completely embed MECs within a polymerized ECM to closely recapitulate the structure and composition of the mammary gland *in vitro*. These models have been modified to study how mechanical properties affect morphogenesis and biochemical processes [146]. In this review, we present an overview of these 3D models and the modifications used to study mechanotransduction. Additionally, engineering approaches to modulating the physical forces applied to cells are discussed.

3D CULTURE SYSTEMS

As discussed in this chapter, ECM composition and architecture are frequently altered in breast transformation and can influence MEC growth, differentiation and migration. Methods to study these biological processes traditionally involve culturing isolated cells on a 2D surface. However, cells *in vivo* exist in a complex 3D environment. To more accurately study MEC morphogenesis *in vitro*, models have been developed to recapitulate the *in vivo* 3D environment. The simplest 3D model involves embedding a single type of cell in a biocompatible scaffold. These biocompatible scaffolds provide cells with a prefabricated ECM, which is often modifiable by the embedded cells. Scaffolding materials commonly used for complete embedment of MECs include recombinant basement membranes (rBMs) produced and isolated from Engelbreth-Holm-Swarm (EHS) mouse tumor matrices, collagen I, and fibrin. Laminin 1, collagen IV, entactin and heparin sulfate proteoglycans are the major components of the EHS rBM. rBM has been utilized extensively to study morphogenesis and transformation in normal, non-transformed MECs, such as MCF-10A cells and S1 cells (from the HMT-3522 progression series) [19, 147-149]. Indeed, when various non-transformed MECs (primary and cell lines) are mixed with rBM they form polarized structures, with hollow lumens, within the polymerized rBM [150][151]. A modified version of this method is to apply a layer of rBM to the tissue culture surface, plate cells on to the rBM and then add another layer of rBM, resulting in a pseudo 3D system [146, 149]. Although the cells are not mixed directly with the rBM, they are nevertheless surrounded by rBM and are able to form acinar structures, presumably by remodeling the rBM. Drawbacks of using rBM matrices are that it is not fully characterized and therefore has an ill-defined content and lot to lot variability. Another commonly used total embedment

scaffold, collagen I, is biologically better defined than rBM derived from EHS cells. While certain epithelial cells types polarize in collagen I, such as MDCK epithelial cells, many other epithelial cell types fail to undergo acinar morphogenesis, or form structures with reverse polarity [152]. One advantage collagen I has over rBM is that the mechanical properties can be adjusted by titrating the collagen concentration and the extent of crosslinking. However, since collagen is biologically derived, there is variability between lots, species and processing techniques (for instances, intact- versus telepeptide free- collagen).

Synthetic materials are now being utilized to more precisely control the substrate stiffness of the matrix presented to the cell. Polyacrylamide gels, traditionally used to separate biomolecules, have been manipulated in the 3D culture system [153]. ~~By varying the concentration of polyacrylamide to bisacrylamide crosslinker, a range of quantifiable stiffnesses can be achieved. The limitation of this system is that polyacrylamide can be cytotoxic to the cells and therefore total embedment can not be utilized. Applying the cells to the top of the polyacrylamide gel may limit the cytotoxic effect, but is not a 3D environment. To circumvent these issues, the gels are modified by crosslinkers that facilitate the binding of rBM or ECM components to the gels [154]. Cells are then applied to these gels and overlaid with more rBM or ECM component to construct a pseudo-3D environment. These gels have a precisely calibrated modulus range (200 – 10,000 Pascals) and have been used successfully to study matrix stiffness and mechanotransduction in normal and malignant mammary development [25].~~

Deleted:

ENGINEERED BIOREACTORS

Knowledge of the types, magnitude and duration of forces throughout the cell are essential in understanding the molecular mechanisms involved in mechanotransduction. The cellular response to mechanical stimulation is dependent on the type of force applied, with tensile and compressive forces being applied perpendicular to the surface of the cell or 3D construct and shear forces being applied parallel to the cell or 3D construct surface. The cellular response is also dependent on the magnitude, frequency and duration of the applied stimuli. To delineate the roles of physical forces in cell behavior and tissue homeostasis, researchers apply physiologically-relevant mechanical stimuli at the cellular and tissue levels using specially engineered devices which have been designed to control temporal, spatial and intensity parameters.

There are two general approaches to studying cellular mechanotransduction. The first approach uses multiple cells, mechanically stimulating a group of cells, and mimicking forces inherent in various

physiological environments. This first set of techniques include the simple application of hydrostatic pressure, compression, tension and shear stress to cell monolayers, or in the context of a tissue (*ex vivo* explant culture or cells embedded in a tissue engineering scaffold). Flow chambers apply shear stress to monolayers of cells, either through pressure-driven systems applying a parabolic laminar flow profile or cone-and-plate flow chambers which apply a uniform shear stress with a linear flow profile [155]. The role of hydrostatic pressure in cell and tissue growth and differentiation can be investigated in 2D by applying a transmembrane pressure to cells plated on a porous, stiff substrate, or in 2D or 3D by directing compressed air or a column of fluid over a culture of cells [15]. Techniques investigating the mechano-response to tensile stress involve the application of static or cyclic, axial or biaxial strains to monolayers of cells on a deformable membrane, or within a deformable 3D scaffold [156][157]. Additionally, mechanical devices have been used since the 70's to deconstruct the roles of static and dynamic compression in cell growth and metabolism [158].

The second and more recent approach to studying cellular mechanotransduction investigates the response by a single, individual cell to a mechanical stimulus. Sophisticated devices apply pico- or nano-Newton forces to individual cell membranes, receptors or cytoskeletal elements. Particle attachment has been used to apply precise forces to the surface of cells, using small microbeads coated with adhesive ligands or antibodies to a specific receptor and then applying a force to the particle [159, 160]. Different techniques for applying forces include optical trapping, micropipette aspiration and the application of both linear and torsional forces with magnetic manipulation [161-163]. Both atomic force microscopy and traction force microscopy have been used to determine the material properties, as well as the forces generated, by single cells [164-166]. Development of these innovative approaches and tools opens endless possibilities for novel insights into fundamental mechanotransduction mechanisms directing interactions between cells and their surrounding microenvironment.

Deleted:

CONCLUSION

Stromal-epithelial interactions drive development and maintain tissue homeostasis through a network of both physical and biochemical factors that operate within a 3D mammary tissue. Specifically, mammary gland development, maintenance, and remodeling, as well as epithelial and stromal cellular responses and functions, are modulated by the mechanical environment. These biomechanical cues contribute crucial information to developmental and disease processes, and influence basic cell fate decisions. The cellular and ECM compositions evolve over time, guiding

and responding to changes in the development of the gland. Integral to this process is the complex interplay between soluble factors, cell-cell and cell-ECM interactions and the mechanical environment, which cooperatively drive mammary morphogenesis and differentiation, and regulate tissue homeostasis.

Mechanical force elicits a myriad of biochemical responses in a cell, altering how a cell responds to an exogenous signal, and dramatically influencing differentiation decisions during development. Given that tumorigenesis is associated with drastic changes in the mechanical characteristics of the mammary gland, including the composition and structure of ECM components, intracellular and extracellular tension, interstitial pressure and tissue elastic modulus, altered mechanotransduction and loss of mechanical-homeostasis constitute a plausible mechanism regulating the pathogenesis of breast tumors. While the overall importance of mechanotransduction is generally acknowledged, much remains to be discovered about cell and tissue mechanotransduction, and how such mechanosensory signals guide behavior. The quest to elucidate how mechanical stimulation induces structural, compositional and functional changes at the cellular level, as well as in 3D tissues, is still in its infancy. It will be critical to clarify the molecular basis of mechanotransduction in the development and homeostasis of the mammary gland, as well as in epithelial transformation.

Deleted:

Deleted:

Deleted:

Deleted:

ACKNOWLEDGEMENTS

We apologize to the many authors whose work is not cited due to space limitations. This work was supported by NIH grant 7R01CA078731-07, DOD grant W81XWH-05-1-330 (BC044791) and DOE grant A107165 to V.M.W., and DOD grant BC062562 to J.K.M.

REFERENCES

1. S. Moulder and G.N. Hortobagyi, *Clin Pharmacol Ther* 83 (2008) 26-36.
2. S. Huang and D.E. Ingber, *Cancer Cell* 8 (2005) 175-6.
3. C.M. Nelson and M.J. Bissell, *Annu Rev Cell Dev Biol* 22 (2006) 287-309.
4. B.S. Wiseman and Z. Werb, *Science* 296 (2002) 1046-9.
5. S. Lelievre, V.M. Weaver and M.J. Bissell, *Recent Prog Horm Res* 51 (1996) 417-32.
6. E. Farge, *Curr Biol* 13 (2003) 1365-77.
7. R. Keller, L.A. Davidson and D.R. Shook, *Differentiation* 71 (2003) 171-205.
8. G. Helmlinger, P.A. Netti, H.C. Lichtenbeld, R.J. Melder and R.K. Jain, *Nat Biotechnol* 15 (1997) 778-83.

9. M. Brancaccio, E. Hirsch, A. Notte, G. Selvetella, G. Lembo and G. Tarone, *Cardiovasc Res* 70 (2006) 422-33.
10. O.P. Hamill and B. Martinac, *Physiol Rev* 81 (2001) 685-740.
11. M. Tamada, M.P. Sheetz and Y. Sawada, *Dev Cell* 7 (2004) 709-18.
12. M. Chiquet, V. Tunc-Civelek and A. Sarasa-Renedo, *Appl Physiol Nutr Metab* 32 (2007) 967-73.
13. F.H. Silver and L.M. Siperko, *Crit Rev Biomed Eng* 31 (2003) 255-331.
14. M.J. Bissell, H.G. Hall and G. Parry, *Journal of Theoretical Biology* 99 (1982) 31-68.
15. M.J. Paszek and V.M. Weaver, *J Mammary Gland Biol Neoplasia* 9 (2004) 325-42.
16. A. Page-McCaw, A.J. Ewald and Z. Werb, *Nat Rev Mol Cell Biol* 8 (2007) 221-33.
17. P. Lu, M.D. Sternlicht and Z. Werb, *J Mammary Gland Biol Neoplasia* 11 (2006) 213-28.
18. M.D. Sternlicht, M.J. Bissell and Z. Werb, *Oncogene* 19 (2000) 1102-13.
19. V.M. Weaver, O.W. Petersen, F. Wang, C.A. Larabell, P. Briand, C. Damsky and M.J. Bissell, *J Cell Biol* 137 (1997) 231-45.
20. J. de Rooij, A. Kerstens, G. Danuser, M.A. Schwartz and C.M. Waterman-Storer, *J Cell Biol* 171 (2005) 153-64.
21. C.A. Carraway and K.L. Carraway, *Sci STKE* 2007 (2007) re3.
22. C. Dickson, B. Spencer-Dene, C. Dillon and V. Fantl, *Breast Cancer Res* 2 (2000) 191-6.
23. F. Lanigan, D. O'Connor, F. Martin and W.M. Gallagher, *Cell Mol Life Sci* 64 (2007) 3159-84.
24. M.D. Marmor, K.B. Skaria and Y. Yarden, *Int J Radiat Oncol Biol Phys* 58 (2004) 903-13.
25. M.J. Paszek, N. Zahir, K.R. Johnson, J.N. Lakins, G.I. Rozenberg, A. Gefen, C.A. Reinhart-King, S.S. Margulies, M. Dembo, D. Boettiger, D.A. Hammer and V.M. Weaver, *Cancer Cell* 8 (2005) ~~241-54~~.
26. A. Samani, J. Zubovits and D. Plewes, *Phys Med Biol* 52 (2007) 1565-76.
27. H.B. Wang, M. Dembo and Y.L. Wang, *Am J Physiol Cell Physiol* 279 (2000) C1345-50.
28. M.A. Wozniak, R. Desai, P.A. Solski, C.J. Der and P.J. Keely, *J Cell Biol* 163 (2003) 583-95.
29. I. Taddei, M.M. Faraldo, J. Teuliere, M.A. Deugnier, J.P. Thiery and M.A. Glukhova, *J Mammary Gland Biol Neoplasia* 8 (2003) 383-94.
30. C.M. Nelson, M.M. Vanduijn, J.L. Inman, D.A. Fletcher and M.J. Bissell, *Science* 314 (2006) 298-300.
31. G.W. Robinson, *Nat Rev Genet* 8 (2007) 963-72.
32. M.A. Chrenek, P. Wong and V.M. Weaver, *Breast Cancer Res* 3 (2001) 224-9.
33. J.R. Hens and J.J. Wysolmerski, *Breast Cancer Res* 7 (2005) 220-4.
34. M.D. Sternlicht, *Breast Cancer Res* 8 (2006) 201.
35. M.D. Sternlicht, H. Kouros-Mehr, P. Lu and Z. Werb, *Differentiation* 74 (2006) 365-81.

Deleted: Submitted

36. J.M. Veltmaat, A.A. Mailleux, J.P. Thiery and S. Bellusci, *Differentiation* 71 (2003) 1-17.
37. L. Hinck and G.B. Silberstein, *Breast Cancer Res* 7 (2005) 245-51.
38. J.E. Fata, Z. Werb and M.J. Bissell, *Breast Cancer Res* 6 (2004) 1-11.
39. S.R. Oakes, H.N. Hilton and C.J. Ormandy, *Breast Cancer Res* 8 (2006) 207.
40. S.M. Anderson, M.C. Rudolph, J.L. McManaman and M.C. Neville, *Breast Cancer Res* 9 (2007) 204.
41. C.J. Watson, *Breast Cancer Res* 8 (2006) 203.
42. M.P. Osborne, *Breast development and anatomy*, Lippincott-Raven Publishers, Philadelphia, 1996.
43. J. Russo and I.H. Russo, *Eur J Cancer Prev* 2 Suppl 3 (1993) 85-100.
44. M. Larsen, V.V. Artym, J.A. Green and K.M. Yamada, *Curr Opin Cell Biol* 18 (2006) 463-71.
45. K. Kimata, T. Sakakura, Y. Inaguma, M. Kato and Y. Nishizuka, *J Embryol Exp Morphol* 89 (1985) 243-57.
46. T. Sakakura, Y. Sakagami and Y. Nishizuka, *Dev Biol* 91 (1982) 202-7.
47. B.S. Wiseman, M.D. Sternlicht, L.R. Lund, C.M. Alexander, J. Mott, M.J. Bissell, P. Soloway, S. Itoharu and Z. Werb, *J Cell Biol* 162 (2003) 1123-33.
48. H. Kouros-Mehr and Z. Werb, *Dev Dyn* 235 (2006) 3404-12.
49. Z. Werb, J. Ashkenas, A. MacAuley and J.F. Wiesen, *Braz J Med Biol Res* 29 (1996) 1087-97.
50. J.E. Fata, K.J. Leco, R.A. Moorehead, D.C. Martin and R. Khokha, *Dev Biol* 211 (1999) 238-54.
51. W.F. Vogel, A. Aszodi, F. Alves and T. Pawson, *Mol Cell Biol* 21 (2001) 2906-17.
52. F. Berditchevski and E. Odintsova, *J Cell Biol* 146 (1999) 477-92.
53. T.C. Klinowska, C.M. Alexander, E. Georges-Labouesse, R. Van der Neut, J.A. Kreidberg, C.J. Jones, A. Sonnenberg and C.H. Streuli, *Dev Biol* 233 (2001) 449-67.
54. J. Chen, T.G. Diacovo, D.G. Grenache, S.A. Santoro and M.M. Zutter, *Am J Pathol* 161 (2002) 337-44.
55. M.J. Naylor, N. Li, J. Cheung, E.T. Lowe, E. Lambert, R. Marlow, P. Wang, F. Schatzmann, T. Wintermantel, G. Schuetz, A.R. Clarke, U. Mueller, N.E. Hynes and C.H. Streuli, *J Cell Biol* 171 (2005) 717-28.
56. T.L. Woodward, A.S. Mienaltowski, R.R. Modi, J.M. Bennett and S.Z. Haslam, *Endocrinology* 142 (2001) 3214-22.
57. J. Trinkaus, *Cells in organs. The forces that shape the embryo.*, second ed., Prentice-Hall Inc., Englewood Cliffs, NJ, 1984.
58. G.F. Oster, J.D. Murray and A.K. Harris, *J Embryol Exp Morphol* 78 (1983) 83-125.
59. J.Y. Wong, A. Velasco, A. Rajagopalan and Q. Pham, *Langmuir* 19 (2003) 1908-1913.
60. S. Goswami, E. Sahai, J.B. Wyckoff, M. Cammer, D. Cox, F.J. Pixley, E.R. Stanley, J.E. Segall and J.S. Condeelis, *Cancer Res* 65 (2005) 5278-83.
61. A. Czirok, B.J. Rongish and C.D. Little, *Dev Biol* 268 (2004) 111-22.

62. E.Y. Chu, J. Hens, T. Andl, A. Kairo, T.P. Yamaguchi, C. Brisken, A. Glick, J.J. Wysolmerski and S.E. Millar, *Development* 131 (2004) 4819-29.
63. D.E. Ingber, *Ann Med* 35 (2003) 564-77.
64. J.C. Howard, V.M. Varallo, D.C. Ross, J.H. Roth, K.J. Faber, B. Alman and B.S. Gan, *BMC Musculoskelet Disord* 4 (2003) 16.
65. J. Yant, L. Buluwela, B. Niranjana, B. Gusterson and T. Kamalati, *Exp Cell Res* 241 (1998) 476-81.
66. B. Niranjana, L. Buluwela, J. Yant, N. Perusinghe, A. Atherton, D. Phippard, T. Dale, B. Gusterson and T. Kamalati, *Development* 121 (1995) 2897-908.
67. C. Dillon, B. Spencer-Dene and C. Dickson, *J Mammary Gland Biol Neoplasia* 9 (2004) 207-15.
68. V. Fleury and T. Watanabe, *C R Biol* 325 (2002) 571-83.
69. S.R. Lubkin and Z. Li, *Biomech Model Mechanobiol* 1 (2002) 5-16.
70. G. Forgacs, *Biol Bull* 194 (1998) 328-29; discussion 329-30.
71. H. Miao, C.H. Nickel, L.G. Cantley, L.A. Bruggeman, L.N. Bennardo and B. Wang, *J Cell Biol* 162 (2003) 1281-92.
72. K.A. Moore, S. Huang, Y. Kong, M.E. Sunday and D.E. Ingber, *J Surg Res* 104 (2002) 95-100.
73. J.T. Emerman and D.R. Pitelka, *In Vitro* 13 (1977) 316-28.
74. M.H. Barcellos-Hoff, J. Aggeler, T.G. Ram and M.J. Bissell, *Development* 105 (1989) 223-35.
75. C.D. Roskelley, A. Srebrow and M.J. Bissell, *Curr Opin Cell Biol* 7 (1995) 736-47.
76. V.M. Weaver and M.J. Bissell, *J Mammary Gland Biol Neoplasia* 4 (1999) 193-201.
77. T.H. Chun, K.B. Hotary, F. Sabeh, A.R. Saltiel, E.D. Allen and S.J. Weiss, *Cell* 125 (2006) 577-91.
78. S.J. Gunst and D.D. Tang, *Eur Respir J* 15 (2000) 600-16.
79. A. Marti, Z. Feng, H.J. Altermatt and R. Jaggi, *Eur J Cell Biol* 73 (1997) 158-65.
80. D.C. Radisky, P.A. Kenny and M.J. Bissell, *J Cell Biochem* 101 (2007) 830-9.
81. J. Condeelis and J.W. Pollard, *Cell* 124 (2006) 263-6.
82. A.A. Rasmussen and K.J. Cullen, *Breast Cancer Res Treat* 47 (1998) 219-33.
83. C. Kuperwasser, T. Chavarria, M. Wu, G. Magrane, J.W. Gray, L. Carey, A. Richardson and R.A. Weinberg, *Proc Natl Acad Sci U S A* 101 (2004) 4966-71.
84. L.M. Coussens and Z. Werb, *Nature* 420 (2002) 860-7.
85. C. Porta, B. Subhra Kumar, P. Larghi, L. Rubino, A. Mancino and A. Sica, *Adv Exp Med Biol* 604 (2007) 67-86.
86. M.J. Bissell, D.C. Radisky, A. Rizki, V.M. Weaver and O.W. Petersen, *Differentiation* 70 (2002) 537-46.
87. G. Akiri, E. Sabo, H. Dafni, Z. Vadasz, Y. Kartvelishvily, N. Gan, O. Kessler, T. Cohen, M. Resnick, M. Neeman and G. Neufeld, *Cancer Res* 63 (2003) 1657-66.

88. T.Y. Eshchenko, V.I. Rykova, A.E. Chernakov, S.V. Sidorov and E.V. Grigorieva, *Biochemistry (Mosc)* 72 (2007) 1016-20.
89. S. Alowami, S. Troup, S. Al-Haddad, I. Kirkpatrick and P.H. Watson, *Breast Cancer Res* 5 (2003) R129-35.
90. D.C. Jinga, A. Blidaru, I. Condrea, C. Ardeleanu, C. Dragomir, G. Szegli, M. Stefanescu and C. Matache, *J Cell Mol Med* 10 (2006) 499-510.
91. B.S. Garra, *Ultrasound Q* 23 (2007) 255-68.
92. E.I. Deryugina and J.P. Quigley, *Cancer Metastasis Rev* 25 (2006) 9-34.
93. T. Yeung, P.C. Georges, L.A. Flanagan, B. Marg, M. Ortiz, M. Funaki, N. Zahir, W. Ming, V. Weaver and P.A. Janmey, *Cell Motil Cytoskeleton* 60 (2005) 24-34.
94. C.M. Lo, H.B. Wang, M. Dembo and Y.L. Wang, *Biophys J* 79 (2000) 144-52.
95. D.S. Gray, J. Tien and C.S. Chen, *J Biomed Mater Res A* 66 (2003) 605-14.
96. E. Vial, E. Sahai and C.J. Marshall, *Cancer Cell* 4 (2003) 67-79.
97. G. Ferretti, A. Felici, P. Papaldo, A. Fabi and F. Cognetti, *Curr Opin Obstet Gynecol* 19 (2007) 56-62.
98. V.M. Weaver, A.H. Fischer, O.W. Peterson and M.J. Bissell, *Biochem Cell Biol* 74 (1996) 833-51.
99. F.G. Giancotti, *Trends Pharmacol Sci* 28 (2007) 506-11.
100. A. Bertotti, P.M. Comoglio and L. Trusolino, *Cancer Res* 65 (2005) 10674-9.
101. S.K. Muthuswamy, D. Li, S. Lelievre, M.J. Bissell and J.S. Brugge, *Nat Cell Biol* 3 (2001) 785-92.
102. W. Guo, Y. Pylayeva, A. Pepe, T. Yoshioka, W.J. Muller, G. Inghirami and F.G. Giancotti, *Cell* 126 (2006) 489-502.
103. C.C. Park, H. Zhang, M. Pallavicini, J.W. Gray, F. Baehner, C.J. Park and M.J. Bissell, *Cancer Res* 66 (2006) 1526-35.
104. J. Condeelis and J.E. Segall, *Nat Rev Cancer* 3 (2003) 921-30.
105. G. Giannelli, J. Falk-Marzillier, O. Schiraldi, W.G. Stetler-Stevenson and V. Quaranta, *Science* 277 (1997) 225-8.
106. J.P. Thiery, *Cell Differ* 15 (1984) 1-15.
107. M.P. Sheetz, D.P. Felsenfeld and C.G. Galbraith, *Trends Cell Biol* 8 (1998) 51-4.
108. G. Fritz, C. Brachetti, F. Bahlmann, M. Schmidt and B. Kaina, *Br J Cancer* 87 (2002) 635-44.
109. C.G. Kleer, Y. Zhang, Q. Pan, G. Gallagher, M. Wu, Z.F. Wu and S.D. Merajver, *Breast Cancer Res* 6 (2004) R110-5.
110. J.T. Erler and A.J. Giaccia, *Cancer Res* 66 (2006) 10238-41.
111. L.J. Martin and N.F. Boyd, *Breast Cancer Res* 10 (2008) 201.
112. C.M. Vachon, C.H. van Gils, T.A. Sellers, K. Ghosh, S. Pruthi, K.R. Brandt and V.S. Pankratz, *Breast Cancer Res* 9 (2007) 217.
113. N.F. Boyd, J.M. Rommens, K. Vogt, V. Lee, J.L. Hopper, M.J. Yaffe and A.D. Paterson, *Lancet Oncol* 6 (2005) 798-808.
114. G. Ursin, L. Hovanesian-Larsen, Y.R. Parisky, M.C. Pike and A.H. Wu, *Breast Cancer Res* 7 (2005) R605-8.

115. P.P. Provenzano, K.W. Eliceiri, J.M. Campbell, D.R. Inman, J.G. White and P.J. Keely, *BMC Med* 4 (2006) 38.
116. M. Egeblad, L.E. Littlepage and Z. Werb, *Cold Spring Harb Symp Quant Biol* 70 (2005) 383-8.
117. S. Ramaswamy, K.N. Ross, E.S. Lander and T.R. Golub, *Nat Genet* 33 (2003) 49-54.
118. D.A. Kirschmann, E.A. Seftor, S.F. Fong, D.R. Nieva, C.M. Sullivan, E.M. Edwards, P. Sommer, K. Csiszar and M.J. Hendrix, *Cancer Res* 62 (2002) 4478-83.
119. Y.P. Guo, L.J. Martin, W. Hanna, D. Banerjee, N. Miller, E. Fishell, R. Khokha and N.F. Boyd, *Cancer Epidemiol Biomarkers Prev* 10 (2001) 243-8.
120. K.Y. Volokh, *Acta Biomater* 2 (2006) 493-504.
121. H. Axelson, E. Fredlund, M. Ovenberger, G. Landberg and S. Pahlman, *Semin Cell Dev Biol* 16 (2005) 554-63.
122. L. Holmquist, T. Lofstedt and S. Pahlman, *Adv Exp Med Biol* 587 (2006) 179-93.
123. T.J. Dennerll, H.C. Joshi, V.L. Steel, R.E. Buxbaum and S.R. Heidemann, *J Cell Biol* 107 (1988) 665-74.
124. Y. Muroi, K. Kakudo and K. Nakata, *J Dent Res* 86 (2007) 786-91.
125. H. Ichimiya, T. Takahashi, W. Ariyoshi, H. Takano, T. Matayoshi and T. Nishihara, *Oral Surg Oral Med Oral Pathol Oral Radiol Endod* 103 (2007) 334-41.
126. T.L. Vincent, C.J. McLean, L.E. Full, D. Peston and J. Saklatvala, *Osteoarthritis Cartilage* 15 (2007) 752-63.
127. F. Reno, P. Grazianetti, M. Stella, G. Magliacani, C. Pezzuto and M. Cannas, *Arch Dermatol* 138 (2002) 475-8.
128. F. Reno, M. Sabbatini, M. Stella, G. Magliacani and M. Cannas, *Wound Repair Regen* 13 (2005) 255-61.
129. J.K. Mouw, J.T. Connelly, C.G. Wilson, K.E. Michael and M.E. Levenston, *Stem Cells* 25 (2007) 655-63.
130. S.K. Leivonen and V.M. Kahari, *Int J Cancer* 121 (2007) 2119-24.
131. B.C. Willis and Z. Borok, *Am J Physiol Lung Cell Mol Physiol* 293 (2007) L525-34.
132. D.J. Tschumperlin, G. Dai, I.V. Maly, T. Kikuchi, L.H. Laiho, A.K. McVittie, K.J. Haley, C.M. Lilly, P.T. So, D.A. Lauffenburger, R.D. Kamm and J.M. Drazen, *Nature* 429 (2004) 83-6.
133. A. Katsumi, A.W. Orr, E. Tzima and M.A. Schwartz, *J Biol Chem* 279 (2004) 12001-4.
134. V. Gupta and K.J. Grande-Allen, *Cardiovasc Res* 72 (2006) 375-83.
135. A. Katsumi, T. Naoe, T. Matsushita, K. Kaibuchi and M.A. Schwartz, *J Biol Chem* 280 (2005) 16546-9.
136. T.P. Quinn, M. Schlueter, S.J. Soifer and J.A. Gutierrez, *Am J Physiol Lung Cell Mol Physiol* 282 (2002) L897-903.
137. H.T. Nguyen, R.M. Adam, S.H. Bride, J.M. Park, C.A. Peters and M.R. Freeman, *Am J Physiol Cell Physiol* 279 (2000) C1155-67.

138. R.M. Adam, J.A. Roth, H.L. Cheng, D.C. Rice, J. Khoury, S.B. Bauer, C.A. Peters and M.R. Freeman, *J Urol* 169 (2003) 2388-93.
139. C. Zhong, M.S. Kinch and K. Burridge, *Mol Biol Cell* 8 (1997) 2329-44.
140. D. Sarrio, S.M. Rodriguez-Pinilla, D. Hardisson, A. Cano, G. Moreno-Bueno and J. Palacios, *Cancer Res* 68 (2008) 989-97.
141. M. Lombaerts, T. van Wezel, K. Philippo, J.W. Dierssen, R.M. Zimmerman, J. Oosting, R. van Eijk, P.H. Eilers, B. van de Water, C.J. Cornelisse and A.M. Cleton-Jansen, *Br J Cancer* 94 (2006) 661-71.
142. P.A. Janmey and D.A. Weitz, *Trends Biochem Sci* 29 (2004) 364-70.
143. J.H. Wang and B.P. Thampatty, *Biomech Model Mechanobiol* 5 (2006) 1-16.
144. R. Paul, P. Heil, J.P. Spatz and U.S. Schwarz, *Biophys J* 94 (2008) 1470-82.
145. R.W. Tilghman and J.T. Parsons, *Semin Cancer Biol* 18 (2008) 45-52.
146. C. Hebnner, V.M. Weaver and J. Debnath, *Annu Rev Pathol* (2007).
147. O.W. Petersen, L. Ronnov-Jessen, A.R. Howlett and M.J. Bissell, *Proc Natl Acad Sci U S A* 89 (1992) 9064-8.
148. V.M. Weaver, A.R. Howlett, B. Langton-Webster, O.W. Petersen and M.J. Bissell, *Semin Cancer Biol* 6 (1995) 175-84.
149. J. Debnath, S.K. Muthuswamy and J.S. Brugge, *Methods* 30 (2003) 256-68.
150. T. Gudjonsson, L. Ronnov-Jessen, R. Villadsen, F. Rank, M.J. Bissell and O.W. Petersen, *J Cell Sci* 115 (2002) 39-50.
151. P.A. Kenny, G.Y. Lee, C.A. Myers, R.M. Neve, J.R. Semeiks, P.T. Spellman, K. Lorenz, E.H. Lee, M.H. Barcellos-Hoff, O.W. Petersen, J.W. Gray and M.J. Bissell, *J Cell Sci* 119 (2007) 84-96.
152. J.G.W. Aunins, D.I.C., *Biotechnology Progress* 6 (1990) 54-61.
153. R.J. Pelham, Jr. and Y. Wang, *Proc Natl Acad Sci U S A* 94 (1997) 13661-5.
154. R.H. Schmedlen, K.S. Masters and J.L. West, *Biomaterials* 23 (2002) 4325-32.
155. P.F. Davies, *Physiol Rev* 75 (1995) 519-60.
156. M.E. Wall, P.S. Weinhold, T. Siu, T.D. Brown and A.J. Banes, *J Biomech* 40 (2007) 173-81.
157. E.J. Vanderploeg, S.M. Imler, K.R. Brodtkin, A.J. Garcia and M.E. Levenston, *J Biomech* 37 (2004) 1941-52.
158. M.M. Panjabi, A.A. White, 3rd and J.W. Wolf, Jr., *Acta Orthop Scand* 50 (1979) 653-61.
159. Y. Gan, *Rev Sci Instrum* 78 (2007) 081101.
160. H. Huang, R.D. Kamm and R.T. Lee, *Am J Physiol Cell Physiol* 287 (2004) C1-11.
161. D. Choquet, D.P. Felsenfeld and M.P. Sheetz, *Cell* 88 (1997) 39-48.
162. R.M. Hochmuth, *Journal of Biomechanics* 33 (2000) 15-22.
163. H. Pommerenke, E. Schreiber, F. Durr, B. Nebe, C. Hahnel, W. Moller and J. Rychly, *Eur J Cell Biol* 70 (1996) 157-64.
164. R. Garcia, R. Magerle and R. Perez, *Nat Mater* 6 (2007) 405-11.
165. B. Sabass, M.L. Gardel, C.M. Waterman and U.S. Schwarz, *Biophys J* 94 (2008) 207-20.
166. S. Munevar, Y. Wang and M. Dembo, *Biophys J* 80 (2001) 1744-57.

Encyclopedia of Cancer
Springer-Verlag Berlin Heidelberg New York 2008
10.1007/978-3-540-47648-1_5727
Manfred Schwab

Tensional Homeostasis

Inkyung Kang² and Valerie M. Weaver²

(2) Department of Surgery, University of California, San Francisco, CA, USA

Without Abstract

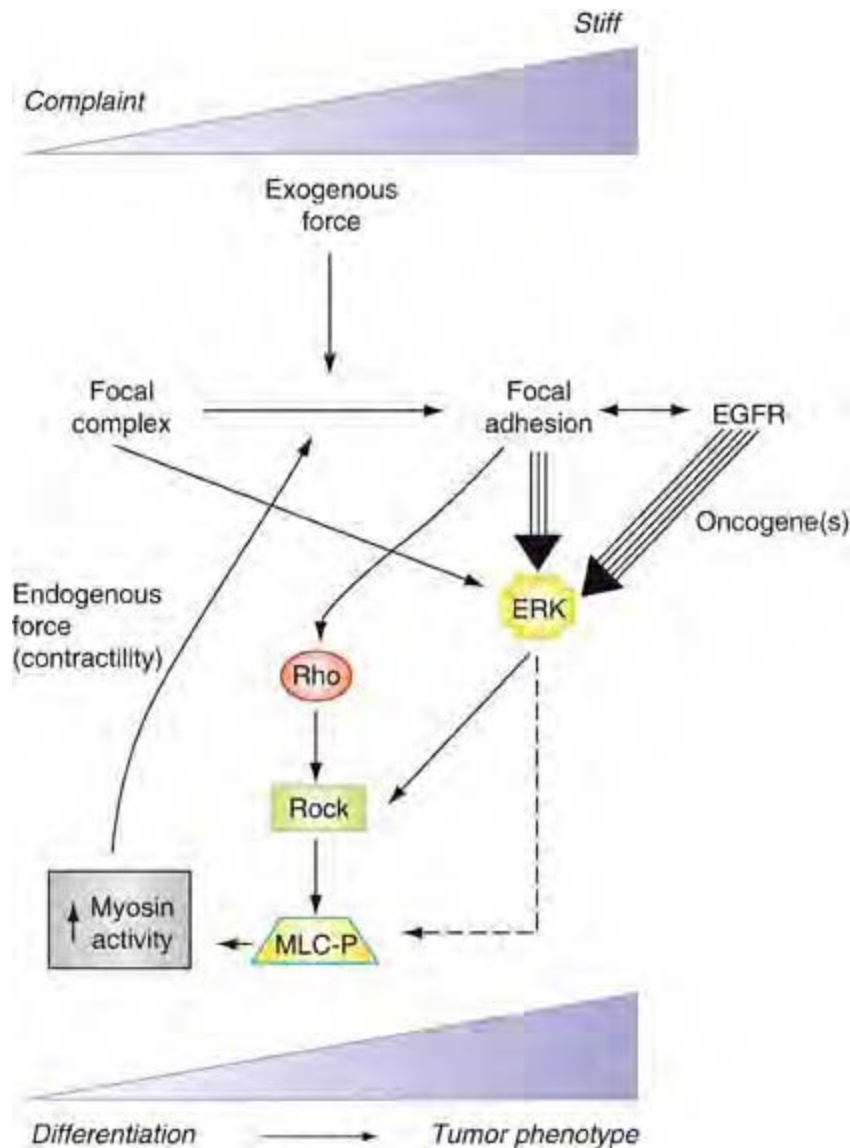
Definition

A mechano-regulatory network that integrates physical and biochemical cues from the tissue [microenvironment](#) through mechano—responsive elements such as transmembrane integrins to evoke cytoskeletal re-organization and actomyosin contractility, thereby altering signal transduction and gene expression to modulate cell and tissue phenotype.

Characteristics

Cells and tissues experience and respond to externally applied mechanical force through mechano-responsive elements that influence signal transduction and result in the generation of reciprocal intracellular force or contractility. The types of [mechanical stress](#) a cell can experience include compressive or tensile stress which is applied perpendicular to the surface of the cell, and shear stress which is applied parallel to the surface of the cell. For example, osteoblasts and chondrocytes within bone and cartilage are subjected to compressive force induced by walking, lung alveolar cells experience tensile load resulting from inhalation-induced alveolar sac expansion, and endothelial cells lining the lumens of blood vessels undergo shear force induced by circulating blood flow. Cells integrate external mechanical force on multiple levels. This includes force-dependent changes in the conformation of the plasma membrane lipid bilayers as well as modifications in the orientation and molecular associations of transmembrane proteins. These changes enhance the activity of calcium and potassium ion channels, the extracellular matrix affinity, and cytoskeletal plaque associations of various adhesion molecules including integrins ([Integrin Signaling and Cancer](#)). Cells also integrate external force cues to generate reciprocal actomyosin-mediated cell contractility and modulate their [mechanical properties](#) through remodeling of the microtubule, intermediate filament and actin cytoskeletal network. Intracellular mechanical force is transduced to the extracellular microenvironment via functional links between transmembrane receptors that bind to extracellular matrix (ECM) proteins and the

intracellular cytoskeletal network and ultimately mediate an equilibrium of extracellular and intracellular forces in the cell. This equilibrium or balance between the extracellular forces and the intracellular forces is called tensional homeostasis. When the extracellular mechanical microenvironment is becomes altered, cells and tissues will coordinately respond by adjusting cell-generated mechanical force or contractility, which in turn elicits changes in cell behavior by modifying the activity and function of signaling pathways and gene expression that determine growth, survival and differentiation. Cells sense and integrate tensional forces by altering the expression and activity of a plethora of putative [mechanosensors](#). Nevertheless, integrins are considered key mechanotransducers by virtue of their external associations with the extracellular matrix and their internal links to various adhesion plaque proteins including vinculin, talin and [focal adhesion kinase](#) (FAK), which in turn mediate interactions with the cytoskeleton and activate various signaling cascades. Extracellular mechanical force can alter the conformation of an integrin from a low ligand-binding affinity state to high ligand-binding affinity state, the conformation of extracellular matrix proteins such as [fibronectin](#) and collagen I to expose or alter ligand binding sites, and the conformation of vinculin and talin to favor intracellular molecular associations. These mechanically-initiated events promote actin assembly and stabilize adhesion plaque protein assembly and clustering of integrins to convert nascent [focal complexes](#) into mature [focal adhesions](#). Force-dependent integrin activation and focal adhesion maturation increase the magnitude and duration of adhesion signaling including ERK [MAP kinase](#) and RhoA GTPase ([Rho family proteins](#)). Elevated and sustained activity of ERK and RhoA GTPase drive actomyosin-mediated intracellular contractility by altering the function of Rho kinase (ROCK) and phosphorylated myosin light chain. The elevated intracellular tension in turn promotes focal adhesion maturation, creating a feedback loop of biochemical signaling pathways resulting in an elevated intracellular force generated by actomyosin cytoskeleton and inside out remodeling of extracellular matrix proteins (see Fig. 1).



Tensional Homeostasis. Figure 1 Key molecular pathways that mediate tensional homeostasis in cells and tissues. Changes in the mechanical environment of cell, such as an increase in ECM stiffness or elevated extracellular tension, promote integrin clustering to drive the maturation of nascent focal contacts into focal adhesions. The assembly of focal adhesions is associated with increased Rho GTPase activity and elevated and sustained ERK signaling. The combination of enhanced Rho and ERK activity increases actomyosin-mediated intracellular contractility by altering the function of Rho kinase (ROCK) and phosphorylated myosin light chain (MLC-P). Elevated cell-generated force promotes focal adhesion assembly and potentiates growth factor dependent ERK activation in a feed forward vicious cycle. Elevated intra cellular force also alters ECM deposition and organization by orienting and further stiffening ECM. Oncogenes which promote RAS-dependent ERK activation and Rho GTPase activity additionally contribute to cell-generated forces by regulating ROCK and MLCK and myosin II activity.

When the balance between the external and intracellular stress is altered, the cell and tissue will adapt to the new mechanical microenvironment challenge, which can result in positive outcomes such as an increase in bone and muscle density due to exercise, or in negative outcomes such as

atherosclerosis mediated by chronically elevated shear force applied by perturbed blood flow and cardiac hypertrophy due to hypertension. Mechanical compression can also regulate gene expression to influence tissue development as has been documented during embryogenesis. Changes in matrix stiffness determine the lineage commitment of mesenchymal stem cells, such that the cells express neurogenic markers when grown in mechanical environment closer to the stiffness of brain (0.1–1 kPa), myogenic markers at an intermediate stiffness (8–17 kPa), and osteogenic markers at a higher stiffness (25–40 kPa). This lineage commitment is regulated by nonmuscle myosin II and is accompanied by an increase in the size of focal adhesions and in the expression of focal adhesion components including talin and phosphoFAK. These results suggest that a cell dynamically probes its mechanical microenvironment through active engagement of integrin adhesion receptors and generation of actomyosin contractility, and that an increase in focal adhesion maturation and intracellular contractility drives downstream signaling events which determine lineage differentiation. Thus, tensional homeostasis is emerging as a critical determinant in cell fate during normal morphogenesis as well as pathophysiological processes.

Solid tumors are characteristically stiffer than normal tissue, which allows detecting tumors by palpation. The elevated stiffness is mediated by increased interstitial tissue pressure and changes in the mechanical properties of malignant cells and the surrounding stroma. The tumor stroma is characterized by an increased deposition and reorganization of matrix proteins including collagen, fibronectin and tenascin, and aberrant ECM cross linking induced by lysyl oxidase, transglutaminase, proteoglycans, and glycation, which contribute to the stiffening of the stroma ([Extracellular matrix remodeling](#)). In addition, transforming [oncogenes](#) such as [RAS](#), ErbB/[HER2 neu](#) and c-Myc ([Myc oncogene](#)) can alter the mechano-responsiveness of cells and cooperate with integrin adhesion signaling molecules to enhance cell proliferation, survival and invasion. Indeed, oncogenes such as Ras and ErbB/HER activate Rho and ERK that induce actomyosin contractility and elevate cell-generated forces to further promote the assembly and maturation of integrin adhesions and enhance growth factor receptor cross-talk. This raises the intriguing possibility that in addition to promoting cell growth and survival by directly modifying the activity of various signaling molecules, some transforming oncogenes might promote malignancy by altering the cells tensional homeostasis. Consistently, Paszek et al demonstrated that increasing ECM stiffness from 140 Pa (approximating the compliance of the normal murine breast) to 1,000–5,000 Pa (similar to the stiffness of a malignant murine breast) compromised mammary morphogenesis and induced the malignant phenotype of non-malignant mammary epithelial cells in culture, as demonstrated by an increase in cell growth and survival, and the loss of mammary tissue integrity (i.e. disruption of cell-cell junctions and loss of tissue polarity). Stiffening of ECM also significantly increased recruitment and activation of FAK and actin-binding proteins such as vinculin to $\beta 1$ integrin adhesion, which was accompanied by an increase of larger, mature focal adhesions, contractility, and enhanced growth-factor dependent ERK activation. More intriguingly, malignantly transformed mammary cells with elevated epidermal growth factor receptor (EGFR) signaling that form colonies of disorganized, invasive and continuously growing cancer cells in response to a compliant normal matrix also exerted higher cell contractility. Strikingly, inhibiting the activity of Rho GTPase or myosin II or ERK was sufficient to reduce the tumor cells contractility and revert the malignant phenotype of these breast cancer cells toward that of a normal breast acini. Likewise, inhibiting Rho or ERK-dependent myosin activity also normalized the phenotype of non-transformed mammary cells interacting with an abnormally stiffened matrix. Together these findings suggest that breast transformation could arise through the combination of oncogenic mutations that promote cell generated contractility and a progressive stiffening of the ECM which compromises the tensional

homeostasis to elevate cell contractility and to increase focal adhesion assembly, which enhance aberrant cell growth, survival and invasion.

Clinical studies indicate that mammographic density is strongly and reproducibly associated with an increased risk of breast cancer, independent of other risk factors ([Mammographic breast density and cancer risk](#)). For example breast cancer risk rises to 30% when greater than 50% of the mammography qualifies as dense. Although the high cancer risk linked with breast density could be attributed to decreased detection sensitivity and increased epithelial mass, recent data indicate that elevated collagen and proteoglycan content are also risk factors that contribute to the enhanced transformation frequency associated with this condition. Elevated mammographic density frequently precedes [ductal carcinoma in situ](#) (DCIS), and DCIS often occurs predominantly in the mammographically dense areas of the breast. Because higher collagen density and elevated proteoglycan-mediated cross linking correlate with an increase in ECM stiffness, these findings are consistent with the prediction that mammographic density could promote carcinogenesis by perturbing the cells tensional homeostasis. If true, an increase in matrix stiffening would herald an altered tissue tensional homeostasis and constitute a tractable predictor of future tissue transformation. Accordingly, an improved understanding of the parameters that promote matrix stiffening and alter tissue tensional homeostasis would assist in the development of improved detection, prognosis and treatment strategies for solid cancers.

To summarize, cells and tissues sense and respond to external force through a process called tensional homeostasis that reciprocally alters the external microenvironment through cell-generated force. Tensional homeostasis is emerging as an important determinant of normal tissue development and adult tissue homeostasis and recent studies indicate that an altered tensional homeostasis likely contributes to the pathogenesis of diseases including cancer and atherosclerosis.

References

1. Keller R, Davidson LA, Shook DR (2003) How we are shaped: the biomechanics of gastrulation. *Differentiation* 71(3):171–205
[PubMed](#)
2. Paszek MJ, Zahir N, Johnson KR et al. (2005) Tensional homeostasis and the malignant phenotype. *Cancer Cell* 8:241–254
[PubMed](#) [ChemPort](#)
3. Engler AJ, Sen S, Sweeney HL et al. (2006) Matrix elasticity directs stem cell lineage specification. *Cell* 126:677–689
[PubMed](#) [ChemPort](#)
4. Boyd NF, Rommens JM, Vogt K et al. (2005) Mammographic breast density as an intermediated phenotype for breast cancer. *Lancet Oncol* 6:798–808
[PubMed](#)

5. Yamaguchi H, Wyckoff J, Condeelis J (2005) Cell migration in tumors. *Curr Opin Cell Biol* 17:559–564

[PubMed](#)[ChemPort](#)

Three-dimensional context regulation of metastasis

Janine T. Erler · Valerie M. Weaver

Received: 5 April 2008 / Accepted: 1 September 2008 / Published online: 24 September 2008
© Springer Science+Business Media B.V. 2008

Abstract Tumor progression ensues within a three-dimensional microenvironment that consists of cellular and non-cellular components. The extracellular matrix (ECM) and hypoxia are two non-cellular components that potently influence metastasis. ECM remodeling and collagen cross-linking stiffen the tissue stroma to promote transformation, tumor growth, motility and invasion, enhance cancer cell survival, enable metastatic dissemination, and facilitate the establishment of tumor cells at distant sites. Matrix degradation can additionally promote malignant progression and metastasis. Tumor hypoxia is functionally linked to altered stromal-epithelial interactions. Hypoxia additionally induces the expression of pro-migratory, survival and invasion genes, and up-regulates expression of ECM components and modifying enzymes, to enhance tumor progression and metastasis. Synergistic interactions between matrix remodeling and tumor hypoxia influence common mechanisms that maximize tumor progression and cooperate to drive metastasis. Thus, clarifying the molecular pathways by which ECM remodeling and tumor hypoxia intersect to promote tumor progression should identify novel therapeutic targets.

Keywords Collagen cross-linking · Hypoxia · Matrix remodeling · Matrix stiffness · Metastasis · Tumor progression

Abbreviations

2D, 3D	2- and 3-dimensional
Pa	Pascals
ECM	Extracellular matrix
MMP	Matrix metalloproteinase
LOX	Lysyl oxidase
HIF	Hypoxia-inducible factor
CAF	Cancer-associated fibroblast
TAM	Tumor-associated macrophage
TGF	Tissue growth factor
BMDC	Bone marrow-derived cell
MEC	Mammary epithelial cell
HMEC	Human mammary epithelial cell

Introduction

Tissue context profoundly influences malignant transformation and tumor progression [1]. This concept was vividly demonstrated experimentally by Mintz and colleagues who showed that the normal mouse embryonic tissue microenvironment could repress expression of the tetracarcoma tumor phenotype [2, 3]. Bissell and colleagues then demonstrated that the normal chicken embryonic microenvironment could suppress transformation mediated by the Rous Sarcoma Virus (RSV) tumor oncogene, and that wounding promoted tumor progression [3]. Experimental data presented by multiple laboratories have since confirmed these seminal observations and demonstrated that the tissue stroma can either promote or restrict tumor progression [4–7]. More recently, the

J. T. Erler (✉)
Hypoxia and Metastasis Team, Section of Cell and Molecular Biology, The Institute of Cancer Research, 237 Fulham Road, London SW3 6JB, UK
e-mail: Janine.erler@icr.ac.uk

V. M. Weaver (✉)
Departments of Surgery, Anatomy, Bioengineering and Therapeutic Sciences, Center for Bioengineering and Tissue Regeneration and Institute for Regenerative Medicine, University of California San Francisco, 513 Parnassus Avenue, San Francisco, CA 94143-0456, USA
e-mail: WeaverV@surgery.ucsf.edu; valeriem.weaver@gmail.com

individual or combined activities of cellular components of the stroma have been shown to modulate various stages of tumor progression. These include, activated endothelial and lymphatic cells, altered fibroblasts, infiltrating immune cells, modified adipocytes and even stimulated mesenchymal stem cells [8–12]. Non-cellular aspects of the tumor microenvironment, such as hypoxia and an altered extracellular matrix (ECM), have additionally been shown to contribute to tumor progression either directly by destabilizing tissue integrity and promoting tumor cell motility, invasion and survival, or indirectly by inducing tumor angiogenesis and enhancing tumor cell survival and selection [4, 13, 14]. Here, we focus on the mammary gland and discuss the critical role of non-cellular microenvironmental factors in normal tissue homeostasis, and in tumor evolution and metastasis. We outline how a synergistic interaction between ECM remodeling and hypoxia, two non-cellular components of the tissue microenvironment, can cooperatively drive tumor metastasis by influencing common molecular targets that may therefore constitute tractable drug targets.

The importance of non-cellular components of the tissue microenvironment on tissue homeostasis

ECM structure determines tissue context

Normal organ and tissue function is determined by the reciprocal communication between cells and their surrounding stroma [15]. The non-cellular component of the stroma includes soluble factors, such as growth factors and cytokines, and an insoluble protein network to which these soluble factors can bind called the extracellular matrix (ECM) [16]. The ECM is a three-dimensional (3D) structure surrounding cells [17]. There are two major categories of ECM. The first type is the basement membrane (BM), which interacts directly with the epithelium and endothelium, and consists primarily of collagen IV, laminins, entactin/nidogen and heparan sulfate proteoglycans [18–20]. The second type is the interstitial matrix, which makes up the bulk of the ECM in the body. The interstitial matrix consists of many collagens including type I and III, which together with fibronectin contribute to the mechanical strength of the tissue [21]. The interstitial matrix additionally consists of tenascin and proteoglycans that provide tissue hydration, growth factor and cytokine binding functions, and cross-link the matrix to enhance its integrity [22]. Although originally thought of as merely a support system for the cells within the tissue, the ECM is now recognized as a central regulator of cell and tissue behavior by providing contextual information for cells to respond to stimuli [23–25]. Indeed, while the basic characteristics and composition

of the basement membrane and interstitial matrix are constant across tissues, variations in ECM component and isoform expression [26], and post-translational modifications, contribute to differences in ECM organization and structure and ensure tissue specificity [22, 27].

ECM topology reflects the organization, orientation and post-translational modifications of the matrix. These parameters determine the mechanical properties of the ECM and modulate cell and tissue phenotype by influencing cytoskeletal remodeling and receptor signaling to influence cell behavior [18, 28]. The architecture of the tissue ECM is influenced by its topology and its biochemical composition [29–32]. Matrix concentration and post-translational modifications, such as glycosylation and cross-linking, significantly affect the mechanical properties of the ECM, including its visco-elasticity or stiffness (which can be measured in Pascals; Pa) [28]. Both the stiffness and topology of the ECM regulate the growth, remodeling, differentiation, migration and phenotype of a wide variety of cell and tissue types [14, 33]. Consistently, mechanical force mediated at the cellular and tissue level specifies tissue organization and cell migration during early embryogenesis, and modulates tissue function and homeostasis in the adult organism [29, 30]. Much of the force mediating these behaviors is functionally linked to ECM architecture and cell-generated actomyosin-dependent contractility [29, 30]. Although it is not clear how ECM topology and stiffness regulate cell fate, it is fast becoming clear that these matrix parameters are likely as important as its biochemical composition, and can profoundly affect cell behavior and influence gene expression to regulate processes as disparate as stem cell differentiation and tumor phenotype [24, 33–39].

Matrix stiffness regulates cell phenotype and function

The importance of matrix stiffness in tissue-specific differentiation is exemplified by the fact that cells grown as monolayers (two dimensional; 2D) on top of either a plastic substrate or a glass cover slip, either with or without ECM ligand, fail to assemble tissue-like structures (3D) and do not express differentiated proteins upon stimulation [14, 28]. These phenotypic disparities can be explained, in part, by the fact that the consistency of living tissues is dramatically softer than conventional 2D substrata such as tissue culture plastic (polystyrene) or borosilicate glass. Specifically, soft tissues such as the breast, liver and lung range between 150 and 3,000 Pa, whereas plastic has a stiffness approaching the GPa range, which is infinitely stiff, and borosilicate glass, is, by comparison 1–2 GPa [14, 28]. Consistently, if epithelial cells and melanocytes are grown in the context of a 3D compliant ECM microenvironment (150–400 Pa) they assemble into tissue-like structures and express differentiated proteins when given the correct

soluble stimuli [9, 40, 41]. The architecture of the interstitial tissue matrix *in vivo* also differs substantially from that found typically in tissue culture plastic experiments, and this too can have dramatic effects on cell behavior [42]. For instance, epithelial cells in a tissue either interact with “other” cells and basally contact a BM (which itself has a complex 3D topology), and tissue fibroblasts are surrounded by interstitial collagen fibrils that can be heavily glycosylated and cross-linked with diameters that range from 0.1 microns upwards to 10 microns. Furthermore, the orientation of these collagen fibers can critically regulate cell and tissue behavior [30, 36]. This 3D contextual information is lost when cells are grown in 2D.

Changes in matrix stiffness and ECM remodeling play a crucial role in embryonic mammary gland development, influence branching mammary gland morphogenesis, and facilitate lactation (functional differentiation) and involution (apoptosis), to orchestrate normal mammary gland homeostasis [18]. Substrate compliancy independently regulates mammary epithelial cell (MEC) shape, mammary tissue morphogenesis, and endogenous BM assembly [14]. For example, functional and morphological differentiation of primary MECs in response to lactogenic hormones can proceed only when mixed mammary cell populations isolated from pre-lactating mice are plated on floating (compliant) collagen gels and permitted to assemble an endogenous BM [28, 43, 44]. Consistently, MEC acini morphogenesis and functional differentiation is not supported by mechanically loaded or cross-linked (stiff) collagen gels because they are too rigid to allow cell rounding and endogenous BM assembly [28].

The ECM stiffness can regulate cell and tissue behavior by initiating biochemical signaling cascades in cells through interactions with a number of specialized transmembrane ECM receptors including integrins, Discoid Domain Receptors (DDR) and syndecans [45–49]. These are mechanosensors critical for mediating outside-in cell signaling to regulate cell behavior. Integrins are perhaps the best characterized ECM receptors that are important for adhesion interactions. They are an excellent model with which to understand how an altered ECM could promote tumor progression. Integrins consist of 24 distinct transmembrane heterodimers that relay cues from the surrounding ECM to regulate cell growth, survival, motility, invasion and differentiation [48]. By virtue of their ability to interact with the ECM externally, and with cytoplasmic adhesion plaque proteins and the cytoskeleton intracellularly, integrins are able to transmit dynamic cues from the tissue microenvironment to influence cell behavior. Integrin-ECM interactions regulate cell fate by activating multiple biochemical signaling circuits and altering cell and nuclear shape [50–52]. This occurs either through direct interactions between ECM receptors and

actin linker proteins or cytoskeletal reorganization induced by activating cytoskeletal remodeling enzymes, such as RhoGTPases [50–52].

Hypoxia regulates normal tissue homeostasis

Hypoxia (low oxygen) is another important non-cellular component of the physiological tissue microenvironment. Similar to ECM stiffness, hypoxia, potently influences cell phenotype, genotype, differentiation and fate [53–58]. Hypoxia itself is a potent regulator of ECM composition, topology and stiffness. Hypoxia-mediated gene expression, signaling and matrix remodeling are critical for embryonic development and wound healing [57–59]. For example, hypoxia regulates the cellular events that occur during the first trimester of pregnancy when fetal trophoblast cells invade the maternal uterine spiral arteries leading to loss of the vascular cells from the vessel wall and remodeling of the ECM [60]. Hypoxic regulation of invasion and ECM remodeling is critical for placental development to ensure that sufficient blood can reach the developing fetus. Furthermore, hypoxia regulates lung branching morphogenesis during embryonic development [61], and oxygen deprivation can stimulate mammary epithelial cell branching morphogenesis *in vitro* through increased HGF expression [62].

Hypoxic conditions stimulate blood cell proliferation and blood vessel formation, and modulate expression of ECM components and remodeling enzymes thereby maintaining tissue homeostasis. Hypoxia-driven changes in gene expression are mediated primarily by hypoxia-inducible factor (HIF)-1 [63]. For example, hypoxia increases ECM accumulation in mesenchymal cells in a HIF-1 dependent fashion, which is required for chondrogenesis and joint development during fetal growth [64]. Moreover, HIF-1 deficient trophoblast stem cells exhibit reduced adhesion and migration toward vitronectin compared with wild-type cells [65], and the defective trophoblast invasion observed in the absence of HIF-1 was associated with decreased cell surface localization of integrin $\alpha v \beta 3$ and reduced levels of focal adhesions containing $\alpha v \beta 3$ integrin [65]. Thus, hypoxia stimulates cell adhesion and migration, as well as angiogenesis and ECM remodeling, and can cooperate with ECM stiffness to synergistically influence cell behavior.

The importance of non-cellular components of the tissue microenvironment on tumor evolution

ECM structural changes during tumorigenesis

Transformation can be regulated by the microenvironment, as was clearly demonstrated by early experiments

exploring the role of RSV in tumor behavior [3]. These and other studies emphasize that tumors are organs whose formation is governed by 3D tissue context [4–7]. Epithelial cancers, such as breast cancer, can be caused by somatic gene mutations but are additionally influenced by sustained alterations of the microenvironment including those associated with ECM remodeling. In fact, the composition of the ECM varies during the development of pathologies such as cancer, and the aberrant expression and organization of matrix components produced by stromal cells in response to stress can direct the malignant behavior of epithelial cells [8, 16, 66].

Many ECM components and remodeling enzymes are elevated in cancer patients [13, 18, 67–69]. In the normal breast tissue, tightly controlled MMPs remodel the breast ECM to promote mammary gland growth and involution. In tumors, however, this stringent control of MMP expression and activity is lost [70]. Overexpression of MMPs 3, 11, 12 and 13 have been demonstrated in the tumor stroma, along with MMP-2 in transformed mammary epithelial cells [71]. Polymorphisms in the promoter region of MMP-3 resulting in elevated expression are associated with increased tumor incidence in patients [72]. Moreover, ectopic expression of MMP-3 within the MECs of transgenic mice induced desmoplasia, precocious branching morphogenesis and malignant transformation of the tissue [73]. Thus, aberrant MMP activity is not merely symptomatic of transformed tissue but additionally plays a causative role. Fibrillar collagens (types I, II, III, V and IX [21]) normally have a low turnover but their metabolism is increased during the ECM remodeling that characterizes tumor evolution [16]. Type I collagen synthesis and remodeling is required for growth factor-induced angiogenesis, endothelial cell invasion and vessel formation, which are necessary to maintain tumor growth [74]. Indeed, the synthesis, concentration and circulating levels (serum concentration) of degradation products of type I collagen are increased during breast, lung, ovarian, prostate and skin malignancy [68, 69, 75–77].

The architecture of tumor-associated ECM is fundamentally different from that of the normal tissue stroma [78]. In particular, whereas type I collagen is in a parallel orientation with respect to the epithelial cells, it is less organized in the stroma surrounding a transformed tissue [79]. While one may expect increased ECM synthesis to encapsulate and limit tumor progression, ECM deposition can in fact enable tumor cell invasion by providing critical biochemical cues that promote chemotaxis or that enhance cell migration by stiffening the matrix [14, 28] as has been observed along type I collagen fibers in invading breast tumors using intravital imaging [80]. Furthermore, elevated ECM deposition and remodeling can directly increase interstitial pressure and impede fluid drainage, as illustrated by the curved matrix sheets formed in melanomas, and

these forces can severely compromise the efficacy of drug delivery [16, 78, 81–84].

Matrix stiffness drives transformation

Matrix stiffening is induced by increased collagen deposition and ECM cross-linking, and can promote malignant transformation by enhancing growth factor signaling and destabilizing tissue integrity [14, 28]. For example, human mammary epithelial cells (HMECs) grown on a highly rigid matrix develop a malignant morphology that is characterized by destabilized E-cadherin adherens junctions, absence of tissue polarity and an invasive behavior (Fig. 1) [14]. Increased matrix stiffness has been observed in fibrotic lungs, in scar tissue, in tissue exposed to high doses of radiation, in aged skin and in women with dense breasts; all conditions that predispose these individuals and tissues to a higher cancer risk. Consistently, tumors are characteristically stiffer than their normal adjacent tissue, and while increased cell mass undoubtedly contributes to the increase in tissue force in tumors, altered stiffness is often detected as a global increase in the physical properties of the transformed tissue [85, 86].

Indeed, over the years imaging methods such as ultrasound sono elastography and MR imaging elastography have been exploited to monitor tissues for evidence of transformation based upon differential stiffness profiles of not only the tumor itself, but also of the surrounding non-transformed tissue [86]. These findings suggest that the stiffening associated with tumor progression is linked to changes in the ECM structure that track with the tumor phenotype. These include elevated levels of collagen, linearization of the collagen fibrils, higher amounts of matrix cross-linking enzymes, and enhanced expression of proteoglycans implicated in matrix cross-linking including lumican and biglycan [87]. Tumor stiffness has additionally been attributed to the elevated interstitial pressure due to leaky blood vessels and lymphatics [88].

Mechanical interactions between cancer cells and ECM can accelerate neoplastic transformation [14, 89, 90]. For instance, normal tissues can be induced to become cancerous *in vivo* by altering ECM structure [73]. The idea that structural or mechanical changes in the microenvironment actively contribute to tumor formation is not a novel concept. Early experiments demonstrated that implantation of a rigid piece of material (metal or plastic) can trigger cancer formation whereas introduction of the same material as a powder did not induce tumor formation in animals [91]. Conversely, there are many studies in experimental systems to suggest that cancers can be induced to become quiescent, differentiate, die or form normal tissues, if provided with the correct set of 3D signals conveyed by the microenvironment [90]. Decades of

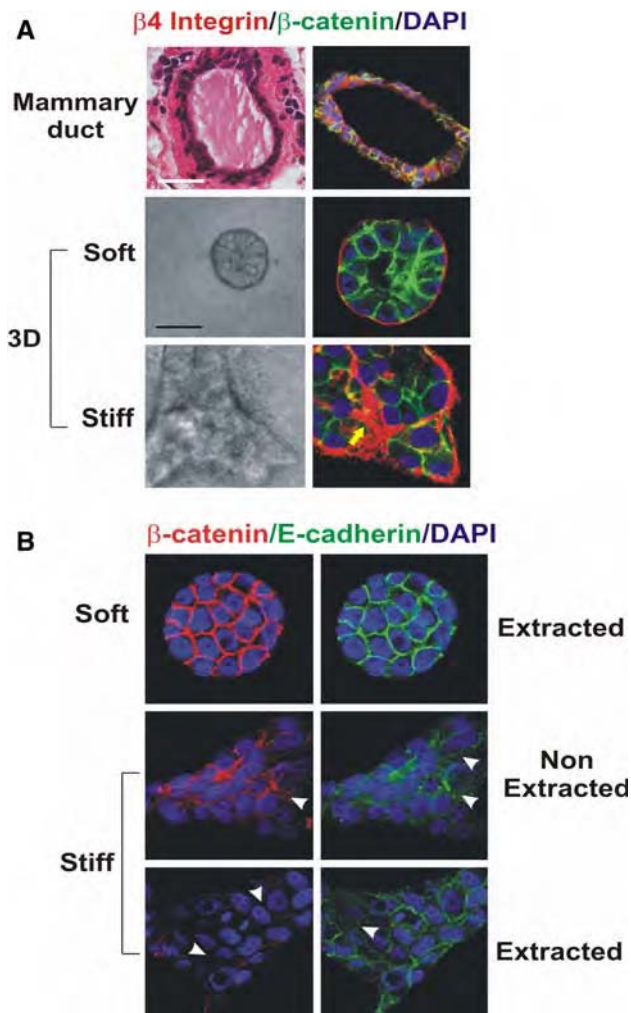


Fig. 1 Mammary epithelial growth and morphogenesis is regulated by matrix stiffness. **(a)** 3D cultures of normal mammary epithelial cells (MECs) within collagen gels of different concentration. Stiffening the ECM through an incremental increase in collagen concentration (soft gels: 1 mg/ml Collagen I, 140 Pa; stiff gels 3.6 mg/ml Collagen I, 1,200 Pa) results in the progressive perturbation of morphogenesis, and the increased growth and modulated survival of MECs. Altered mammary acini morphology is illustrated by the destabilization of cell–cell adherens junctions and disruption of basal tissue polarity indicated by the gradual loss of cell–cell localized β -catenin (green) and disorganized $\beta 4$ integrin (red) visualized through immunofluorescence and confocal imaging. **(b)** Confocal immunofluorescence images of MEC colonies on soft and stiff gels (140 vs. >5,000 Pa) stained for β -catenin (red) and E-cadherin (green), and counterstained with DAPI (blue) after triton X-100 extraction. β -catenin could be extracted from the sites of cell–cell interaction in MEC colonies formed on a stiff but not on a soft gel, indicating that adherens junctions are less stable in MEC structures formed on stiff gels. White arrows indicate diffuse staining patterns of β -catenin and E-cadherin (Modified from Kass et al. [18])

research has shown that combining epithelial tumor cells with normal mesenchyme (stroma), embryonic tissues, or with ECMs that are deposited as a result of these interactions, reverts their cancerous phenotype and restores their

normal tumor morphology [90, 92–96]. For example, stroma from healthy animals can prevent neoplastic transformation of grafted epithelial cancer cells and encourage their normal growth [93, 94]. The growth and differentiation of mammary epithelial tumors can be reverted to normal by modulating cell adhesion to the ECM [4]. These studies suggest that it may be possible to prevent tumor progression by “normalizing” the ECM microenvironment [90, 94].

Hypoxia drives pro-tumor ECM remodeling

Hypoxia is present in all solid tumors over 1 cm^3 , and is clinically associated with metastasis and poor patient outcome [54, 57]. Transformation of cells may also be driven by hypoxia, which induces oncogene expression, enhances DNA mutation rate, and selects for cells with increased apoptotic thresholds [54, 97–99]. In addition hypoxia can drive tumor evolution through increased matrix deposition, cross-linking and remodeling. Hypoxia increases collagen biosynthesis [100, 101], collagen fibril deposition [102, 103], and collagen remodeling [103], and processing [104]. For example, hypoxia up-regulates the P4H $\alpha 1$ subunit of collagen prolyl 4-hydroxylase (P4H) which is the rate-limiting subunit for the hydroxylation of proline residues of procollagens [104]. The formation of hydroxyproline is an essential post-transcriptional process for stabilization of the helical trimer of procollagen polypeptides. Prolonged hypoxic incubation of fetal rat lung fibroblasts enhanced this post-transcriptional step of collagen synthesis and accelerated the deposition of collagen molecules and fibrils [102]. In addition, cytoplasmic P4Hs play a critical role in the regulation of the HIF α [105].

In addition, hypoxia increases expression of matrix remodeling enzymes, including MMPs [106]. Micro-array analysis revealed that expression of a secreted protein, lysyl oxidase (LOX), was consistently over-expressed by hypoxic human tumor cells [107]. LOX initiates the covalent cross-linking of collagens and elastins, thereby increasing insoluble matrix deposition and tensile strength [108]. LOX expression is induced by hypoxia-inducible factor (HIF)-1 and is associated with experimental hypoxia in vitro and in vivo, and clinically in breast and head and neck cancer patients [13]. LOX is synthesized in fibrogenic cells as a pre-pro-enzyme that is cleaved and glycosylated prior to its secretion [108]. After secretion, the LOX pro-enzyme is proteolytically processed by procollagen C-proteinase (bone morphogenic protein-1) which releases the 32-kDa biologically active mature form of the protein. Procollagen C-proteinase (bone morphogenic protein-1) is also hypoxia-induced [107], and cleaves pro-collagens thereby permitting processing and collagen fibril assembly, in addition to activating LOX.

LOX mediates stiffness-induced transformation

The importance of collagen remodeling, cross-linking and stiffening to tumor progression was emphasized by our recent unpublished work in which we primed the mammary stroma of nude mice with fibroblasts expressing a constitutively active LOX (Levental et al., unpublished). In these studies, LOX-dependent collagen cross-linking of the mammary fat pad promoted the linearization of the interstitial collagens, stiffened the gland and induced the neoplastic progression of Ha-Ras pre-malignant HMECs. Consistently, we found that the elastic modulus (indenter) and the storage modulus (shear) (i.e. stiffness) of the mammary tissue in MMTV-Her2/neu transgenic mice increased incrementally, coincident with and prior to the establishment of large, invasive tumors. Although the tissue stiffening could be attributed in part to an increase in cell mass, we noted that both the tumor and the surrounding stroma were significantly stiffer than normal tissue [14]. Moreover, second generation harmonics imaging as well as polarized light scanning of picosirius-stained tissues revealed that tissue stiffening correlated with collagen linearization. Importantly, we found that collagen linearization was associated with elevated levels of the collagen cross-linker LOX, which we could detect in the stroma prior to tumor formation. Matrix stiffening and cross-linking were additionally associated with enhanced mechano-responsiveness of the epithelium, as evidenced by elevated activated focal adhesion kinase, and p130 Cas. Intriguingly, inhibiting LOX-dependent collagen cross-linking in Her2/neu mice, tempered collagen linearization, reduced gland stiffening and enhanced the latency and decreased the incidence of breast transformation. These data imply that altering the cell's mechano homeostasis could promote the malignant behavior of an epithelium in culture and promote transformation in vivo, and that inhibiting matrix stiffening could temper reducing matrix stiffness can diminish breast transformation in vivo.

Metastasis driven by non-cellular components of the tumor microenvironment

3D context dictates malignant progression

Deregulated growth is not sufficient to make a tissue cancerous. What makes a growing cancer malignant is its ability to break down tissue architecture, invade through disrupted boundaries, and metastasize to distant organs. Malignant progression is completely dependent upon the 3D context of the tissue microenvironment. In fact, the multistep process of metastasis can only be successful if the 3D microenvironment is permissive for tumor cell

invasion, metastatic dissemination and metastatic growth. Non-cellular components of the tumor microenvironment, such as the ECM and hypoxia, critically drive tumor progression through increased ECM deposition, cross-linking and remodeling. This ECM remodeling creates a micro-environmental context that enhances tumor cell survival, migration, growth, tumor angiogenesis and lymph angiogenesis [67, 109, 110]. Indeed, hypoxia and matrix remodeling that lead to a progressive stiffening of the ECM are associated with tumor progression, and many ECM components and remodeling enzymes are associated with metastasis in cancer patients [13, 18, 67–69].

The 3D organization and architecture of the ECM and stroma are dynamic [16, 18]. Ultrastructural studies, immunohistochemistry, and biochemical analysis have demonstrated changes in stroma, ECM composition and architecture occur at critical steps during malignant progression [109, 111]. The dramatic changes in the organization and composition of the ECM during tumor progression alter tumor behavior and contribute to tumor metastasis. For instance, the mammary gland matrix stiffens progressively during tumor progression and this mechanical alteration is associated with increased collagen, fibronectin and tenascin deposition, and elevated collagen cross-linking and linearization [14]. Matrix stiffness in association with growth factors, enhances cell survival and increases cell contractility [14]. Matrix stiffness and/or exogenous force independently induce cell-generated contractility to promote focal adhesion maturation and enhance integrin-dependent signaling, thus compromising multi-cellular tissue morphogenesis and promoting a tumor-like behavior in mammary cells [14]. This suggests that matrix stiffness likely promotes breast tumorigenesis through altering integrins and their adhesion interactions. Conversely, blocking integrin or growth factor-dependent cell contractility can revert the malignant phenotype in culture [40]. Consistent with these findings, ectopic expression of $\beta 1$ integrin mutants with increased transmembrane molecular associations (V737 N, G744 N), elevated cellular contractility and forced focal adhesion maturation increase integrin/growth factor-dependent signaling, again to compromise multi-cellular tissue morphogenesis and promote tumorigenic behavior in culture and in vivo [14].

ECM structural changes disrupt cell–cell relations

Deregulated cell growth and loss of cell–cell relations correlate with compromised structural integrity of the basement membrane (BM) [92]. Tumor cell growth can be suppressed and cells can be induced to re-form polarized epithelium when they come into contact with intact BM in vivo or are cultured on intact BM in vitro [92, 95, 96, 112]. Structural alterations in the BM occur early on in cancer,

even before the development of a palpable tumor [113]. These include gaps, thickening, loosening of cells from each other and the surrounding stroma [90], and can be considered a hallmark of malignant invasion because tumors surrounded by an intact BM generally do not penetrate into surrounding tissues [114–116].

Loss of cell–cell contact occurs during epithelial-to-mesenchyme transition (EMT), and is a key step in malignant progression of many epithelial cancer cells [117]. EMT often occurs as a consequence of transcriptional repression of E-cadherin mediated by transcription factors such as TWIST, Snail and Slug [117]. Hypoxia drives EMT through hypoxia-inducible factor (HIF) [118], uPAR [119] and TWIST [120]. TWIST expression is increased by mechanical force [121], and EMT can be induced by TGF- β released as a result of hydrostatic compression [122–126]. Intriguingly, murine MECs expressing oncogenic Ras expressed higher levels and secreted more ILEI, a novel interleukin-related protein, following EMT induction by TGF- β [127]. ILEI knock-down normalized the morphology and gene expression of the MECs and prevented the transformation and metastasis of normal epithelial cells [127]. Importantly, EMT induces cytoskeletal reorganization and alters cell adhesion to increase tensional force illustrating how an exogenous mechanical force can modulate cellular tension through a positive feed-forward mechanism [32, 128].

Transformed MECs often exert greater cell-generated force in response to physical interactions with the ECM [14]. These cellular forces are mediated through actomyosin contractility and cytoskeletal remodeling that are induced by ERK and Rho GTPase signaling. Matrix stiffening can establish a mechanical autocrine loop in which Rho GTPases are activated by the transmission of force through transmembrane integrin receptor interactions with the ECM and that can be suppressed by tension dissipation in the cytoskeleton [28, 90]. Mechanotransduction modulates cell behavior by altering the function and activity of multiple signaling pathways including those regulated by ERK, MAPK, calcium, SRC, and G-coupled receptor proteins [28, 90]. Force can significantly enhance growth factor signaling and even modify the requirement of cytokine binding for receptor activation [28, 90, 129]. ECM rigidity enhances cell contractibility largely by activating RhoGTPases, and by so doing drives cell spreading and growth, promotes ECM fibril alignment and can further increase ECM stiffness and induce matrix tension by facilitating cell pulling through ECM adhesions [14]. Furthermore, Rho can alter cell and tissue tension by promoting EMT [130]. Finally, tensional stress can facilitate cell invasion by elevating MMP-9 release and activation [131].

ECM remodeling and hypoxia enable invasion, metastatic growth and dissemination

The acquisition of the metastatic phenotype is not simply the result of deregulated signal transduction pathways, but instead is achieved through a stepwise selection process driven by microenvironmental pressures including hypoxia and ECM remodeling. For example, invasion into surrounding tissue requires destruction of the BM and remodeling of the ECM. This is governed by microenvironmental cues that determine ECM degradation and synthesis. Hypoxia can disrupt tissue integrity and enhance cell motility and invasion directly by repressing E-cadherin and enhancing N-cadherin expression and hepatocyte growth factor (HGF)-MET receptor signaling [132]. Hypoxia can disrupt tissue integrity indirectly by promoting cell-ECM interactions through enhancement of $\alpha v \beta 3$ integrin membrane localization [65], or by fostering ECM remodeling through up-regulation of uPAR and uPAR-dependent MMP activation [132]. In addition, hypoxia can induce ECM stiffening through elevated expression of LOX and LOX-dependent collagen cross-linking [13]. In addition, hypoxia indirectly enhances tumor dissemination by directly regulating the expression and activity of hypoxia-induced vascular endothelial growth factor (VEGF) to promote angiogenesis and lymphangiogenesis, and increase vascular permeability to promote both intravasation at the primary tumor site and extravasation at the distant metastatic site [132].

Disordered ECM architecture is a characteristic of the tumor invasive front where increased matrix deposition and remodeling is observed [133, 134]. Hypoxia enhances the proteolytic activity at the invasive tumor front and alters interactions between integrins and components of the ECM, enabling tumor cell invasion [132]. Invasive branching of breast cancer cells growing in 3D matrix is observed in oxygen-deprived conditions due to hypoxia-induced HGF expression [62]. Furthermore, hypoxia-induced LOX is needed for invasive branching of oxygen-deprived human cancer cells in 3D matrix and its expression is elevated at the leading edge of invading cells [13]. LOX expression is not only associated with hypoxia but is also associated with metastasis and decreased survival in human cancer patients [13]. Inhibition of LOX expression or activity was found to prevent *in vitro* invasion and *in vivo* metastasis in an orthotopic model of breast cancer [13]. LOX activity outside of the cell resulted in matrix remodeling and activation of focal adhesion kinase (FAK) enabling cell motility. LOX inhibition resulted in decreased cell–matrix adhesion interactions critical for invasive migration and metastatic dissemination. A dependence on LOX expression for metastatic growth was additionally observed and may be explained by LOX's role in the formation and maintenance

of the metastatic niche (see below). LOX-induced matrix cross-linking can activate MMPs (Erler/Bennewith et al., unpublished). Increased MMP activity results in both matrix remodeling and release of chemokines, cytokines and growth factors trapped within the ECM [16]. Taken together, these studies demonstrate that hypoxia can enhance ECM remodeling thereby enabling tumor cell invasion.

Angiogenesis is required for metastatic dissemination and to sustain metastatic growth. Mechanical interactions between capillary cells and ECM control capillary cell growth and angiogenesis through Rho signaling [135]. Angiogenesis is also potently induced by hypoxia through increased expression of vascular endothelial growth factor, erythropoietin, and other pro-angiogenic factors [54]. Under physiological non-hypoxic conditions, angiogenesis can be driven by mechanical forces. For example, capillary endothelial cells subjected to mechanical stretch demonstrate elevated MMP-2 and HIF-1 α expression, and MMP-2 activity [136]. These findings additionally suggest that ECM remodeling can increase hypoxic responses, a phenomenon supported by the presence of hypoxia as a result of increased ECM remodeling and fibrosis during wound-healing [58]. Hypoxia in turn increases the expression and activity of genes involved in fibrosis and ECM remodeling, resulting in a feed-forward mechanism that increases matrix stiffness and drives tumor progression (Fig. 2). This synergistic relationship is further exemplified by the fact that tumor-associated compression stress can induce tumor angiogenesis by directly increasing expression of VEGF or indirectly by blocking the vasculature surrounding the tumor mass to promote hypoxia and VEGF secretion [137].

The importance of cellular components of the tissue microenvironment on tumor progression

Metastatic progression depends on stromal cell involvement

The non-tumor cellular component of the microenvironment consists of activated and/or recruited host cells such as fibroblasts and immune cells [8, 138]. It is the reciprocal interactions between these host cells, the tumor cells and the ECM that drive tumor progression including metastatic dissemination [16, 109]. Altering stromal cells alone can induce cancer [5], and mutations in stromal cells contribute to the formation of epithelial tumors [139]. Thus, persistence of abnormal signals from the stroma can create an interdependent cancerous tissue [16]. In addition, solid tumor growth cannot be sustained unless the tumor resets the balance between ECM remodeling/degradation and ECM synthesis, and growth cannot be maintained without sufficient blood supply [79]. To do this, the tumor must recruit stromal cells (fibroblasts, inflammatory cells and vascular cells) to increase ECM deposition, MMP-mediated matrix degradation, and increase angiogenesis [16]. Stromal cells therefore play a critical role in tumor evolution and metastasis [140].

Alterations in matrix compliance, such as changes in stiffness, influence MEC malignant behavior directly through mechanotransduction pathways (described above) or indirectly by activating resident fibroblasts to release cytokines, growth factors and ECM degrading enzymes [28, 141–143]. Fibroblasts are the predominant cell

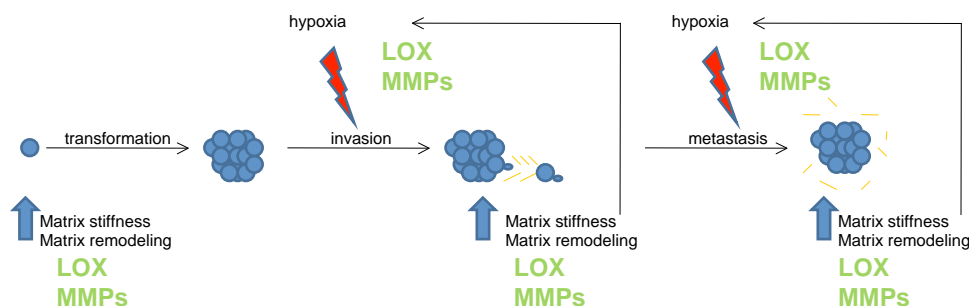


Fig. 2 Schematic to demonstrate the interplay between hypoxia and matrix remodeling, using lysyl oxidase (LOX) as an example. LOX expression is increased in pre-malignant tissue, where it cross-links collagens in the ECM increasing matrix stiffness and enabling ECM remodeling. This allows for malignant transformation and primary tumor growth. As the tumor grows larger, regions become subjected to hypoxic conditions. In response to hypoxia, tumor cells increase expression of proteins involved in collagen biosynthesis and processing, including LOX. This results in increased matrix deposition, collagen cross-linking, matrix remodeling and matrix stiffness, which in turn encourage a hypoxic environment. LOX secreted by hypoxic tumor cells is additionally involved in the formation of a pre-metastatic niche at distant sites of future metastasis. Increased

collagen cross-linking and matrix remodeling attract bone marrow-derived cells to the site, which create a niche permissive for metastatic tumor cell attachment and growth. Again, subsequent matrix remodeling and increased stiffness at these metastatic sites would enhance hypoxia, which in turn elevates expression of proteins involved in collagen biosynthesis and processing, further increasing matrix remodeling and matrix stiffness. This feed forward mechanism is further enhanced by matrix metalloproteinase (MMP) activity. MMP expression and activity is elevated by both increased matrix stiffness and by hypoxia. Thus, the symbiotic interaction between ECM remodeling and hypoxia, two non-cellular components of the tissue microenvironment, can cooperatively drive tumor metastasis by influencing common targets

population in the stroma, and are the largest producers of ECM components (collagen I and fibronectin, in particular) [110]. Each organ has their own specific set of fibroblasts that regulate normal tissue homeostasis [144]. Fibroblasts associated with the tumor stroma are myofibroblasts, peritumor fibroblasts, and cancer associated fibroblasts (CAFs) [16]. CAFs can stimulate oncogenic signaling and malignancy in non-tumorigenic epithelial cells [145]. In addition, CAFs produce abundant quantities of collagen changing the biochemistry and structure of the ECM, which can encourage tumor development and progression [146, 147]. One of hallmarks of fibroblasts is that they are surrounded by dense accumulations of fibrillar collagen [110, 148]. This desmoplastic response is frequently seen cancers such as breast, pancreatic, prostate, colon and lung, and is associated with the recruitment of inflammatory cells and with the induction of angiogenesis [16]. Furthermore, hypoxia is associated with desmoplasia and poor prognosis in breast cancer patients [149].

Stromal cells mediate pro-metastatic ECM remodeling

Fibroblasts

Fibroblasts and vascular cells create a similar fibrotic environment during wound healing to enable tissue repair. In fact, both tissue fibrosis and inflammation increase cancer risk in patients [138], and there is an increased incidence of tumor formation at sites of scarred tissue [150]. Interestingly, wounding in RSV infected chickens induces tumor formation [151] possibly by stimulating TGF- β which can [151] increase collagen production and smooth muscle actin expression in fibroblasts and induce tissue desmoplasia [152]. In this regard, cancer has been defined as a wound that fails to heal [1, 153], because tumor progression and the wound-response are both characterized by ECM remodeling, hypoxia, angiogenesis, and the recruitment of a repertoire of non-transformed host cells.

Fibroblasts themselves are strongly regulated by their 3D environment. For example, fibroblasts embedded within 3D compliant floating collagen gels are quiescent [154] in contrast to fibroblasts growing on rigid 2D substrata. However, a mechanical challenge can stimulate the fibroblasts, to increase mechanical loading and alter fibroblast behavior [28]. This is because mechanical loading induces fibroblasts to up regulate the synthesis, secretion and deposition of many ECM components and their cross-linking enzymes such as LOX, and by so doing increases the local stiffness of the matrix and enhances the tensile properties of the gel [28]. These matrix modifications further activate fibroblasts and result in a feed-forward mechanism to maximize tumor progression. Hypoxia

results in similar activation of fibroblasts, and increases the expression of ECM components and remodeling enzymes, such as LOX, to further enhances tissue desmoplasia and promote metastatic progression [54, 149, 155].

Leukocytes

Innate immune cells are strong mediators of disease progression because they release potent soluble factors that enable growth, motility and angiogenesis [16, 138]. Leukocytes play a key role in tumor progression. They are loaded with chemokines, cytokines, reactive oxygen species, proteases, TNF- α , interleukins and interferons [16]. These factors are all known to mediate inflammation responses, recruit/activate innate immune cells, tissue remodeling and angiogenesis [16]. For instance, leukocytes produce abundant MMPs, which remodel the ECM and release chemokines, cytokines and growth factors, such as TNF- α , bFGF and VEGF which are sequestered to ECM molecules or tethered to cells [156, 157, 106, 108]. In particular, MMP2 and MMP9 activate latent TGF- β in ECM which drives EMT, induces tissue desmoplasia and elevates LOX expression [158]. In addition, leukocyte-mediated matrix modifications stimulate cell–cell and cell–matrix adhesion molecules thereby increasing invasion, angiogenesis and inflammation [156, 157]. While the majority of matrix remodeling creates an environment permissive for malignant conversion and cancer development, peptides released from collagen remodeling can also exert anti-angiogenic effects. These released factors include endostatin released from the NC1 fragment of type XVIII collagen [159], restin released from type XV collagen [160], arrestin released from type IV collagen [161], and all three chains of type IV collagen [27, 161, 162]. Thus, protease-generated cleavage products released from the interstitial ECM and BM can act as either suppressors or activators of angiogenesis.

TAMs

Tumor-associated macrophages (TAMs) are determinants of malignant progression [16]. TAMs are present in many cancer types including melanoma, cervical squamous cell carcinoma and mammary adenocarcinoma [163–166]. Furthermore, TAMs are associated with metastasis and poor patient outcome [167]. TAM-induced ECM remodeling increases angiogenic and lymphangiogenic responses thereby promoting tumor growth, survival and dissemination [168, 169]. In addition, TAMs enhance tumor cell invasion [80, 165] as revealed by elegant intravital imaging that showed how TAMs secrete growth factors to direct tumor cell migration towards blood vessels and enable intravasation [80]. Interestingly, TAMs are known to

accumulate in regions of hypoxia raising the intriguing possibility that hypoxia might additionally promote tumor metastasis by recruiting factors that stimulate TAM recruitment [167, 170].

ECM remodeling and recruited BMDCs establish the pre-metastatic niche

Recent *in vivo* data has suggested that formation of a pre-metastatic niche is essential for the growth and survival of extravasating metastatic tumor cells [171]. These studies showed that factors secreted by primary tumor cells stimulate the recruitment of bone marrow-derived cells (BMDCs) to sites of future metastasis. The bone marrow-derived cells express VEGFR-1, c-kit, CD133, CD34 and integrin VLA-4, and increase angiogenesis at the pre-metastatic sites thereby creating tissue-specific niches that permit the growth and survival of metastatic tumor cells. Consistently, targeted inhibition of VEGFR-1 prevented niche formation and inhibited subsequent metastatic progression. Such localized tissue pre-conditioning may thus represent a key step during tumor metastasis that could be targeted therapeutically.

Elevated fibronectin expression in fibroblasts and fibroblast-like cells resident at pre-metastatic sites appears to be a critical factor in the development of the pre-metastatic niche. The key tumor-secreted factors that determine metastatic sites and mediate pre-metastatic niche formation have yet to be identified, although TNF- α , TGF- β and VEGF- α signaling have all been implicated [172]. MMPs might also play a role in the formation of the metastatic niche. For example, VEGF-R1 signaling is required for the pre-metastatic induction of MMP-9 expression in endothelial cells and macrophages of the lungs by distant primary tumors [173]. This is thought to make the lung microenvironment more hospitable for the subsequent invasion and survival of metastatic cells. Indeed, pericyte recruitment and angiogenesis are not observed in tumor-bearing mice with MMP-9 knock-out bone marrow cells [174], whereas stromal-derived MMP-2 and MMP-9 facilitate the establishment and growth of metastatic tumors [175].

Exactly what determines where these niches form remains unresolved. Studies have shown that cell growth rate is increased at sites where mechanical stresses concentrate [176] and that continuous mechanical perturbation induces tumors in rodents [91]. Furthermore, there are many accounts of cancer forming at sites of repeated physical injury, and chronic wounding can promote malignant transformation and foster tumor metastasis [90]. These observations raise the intriguing possibility that pre-metastatic niches might occur at sites exposed to repetitive mechanical strain.

Recently, we found that LOX secreted by hypoxic tumor cells plays a critical role *in vivo* in the formation of the pre-metastatic niche [Erler/Bennewith et al., unpublished]. We could show that the activity of tumor-secreted LOX at pre-metastatic sites is required for BMDC recruitment. *In vitro* data suggested this effect was likely mediated through LOX-dependent matrix remodeling and MMP activity induced by collagen cross-linking. BMDC recruitment enabled pre-metastatic niche formation that was able to support metastatic growth, and this process could be disrupted by administering LOX-targeting therapies. These studies stress the importance of ECM remodeling and the interplay between the tumor cells and the stroma in transformation and metastasis, and highlight the therapeutic potential of targeting the tissue stroma to prevent tumor progression.

Future directions

There is a critical reciprocal and functional link between multiple non-cellular micro-environmental components that control tumor evolution and metastatic progression. These include the ECM and hypoxia, which are potent driving forces of tumor progression. Emerging evidence indicate that changes at the primary tumor, including those driven by stiffness and hypoxia, profoundly influence distant metastatic sites. Preliminary studies suggest that a complex interplay between matrix remodeling and tumor hypoxia likely “primes” the metastatic niche. Nevertheless, in order to develop effective anti-metastatic therapies, it will be critical to understand and identify the key molecular mechanisms whereby tissue context, as exemplified by mechanical force and hypoxia, regulate tumor metastasis.

Acknowledgements We apologize to those authors whose excellent work could not be cited due to space limitations. This work was supported by DOD BCRP W81XWH-05-1-330, NCI CA078731, and DOE A107165 (VMW); and by The Institute of Cancer Research, and Cancer Research UK (JTE).

References

1. Bissell MJ, Radisky D (2001) Putting tumours in context. *Nat Rev Cancer* 1:46–54. doi:10.1038/35094059
2. Mintz B, Illmensee K (1975) Normal genetically mosaic mice produced from malignant teratocarcinoma cells. *Proc Natl Acad Sci USA* 72:3585–3589. doi:10.1073/pnas.72.9.3585
3. Dolberg DS, Bissell MJ (1984) Inability of Rous sarcoma virus to cause sarcomas in the avian embryo. *Nature* 309:552–556. doi:10.1038/309552a0
4. Weaver VM, Petersen OW, Wang F, Larabell CA, Briand P, Damsky C et al (1997) Reversion of the malignant phenotype of human breast cells in three-dimensional culture and *in vivo* by

- integrin blocking antibodies. *J Cell Biol* 137:231–245. doi:10.1083/jcb.137.1.231
5. Barcellos-Hoff MH, Ravani SA (2000) Irradiated mammary gland stroma promotes the expression of tumorigenic potential by unirradiated epithelial cells. *Cancer Res* 60:1254–1260
 6. Wiseman BS, Werb Z (2002) Stromal effects on mammary gland development and breast cancer. *Science* 296:1046–1049. doi:10.1126/science.1067431
 7. Burdelya LG, Komarova EA, Hill JE, Browder T, Tararova ND, Mavrakis L et al (2006) Inhibition of p53 response in tumor stroma improves efficacy of anticancer treatment by increasing antiangiogenic effects of chemotherapy and radiotherapy in mice. *Cancer Res* 66:9356–9361. doi:10.1158/0008-5472.CAN-06-1223
 8. Bhowmick NA, Moses HL (2005) Tumor-stroma interactions. *Curr Opin Genet Dev* 15:97–101. doi:10.1016/j.gde.2004.12.003
 9. Haass NK, Smalley KS, Herlyn M (2004) The role of altered cell-cell communication in melanoma progression. *J Mol Histol* 35:309–318. doi:10.1023/B:HIJO.0000032362.35354.bb
 10. Karnoub AE, Dash AB, Vo AP, Sullivan A, Brooks MW, Bell GW et al (2007) Mesenchymal stem cells within tumour stroma promote breast cancer metastasis. *Nature* 449:557–563. doi:10.1038/nature06188
 11. Coussens LM, Raymond WW, Bergers G, Laig-Webster M, Behrendtsen O, Werb Z et al (1999) Inflammatory mast cells up-regulate angiogenesis during squamous epithelial carcinogenesis. *Genes Dev* 13:1382–1397. doi:10.1101/gad.13.11.1382
 12. Iyengar P, Combs TP, Shah SJ, Gouon-Evans V, Pollard JW, Albanese C et al (2003) Adipocyte-secreted factors synergistically promote mammary tumorigenesis through induction of anti-apoptotic transcriptional programs and proto-oncogene stabilization. *Oncogene* 22:6408–6423. doi:10.1038/sj.onc.1206737
 13. Erler JT, Bennewith KL, Nicolau M, Dornhofer N, Kong C, Le QT et al (2006) Lysyl oxidase is essential for hypoxia-induced metastasis. *Nature* 440:1222–1226. doi:10.1038/nature04695
 14. Paszek MJ, Zahir N, Johnson KR, Lakins JN, Rozenberg GI, Gefen A et al (2005) Tensional homeostasis and the malignant phenotype. *Cancer Cell* 8:241–254. doi:10.1016/j.ccr.2005.08.010
 15. Bissell MJ, Aggeler J (1987) Dynamic reciprocity: how do extracellular matrix and hormones direct gene expression? *Prog Clin Biol Res* 249:251–262
 16. Tlsty TD, Coussens LM (2006) Tumor stroma and regulation of cancer development. *Annu Rev Pathol* 1:119–150. doi:10.1146/annurev.pathol.1.110304.100224
 17. Aumailley M, Gayraud B (1998) Structure and biological activity of the extracellular matrix. *J Mol Med* 76:253–265. doi:10.1007/s001090050215
 18. Kass L, Erler JT, Dembo M, Weaver VM (2007) Mammary epithelial cell: influence of extracellular matrix composition and organization during development and tumorigenesis. *Int J Biochem Cell Biol* 39:1987–1994. doi:10.1016/j.biocel.2007.06.025
 19. Sinkus R, Lorenzen J, Schrader D, Lorenzen M, Dargatz M, Holz D (2000) High-resolution tensor MR elastography for breast tumour detection. *Phys Med Biol* 45:1649–1664. doi:10.1088/0031-9155/45/6/317
 20. Myllyharju J, Kivirikko KI (2004) Collagens, modifying enzymes and their mutations in humans, flies and worms. *Trends Genet* 20:33–43. doi:10.1016/j.tig.2003.11.004
 21. Vuorio E, de Crombrughe B (1990) The family of collagen genes. *Annu Rev Biochem* 59:837–872. doi:10.1146/annurev.bi.59.070190.004201
 22. Bosman FT, Stamenkovic I (2003) Functional structure and composition of the extracellular matrix. *J Pathol* 200:423–428. doi:10.1002/path.1437
 23. Howe A, Aplin AE, Alahari SK, Juliano RL (1998) Integrin signaling and cell growth control. *Curr Opin Cell Biol* 10:220–231. doi:10.1016/S0955-0674(98)80144-0
 24. Weaver VM, Lelievre S, Lakins JN, Chrenek MA, Jones JC, Giancotti F et al (2002) beta4 Integrin-dependent formation of polarized three-dimensional architecture confers resistance to apoptosis in normal and malignant mammary epithelium. *Cancer Cell* 2:205–216. doi:10.1016/S1535-6108(02)00125-3
 25. Bissell MJ, Radisky DC, Rizki A, Weaver VM, Petersen OW (2002) The organizing principle: microenvironmental influences in the normal and malignant breast. *Differentiation* 70:537–546. doi:10.1046/j.1432-0436.2002.700907.x
 26. Sugawara K, Tsuruta D, Ishii M, Jones JC, Kobayashi H (2008) Laminin-332 and -511 in skin. *Exp Dermatol* 17:473–480. doi:10.1111/j.1600-0625.2008.00721.x
 27. Kalluri R (2003) Basement membranes: structure, assembly and role in tumour angiogenesis. *Nat Rev Cancer* 3:422–433. doi:10.1038/nrc1094
 28. Paszek MJ, Weaver VM (2004) The tension mounts: mechanics meets morphogenesis and malignancy. *J Mammary Gland Biol Neoplasia* 9:325–342. doi:10.1007/s10911-004-1404-x
 29. Discher DE, Janmey P, Wang YL (2005) Tissue cells feel and respond to the stiffness of their substrate. *Science* 310:1139–1143. doi:10.1126/science.1116995
 30. Pedersen JA, Swartz MA (2005) Mechanobiology in the third dimension. *Ann Biomed Eng* 33:1469–1490. doi:10.1007/s10439-005-8159-4
 31. Georges PC, Janmey PA (2005) Cell type-specific response to growth on soft materials. *J Appl Physiol* 98:1547–1553. doi:10.1152/jappphysiol.01121.2004
 32. Janmey PA, Weitz DA (2004) Dealing with mechanics: mechanisms of force transduction in cells. *Trends Biochem Sci* 29:364–370. doi:10.1016/j.tibs.2004.05.003
 33. Engler AJ, Sen S, Sweeney HL, Discher DE (2006) Matrix elasticity directs stem cell lineage specification. *Cell* 126:677–689. doi:10.1016/j.cell.2006.06.044
 34. Zahir N, Lakins JN, Russell A, Ming W, Chatterjee C, Rozenberg GI et al (2003) Autocrine laminin-5 ligates alpha6beta4 integrin and activates RAC and NFKappaB to mediate anchorage-independent survival of mammary tumors. *J Cell Biol* 163:1397–1407. doi:10.1083/jcb.200302023
 35. Hotary KB, Allen ED, Brooks PC, Datta NS, Long MW, Weiss SJ (2003) Membrane type I matrix metalloproteinase usurps tumor growth control imposed by the three-dimensional extracellular matrix. *Cell* 114:33–45. doi:10.1016/S0092-8674(03)00513-0
 36. O'Brien LE, Jou TS, Pollack AL, Zhang Q, Hansen SH, Yurchenco P et al (2001) Rac1 orientates epithelial apical polarity through effects on basolateral laminin assembly. *Nat Cell Biol* 3:831–838. doi:10.1038/ncb0901-831
 37. Cukierman E, Pankov R, Stevens DR, Yamada KM (2001) Taking cell-matrix adhesions to the third dimension. *Science* 294:1708–1712. doi:10.1126/science.1064829
 38. Yamada KM, Pankov R, Cukierman E (2003) Dimensions and dynamics in integrin function. *Braz J Med Biol Res* 36:959–966. doi:10.1590/S0100-879X2003000800001
 39. Beacham DA, Cukierman E (2005) Stromagenesis: the changing face of fibroblastic microenvironments during tumor progression. *Semin Cancer Biol* 15:329–341. doi:10.1016/j.semcancer.2005.05.003
 40. Bogenrieder T, Herlyn M (2002) Cell-surface proteolysis, growth factor activation and intercellular communication in the progression of melanoma. *Crit Rev Oncol Hematol* 44:1–15. doi:10.1016/S1040-8428(01)00196-2
 41. Haass NK, Smalley KS, Li L, Herlyn M (2005) Adhesion, migration and communication in melanocytes and melanoma.

- Pigment Cell Res 18:150–159. doi:[10.1111/j.1600-0749.2005.00235.x](https://doi.org/10.1111/j.1600-0749.2005.00235.x)
42. Yamada KM, Cukierman E (2007) Modeling tissue morphogenesis and cancer in 3D. *Cell* 130:601–610. doi:[10.1016/j.cell.2007.08.006](https://doi.org/10.1016/j.cell.2007.08.006)
 43. Emerman JT, Pitelka DR (1977) Maintenance and induction of morphological differentiation in dissociated mammary epithelium on floating collagen membranes. *In Vitro* 13:316–328. doi:[10.1007/BF02616178](https://doi.org/10.1007/BF02616178)
 44. Barcellos-Hoff MH, Aggeler J, Ram TG, Bissell MJ (1989) Functional differentiation and alveolar morphogenesis of primary mammary cultures on reconstituted basement membrane. *Development* 105:223–235
 45. Leitinger B, Hohenester E (2007) Mammalian collagen receptors. *Matrix Biol* 26:146–155. doi:[10.1016/j.matbio.2006.10.007](https://doi.org/10.1016/j.matbio.2006.10.007)
 46. Vogel WF, Abdulhussein R, Ford CE (2006) Sensing extracellular matrix: an update on discoidin domain receptor function. *Cell Signal* 18:1108–1116. doi:[10.1016/j.cellsig.2006.02.012](https://doi.org/10.1016/j.cellsig.2006.02.012)
 47. Avraamides CJ, Garmy-Susini B, Varner JA (2008) Integrins in angiogenesis and lymphangiogenesis. *Nat Rev Cancer* 8(8):604–617
 48. Hynes RO (2002) Integrins: bidirectional, allosteric signaling machines. *Cell* 110:673–687. doi:[10.1016/S0092-8674\(02\)00971-6](https://doi.org/10.1016/S0092-8674(02)00971-6)
 49. Morgan MR, Humphries MJ, Bass MD (2007) Synergistic control of cell adhesion by integrins and syndecans. *Nat Rev Mol Cell Biol* 8:957–969. doi:[10.1038/nrm2289](https://doi.org/10.1038/nrm2289)
 50. Miranti CK, Brugge JS (2002) Sensing the environment: a historical perspective on integrin signal transduction. *Nat Cell Biol* 4:E83–E90. doi:[10.1038/ncb0402-e83](https://doi.org/10.1038/ncb0402-e83)
 51. Clark EA, Brugge JS (1995) Integrins and signal transduction pathways: the road taken. *Science* 268:233–239. doi:[10.1126/science.7716514](https://doi.org/10.1126/science.7716514)
 52. Caswell PT, Norman JC (2006) Integrin trafficking and the control of cell migration. *Traffic* 7:14–21. doi:[10.1111/j.1600-0854.2005.00362.x](https://doi.org/10.1111/j.1600-0854.2005.00362.x)
 53. Huang LE, Bindra RS, Glazer PM, Harris AL (2007) Hypoxia-induced genetic instability—a calculated mechanism underlying tumor progression. *J Mol Med* 85:139–148. doi:[10.1007/s00109-006-0133-6](https://doi.org/10.1007/s00109-006-0133-6)
 54. Lunt SJ, Chaudary N, Hill RP (2008) The tumor microenvironment and metastatic disease. *Clin Exp Metastasis*. doi:[10.1007/s10585-008-9182-2](https://doi.org/10.1007/s10585-008-9182-2)
 55. Parmar K, Mauch P, Vergilio JA, Sackstein R, Down JD (2007) Distribution of hematopoietic stem cells in the bone marrow according to regional hypoxia. *Proc Natl Acad Sci USA* 104:5431–5436. doi:[10.1073/pnas.0701152104](https://doi.org/10.1073/pnas.0701152104)
 56. Axelson H, Fredlund E, Ovenberger M, Landberg G, Pahlman S (2005) Hypoxia-induced dedifferentiation of tumor cells—a mechanism behind heterogeneity and aggressiveness of solid tumors. *Semin Cell Dev Biol* 16:554–563. doi:[10.1016/j.semdb.2005.03.007](https://doi.org/10.1016/j.semdb.2005.03.007)
 57. Hockel M, Vaupel P (2001) Tumor hypoxia: definitions and current clinical, biologic, and molecular aspects. *J Natl Cancer Inst* 93:266–276. doi:[10.1093/jnci/93.4.266](https://doi.org/10.1093/jnci/93.4.266)
 58. Rodriguez PG, Felix FN, Woodley DT, Shim EK (2008) The role of oxygen in wound healing: a review of the literature. *Dermatol Surg*
 59. Simon MC, Keith B (2008) The role of oxygen availability in embryonic development and stem cell function. *Nat Rev Mol Cell Biol* 9:285–296. doi:[10.1038/nrm2354](https://doi.org/10.1038/nrm2354)
 60. Cartwright JE, Keogh RJ, Tissot van Patot MC (2007) Hypoxia and placental remodelling. *Adv Exp Med Biol* 618:113–126. doi:[10.1007/978-0-387-75434-5_9](https://doi.org/10.1007/978-0-387-75434-5_9)
 61. van Tuyll M, Liu J, Wang J, Kuliszewski M, Tibboel D, Post M (2005) Role of oxygen and vascular development in epithelial branching morphogenesis of the developing mouse lung. *Am J Physiol Lung Cell Mol Physiol* 288:L167–L178. doi:[10.1152/ajplung.00185.2004](https://doi.org/10.1152/ajplung.00185.2004)
 62. Pennacchiotti S, Michieli P, Galluzzo M, Mazzone M, Giordano S, Comoglio PM (2003) Hypoxia promotes invasive growth by transcriptional activation of the met protooncogene. *Cancer Cell* 3:347–361. doi:[10.1016/S1535-6108\(03\)00085-0](https://doi.org/10.1016/S1535-6108(03)00085-0)
 63. Semenza GL (2003) Targeting HIF-1 for cancer therapy. *Nat Rev Cancer* 3:721–732. doi:[10.1038/nrc1187](https://doi.org/10.1038/nrc1187)
 64. Provot S, Schipani E (2007) Fetal growth plate: a developmental model of cellular adaptation to hypoxia. *Ann NY Acad Sci* 1117:26–39. doi:[10.1196/annals.1402.076](https://doi.org/10.1196/annals.1402.076)
 65. Cowden Dahl KD, Robertson SE, Weaver VM, Simon MC (2005) Hypoxia-inducible factor regulates alphavbeta3 integrin cell surface expression. *Mol Biol Cell* 16:1901–1912. doi:[10.1091/mbc.E04-12-1082](https://doi.org/10.1091/mbc.E04-12-1082)
 66. Radisky D, Hagios C, Bissell MJ (2001) Tumors are unique organs defined by abnormal signaling and context. *Semin Cancer Biol* 11:87–95. doi:[10.1006/scbi.2000.0360](https://doi.org/10.1006/scbi.2000.0360)
 67. Mackie EJ, Chiquet-Ehrismann R, Pearson CA, Inaguma Y, Taya K, Kawarada Y et al (1987) Tenascin is a stromal marker for epithelial malignancy in the mammary gland. *Proc Natl Acad Sci USA* 84:4621–4625. doi:[10.1073/pnas.84.13.4621](https://doi.org/10.1073/pnas.84.13.4621)
 68. Kauppila S, Stenback F, Risteli J, Jukkola A, Risteli L (1998) Aberrant type I and type III collagen gene expression in human breast cancer in vivo. *J Pathol* 186:262–268. doi:[10.1002/\(SICI\)1096-9896\(199811\)186:3<262::AID-PATH191>3.0.CO;2-3](https://doi.org/10.1002/(SICI)1096-9896(199811)186:3<262::AID-PATH191>3.0.CO;2-3)
 69. Zhu GG, Risteli L, Makinen M, Risteli J, Kauppila A, Stenback F (1995) Immunohistochemical study of type I collagen and type I pN-collagen in benign and malignant ovarian neoplasms. *Cancer* 75:1010–1017. doi:[10.1002/1097-0142\(19950215\)75:4<1010::AID-CNCR2820750417>3.0.CO;2-O](https://doi.org/10.1002/1097-0142(19950215)75:4<1010::AID-CNCR2820750417>3.0.CO;2-O)
 70. Strongin AY (2006) Mislocalization and unconventional functions of cellular MMPs in cancer. *Cancer Metastasis Rev* 25:87–98. doi:[10.1007/s10555-006-7892-y](https://doi.org/10.1007/s10555-006-7892-y)
 71. Jodele S, Blavier L, Yoon JM, DeClerck YA (2006) Modifying the soil to affect the seed: role of stromal-derived matrix metalloproteinases in cancer progression. *Cancer Metastasis Rev* 25:35–43. doi:[10.1007/s10555-006-7887-8](https://doi.org/10.1007/s10555-006-7887-8)
 72. Biondi ML, Turri O, Leviti S, Seminati R, Cecchini F, Bernini M et al (2000) MMP1 and MMP3 polymorphisms in promoter regions and cancer. *Clin Chem* 46:2023–2024
 73. Sternlicht MD, Lochter A, Sympon CJ, Huey B, Rougier JP, Gray JW et al (1999) The stromal proteinase MMP3/stromelysin-1 promotes mammary carcinogenesis. *Cell* 98:137–146. doi:[10.1016/S0092-8674\(00\)81009-0](https://doi.org/10.1016/S0092-8674(00)81009-0)
 74. Seandel M, Noack-Kunmann K, Zhu D, Aimes RT, Quigley JP (2001) Growth factor-induced angiogenesis in vivo requires specific cleavage of fibrillar type I collagen. *Blood* 97:2323–2332. doi:[10.1182/blood.V97.8.2323](https://doi.org/10.1182/blood.V97.8.2323)
 75. Santala M, Simojoki M, Risteli J, Risteli L, Kauppila A (1999) Type I and III collagen metabolites as predictors of clinical outcome in epithelial ovarian cancer. *Clin Cancer Res* 5:4091–4096
 76. Burns-Cox N, Avery NC, Gingell JC, Bailey AJ (2001) Changes in collagen metabolism in prostate cancer: a host response that may alter progression. *J Urol* 166:1698–1701. doi:[10.1016/S0022-5347\(05\)65656-X](https://doi.org/10.1016/S0022-5347(05)65656-X)
 77. Ylisirnio S, Hoyhtya M, Makitaro R, Paaakko P, Risteli J, Kinnula VL et al (2001) Elevated serum levels of type I collagen degradation marker ICTP and tissue inhibitor of metalloproteinase (TIMP) 1 are associated with poor prognosis in lung cancer. *Clin Cancer Res* 7:1633–1637
 78. Clarijs R, Ruiter DJ, De Waal RM (2003) Pathophysiological implications of stroma pattern formation in uveal melanoma. *J Cell Physiol* 194:267–271. doi:[10.1002/jcp.10214](https://doi.org/10.1002/jcp.10214)

79. Ruiter D, Bogenrieder T, Elder D, Herlyn M (2002) Melanoma-stroma interactions: structural and functional aspects. *Lancet Oncol* 3:35–43. doi:[10.1016/S1470-2045\(01\)00620-9](https://doi.org/10.1016/S1470-2045(01)00620-9)
80. Condeelis J, Pollard JW (2006) Macrophages: obligate partners for tumor cell migration, invasion, and metastasis. *Cell* 124:263–266. doi:[10.1016/j.cell.2006.01.007](https://doi.org/10.1016/j.cell.2006.01.007)
81. Jain RK (2005) Antiangiogenic therapy for cancer: current and emerging concepts. *Oncology* 19:7–16 Williston Park
82. Clarijs R, Schalkwijk L, Ruiter DJ, de Waal RM (2001) Lack of lymphangiogenesis despite coexpression of VEGF-C and its receptor Flt-4 in uveal melanoma. *Invest Ophthalmol Vis Sci* 42:1422–1428
83. Clarijs R, Otte-Holler I, Ruiter DJ, de Waal RM (2002) Presence of a fluid-conducting meshwork in xenografted cutaneous and primary human uveal melanoma. *Invest Ophthalmol Vis Sci* 43:912–918
84. Hendrix MJ, Seftor EA, Hess AR, Seftor RE (2003) Vasculogenic mimicry and tumour-cell plasticity: lessons from melanoma. *Nat Rev Cancer* 3:411–421. doi:[10.1038/nrc1092](https://doi.org/10.1038/nrc1092)
85. Krouskop TA, Wheeler TM, Kallel F, Garra BS, Hall T (1998) Elastic moduli of breast and prostate tissues under compression. *Ultrason Imaging* 20:260–274
86. Khaled W, Reichling S, Bruhns OT, Boese H, Baumann M, Monkman G et al (2004) Palpation imaging using a haptic system for virtual reality applications in medicine. *Stud Health Technol Inform* 98:147–153
87. Decitre M, Gleyzal C, Raccurt M, Peyrol S, Aubert-Foucher E, Csiszar K et al (1998) Lysyl oxidase-like protein localizes to sites of de novo fibrinogenesis in fibrosis and in the early stromal reaction of ductal breast carcinomas. *Lab Invest* 78:143–151
88. Padera TP, Stoll BR, Tooredman JB, Capen D, di Tomaso E, Jain RK (2004) Pathology: cancer cells compress intratumour vessels. *Nature* 427:695. doi:[10.1038/427695a](https://doi.org/10.1038/427695a)
89. Huang S, Ingber DE (2005) Cell tension, matrix mechanics, and cancer development. *Cancer Cell* 8:175–176. doi:[10.1016/j.ccr.2005.08.009](https://doi.org/10.1016/j.ccr.2005.08.009)
90. Ingber DE (2008) Can cancer be reversed by engineering the tumor microenvironment? *Semin Cancer Biol* 18:356–364. doi:[10.1016/j.semcancer.2008.03.016](https://doi.org/10.1016/j.semcancer.2008.03.016)
91. Bischoff F, Bryson G (1964) Carcinogenesis through solid state surfaces. *Prog Exp Tumor Res* 5:85–133
92. Ingber DE, Madri JA, Jamieson JD (1981) Role of basal lamina in neoplastic disorganization of tissue architecture. *Proc Natl Acad Sci USA* 78:3901–3905. doi:[10.1073/pnas.78.6.3901](https://doi.org/10.1073/pnas.78.6.3901)
93. Maffini MV, Calabro JM, Soto AM, Sonnenschein C (2005) Stromal regulation of neoplastic development: age-dependent normalization of neoplastic mammary cells by mammary stroma. *Am J Pathol* 167:1405–1410
94. Kenny PA, Bissell MJ (2003) Tumor reversion: correction of malignant behavior by microenvironmental cues. *Int J Cancer* 107:688–695. doi:[10.1002/ijc.11491](https://doi.org/10.1002/ijc.11491)
95. Watanabe TK, Hansen LJ, Reddy NK, Kanwar YS, Reddy JK (1984) Differentiation of pancreatic acinar carcinoma cells cultured on rat testicular seminiferous tubular basement membranes. *Cancer Res* 44:5361–5368
96. Ingber DE, Madri JA, Jamieson JD (1986) Basement membrane as a spatial organizer of polarized epithelia. Exogenous basement membrane reorients pancreatic epithelial tumor cells in vitro. *Am J Pathol* 122:129–139
97. Young SD, Marshall RS, Hill RP (1988) Hypoxia induces DNA overreplication and enhances metastatic potential of murine tumor cells. *Proc Natl Acad Sci USA* 85:9533–9537. doi:[10.1073/pnas.85.24.9533](https://doi.org/10.1073/pnas.85.24.9533)
98. Erler JT, Cawthorne CJ, Williams KJ, Koritzinsky M, Wouters BG, Wilson C et al (2004) Hypoxia-mediated down-regulation of Bid and Bax in tumors occurs via hypoxia-inducible factor 1-dependent and -independent mechanisms and contributes to drug resistance. *Mol Cell Biol* 24:2875–2889. doi:[10.1128/MCB.24.7.2875-2889.2004](https://doi.org/10.1128/MCB.24.7.2875-2889.2004)
99. Graeber TG, Osmanian C, Jacks T, Housman DE, Koch CJ, Lowe SW et al (1996) Hypoxia-mediated selection of cells with diminished apoptotic potential in solid tumours. *Nature* 379:88–91. doi:[10.1038/379088a0](https://doi.org/10.1038/379088a0)
100. Tamamori M, Ito H, Hiroe M, Marumo F, Hata RI (1997) Stimulation of collagen synthesis in rat cardiac fibroblasts by exposure to hypoxic culture conditions and suppression of the effect by natriuretic peptides. *Cell Biol Int* 21:175–180. doi:[10.1006/cbir.1997.0130](https://doi.org/10.1006/cbir.1997.0130)
101. Lu SY, Wang DS, Zhu MZ, Zhang QH, Hu YZ, Pei JM (2005) Inhibition of hypoxia-induced proliferation and collagen synthesis by vasonatrin peptide in cultured rat pulmonary artery smooth muscle cells. *Life Sci* 77:28–38. doi:[10.1016/j.lfs.2004.11.026](https://doi.org/10.1016/j.lfs.2004.11.026)
102. Horino Y, Takahashi S, Miura T, Takahashi Y (2002) Prolonged hypoxia accelerates the posttranscriptional process of collagen synthesis in cultured fibroblasts. *Life Sci* 71:3031–3045. doi:[10.1016/S0024-3205\(02\)02142-2](https://doi.org/10.1016/S0024-3205(02)02142-2)
103. Kukacka J, Bibova J, Ruskoaho H, Pelouch V (2007) Protein remodeling of extracellular matrix in rat myocardium during four-day hypoxia: the effect of concurrent hypercapnia. *Gen Physiol Biophys* 26:133–142
104. Takahashi Y, Takahashi S, Shiga Y, Yoshimi T, Miura T (2000) Hypoxic induction of prolyl 4-hydroxylase alpha (I) in cultured cells. *J Biol Chem* 275:14139–14146. doi:[10.1074/jbc.275.19.14139](https://doi.org/10.1074/jbc.275.19.14139)
105. Myllyharju J (2003) Prolyl 4-hydroxylases, the key enzymes of collagen biosynthesis. *Matrix Biol* 22:15–24. doi:[10.1016/S0945-053X\(03\)00006-4](https://doi.org/10.1016/S0945-053X(03)00006-4)
106. Le QT, Denko NC, Giaccia AJ (2004) Hypoxic gene expression and metastasis. *Cancer Metastasis Rev* 23:293–310. doi:[10.1023/B:CANC.0000031768.89246.d7](https://doi.org/10.1023/B:CANC.0000031768.89246.d7)
107. Denko NC, Fontana LA, Hudson KM, Sutphin PD, Raychaudhuri S, Altman R et al (2003) Investigating hypoxic tumor physiology through gene expression patterns. *Oncogene* 22:5907–5914. doi:[10.1038/sj.onc.1206703](https://doi.org/10.1038/sj.onc.1206703)
108. Kagan HM, Li W (2003) Lysyl oxidase: properties, specificity, and biological roles inside and outside of the cell. *J Cell Biochem* 88:660–672. doi:[10.1002/jcb.10413](https://doi.org/10.1002/jcb.10413)
109. van den Hoff A (1988) Stromal involvement in malignant growth. *Adv Cancer Res* 50:159–196. doi:[10.1016/S0065-230X\(88\)60437-6](https://doi.org/10.1016/S0065-230X(88)60437-6)
110. Sappino AP, Schurch W, Gabbiani G (1990) Differentiation repertoire of fibroblastic cells: expression of cytoskeletal proteins as marker of phenotypic modulations. *Lab Invest* 63:144–161
111. Ronnov-Jessen L, Petersen OW, Bissell MJ (1996) Cellular changes involved in conversion of normal to malignant breast: importance of the stromal reaction. *Physiol Rev* 76:69–125
112. Ingber DE, Madri JA, Jamieson JD (1985) Neoplastic disorganization of pancreatic epithelial cell-cell relations. Role of basement membrane. *Am J Pathol* 121:248–260
113. Lu S, Huang M, Kobayashi Y, Komiyama A, Li X, Katoh R et al (2000) Alterations of basement membrane in di-isopropanolnitrosamine-induced carcinogenesis of the rat thyroid gland: an immunohistochemical study. *Virchows Arch* 436:595–601. doi:[10.1007/s004280000180](https://doi.org/10.1007/s004280000180)
114. Ozzello L (1959) The behavior of basement membranes in intraductal carcinoma of the breast. *Am J Pathol* 35:887–899
115. Luibel FJ, Sanders E, Ashworth CT (1960) An electron microscopic study of carcinoma in situ and invasive carcinoma of the cervix uteri. *Cancer Res* 20:357–361
116. Rubio CA, Biberfeld P (1979) The basement membrane in experimentally induced atypias and carcinoma of the uterine

- cervix in mice. An immunofluorescence study. *Virchows Arch A Pathol Anat Histol* 381:205–209. doi:[10.1007/BF01257885](https://doi.org/10.1007/BF01257885)
117. Lee JM, Dedhar S, Kalluri R, Thompson EW (2006) The epithelial-mesenchymal transition: new insights in signaling, development, and disease. *J Cell Biol* 172:973–981. doi:[10.1083/jcb.200601018](https://doi.org/10.1083/jcb.200601018)
 118. Higgins DF, Kimura K, Bernhardt WM, Shrimanker N, Akai Y, Hohenstein B et al (2007) Hypoxia promotes fibrogenesis in vivo via HIF-1 stimulation of epithelial-to-mesenchymal transition. *J Clin Invest* 117:3810–3820
 119. Lester RD, Jo M, Montel V, Takimoto S, Gonias SL (2007) uPAR induces epithelial-mesenchymal transition in hypoxic breast cancer cells. *J Cell Biol* 178:425–436. doi:[10.1083/jcb.200701092](https://doi.org/10.1083/jcb.200701092)
 120. Yang MH, Wu MZ, Chiou SH, Chen PM, Chang SY, Liu CJ et al (2008) Direct regulation of TWIST by HIF-1 α promotes metastasis. *Nat Cell Biol* 10:295–305. doi:[10.1038/ncb1691](https://doi.org/10.1038/ncb1691)
 121. Farge E (2003) Mechanical induction of twist in the *Drosophila* foregut/stomodaeal primordium. *Curr Biol* 13:1365–1377. doi:[10.1016/S0960-9822\(03\)00576-1](https://doi.org/10.1016/S0960-9822(03)00576-1)
 122. Tschumperlin DJ, Shively JD, Kikuchi T, Drazen JM (2003) Mechanical stress triggers selective release of fibrotic mediators from bronchial epithelium. *Am J Respir Cell Mol Biol* 28:142–149. doi:[10.1165/rcmb.2002-0121OC](https://doi.org/10.1165/rcmb.2002-0121OC)
 123. Oft M, Peli J, Rudaz C, Schwarz H, Beug H, Reichmann E (1996) TGF- β 1 and Ha-Ras collaborate in modulating the phenotypic plasticity and invasiveness of epithelial tumor cells. *Genes Dev* 10:2462–2477. doi:[10.1101/gad.10.19.2462](https://doi.org/10.1101/gad.10.19.2462)
 124. Miettinen PJ, Ebner R, Lopez AR, Derynck R (1994) TGF- β 1 induced transdifferentiation of mammary epithelial cells to mesenchymal cells: involvement of type I receptors. *J Cell Biol* 127:2021–2036. doi:[10.1083/jcb.127.6.2021](https://doi.org/10.1083/jcb.127.6.2021)
 125. Hosobuchi M, Stampfer MR (1989) Effects of transforming growth factor beta on growth of human mammary epithelial cells in culture. *In Vitro Cell Dev Biol* 25:705–713. doi:[10.1007/BF02623723](https://doi.org/10.1007/BF02623723)
 126. Akhurst RJ, Derynck R (2001) TGF- β 1 signaling in cancer—a double-edged sword. *Trends Cell Biol* 11:S44–S51
 127. Waerner T, Alacakaptan M, Tamir I, Oberauer R, Gal A, Brabletz T et al (2006) ILE1: a cytokine essential for EMT, tumor formation, and late events in metastasis in epithelial cells. *Cancer Cell* 10:227–239. doi:[10.1016/j.ccr.2006.07.020](https://doi.org/10.1016/j.ccr.2006.07.020)
 128. Huang H, Kamm RD, Lee RT (2004) Cell mechanics and mechanotransduction: pathways, probes, and physiology. *Am J Physiol Cell Physiol* 287:C1–C11. doi:[10.1152/ajpcell.00559.2003](https://doi.org/10.1152/ajpcell.00559.2003)
 129. Bershadsky AD, Balaban NQ, Geiger B (2003) Adhesion-dependent cell mechanosensitivity. *Annu Rev Cell Dev Biol* 19:677–695. doi:[10.1146/annurev.cellbio.19.111301.153011](https://doi.org/10.1146/annurev.cellbio.19.111301.153011)
 130. Bellovin DI, Simpson KJ, Danilov T, Maynard E, Rimm DL, Oettgen P et al (2006) Reciprocal regulation of RhoA and RhoC characterizes the EMT and identifies RhoC as a prognostic marker of colon carcinoma. *Oncogene* 25:6959–6967. doi:[10.1038/sj.onc.1209682](https://doi.org/10.1038/sj.onc.1209682)
 131. Reno F, Grazianetti P, Stella M, Magliacani G, Pezzuto C, Cannas M (2002) Release and activation of matrix metalloproteinase-9 during in vitro mechanical compression in hypertrophic scars. *Arch Dermatol* 138:475–478. doi:[10.1001/archderm.138.4.475](https://doi.org/10.1001/archderm.138.4.475)
 132. Sullivan R, Graham CH (2007) Hypoxia-driven selection of the metastatic phenotype. *Cancer Metastasis Rev* 26:319–331. doi:[10.1007/s10555-007-9062-2](https://doi.org/10.1007/s10555-007-9062-2)
 133. van Kempen LC, Ruitter DJ, van Muijen GN, Coussens LM (2003) The tumor microenvironment: a critical determinant of neoplastic evolution. *Eur J Cell Biol* 82:539–548. doi:[10.1078/0171-9335-00346](https://doi.org/10.1078/0171-9335-00346)
 134. Berndt A, Borsi L, Hycckel P, Kosmehl H (2001) Fibrillary co-deposition of laminin-5 and large unspliced tenascin-C in the invasive front of oral squamous cell carcinoma in vivo and in vitro. *J Cancer Res Clin Oncol* 127:286–292. doi:[10.1007/s004320000205](https://doi.org/10.1007/s004320000205)
 135. Mammoto A, Mammoto T, Ingber DE (2008) Rho signaling and mechanical control of vascular development. *Curr Opin Hematol* 15:228–234. doi:[10.1097/MOH.0b013e3282fa7445](https://doi.org/10.1097/MOH.0b013e3282fa7445)
 136. Milkiewicz M, Haas TL (2005) Effect of mechanical stretch on HIF-1 α and MMP-2 expression in capillaries isolated from overloaded skeletal muscles: laser capture microdissection study. *Am J Physiol Heart Circ Physiol* 289:H1315–H1320. doi:[10.1152/ajpheart.00284.2005](https://doi.org/10.1152/ajpheart.00284.2005)
 137. Harris AL (2002) Hypoxia—a key regulatory factor in tumour growth. *Nat Rev Cancer* 2:38–47. doi:[10.1038/nrc704](https://doi.org/10.1038/nrc704)
 138. Coussens LM, Werb Z (2002) Inflammation and cancer. *Nature* 420:860–867. doi:[10.1038/nature01322](https://doi.org/10.1038/nature01322)
 139. Moinfar F, Man YG, Arnould L, Brathauer GL, Ratschek M, Tavassoli FA (2000) Concurrent and independent genetic alterations in the stromal and epithelial cells of mammary carcinoma: implications for tumorigenesis. *Cancer Res* 60:2562–2566
 140. Bhowmick NA, Neilson EG, Moses HL (2004) Stromal fibroblasts in cancer initiation and progression. *Nature* 432:332–337. doi:[10.1038/nature03096](https://doi.org/10.1038/nature03096)
 141. Yeung T, Georges PC, Flanagan LA, Marg B, Ortiz M, Funaki M et al (2005) Effects of substrate stiffness on cell morphology, cytoskeletal structure, and adhesion. *Cell Motil Cytoskeleton* 60:24–34. doi:[10.1002/cm.20041](https://doi.org/10.1002/cm.20041)
 142. Huang S, Ingber DE (1999) The structural and mechanical complexity of cell-growth control. *Nat Cell Biol* 1:E131–E138. doi:[10.1038/13043](https://doi.org/10.1038/13043)
 143. Ebihara T, Venkatesan N, Tanaka R, Ludwig MS (2000) Changes in extracellular matrix and tissue viscoelasticity in bleomycin-induced lung fibrosis. Temporal aspects. *Am J Respir Crit Care Med* 162:1569–1576
 144. Chang HY, Sneddon JB, Alizadeh AA, Sood R, West RB, Montgomery K et al (2004) Gene expression signature of fibroblast serum response predicts human cancer progression: similarities between tumors and wounds. *PLoS Biol* 2:E7. doi:[10.1371/journal.pbio.0020007](https://doi.org/10.1371/journal.pbio.0020007)
 145. Olumi AF, Grossfeld GD, Hayward SW, Carroll PR, Tlsty TD, Cunha GR (1999) Carcinoma-associated fibroblasts direct tumor progression of initiated human prostatic epithelium. *Cancer Res* 59:5002–5011
 146. Bauer EA, Uitto J, Walters RC, Eisen AZ (1979) Enhanced collagenase production by fibroblasts derived from human basal cell carcinomas. *Cancer Res* 39:4594–4599
 147. Knudson W, Biswas C, Toole BP (1984) Interactions between human tumor cells and fibroblasts stimulate hyaluronate synthesis. *Proc Natl Acad Sci USA* 81:6767–6771. doi:[10.1073/pnas.81.21.6767](https://doi.org/10.1073/pnas.81.21.6767)
 148. Willis RA (1967) The unusual in tumour pathology. *Can Med Assoc J* 97:1466–1479
 149. Colpaert CG, Vermeulen PB, Fox SB, Harris AL, Dirix LY, Van Marck EA (2003) The presence of a fibrotic focus in invasive breast carcinoma correlates with the expression of carbonic anhydrase IX and is a marker of hypoxia and poor prognosis. *Breast Cancer Res Treat* 81:137–147. doi:[10.1023/A:1025702330207](https://doi.org/10.1023/A:1025702330207)
 150. Jacobs TW, Byrne C, Colditz G, Connolly JL, Schnitt SJ (1999) Radial scars in benign breast-biopsy specimens and the risk of breast cancer. *N Engl J Med* 340:430–436. doi:[10.1056/NEJM199902113400604](https://doi.org/10.1056/NEJM199902113400604)
 151. Sieweke MH, Thompson NL, Sporn MB, Bissell MJ (1990) Mediation of wound-related Rous sarcoma virus tumorigenesis

- by TGF- β . *Science* 248:1656–1660. doi:[10.1126/science.2163544](https://doi.org/10.1126/science.2163544)
152. Roberts AB, Sporn MB, Assoian RK, Smith JM, Roche NS, Wakefield LM et al (1986) Transforming growth factor type beta: rapid induction of fibrosis and angiogenesis in vivo and stimulation of collagen formation in vitro. *Proc Natl Acad Sci USA* 83:4167–4171. doi:[10.1073/pnas.83.12.4167](https://doi.org/10.1073/pnas.83.12.4167)
 153. Unger M, Weaver VM (2003) The tissue microenvironment as an epigenetic tumor modifier. *Methods Mol Biol* 223:315–347
 154. Fringer J, Grinnell F (2003) Fibroblast quiescence in floating collagen matrices: decrease in serum activation of MEK and Raf but not Ras. *J Biol Chem* 278:20612–20617. doi:[10.1074/jbc.M212365200](https://doi.org/10.1074/jbc.M212365200)
 155. Erler JT, Giaccia AJ (2006) Lysyl oxidase mediates hypoxic control of metastasis. *Cancer Res* 66:10238–10241. doi:[10.1158/0008-5472.CAN-06-3197](https://doi.org/10.1158/0008-5472.CAN-06-3197)
 156. Egeblad M, Werb Z (2002) New functions for the matrix metalloproteinases in cancer progression. *Nat Rev Cancer* 2:161–174. doi:[10.1038/nrc745](https://doi.org/10.1038/nrc745)
 157. de Visser KE, Korets LV, Coussens LM (2004) Early neoplastic progression is complement independent. *Neoplasia* 6:768–776. doi:[10.1593/neo.04250](https://doi.org/10.1593/neo.04250)
 158. Dallas SL, Rosser JL, Mundy GR, Bonewald LF (2002) Proteolysis of latent transforming growth factor- β (TGF- β)-binding protein-1 by osteoclasts. A cellular mechanism for release of TGF- β from bone matrix. *J Biol Chem* 277:21352–21360. doi:[10.1074/jbc.M111663200](https://doi.org/10.1074/jbc.M111663200)
 159. O'Reilly MS, Boehm T, Shing Y, Fukai N, Vasios G, Lane WS et al (1997) Endostatin: an endogenous inhibitor of angiogenesis and tumor growth. *Cell* 88:277–285. doi:[10.1016/S0092-8674\(00\)81848-6](https://doi.org/10.1016/S0092-8674(00)81848-6)
 160. Ramchandran R, Dhanabal M, Volk R, Waterman MJ, Segal M, Lu H et al (1999) Antiangiogenic activity of restin, NC10 domain of human collagen XV: comparison to endostatin. *Biochem Biophys Res Commun* 255:735–739. doi:[10.1006/bbrc.1999.0248](https://doi.org/10.1006/bbrc.1999.0248)
 161. Colorado PC, Torre A, Kamphaus G, Maeshima Y, Hopfer H, Takahashi K et al (2000) Anti-angiogenic cues from vascular basement membrane collagen. *Cancer Res* 60:2520–2526
 162. Maeshima Y, Colorado PC, Torre A, Holthaus KA, Grunke-meyer JA, Ericksen MB et al (2000) Distinct antitumor properties of a type IV collagen domain derived from basement membrane. *J Biol Chem* 275:21340–21348. doi:[10.1074/jbc.M001956200](https://doi.org/10.1074/jbc.M001956200)
 163. Coussens LM, Tinkle CL, Hanahan D, Werb Z (2000) MMP-9 supplied by bone marrow-derived cells contributes to skin carcinogenesis. *Cell* 103:481–490. doi:[10.1016/S0092-8674\(00\)00139-2](https://doi.org/10.1016/S0092-8674(00)00139-2)
 164. Lin EY, Nguyen AV, Russell RG, Pollard JW (2001) Colony-stimulating factor 1 promotes progression of mammary tumors to malignancy. *J Exp Med* 193:727–740. doi:[10.1084/jem.193.6.727](https://doi.org/10.1084/jem.193.6.727)
 165. Lin EY, Guon-Evans V, Nguyen AV, Pollard JW (2002) The macrophage growth factor CSF-1 in mammary gland development and tumor progression. *J Mammary Gland Biol Neoplasia* 7:147–162. doi:[10.1023/A:1020399802795](https://doi.org/10.1023/A:1020399802795)
 166. Kobayashi A, Greenblatt RM, Anastos K, Minkoff H, Massad LS, Young M et al (2004) Functional attributes of mucosal immunity in cervical intraepithelial neoplasia and effects of HIV infection. *Cancer Res* 64:6766–6774. doi:[10.1158/0008-5472.CAN-04-1091](https://doi.org/10.1158/0008-5472.CAN-04-1091)
 167. Lewis CE, Pollard JW (2006) Distinct role of macrophages in different tumor microenvironments. *Cancer Res* 66:605–612. doi:[10.1158/0008-5472.CAN-05-4005](https://doi.org/10.1158/0008-5472.CAN-05-4005)
 168. Skobe M, Hamberg LM, Hawighorst T, Schirner M, Wolf GL, Alitalo K et al (2001) Concurrent induction of lymphangiogenesis, angiogenesis, and macrophage recruitment by vascular endothelial growth factor-C in melanoma. *Am J Pathol* 159:893–903
 169. Schoppmann SF, Birner P, Stockl J, Kalt R, Ullrich R, Caucig C et al (2002) Tumor-associated macrophages express lymphatic endothelial growth factors and are related to peritumoral lymphangiogenesis. *Am J Pathol* 161:947–956
 170. Knowles HJ, Harris AL (2007) Macrophages and the hypoxic tumour microenvironment. *Front Biosci* 12:4298–4314. doi:[10.2741/2389](https://doi.org/10.2741/2389)
 171. Kaplan RN, Riba RD, Zacharoulis S, Bramley AH, Vincent L, Costa C et al (2005) VEGFR1-positive haematopoietic bone marrow progenitors initiate the pre-metastatic niche. *Nature* 438:820–827. doi:[10.1038/nature04186](https://doi.org/10.1038/nature04186)
 172. Hiratsuka S, Watanabe A, Aburatani H, Maru Y (2006) Tumour-mediated upregulation of chemoattractants and recruitment of myeloid cells predetermines lung metastasis. *Nat Cell Biol* 8:1369–1375. doi:[10.1038/ncb1507](https://doi.org/10.1038/ncb1507)
 173. Hiratsuka S, Nakamura K, Iwai S, Murakami M, Itoh T, Kijima H et al (2002) MMP9 induction by vascular endothelial growth factor receptor-1 is involved in lung-specific metastasis. *Cancer Cell* 2:289–300. doi:[10.1016/S1535-6108\(02\)00153-8](https://doi.org/10.1016/S1535-6108(02)00153-8)
 174. Chantrain CF, Shimada H, Jodele S, Groshen S, Ye W, Shalinsky DR et al (2004) Stromal matrix metalloproteinase-9 regulates the vascular architecture in neuroblastoma by promoting pericyte recruitment. *Cancer Res* 64:1675–1686. doi:[10.1158/0008-5472.CAN-03-0160](https://doi.org/10.1158/0008-5472.CAN-03-0160)
 175. Masson V, de la Ballina LR, Munaut C, Wielockx B, Jost M, Maillard C et al (2005) Contribution of host MMP-2 and MMP-9 to promote tumor vascularization and invasion of malignant keratinocytes. *FASEB J* 19:234–236
 176. Nelson CM, Jean RP, Tan JL, Liu WF, Sniadecki NJ, Spector AA et al (2005) Emergent patterns of growth controlled by multicellular form and mechanics. *Proc Natl Acad Sci USA* 102:11594–11599. doi:[10.1073/pnas.0502575102](https://doi.org/10.1073/pnas.0502575102)

A tense situation: forcing tumour progression

Darci T. Butcher*, Tamara Alliston^{†§||} and Valerie M. Weaver^{*§||†#}

Abstract | Cells within tissues are continuously exposed to physical forces including hydrostatic pressure, shear stress, and compression and tension forces. Cells dynamically adapt to force by modifying their behaviour and remodelling their microenvironment. They also sense these forces through mechanoreceptors and respond by exerting reciprocal actomyosin- and cytoskeletal-dependent cell-generated force by a process termed 'mechanoreciprocity'. Loss of mechanoreciprocity has been shown to promote the progression of disease, including cancer. Moreover, the mechanical properties of a tissue contribute to disease progression, compromise treatment and might also alter cancer risk. Thus, the changing force that cells experience needs to be considered when trying to understand the complex nature of tumorigenesis.

Force modulates cell fate and directs tissue development and post-natal function. Although we know much about the biochemical pathways that direct cell behaviour, by comparison we know less about how force can regulate cell fate and tissue phenotype. Nevertheless, cells in tissues such as the heart, lung and skeleton encounter nanoscale to macroscale forces that are integral to their function. The nature of these tissue-associated forces can be parallel, such as the shear stress induced by blood flow on a vessel wall, or perpendicular, such as the compressive or tensile stress induced by weight bearing on bone. In fact, all cells, including those incorporated into traditionally mechanically static tissues, such as the breast or the brain, are exposed to isometric force or tension that is generated locally at the nanoscale level by cell–cell or cell–extracellular matrix (ECM) interactions. These nanoscale forces influence cell function through actomyosin contractility and actin dynamics, and it is increasingly clear that force collaborates with biochemical cues to modulate cell and tissue behaviour.

In this Review we summarize the current understanding of tensional homeostasis in tissue development, homeostasis and cancer, and identify important areas for investigation. Defining the role of force on cell and tissue behaviour depends on understanding what contributes to force generation in the tissue, how the cell senses and integrates exogenous mechanical signals within its tissue microenvironment, and thereafter how the cell coordinates its response as part of a multicellular, organized tissue structure within its three-dimensional ECM microenvironment. To focus our Review, we have

detailed how force modulates the normal and malignant behaviour of mammary epithelial cells in the context of the breast, illustrating, where pertinent, major concepts with examples from experimental findings.

Forcing form and function

The importance of mechanical force in biological systems is illustrated by exploring its role in normal tissue development and function. The mechanical stress that a cell is subjected to is quantified in Pascals (Pa) and measured as force per unit area, or N per m² (BOX 1). This mechanical stress or force, in turn, is perceived and integrated in the cell at the molecular level through mechanically responsive sensors that interface with biochemical signalling cascades to elicit a specific cellular response through mechano-effectors. For example, force and growth factor receptor signalling can each influence cell growth, survival, motility, differentiation, shape and gene expression by regulating the activity of RhoGTPases that modulate actomyosin contractility and actin dynamics^{1–7}. Similarly, integrin-dependent extracellular-signal regulated kinase (Erk) signalling and focal adhesion assembly are regulated by both growth factor signalling and force from the ECM^{8,9} (BOX 2).

Force and embryogenesis. Force has a fundamental role in directing stem cell fate and in dictating embryonic development^{10–12}. For instance, embryonic stem cells progressively stiffen as cells differentiate¹³, whereas stem cell shape and specification are influenced by Rho-dependent contractility that is modulated by the

*Department of Surgery and Center for Bioengineering and Tissue Regeneration, University of California at San Francisco, San Francisco, California 94143, USA.

†Department of Orthopaedic Surgery, University of California at San Francisco, San Francisco, California 94143-0512, USA.

§Institute for Regenerative Medicine, University of California at San Francisco, San Francisco, California 94143, USA.

||Department of Bioengineering and Therapeutic Sciences, University of California at San Francisco, San Francisco, California 94143, USA.

#Department of Anatomy, University of California at San Francisco, San Francisco, California 94143, USA.

#Department of Bioengineering, University of Pennsylvania, Philadelphia, Pennsylvania 19104, USA. Correspondence to V.M.W. e-mail: Valerie.Weaver@ucsfmedctr.org
doi:10.1038/nrc2544

At a glance

- Cells within tissues are continuously exposed to physical forces, including hydrostatic pressure, shear stress and compression and tension forces. The nature of these forces can change in pathologies such as cardiovascular disease and cancer.
- Cells sense force through mechanoreceptors and, regardless of the type of force applied, cells respond by exerting reciprocal actomyosin- and cytoskeleton-dependent cell-generated force by a process termed mechanoreciprocity.
- Mechanoreciprocity maintains tensional homeostasis in the tissue and is necessary for development and tissue-specific differentiation. Its loss promotes disease progression, including liver fibrosis, atherosclerosis and cancer.
- Cells dynamically adapt to force by modifying their behaviour and remodelling their microenvironment. This adaptation probably involves a combination of epigenetic chromatin remodelling events and direct physical links between the matrix and nucleus that regulate gene expression. These gene-regulatory processes are altered in diseases such as cancer.
- Breast cancer is characterized by changes in cellular rheology and tissue level forces, a stiffening of the tissue and a progressive loss of tensional homeostasis that has been exploited to detect tumours. The mechanical properties of a tissue contribute to disease progression, compromise treatment and might also alter cancer risk.

mechanical properties of the tissue microenvironment^{3,5}. Indeed, mesenchymal stem cells undergo lineage selection in response to the elasticity of the matrix substrate. Soft matrices, similar to the brain, direct stem cells into a neurogenic lineage, whereas stiffer matrices, similar to muscle and newly deposited bone, direct them into myogenic and osteogenic lineages³. As development proceeds, tension fields mediated by cell compression that result from normal morphogenic movements also shape the embryo. Indeed, external micropipette-applied force, which mimics these developmental forces, drives nuclear translocation of the transcription factor Armadillo to activate the transcription of *twist*, which controls the formation of the dorsal–ventral axis in the early *Drosophila melanogaster* embryo¹⁴. Tissue development depends not only on the precisely timed application of force, but also on its correct spatial localization, as in the distinctly patterned tissue domains that specify cell polarity, shape and motility in the trunk and head mesoderm in *Xenopus laevis* embryos^{15,16}. By contrast, mislocalization of Rho and Rac, which regulate cell contractility, prevents blastula gastrulation^{15,16}.

Force is essential for normal tissue-specific development, in which it orchestrates tissue organization and function, and regulates cell growth, survival and migration. The lung epithelium, for example, undergoes branching morphogenesis as a result of progressive end bud enlargement and expansion to form the respiratory tree¹⁷. Interestingly, like the branching of the adolescent mammary gland, branch patterning in the lung epithelium is dictated by localized remodelling of the ECM and the corresponding stretching of lung epithelial cells at these locations. Force also regulates the integrity of the final lung ductal tree, which is governed by the cyclic shear stress of fetal breathing movements^{18,19}. Indeed, compromising Rho-dependent cytoskeletal tension perturbs basement membrane thickness, disrupts terminal bud formation and compromises lung epithelial duct organization²⁰.

Adult tissue homeostasis and the ECM. A balance of forces is required to maintain adult tissue homeostasis. Skeletal health depends on mechanical loading, such that exercise increases the proteoglycan content of articular cartilage whereas reduced mobility leads to loss of proteoglycan content and exacerbates arthritis-associated joint degeneration^{21,22}. Force also facilitates bone matrix deposition to accommodate skeletal loading such that immobilization of the organism, unilateral lower limb suspension or microgravity leads to loss of bone mineral density, which in turn compromises bone strength^{23,24}. Similarly, vascular function is largely determined by fluid shear stress^{25,26}. The shear stress induced by blood flow permits artery maturation by directing endothelial cells and their filamentous cytoskeletal networks to elongate and align with the direction of flow²⁷.

It is becoming increasingly apparent that each tissue has a characteristic ‘stiffness phenotype’ (FIG. 1) and that each cellular component within a tissue has a unique rheology and a stiffness optimum that can change over the course of development (as in lung branching morphogenesis), in response to function (as during mammary gland lactation) or in pathological situations (as in atherosclerotic plaque formation or in tumours)^{28,29}. Furthermore, the physical properties of the ECM and cellular rheology can profoundly influence cellular behaviours as diverse as differentiation, tissue organization and cell migration^{6,30–32}.

A cell within a tissue is subjected to isometric force through dynamic interactions with the ECM and its neighbouring cells, and these forces exert profound effects on cellular behaviour. For example, endothelial cells form branched capillary-like vessels when cultured within compliant gels, but form vessels with larger lumens in more rigid matrices. Compliance-dependent cell behaviour has also been observed in neural, muscle and mesenchymal cell populations. Therefore, ECM stiffness is an isometric force that exerts its effects gradually and chronically on cell behaviour, predominantly at the nanoscale level. An increase in ECM protein concentration, increased matrix crosslinking or parallel reorientation of matrix fibrils within a stromal matrix can stiffen a tissue locally to alter cell growth or direct cell migration, albeit to differing degrees. This phenomenon permits fine-tuning of cellular function within a heterogeneous tissue.

Interstitial collagens are major contributors to tissue materials properties. Collagens undergo a myriad of post-translational modifications, including matrix metalloproteinase (MMP)-dependent cleavage, glycosylation and crosslinking, that modify their tensile strength and viscoelasticity. During extracellular processing, collagen propeptides are cleaved by specific endoproteases. Thereafter, enzymes such as the lysyl oxidases (LOX) and the lysyl hydroxylases catalyse covalent intermolecular crosslinks between collagens and with elastin. LOX-mediated crosslinking increases insoluble matrix deposition, tissue tensile strength and matrix stiffness³³. However, chronically increased LOX activity increases collagen crosslinking and this can stiffen heart muscle to compromise cardiac function³⁴. Importantly, non-enzymatic collagen crosslinking, such as glycation

Rheology

The study of the deformation and flow of matter.

Viscoelasticity

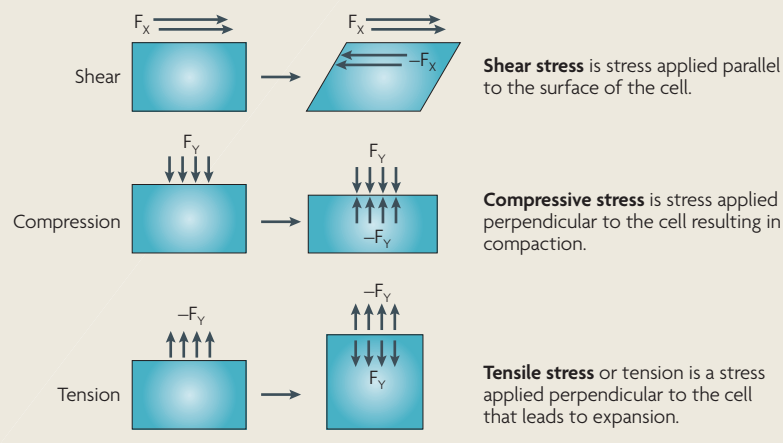
Soft biological tissues can be described as viscoelastic materials. A viscous fluid resists shear flow and strain linearly with time under stress. An elastic solid undergoes deformation under stress and rapidly returns to its original state. Viscoelastic biological materials exhibit characteristics of both a viscous fluid and an elastic solid.

Endoproteinase

An enzyme that proteolytically cleaves peptides at internal amino acids.

Box 1 | Types of forces experienced by a cell

Normal physiological processes expose cells to a variety of mechanical stimuli including hydrostatic pressure, shear, compression and tensile force. The right-hand images in the figure depict the balance of forces once equilibrium is achieved following the application of a mechanical force. Newton's third law states that for every action there is an equal and opposite reaction and, following this law, cells *in vivo* will respond to alterations in the mechanical properties of their surrounding matrix by adjusting their intracellular tension through the cytoskeletal network. Conversely, changes in cell tension will result in alterations in extracellular matrix (ECM) organization, thereby changing the mechanical properties of the ECM. Stress is defined as a normalized load, where the force or load is divided by the cross-sectional area available to support the load, and the units of stress are Newtons per square metre (N/m²) or Pascals (Pa). The deformation of a material in response to a given load varies with the geometry and the composition of the specimen. Strain is a normalized deformation, in which the change in length is divided by the original length of the specimen, and is a unitless quantity. We and others have previously measured the stiffness or Young's modulus of tissues *in vivo* and reported values in units of Pascals⁶. Soft biological tissues can be described as viscoelastic materials. A viscous fluid resists shear flow and strain linearly with time under stress. An elastic solid undergoes deformation under stress and rapidly returns to its original state. Viscoelastic biological materials exhibit the characteristics of both a viscous fluid and an elastic solid.



and transglutamination, or increased biglycan and fibromodulin proteoglycan levels also stiffen the matrix³⁵. The excessive deposition of proteoglycans in injured lungs contributes to fibrosis by stiffening the parenchyma³⁶, whereas inappropriate glycation-mediated crosslinking compromises wound healing and cardiac function in diabetic patients in whom glycation is increased owing to high blood glucose levels^{37,38}. Therefore, isometric and active forces have crucial roles in tissue behaviour. Force directs the differentiation of stem cells, drives the assembly of differentiated tissues and maintains tissue homeostasis.

Mechanotransduction and mechanoreciprocity

Given that cells are exposed to a myriad of active and isometric forces, it follows that cells must have derived an array of generic and specialized force-sensory mechanisms. Examples of specialized mechanosensors include the primary cilia in the hair cells of the inner ear and calcium-gated ion channels in cardiac muscle^{39,40}. Activation of stretch-activated potassium channels⁴¹, activation and oligomerization of transmembrane integrins, and remodelling of the cytoskeleton in response to shear flow are examples of conserved mechanosensory mechanisms⁴².

The current contention is that all force sensors directly undergo controllable molecular changes in response to force, regardless of their nature. This behaviour is illustrated by the sequential unfolding of p130Cas (also known as *BCAR1*) and conformational changes in the integrin-associated molecule *talin 1* in response to force^{43,44}. Elegant experiments demonstrated that direct application of a piconewton force can stimulate the mechanical extension of p130Cas, revealing a domain that is a substrate of Src family kinases^{45,46}. Phosphorylation by Src family kinases subsequently activates the small GTPase *RAP1* and initiates a sequence of events that propagates integrin signalling^{45,47}. Force-induced conformational changes in talin 1 also reveal a binding site for *vinculin*, and force can modify extracellular *fibronectin* to alter integrin adhesion⁴⁸, suggesting other plausible mechanisms by which force could link the ECM to the inside of the cell (FIG. 2a).

Once mechanical cues have been detected, cells must propagate and amplify the physical cue within the cell and translate the signal into either a transient response or sustained cellular behaviour. Integrins, by virtue of their extracellular interaction with the ECM and intracellular interaction with plaque proteins and the cytoskeleton, are an excellent example of one such ubiquitous mechanotransducer^{49,50} (FIG. 2a). Either exogenous or endogenous force can activate integrins, facilitate their nucleation and clustering, and drive their maturation into focal adhesions^{6,51-55}. Integrin oligomerization in turn facilitates RhoGTPase-dependent actomyosin contractility and cytoskeletal reinforcement⁶. Integrin clustering and cytoskeletal reinforcement lead to the phosphorylation of focal adhesion kinase (*FAK*) at tyrosine 397 (REF. 56), which stabilizes the focal adhesions through activation of small RhoGTPases and actin remodelling. The assembly of focal adhesions perpetuates downstream signalling through kinases and initiates cytoskeletal remodelling through the nucleation of an assortment of adhesion plaque proteins and signalling molecules, including Ras, Rac and Rho^{57,58}. Ras couples force-dependent integrin signalling to MAPKs including Erk, as has been illustrated in lung epithelial cells in response to mechanical strain⁵⁹ and increased Erk phosphorylation in endothelial cells in response to cyclic strain⁶⁰. Importantly, however, what has yet to be determined is whether any cellular or extracellular protein whose activated conformation can be enhanced by force constitutes a viable mechanosignalling mechanism and, if so, what then dictates mechanospecificity. Indeed, do mechanohierarchies exist?

Force-dependent activation of signalling cascades allows cells to respond quickly to a dynamic force environment, and the same pathways also lead to sustained changes in cell behaviour. Force-activated Erk cooperates with other kinases, such as Src and FAK, to induce cell proliferation or sustain cell survival⁶¹, as shown for MAPK-dependent growth of keratinocytes in response to mechanical stretch⁶² and the load-dependent survival of osteocytes⁶³. In addition to changes in cell growth and survival, compression stress affects microtubule dynamics⁶⁴ to induce quantifiable changes in cell shape,

Box 2 | Three-dimensional model systems to study the effect of force

Three-dimensional cell culture models offer a distinct advantage over conventional two-dimensional systems because they recapitulate both the architecture and the phenotypical behaviour of differentiated tissues with reasonable fidelity. Three-dimensional model systems can be used to study force and its effects on cell behaviour in the context of an organized tissue structure *in vitro*. These systems use primary or immortalized cells and natural or synthetic hydrogels (for example, collagen I, reconstituted basement membrane, alginate, agarose, synthetic peptides and polyacrylamide). By various means, protein and polysaccharide gels can be manipulated to modify their mechanical properties. An increase in the total protein concentration of protein gels, such as collagen or fibrin, results in an increased stiffness of the polymerized network. In this case, the elastic modulus has been approximated to be proportional to the square of the protein concentration¹⁸⁵. Free-floating or relaxed gels present a more compliant three-dimensional environment to cells than anchored or stressed gels and are more sensitive to cell force generation¹⁸⁶. Glycation by the addition of reducing sugars such as glucose or ribose results in non-enzymatic crosslinking of collagen fibres that can further stiffen the three-dimensional collagen gels¹⁸⁷. The stiffness of fibrin gels can be increased by the addition of salts at physiological pH or by activation of the plasma transglutaminase factor XIII^{188,189}. Altering the protein concentration to change gel stiffness can introduce additional variables into the model system. The use of polyacrylamide gels allows for precise control of the gel stiffness while maintaining ligand density and chemical content and changing either the bis-acrylamide (a polyacrylamide crosslinking agent) or the acrylamide components of the gel can alter the gel mechanics¹⁹⁰. Pelham and Wang pioneered polyacrylamide gels for cell culture less than 10 years ago and numerous investigators have used this model system with many different cell types to address the question of cell response to ECM force. This technique has proved exceptionally adaptable, such that gels of varying stiffness can be combined to resemble the mechanical properties of, for example, the alveolar basement membrane and breast stroma^{6,191}.

whereas *durotactic* gradients of ECM stiffness^{30,65} direct cell motility and the migration of fibroblasts and smooth muscle cells. In response to mechanical loading, fibroblasts synthesize and secrete many ECM proteins, including fibronectin, *tenascin* and collagen, and direct matrix remodelling through the expression, secretion and activation of MMPs and crosslinking enzymes. These sustained cellular responses to force must be coordinated. One factor implicated in this orchestrated response is transforming growth factor- β (TGF β). Mechanical force initiates post-translational activation of secreted TGF β from a latent complex into the functional ligand⁶⁶. TGF β , in turn, can stimulate the production of matrix proteins and matrix-modifying enzymes such as MMPs and LOX that dramatically alter the characteristics of the extracellular stroma⁶⁷. In extreme cases, chronic activation of TGF β can even induce tissue fibrosis and disease in soft tissues such as the liver and kidney⁶⁸. In this manner, cells can dramatically change the composition, topology and elasticity of their tissue microenvironment and alter their adhesions and cell shape and orientation to tune their behaviour according to the magnitude, direction and nature of applied mechanical stress.

Push-me-pull-you. Cells are not simply passive force recipients but also respond dynamically to externally applied force or stiff matrices with a proportional reciprocal cell-generated force. This reciprocal force response depends on actomyosin contractility and cytoskeletal remodelling. For instance, inside the cell, adaptor proteins associated with focal adhesions such as talin and

α -actinin directly link the cytoplasmic domains of β integrin subunits with actin filaments^{69,70}. Actin stress fibres polymerized at the focal adhesion act like viscoelastic cables and respond to the extracellular mechanical environment with myosin-induced cell contractility^{71,72}. Cells anchor to and pull on ECM fibrils, creating intracellular tension⁷³. This intracellular tension, which can be induced experimentally by local application of mechanical stress to the extracellular domains of integrins, redirects cytoskeletal reorganization and ultimately activates RhoGTPases to generate large traction forces that can be measured using traction force microscopy⁷⁴ (FIG. 2b,c). Such approaches have revealed that cell-generated force or mechanoreciprocity can profoundly influence cell behaviour by enhancing cell spreading, growth, survival and motility^{6,30,65}. Indeed, cellular tension and microrheology are finely tuned to the properties of their surrounding matrix, and the nature and magnitude of applied force they experience within their tissue microenvironment. The magnitude of cellular contractility reflects the cell type and state^{75,76}. For instance, cells on stiff substrates tolerate excision of a single stress fibre by exerting greater myosin-dependent force, whereas the same manipulation in cells grown on a compliant substrate disrupts the cellular force balance and cell shape⁷⁷. We have observed that normal mammary epithelial cells generate greater force and occupy more surface area on a stiff matrix (5,000 Pa) than similar cells interacting with a soft matrix of 140 Pa (FIG. 2b).

So, at the single cell level, cell-generated force can increase adhesion strength, enhance integrin-dependent signalling and drive cytoskeletal remodelling to change cell rheology and shape and modify cell behaviour. In multicellular tissues increased cell contractility can destabilize cell–cell adhesions and promote cell invasion to facilitate wound healing or drive MMP-dependent branching morphogenesis^{78,79}. As well as changing cell shape and behaviour, mechanical forces can also alter gene expression.

Gene expression and force

Changes in microenvironment or cell behaviour that permit the long-term adaptation to exogenous forces or alterations in matrix compliance require a change in gene expression. Integrin expression, for example, is much higher in fibroblasts and epithelial cells that are grown on rigid substrates than those that are grown on compliant gels, and the expression of $\alpha 5$ integrin is induced following sustained exposure to a stiffer matrix^{80,81}. So, how might force regulate gene expression? Many of the signalling networks that are activated in response to force, such as Erk and Jun N-terminal kinase (JNK), activate and induce nuclear translocation of transcription factors such as AP1, p53, signal transducer and activator of transcription 1 (STAT1), STAT3, MYC, CCAAT/enhancer-binding protein (C/EBP), cAMP response element-binding protein (CREB) and nuclear factor- κ B (NF- κ B)^{33,82–85}. Therefore, force probably modifies cell fate by altering the activity of various adhesion and growth factor-dependent transcriptional networks. However, acinar morphogenesis

Durotactic

Directed movement of cells up or down the stiffness gradient of a biomaterial.

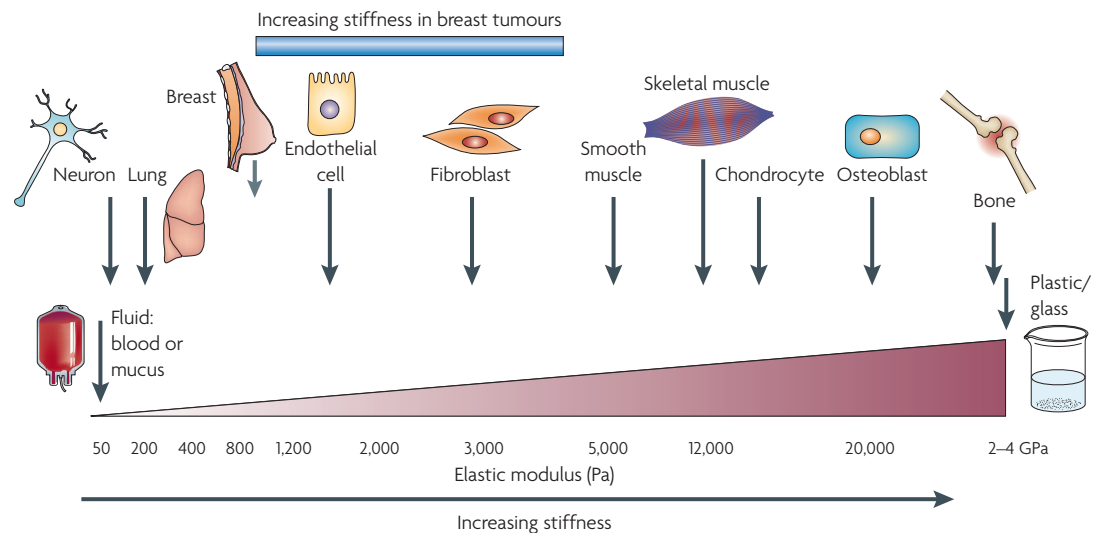


Figure 1 | Cells are tuned to the materials properties of their matrix. All cells, including those in traditionally mechanically static tissues, such as the breast or the brain, are exposed to isometric force or tension that is generated locally at the nanoscale level by cell–cell or cell–extracellular matrix interactions and that influences cell function through actomyosin contractility and actin dynamics. Moreover, each cell type is specifically tuned to the specific tissue in which it resides. The brain, for instance, is infinitely softer than bone tissue. Consequently, neural cell growth, survival and differentiation are favoured by a highly compliant matrix. By contrast, osteoblast differentiation and survival occurs optimally on stiffer extracellular matrices with material properties more similar to newly formed bone. Normal mammary epithelial cell growth, survival, differentiation and morphogenesis are optimally supported by interaction with a soft matrix. Following transformation, however, breast tissue becomes progressively stiffer and tumour cells become significantly more contractile and hyper-responsive to matrix compliance cues. Normalizing the tensional homeostasis of tumour cells, however, can revert them towards a non-malignant phenotype⁶, thereby illustrating the functional link between matrix materials properties, cellular tension and normal tissue behaviour. Importantly, however, although breast tumours are much stiffer than the normal breast, the materials properties of a breast tumour remain significantly softer than those of muscle or bone, emphasizing the critical association between tissue phenotype and matrix rigidity.

within a compliant reconstituted basement membrane (rBM) or in response to mechanical loading is associated with the repression and induction of hundreds of genes, and we determined that human mammary epithelial cells (HMEC) respond to matrix stiffness by altering the expression of at least 1,500 genes that span multiple functional categories⁸⁶ (K. C. Tsai *et al.*, unpublished data). Likewise, although we showed that breast tumour progression in the HMT-3522 human breast cancer model is associated with specific genomic alterations, the accompanying gene expression profile differs markedly between those cells grown on either a rigid tissue culture plastic or stiff rBM-conjugated polyacrylamide gels and those within compliant rBM or on soft rBM-conjugated polyacrylamide gels⁸⁷. This suggests that additional gene regulatory mechanisms, possibly linked to chromatin remodelling, must also be regulated by force.

A direct mechanical link from the ECM to nuclear chromatin could dynamically alter gene expression in response to exogenous force¹ through a solid-state signalling mechanism that is governed by the principles of ‘tensegrity’ (tensional integrity). The tensegrity model implies that integrins are linked to the nucleus through the cytoskeleton, that an applied force is transmitted to the DNA through the cytoskeleton by nuclear lamins and nuclear envelope receptor complexes, and that this then modulates gene expression by inducing

conformational changes in chromatin either by altering the nature of the protein complexes at the telomeres of chromosomes or by changing the activity of DNA remodelling enzymes^{88–92}. Support for this paradigm has come from studies demonstrating how application of force on the integrin–ECM interface can induce nuclear and chromatin distortion⁹³, that tension can alter DNA wrapping⁹⁴, and that spooled chromatin can be excised from the nucleus as a continuum that remains physically linked to the cytoskeleton and adhesion interface⁹⁵. Alternately, epigenetic changes regulate gene expression during embryogenesis and tissue-specific development. Given that force also modulates these processes, it follows that mechanotransduction might influence chromatin remodelling to regulate histone acetylation and methylation. For example, HMEC morphogenesis and differentiation in a compliant rBM but not on a stiff two-dimensional substrate is associated with pronounced chromatin remodelling, changes in histone deacetylase (HDAC) expression and activity, and increased expression of the methyl-CpG-binding protein *MECP2* (REFS 96,97) (Tsai *et al.*, unpublished data). In addition, we and others have found that rBM compliance dictates the response of differentiated HMEC acini to the methylation inhibitor *5-azacytidine* or the HDAC inhibitor trichostatin A. Only on compliant matrices do these inhibitors induce gene expression to sensitize a mammary epithelium to exogenous growth and death

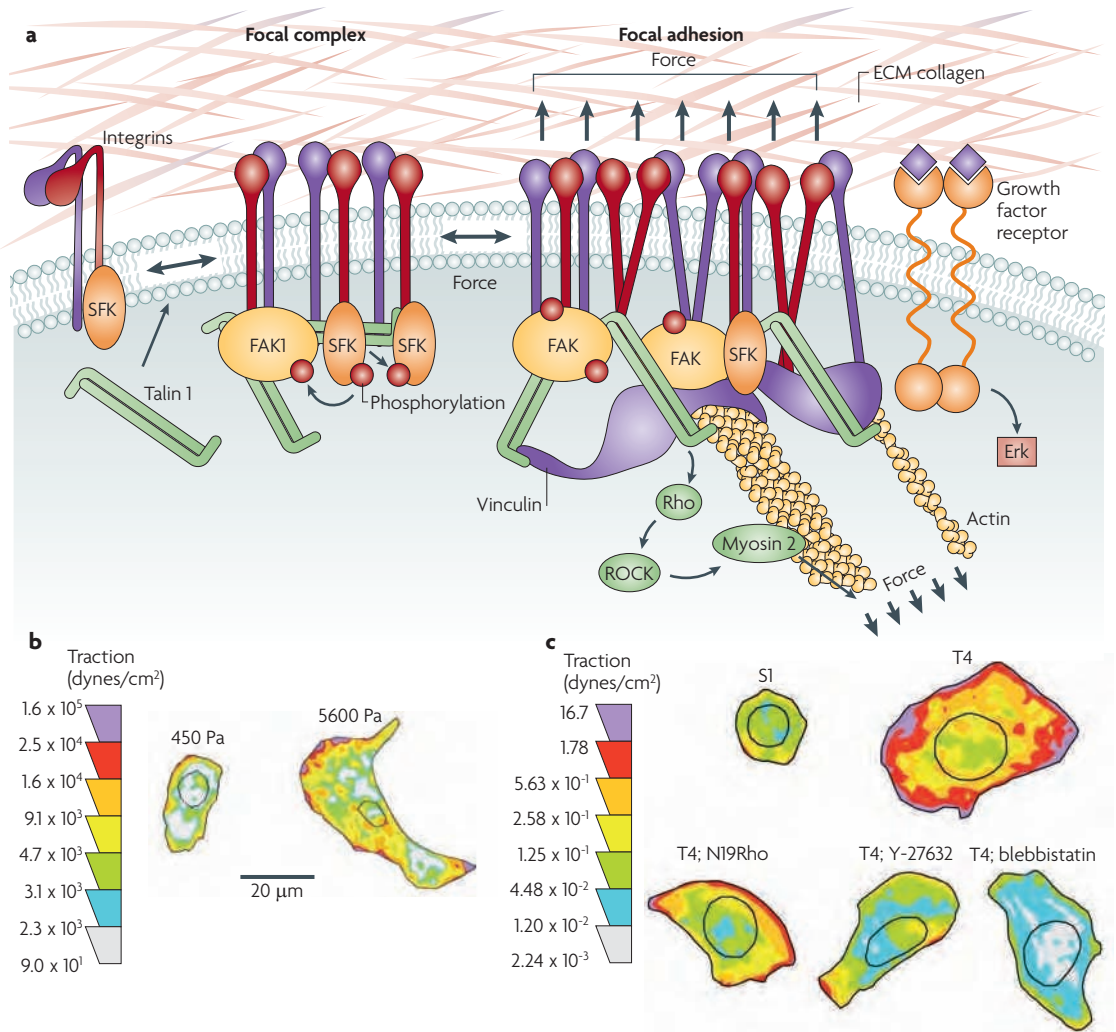


Figure 2 | Mechanotransduction and focal adhesion maturation. a | The majority of integrins exist at the plasma membrane in a resting, inactive state in which they can be activated by inside–out or outside–in cues. With regard to outside–in activation, when cells encounter a mechanically rigid matrix or are exposed to an exogenous force integrins become activated, which favours integrin oligomerization or clustering, talin 1 and p130Cas protein unfolding, vinculin–talin association, and Src and focal adhesion kinase (FAK) stimulation of RhoGTPase-dependent actomyosin contractility and actin remodelling. Focal adhesions mature with the recruitment of a repertoire of adhesion plaque proteins, including α -actinin to facilitate actin association, and adaptor proteins such as *paxillin*, which foster interactions between multiple signalling complexes to promote growth, migration and differentiation. **b** | Normal cells tune their contractility in response to matrix stiffness cues, but tumours exhibit altered tensional homeostasis. Cells exert actomyosin contractility and cytoskeleton-dependent force in response to matrix stiffness cues. These forces can be measured using traction force microscopy. Thus, non-malignant human mammary epithelial cells spread more and exert more force on a stiff matrix than on a soft matrix. **c** | By comparison, breast tumour cells (T4) are highly contractile and spread considerably more than their non-malignant counterparts (S1) in response to the same compliant matrix. Importantly, inhibiting RhoGTPase signalling in tumour cells, by expressing a dominant-negative N19Rho or treating tumours with an inhibitor of Rho-associated, coiled-coil-containing protein kinase (ROCK; Y-27632) or myosin 2 (blebbistatin), reduces tumour cell contractility and spreading to levels exhibited by non-malignant breast epithelial cells. These data illustrate the importance of Rho signalling and actomyosin contractility in cell force generation and show how transformation alters cell force sensing. The traction map is shown in pseudocolour indicating regions of low (grey) and high (purple) forces in dynes per cm^2 . ECM, extracellular matrix; SFK, Src family kinase. Reproduced, with permission, from REF. 6 © (2005) Elsevier Inc.

stimuli, coincident with a disruption of morphology and cytoskeletal organization^{96,97} (K. Levental, V.M.W. and N. Zahir, unpublished observations). These results indirectly implicate the properties of matrix materials in the control of cell shape, cytoskeleton morphology and chromatin remodelling.

Several studies have highlighted the interactions between force, Rho signalling, cell shape and histone acetylation^{98,99}. Adhesion-induced changes in HMEC shape are associated with altered actin organization, RhoGTPase activity, actomyosin contractility and modified global patterns of chromatin histone acetylation^{6,100}.

Similarly, modifying fibroblast adhesion and changing cell shape alters cytoskeletal organization and shrinks the nucleus and nuclear lamina of cultured cells. These changes in the cytoskeleton and nuclear morphology are associated with impaired polymerase access to chromosomal territories and a concomitant reduction in gene transcription^{91,101–103}. More convincingly, Rho-family GTPases indirectly regulate histone H4 acetylation by shifting the balance of cellular and nuclear pools of F and G actin, which in turn, modifies the association between serum response factor (SRF) and its co-activator MAL (also known as MKL1)^{104–106}. These and other data argue convincingly that mechanical force regulates gene expression to alter cell behaviour either by directly altering the DNA or by modulating the function of chromatin remodelling molecules. The current challenge facing biologists then is to delineate the molecular mechanisms underlying these provocative phenomenological observations.

Changes in mechanical stress and cancer

Loss of tissue homeostasis is a hallmark of disease. Given the pluripotent role of force in tissue function, it is not surprising that multiple pathologies, including cancer, are characterized by compromised tensional homeostasis^{6,68,107}. Indeed, tumours are often detected as a palpable ‘stiffening’ of the tissue, and approaches such as magnetic resonance imaging elastography and sono-elastography have been developed to exploit this observation to enhance cancer detection^{108,109}. More provocatively, altered stromal–epithelial interactions precede and can even contribute to malignant transformation (K. Levantal and V.M.W., unpublished observations), and the desmoplastic stroma that is present in many solid tumours is typically significantly stiffer than normal⁶. This raises the interesting possibility that preventing tissue stiffening could impede cancer progression, and that genetically susceptible individuals predisposed to matrix stiffening might be at greater risk for tumours and could benefit from enhanced screening programmes^{37,110,111}. To discuss these ideas further, we focus on the role of mechanical stimuli in the regulation of normal breast development and the implications these have for breast cancer.

The mechanics of mammary morphogenesis and maintenance. Force modulates all stages of breast development and is vital to the proper functioning of the differentiated tissue. Together with hormonal and growth cues, force specifies the architecture of the mature ductal tree and mediates efficient delivery of milk to the young. In mammals the breast is the source of nutrients and passive immunity for the offspring, so abnormalities in tensional homeostasis not only impair the structural organization and health of the tissue, but could also compromise the survival of the species. As such, understanding how force orchestrates the behaviour of such a crucial tissue as the breast should provide insight into how mechanics regulates the behaviour of other seemingly mechanically inert tissues.

The mammary gland comprises an organized ductal tree consisting of a single polarized layer of luminal epithelial cells that interact at their basal surface with a network of contractile myoepithelial cells (FIG. 3). Each intralobular ductal tree terminates in a cluster of alveoli, which comprise the basic structural unit of the breast. It is this basic acini unit that will differentiate to produce milk on exposure to lactogenic hormones¹¹². Surrounding the ducts and alveoli of each lobule is the intralobular stroma, which is a loose connective tissue containing microvasculature, small lymphatic channels, adipocytes, resident fibroblasts and inflammatory cells¹¹³. Adjacent to and encompassing the intralobular stroma and ductal network is the interstitial stroma, which comprises over 80% of the human breast volume^{114,115}. Unlike the loose and cellular intralobular stroma, the connective tissue of the interstitial stroma is dense, less cellular and contains variable proportions of ECM and adipose tissue.

A highly organized ECM supports the tissue and cellular level architecture of the breast. Collagen IV, heparin proteoglycans, perlecan and various laminin isoforms comprise the basement membrane that surrounds the mammary epithelial cell (MEC) bilayer. Together these provide mechanical stress shielding that is crucial for functional integrity of the ductal tree^{116,117}. The intralobular stromal matrix, which surrounds the ductal tree, is secreted primarily by stromal fibroblasts and is composed of structural matrix proteins — including collagens I and III, elastin, proteoglycans, glycosaminoglycans and glycoproteins — that interact to form a large complex network in the extracellular space that is contiguous with the basement membrane¹¹⁸. The organization, concentration and crosslinking of the structural components of the basement membrane and the intralobular matrix contribute to their material properties¹¹⁹. Together, the basement membrane, intralobular matrix and interstitial stroma are a continuum that cooperates to define the form and function of the breast through their ability to act as a physical scaffold, to function as a repository for growth factors and cytokines, and to provide specific biochemical and tensional cues through specialized cellular receptors. Thus, the ECM can be considered a highway by which MECs are able to communicate with one another and with stromal cells locally and distally through biochemical and mechanical cues.

Forces that operate from the nanoscale to the macroscale facilitate normal functioning of the differentiated breast. The nature and magnitude of these forces reflect the organization, composition, topology and post-translational modification state of the ECM and the organization of the ductal tree. Thus, the matrix surrounding the large ducts is more linear and stiffer, whereas the collagen surrounding the terminal ductal units is more relaxed and the matrix is more compliant (K. Levantal and V.M.W., unpublished observations). During lactation, the breast is subjected to compressive stress on the luminal and myoepithelial cells and the basement membrane owing to the accumulation of milk and distension of the ducts, which is facilitated by the highly compliant, relaxed collagen matrix surrounding the differentiated acini. Upon suckling, the luminal epithelial

Desmoplastic stroma
Stromal tissue responds to tumour cells with a characteristic desmoplasia resulting from fibroblast recruitment, collagen deposition and angiogenesis.

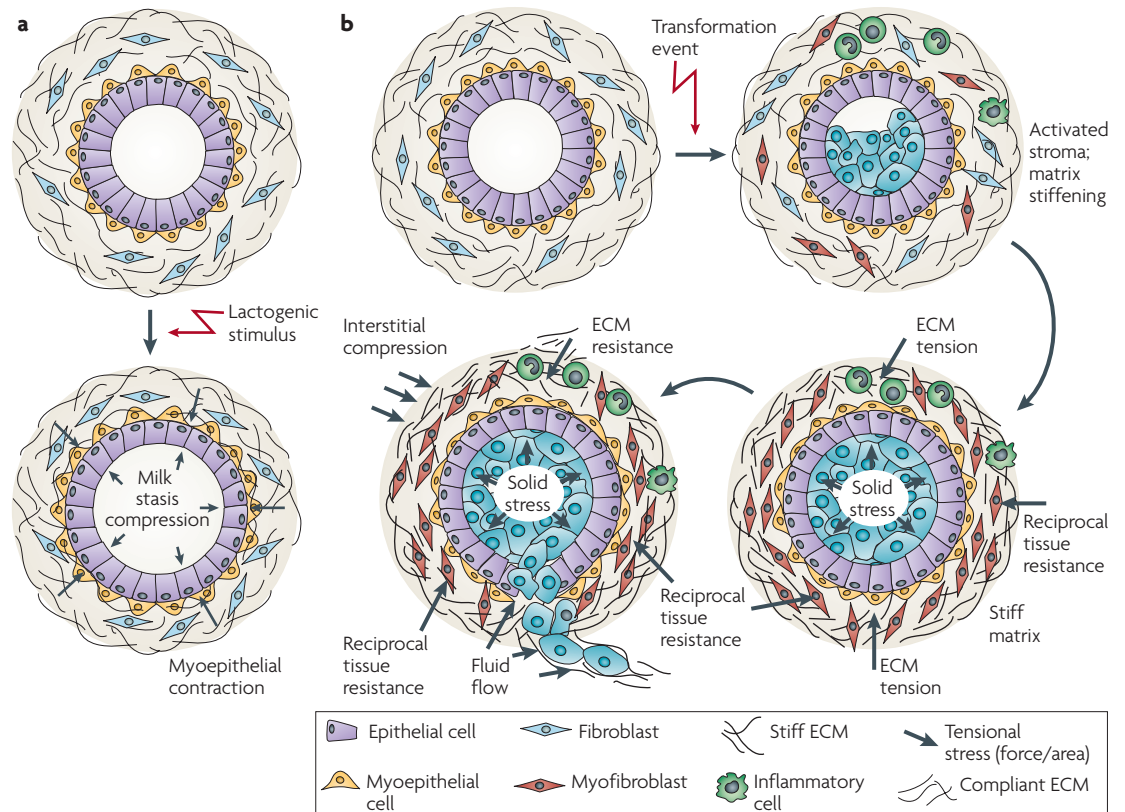


Figure 3 | The normal mammary gland as a mechanically active tissue. a | The developing breast is subjected to a number of forces that facilitate its normal function. During lactation, for instance, the normal breast experiences compressive stress on the luminal epithelial cells and the basement membrane owing to the accumulation of milk and alveolar distension. Upon sucking and oxytocin stimulation, epithelial cells encounter inward tensile stress as the myoepithelium contracts to force the milk out of the alveolar sacs. In the absence of this stimulus, milk will accumulate within the acinus and eventually exert an outward projecting compressive force on the surrounding epithelium. This compressive force is countered by a compensatory inward projecting resistance force and the combination of these two forces eventually compromises the integrity of the tight junctions between alveolar cells. Chronic exposure to these forces and perturbed tissue integrin sensitize the gland to apoptotic cues so that the gland undergoes involution accompanied by extensive remodelling of the epithelium and the cellular and extracellular components of the stroma. **b** | Transformation (blue cells) resulting from the accumulation of genetic and epigenetic alterations in the epithelium along with an altered stromal matrix leads to unchecked proliferation and enhanced survival of luminal epithelial cells within the ductal tree, which compromises normal ductal architecture. With prolonged growth and abnormal survival, the abnormal pre-neoplastic luminal mammary epithelial cells eventually expand to fill the breast ducts. The expanding luminal epithelial mass exerts outward projecting compression forces of increasing magnitude on the basement membrane and adjacent myoepithelium. These forces are countered by an inward projecting resistance force. Importantly, the pre-neoplastic lesion secretes a plethora of soluble factors that stimulate immune cell infiltration and activation of resident fibroblasts to induce a desmoplastic response in the breast stroma. The desmoplastic stroma, which is characterized by dramatic changes in the composition, post-translational modifications and topology of the extracellular matrix (ECM), stiffens over time. This rigid parenchyma exerts a progressively greater inward projecting resistance force on the expanding pre-neoplastic duct. Over time, the number of myoepithelial cells surrounding the pre-neoplastic mass decreases and the basement membrane thins, probably owing to increased matrix metalloproteinase (MMP) activity, decreased protein deposition and compromised assembly (adapted from REF. 128). In parallel, there is a build-up of interstitial fluid pressure contributed by a leaky vasculature and compromised lymphatic drainage. In response to their genetic modifications and the altered materials properties of the matrix, the pre-neoplastic luminal epithelial cells exhibit modified tensional homeostasis and respond to the combination of forces and stromal cues to invade the breast parenchyma. Some resident fibroblasts transdifferentiate into myofibroblasts and facilitate tumour migration and invasion by promoting the assembly of linearized collagen fibrils surrounding the distended pre-neoplastic epithelial ducts.

cells encounter inward projecting tensile stress as the myoepithelium contracts in response to oxytocin to force the milk out of the aveolar sacs and into the larger ducts to facilitate efficient feeding of the young. In the absence of the suckling stimulus, lactation ceases and milk accumulates within the acini, slowly exerting an outwardly

projecting compressive force of increasing magnitude on the surrounding luminal epithelium and myoepithelium. With prolonged milk stasis and continued gland distension, this compressive force eventually compromises the integrity of the tight junctions between luminal alveolar cells, and the gland undergoes involution accompanied

by extensive remodelling of the cellular and extracellular stroma^{120,121}. Importantly, gland remodelling dramatically changes the composition and architecture of the stroma. The remodelled stroma consequently alters the signals and the force encountered by the MECs within the ducts and by so doing sets the stage for a subsequent round of epithelial proliferation and differentiation¹²². For example, primary cultures of murine MECs form polarized mammary acini with an endogenous basement membrane and differentiate in response to lactogenic hormones when embedded within a floating collagen gel. By contrast, these same cells will spread and continue proliferating in response to identical stimuli when interacting with a stiff two-dimensional scaffold or incorporated into a mechanically loaded collagen gel¹²³. Similarly, immortalized MECs fail to express one of the major milk proteins, β -casein, unless they interact with a compliant basement membrane^{123–125}.

The crucial role of matrix compliance in MEC morphogenesis was illustrated by studies using matrices with defined viscoelastic properties. HMECs embedded within collagen-rBM gels or interacting with rBM-crosslinked polyacrylamide gels with matrix compliance comparable to the normal murine mammary gland proliferated until they formed growth-arrested, polarized mammary acinus-like structures with a central lumen and an external endogenous basement membrane. When the matrix is progressively stiffened, cell growth is enhanced, cell-cell junction integrity is compromised and lumen formation is impeded. MECs interacting with the most rigid matrices form continuously growing, non-polarized, disorganized and invasive colonies that lack detectable cell-cell junction proteins and exhibit irregular cell shapes with detectable actin stress fibres. Whereas MECs interacting with the highly compliant matrix form nascent focal contacts, those within the stiff gels assemble mature focal adhesions with active FAK phosphorylated on Tyr397, vinculin and p130Cas (REF. 6). Importantly, when MECs engineered to express a constitutively active V14Rho or a mutant V737N integrin that promotes integrin clustering interact with a compliant basement membrane, they exert higher contractility, assemble focal adhesions and display tissue phenotypes characteristic of MECs interacting with a stiff matrix. Such observations underscore the importance of integrin signalling and Rho-dependent actomyosin contractility in multicellular tissue morphogenesis. This work also highlights the central role of active and isometric force in the functional integrity of soft tissues such as the breast, where small changes in matrix stiffness or mechanical cues can profoundly alter cell behaviour.

Cancer: forcing transformation. Epithelial cancers are characterized by an altered tissue tensional homeostasis that reflects differences in rheology and increased cell-generated force in the transformed cells^{126–128}, increased compression force due to the solid state pressure exerted by the expanding tumour mass¹²⁹, matrix stiffening due to the desmoplastic response⁶, and increased interstitial pressure due a leaky vasculature and poor lymphatic drainage¹³⁰. For instance,

transformed epithelial cells express vastly different intermediate filament profiles and cytoarchitecture to normal cells and consequently have an altered microrheology that could provide a distinct advantage to the cell during intravasation and extravasation of the vasculature, thereby facilitating cancer metastasis^{29,128,130}. Transformed cells also show compromised mechanoreciprocity such that they often exert abnormally high force in response to a compliant matrix and these increased cell-generated forces disrupt cell-cell junction integrity, compromise tissue polarity, promote anchorage-independent survival and enhance invasion (FIG. 4). It is also plausible that altered cellular force could account for the increased invadopodia⁶ observed in transformed, invasive cells¹³¹. Increased cell contractility probably reflects increased expression and activity of RhoGTPases and Rho-associated, coiled-coil-containing protein kinase 1 (ROCK1), as well as high levels of growth factor-induced Erk activity. The increased cell-generated forces exhibited by tumours enhance their growth, survival and invasion by promoting focal adhesion maturation and signalling through actomyosin contractility^{6,128,130,132–135}. The increased contractility of tumour cells and their associated stromal fibroblasts also induce tension-dependent matrix remodelling to promote the linear reorientation of collagen fibrils surrounding the invasive front of the tumour^{136,137}. Rapidly migrating transformed mammary epithelial cells have been observed on prominent linear bundles of collagen fibres adjacent to blood vessels^{138–140}.

The expanding tumour mass exerts compressive stress on the surrounding tissue extracellular matrix, vasculature, lymphatics and interstitial space. The solid stress induced by tumour expansion could also promote tumour progression. For example, tumours in soft tissues such as the pancreas typically show compromised laminin and type IV collagen basement membrane organization and thinning that, when combined with outward projecting compression force, facilitates tumour cell invasion into the parenchyma^{6,141} (FIG. 3). Tumour-associated compression stress can induce tumour angiogenesis by directly increasing expression of vascular endothelial growth factor A (VEGFA) or by indirectly blocking the existing vasculature surrounding the tumour mass to promote hypoxia and VEGFA secretion^{142,143}. In addition, compression can increase the interstitial pressure in the tumour to up to 10× that of normal tissue. This pressure induces the accumulation of fluid from leaky blood and lymphatic vessels^{144,145}. Compression force can also shrink the interstitial space surrounding the ductal structures, which increases the local concentration of growth factors and cytokines to facilitate autocrine and paracrine signalling and promote tumour growth¹⁴⁶. Tumour-associated changes in interstitial pressure and compressive stress also present real challenges for the treatment of solid tumours with chemotherapeutic drugs¹⁴⁷.

Breast cancer progression is accompanied by a desmoplastic response that includes inflammatory cell infiltration, angiogenesis, fibroblast

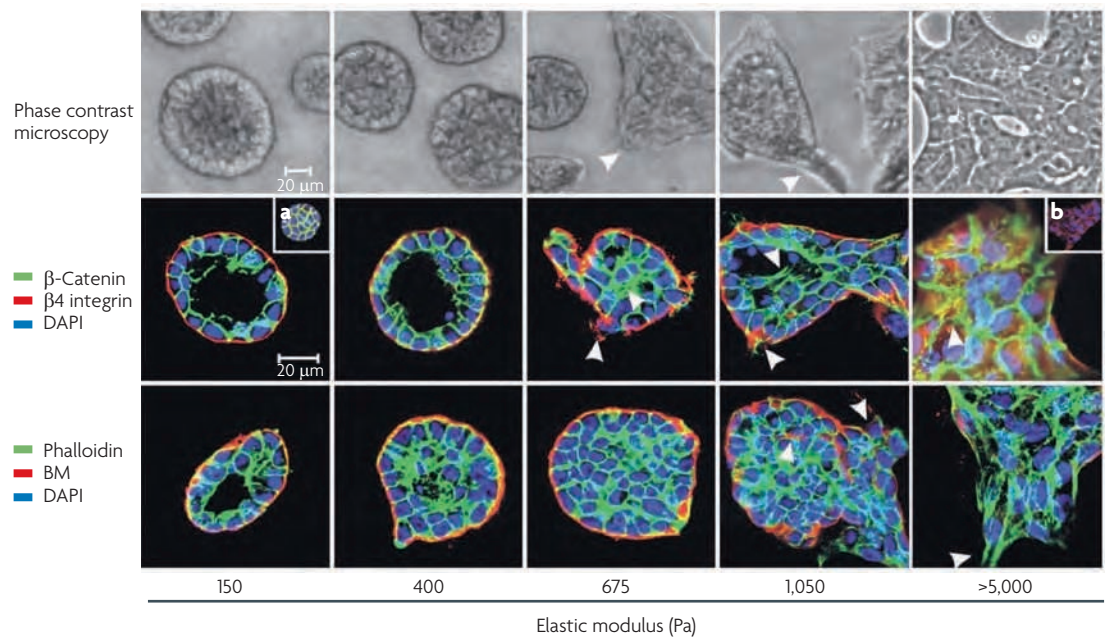


Figure 4 | Matrix stiffness modulates cellular morphology and epidermal growth factor (EGF)-dependent growth. Phase contrast microscopy and confocal immunofluorescence images of non-malignant immortalized human mammary epithelial cell (HMEC; MCF10A) colonies interacting with a three-dimensional reconstituted basement membrane (BM)-laminated polyacrylamide gel of increasing stiffness (150–5,000 Pa) showing colony morphogenesis after 20 days of culture. On compliant gels with materials properties similar to that measured in the normal murine mammary gland (150 Pa) non-malignant MECs proliferate for 6–12 days to eventually form growth-arrested, polarized acini analogous to the terminal ductal lobular units observed at the end buds of the differentiated breast. These structures have intact adherens junctions and insoluble cell–cell localized β -catenin before (main images) and after (inset a) Triton extraction, and polarity, as shown by the basal localization of $(\alpha 6)$ $\beta 4$ integrin, the apical–lateral localization of cortical actin (Phalloidin), and the assembly of an endogenous laminin 5 basement membrane. Incremental stiffening of the basement membrane gel progressively compromises tissue morphogenesis and alters EGF-dependent growth of these cells. Thus, colony size progressively increases with matrix stiffening, lumen formation is compromised, cell–cell junctions are disrupted, as revealed by loss of cell–cell-associated β -catenin (inset b), and tissue polarity is inhibited, as indicated by disorganized $(\alpha 6)$ $\beta 4$ integrin localization and loss of the endogenous laminin 5 basement membrane. Interestingly, actin stress fibres were not observed in the structures until the stiffness of the matrix reached 5,000 Pa, as has been observed in murine breast tumours *in vivo*⁶. The arrows indicate loss of the endogenous basement membrane and disruption of basal polarity. Reproduced, with permission, from REF. 6 © (2005) Elsevier Inc.

transdifferentiation and changes in ECM composition, integrity and topology^{114,148,149}. The ECM remodelling observed in tumours includes increased deposition of fibronectin, tenascin, collagen types I, III and IV, and proteoglycans^{150–152}, substantial MMP-dependent cleavage and increased levels of LOX-dependent matrix crosslinking^{33,153}. In the normal breast, tightly controlled MMPs remodel the ECM to promote mammary gland growth or involution. In tumours, however, this stringent control of MMP expression and function is lost¹⁵⁴. Overexpression of *MMP3*, *MMP11*, *MMP12* and *MMP13* have each been demonstrated in the tumour stroma, along with *MMP2* in the transformed mammary epithelial cells¹⁵⁵. Moreover, aberrant MMP activity is not merely symptomatic of a transformed tissue but rather has a causative role, as illustrated by the observation that polymorphisms in the human *MMP3* promoter that increase its expression are associated with an increased tumour incidence¹⁵⁶. Likewise, transgenic mice that overexpress *MMP3* displayed marked desmoplasia and precocious branching of the mammary epithelium, and developed

tumours with marked genetic abnormalities¹⁵⁷. However, tumour progression is also associated with substantial post-translational modifications of matrix proteins including altered deposition of proteoglycans and increased expression and activity of collagen crosslinking enzymes such as *LOX* and *LOXL*^{158,159}. We showed that experimentally induced breast tumour progression in transgenic mice is accompanied by a significant increase in reversible and irreversible collagen crosslinking, increased expression of *LOX* and an incremental increase in tissue and ECM stiffness (K. Levental *et al.*, unpublished information). Inducing collagen crosslinking and stiffening either in three-dimensional collagen hydrogels or *in vivo* in a modified breast stroma promoted MEC transformation that was associated with increased mechanosignalling. Provocatively, inhibiting LOX-dependent collagen crosslinking tempered tissue desmoplasia, decreased tumour incidence, reduced tumour growth and reduced mechanotransduction in the mammary epithelium; thereby directly implicating changes in the properties of matrix materials in tumour evolution.

Tumour evolution is accompanied by dramatic changes in interstitial pressure and fluid flow. Fluid flow dynamics within soft tumour tissues has largely been ignored but is especially relevant to tissue development and tumour metastasis and for optimal treatment efficacy¹⁴⁵. For instance, fluid flow facilitates lymphatic clearance and induces cytokine differentials that promote cell motility and invasion through the creation of chemotactic C-C chemokine receptor 7 (CCR7) gradients that are highly important for cancer cell metastasis through the lymphatics¹⁶⁰. The increased interstitial pressure in an epithelial tumour mass, with fluids accumulating from leaky blood vessels and impaired lymphatic drainage, can greatly impede the delivery of tumour therapies¹³⁰. Clearly, tumour cells are exposed to a myriad of altered mechanical forces that could dramatically modify their behaviour. A better understanding of how these force cues regulate tumour progression and metastasis and affect cancer therapy could significantly aid the development of improved treatments¹⁶¹.

Breast density and age: a new perspective

Clinicians have long recognized that there is a connection between breast density and breast cancer risk^{6,162–164}. Increased mammographic density for instance, is associated with a four- to six-fold increase in the relative risk of developing breast cancer^{165,166}. Unfortunately, however, deciphering the functional relationship between mammographic density and breast transformation has proved quite challenging^{111,167}. For instance, although dense breasts have more collagen and increased cell density (reflected by a greater nuclear area), other factors such as altered levels of the tissue inhibitor of metalloprotease 3 (TIMP3) and insulin-like growth factor I (IGFI) are also associated with mammographic density and need

to be considered^{165,168,169}. In fact, the composition of the ECM differs in women with dense breasts, such that the proteoglycans *lumican* and *decorin* are often disproportionately increased in women with mammographically dense breasts^{165,169}. Proteoglycan deposition often precedes fibrosis and may enhance tissue inflammation, raising the intriguing possibility that women with mammographically dense breasts could be more susceptible to chronic inflammation¹⁷⁰. Interestingly, proteoglycans such as lumican and *biglycan* not only bind growth factors and maintain tissue hydration but also contribute crucially to the mechanical integrity of the stroma, suggesting that in some instances mammographic density could reflect a stiffer breast parenchyma^{36,171}. Given that matrix stiffness can modify cell and tissue behaviour by altering adhesion and growth factor receptor signalling and cytoskeletal dynamics to change cell shape and tissue organization, it seems reasonable to predict that the increased breast cancer risk associated with dense breasts could be attributed in some instances to an aberrant tensional homeostasis in these tissues. In this regard, sonoelastography, which measures the stiffness of a tissue in real time *in situ*, might offer a tractable auxiliary screening strategy to diagnose high-risk women who are identified initially using imaging mammography¹⁷² (FIG. 5).

As women age, mammographic density decreases yet cancer incidence rises^{169,173}. Indeed, the post-menopausal breast has proportionately less collagen and more fatty tissue than the young breast, implying that older breast tissue must be softer¹⁶⁹. Consistently, in old skin and bone, collagen deposition decreases and MMP-dependent degradation increases, and old bone and skin are mechanically weaker than their younger tissue counterparts^{174,175}. How can we reconcile this seeming paradox between the increased cancer risk with age and the decreased mechanical strength of tissues? One explanation is that ageing is associated with a disproportionate increase in inappropriate post-translational modifications of ECM proteins, including increased collagen glycation and ultraviolet crosslinking, yielding old tissue matrices with less total collagen but a greater amount of disorganized collagen fibrils than young tissues. Consistently, although old skin has lower tensile properties (that is, is mechanically weaker) it is paradoxically stiffer (less elastic) and less functional than young skin^{176,177}. Wound healing in old skin is severely compromised, which could be attributed to altered mechanical properties of the extracellular collagens^{178,179}. Therefore, there is a positive association between age, matrix stiffening, aberrant matrix crosslinking and increased cancer incidence. Although the post-menopausal breast has less collagen, the collagen may be less mechanically elastic, stiffer, more disorganized and less functional, a possibility that now needs to be examined.

These findings underscore the need to understand the complex relationship between matrix remodelling and topology, and cell and tissue behaviour. Indeed, although hormone replacement therapy can increase breast density and *tamoxifen* treatment can reduce breast density, these mammographic changes do not

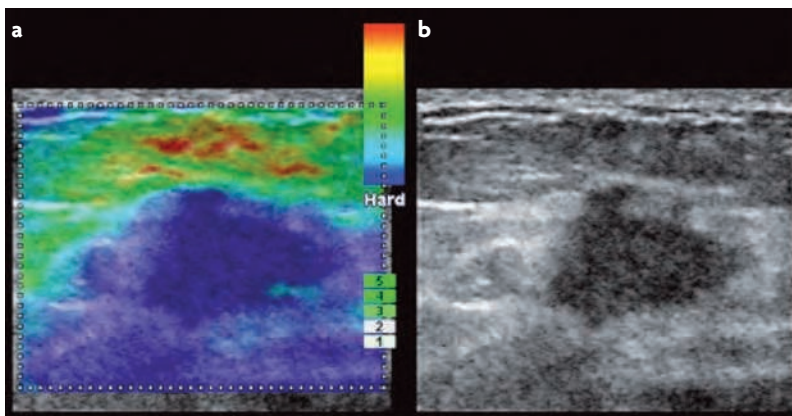


Figure 5 | Imaging elastography of a breast tumour. Tissue imaging elastography is a spatial 'visual' qualitative measurement of the stiffness of a tissue that is generated by extrapolating tissue viscoelastic characteristics from ultrasound wave reflection in real-time. Photographs of sonoelastography images compare an elastogram image (a) with a B mode ultrasound scan (b) of a breast tumour¹⁷⁰. Ultrasound imaging elastography, as shown here, is an *in situ* mechanical imaging method that could improve the sensitivity and the specificity of breast cancer detection and may be a useful tool to advance our understanding of the link between mammographic density and the matrix materials properties of the breast. Image courtesy of A. Thomas & T. Fischer, Charité, Berlin, Germany.

always reflect modified cancer risk, emphasizing our need to develop additional metrics to understand the relationship between ECM remodelling and tissue phenotype^{23,180}. Such insight would be highly beneficial for clarifying those issues encountered with the recent clinical trials of MMP inhibitors in cancer treatment¹⁸¹.

Summary

Realizing that force is a crucial determinant of tissue development, cell differentiation and homeostasis leads us to conclude that the loss of the ability to sense, respond and adapt appropriately to force contributes to disease. Indeed, we and others showed that pathological changes in cells and in the architecture, topology and material properties of their matrix microenvironments constitutes a positive feedback loop that propels carcinogenesis and other diseases. However, many questions still need to be resolved. Such issues include how the unique material properties of specific differentiated tissues are established and maintained, how cells coordinate their function and adaptation to external cues with their microenvironments, and how physical signals might interface with and modulate the activity of biochemical signalling pathways. Addressing these questions is particularly important if we are to understand lethal processes such as tumour metastasis, which clearly is profoundly influenced by the primary

tissue microenvironment. Metastasis is also acutely regulated by the inherent cellular rheology and the forces that the cells experience during their metastatic spread, and is chronically regulated by the material properties of their targeted distal metastatic niche^{29,182}. It may be that this niche is defined by proteins such as LOX or TGFβ, which have the capacity to modify tumour cell adhesion and the material properties of ECM in tissues targeted by these cells, respectively^{183,184}. In this regard, recent work suggests that tumour cells select their metastatic microenvironments in part through compliance matching but also by pre-conditioning their metastatic niche. This raises a number of intriguing questions, including defining the part that mechanical force might play in modulating the function of tumour stem cells, why specific tumour types characteristically metastasize to distinct tissues, and whether tumour cells might be mechanically pre-conditioning their metastatic sites. Clearly, addressing such outstanding issues falls outside the realm of traditional cell biology approaches and instead requires the cooperative effort of biologists, materials scientists, physicists and engineers. Indeed, this exciting force ‘frontier’ is fertile territory for scientific exploration of development and cancer biology that will undoubtedly yield new insights into cancer evolution and identify novel anticancer therapeutic targets.

1. Gieni, R. S. & Hendzel, M. J. Mechanotransduction from the ECM to the genome: are the pieces now in place? *J. Cell Biochem.* **104**, 1964–1987 (2008).
2. Engler, A. J. *et al.* Myotubes differentiate optimally on substrates with tissue-like stiffness: pathological implications for soft or stiff microenvironments. *J. Cell Biol.* **166**, 877–887 (2004).
3. Engler, A. J., Sen, S., Sweeney, H. L. & Discher, D. E. Matrix elasticity directs stem cell lineage specification. *Cell* **126**, 677–689 (2006).
- Contractile myocytes were used to demonstrate that cells sense their mechanical environment. Myotubes form independently of matrix stiffness but myosin–actin striations emerge only on gels with stiffness typical of normal muscle, and not on matrices that are softer or stiffer.**
4. Georges, P. C., Miller, W. J., Meaney, D. F., Sawyer, E. S. & Janmey, P. A. Matrices with compliance comparable to that of brain tissue select neuronal over glial growth in mixed cortical cultures. *Biophys. J.* **90**, 3012–3018 (2006).
5. McBeath, R., Pirone, D. M., Nelson, C. M., Bhadriraju, K. & Chen, C. S. Cell shape, cytoskeletal tension, and rhoa regulate stem cell lineage commitment. *Dev. Cell* **6**, 483–495 (2004).
6. Paszek, M. J. *et al.* Tensional homeostasis and the malignant phenotype. *Cancer Cell* **8**, 241–254 (2005).
- The first paper to describe tensional homeostasis regulation of the tumour phenotype and the molecular link between ECM stiffness, Rho-dependent cell contractility and oncogene-mediated transformation.**
7. Vial, E., Sahai, E. & Marshall, C. J. ERK–MAPK signaling coordinately regulates activity of Rac1 and RhoA for tumor cell motility. *Cancer Cell* **4**, 67–79 (2003).
8. Lee, M. K. & Nikodem, V. M. Differential role of ERK in cAMP-induced *Nurr1* expression in N2A and C6 cells. *Neuroreport* **15**, 99–102 (2004).
9. Chrzanowska-Wodnicka, M. & Burridge, K. Rho-stimulated contractility drives the formation of stress fibers and focal adhesions. *J. Cell Biol.* **133**, 1403–1415 (1996).
10. Krieg, M. *et al.* Tensile forces govern germ-layer organization in zebrafish. *Nature Cell Biol.* **10**, 429–436 (2008).
- This article defined the mechanical properties of progenitor cells of the ectoderm, mesoderm and endoderm in gastrulating zebrafish embryos and demonstrated that differential actomyosin-dependent cell–cortex tension is regulated by Nodal–TGFβ signalling.**
11. Page-McCaw, A., Ewald, A. J. & Werb, Z. Matrix metalloproteinases and the regulation of tissue remodelling. *Nature Rev. Mol. Cell Biol.* **8**, 221–233 (2007).
12. Czirok, A., Rongish, B. J. & Little, C. D. Extracellular matrix dynamics during vertebrate axis formation. *Dev. Biol.* **268**, 111–122 (2004).
13. Pajerowski, J. D., Dahl, K. N., Zhong, F. L., Sammak, P. J. & Discher, D. E. Physical plasticity of the nucleus in stem cell differentiation. *Proc. Natl Acad. Sci. USA* **104**, 15619–15624 (2007).
14. Farge, E. Mechanical induction of Twist in the *Drosophila* foregut/stomodaeal primordium. *Curr. Biol.* **13**, 1365–1377 (2003).
15. Ren, R., Nagel, M., Tahinci, E., Winklbauer, R. & Symes, K. Migrating anterior mesoderm cells and intercalating trunk mesoderm cells have distinct responses to Rho and Rac during *Xenopus* gastrulation. *Dev. Dyn.* **235**, 1090–1099 (2006).
16. Tahinci, E. & Symes, K. Distinct functions of Rho and Rac are required for convergent extension during *Xenopus* gastrulation. *Dev. Biol.* **259**, 318–335 (2003).
17. Cardoso, W. V. & Lu, J. Regulation of early lung morphogenesis: questions, facts and controversies. *Development* **133**, 1611–1624 (2006).
18. Kitterman, J. A. The effects of mechanical forces on fetal lung growth. *Clin. Perinatol.* **23**, 727–740 (1996).
19. Liu, M., Tanswell, A. K. & Post, M. Mechanical force-induced signal transduction in lung cells. *Am. J. Physiol.* **277**, L667–L683 (1999).
20. Moore, K. A. *et al.* Control of basement membrane remodeling and epithelial branching morphogenesis in embryonic lung by Rho and cytoskeletal tension. *Dev. Dyn.* **232**, 268–281 (2005).
21. Bird, J. L., Platt, D., Wells, T., May, S. A. & Bayliss, M. T. Exercise-induced changes in proteoglycan metabolism of equine articular cartilage. *Equine Vet. J.* **32**, 161–163 (2000).
22. Haapala, J. *et al.* Coordinated regulation of hyaluronan and aggrecan content in the articular cartilage of immobilized and exercised dogs. *J. Rheumatol.* **23**, 1586–1593 (1996).
23. Ebbesen, E. N., Thomsen, J. S. & Mosekilde, L. Nondestructive determination of iliac crest cancellous bone strength by pOCT. *Bone* **21**, 535–540 (1997).
24. Rittweger, J. *et al.* Bone loss from the human distal tibia epiphysis during 24 days of unilateral lower limb suspension. *J. Physiol.* **577**, 331–337 (2006).
25. Takahashi, M., Ishida, T., Traub, O., Corson, M. A. & Berk, B. C. Mechanotransduction in endothelial cells: temporal signaling events in response to shear stress. *J. Vasc. Res.* **34**, 212–219 (1997).
26. Davies, P. F. Flow-mediated endothelial mechanotransduction. *Physiol. Rev.* **75**, 519–560 (1995).
27. Davies, P. F., Remuzzi, A., Gordon, E. J., Dewey, C. F. Jr & Gimbrone, M. A. Jr. Turbulent fluid shear stress induces vascular endothelial cell turnover *in vitro*. *Proc. Natl Acad. Sci. USA* **83**, 2114–2117 (1986).
28. Guck, J. *et al.* Optical deformability as an inherent cell marker for testing malignant transformation and metastatic competence. *Biophys. J.* **88**, 3689–3698 (2005).
29. Cross, S. E., Jin, Y. S., Rao, J. & Gimzewski, J. K. Nanomechanical analysis of cells from cancer patients. *Nature Nanotech.* **2**, 780–783 (2007).
30. Wong, J. Y., Velasco, A., Rajagopalan, P. & Pham, Q. Directed movement of vascular smooth muscle cells on gradient-compliant hydrogels. *Langmuir* **19**, 1908–1913 (2003).
- This article demonstrates the durotactic movement of cells along a stiffness gradient on polyacrylamide gels.**
31. Gaudet, C. *et al.* Influence of type I collagen surface density on fibroblast spreading, motility, and contractility. *Biophys. J.* **85**, 3329–3335 (2003).
32. Discher, D. E., Janmey, P. & Wang, Y. L. Tissue cells feel and respond to the stiffness of their substrate. *Science* **310**, 1139–1143 (2005).
33. Payne, S. L., Hendrix, M. J. & Kirschmann, D. A. Paradoxical roles for lysyl oxidases in cancer — a prospect. *J. Cell Biochem.* **101**, 1338–1354 (2007).
34. Sivakumar, P., Gupta, S., Sarkar, S. & Sen, S. Upregulation of lysyl oxidase and MMPs during cardiac remodeling in human dilated cardiomyopathy. *Mol. Cell Biochem.* **307**, 159–167 (2008).
35. Avery, N. C. & Bailey, A. J. The effects of the Maillard reaction on the physical properties and cell interactions of collagen. *Pathol. Biol. (Paris)* **54**, 387–395 (2006).
36. Ebihara, T., Venkatesan, N., Tanaka, R. & Ludwig, M. S. Changes in extracellular matrix and tissue viscoelasticity in bleomycin-induced lung fibrosis. Temporal aspects. *Am. J. Respir. Crit. Care Med.* **162**, 1569–1576 (2000).

37. Susic, D. Cross-link breakers as a new therapeutic approach to cardiovascular disease. *Biochem. Soc. Trans.* **35**, 853–856 (2007).
38. Robins, S. P. *et al.* Increased skin collagen extractability and proportions of collagen type III are not normalized after 6 months healing of human excisional wounds. *J. Invest. Dermatol.* **121**, 267–272 (2005).
39. Nayak, G. D., Ratnayaka, H. S., Goodyear, R. J. & Richardson, G. P. Development of the hair bundle and mechanotransduction. *Int. J. Dev. Biol.* **51**, 597–608 (2007).
40. Parker, K. K. & Ingber, D. E. Extracellular matrix, mechanotransduction and structural hierarchies in heart tissue engineering. *Philos. Trans. R. Soc. Lond. B Biol. Sci.* **362**, 1267–1279 (2007).
41. Brakemeier, S., Eichler, I., Hopp, H., Kohler, R. & Hoyer, J. Up-regulation of endothelial stretch-activated cation channels by fluid shear stress. *Cardiovasc. Res.* **53**, 209–218 (2002).
42. Helmke, B. P., Rosen, A. B. & Davies, P. F. *Biophys. J.* **84**, 2691–2699 (2003).
43. del Pozo, M. A. *et al.* Integrins regulate Rac targeting by internalization of membrane domains. *Science* **303**, 839–842 (2004).
44. Chen, Y. & Dokholyan, N. V. Insights into allosteric control of vinculin function from its large scale conformational dynamics. *J. Biol. Chem.* **281**, 29148–29154 (2006).
- This paper demonstrates the large-scale conformational dynamics of full-length vinculin.**
45. Defilippi, P., Di Stefano, P. & Cabodi, S. p130Cas: a versatile scaffold in signaling networks. *Trends Cell Biol.* **16**, 257–263 (2006).
46. Tamada, M., Sheetz, M. P. & Sawada, Y. Activation of a signaling cascade by cytoskeleton stretch. *Dev. Cell* **7**, 709–718 (2004).
47. Sawada, Y. *et al.* Force sensing by mechanical extension of the Src family kinase substrate p130Cas. *Cell* **127**, 1015–1026 (2006).
- References 45 and 46 describe the changes in conformation of RAP1 and p130 Cas in response to mechanical stretch.**
48. Hattori, M. & Minato, N. Rap1 GTPase: functions, regulation, and malignancy. *J. Biochem.* **134**, 479–484 (2003).
49. Friedland, J. C., Lee, M. H. & Boettiger, D. Mechanically activated integrin switch controls $\alpha 5 \beta 1$ function. *Science* (in press).
50. Ginsberg, M. H., Du, X. & Plow, E. F. Inside-out integrin signalling. *Curr. Opin. Cell Biol.* **4**, 766–771 (1992).
51. Hynes, R. O. Integrins: versatility, modulation, and signaling in cell adhesion. *Cell* **69**, 11–25 (1992).
52. Galbraith, C. G., Yamada, K. M. & Sheetz, M. P. The relationship between force and focal complex development. *J. Cell Biol.* **159**, 695–705 (2002).
53. Giancotti, F. G. & Ruoslahti, E. Integrin signaling. *Science* **285**, 1028–1032 (1999).
54. Riveline, D. *et al.* Focal contacts as mechanosensors: externally applied local mechanical force induces growth of focal contacts by an mDia1-dependent and ROCK-independent mechanism. *J. Cell Biol.* **153**, 1175–1186 (2001).
55. Tzima, E., del Pozo, M. A., Shattil, S. J., Chien, S. & Schwartz, M. A. Activation of integrins in endothelial cells by fluid shear stress mediates Rho-dependent cytoskeletal alignment. *EMBO J.* **20**, 4639–4647 (2001).
56. Watanabe, Y. & Akaïke, T. Possible involvement of caspase-like family in maintenance of cytoskeleton integrity. *J. Cell Physiol.* **179**, 45–51 (1999).
57. Shi, Q. & Boettiger, D. A novel mode for integrin-mediated signaling: tethering is required for phosphorylation of FAK Y397. *Mol. Biol. Cell* **14**, 4306–4315 (2003).
58. Clark, E. A., King, W. G., Brugge, J. S., Symons, M. & Hynes, R. O. Integrin-mediated signals regulated by members of the rho family of GTPases. *J. Cell Biol.* **142**, 573–586 (1998).
59. Cox, E. A., Sastry, S. K. & Huttenlocher, A. Integrin-mediated adhesion regulates cell polarity and membrane protrusion through the Rho family of GTPases. *Mol. Biol. Cell* **12**, 265–277 (2001).
60. Chess, P. R., Toia, L. & Finkelstein, J. N. Mechanical strain-induced proliferation and signaling in pulmonary epithelial H441 cells. *Am. J. Physiol. Lung Cell. Mol. Physiol.* **279**, L43–51 (2000).
61. Milkiewicz, M., Mohammadzadeh, F., Ispanovic, E., Gee, E. & Haas, T. L. Static strain stimulates expression of matrix metalloproteinase-2 and VEGF in microvascular endothelium via JNK- and ERK-dependent pathways. *J. Cell Biochem.* **100**, 750–761 (2007).
62. Chaturvedi, L. S., Marsh, H. M. & Basson, M. D. Src and focal adhesion kinase mediate mechanical strain-induced proliferation and ERK1/2 phosphorylation in human H441 pulmonary epithelial cells. *Am. J. Physiol. Cell Physiol.* **292**, C1701–C1713 (2007).
63. Kippenberger, S. *et al.* Signaling of mechanical stretch in human keratinocytes via MAP kinases. *J. Invest. Dermatol.* **114**, 408–412 (2000).
64. Plotkin, L. I. *et al.* Mechanical stimulation prevents osteocyte apoptosis: requirement of integrins, Src kinases, and ERKs. *Am. J. Physiol. Cell Physiol.* **289**, C633–C643 (2005).
65. Dennerll, T. J., Joshi, H. C., Steel, V. L., Buxbaum, R. E. & Heidemann, S. R. Tension and compression in the cytoskeleton of PC-12 neurites. II: Quantitative measurements. *J. Cell Biol.* **107**, 665–674 (1988).
66. Wang, H. B., Dembo, M., Hanks, S. K. & Wang, Y. Focal adhesion kinase is involved in mechanosensing during fibroblast migration. *Proc. Natl Acad. Sci. USA* **98**, 11295–11300 (2001).
- This paper demonstrates that FAK is important for migrating fibroblasts to respond to mechanical force. FAK-null cells are unable to migrate at the same speed or in a sustained direction when compared with wild-type cells.**
67. Wipff, P. J., Rifkin, D. B., Meister, J. J. & Hinz, B. Myofibroblast contraction activates latent TGF- β 1 from the extracellular matrix. *J. Cell Biol.* **179**, 1311–1323 (2007).
- This paper demonstrates that myofibroblast contraction, through integrin activation, directly activates TGF β 1 from ECM stores.**
68. Heinemeier, K. M. *et al.* Expression of collagen and related growth factors in rat tendon and skeletal muscle in response to specific contraction types. *J. Physiol.* **582**, 1303–1316 (2007).
69. Wells, R. G. The role of matrix stiffness in hepatic stellate cell activation and liver fibrosis. *J. Clin. Gastroenterol.* **39**, S158–161 (2005).
70. Geiger, B., Bershadsky, A., Pankov, R. & Yamada, K. M. Transmembrane crosstalk between the extracellular matrix–cytoskeleton crosstalk. *Nature Rev. Mol. Cell Biol.* **2**, 793–805 (2001).
71. Liu, B. P. & Burridge, K. Yav2 activates Rac1, Cdc42, and RhoA downstream from growth factor receptors but not $\beta 1$ integrins. *Mol. Cell Biol.* **20**, 7160–7169 (2000).
72. Bresnick, A. R. Molecular mechanisms of nonmuscle myosin-II regulation. *Curr. Opin. Cell Biol.* **11**, 26–33 (1999).
73. Mogilner, A. & Oster, G. Force generation by actin polymerization II: the elastic ratchet and tethered filaments. *Biophys. J.* **84**, 1591–1605 (2003).
74. Beningo, K. A. & Wang, Y. L. Flexible substrata for the detection of cellular traction forces. *Trends Cell Biol.* **12**, 79–84 (2002).
75. Dembo, M. & Wang, Y. L. Stresses at the cell-to-substrate interface during locomotion of fibroblasts. *Biophys. J.* **76**, 2307–2316 (1999).
- This paper demonstrates a method to determine the traction forces exerted by a single fibroblast during steady locomotion, revealing that the lamellipodia generate larger traction forces than the body of the cell.**
76. Sirghi, L., Ponti, J., Broggi, F. & Rossi, F. Probing elasticity and adhesion of live cells by atomic force microscopy indentation. *Eur. Biophys. J.* **37**, 935–945, (2008).
77. Solon, J., Levental, I., Sengupta, K., Georges, P. C. & Janmey, P. A. Fibroblast adaptation and stiffness matching to soft elastic substrates. *Biophys. J.* **93**, 4453–4461 (2007).
78. Kumar, S. *et al.* Viscoelastic retraction of single living stress fibers and its impact on cell shape, cytoskeletal organization, and extracellular matrix mechanics. *Biophys. J.* **90**, 3762–3773 (2006).
79. Hamelers, I. H. *et al.* The Rac activator Tiam1 is required for $\alpha 3 \beta 1$ -mediated laminin-5 deposition, cell spreading, and cell migration. *J. Cell Biol.* **171**, 871–881 (2005).
80. Ewald, A. J., Brenot, A., Duong, M., Chan, B. S. & Werb, Z. Collective epithelial migration and cell rearrangements drive mammary branching morphogenesis. *Dev. Cell* **14**, 570–581 (2008).
81. Yeung, T. *et al.* Effects of substrate stiffness on cell morphology, cytoskeletal structure, and adhesion. *Cell Motil. Cytoskeleton* **60**, 24–34 (2005).
82. Delcommenne, M. & Streuli, C. H. Control of integrin expression by extracellular matrix. *J. Biol. Chem.* **270**, 26794–26801 (1995).
83. Triplett, J. W., O’Riley, R., Tekulke, K., Norvell, S. M. & Pavalko, F. M. Mechanical loading by fluid shear stress enhances IGF-1 receptor signaling in osteoblasts in a PKC ζ -dependent manner. *Mol. Cell Biomech.* **4**, 13–25 (2007).
84. Reichelt, J. Mechanotransduction of keratinocytes in culture and in the epidermis. *Eur. J. Cell Biol.* **86**, 807–816 (2007).
85. Chien, S. Effects of disturbed flow on endothelial cells. *Ann. Biomed. Eng.* **36**, 554–562 (2008).
86. Awisato, C. L. *et al.* Mechanical force modulates global gene expression and β -catenin signaling in colon cancer cells. *J. Cell Sci.* **120**, 2672–2682 (2007).
87. Alcaraz, J. *et al.* Laminin and biomimetic extracellular elasticity enhance functional differentiation in mammary epithelia. *EMBO J.* **27**, 2829–2838 (2008).
88. Rizki, A. *et al.* A human breast cell model of preinvasive to invasive transition. *Cancer Res.* **68**, 1378–1387 (2008).
89. Ingber, D. E. Tensegrity II. How structural networks influence cellular information processing networks. *J. Cell Sci.* **116**, 1397–1408 (2003).
90. Ingber, D. E. Tensegrity I. Cell structure and hierarchical systems biology. *J. Cell Sci.* **116**, 1157–1173 (2003).
91. Bloom, S., Lockard, V. G. & Bloom, M. Intermediate filament-mediated stretch-induced changes in chromatin: a hypothesis for growth initiation in cardiac myocytes. *J. Mol. Cell Cardiol.* **28**, 2123–2127 (1996).
92. Molenaar, C. *et al.* Visualizing telomere dynamics in living mammalian cells using PNA probes. *EMBO J.* **22**, 6631–6641 (2003).
93. Bustamante, C., Bryant, Z. & Smith, S. B. Ten years of tension: single-molecule DNA mechanics. *Nature* **421**, 423–427 (2003).
94. Ingber, D. E. Cellular mechanotransduction: putting all the pieces together again. *FASEB J.* **20**, 811–827 (2006).
95. Gore, J. *et al.* Mechanochemical analysis of DNA gyrase using rotor bead tracking. *Nature* **439**, 100–104 (2006).
96. Maniatis, A. J., Bojanowski, K. & Ingber, D. E. Mechanical continuity and reversible chromosome disassembly within intact genomes removed from living cells. *Cell Biochem.* **65**, 114–130 (1997).
97. Plachot, C. & Lelievre, S. A. DNA methylation control of tissue polarity and cellular differentiation in the mammary epithelium. *Exp. Cell Res.* **298**, 122–132 (2004).
98. Lelievre, S. *et al.* Tissue phenotype is dependent on reciprocal interactions between the extracellular matrix and the structural organization of the nucleus. *Proc. Natl. Acad. Sci. USA* **95**, 14711–14716 (1998).
99. Kim, Y. B. *et al.* Cell adhesion status-dependent histone acetylation is regulated through intracellular contractility-related signaling activities. *J. Biol. Chem.* **280**, 28357–28364 (2005).
- This paper shows a link between cell adhesion and contractility and a decrease in acetylation of histone H3 and higher HDAC activity, suggesting that histone modifications can be regulated by mechanical cues.**
100. Destaing, O. *et al.* A novel Rho–mDia2–HDAC6 pathway controls podosome patterning through microtubule acetylation in osteoclasts. *J. Cell Sci.* **118**, 2901–2911 (2005).
101. Le Beyec, J. *et al.* Cell shape regulates global histone acetylation in human mammary epithelial cells. *Exp. Cell Res.* **313**, 3066–3075 (2007).
102. Dalby, M. J., Riehle, M. O., Sutherland, D. S., Agheli, H. & Curtis, A. S. Morphological and microarray analysis of human fibroblasts cultured on nanocolumns produced by colloidal lithography. *Eur. Cell Mater.* **9**, 1–8; discussion 8 (2005).
103. Dalby, M. J. *et al.* Nanomechanotransduction and interphase nuclear organization influence on genomic control. *J. Cell Biochem.* **102**, 1234–1244 (2007).
- This paper demonstrated that changes in cell shape owing to cell spreading altered the location of chromosomes within the nucleus and the chromosomal sites of regulated gene expression.**
104. Dalby, M. J. *et al.* Group analysis of regulation of fibroblast genome on low-adhesion nanostructures. *Biomaterials* **28**, 1761–1769 (2007).

104. Alberts, A. S., Geneste, O. & Treisman, R. Activation of SRF-regulated chromosomal templates by Rho-family GTPases requires a signal that also induces H4 hyperacetylation. *Cell* **92**, 475–487 (1998).
105. Posern, G., Miralles, F., Guettler, S. & Treisman, R. Mutant actins that stabilise F-actin use distinct mechanisms to activate the SRF coactivator MAL. *EMBO J.* **23**, 3973–3983 (2004).
106. Vartiainen, M. K., Guettler, S., Larjani, B. & Treisman, R. Nuclear actin regulates dynamic subcellular localization and activity of the SRF cofactor MAL. *Science* **316**, 1749–1752 (2007).
107. Davies, P. F., Spaan, J. A. & Krams, R. Shear stress biology of the endothelium. *Ann. Biomed. Eng.* **33**, 1714–1718 (2005).
108. Glaser, K. J., Felmlee, J. P., Manduca, A., Kannan Mariappan, Y. & Ehman, R. L. Stiffness-weighted magnetic resonance imaging. *Magn. Reson. Med.* **55**, 59–67 (2006).
109. Garra, B. S. Imaging and estimation of tissue elasticity by ultrasound. *Ultrasound Q.* **23**, 255–268 (2007).
110. Reihnsner, R., Melling, M., Pfeiler, W. & Menzel, E. J. Alterations of biochemical and two-dimensional biomechanical properties of human skin in diabetes mellitus as compared to effects of *in vitro* non-enzymatic glycation. *Clin. Biomech. (Bristol, Avon)* **15**, 379–386 (2000).
111. Stone, J. *et al.* The heritability of mammographically dense and nondense breast tissue. *Cancer Epidemiol. Biomarkers Prev.* **15**, 612–617 (2006).
112. Nelson, C. M., Vanduijn, M. M., Inman, J. L., Fletcher, D. A. & Bissell, M. J. Tissue geometry determines sites of mammary branching morphogenesis in organotypic cultures. *Science* **314**, 298–300 (2006). **This article demonstrates that tissue geometry is a crucial factor in establishing the morphogen microenvironments that dictate branch formation.**
113. Elston, C. W. & Ellis, I. O. (eds) *The Breast* vol. 13 356–384 (Churchill Livingstone, Edinburgh; New York, 1998).
114. Ronnov-Jessen, L., Petersen, O. W. & Bissell, M. J. Cellular changes involved in conversion of normal to malignant breast: importance of the stromal reaction. *Physiol. Rev.* **76**, 69–125 (1996).
115. Weaver, V. M., Fischer, A. H., Peterson, O. W. & Bissell, M. J. The importance of the microenvironment in breast cancer progression: recapitulation of mammary tumorigenesis using a unique human mammary epithelial cell model and a three-dimensional culture assay. *Biochem. Cell Biol.* **74**, 833–851 (1996).
116. Timpl, R. Macromolecular organization of basement membranes. *Curr. Opin. Cell Biol.* **8**, 618–624 (1996).
117. Griffith, L. G. & Swartz, M. A. Capturing complex 3D tissue physiology *in vitro*. *Nature Rev. Mol. Cell Biol.* **7**, 211–224 (2006).
118. Kreis, T. & Vale, R. (eds). *Guidebook to the ECM, Anchor, and Adhesion Proteins* (Oxford Univ. Press, New York, 1999).
119. Kleinman, H. K. & Martin, G. R. Matrigel: basement membrane matrix with biological activity. *Semin. Cancer Biol.* **15**, 378–386 (2005).
120. Green, K. A. & Lund, L. R. ECM degrading proteases and tissue remodelling in the mammary gland. *Bioessays* **27**, 894–903 (2005).
121. Watson, C. J. Post-lactational mammary gland regression: molecular basis and implications for breast cancer. *Expert Rev. Mol. Med.* **8**, 1–15 (2006).
122. McDaniel, S. M. *et al.* Remodeling of the mammary microenvironment after lactation promotes breast tumor cell metastasis. *Am. J. Pathol.* **168**, 608–620 (2006).
123. Barcellos-Hoff, M. H., Aggeler, J., Ram, T. G. & Bissell, M. J. Functional differentiation and alveolar morphogenesis of primary mammary cultures on reconstituted basement membrane. *Development* **105**, 223–235 (1989). **This article demonstrates that growth of mammary epithelial cells in RBM permits the assembly of polarized alveolus-like structures that secrete milk proteins into the luminal space.**
124. Weaver, V. M. *et al.* Reversion of the malignant phenotype of human breast cells in three-dimensional culture and *in vivo* by integrin blocking antibodies. *J. Cell Biol.* **137**, 231–245 (1997). **Blocking integrin function reverted tumour cells grown in three-dimensional culture to a normal phenotype, demonstrating that the ECM and its receptors determine the phenotype and can override genotype in this model system.**
125. Li, M. L. *et al.* Influence of a reconstituted basement membrane and its components on casein gene expression and secretion in mouse mammary epithelial cells. *Proc. Natl Acad. Sci. USA* **84**, 136–140 (1987).
126. Bao, G. & Suresh, S. Cell and molecular mechanics of biological materials. *Nature Mater.* **2**, 715–725 (2003).
127. Samani, A., Bishop, J., Luginbuhl, C. & Plewes, D. B. Measuring the elastic modulus of *ex vivo* small tissue samples. *Phys. Med. Biol.* **48**, 2183–2198 (2003).
128. Suresh, S. Biomechanics and biophysics of cancer cells. *Acta Biomater.* **3**, 413–438 (2007).
129. Paszek, M. J. & Weaver, V. M. The tension mounts: mechanics meets morphogenesis and malignancy. *J. Mammary Gland Biol. Neoplasia* **9**, 325–342 (2004).
130. Netti, P. A., Berk, D. A., Swartz, M. A., Grodzinsky, A. J. & Jain, R. K. Role of extracellular matrix assembly in interstitial transport in solid tumors. *Cancer Res.* **60**, 2497–2503 (2000). **This article demonstrates that increased elastic modulus resulting from increased ECM collagen content influences the resistance of tissues to macromolecule transport, including chemotherapeutic agents.**
131. Dalby, M. J., Riehle, M. O., Johnstone, H., Affrossman, S. & Curtis, A. S. Investigating the limits of filopodial sensing: a brief report using SEM to image the interaction between 10 nm high nano-topography and fibroblast filopodia. *Cell Biol. Int.* **28**, 229–236 (2004).
132. Chaw, K. C., Manimaran, M., Tay, F. E. & Swaminathan, S. A quantitative observation and imaging of single tumor cell migration and deformation using a multi-gap microfluidic device representing the blood vessel. *Microvasc. Res.* **72**, 153–160 (2006).
133. Croft, D. R. *et al.* Conditional ROCK activation *in vivo* induces tumor cell dissemination and angiogenesis. *Cancer Res.* **64**, 8994–9001 (2004).
134. O'Brien, L. E. *et al.* Rac1 orientates epithelial apical polarity through effects on basolateral laminin assembly. *Nature Cell Biol.* **3**, 831–838 (2001).
135. Wang, F. *et al.* Reciprocal interactions between beta 1-integrin and epidermal growth factor receptor in three-dimensional basement membrane breast cultures: a different perspective in epithelial biology. *Proc. Natl Acad. Sci. USA* **95**, 14821–14826 (1998). **This article demonstrates that the spatial organization of breast cells in three-dimensions is important for correct signalling through integrin and EGFR–MAPK pathways.**
136. Provenzano, P. P. *et al.* Collagen reorganization at the tumor-stromal interface facilitates local invasion. *BMC Med.* **4**, 38 (2006).
137. Rhee, S. & Grinnell, F. Fibroblast mechanics in 3D collagen matrices. *Adv. Drug Deliv. Rev.* **59**, 1299–1305 (2007).
138. Ingman, W. V., Wyckoff, J., Gouon-Evans, V., Condeelis, J. & Pollard, J. W. Macrophages promote collagen fibrillogenesis around terminal end buds of the developing mammary gland. *Dev. Dyn.* **235**, 3222–3229 (2006).
139. Provenzano, P. P. *et al.* Collagen density promotes mammary tumor initiation and progression. *BMC Med.* **6**, 11 (2008).
140. Wyckoff, J. B., Pinner, S. E., Gschmeissner, S., Condeelis, J. S. & Sahai, E. ROCK- and myosin-dependent matrix deformation enables protease-independent tumor-cell invasion *in vivo*. *Curr. Biol.* **16**, 1515–1523 (2006). **This paper describes the mechanism by which cells move through a dense ECM without proteolysis by MMPs. The tumour cells generated actomyosin forces that deformed the collagen fibres to push through the ECM.**
141. Ingber, D. E., Madri, J. A. & Jamieson, J. D. Role of basal lamina in neoplastic disorganization of tissue architecture. *Proc. Natl Acad. Sci. USA* **78**, 3901–3905 (1981).
142. Roose, T., Netti, P. A., Munn, L. L., Boucher, Y. & Jain, R. K. Solid stress generated by spheroid growth estimated using a linear poroelasticity model small star, filled. *Microvasc. Res.* **66**, 204–212 (2003).
143. Harris, A. L. Hypoxia — a key regulatory factor in tumour growth. *Nature Rev. Cancer* **2**, 38–47 (2002).
144. Jain, R. K. Transport of molecules, particles, and cells in solid tumors. *Annu. Rev. Biomed. Eng.* **1**, 241–263 (1999).
145. Rutkowski, J. M. & Swartz, M. A. A driving force for change: interstitial flow as a morphoregulator. *Trends Cell Biol.* **17**, 44–50 (2007).
146. Tschumperlin, D. J. *et al.* Mechanotransduction through growth-factor shedding into the extracellular space. *Nature* **429**, 83–86 (2004). **This article demonstrates for the first time how compressive force can modify growth factor receptor signalling by increasing the local ligand concentration.**
147. Minchinton, A. I. & Tannock, I. F. Drug penetration in solid tumours. *Nature Rev. Cancer* **6**, 583–592 (2006).
148. Walker, R. A. The complexities of breast cancer desmoplasia. *Breast Cancer Res.* **3**, 143–145 (2001).
149. Willis, R. *Pathology of Tumors* (Butterworth and Company, London, 1967).
150. Goepel, C., Buchmann, J., Schultka, R. & Koelbl, H. Tenascin — a marker for the malignant potential of preinvasive breast cancers. *Gynecol. Oncol.* **79**, 372–378 (2000).
151. Gorczyca, W., Holm, R. & Nesland, J. M. Laminin production and fibronectin immunoreactivity in breast carcinomas. *Anticancer Res.* **13**, 851–858 (1993).
152. Guarino, M., Reale, D. & Micoli, G. The extracellular matrix in sarcomatoid carcinomas of the breast. *Virchows Arch. A Pathol. Anat. Histopathol* **423**, 131–136 (1993).
153. Rodríguez, C., Rodríguez-Sinovas, A. & Martínez-González, J. Lysyl oxidase as a potential therapeutic target. *Drug News Perspect.* **21**, 218–224 (2008).
154. Strongin, A. Y. Mislocalization and unconventional functions of cellular MMPs in cancer. *Cancer Metastasis Rev.* **25**, 87–98 (2006).
154. Jodele, S., Blavier, L., Yoon, J. M. & DeClerck, Y. A. Modifying the soil to affect the seed: role of stromal-derived matrix metalloproteinases in cancer progression. *Cancer Metastasis Rev.* **25**, 35–43 (2006).
156. Biondi, M. L. *et al.* MMP1 and MMP3 polymorphisms in promoter regions and cancer. *Clin. Chem.* **46**, 2023–2024 (2000).
157. Sternlicht, M. D., Safarians, S., Rivera, S. P. & Borsky, S. H. Characterizations of the extracellular matrix and protease inhibitor content of human myoepithelial tumors. *Lab. Invest.* **74**, 781–796 (1996).
158. Akiri, G. *et al.* Lysyl oxidase-related protein-1 promotes tumor fibrosis and tumor progression *in vivo*. *Cancer Res.* **63**, 1657–1666 (2003).
159. Decitre, M. *et al.* Lysyl oxidase-like protein localizes to sites of *de novo* fibrinogenesis in fibrosis and in the early stromal reaction of ductal breast carcinomas. *Lab. Invest.* **78**, 143–151 (1998).
160. Shields, J. D. *et al.* Autologous chemotaxis as a mechanism of tumor cell homing to lymphatics via interstitial flow and autocrine CCR7 signaling. *Cancer Cell* **11**, 526–538 (2007). **This paper demonstrates that interstitial flow establishes an autocrine CCR7 gradient that guides tumour cells to lymphatic vessels during metastasis.**
161. Lieber, M. M. Towards an understanding of the role of forces in carcinogenesis: a perspective with therapeutic implications. *Riv. Biol.* **99**, 131–160 (2006).
162. Wolfe, J. N. Risk for breast cancer development determined by mammographic parenchymal pattern. *Cancer* **37**, 2486–2492 (1976).
163. Wolfe, J. N. Breast patterns as an index of risk for developing breast cancer. *AJR Am. J. Roentgenol.* **126**, 1130–1137 (1976). **References 162 and 163 were the first to describe the link between mammographic density and breast cancer risk.**
164. Couzin, J. Breast cancer. Fine-tuning breast density measures. *Science* **309**, 1665 (2005).
165. Boyd, N. F. *et al.* Mammographic density and the risk and detection of breast cancer. *N. Engl. J. Med.* **356**, 227–236 (2007).
166. Boyd, N. F. *et al.* Mammographic densities and breast cancer risk. *Breast Dis.* **10**, 113–126 (1998).
167. Boyd, N. F. *et al.* Heritability of mammographic density, a risk factor for breast cancer. *N. Engl. J. Med.* **347**, 886–894 (2002).
168. Guo, Y. P. *et al.* Growth factors and stromal matrix proteins associated with mammographic densities. *Cancer Epidemiol. Biomarkers Prev.* **10**, 243–248 (2001).
169. Li, T. *et al.* The association of measured breast tissue characteristics with mammographic density and other risk factors for breast cancer. *Cancer Epidemiol. Biomarkers Prev.* **14**, 343–349 (2005). **This article demonstrated that collagen levels are increased in breast tissues with high mammographic density**

170. Radisky, E. S. & Radisky, D. C. Stromal induction of breast cancer: inflammation and invasion. *Rev. Endocr. Metab. Disord.* **8**, 279–287 (2007).
171. Martin, L. J. & Boyd, N. F. Mammographic density. Potential mechanisms of breast cancer risk associated with mammographic density: hypotheses based on epidemiological evidence. *Breast Cancer Res.* **10**, 201 (2008).
172. Thomas, A. *et al.* Real-time elastography—an advanced method of ultrasound: First results in 108 patients with breast lesions. *Ultrasound Obstet. Gynecol.* **28**, 335–340 (2006).
173. Woloshin, S., Schwartz, L. M. & Welch, H. G. The risk of death by age, sex, and smoking status in the United States: putting health risks in context. *J. Natl Cancer Inst.* **100**, 845–853 (2008).
174. Tang, S. Y., Zeenath, U. & Vashishth, D. Effects of non-enzymatic glycation on cancellous bone fragility. *Bone* **40**, 1144–1151 (2007).
175. Varani, J. *et al.* Vitamin A antagonizes decreased cell growth and elevated collagen-degrading matrix metalloproteinases and stimulates collagen accumulation in naturally aged human skin. *J. Invest. Dermatol.* **114**, 480–486 (2000).
176. Gosain, A. K., Recinos, R. F., Agresti, M. & Khanna, A. K. TGF- β 1, FGF-2, and receptor mRNA expression in suture mesenchyme and dura versus underlying brain in fusing and nonfusing mouse cranial sutures. *Plast. Reconstr Surg.* **113**, 1675–1684 (2004).
177. Alexander, H. & Cook, T. Variations with age in the mechanical properties of human skin *in vivo*. *J. Tissue Viability* **16**, 6–11 (2006).
178. Agah, A., Kyriakides, T. R., Letrondo, N., Bjorkblom, B. & Bornstein, P. Thrombospondin 2 levels are increased in aged mice: consequences for cutaneous wound healing and angiogenesis. *Matrix Biol.* **22**, 539–547 (2004).
179. Bornstein, P., Agah, A. & Kyriakides, T. R. The role of thrombospondins 1 and 2 in the regulation of cell–matrix interactions, collagen fibril formation, and the response to injury. *Int. J. Biochem. Cell Biol.* **36**, 1115–1125 (2004).
180. Lasco, A. *et al.* Effect of long-term treatment with raloxifene on mammary density in postmenopausal women. *Menopause* **13**, 787–792 (2006).
181. Coussens, L. M., Fingleton, B. & Matrisian, L. M. Matrix metalloproteinase inhibitors and cancer: trials and tribulations. *Science* **295**, 2387–2392 (2002).
182. Psaila, B., Kaplan, R. N., Port, E. R. & Lyden, D. Priming the 'soil' for breast cancer metastasis: the pre-metastatic niche. *Breast Dis.* **26**, 65–74 (2006).
183. Balooch, G. *et al.* TGF- β regulates the mechanical properties and composition of bone matrix. *Proc. Natl Acad. Sci. USA* **102**, 18813–18818 (2005).
184. Eler, J. T. *et al.* Lysyl oxidase is essential for hypoxia-induced metastasis. *Nature* **440**, 1222–1226 (2006).
185. MacKintosh, F. C., Kas, J. & Janmey, P. A. Elasticity of semiflexible biopolymer networks. *Phys. Rev. Lett.* **75**, 4425–4428 (1995).
186. Halliday, N. L. & Tomasek, J. J. Mechanical properties of the extracellular matrix influence fibronectin fibril assembly *in vitro*. *Exp. Cell Res.* **217**, 109–117 (1995).
187. Cirton, T. S., Oegema, T. R. & Tranquillo, R. T. Exploiting glycation to stiffen and strengthen tissue equivalents for tissue engineering. *J. Biomed. Mater. Res.* **46**, 87–92 (1999).
188. Marx, G. Elasticity of fibrin and protofibrin gels is differentially modulated by calcium and zinc. *Thromb. Haemost.* **59**, 500–503 (1988).
189. Carr, M. E. Jr, Gabriel, D. A. & McDonagh, J. Influence of factor XIII and fibronectin on fiber size and density in thrombin-induced fibrin gels. *J. Lab. Clin. Med.* **110**, 747–752 (1987).
190. Pelham, R. J. Jr & Wang, Y. Cell locomotion and focal adhesions are regulated by substrate flexibility. *Proc. Natl Acad. Sci. USA* **94**, 13661–13665 (1997).

This article illustrated the development of polyacrylamide gels of defined mechanical stiffness for use in tissue culture, facilitating the study of cell response to extracellular matrix force and demonstrated that focal adhesions are irregular and dynamic on flexible matrices and have normal morphology and stability on stiff matrices.

191. Debnath, J. & Brugge, J. S. Modelling glandular epithelial cancers in three-dimensional cultures. *Nature Rev. Cancer* **5**, 675–688 (2005).

Acknowledgements.

We apologize to the many authors whose work is not cited due to space limitations. A special thank you is extended to N. Zahir for her efforts on the text boxes, M. Paszek for his contribution to the traction force images in FIG. 1 and S. Cersosimo for administrative support. This work was supported by National Institutes of Health grant 7R01CA078731-07, Department of Defense Breast Cancer Research Era of Hope grant W81XWH-05-1-330 (BC044791), California Institute for Regenerative Medicine grant RS1-00449 and DOE grant A107165 to V.M.W., and a Sandler Family Foundation Award and National Institutes of Health grant RO3DE016868 to T.A.

DATABASES

National Cancer Institute Drug Dictionary: <http://www.cancer.gov/drugdictionary/5-azacytidine|tamoxifen>
 UniProtKB: <http://www.uniprot.org>
 β 5 integrin | β -casein | biglycan | BCAR1 | CCR7 | CREB | decorin | EAK | fibronectin | LOX | lumican | MAL | MECP2 | MMP2 | MMP3 | MMP11 | MMP12 | MMP13 | MYC | NF- κ B | p53 | paxillin | RAP1 | SRF | STAT1 | STAT3 | talin 1 | tenascin | TGF β | TIMP3 | TWIST1 | VEGFA | vinculin

ALL LINKS ARE ACTIVE IN THE ONLINE PDF

Mechanics, malignancy, and metastasis: The force journey of a tumor cell

Sanjay Kumar · Valerie M. Weaver

Published online: 21 January 2009

© The Author(s) 2009. This article is published with open access at Springerlink.com

Abstract A cell undergoes many genetic and epigenetic changes as it transitions to malignancy. Malignant transformation is also accompanied by a progressive loss of tissue homeostasis and perturbations in tissue architecture that ultimately culminates in tumor cell invasion into the parenchyma and metastasis to distant organ sites. Increasingly, cancer biologists have begun to recognize that a critical component of this transformation journey involves marked alterations in the *mechanical* phenotype of the cell and its surrounding microenvironment. These mechanical differences include modifications in cell and tissue structure, adaptive force-induced changes in the environment, altered processing of micromechanical cues encoded in the extracellular matrix (ECM), and cell-directed remodeling of the extracellular stroma. Here, we review critical steps in this “force journey,” including mechanical contributions to tissue dysplasia, invasion of the ECM, and metastasis. We discuss the biophysical basis of this force journey and present recent advances in the measurement of cellular mechanical properties *in vitro* and *in vivo*. We end by describing examples of molecular mechanisms through which tumor cells sense, process and respond to mechanical forces in their environment. While our understanding of the mechanical components of tumor growth, survival and

motility remains in its infancy, considerable work has already yielded valuable insight into the molecular basis of force-dependent tumor pathophysiology, which offers new directions in cancer chemotherapeutics.

Keywords Cancer · Extracellular matrix · Cell mechanics · Atomic force microscopy · Subcellular laser ablation · Rho kinase · Focal adhesion kinase

1 Introduction

Cancer biologists have long understood that tumor transformation and metastasis are driven by both intrinsic genomic changes in the constituent tumor cells and the integrated response of the tissue or organ to extrinsic soluble cues, such as growth factors, cytokines, and chemotactic stimuli. Indeed, cancer progression is often collectively conceptualized and portrayed as a “journey” in which a cell morphs over time from a benign phenotype into an invasive or metastatic entity, with many potential intermediate steps along the way. In practice, the stages of this journey are marked by a variety of genetic and histopathological checkpoints, including amplification or inactivation of specific genes, expression of tumor markers, and stereotypic alterations in cell and tissue architecture. Over the past two decades, however, the field has begun to appreciate that an important part of this journey involves changes in the *mechanical* phenotype of the cell and tissue, as reflected both in intrinsic changes in cell and tissue structure and mechanics and in the biophysical properties of the cell’s microenvironment, such as the mechanics, geometry, and topology of the extracellular matrix (ECM) [1–3]. The interplay between the biophysical properties of the cell and ECM establishes a dynamic, mechanical

S. Kumar (✉)
Department of Bioengineering, University of California,
Berkeley, USA
e-mail: skumar@berkeley.edu

V. M. Weaver
Department of Surgery and Center for Bioengineering
and Tissue Regeneration, Department of Anatomy,
Department of Bioengineering and Therapeutics,
Institute for Regeneration Medicine, University of California,
San Francisco, USA
e-mail: Valerie.Weaver@ucsfmedctr.org

reciprocity between the cell and the ECM in which the cell's ability to exert contractile stresses against the extracellular environment balances the elastic resistance of the ECM to that deformation (i.e., ECM rigidity or elasticity). It has now become clear that this force balance can regulate a surprisingly wide range of cellular properties that are all critical to tumorigenesis, including structure, motility, proliferation, and differentiation.

Cells sense, process, and respond to mechanical and other biophysical cues from the ECM using an interconnected hierarchy of mechanochemical systems that includes adhesion receptors (e.g., integrins), intracellular focal adhesions, cytoskeletal networks, and molecular motors. The integrated mechanics and dynamics of these systems enable cells to control their shape, generate force, and ultimately remodel the ECM [4–8]. These structural networks also interact in very specific ways with canonical signal transduction pathways to orchestrate cell behavior. For example, mammary epithelial cells (MECs) form normal acinar structures when cultured in ECMs of physiological stiffness but display the structural and transcriptional hallmarks of a developing tumor when cultured in ECMs of a stiffness that more closely resembles tumor stroma. Processing of these signals requires integrin clustering, ERK activation, cytoskeletal remodeling and Rho GTPase-dependent contractility, illustrating functional connections between growth factor signaling, mechano-transductive signaling, and the cell's cytoskeletal, adhesive, and contractile machinery [9]. In other words, micro-mechanical signals from the ECM and cell structural control are intimately connected and interface with signal transduction networks to control fundamental behaviors relevant to tumor transformation, invasion, and metastasis.

In this review, we discuss the evolution of the mechanical phenotype of tumor cells, which we conceptualize as a “force journey.” We begin by discussing the various stages of this journey, including mechanical forces that cells within tissues must encounter and generate while transforming from a normal to an invasive or metastatic phenotype. We then review methods for measuring cellular mechanical properties *in vitro* and *in vivo*, including a description of probes of both cortical and intracellular mechanics. Finally, we briefly describe emerging molecular mechanisms for mechanotransduction in tumor cells, with a special emphasis on Rho GTPase and focal adhesion kinase.

2 The mechanical force journey of a tumor cell

2.1 Tissue assembly and morphogenesis

Even in tissues that are seemingly static, cells constantly encounter a variety of mechanical forces and, in turn,

actively exert mechanical force on their surroundings (Fig. 1A). These forces can originate from neighboring cells or the ECM and are channeled through specific adhesion receptors [10], as well as through mechanical loads applied nonspecifically to the entire tissue, including interstitial forces and shear flows [11]. Indeed, cells continuously interrogate their mechanical microenvironment and integrate these force cues by exerting a reciprocal compensatory contractile force derived from the coordinated action of cytoskeletal remodeling and motor protein activity. At the tissue and organismal levels, these cell-derived contractile forces are essential for sculpting the organism during embryogenesis and organ development. For example, application of mechanical force to the developing *Drosophila* embryo induces expression of the mechanosensitive gene *Twist* throughout the embryo and induces ventralization; moreover, developmental deficits in mutants with abnormal *Twist* expression may be rescued by application of compressive forces [12]. Force transmission between cells in this system may be quantified and directly manipulated through the use of femtosecond laser ablation [13]. These force interactions play similar roles in vertebrate embryogenesis [14] and the development of specific organ systems; for example, pharmacologic disruption of cellular contractility interferes with lung branching morphogenesis [15]. More recently, the mechanical force environment has been exploited as an engineering tool to direct stem cell differentiation *in vitro*, with an eye towards tissue engineering and regenerative medicine applications. Human mesenchymal stem cells (hMSCs) cultured on highly compliant and rigid ECMs preferentially differentiate into neurons and osteocytes, respectively. In this case, the ECM directs hMSCs to differentiate towards a tissue type whose stiffness matches that of the ECM [16]. Interestingly, these stiffness-dependent lineage effects depend on the specific ECM protein presented to the cells, with compliant ECMs promoting neurogenesis on collagen-based ECMs and adipogenesis on fibronectin-based ECMs [17]. Even stem cell populations not traditionally regarded as “load-bearing” are sensitive to these mechanical cues; for example, when adult neural stem cells are presented with ECMs of various mechanical rigidities and cultured in mixed differentiation media, soft matrices promote neuronal cultures and rigid matrices promote glial cultures [18].

Alterations in the mechanical interactions between cells and their environment contribute to the tissue dysplasia associated with tumor initiation. For example, transformed epithelial cells express vastly different intermediate filament profiles and cytoskeletal architectures than their normal counterparts; indeed, replacement of a keratin-based cytoskeleton with a vimentin-based cytoskeleton is a defining hallmark of epithelial-to-mesenchymal transition in mammary tissue [19–21]. When presented with compli-

ant substrates that suppress spreading and proliferation of normal cells, transformed cells both proliferate extensively [22] and exert abnormally high tractional forces, which can in turn disrupt cell-cell junctional integrity, compromise tissue polarity, promote anchorage-independent survival and enhance invasion (Fig. 2). This increased contractility reflects increased expression and activity of Rho GTPase and its downstream effectors, as well as high levels of growth factor-induced ERK activity. Most compellingly, manipulation of ECM stiffness and stiffness-dependent cell contractility is sufficient to induce epithelial transformation in cultured cells. For example, as discussed earlier, use of high-stiffness ECM gels alters integrin subtype expression, enhances focal adhesion assembly, disrupts acinar architecture, and promotes invasion in cultured MECs through an elevation of Rho- and ERK-dependent contractility [9]. Intriguingly, similar comparative effects may be induced by culturing transformed MECs on collagen gels affixed to a

rigid substrate versus gels allowed to freely float [23], implying that intracellular tension channeled through the ECM is a governing cue that regulates tissue assembly and morphogenesis.

2.2 Detachment and invasion

As an individual cell frees itself from a tumor and begins to invade the surrounding parenchyma, additional force-generating mechanisms begin to regulate its behavior (Fig. 1B). This phenomenon is perhaps best illustrated by recent work on the role of protrusive processes known as invadopodia in facilitating initial digestion and invasion of the ECM [24, 25]. While the structure and molecular composition of invadopodia remain incompletely understood, from these studies it is now clear that formation of these structures requires highly localized actin polymerization and the coordinated action of multiple actin binding

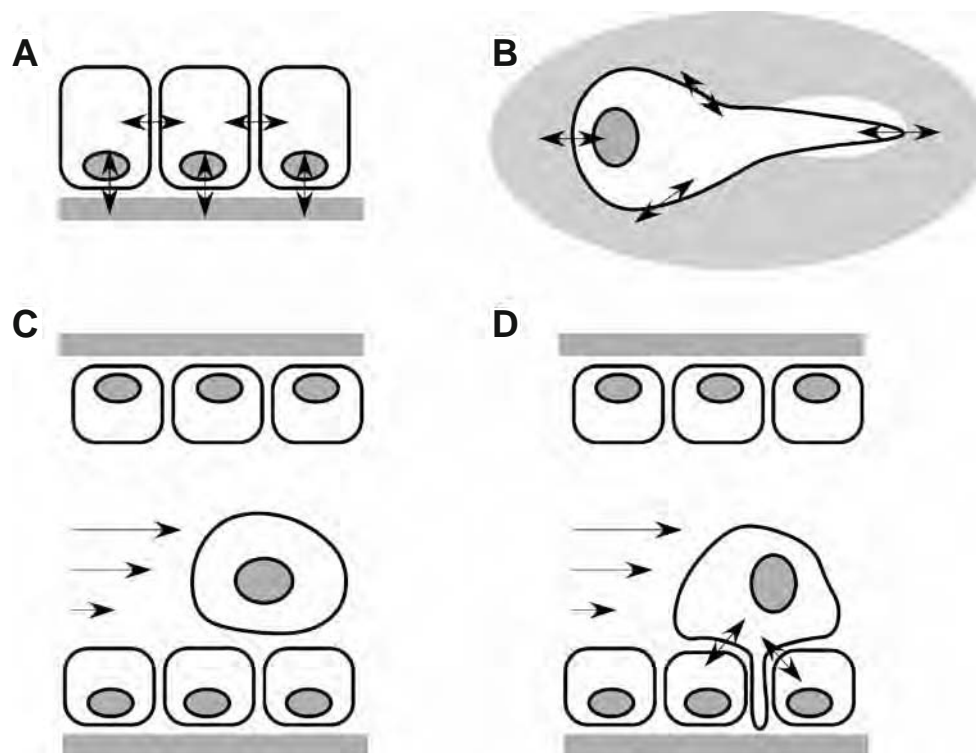
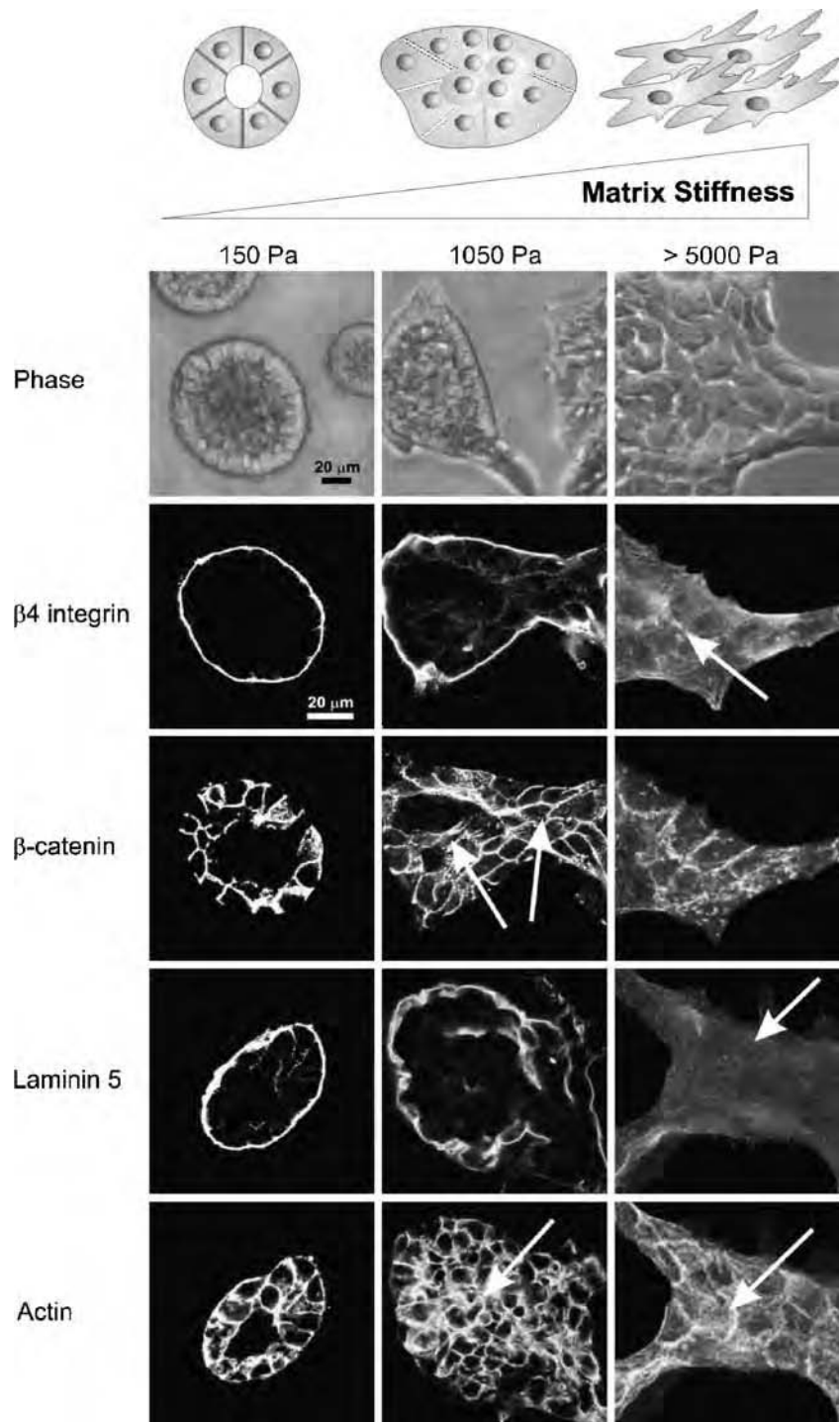


Fig. 1 The force journey of a tumor cell. Starting from their participation in normal tissue homeostasis and continuing through all stages of tissue dysplasia, tumor cell invasion, and metastasis, tumor cells both absorb and exert mechanical force. This interplay establishes a dynamic, mechanical reciprocity between tumor cells and their environment (represented schematically as arrows). **a** Even in normal tissues, such as the epithelium depicted here, cells experience mechanical force from their neighbors and the extracellular matrix, which are often channeled through specific receptor-ligand interactions to trigger signaling events. Cells may also be subject to nonspecific forces applied to the whole tissue, such as interstitial pressure and shear flow. **b** As a tumor cell detaches from the primary tumor mass and invades the surrounding parenchyma, it continues to

exchange mechanical force with its environment, including tractional forces associated with locomotion and protrusive forces of the leading edge of the cell. In some cases, protrusive structures are also used to spatially focus secretion of matrix metalloproteases, e.g., invadopodia. **c** If a tumor cell escapes its primary tissue and reaches the vasculature, it must withstand shear forces associated with blood flow. Shear has been demonstrated to activate gene programs associated with cytoskeletal remodeling and altered cell-cell adhesion. **d** In order for a tumor cell to escape the vasculature and metastasize to a distal tissue, it must undergo diapedesis through the endothelial wall, which introduces additional mechanical interactions between the tumor cell and endothelial cells and precedes a transition from cell-cell adhesion to cell-ECM adhesion

Fig. 2 Effect of extracellular matrix stiffness on mammary epithelial morphogenesis. Phase and immunofluorescence images of mammary epithelial cells (MECs) cultured on ECM substrates of Young's moduli of 150 Pa (left column), 1050 Pa (middle column) and >5000 Pa (right column). Cells cultured on substrates with elasticities of 150 Pa, which is similar to the elasticity of normal mammary tissue, form patent acinar structures with clearly defined cell-cell junctions and integrin distributions. A modest increase in ECM elasticity to 1050 Pa leads to loss of luminal patency, disruption of cell-cell contacts, and altered acinar morphology. For ECM elasticities greater than 5000 Pa, acinar organization, cell-cell junctions, and cellular ECM deposition are all completely disrupted. Figure reproduced with permission from [149]



proteins, including cofilin, Arp2/3, and N-WASP [26]. Importantly, although invadopodia share many structural and functional similarities to the filopodia that are observed during two-dimensional migration, they can be distinguished by their ability to spatially focus proteolytic secretion, thereby facilitating the remodeling of existing matrix, secretion of new matrix, and ultimately the establishment of “tracks” that support subsequent invasion.

This process was recently captured in real time through elegant multimodal dynamic imaging conducted by Wolf, Friedl, and colleagues [27]. These authors could observe how cells proteolytically degrade and rearrange local ECM fibrils while they migrate through three-dimensional collagen gels. Importantly, broad-spectrum pharmacological inhibition of matrix metalloprotease (MMP) activity forces the cells to “squeeze” through the existing collagen fibers

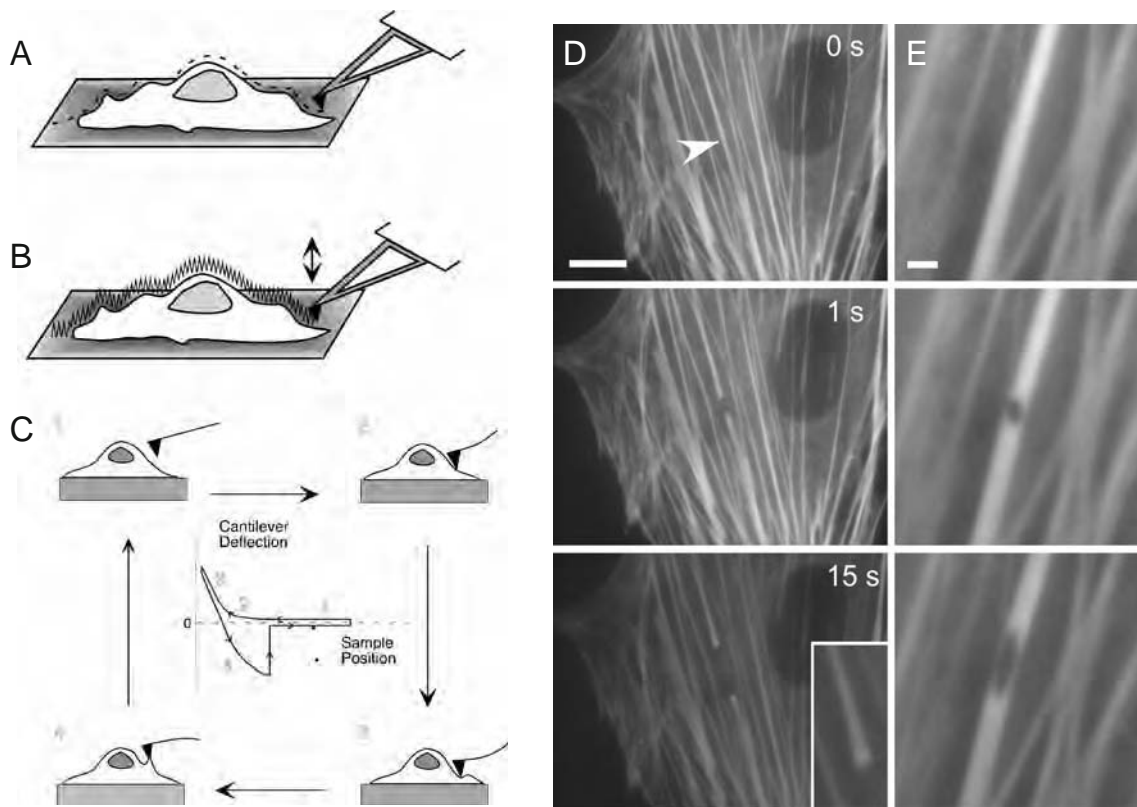


Fig. 3 Methods for characterizing the mechanical phenotype. **(a-c)** Atomic force microscopy (AFM). AFM may be used to obtain topographic images of living cells by scanning a nanoscale probe mounted on a force-sensitive cantilever. This may be accomplished by maintaining the probe in **a** constant contact or **b** oscillatory contact with the cell and using the deflections of the cantilever to reconstruct an image. **c** AFM may also be used to obtain mechanical properties of living cells by indenting the surface of the cell with the probe and recording the resistive force of the cell during indentation. **(d-e)**

Subcellular laser ablation (SLA). In SLA, sub-micron structures inside living cells are irradiated with a high-intensity and tightly-focused laser, resulting in nonlinear absorption and optical breakdown. SLA has been used to **d** sever and **e** puncture actomyosin stress fiber bundles in endothelial cells, and the response of these structures (e.g., the retraction of the severed ends) have been used to measure stress fiber mechanical properties and contribution to cell shape. **(a)-(c)** reproduced from [71] with permission from Blackwell; **(d)** and **(e)** reproduced from [80] with permission from Biophysical Society

(analogous to amoeboid motion), and this migratory behavior is accompanied by dramatic cell and nuclear deformations. By definition, all of these processes—invadopodia extension, matrix track formation, and cell and nuclear deformation—require local, dramatic, and highly dynamic changes in cytoskeletal organization and cellular mechanics. Quantification of these changes and elucidation of the underlying molecular mechanisms represents a significant and ongoing challenge in this emerging field but also has the potential to uncover novel insights into how cells invade and metastasize, and to identify new therapeutic targets.

The alterations in tumor cell structure and mechanics during detachment and invasion are accompanied by reciprocal changes in ECM topology (organization) and materials properties (mechanics). As described above, cellular contractility can directly promote microscale remodeling of the ECM, which can create matrix bundles or motility tracks that could facilitate three-dimensional cell migration. In addition, tumor formation *in vivo* is accompanied by a progressive stiffening of the tissue and ECM, as

evidenced by the finding that mammary tumor tissue and tumor-adjacent stroma are between 5–20 times stiffer than normal mammary gland, respectively [9]. While such differences in tissue stiffness have not been as well characterized in other tumor systems, they plainly exist and are regularly exploited for cancer diagnosis and therapy. For example, palpable tissue stiffening is routinely used to screen and diagnose virtually all superficial soft-tissue tumors [28]. More recently, ultrasound imaging, which derives its contrast from mechanical compliance differences within tissue, has found a role in tumor diagnosis [29] and intraoperative localization of tumor tissue during resection of gliomas [30, 31]. These increases in ECM stiffness in turn enable cells to generate increased tractional forces on their surroundings, which enhances their growth, survival, and invasion by promoting focal adhesion maturation and signaling through actomyosin contractility [39, 32–34]. As described above, the elevated contractility of tumor cells and their associated stromal fibroblasts also induce tension-dependent matrix remodeling to promote the linear reorientation of collagen

fibrils surrounding the invasive front of the tumor. Rapidly migrating transformed mammary epithelial cells have been observed on these prominent linear bundles of collagen fibers adjacent to blood vessels [35–37].

2.3 Interstitial forces

In addition to the microscale, molecularly-specific issues described above, an important component of the force journey of a tumor cell involves its ability to withstand nonspecific mechanical forces that arise from the growth of the tumor itself, tissue homeostasis, and transport in the lymphatic system and bloodstream. Even before the initiation of invasion and metastasis, tumor expansion compresses the surrounding ECM, which in turn constricts flow in the vasculature, lymphatic system, and interstitial space. When these compressive stresses occur in the setting of tissue that is highly compliant at baseline, such as pancreas and brain, one observes compromised basement membrane organization and thinning, which combined with the outward projecting compression force, facilitates tumor cell invasion into the parenchyma [9, 38]. These compressive forces clearly also contribute directly to the initial clinical presentation of tumors, such as the symptoms of increased intracranial pressure which commonly prompt presentation in glioblastoma multiforme [39, 40] and the biliary obstructions that are often the initial sign of pancreatic cancer [41]. At the histopathologic level, these stresses can facilitate tumor angiogenesis by enhancing VEGF expression, either through direct upregulation of VEGF secretion or indirectly through induction of hypoxia [42, 43]. Compression forces can also shrink the interstitial space surrounding the ductal structures, which can in turn concentrate growth factors and cytokines to facilitate autocrine and paracrine signaling and promote tumor growth [44]. Tumor-associated changes in interstitial pressure and compressive stress also present significant challenges for drug delivery to solid tumors [45]. These pressures may be compounded by tumor-induced stromal stiffening, which forces the tumor to exert even higher stresses to expand than would be needed in normal tissue. Ironically, while tumor expansion is commonly associated with massive MMP secretion and matrix digestion, tumor-adjacent ECM is frequently quite dense, with increased matrix deposition, crosslinking, and bundling [9].

2.4 Shear Forces

If a tumor cell successfully escapes the confines of its primary tissue of presentation and arrives at the vasculature or lymphatic system en route to metastasis, it must deal with an entirely new set of mechanical forces, in particular those associated with fluid flow and shear (Fig. 1C). Even

if the primary tumor is successfully excised, surgical manipulations such as irrigation and suction may subject tumor cells to substantial shear forces or altered patterns of flow [46]. Exposure to shear can activate specific signaling pathways in tumor cells that can in turn induce dramatic reorganization of the cytoskeleton and adhesive machinery and ultimately facilitate reinforcement of cell structure and attachment to the vascular wall [47]. Recently, Basson and colleagues demonstrated that shear can paradoxically *enhance* adhesion to collagen-based ECM substrates *in vitro* through a process that involves activation of Src and subsequent assembly of the actin cytoskeleton and formation of focal adhesions [48]. Similarly, Haier and colleagues demonstrated that shear can enhance FAK phosphorylation in colon carcinoma cells, thereby strengthening adhesion to collagen-based ECMs. Impressively, parallel *in vivo* studies illustrated that overexpression of dominant-negative FAK significantly diminished the ability of tumor cells to adhere to vasculature within the hepatic microcirculation [49].

2.5 Diapedesis and distal metastasis

Once a circulating tumor cell has survived the vasculature and adhered to the endothelium of a target tissue, it must cross the endothelial barrier in order to colonize that tissue (Fig. 1D). Much like leukocytes during an inflammatory response, adherent tumor cells undergo diapedesis, a process by which they extend pseudopodial process that penetrate cell-cell junctions in the endothelium, which requires local and dynamic changes in cellular mechanics driven by cytoskeletal remodeling. This in turn is accompanied by rearrangements in the actin cytoskeletons of the endothelial cells (and changes in their own mechanical phenotype), although the molecular details of this complex process are poorly understood [50]. As the tumor cell makes its way towards the subendothelial basement membrane, these cellular rheological changes are accompanied by changes in expression of adhesion molecules, portending a phenotypic switch from cell-cell adhesion to cell-ECM adhesion. The mechanisms underlying this switch may include conformational activation of existing integrins [51] and expression of entirely new integrin subunit combinations [52]. Recently, Mierke et al. screened 51 tumor lines for their ability to transmigrate in an endothelial co-culture system and showed that the propensity of a cell line to invade correlated with (and was enhanced by) expression of the chemokine receptor CXCR2. Importantly, parallel cellular mechanics measurements revealed that siRNA-mediated knockdown of CXCR2 expression increased cytoskeletal remodeling dynamics and contractility, leading to a model in which CXCR2-mediated signaling promotes tumor cell transmigration through modulation of cytoskeletal assembly and contractility [53].

In summary, tumor cells both withstand and exert mechanical force on their environment in their transformative journey, and these processes require profound and highly dynamic changes in cellular mechanical properties. We now discuss specific biophysical methods that permit direct measurement of these properties.

3 Characterizing the mechanical phenotype

3.1 Stress, strain, elasticity, and viscoelasticity

Before embarking on a detailed discussion of how cellular mechanical properties can be measured, it is first necessary to define some terms. Mechanical stress is the force applied per unit area to an object (e.g., a cell), and strain is that object's deformation normalized by its initial size. Thus, mechanical stress is expressed in units of force/area (e.g., N/m^2 or Pascals (Pa)), and strain is a dimensionless quantity. The Young's Modulus (also known as the elastic modulus or elasticity (E)), a measure of the deformability of the material, is stress divided by strain; the higher the Young's Modulus, the stiffer the material. Because strain is a dimensionless quantity, the Young's Modulus has the same units as stress, e.g., Pa. The Young's Modulus offers a way to quantify mechanical differences between tissues, and indeed the measured bulk elasticities of human tissues span some five orders of magnitude, e.g., fat (17 Pa), mammary gland (160 Pa), brain (260–490 Pa), liver (640 Pa), kidney (2.5 kPa), skeletal muscle (50 kPa), cartilage (950 kPa) [54]. Strictly speaking, elasticity describes the mechanical properties associated with the ability of a material to internally store mechanical energy and is therefore independent of the rate of deformation. However, many biological materials, including living cells, are capable of both storing and dissipating applied mechanical energy through internal frictional interactions, and do so in a way that depends strongly on the rate of deformation. For this reason, when measuring the mechanical properties of these materials, it is critical to capture both the elastic, or "storage" properties and the viscous, or "loss" properties. Such materials are referred to as viscoelastic materials, and the aggregate viscous and elastic response of a material to mechanical deformation is collectively referred to as its *rheology* [55].

3.2 Measuring cellular rheology in two-dimensional cell culture

Over the past decade, a sophisticated suite of technologies has been developed with the primary goal of quantifying the viscoelastic properties of cultured cells [8, 56]. These include methods for measuring mean rheological properties

of whole cells, such as optical stretching [57–60], micropipette aspiration [61–65], traction force microscopy (TFM) [66–69], atomic force microscopy (AFM) [70–73], and magnetic twisting microrheometry [10, 74–77]; and micro-scale mechanics of portions of cells, such as subcellular laser ablation (SLA) [78–82], micropost array detectors [83–88], and particle tracking microrheometry [89–93]. Some of these methods can be applied to both the subcellular and whole-cell scale; for example, AFM may be used both at low resolution to obtain mean indentational modulus of a population cells and at high resolution to spatially map mechanical properties across the surface of a single cell. All of these methods have been reviewed extensively elsewhere; to offer examples of how these techniques can be applied to cellular rheology in the context of tumor biology, we focus here on AFM and SLA.

1. Atomic force microscopy (AFM)

In atomic force microscopy (AFM), one measures the interaction force between a sample surface, such as a living cell, and a microscale probe ("tip") attached to a spring-like cantilever (Fig. 3A-C). The encounter between the tip and sample creates a force that deflects the cantilever, which in turn can be optically tracked and converted to an interaction force if the spring constant of the cantilever is known. Because contrast in AFM originates entirely from the interaction force between the tip and sample, it typically requires no fixation or staining and may readily be conducted in cell culture media. Thus, the method is perfectly suited to capture dynamic processes in living systems. One may acquire two types of information from the tip-sample interaction with the AFM: topographical images and force measurements. In the former measurement, the surface of a sample is scanned at constant force, and the compensatory motions of the stage needed to maintain force constant as the sample topography changes can be used to reconstruct an image. In the latter approach, the sample is vertically indented by the tip at a fixed position, and the resistance of the sample to that deformation may be analyzed to extract the material's viscoelastic properties. AFM has been employed to image superficial cytoskeletal structures in living cells that may not be readily optically imaged, including cortical actin bundles [94, 95]. Similarly, the force measurement capability of AFM has been used quite successfully to quantitatively measure properties relevant to cellular mechanics at length scales ranging from single molecules to whole cells. In the area of single molecule mechanics, AFM has been used to measure both the force-dependent unfolding of ECM proteins [96] and cell-ECM adhesion proteins [97] in an effort to understand how these systems accomplish mechanochemical conversions. AFM has also demonstrated tremendous value for quantifying the indentational rheology of living

cells, including cellular elasticity [98], spatial maps of elasticity across the cell surface [99], and transduction of local compressive forces into biochemical signals [100].

One of the more innovative recent applications of AFM to cellular mechanics is the measurement of protrusive forces generated by growing actin networks, such as those found in invadopodia and pseudopodia. For example, Fletcher and coworkers recently nucleated a dendritic actin network from an AFM cantilever and allowed the network to polymerize against a solid support and deflect the cantilever [101]. With this system, they measured network protrusive forces under various applied loads, analogous to a pseudopodium squeezing its way through an endothelial barrier. Surprisingly, these studies show that the growth velocity depends on the loading history of the network and not merely the instantaneous load. These data therefore suggest that these cytoskeletal networks likely remodel to adapt to applied loads (e.g., by recruiting additional actin filaments), and that these remodeling events are progressively recorded in the evolving structure of the network. These investigators later used a similar approach to measure the oscillatory viscoelastic properties of these growing networks and were able to observe predictable and reversible stress-softening phenomena [102]. These results are particularly exciting in light of the parallel efforts of Radmacher and colleagues to measure forces associated with cell migration in living cells [103]. By orienting the AFM cantilever perpendicularly to a glass coverslip containing a culture of migrating keratocytes, these authors could directly measure cellular propulsive forces as individual cells encountered the cantilever during migration and attempted to push the cantilever by extending a lamellipodium against it.

AFM has also recently been employed as a diagnostic tool for measuring stiffness differences in leukemia cells, and for tracking changes in stiffness in response to chemotherapy [104–106]. In these studies, myeloblastic cell lines were found to be more than an order of magnitude stiffer than corresponding lymphoblastic cell lines. Taken together with the clinical observation that acute myelogenous leukemia produces leukostasis much more frequently than acute lymphocytic leukemia, these observations serve as a conceptual basis for a model in which low cell deformability likely contributes directly to cellular occlusion of blood vessels. This model has been further supported by the observation that when these cells are treated with chemotherapeutic agents and undergo apoptosis, they stiffen further, consistent with the clinical observation that leukostatic episodes often correlate with the induction of chemotherapy.

2. Subcellular laser ablation

Although AFM has yielded much insight into cellular rheological properties relevant to tumor cell invasion and

metastasis, it suffers from two important limitations. First, it can only probe the exterior surface of a living cell, thereby offering limited access to the mechanical properties of internal structures. Second, AFM measurements represent the collective contribution of many cytoskeletal filaments and motor proteins and do not permit dissection of the contribution of individual structural elements in localized microscale regions within the cell. As described earlier, the elucidation of specific cytoskeletal structures in specific places and times in the cell (e.g., stress fibers, filopodial actin bundles) are likely to be critical as the cell journeys towards invasion and metastasis.

Subcellular laser ablation (SLA) has emerged as a complementary method that is capable of overcoming both limitations (Fig. 3D-E). First applied towards cell biology by Michael Berns and coworkers [78, 107–111], SLA uses a tightly focused laser beam to irradiate and vaporize nano- to microscale structures in living cells. Upon irradiation, material at the laser focus undergoes nonlinear multiphoton absorption, leading to optical breakdown and material destruction. Importantly, if the pulse energy, pulse width, and repetition rate are chosen correctly, structures in living cells may be selectively incised with sub-micrometer precision without compromising the plasma membrane or killing the cell. For example, it was recently demonstrated that delivery of femtosecond laser pulses at kilohertz repetition rates and at pulse energies ranging from 1.4 nJ–2.3 nJ can produce zones of photodamage as small as ~150 nm [79].

In the context of understanding biophysical signaling between capillary endothelial cells and the ECM in tumor angiogenesis [112], SLA has been employed to probe the micromechanical properties of actomyosin stress fiber bundles (stress fibers), which are the contractile structures that anchor and enable endothelial cells to exert tractional forces against the ECM [80]. These tractional forces play central roles in endothelial and epithelial cell shape, polarity, and motility both *in vitro* [113–116] and *in vivo* [117, 118]. The actin cytoskeletons of living endothelial cells were visualized using yellow fluorescent protein (YFP)-tagged actin, and selected stress fibers at the cell base were irradiated and severed with femtosecond laser pulses. These studies show that severed stress fibers retract in parallel with the axis of the fiber, providing *prima facie* evidence that these structures bear tensile loads; and that the quantitative retraction kinetics are consistent with that of a viscoelastic cable. Perhaps the most surprising result to emerge from this study is that the coupling between one fiber and the cytoskeletal architecture and shape of the rest of the cell depend strongly on the stiffness of the ECM onto which cells are cultured. For cells cultured on rigid substrates with an elasticity on the order of 1 MPa–1 GPa (e.g., glass), severing a single stress fiber, or even multiple parallel fibers,

does not appreciably alter cell shape. Conversely, severing a stress fiber in cells cultured on relatively soft (~4 kPa) polyacrylamide-based substrates produces a 4–5% elongation of the cell along the axis of the stress fiber, as well as a thinning and extension of cytoskeletal structures tens of microns from the site of incision. Parallel studies with TFM revealed that a single stress fiber contributes to ECM strain across nearly the entire cell-ECM interface and strains the ECM most strongly near the points at which the cytoskeletal element inserts into the focal adhesion. Thus, these studies illustrate how SLA can be used to show direct connections between individual micron-scale cellular contractile structures and tractional forces exerted by cells that are distributed over hundreds of square microns.

3.3 Measuring cellular mechanics in three dimensions and *in vivo*

The application of AFM and SLA to the measurement of cellular mechanics has largely been limited to cells in two-dimensional culture formats. Recently, however, both of these methods have been extended to more physiologically relevant systems. For example, AFM has been used to measure the regional elasticity of cultured brain slices [119] and excised mammary tissue (VMW, unpublished observations). And as described earlier, laser ablation has been used to disrupt mechanical interactions between groups of cells in the developing three-dimensional embryo [13]. Recently, in an effort to understand biophysical mechanisms regulating cadherin-mediated cell-cell adhesion in living epithelia, Cavey and colleagues successfully used SLA to sever junctional actin networks in *Drosophila* embryonic epithelia in the presence of actin-severing agents and Rho kinase inhibitors, and in the context of siRNA-mediated knockdown of α -catenin [120]. Similar efforts have been used to extend other cellular mechanics methods to living, three-dimensional organisms, including particle-tracking microrheology [121].

Additional new methods are emerging that enable real-time tracking of cell-directed ECM dynamics during various stages of tumorigenesis. In many cases, this has involved creative extensions of two-dimensional mechanics approaches to three-dimensional cultures. For example, three-dimensional particle tracking microrheology has recently been used to quantify both cellular mechanics [122] and matrix remodeling during migration of cells within hydrogels [123]. Similarly, modified versions of TFM have been used to track ECM stresses and strains in three dimensions [124]. These methods have also been correlated with molecular-scale events during cell migration, such as the formation and disassembly of focal adhesions [125] and generation of contractile forces [126]. An important challenge for the future will be to develop

mechanical methodologies that are as quantitatively sophisticated as current two-dimensional approaches but that also allow access to more complex and physiologically relevant ECM environments.

4 Future prospects: Towards molecular mechanisms

One of the central challenges in understanding the role of the mechanical phenotype in cancer is elucidation of the molecular mechanisms that enable tumor cells to modulate their mechanical responses and phenotype and their ability to sense and actively direct the biophysical properties of the ECM. This problem is particularly daunting because it requires facility with cell biology, biophysics, materials science, and imaging. It also requires a willingness to integrate new knowledge about mechanics and mechanobiology into our existing understanding of the molecular and cellular biology of cancer. That said, the field has made tremendous strides over the past decade towards identifying key molecules and signaling pathways relevant to cellular mechanobiology in cancer. While a detailed discussion of these mechanisms is beyond the scope of this review, we briefly discuss evidence for two such systems: Rho GTPase and focal adhesion kinase (FAK).

4.1 Rho GTPase

The small GTPase Rho has long been known to contribute to many steps in cancer progression, including proliferation, evasion of apoptosis, invasion, and metastasis [127]. In the specific context of cell mechanics, Rho can stimulate cellular contractility through its ability to activate Rho-associated kinase (ROCK), which in turn inhibits myosin light chain (MLC) phosphatase and activates MLC kinase, thereby promoting net phosphorylation of MLC. As with all of the small GTPases, Rho acts as a molecular switch in which the GTP-bound form is “active” and the GDP-bound form is “inactive.” Indeed, the expression levels and subtype distributions of accessory factors that facilitate this switching, chiefly guanine nucleotide exchange factors (GEFs) and GTPase activating proteins (GAPs), are frequently markedly altered in tumors. Rho activation has been linked in a wide variety of culture systems to actomyosin contractility, formation of stress fiber bundles, and reinforcement and maturation of focal adhesions [128]. In three-dimensional culture models, Rho GTPases play a central role in both pseudopodial protrusion, focal contact and adhesion formation, and trailing-edge retraction, thereby contributing to amoeboid motion [129]. Rho can also regulate and spatially focus secretion of MMPs, which can in turn facilitate matrix remodeling [130]. Recently, ROCK has

been explored as a clinical target; for example, the ROCK inhibitor fasudil has been shown to slow the progression of lung and breast tumors in a series of animal models [131].

4.2 Focal adhesion kinase

As discussed earlier, focal adhesions are micron-scale macromolecular complexes at the intracellular face of the cell-ECM interface that serve the dual purpose of physically anchoring cell adhesion receptors to the cytoskeleton and coordinating mechanotransductive signaling. More than one hundred distinct focal adhesion proteins have been identified to date [132], with a rich diversity of functional properties that includes binding to integrins [133], binding to cytoskeletal proteins [134], binding to membrane lipids [135], internal coordination of other focal adhesion proteins [136], and participation in canonical signal transduction pathways [137]. While focal adhesions seem endlessly complex, a few key proteins appear to play a particularly central role in organizing structure and signaling; one such protein is focal adhesion kinase (FAK) [138]. FAK is a nonreceptor tyrosine kinase that is widely overexpressed and activated in tumor cells [139–142]. For this reason, FAK has emerged as an important therapeutic target in cancer; FAK inhibitors have been demonstrated to inhibit the proliferation of tumor cells in culture [143] and are now currently in phase I clinical trials [138]. In addition to its kinase domain, FAK contains a focal adhesion targeting (FAT) domain that is required for its localization to focal adhesions and binds other focal adhesions proteins (e.g., vinculin) and modulators of Rho GTPase signaling (e.g., p190RhoGEF), and a proline-rich domain that enables docking of SH3-containing proteins (e.g., p130Cas) [144]. FAK also contributes indirectly to focal adhesion structure and function by phosphorylating and functionally activating a wide variety of focal adhesion proteins including the F-actin crosslinking protein α -actinin [145]. While the importance of FAK to regulating all steps in the force journey of tumor cells, including tumor de-adhesion, invasion, and distal metastasis, is well documented, the molecular mechanisms through which FAK senses and transduces mechanical signals remains unclear. Evidence for the importance of FAK in mechanosensing comes from a number of sources. For example, the migration and focal adhesion dynamics of FAK $-/-$ fibroblasts are substantially less sensitive to ECM rigidity than wild-type cells [146], and FAK phosphorylation is dramatically stimulated with application of mechanical force [147]. Recently, Mofrad and colleagues used steered molecular dynamics simulations to show that application of tensile forces to the FAT domain of FAK strongly modulates its binding affinity for vinculin [148].

5 Conclusions

One of the most exciting and challenging developments in cancer biology over the past decade is the recognition that tumor growth, invasion, and metastasis are all intricately tied to the constituent cells' ability to sense, process, and adapt to mechanical forces in their environment. In this review, we have conceptualized this process as a “force journey” through which a cell progresses that includes dramatic changes in tumor cell shape, mechanics, motility, and actuation of mechanical cues in the tumor microenvironment. It is important to emphasize that while this force journey represents a crucial element in the evolution of a tumor, it exists in an equally important context that includes all of the genetic and epigenetic lesions traditionally associated with cancer, such as genomic disruptions and instability, altered sensitivity to soluble growth and inhibitory factors, and secretion of soluble signals that facilitate matrix remodeling and angiogenesis. The challenge is to determine how these two parallel journeys interact, which portions of each are necessary and sufficient for tumor progression, and under what circumstances elements of one can offset or potentiate elements of the other. An important part of interfacing these two paradigms will be to bring together the quantitative power of mechanobiology with the biological sophistication of traditional cancer biology. In particular, progress in this area will require a willingness to broaden the scope of cancer cell biology to include the concepts, methods, and formalisms normally associated with cellular biophysics and engineering that are needed to synthesize and characterize physically-defined microenvironments, precisely measure mechanobiological properties of living cells, and incorporate applied mechanical force into traditional experimental paradigms. This will also require biophysicists and bioengineers to work closely with traditionally-trained cancer biologists to direct their tools towards experimental problems of maximal physiologic relevance and potential clinical impact. While forging these connections is far from trivial, the examples discussed in this review suggest that the benefits to our understanding of the cellular basis of cancer more than justify the effort.

Acknowledgments We apologize to the many authors whose work is not cited due to space limitations. SK acknowledges grant support from the University of California Cancer Research Coordinating Committee, the Arnold and Mabel Beckman Foundation, the American Heart Association (0765128Y), the National Science Foundation (CMMI-0727420), and the NIH Director's New Innovator Award (1DP2OD004213), a part of the NIH Roadmap for Medical Research. VMW acknowledges grant support from NIH NCI grant 7R01CA078731-07, DOD Breast Cancer Research Era of Hope grant W81XWH-05-1-330 (BC044791), CIRM grant RS1-00449 and DOE Low Dose Radiation grant A107165.

Open Access This article is distributed under the terms of the Creative Commons Attribution Noncommercial License which per-

mits any noncommercial use, distribution, and reproduction in any medium, provided the original author(s) and source are credited.

References

- Lelievre, S. A., Weaver, V. M., Nickerson, J. A., Larabell, C. A., Bhaumik, A., Petersen, O. W., et al. (1998). Tissue phenotype depends on reciprocal interactions between the extracellular matrix and the structural organization of the nucleus. *Proceedings of the National Academy of Sciences of the United States of America*, *95*(25), 14711–14716.
- Nelson, C. A., & Bissell, M. J. (2005). Modeling dynamic reciprocity: Engineering three-dimensional culture models of breast architecture, function, and neoplastic transformation. *Seminars in Cancer Biology*, *15*(5), 342–352.
- Paszek, M. J., & Weaver, V. M. (2004). The tension mounts: Mechanics meets morphogenesis and malignancy. *Journal of Mammary Gland Biology and Neoplasia*, *9*(4), 325–342.
- Bershadsky, A. D., Balaban, N. Q., & Geiger, B. (2003). Adhesion-dependent cell mechanosensitivity. *Annual Review of Cell and Developmental Biology*, *19*, 677–695.
- Giancotti, F. G., & Ruoslahti, E. (1999). Transduction — Integrin signaling. *Science*, *285*(5430), 1028–1032.
- Ingber, D. E. (2008). Tensegrity-based mechanosensing from macro to micro. *Progress in Biophysics & Molecular Biology*, *97* (2–3), 163–179.
- Janmey, P. A. (1998). The cytoskeleton and cell signaling: Component localization and mechanical coupling. *Physiological Reviews*, *78*(3), 763–781.
- Lele, T. P., & Kumar, S. (2007). Brushes, cables, and anchors: Recent insights into multiscale assembly and mechanics of cellular structural networks. *Cell Biochemistry and Biophysics*, *47*(3), 348–360.
- Paszek, M. J., Zahir, N., Johnson, K. R., Lakins, J. N., Rozenberg, G. I., Gefen, A., et al. (2005). Tensional homeostasis and the malignant phenotype. *Cancer Cell*, *8*, 241–254.
- Wang, N., Butler, J. P., & Ingber, D. E. (1993). Mechanotransduction across the cell surface and through the cytoskeleton. *Science*, *260*(5111), 1124–1127.
- Ingber, D. E. (2003). Mechanobiology and diseases of mechanotransduction. *Annals of Medicine*, *35*(8), 564–577.
- Farge, E. (2003). Mechanical induction of Twist in the Drosophila foregut/stomodaeal primordium. *Current Biology*, *13* (16), 1365–1377.
- Supatto, W., Debarre, D., Moulia, B., Brouzes, E., Martin, J. L., Farge, E., et al. (2005). *In vivo* modulation of morphogenetic movements in Drosophila embryos with femtosecond laser pulses. *Proceedings of the National Academy of Sciences of the United States of America*, *102*(4), 1047–1052.
- Wei, L., Roberts, W., Wang, L., Yamada, M., Zhang, S., Zhao, Z., et al. (2001). Rho kinases play an obligatory role in vertebrate embryonic organogenesis. *Development*, *128*(15), 2953–2962.
- Ewald, A. J., Brenot, A., Duong, M., Chan, B. S., & Werb, Z. (2008). Collective epithelial migration and cell rearrangements drive mammary branching morphogenesis. *Developmental Cell*, *14*(4), 570–581.
- Engler, A. J., Sen, S., Sweeney, H. L., & Discher, D. E. (2006). Matrix elasticity directs stem cell lineage specification. *Cell*, *126* (4), 677–689.
- Winer, J. P., Janmey, P. A., McCormick, M. E., & Funaki, M. (2009). Bone Marrow-Derived Human Mesenchymal Stem Cells Become Quiescent on Soft Substrates but Remain Responsive to Chemical or Mechanical Stimuli. *Tissue Engineering Part A*, *15* (1), 147–154.
- Saha, K., Keung, A. J., Irwin, E. F., Li, Y., Little, L., Schaffer, D. V., et al. (2008). Substrate modulus directs neural stem cell behavior. *Biophysical Journal*, *95*(9), 4426–4438.
- Kokkinos, M. I., Wafai, R., Wong, M. K., Newgreen, D. F., Thompson, E. W., & Waltham, M. (2007). Vimentin and epithelial-mesenchymal transition in human breast cancer—Observations *in vitro* and *in vivo*. *Cells Tissues Organs*, *185* (1–3), 191–203.
- Pagan, R., Martin, I., Alonso, A., Llobera, M., & Vilaro, S. (1996). Vimentin filaments follow the preexisting cytokeratin network during epithelial-mesenchymal transition of cultured neonatal rat hepatocytes. *Experimental Cell Research*, *222*(2), 333–344.
- Willipinski-Stapelfeldt, B., Riethdorf, S., Assmann, V., Woelfle, U., Rau, T., Sauter, G., et al. (2005). Changes in cytoskeletal protein composition indicative of an epithelial-mesenchymal transition in human micrometastatic and primary breast carcinoma cells. *Clinical Cancer Research*, *11*(22), 8006–8014.
- Wang, H. B., Dembo, M., & Wang, Y. L. (2000). Substrate flexibility regulates growth and apoptosis of normal but not transformed cells. *American Journal of Physiology — Cell Physiology*, *279*(5), C1345–1350.
- Wozniak, M. A., Desai, R., Solski, P. A., Der, C. J., & Keely, P. J. (2003). ROCK-generated contractility regulates breast epithelial cell differentiation in response to the physical properties of a three-dimensional collagen matrix. *Journal of Cell Biology*, *163* (3), 583–595.
- Wolf, K., Friedl, P. (2008). Mapping proteolytic cancer cell-extracellular matrix interfaces. *Clinical and Experimental Metastasis*, (in press).
- Yamaguchi, H., Wyckoff, J., & Condeelis, J. (2005). Cell migration in tumors. *Current Opinion in Cell Biology*, *17*(5), 559–564.
- Yamaguchi, H., Lorenz, M., Kempiak, S., Sarmiento, C., Coniglio, S., Symons, M., et al. (2005). Molecular mechanisms of invadopodium formation: the role of the N-WASP-Arp2/3 complex pathway and cofilin. *Journal of Cell Biology*, *168*(3), 441–452.
- Wolf, K., Wu, Y. I., Liu, Y., Geiger, J., Tam, E., Overall, C., et al. (2007). Multi-step pericellular proteolysis controls the transition from individual to collective cancer cell invasion. *Nature Cell Biology*, *9*(8), 893–904.
- Khaled, W., Reichling, S., Bruhns, O. T., Boese, H., Baumann, M., Monkman, G., et al. (2004). Palpation imaging using a haptic system for virtual reality applications in medicine. *Studies in Health Technology and Informatics*, *98*, 147–153.
- Khaled, W., Reichling, S., Bruhns, O. T., & Ermert, H. (2006). Ultrasonic strain imaging and reconstructive elastography for biological tissue. *Ultrasonics*, *44*(Suppl 1), e199–202.
- Selbekk, T., Bang, J., & Unsgaard, G. (2005). Strain processing of intraoperative ultrasound images of brain tumours: initial results. *Ultrasound in Medicine and Biology*, *31*(1), 45–51.
- Unsgaard, G., Rygh, O. M., Selbekk, T., Muller, T. B., Kolstad, F., Lindseth, F., et al. (2006). Intra-operative 3D ultrasound in neurosurgery. *Acta Neurochir (Wien)*, *148*(3), 235–253 discussion 253.
- Croft, D. R., Sahai, E., Mavria, G., Li, S., Tsai, J., Lee, W. M., et al. (2004). Conditional ROCK activation *in vivo* induces tumor cell dissemination and angiogenesis. *Cancer Research*, *64*(24), 8994–9001.
- O'Brien, L. E., Jou, T. S., Pollack, A. L., Zhang, Q., Hansen, S. H., Yurchenco, P., et al. (2001). Rac1 orientates epithelial apical polarity through effects on basolateral laminin assembly. *Nature Cell Biology*, *3*(9), 831–838.
- Wang, F., Weaver, V. M., Petersen, O. W., Larabell, C. A., Dedhar, S., Briand, P., et al. (1998). Reciprocal interactions

- between beta1-integrin and epidermal growth factor receptor in three-dimensional basement membrane breast cultures: a different perspective in epithelial biology. *Proceedings of the National Academy of Sciences of the United States of America*, 95(25), 14821–14826.
35. Ingman, W. V., Wyckoff, J., Gouon-Evans, V., Condeelis, J., & Pollard, J. W. (2006). Macrophages promote collagen fibrillogenesis around terminal end buds of the developing mammary gland. *Developmental Dynamics*, 235(12), 3222–3229.
 36. Provenzano, P. P., Inman, D. R., Eliceiri, K. W., Knittel, J. G., Yan, L., Rueden, C. T., et al. (2008). Collagen density promotes mammary tumor initiation and progression. *BMC Medicine*, 6(1), 1–11.
 37. Wyckoff, J. B., Pinner, S. E., Gschmeissner, S., Condeelis, J. S., & Sahai, E. (2006). ROCK- and myosin-dependent matrix deformation enables protease-independent tumor-cell invasion *in vivo*. *Current Biology*, 16(15), 1515–1523.
 38. Ingber, D. E., Madri, J. A., & Jamieson, J. D. (1981). Role of basal lamina in neoplastic disorganization of tissue architecture. *Proceedings of the National Academy of Sciences of the United States of America*, 78(6), 3901–3905.
 39. Black, P. (1998). Management of malignant glioma: role of surgery in relation to multimodality therapy. *Journal of Neurovirology*, 4(2), 227–236.
 40. Schankin, C. J., Ferrari, U., Reinisch, V. M., Birnbaum, T., Goldbrunner, R., & Straube, A. (2007). Characteristics of brain tumour-associated headache. *Cephalalgia*, 27(8), 904–911.
 41. Watanapa, P., & Williamson, R. C. N. (1992). Surgical Palliation for Pancreatic-Cancer—Developments during the Past 2 Decades. *British Journal of Surgery*, 79(1), 8–20.
 42. Harris, A. L. (2002). Hypoxia—a key regulatory factor in tumour growth. *Nature Reviews Cancer*, 2(1), 38–47.
 43. Roose, T., Netti, P. A., Munn, L. L., Boucher, Y., & Jain, R. K. (2003). Solid stress generated by spheroid growth estimated using a linear poroelasticity model small star, filled. *Microvascular Research*, 66(3), 204–212.
 44. Tschumperlin, D. J., Dai, G., Maly, I. V., Kikuchi, T., Laiho, L. H., McVittie, A. K., et al. (2004). Mechanotransduction through growth-factor shedding into the extracellular space. *Nature*, 429(6987), 83–86.
 45. Minchinton, A. I., & Tannock, I. F. (2006). Drug penetration in solid tumours. *Nature Reviews Cancer*, 6(8), 583–592.
 46. Marshburn, P. B., & Hulka, J. F. (1990). A simple irrigator-aspirator cannula for laparoscopy: the Stewart system. *Obstetrics and Gynecology*, 75(3 Pt 1), 458–460.
 47. Davies, P. F., Spaan, J. A., & Krams, R. (2005). Shear stress biology of the endothelium. *Annals of Biomedical Engineering*, 33(12), 1714–1718.
 48. Thamilselvan, V., Craig, D. H., & Basson, M. D. (2007). FAK association with multiple signal proteins mediates pressure-induced colon cancer cell adhesion via a Src-dependent PI3K/Akt pathway. *FASEB Journal*, 21(8), 1730–1741.
 49. von Sengbusch, A., Gassmann, P., Fisch, K. M., Enns, A., Nicolson, G. L., & Haier, J. (2005). Focal adhesion kinase regulates metastatic adhesion of carcinoma cells within liver sinusoids. *American Journal of Pathology*, 166(2), 585–596.
 50. Miles, F. L., Pruitt, F. L., van Golen, K. L., & Cooper, C. R. (2008). Stepping out of the flow: capillary extravasation in cancer metastasis. *Clinical and Experimental Metastasis*, 25(4), 305–324.
 51. Stewart, D. A., Cooper, C. R., & Sikes, R. A. (2004). Changes in extracellular matrix (ECM) and ECM-associated proteins in the metastatic progression of prostate cancer. *Reproductive Biology and Endocrinology*, 2, 2.
 52. Heino, J., & Massague, J. (1989). Transforming growth factor-beta switches the pattern of integrins expressed in MG-63 human osteosarcoma cells and causes a selective loss of cell adhesion to laminin. *Journal of Biological Chemistry*, 264(36), 21806–21811.
 53. Mierke, C. T., Zitterbart, D. P., Kollmannsberger, P., Raupach, C., Schlotzer-Schrehardt, U., Goecke, T. W., et al. (2008). Breakdown of the endothelial barrier function in tumor cell transmigration. *Biophysical Journal*, 94(7), 2832–2846.
 54. Levental, I., Georges, P. C., & Janmey, P. A. (2007). Soft biological materials and their impact on cell function. *Soft Matter*, 3(3), 299–306.
 55. Janmey, P. A., Georges, P. C., & Hvidt, S. (2007). Basic rheology for biologists. *Methods in Cell Biology*, 83(1), 3–27.
 56. Chown, M. G., & Kumar, S. (2007). Imaging and manipulating the structural machinery of living cells on the micro- and nanoscale. *International Journal of Nanomedicine*, 2(3), 333–344.
 57. Dao, M., Lim, C. T., & Suresh, S. (2003). Mechanics of the human red blood cell deformed by optical tweezers. *Journal of the Mechanics and Physics of Solids*, 51(11–12), 2259–2280.
 58. Guck, J., Schinkinger, S., Lincoln, B., Wottawah, F., Ebert, S., Romeyke, M., et al. (2005). Optical deformability as an inherent cell marker for testing malignant transformation and metastatic competence. *Biophysical Journal*, 88(5), 3689–3698.
 59. Lincoln, B., Wottawah, F., Schinkinger, S., Ebert, S., & Guck, J. (2007). High-throughput rheological measurements with an optical stretcher. *Methods in Cell Biology*, 83(1), 397–423.
 60. Trepap, X., Grabulosa, M., Puig, F., Maksym, G. N., Navajas, D., & Farre, R. (2004). Viscoelasticity of human alveolar epithelial cells subjected to stretch. *American Journal of Physiology-Lung Cellular and Molecular Physiology*, 287(5), L1025–L1034.
 61. Drury, J. L., & Dembo, M. (2001). Aspiration of human neutrophils: Effects of shear thinning and cortical dissipation. *Biophysical Journal*, 81(6), 3166–3177.
 62. Hochmuth, R. M. (2000). Micropipette aspiration of living cells. *Journal of Biomechanics*, 33(1), 15–22.
 63. Jones, W. R., Ting-Beall, H. P., Lee, G. M., Kelley, S. S., Hochmuth, R. M., & Guilak, F. (1999). Alterations in the Young's modulus and volumetric properties of chondrocytes isolated from normal and osteoarthritic human cartilage. *Journal of Biomechanics*, 32(2), 119–127.
 64. Koay, E. J., Shieh, A. C., & Athanasiou, K. A. (2003). Creep indentation of single cells. *Journal of Biomechanical Engineering-Transactions of the ASME*, 125(3), 334–341.
 65. Trickey, W. R., Baaijens, F. P. T., Laursen, T. A., Alexopoulos, L. G., & Guilak, F. (2006). Determination of the Poisson's ratio of the cell: recovery properties of chondrocytes after release from complete micropipette aspiration. *Journal of Biomechanics*, 39(1), 78–87.
 66. Beningo, K. A., Dembo, M., Kaverina, I., Small, J. V., & Wang, Y. L. (2001). Nascent focal adhesions are responsible for the generation of strong propulsive forces in migrating fibroblasts. *Journal of Cell Biology*, 153(4), 881–887.
 67. Butler, J. P., Tolic-Norrelykke, I. M., Fabry, B., & Fredberg, J. J. (2002). Traction fields, moments, and strain energy that cells exert on their surroundings. *American Journal of Physiology-Cell Physiology*, 282(3), C595–C605.
 68. Munevar, S., Wang, Y. L., & Dembo, M. (2001). Traction force microscopy of migrating normal and H-ras transformed 3T3 fibroblasts. *Biophysical Journal*, 80(4), 1744–1757.
 69. Pelham, R. J., & Wang, Y. L. (1999). High resolution detection of mechanical forces exerted by locomoting fibroblasts on the substrate. *Molecular Biology of the Cell*, 10(4), 935–945.
 70. Hansma, H. G., & Hoh, J. H. (1994). Biomolecular Imaging with the Atomic-Force Microscope. *Annual Review of Biophysics and Biomolecular Structure*, 23(1), 115–139.
 71. Kumar, S., & Hoh, J. H. (2001). Probing the machinery of intracellular trafficking with the atomic force microscope. *Traffic*, 2(11), 746–756.

72. Lal, R., & John, S. A. (1994). Biological Applications of Atomic-Force Microscopy. *American Journal of Physiology*, 266(1), C1–&
73. Radmacher, M. (2002). Measuring the elastic properties of living cells by the atomic force microscope. *Methods in Cell Biology*, 68(1), 67–90.
74. An, S. S., Laudadio, R. E., Lai, J., Rogers, R. A., & Fredberg, J. J. (2002). Stiffness changes in cultured airway smooth muscle cells. *American Journal of Physiology-Cell Physiology*, 283(3), C792–C801.
75. Ingber, D. E., Prusty, D., Sun, Z. Q., Betensky, H., & Wang, N. (1995). Cell shape, cytoskeletal mechanics, and cell cycle control in angiogenesis. *Journal of Biomechanics*, 28(12), 1471–1484.
76. Maksym, G. N., Fabry, B., Butler, J. P., Navajas, D., Tschumperlin, D. J., Laporte, J. D., et al. (2000). Mechanical properties of cultured human airway smooth muscle cells from 0.05 to 0.4 Hz. *Journal of Applied Physiology*, 89(4), 1619–1632.
77. Wang, N., Tolic-Norrellykke, I. M., Chen, J. X., Mijailovich, S. M., Butler, J. P., Fredberg, J. J., et al. (2002). Cell prestress. I. Stiffness and prestress are closely associated in adherent contractile cells. *American Journal of Physiology-Cell Physiology*, 282(3), C606–C616.
78. Berns, M. W., Aist, J., Edwards, J., Strahs, K., Girton, J., McNeill, P., et al. (1981). Laser microsurgery in cell and developmental biology. *Science*, 213(4507), 505–513.
79. Heisterkamp, A., Maxwell, I. Z., Mazur, E., Underwood, J. M., Nickerson, J. A., Kumar, S., et al. (2005). Pulse energy dependence of subcellular dissection by femtosecond laser pulses. *Optics Express*, 13(10), 3690–3696.
80. Kumar, S., Maxwell, I. Z., Heisterkamp, A., Polte, T. R., Lele, T. P., Salanga, M., et al. (2006). Viscoelastic retraction of single living stress fibers and its impact on cell shape, cytoskeletal organization, and extracellular matrix mechanics. *Biophysical Journal*, 90(10), 3762–3773.
81. Lele, T. P., Pendse, J., Kumar, S., Salanga, M., Karavitis, J., & Ingber, D. E. (2006). Mechanical forces alter zyxin unbinding kinetics within focal adhesions of living cells. *Journal of Cellular Physiology*, 207(1), 187–194.
82. Shen, N., Colvin, M., Genin, F., Huser, T., Cortopassi, G. A., Stearns, T., et al. (2004). Using femtosecond laser subcellular surgery to study cell biology. *Biophysical Journal*, 86(1), 520A–520A.
83. du Roure, O., Saez, A., Buguin, A., Austin, R. H., Chavrier, P., Siberzan, P., et al. (2005). Force mapping in epithelial cell migration. *Proceedings of the National Academy of Sciences of the United States of America*, 102(7), 2390–2395.
84. Nelson, C. M., Jean, R. P., Tan, J. L., Liu, W. F., Sniadecki, N. J., Spector, A. A., et al. (2005). Emergent patterns of growth controlled by multicellular form and mechanics. *Proceedings of the National Academy of Sciences of the United States of America*, 102(33), 11594–11599.
85. Poujade, M., Grasland-Mongrain, E., Hertzog, A., Jouanneau, J., Chavrier, P., Ladoux, B., et al. (2007). Collective migration of an epithelial monolayer in response to a model wound. *Proceedings of the National Academy of Sciences of the United States of America*, 104(41), 15988–15993.
86. Rabadzey, A., Alcaide, P., Luscinskas, F. W., & Ladoux, B. (2008). Mechanical forces induced by the transendothelial migration of human neutrophils. *Biophysical Journal*, 95(3), 1428–1438.
87. Sniadecki, N. J., Anguelouch, A., Yang, M. T., Lamb, C. M., Liu, Z., Kirschner, S. B., et al. (2007). Magnetic microposts as an approach to apply forces to living cells. *Proceedings of the National Academy of Sciences of the United States of America*, 104(37), 14553–14558.
88. Tan, J. L., Tien, J., Pirone, D. M., Gray, D. S., Bhadriraju, K., & Chen, C. S. (2003). Cells lying on a bed of microneedles: An approach to isolate mechanical force. *Proceedings of the National Academy of Sciences of the United States of America*, 100(4), 1484–1489.
89. Bausch, A. R., Ziemann, F., Boulbitch, A. A., Jacobson, K., & Sackmann, E. (1998). Local measurements of viscoelastic parameters of adherent cell surfaces by magnetic bead microrheometry. *Biophysical Journal*, 75(4), 2038–2049.
90. Tseng, Y., Kole, T. P., & Wirtz, D. (2002). Micromechanical mapping of live cells by multiple-particle-tracking microrheology. *Biophysical Journal*, 83(6), 3162–3176.
91. Valentine, M. T., Perlman, Z. E., Gardel, M. L., Shin, J. H., Matsudaira, P., Mitchison, T. J., et al. (2004). Colloid surface chemistry critically affects multiple particle tracking measurements of biomaterials. *Biophysical Journal*, 86(6), 4004–4014.
92. Yamada, S., Wirtz, D., & Kuo, S. C. (2000). Mechanics of living cells measured by laser tracking microrheology. *Biophysical Journal*, 78(4), 1736–1747.
93. Yap, B., & Kamm, R. D. (2005). Mechanical deformation of neutrophils into narrow channels induces pseudopod projection and changes in biomechanical properties. *Journal of Applied Physiology*, 98(5), 1930–1939.
94. Pesen, D., & Hoh, J. H. (2005). Modes of remodeling in the cortical cytoskeleton of vascular endothelial cells. *FEBS Letters*, 579(2), 473–476.
95. Pesen, D., & Hoh, J. H. (2005). Micromechanical architecture of the endothelial cell cortex. *Biophysical Journal*, 88(1), 670–679.
96. Oberhauser, A. F., Badilla-Fernandez, C., Carrion-Vasquez, M., & Fernandez, J. M. (2002). The mechanical hierarchies of fibronectin observed with single-molecule AFM. *Journal of Molecular Biology*, 319, 433–447.
97. Carl, P., Kwok, C. H., Manderson, G., Speicher, D. W., & Discher, D. E. (2001). Forced unfolding modulated by disulfide bonds in the Ig domains of a cell adhesion molecule. *Proceedings of the National Academy of Sciences of the United States of America*, 98, 1565–1570.
98. Rotsch, C., Jacobson, K., & Radmacher, M. (1999). Dimensional and mechanical dynamics of active and stable edges in motile fibroblasts investigated by using atomic force microscopy. *Proceedings of the National Academy of Sciences of the United States of America*, 96(3), 921–926.
99. A-Hassan, E., Heinz, W. F., Antonik, M. D., D’Costa, N. P., Nageswaran, S., Schoenenberger, C. A., et al. (1998). Relative microelastic mapping of living cells by atomic force microscopy. *Biophysical Journal*, 74(3), 1564–1578.
100. Charras, G. T., & Horton, M. A. (2002). Single cell mechanotransduction and its modulation analyzed by atomic force microscope indentation. *Biophysical Journal*, 82(6), 2970–2981.
101. Parekh, S. H., Chaudhuri, O., Theriot, J. A., & Fletcher, D. A. (2005). Loading history determines the velocity of actin-network growth. *Nature Cell Biology*, 7(12), 1219–1223.
102. Chaudhuri, O., Parekh, S. H., & Fletcher, D. A. (2007). Reversible stress softening of actin networks. *Nature*, 445(7125), 295–298.
103. Prass, M., Jacobson, K., Mogilner, A., & Radmacher, M. (2006). Direct measurement of the lamellipodial protrusive force in a migrating cell. *Journal of Cell Biology*, 174(6), 767–772.
104. Lam, W. A., Rosenbluth, M. J., & Fletcher, D. A. (2008). Increased leukaemia cell stiffness is associated with symptoms of leucostasis in paediatric acute lymphoblastic leukaemia. *British Journal of Haematology*, 142(3), 497–501.
105. Lam, W. A., Rosenbluth, M. J., & Fletcher, D. A. (2007). Chemotherapy exposure increases leukemia cell stiffness. *Blood*, 109(8), 3505–3508.

106. Rosenbluth, M. J., Lam, W. A., & Fletcher, D. A. (2006). Force microscopy of nonadherent cells: A comparison of leukemia cell deformability. *Biophysical Journal*, *90*(8), 2994–3003.
107. Strahs, K. R., Burt, J. M., & Berns, M. W. (1978). Contractility changes in cultured cardiac cells following laser microirradiation of myofibrils and the cell surface. *Experimental Cell Research*, *113*(1), 75–83.
108. Strahs, K. R., & Berns, M. W. (1979). Laser microirradiation of stress fibers and intermediate filaments in non-muscle cells from cultured rat heart. *Experimental Cell Research*, *119*(1), 31–45.
109. Koonce, M. P., Strahs, K. R., & Berns, M. W. (1982). Repair of laser-severed stress fibers in myocardial non-muscle cells. *Experimental Cell Research*, *141*(2), 375–384.
110. Burt, J. M., Strahs, K. R., & Berns, M. W. (1979). Correlation of cell surface alterations with contractile response in laser microbeam irradiated myocardial cells. A scanning electron microscope study. *Experimental Cell Research*, *118*(2), 341–351.
111. Botvinick, E. L., Venugopalan, V., Shah, J. V., Liaw, L. H., & Berns, M. W. (2004). Controlled ablation of microtubules using a picosecond laser. *Biophysical Journal*, *87*(6), 4203–4212.
112. Ingber, D. E. (2002). Mechanical signalling and the cellular response to extracellular matrix in angiogenesis and cardiovascular physiology. *Circulation Research*, *91*(10), 877–887.
113. Assoian, R. K., & Klein, E. A. (2008). Growth control by intracellular tension and extracellular stiffness. *Trends in Cell Biology*, *18*(7), 347–352.
114. Burridge, K., & Chrzanowska-Wodnicka, M. (1996). Focal adhesions, contractility, and signaling. *Annual Review of Cell and Developmental Biology*, *12*, 463–518.
115. Etienne-Manneville, S., & Hall, A. (2002). Rho GTPases in cell biology. *Nature*, *420*(6916), 629–635.
116. Hotulainen, P., & Lappalainen, P. (2006). Stress fibers are generated by two distinct actin assembly mechanisms in motile cells. *Journal of Cell Biology*, *173*(3), 383–394.
117. Sipkema, P., van der Linden, P. J. W., Westerhof, N., & Yin, F. C. P. (2003). Effect of cyclic axial stretch of rat arteries on endothelial cytoskeletal morphology and vascular reactivity. *Journal of Biomechanics*, *36*(5), 653–659.
118. Hayes, A. J., Benjamin, M., & Ralphs, J. R. (1999). Role of actin stress fibres in the development of the intervertebral disc: Cytoskeletal control of extracellular matrix assembly. *Developmental Dynamics*, *215*(3), 179–189.
119. Elkin, B. S., Azeloglu, E. U., Costa, K. D., & Morrison, B. (2007). Mechanical heterogeneity of the rat hippocampus measured by atomic force microscope indentation. *Journal of Neurotrauma*, *24*(5), 812–822.
120. Cavey, M., Rauzi, M., Lenne, P. F., & Lecuit, T. (2008). A two-tiered mechanism for stabilization and immobilization of E-cadherin. *Nature*, *453*(7196), 751–U2.
121. Daniels, B. R., Masi, B. C., & Wirtz, D. (2006). Probing single-cell micromechanics *in vivo*: The microrheology of C-elegans developing embryos. *Biophysical Journal*, *90*(12), 4712–4719.
122. Panorchan, P., Lee, J. S. H., Kole, T. P., Tseng, Y., & Wirtz, D. (2006). Microrheology and ROCK signaling of human endothelial cells embedded in a 3D matrix. *Biophysical Journal*, *91*(9), 3499–3507.
123. Bloom, R. J., George, J. P., Celedon, A., Sun, S. X., & Wirtz, D. (2008). Mapping local matrix remodeling induced by a migrating tumor cell using 3-D multiple-particle tracking. *Biophysical Journal*, *95*(8), 4077–4088.
124. Roy, P., Petroll, W. M., Cavanagh, H. D., & Jester, J. V. (1999). Exertion of tractional force requires the coordinated up-regulation of cell contractility and adhesion. *Cell Motility and the Cytoskeleton*, *43*(1), 23–34.
125. Petroll, W. M., Ma, L., & Jester, J. V. (2003). Direct correlation of collagen matrix deformation with focal adhesion dynamics in living corneal fibroblasts. *Journal of Cell Science*, *116*(8), 1481–1491.
126. Vanni, S., Lagerholm, B. C., Otey, C., Taylor, D. L., & Lanni, F. (2003). Internet-Based image analysis quantifies contractile behavior of individual fibroblasts inside model tissue. *Biophysical Journal*, *84*(4), 2715–2727.
127. Vega, F. M., & Ridley, A. J. (2008). Rho GTPases in cancer cell biology. *FEBS Letters*, *582*(14), 2093–2101.
128. Raftopoulos, M., & Hall, A. (2004). Cell migration: Rho GTPases lead the way. *Developmental Biology*, *265*(1), 23–32.
129. Friedl, P., & Wolf, K. (2003). Tumour-cell invasion and migration: Diversity and escape mechanisms. *Nature Reviews Cancer*, *3*(5), 362–374.
130. Lozano, E., Betson, M., & Braga, V. M. M. (2003). Tumor progression: small GTPases and loss of cell-cell adhesion. *Bioessays*, *25*(5), 452–463.
131. Ying, H., Biroc, S. L., Li, W. W., Alicke, B., Xuan, J. A., Pagila, R., et al. (2006). The Rho kinase inhibitor fasudil inhibits tumor progression in human and rat tumor models. *Molecular Cancer Therapeutics*, *5*(9), 2158–2164.
132. Bershadsky, A., Kozlov, M., & Geiger, B. (2006). Adhesion-mediated mechanosensitivity: a time to experiment, and a time to theorize. *Current Opinion in Cell Biology*, *18*(5), 472–481.
133. Schlaepfer, D. D., Hanks, S. K., Hunter, T., & Vandergeer, P. (1994). Integrin-Mediated Signal-Transduction Linked to Ras Pathway by Grb2 Binding to Focal Adhesion Kinase. *Nature*, *372*(6508), 786–791.
134. Ridley, A. J., & Hall, A. (1992). The Small Gtp-Binding Protein Rho Regulates the Assembly of Focal Adhesions and Actin Stress Fibers in Response to Growth-Factors. *Cell*, *70*(3), 389–399.
135. Sechi, A. S., & Wehland, J. (2000). The actin cytoskeleton and plasma membrane connection: PtdIns(4,5)P-2 influences cytoskeletal protein activity at the plasma membrane. *Journal of Cell Science*, *113*(21), 3685–3695.
136. Gilmore, A. P., & Burridge, K. (1996). Regulation of vinculin binding to talin and actin by phosphatidylinositol-4-5-bisphosphate. *Nature*, *381*(6582), 531–535.
137. Schwartz, M. A., Schaller, M. D., & Ginsberg, M. H. (1995). Integrins: Emerging paradigms of signal transduction. *Annual Review of Cell and Developmental Biology*, *11*, 549–599.
138. Tilghman, R. W., & Parsons, J. T. (2008). Focal adhesion kinase as a regulator of cell tension in the progression of cancer. *Seminars in Cancer Biology*, *18*(1), 45–52.
139. Gabarra-Niecko, V., Schaller, M. D., & Dunty, J. M. (2003). FAK regulates biological processes important for the pathogenesis of cancer. *Cancer and Metastasis Reviews*, *22*(4), 359–374.
140. Mitra, S. K., Hanson, D. A., & Schlaepfer, D. D. (2005). Focal adhesion kinase: In command and control of cell motility. *Nature Reviews Molecular Cell Biology*, *6*(1), 56–68.
141. Parsons, J. T. (2003). Focal adhesion kinase: the first ten years. *Journal of Cell Science*, *116*(8), 1409–1416.
142. Schlaepfer, D. D., Mitra, S. K., & Ilic, D. (2004). Control of motile and invasive cell phenotypes by focal adhesion kinase. *Biochimica et Biophysica Acta-Molecular Cell Research*, *1692*(2–3), 77–102.
143. Liu, T. J., LaFortune, T., Honda, T., Ohmori, O., Hatakeyama, S., Meyer, T., et al. (2007). Inhibition of both focal adhesion kinase and insulin-like growth factor-I receptor kinase suppresses glioma proliferation *in vitro* and *in vivo*. *Molecular Cancer Therapeutics*, *6*(4), 1357–1367.
144. Shen, T. L., & Guan, J. L. (2001). Differential regulation of cell migration and cell cycle progression by FAK complexes with Src, PI3K, Grb7 and Grb2 in focal contacts. *FEBS Letters*, *499*(1–2), 176–181.
145. Izaguirre, G., Aguirre, L., Hu, Y. P., Lee, H. Y., Schlaepfer, D. D., Aneskievich, B. J., et al. (2001). The cytoskeletal/non-muscle

- isoform of alpha-actinin is phosphorylated on its actin-binding domain by the focal adhesion kinase. *Journal of Biological Chemistry*, 276(31), 28676–28685.
146. Wang, H. B., Dembo, M., Hanks, S. K., & Wang, Y. L. (2001). Focal adhesion kinase is involved in mechanosensing during fibroblast migration. *Proceedings of the National Academy of Sciences of the United States of America*, 98(20), 11295–11300.
147. Hamasaki, K., Mimura, T., Furuya, H., Morino, N., Yamazaki, T., Komuro, I., et al. (1995). Stretching Mesangial Cells Stimulates Tyrosine Phosphorylation of Focal Adhesion Kinase Pp125(Fak). *Biochemical and Biophysical Research Communications*, 212(2), 544–549.
148. Mofrad, M. R., Golji, J., Abdul Rahim, N. A., & Kamm, R. D. (2004). Force-induced unfolding of the focal adhesion targeting domain and the influence of paxillin binding. *Mechanics and Chemistry of Biosystems*, 1(4), 253–65.
149. Johnson, K. R., Leight, J. L., & Weaver, V. M. (2007). Demystifying the effects of a three-dimensional microenvironment in tissue morphogenesis. *Methods in Cell Biology*, 83(1), 547–583.



Multiscale Modeling of Form and Function

Adam J. Engler, *et al.*
Science **324**, 208 (2009);
DOI: 10.1126/science.1170107

The following resources related to this article are available online at www.sciencemag.org (this information is current as of April 29, 2009):

Updated information and services, including high-resolution figures, can be found in the online version of this article at:

<http://www.sciencemag.org/cgi/content/full/324/5924/208>

A list of selected additional articles on the Science Web sites **related to this article** can be found at:

<http://www.sciencemag.org/cgi/content/full/324/5924/208#related-content>

This article **cites 78 articles**, 30 of which can be accessed for free:

<http://www.sciencemag.org/cgi/content/full/324/5924/208#otherarticles>

This article appears in the following **subject collections**:

Biochemistry

<http://www.sciencemag.org/cgi/collection/biochem>

Information about obtaining **reprints** of this article or about obtaining **permission to reproduce this article** in whole or in part can be found at:

<http://www.sciencemag.org/about/permissions.dtl>

Multiscale Modeling of Form and Function

Adam J. Engler,¹ Patrick O. Humbert,² Bernhard Wehrle-Haller,³ Valerie M. Weaver^{4,5*}

Topobiology posits that morphogenesis is driven by differential adhesive interactions among heterogeneous cell populations. This paradigm has been revised to include force-dependent molecular switches, cell and tissue tension, and reciprocal interactions with the microenvironment. It is now appreciated that tissue development is executed through conserved decision-making modules that operate on multiple length scales from the molecular and subcellular level through to the cell and tissue level and that these regulatory mechanisms specify cell and tissue fate by modifying the context of cellular signaling and gene expression. Here, we discuss the origin of these decision-making modules and illustrate how emergent properties of adhesion-directed multicellular structures sculpt the tissue, promote its functionality, and maintain its homeostasis through spatial segregation and organization of anchored proteins and secreted factors and through emergent properties of tissues, including tension fields and energy optimization.

Morphogenesis is the process whereby a complex living system is created from individual components that are systematically developed to yield a functionally stable unit with a defined form and function. As proposed by Edelman and colleagues (1), topobiology is the process that sculpts and maintains differentiated tissues and is acquired by the energetically favored segregation of cells through heterologous cellular interactions. That “tissue affinity” is the primary morphogenetic driver was first demonstrated by Townes and Holtfreter, who showed that disaggregated amphibian cells self-organize into tissue structures with distinct cell fates (2). This concept was confirmed by the identification of cell adhesion molecules, which facilitate the assembly of multiprotein “signaling modules” that mediate, integrate, and stabilize multicellular interactions (3). Phenotypic cues mediated through gradients of secreted “soluble” factors such as fibroblast growth factor, transforming growth factor- β (TGF β), and Wnt also control tissue patterning by activating genetic programs such as HOX gene clusters, thereby inducing and maintaining cellular identity and directing higher-order tissue architecture (4). Tensile forces also govern the self-organization of heterologous cellular interactions during embryogenesis and modulate tissue movements in

development by altering the activity of critical transcriptional regulators such as twist, implicating physical cues as key morphometric integrators (5, 6). Indeed, composition and topology of the extracellular matrix (ECM) stroma, which is secreted and modified by cells as they develop, changes throughout morphogenesis and directly regulates cell and tissue fate by inducing signaling within cells through specific matrix adhesion receptors to modify cytoskeletal orga-

nization and cell shape (7). Soluble factors such as hepatocyte growth factor and TGF β also modulate cell fate either by directly destabilizing multicellular tissue organization through Rho guanosine triphosphatase (GTPase)-dependent actomyosin contractility (8) or by changing ECM composition and posttranslational processing through altered transcription to stiffen the matrix (9). Thus, while morphogenesis might depend upon cell adhesion, it is orchestrated by a highly coordinated series of events that are initiated by soluble factors that activate cellular signaling at the adhesions and that are integrated by mechanical cues operating at the molecular, cellular, and tissue level. Here, we discuss how topobiological cues are arranged from the molecular to the organism level based on the repetitive use of basic conserved “decision-making modules” (Fig. 1 and Table 1). We describe how these decision-making modules not only orchestrate rapid and highly adaptive changes in non-structured masses of cells as they mature into highly defined tissues and organs but also are dynamic—displaying exquisite sensitivity to mechanical cues and undergoing reciprocal state transitions that permit the fine tuning of the organism. Finally, we speculate how emergent properties of organized multicellular tissues dictate specialized functions and modulate the functional integrity of cell and tissue fate so that altered expression, organization, or structure of any of these decision-making modules

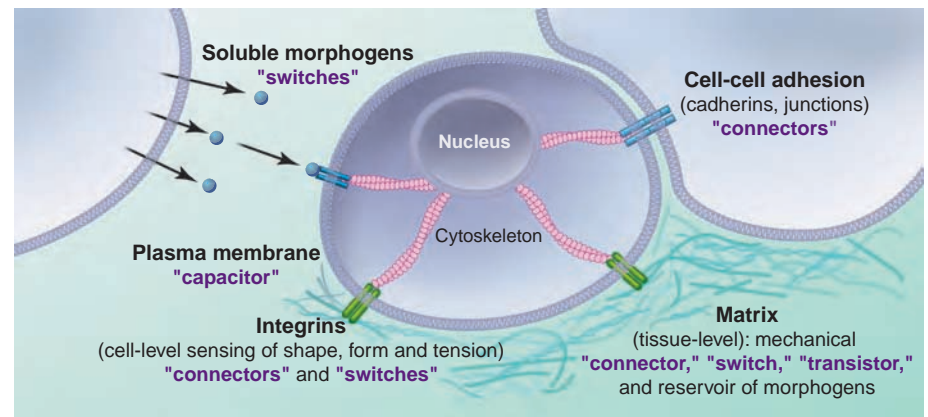


Fig. 1. Basic biological modules operate in tissues at multiple length scales. Variations and repetitions of the critical biological modules through many length scales and systems allow the formation and maintenance of increasingly complex multicellular structures with highly evolved functions. Different elements can “connect” one cell to its neighbor by homophilic receptors such as cadherins. Other connectors, such as integrins, mechanically link cells to the extracellular matrix, a three-dimensional (3D) scaffold to which different cell types can adhere. This mechanical connection allows the contraction or cell shape change of one cell to be transmitted by matrix fibrils through the cytoskeleton to a cohort of cells embedded in the same matrix, amplifying small perturbations to cause the matrix to act as a “transistor.” Upon matrix binding, conformational changes within integrin adhesions recruit adapter proteins, which modify the cytoskeleton and act as individual switches to control adhesion, migration, and the like. Cytokine stimulation can also act as a switch, turning on and off to fine-tune cellular behavior. The plasma membrane with its intracellular recycling and storage compartment consists of a reservoir of receptors, the dynamic reshuffling of which controls the degree of signaling by acting as a capacitor. Complex interactions and repetitions of these modules through various length scales is the critical mechanism controlling morphogenesis and form.

¹Department of Bioengineering, University of California, San Diego, La Jolla, CA 92093, USA. ²Cell Cycle and Cancer Genetics Laboratory, Research Division, Peter MacCallum Cancer Center, Melbourne, Victoria, Australia. ³Department of Cell Physiology and Metabolism, Centre Medical Universitaire, 1211 Geneva 4, Switzerland. ⁴Center for Bioengineering and Tissue Regeneration and Department of Surgery, University of California, San Francisco (UCSF), San Francisco, CA 94143, USA. ⁵Department of Anatomy, Centre of Bioengineering and Therapeutic Sciences, Center for Regenerative Medicine and UCSF Comprehensive Cancer Center, San Francisco, CA 94143, USA.

*To whom correspondence should be addressed. E-mail: Valerie.weaver@ucsfmedctr.org

will alter cell and tissue architecture and perturb homeostasis and ultimately lead to disease.

Phenotypic Complexity Through Modular Sensors, Transistors, and Amplifiers

The first niche requirement for a multicellular organism is the development of cell-cell adhesions, which act as “connector” modules that define which cells will adhere to each other as they segregate. These modules are also the nucleation point for signaling molecules and cytoskeletal elements that regulate cell and tissue shape and function, giving them “switchlike” properties. A

mass and will dictate the ultimate stability, size, and shape of the multicellular structure. Cellular rearrangements and coordinated tissue migration are also guided by the extracellular milieu of the tissue. Thus, the assembled ECM at the exterior of the blastula provides a qualitatively different anchorage site for the actin cytoskeleton that permits the differentiation of cell-cell from cell-ECM interactions (12). Integrins, which comprise the best characterized class of cell-ECM adhesion molecules, are heterodimeric transmembrane proteins that upon activation bind to specific ECM sites. After their binding, integrins recruit a host

adhesions through competitive associations between conserved signaling complexes and function globally to efficiently transmit information from the cellular to the tissue level by directed cytoskeletal remodeling and cellular and tissue tension. For instance, blastula assembly is followed by blastocoel cavity formation and the assembly of a fibrillar fibronectin matrix, both of which are regulated by the integrin-linked kinase (ILK)/pinch/parvin complex (17). Consistently, blastocoel formation fails in ILK-null embryos (18), and inhibition of fibronectin-integrin interactions inhibits the epithelial-mesenchymal transition that is critical for gastrulation (19). Although the processes occur at dramatically different length scales, both require specific gene expression (e.g., Rho GTPase) and activation to drive tension-dependent processes—for example, cell-cell adhesion maturation and focal adhesion assembly—and act by initiating actin remodeling (3).

Cell-cell and cell-ECM modules share many conserved features; however, they have also evolved fundamental differences that optimize environmental responses and permit fine-tuning of the multicellular organism throughout its life span. Whereas adherens junctions are tightly regulated by receptor number and density to maximize structural variability, integrins evolved to transduce environmental cues, thereby maximizing survival advantage and adaptability for the organism (Fig. 1). Indeed, homotypic adhesion systems appeared in primitive organisms such as the *Dictyostelium* fruiting body to maintain its integrity through aggregation. *Dictyostelium* use at least two independent homotypic adhesion systems that are related to metazoan adhesion molecules (20): the Cadherin super family member DdCAD-1 and the immunoglobulin-like domain protein gp80. These connector modules have weak interactions that allow dynamic rearrangement to cluster, sort, stream migrate, and maintain the rigidity of the organism. A fundamental feature of these early adhesion molecules is their enrichment at filipodial extensions, which, together with actin, form transient spot adhesions required for their initial clustering. These molecules are then rapidly replaced with adhesion plaque proteins such as the glycosylphosphatidylinositol-anchored protein gp80, which establishes more stable cell contacts that act as storage modules through associations with lipid-rich membrane micro domains. Although similar principles operate in higher organisms to facilitate multicellular integrity, the nature of the adhesions has become more complex so that spot-like junctions have been extended into beltlike structures such as those found in adherens and in occluding, tight, and septate junctions in higher organisms (21). A common framework for these diverse junctional complexes is that they all are organized into large complexes made up of highly clustered modules that, through adaptor proteins, i.e., “switch” modules, initiate signaling cascades,

Table 1. Other examples of basic biological modules that could regulate form and function.

Module	Type	Major concept	References
Switch	Soluble morphogen	Spatial modulation of growth factor receptors in oogenesis	(66, 67)
		Morphogen regulation of PCP	(68, 69)
	Focal adhesion	Force-dependent signaling of adhesion complexes	(70, 71)
Connector	Cell-cell binding	Adherens junctions and β -catenin in nonmetazoans	(72)
		Cell sorting and segregation scales with cadherin levels	(73)
		Peripheral myosin regulates cell intercalation	(74)
	Focal adhesion	Molecular clutch hypothesis for focal adhesions	(75, 76)
Capacitor	Plasma membrane	Lipid raft-induced membrane curvature	(77)
Transistor	ECM	Storage of growth factors to guide tissue development and direct cancer progression	(78, 79)

myriad of cell-cell adhesion molecules have evolved and have gained increasing complexity to facilitate cell-cell adhesion based on conserved components consisting of cytoplasmic, transmembrane, and 3 to 5 repeated extracellular domains, such as in neural cell adhesion molecules, that homotypically bind to each other. Evolution of these repeated domains has precisely set cell-cell spacing and has also regulated the amount of force that the bond can resist (10). Nevertheless, as exemplified by the ability of classic cadherins to link the actin cytoskeleton and adjacent cells, the major function of these modules is to mediate the efficient segregation of heterogeneous cell populations into distinct entities (11). This task is achieved by constant actomyosin-mediated pushing and pulling and the initiation of signaling that optimizes connections among neighboring cells and leads to phenomena such as cell compaction, as occurs at the blastula stage during embryogenesis. Thus, cell compaction is determined by the strength and number of connectors expressed on the cell surface and is likely dictated by the tension induced at the cellular and tissue levels. For example, cortical tension enhances the strength of cell adhesion in zebrafish such that the distinct germ layers display differing adhesion strengths (6). Assuming equal module density, the number of engaged connectors and the overall energy dynamics of the system will enable cells to determine whether they are sitting within or at the periphery of a given cell

of structural and signaling modules, such as talin and Rho GTPases, respectively, to the plasma membrane, thereby responding to matrix tension and reciprocally exerting contractility at the cell periphery (13, 14). Similar conserved modules occur in cell-cell adhesions, where structural and signaling modules act to hold cells together and communicate with the transcriptional apparatus in the nucleus to which the cellular cytoskeleton is tethered. Although they contain similar modules, integrin-matrix adhesions segregate from cadherins to define multicellular properties such as cell and tissue polarity. Thus, mice lacking $\beta 1$ integrin fail to deposit ECM (e.g., laminin) at the blastula surface, leading to developmental arrest after implantation (15) that can be rescued by coating the blastula with purified laminin (16). In this manner, coordinated and dynamic interactions between cell-cell and cell-ECM are thought to direct multicellular tissue development. Nevertheless, how these events are executed and integrated at the tissue level is poorly understood and remains an area of intense investigation.

Phenotype Is Dominant over Genotype: Clues from the Evolution of Cell-Cell Interactions

Reciprocal and dynamic cell-cell and cell-ECM adhesion communication is essential for multicellular tissue morphogenesis and homeostasis. Consistently, mechanisms intersecting at different length scales have evolved to facilitate this dialogue. These mechanisms act locally at

Protein Dynamics

and act as connector modules to strengthen the cytoskeletal link in response to increasing tension. Whether adhesion or signaling function came first for this class of cell adhesion complexes is still a matter of contention, but it is now clear that similar downstream signaling components are used by both cadherins and junctional complexes. Yet, while the modular nature of these switches is undisputed, the molecular and physical factors that regulate their function remain unknown.

Phenotype Is Dominant over Genotype: Clues from the Evolution of Cell-Matrix Interactions

Modern heterodimeric integrins developed to link the onset of multicellular structures with the appearance of a stable form in metazoans such as *Dictyostelium discoideum*, where they developed as specialized sensory modules to regulate adhesion, survival, and phagocytosis (22, 23). These primitive integrin-like proteins called “sib receptors” contain several conserved motifs identical to β integrins, in addition to having tandem NPXY repeat motifs in the cytoplasmic tail (22), suggesting that sib is a cation-dependent, low-affinity receptor for exposed acidic residues in extracellular proteins. Sib also appears to act as a mechanical connector to the actin cytoskeleton through the recruitment of FERM domain-containing proteins such as talin (22). In addition to a mechanical role, sib’s recruitment into the phagocytic cup, as with integrin clustering in the membrane for metazoans, likely serves as an important signaling transistor for prey recognition and feeding stimulation (13). Thus, integrins evolved to permit organisms to respond rapidly to biochemical and physical cues from their microenvironment with specialized features that include adhesion to substrate, active mobility, and detection and capture of prey by phagocytosis (Fig. 2) (24–39).

A second distinguishing feature of integrin-matrix adhesion modules is their ability to function as molecular switches through adaptor molecules that are activated to initiate a cascade of downstream events that amplify the original signal. When compared with adenosine triphosphate-driven signaling enzymes, such as kinases that are

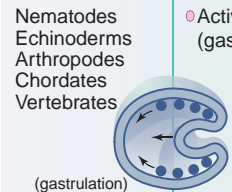
Organism	Feeding	Mobility	Adhesion & scaffold
Bacteria 	○ Passive (food absorption & assimilation)	○ Swimming ○ Chemotaxis	○ Polysaccharide-based biofilm formation (24)
Fungi 	○ Passive	○ Pseudohyphal growth	○ GPI-anchored (25) cell-cell & cell-substrate receptors (26)
Amoebozoa 	○ Active “hunting” β -integrin-like (sib)-dependent phagocytosis	○ Migration (β -integrin-like (sib)-dependent)	○ Cellulose-based, cysrich & laminin-like ECM (27) ○ β -integrin-like & paxillin-dependent (28, 29)
Choanoflagellates <i>M. brevicollis</i> 	○ Passive	○ Swimming (no adhesion)	○ Collagens, laminins ○ but no β -integrin (30)
Porifera 	○ Filtration	○ Sessile (secretion of ECM-like scaffold)	○ Collagens (31) ○ α & β -integrins (32, 33)
Placozoans <i>T. adhaerens</i> 	○ Active (extra-organismal gastric cavity)	○ Migration on surfaces	○ Collagens, laminins, fibrin, no visible ECM scaffold ○ α & β -integrins (34)
Cnidarians 	○ Active “hunting” (gastric cavity)	○ Sessile (polyp) ○ Swimming (medusae)	○ Collagens, laminins, ECM scaffold (35) ○ α & β -integrins (36)
Nematodes Echinoderms Arthropods Chordates Vertebrates  (gastrulation)	○ Active “hunting” (gastric cavity)	○ Specific organelles for mobility	○ Collagens, laminins, ○ α & β -integrins (37, 38) ○ fibronectin, tenascins (from chordates on) (39)

Fig. 2. Functional evolution of adhesion-dependent form and function, from bacteria to vertebrates. Although the mechanisms for replication are directly linked to the multiplication and management of the genetic information, the capacity to form complex multilayer organisms is likely based on the evolutionary advantage to adhere to new environments and survive in potentially hostile environments. Although bacteria and fungi use rather simple strategies to create multicellular structures, the evolution of “hunters,” such as amoeba, introduced new dynamic and controllable cell-cell and cell-substrate adhesion systems, such as integrins, allowing the capture of prey and formation of complex multicellular structures. In parallel, the evolution from polysaccharide- or cellulose-based to protein-based extracellular scaffold increased the versatility of cell-to-substrate adhesion systems. Interestingly, the emergence of integrin α/β -heterodimers correlates with the appearance of metazoans (dashed line), indicating that the intracellular perception of the extracellular scaffold is critical to the stable generation of form and function. Details can be found in (24–39).

typical of this type of switch module, the function of adaptor proteins in cell adhesions may, at least at first glance, seem neither similar nor switchlike. However, many adaptor proteins bind to both a cytoskeletal protein and an integrin-based adhesion protein to form a complex, where stability of the adaptor protein is greatly increased by the initial binding reaction and subsequent change in conformation, for example, vinculin (40). Structural changes, such as those brought on by forces imposed on the adaptor protein (41), could liberate

cell proteins, this is perhaps suggestive of the evolutionary force behind integrin-driven tissue morphogenesis, which relies heavily on its binding partner, the ECM, to aid in the drive to undergo morphogenesis.

These integrin features enable the organism to discriminate noise from critical external cues as well as ensure a quick response to these stimuli, both necessary elements required for multicellular organisms to maintain their survival advantage in a rapidly changing environment.

additional protein-protein interaction sites in a cooperative manner, and the immediate influx of new binding opportunities for signaling molecules could switch on previously dormant cell behaviors and alter properties like cell shape. Another efficient way to create a switch module for adhesion is to limit protein-protein interactions by immobilizing individual binding partners to a surface. Adsorption-limited diffusion of the binding partners restricts the conformational changes that would inactivate the connector module in examples that range from the rapid rise of phosphatidylinositol biphosphate in the plasma membrane that stabilizes the integrin/talin complex (42) to the regulation of cell motility by ECM sheets like basement membrane (43). For protein interactions, receptor-like protein tyrosine phosphatase- α binding to α , integrin acts as a switch to form the nucleation site for a focal adhesion. One characteristic aspect of this switch is its response to the external application of force, resulting in new protein-protein binding sites, such as with the Src family kinase Fyn (44). In fact, integrin receptors themselves react in response to force by increasing their binding affinities to ligands through conformational changes (45), resulting in the formation of a catch bond that holds under force and gets released in the absence of force (46). An analogy to an old fashioned “finger trap” is perhaps insightful: force-dependent integrin extension acts to increase affinity, much like the pulling force by fingers stuck in the trap further tightens the trap on the fingers. Given their shape and functional differences with lower organisms as well as cell-

Accordingly, cells use both cadherins and integrins to assemble into multicellular tissues, to distinguish and rapidly respond to external cues, and to amplify the signal to launch an appropriate and coordinated response. Tissues achieve this task by a series of evolutionarily conserved modules that are initiated through the adhesion sensor, transduced through a series of molecular switches, and propagated through amplifiers (21, 47, 48) (Fig. 3).

Signaling in Context: Emergent Properties of Complex Systems

Multicellular organisms require stable adhesion between neighboring cells and coordination of cell behaviors through cell-cell signaling to develop shape and compartmentalize function into tissues. The first coordinated event to occur in metazoa is gastrulation, which imparts a body pattern. Given the level of reorganization required to establish the resulting form (49), it is evolutionarily advantageous to ensure tighter regulation and spatial arrangement of proliferative ectodermal cells covering the embryo versus motile, involuting cells during gastrulation. The impetus to rearrange and expand the multiple layers of tissue, however, may be due to the microtubule organizing center having competing roles in motility and cell division (50). As a result, metazoans employ additional cell-cell adhesion-based mechanisms to control the identity and spatial distribution of differentiated cells, including cell polarity, tension, and morphogen gradients, rather than relying on proliferation alone. Cell polarity refers to the asymmetric distribution of cell constituents and organelles, and, if coordinated through cell-cell connectors, cell orientation can effect tissue-wide polarity, known as planar cell polarity (PCP), using a highly conserved set of polarity protein complexes (51). This behavior is likely to have arisen from unicellular organisms that would distribute unequally damaged cell components to bypass senescence (52). The advent of stable connector modules such as adherens or tight junctions further contributed to the development of apical-basal membrane segregation, permitting the establishment of cell sheets as well as outside and inside separation of an organism. Orientated cell division and polarized cell shape changes, such as those seen in the convergence and extension phase of gastrulation, can also be used to rotate the body axis out of the plane of a tissue, to contribute to the differential spatial orientation of cells, and to establish anisotropic mechanical properties (49). The latter of these characteristics can establish differences in ECM properties by secretion or cross-linking, setting up spatially controlled matrix topography and elasticity, both of which are known regulators of differentiation (53, 54). Interplay among polarity, ECM, and adhesions has also been shown in mammary acini, where increased matrix elasticity altered tensional homeostasis, perturbed

tissue polarity, and promoted a malignant phenotype (55). Polarity, however, should be thought of not just in terms of how it modulates matrix and restricts secretion but also how it changes the context of signaling; for example, loss of Scribble in mammary epithelia can block morphogenesis and induce dysplasia by disrupting cell polarity and inhibiting apoptosis (56). Cells organized into polarized tissue structures respond very differently to external signaling cues than do cell

tension in the blastula (6). Mechanoregulation of homeostasis by morphogen gradients likely continues through gastrulation, the formation of organs, and internal assembly, because evidence shows that they can direct cells to stop proliferating to maintain size (60), as well as cease migration (11) once cells are appropriately segregated.

Morphogen gradients are not always present in nonstereotyped organs such as the heart or

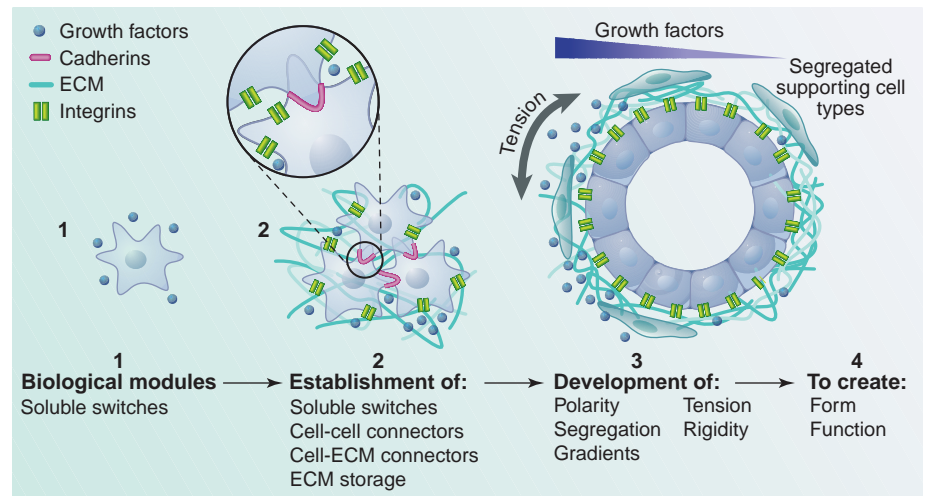


Fig. 3. Tensional homeostasis and emergent properties of multicellular systems. At a single-cell level, filopodial projections probe the cellular environment while cells secrete and ingest growth factors that act as switches to turn on behaviors. With the onset of multicellular aggregates, adhesive “connectors,” for example, cadherins, form and link the lamellipodia to a lattice of individual actin filaments within the cell, permitting adhesion to and migration on surfaces or dense fibrillar network. Whereas these structures can contribute to cell sheets such as an epithelial cell layer adhered to a basement membrane, the development of segregated adhesion structures establishes cell polarity, morphogen gradients signal to cells to regulate cell coordinates within the body plan, and actomyosin-based contractions allow cells to integrate within a 3D environment in a particular structure. Within this framework, the continuous contraction against a compliant ECM maintains tensional homeostasis to create form and function through the incorporation of all of these conserved modules.

sheets or isolated cells (57). In fact, by forcing a polarized tissue structure on both normal and teratocarcinoma cells, the signaling milieu that the cells inhabit can give rise to animals that retain tumor cells but exhibit no detectable tumor phenotype (58). These observations argue that additional emergent properties arise in polarized tissue structures that regulate cell and tissue behavior.

In addition to polarity, positional information within the organism and tissue also need to be programmed after initial cell segregation. Body plan axis and length, for example, are regulated by morphogen gradients, where local signal concentrations define the coordinates for each cell, based on source distance (59). Progenitor cell phenotype can be regulated by these gradients, where cells from one location transplanted to another will express the phenotype of the new niche (4). In fact, nodal gradients in the developing embryo even modulate the development of

mammary acini, where homeostasis is maintained by a balance between matrix compliance and cell tension in a manner that may parallel proposed intracellular tension balances, such as with the concept of tensegrity (61). This argues for a set of newly emerging properties that can shape tissue and organ level form and function. Recent evidence implicates tension as such a regulator, not only to shape cell form as previously shown but also to control tissue formation (62). As mammary acini secrete milk proteins, this generates outward pressure on the cells, tensing their adhesive modules and forcing them into a spherical structure, which maximizes their surface area to volume ratio so that they hold as much fluid as possible while at the same time minimizing the energetics of the system to promote stability. When tension is misregulated at this length scale, as with constitutively active Rho, it can shift the acinar force balance to compromise morphogenesis and integrity and induce a cancer-like phenotype. As a

disease parallel to this, breast cancer is characterized by increased matrix stiffness and cell contractility, altered rheology, and changes in cell shape and tissue architecture (55). In addition to these force-induced changes in cell and tissue behavior, matrix stiffness and elevated cell tension stimulate excessive fibronectin production that compromises tissue integrity and perturbs tissue polarity (63), illustrating how cell and matrix tension operate at multiple length scales to influence malignancy. Conversely, normal acinar morphology can be a powerful tumor suppressor, preventing expression of the malignant phenotype even in cells with a multitude of genomic alterations, including amplifications in key oncogenes (64). Heart looping also appears to be force sensitive, such that a threefold gradient in matrix deposition corresponds to a similar gradient in stiffness for the inner versus outer curvature of the heart tube. As hemodynamic forces differentially press against the softer basal wall, it induces cell shape changes that create the looped form of the embryonic heart (65). Altered differences in matrix gradients could easily upset how cells at the outer curve extend by changing the cell tension that cells along the curve can generate (7). The underpinnings of tension-driven regulation may rest in clarifying why changing membrane tension or curvature induced by matrix or shape perturbations can exert such a profound effect on the lineage specification of stem cells (14, 54). Although tissue development and homeostasis clearly require reciprocal cross-talk between the cell and its extracellular matrix mediated through dynamic adhesion interactions (64), scaling up these cell-ECM changes to tissue level behaviors, much like has been done with morphogen gradients and polarity, will greatly advance our understanding of these modules and their economies of scale.

Unresolved Issues?

Although emergent properties of multicellular tissues and signaling modules clearly regulate processes such as gastrulation and acini formation, it is not clear how these morphogenetic events shape an organ, tissue, or cell at large distances where diffusion of morphogens may be limited, direct cell-cell contacts are out of range, and the matrix is discontinuous. Do processes that sculpt multicellular tissues and maintain homeostasis at short length scales and acute time frames operate similarly in the organism at larger length scales in complex tissues or organ systems with multiple cell types and variable chronologies? For some of the open developmental questions posed above, modular analogies (Fig. 1) perhaps improve our ability to describe the toolbox of tissue homeostasis and clarify the circuitry rules required to use them, i.e., combining connectors

in series. However, much of our circuitry diagram is missing, and key integrators that operate at multilength scales and that retain the molecular memory necessary for the long-term viability and adaptability demanded of complex organisms have yet to be identified. The solution to understanding how this enormous task is achieved likely rests on discovering new modules and alternate signaling paradigms. Nevertheless, it is clear that without including a comprehensive description of all the environmental players and clarifying their interrelations—for example, matrix, cadherins, and integrins—an explanation of the origin of form and function will remain incomplete.

References and Notes

- G. M. Edelman, *Topobiology: An Introduction to Molecular Embryology* (Basic Books, New York 1988).
- P. Townes, J. Holtfreter, *J. Exp. Zool.* **128**, 53 (1955).
- E. Brouzes, E. Farge, *Curr. Opin. Genet. Dev.* **14**, 367 (2004).
- F. V. Mariani, G. R. Martin, *Nature* **423**, 319 (2003).
- N. Desprat, W. Supatto, P. A. Pouille, E. Beaupaire, E. Farge, *Dev. Cell* **15**, 470 (2008).
- M. Krieg *et al.*, *Nat. Cell Biol.* **10**, 429 (2008).
- C. M. Nelson *et al.*, *Proc. Natl. Acad. Sci. U.S.A.* **102**, 11594 (2005).
- J. de Rooij, A. Kerstens, G. Danuser, M. A. Schwartz, C. M. Waterman-Storer, *J. Cell Biol.* **171**, 153 (2005).
- K. M. Heinemeier *et al.*, *J. Physiol.* **582**, 1303 (2007).
- C. P. Johnson, I. Fujimoto, C. Perrin-Tricaud, U. Rutishauser, D. Leckband, *Proc. Natl. Acad. Sci. U.S.A.* **101**, 6963 (2004).
- B. M. Gumbiner, *Cell* **84**, 345 (1996).
- T. Rozario, B. Dzamba, G. F. Weber, L. A. Davidson, D. W. Desimone, *Dev. Biol.* **327**, 386 (2008).
- S. Miyamoto, S. K. Akiyama, K. M. Yamada, *Science* **267**, 883 (1995).
- R. McBeath, D. M. Pirone, C. M. Nelson, K. Bhadriraju, C. S. Chen, *Dev. Cell* **6**, 483 (2004).
- L. E. Stephens *et al.*, *Genes Dev.* **9**, 1883 (1995).
- S. Li *et al.*, *J. Cell Biol.* **157**, 1279 (2002).
- S. Li *et al.*, *J. Cell Sci.* **118**, 2913 (2005).
- T. Sakai *et al.*, *Genes Dev.* **17**, 926 (2003).
- T. Darriberre, J. E. Schwarzbauer, *Mech. Dev.* **92**, 239 (2000).
- C. H. Siu, T. J. Harris, J. Wang, E. Wong, *Semin. Cell Dev. Biol.* **15**, 633 (2004).
- C. R. Magie, M. Q. Martindale, *Biol. Bull.* **214**, 218 (2008).
- S. Cornillon *et al.*, *EMBO Rep.* **7**, 617 (2006).
- A. L. Hughes, *J. Mol. Evol.* **52**, 63 (2001).
- C. Ryder, M. Byrd, D. J. Wozniak, *Curr. Opin. Microbiol.* **10**, 644 (2007).
- F. Li, S. P. Palecek, *Microbiology* **154**, 1193 (2008).
- A. Halme, S. Bumgarner, C. Styles, G. R. Fink, *Cell* **116**, 405 (2004).
- L. Eichinger *et al.*, *Nature* **435**, 43 (2005).
- S. Cornillon, R. Froquet, P. Cosson, *Eukaryot. Cell* **7**, 1600 (2008).
- T. Bukahrova *et al.*, *J. Cell Sci.* **118**, 4295 (2005).
- N. King *et al.*, *Nature* **451**, 783 (2008).
- J. Y. Exposito *et al.*, *J. Biol. Chem.* **283**, 28226 (2008).
- Z. Pancer, M. Kruse, I. Muller, W. E. Muller, *Mol. Biol. Evol.* **14**, 391 (1997).
- D. L. Brower, S. M. Brower, D. C. Hayward, E. E. Ball, *Proc. Natl. Acad. Sci. U.S.A.* **94**, 9182 (1997).
- M. Srivastava *et al.*, *Nature* **454**, 955 (2008).
- J. Heino, M. Huhtala, J. Kapyla, M. S. Johnson, *Int. J. Biochem. Cell Biol.* **41**, 341 (2009).
- B. A. Knack *et al.*, *BMC Evol. Biol.* **8**, 136 (2008).
- N. H. Brown, *Matrix Biol.* **19**, 191 (2000).
- C. A. Whittaker *et al.*, *Dev. Biol.* **300**, 252 (2006).
- R. P. Tucker, R. Chiquet-Ehrmann, *Int. J. Biochem. Cell Biol.* **41**, 424 (2009).
- H. Chen, D. M. Cohen, D. M. Choudhury, N. Kioka, S. W. Craig, *J. Cell Biol.* **169**, 459 (2005).
- C. P. Johnson, H. Y. Tang, C. Carag, D. W. Speicher, D. E. Discher, *Science* **317**, 663 (2007).
- C. Cluzel *et al.*, *J. Cell Biol.* **171**, 383 (2005).
- M. Paulsson, *Crit. Rev. Biochem. Mol. Biol.* **27**, 93 (1992).
- G. von Wichert *et al.*, *J. Cell Biol.* **161**, 143 (2003).
- J. Zhu *et al.*, *Mol. Cell* **32**, 849 (2008).
- J. C. Friedland, M. H. Lee, D. Boettiger, *Science* **323**, 642 (2009).
- V. M. Bowers-Morrow, S. O. Ali, K. L. Williams, *Biol. Rev. Camb. Philos. Soc.* **79**, 611 (2004).
- N. King, C. T. Hittinger, S. B. Carroll, *Science* **301**, 361 (2003).
- R. Keller, L. A. Davidson, D. R. Shook, *Differentiation* **71**, 171 (2003).
- N. King, *Dev. Cell* **7**, 313 (2004).
- P. A. Lawrence, G. Struhl, J. Casal, *Nat. Rev. Genet.* **8**, 555 (2007).
- I. G. Macara, S. Mili, *Cell* **135**, 801 (2008).
- M. J. Dalby *et al.*, *Nat. Mater.* **6**, 997 (2007).
- A. J. Engler, S. Sen, H. L. Sweeney, D. E. Discher, *Cell* **126**, 677 (2006).
- M. J. Paszek *et al.*, *Cancer Cell* **8**, 241 (2005).
- L. Zhan *et al.*, *Cell* **135**, 865 (2008).
- V. M. Weaver *et al.*, *Cancer Cell* **2**, 205 (2002).
- B. Mintz, K. Ilimensee, *Proc. Natl. Acad. Sci. U.S.A.* **72**, 3585 (1975).
- J. Jaeger *et al.*, *Nature* **430**, 368 (2004).
- D. Rogulja, C. Rauskolb, K. D. Irvine, *Dev. Cell* **15**, 309 (2008).
- D. E. Ingber, *Sci. Am.* **278**, 48 (1998).
- C. M. Nelson, M. J. Bissell, *Annu. Rev. Cell Dev. Biol.* **22**, 287 (2006).
- C. M. Williams, A. J. Engler, R. D. Slone, L. L. Galante, J. E. Schwarzbauer, *Cancer Res.* **68**, 3185 (2008).
- V. M. Weaver *et al.*, *J. Cell Biol.* **137**, 231 (1997).
- E. A. Zamir, V. Srinivasan, R. Perucchio, L. A. Taber, *Ann. Biomed. Eng.* **31**, 1327 (2003).
- S. Y. Shvartsman, C. B. Muratov, D. A. Lauffenburger, *Development* **129**, 2577 (2002).
- H. Strutt, D. Strutt, *Curr. Biol.* **13**, 1451 (2003).
- K. Amonlirdviman *et al.*, *Science* **307**, 423 (2005).
- U. Weber, C. Pataki, J. Mihalý, M. Młodzik, *Dev. Biol.* **316**, 110 (2008).
- A. del Rio *et al.*, *Science* **323**, 638 (2009).
- B. Geiger, J. P. Spatz, A. D. Bershadsky, *Nat. Rev. Mol. Cell Biol.* **10**, 21 (2009).
- M. J. Grimson *et al.*, *Nature* **408**, 727 (2000).
- R. A. Foty, M. S. Steinberg, *Dev. Biol.* **278**, 255 (2005).
- C. Bertet, L. Sulak, T. Lecuit, *Nature* **429**, 667 (2004).
- C. E. Chan, D. J. Odde, *Science* **322**, 1687 (2008).
- M. L. Gardel *et al.*, *J. Cell Biol.* **183**, 999 (2008).
- T. Baumgart, S. T. Hess, W. W. Webb, *Nature* **425**, 821 (2003).
- A. R. Small *et al.*, *J. Theor. Biol.* **252**, 593 (2008).
- X. Wang, R. E. Harris, L. J. Bayston, H. L. Ashe, *Nature* **455**, 72 (2008).
- We apologize to the many authors whose work is not cited due to space limitations. This work was supported by grants NIH R01-CA078731, Department of Defense Era of Hope Breast Cancer Research Grant W81XWH-05-1-330, Department of Energy A107165, and California Institute for Regenerative Medicine R51-00449 to V.M.W.; American Heart Association 0865150F to A.J.E.; the Australian NHMRC, CCV, Prostate Cancer Foundation of Australia; the AICR UK and NHMRC Career Development Award to P.O.H.; and the Swiss National Science Foundation and Nevus Outreach to B.W.-H.

The Tissue Diagnostic Instrument

Paul Hansma¹, Hongmei Yu², David Schultz³, Azucena Rodriguez³, Eugene A. Yurtsev¹, Jessica Orr³, Simon Tang³, Jon Miller⁴, Joseph Wallace⁵, Frank Zok⁶, Cheng Li⁷, Richard Souza⁸, Alexander Proctor⁹, Davis Brimer⁹, Xavier Nogues-Solan¹⁰, Leonardo Mellbovsky¹⁰, M. Jesus Peña¹⁰, Oriol Diez-Ferrer¹⁰, Phillip Mathews¹, Connor Randall¹, Alfred Kuo³, Carol Chen³, Mathilde Peters⁴, David Kohn⁵, Jenni Buckley³, Xiaojuan Li⁸, Lisa Pruitt⁷, Adolfo Diez-Perez¹⁰, Tamara Alliston³, Valerie Weaver², Jeffrey Lotz³

1. Department of Physics, University of California, Santa Barbara, CA, 93106

2. Center for Bioengineering and Tissue Regeneration and Departments of Surgery, Anatomy and Bioengineering and Therapeutics, University of California, San Francisco, CA, 94143

3. Department of Orthopaedic Surgery, University of California, San Francisco, CA, 94143

4. Department of Dentistry, University of Michigan, Ann Arbor, MI, 48109

5. Departments of Biologic and Materials Sciences, and Biomedical Engineering, University of Michigan, Ann Arbor, MI, 48109

6. Materials Department, University of California, Santa Barbara, CA, 93106

7. UC Berkeley & UCSF Joint Graduate Group in Bioengineering, Berkeley, CA 94720

8. Department of Mechanical Engineering, University of California, Berkeley, 94720

9. Active Life Technologies, 629 State St., Suite 213, Santa Barbara, CA 93101

10. Autonomous University of Barcelona, Department of Internal Medicine, Hospital del Mar, P. Maritim 25-29, 08003 Barcelona, Spain

Abstract

Tissue mechanical properties reflect extracellular matrix composition and organization, and as such, their changes can be a signature of disease. Examples of such diseases include intervertebral disc degeneration, cancer, atherosclerosis, osteoarthritis, osteoporosis, and tooth decay. Here we introduce the Tissue Diagnostic Instrument (TDI), a device designed to probe the mechanical properties of normal and diseased soft and hard tissues not only in the laboratory, but also in patients. The TDI can distinguish between the nucleus and the annulus of spinal discs, between young and degenerated

cartilage, and between normal and cancerous mammary glands. It can quantify the elastic modulus and hardness of the wet dentin left in a cavity after excavation. It can perform an indentation test of bone tissue quantifying the indentation depth increase and other mechanical parameters. With local anesthesia and disposable, sterile, probe assemblies, there has been neither pain nor complications in tests on patients. We anticipate that this unique device will facilitate research on many tissue systems in living organisms, including plants, leading to new insights into disease mechanisms and methods for their early detection.

Introduction

The Tissue Diagnostic Instrument, TDI, was redesigned from the Bone Diagnostic Instrument^{1,2} so as to measure tissue mechanical properties subcutaneously and in vivo with additional probe assemblies and an adjustable compliance (Fig. 1). It consists of a thin probe assembly that can penetrate skin and soft tissue to reach deep tissues. The disposable, sterilizable probe assembly consists of an outer reference probe made from a 23 gauge hypodermic needle and an inner test probe made from stainless steel wire ranging from 175 to 300 micrometers in diameter and from 2 millimeters to 90 millimeters in length. Since friction between the test probe and the reference probe increases with length it is desirable to use only the length needed to access the desired tissue location. The test probe is held in a nickel tube that couples to a magnet which in turn is linked to a force generator. During operation the force generator oscillates the probe within the tissue of interest and concurrently measures the force and displacement. The maximum values for force and displacement are 12 N and 600 micrometers. The probe is typically operated at a frequency of 4 Hz because this is rapid enough to allow hand holding, yet sufficiently slow to allow easy decoupling of the elastic and viscous response of the tissue (see supplementary material³ for more details including force and displacement ranges.)

Measurements

We first illustrate TDI use in human spinal discs, that are composed of a thick outer ligament (annulus fibrosus) and a central swelling hydrogel (nucleus pulposus). Spinal

disc degeneration can be the underlying cause of back pain leading to significant morbidity and societal expense. Intervertebral discs are one of the most highly loaded tissues in the body, and consequently material property insufficiency can lead to damage accumulation, inflammation, and pain. Disc degeneration is currently diagnosed using imaging techniques, such as magnetic resonance ⁴. Unfortunately, these methods can only indirectly suggest disc mechanical properties, which currently cannot be measured in vivo.

Using image-guided, percutaneous placement (Fig. 2(a) and 2(b)), disc material properties can now be measured safely in vivo using a Type N probe assembly (Fig. 1(c)). The novel sharpening of the reference probe for Type N probe assembly decreases the problem of tissue being caught between the test probe and the reference probe during insertion and thus decreases the friction between the test probe and the reference probe. The friction between the test and reference probes is typically ~0.02 N. The specific value is recorded by the software before testing a sample and is removed from the samples' Force vs. Distance plot before analysis. The Force vs. Displacement data are plotted in real time and recorded digitally (Fig. 2(c) and 2(d)). The slope of the Force vs. Displacement curve provides a measure of disc elasticity: in the case of a simple spring, the slope would be the spring constant. The energy dissipation in the Force vs. Displacement curve is the area inside the curve and is a measure of the viscous behavior. Viscosity is absent from a simple spring, yet is large for a purely viscous material such as petroleum jelly, which has an elasticity near zero.

There are significant differences (p values < 0.01) in slope (N/m) and energy dissipation (μ J) between the annulus fibrosus and the nucleus pulposus (Fig. 2). The annulus fibrosus has both higher slope and energy dissipation. These results are representative of our measurements on 11 discs: the slope and energy dissipation are always greater in the annulus than the nucleus. This observation of higher slope or stiffness in the annulus is consistent with previous experiments measuring the compressive properties of both annulus and nucleus ^{5,6}. However, a precise comparison with established mechanical data is not readily available because mechanical testing in this manner at high spatial

resolution has not been possible previously. Because these properties are known to change with age and degeneration, an eventual goal would be to determine whether in vivo measures of annulus and nucleus material properties provide novel data that improve back pain diagnosis and treatment. We note that the 23 gauge needle is consistent with the recent recommendation ⁷ that a spinal needle smaller than or equal to 22 gauge should be used to prevent postsurgery leakage.

An epithelial tissue such as the mammary gland is an example of the softest tissue that can be probed with the current TDI. Figure 3 shows a paired-comparison of the mammary glands #2/3 and #4 from normal FVB mice and tumors arising in the matched mammary glands of their MMTV-PyMT+/- littermates. These data are representative of the data in an ongoing study of various tumors. The results of that study are beyond the scope of this paper, but we can report that all 30 tumors are stiffer (have higher slope) than all 15 normal mammary glands in tissue site-matched and age-matched mice. Normal murine mammary glands have elastic modulus below 1 kPa as measured with a conventional rheometer and with the TDI device. This value is comparable with our calibration curves on polyacrylamide gels (see supplementary material) that demonstrate TDI sensitivity below 1 kPa. Normal and transformed human breast tissue is considerably stiffer than mouse tissue ⁸, and is therefore well within the range of the TDI. Tissue stiffness increases in many breast cancers. To quantify stiffness and improve breast tumor detection, imaging modalities such as sonoelastography and MR elastography have been used ^{9,10}. The TDI offers a tractable and economical approach to measure breast stiffness in situ with millimeter resolution. Our preliminary trials on human breast tissue from cadavers showed detectable variations in mechanical properties between different locations in the same specimen with a spatial resolution of 2 mm. (Data not shown). Based on these observations an eventual goal would be to use the TDI for localization of human breast cancer in situ. A foreseeable clinical application includes using the device to define margins of affected tissue and sites for biopsy. The TDI measurement could easily be combined with biopsy; the test probe could be withdrawn into the reference probe to collect a biopsy sample after mechanical testing. We are currently investigating the molecular mechanism of how the mechanical

properties contribute to breast cancer; the TDI can be applied to clarify the molecular link between matrix materials properties of tissues and tumor risk (i.e. breast cancer in women with mammographically dense breasts ^{11, 12}).

Prior to clinically apparent symptoms of osteoarthritis, the material quality and mechanical function of cartilage matrix is compromised ¹³. The ability to non-invasively probe the material quality of this stratified tissue will complement and extend current diagnostic capabilities ¹³. Furthermore, detection of cartilage degeneration early in osteoarthritis may increase the success of therapeutic intervention. To that end, the ability of the TDI to distinguish the elastic modulus of synthetic materials with moduli comparable to cartilage was validated against well-established methods including atomic force microscopy, nanoindentation, and bulk stress relaxation (Fig. 4). In addition to accurately measuring the elastic modulus of polyacrylamide gels with a range of moduli from 0.2-1 MPa, the TDI could measure the elastic modulus of a stiff gel that was inferior to a compliant gel, demonstrating its ability to non-invasively evaluate a stratified material (Fig. 4d). When applied to cartilage, the TDI readily discriminated between a young healthy cadaveric specimen and an old degenerated surgical specimen that were probed in situ (Fig. 4f).

Human dentin is an example of the hard tissue that can be probed with our current device (Fig. 5). One unsolved problem for practicing dentists is deciding when a sufficient depth has been reached when drilling to remove carious dentin from a cavity. One proposed solution has been the development of a new experimental polymer bur (EPB from SS White Burs, Inc., Lakewood, NJ) which is designed to remove soft, decaying dentin, but blunt on harder, healthy dentin and thus self limit the tissue amount removed. Here we show the properties of the remaining dentin after a 1st excavation by such a bur and then after a 2nd excavation with a second polymer bur of the same type (Fig. 5). Next was a 3rd excavation with a #4 round carbide bur and finally a cavity preparation into presumably sound dentin using a #330 carbide bur. Note that even after the cavity preparation the dentin did not have the full elastic modulus of the healthy dentin. Our primary focus was on relative values as excavation proceeded. The Elastic Modulus, as

calculated from Force vs. Displacement curves generated by the TDI and analyzed using a modified Oliver and Pharr method¹⁴, for the dentin left in the cavity by the polymer bur was below that for healthy dentin far from the cavity (Fig. 5c). Please see the appendix for the details of the modified method. The Hardness, as calculated from Force vs. Displacement curves generated by the TDI and analyzed using a modified Oliver and Pharr method¹⁴, for the dentin left in the cavity by the polymer bur was below that for healthy dentin far from the cavity (Fig. 5c). One-way Analysis of Variance (ANOVA) gives values of $P < 0.0001$ for the Elastic Modulus and $P = 0.0008$ for the Hardness indicating that the variation among means is significantly greater than expected by chance. Thus the TDI has the potential to quantify the properties of dentin left in a cavity and could be used to study the outcome of various treatment strategies for how much degenerated dentin is removed before filling the cavity.

The absolute value for the elastic modulus of our "healthy dentin" is well within the range of existing measurements, but below the value of 20 -25 GPa recommended in a recent critical reevaluation of the literature¹⁵. The reason is probably the storage of the teeth in water for weeks before measurement¹⁶. To our knowledge, the TDI is the first instrument that can measure elastic modulus and hardness inside irregularly shaped, fully-hydrated dentin cavities. It could be used for research projects without further modification. For individual clinical use, a smaller, less expensive version with an angled probe would be desirable. The experiments on dentin reported here build on a rich history of measuring mechanical properties with indentation methods^{14, 17, 18}. Of special interest is recent work modeling size effects with finite element analysis¹⁹ because extensions of work like this may lead to a more quantitative understanding of TDI measurements on soft tissue as well as hard tissue.

The hard tissue, bone, is of particular interest medically because of the growing incidence of debilitating bone fracture as our population ages²⁰. Changes in bone material properties are believed to play a role in fracture risk²¹⁻²³. With the top screw backed off, as discussed in the supplementary materials, the TDI functions as a Bone Diagnostic Instrument^{1, 2}, which may, after clinical tests, prove useful in quantifying the component

of bone fragility due to degraded material properties. Figure 6 shows tests of the TDI, working as a Bone Diagnostic Instrument, on a living patient to determine if the procedure is painful or results in complications. Neither this patient nor the others tested to date experienced any pain beyond the initial “stick” when the local anesthesia was injected. There have been no complications.

Discussion of New Possibilities

It might, in the future, be possible for the TDI to measure the interaction forces between antibody coated test probes and tissues. This would allow measurements of single molecule interactions as is currently achieved with an atomic force microscope²⁴. Rupture forces in the range of 20 to 140 pN have been measured for many receptor-ligand interactions with single-cell force spectroscopy²⁵. With these interaction forces, we can make order of magnitude estimates of forces we might find when trying to rotate or translate a test probe that had bound to a tissue with many molecular bonds in parallel. Assuming a molecular density of one molecule per 10 nm^2 , an interaction force per molecule of 50 pN, a coated region of area $4 \times 10^{-6} \text{ m}^2$ (the exposed area of the Type D probe) and a fractional binding of 1% we would get a force of $50 \text{ pN/molecule} \times 4 \times 10^{-6} \text{ m}^2 \times 1 \text{ molecule}/10 \text{ nm}^2 \times .01 = 200 \text{ mN}$. The current lower limits of sensitivity of the TDI for forces come from the friction between the test probe and the reference probe, of order 10 mN, and from the force noise in our force transducer, of order 5 mN in a 1 kHz bandwidth. Thus forces of the magnitude that could be expected from molecular interactions with coated tips should be measurable. A big problem could be non-specific interaction masking specific interactions. A proof of concept experimental approach to overcoming this masking effect would be to use a test probe coated on just one side that was exposed to the tissue under test through a window in the wall of a closed-end reference probe. The difference in the forces between the test probe and the tissue under test for the coated vs. uncoated side could be measured. This could naturally be extended with multiple coatings on multiple strips on the test probe, each exposed one by one through a slit in the wall of the closed-end reference probe. We emphasize, however, that proof of concept experiments will be necessary to evaluate this potential application of the Tissue Diagnostic Instrument.

It is important to note that though the present instrument is able to make basic measurements in a wide range of tissues (almost all tissues in the human body from very soft breast tissue to hard, mineralized tissues), it is in a very early stage of development. More versatile instruments with more measurement modalities, such as mentioned above, and more user convenience features, such as wireless operation, are possible. Specialized instruments for specific measurements in specific tissues could be developed at a small fraction of the cost of the fully versatile instrument. The device could also be modified to assess materials properties of various bioengineered artificial three dimensional tissues^{26, 27}.

Acknowledgements: We thank the NIH for support of this work under grants RO1 GM 065354, RO1 AR 049770, and NIH Grant AR049770, the DOD under W81XWH-05-1-330 and the Fondo de Investigaciones Sanitarias (FIS) PI07/90912. We thank Angus Scrimgeour for asking us to do indentation measurements on bone, Robert Recker for encouraging us to plan for clinical trials even when the BDI was at an early stage of development, and Georg Fantner, Jonathan Adams, Patricia Turner, Doug Rhen, Jason Lelujian, and Ralf Jungman for helping develop prototype BDIs, which then stimulated development of the more general TDI.

Author contributions: D. S., A. R., J. B. and J. L. planned the spinal disc experiment, which was preformed by D. S. and A. R. on tissue obtained by J. B. and A. R.; H.Y. and V.W. planned the mouse breast experiment, which was preformed by H. Y.; the dentin experiments were planned by T. P.; J.O. made the gels to model cartilage. J.O., S.T., A.K., C.C., and R.S. made measurements on gels and cartilage. T.A., C.C., X.L. and L.P. planned the cartilage experiments and supervised the students and postdocs who were involved. J. W. in the laboratory of D. K. preformed preliminary dentin measurements on teeth prepared by T. P.; J. M. preformed the final set of measurements, which are presented here, on teeth prepared by T. P.; The bone measurements were done by A. D. P., X.N.S. and L.M. with the assistance of D.B., A.P. and M.J.P. O.D.F. documented human tests on a video from which a still was taken for figure 6. P.M. and C.R. developed tip assemblies and protocols for the human tests and assisted with the preparation of figures. E. Y. wrote the computer programs that operate the TDI; D.S.

prepared Fig. 7; H.Y. took the data and prepared Fig. 8, which also included data from Inkyung Kang. P.H. invented the TDI, was a co-inventor of the BDI and participated in most of the measurements reported here.

Author information: Competing financial interests: P. H., D.B. and A.P. are members of Active Life™ Technologies, which sells the Biodent™ product line of Bone and Tissue Diagnostic Instruments for research use only.

Figure Captions:

Fig. 1 The Tissue Diagnostic Instrument, TDI. (a) The TDI can measure mechanical properties of tissues under test even if they are covered with skin and other soft tissues because it has a probe assembly that can be inserted subcutaneously into the tissue under test. (b) It can be handheld and is connected to a computer for data generation, acquisition and processing. In this photo it is being used to measure differences in the mechanical properties of fruit and gel in a snack food. (c) A probe assembly for the TDI consists of a test probe, which moves displacements of order 200 micrometers relative to the reference probe. The reference probe serves to shield the test probe from the influence of the skin and soft tissue that must be penetrated to reach the tissue under test. Type D probes are good for very soft tissue, such as the murine breast tissue of Fig. 3. Type N probes are good for stiffer tissue, such as the spinal disc tissue of Fig. 2. The screw at the top of the TDI (a) can adjust the compliance of the TDI, as discussed in the supplementary material.

Fig. 2: Demonstration of the ability of the TDI to distinguish between the annulus and nucleus of a human intervertebral disc. (a) X-ray image of transverse view of a cadaver lumbar motion segment L12 with test probe located in annulus. (b) Similar view with probe centered in the nucleus. (c) Force vs. displacement curve measured by the TDI during a cyclic load cycle (4 Hz) in the annulus. (d) Force vs. displacement curve

measured in the nucleus. Note that the annulus is much stiffer (higher slope) and dissipates more energy (higher area enclosed by the curve). (e) Histogram comparing the average least squares slope for 10 cycles in the annulus versus in the nucleus. (f) Histogram comparing the average energy dissipation for 10 measurements in the annulus versus in the nucleus ($31.8 \pm 1.1 \mu\text{J}$ vs. $9.7 \pm 0.6 \mu\text{J}$; $p < 0.01$). The error bars indicate standard deviation for the 10 measurement within the annulus and within the nucleus in the disc.

Fig. 3: Demonstration of the ability of the TDI to distinguish between normal mammary glands and tumors. Hematoxylin and eosin (H&E) staining of (a) the representative normal FVB murine mammary gland and (b) the matched, malignant MMTV-PyMT^{+/-} murine mammary gland that were tested in this experiment. (c) The mammary tumors have significantly ($P < 0.001$) higher slopes, a measure of elasticity, for both the thoracic # 2/3 and the inguinal #4 tissues. (d) The mammary tumors have significantly higher energy dissipation for the thoracic # 2/3 tissue ($P < 0.01$) but the difference for the inguinal # 4 tumor was not significant. Histogram comparing (e) the Elastic Modulus and (f) the Loss Modulus, as measured by Rheology, for the normal mammary glands and mammary tumors after the TDI measurements (2 sub-regions for each mammary gland, 10 measurements for each region). Note that the results for elasticity and loss modulus for the two techniques reproduce the same general trends. The error bars in the measurements indicate standard deviation for all the measurements.

Fig. 4: Demonstration of the ability of the TDI to distinguish differences in moduli of stratified materials such as cartilage. (a) The elastic modulus can be determined with the type V probe assembly that indents soft materials rather than penetrating them, as above. (b) Polyacrylamide (PA) gels with elastic moduli in the range previously reported for cartilage (0.2 – 1 MPa) were used to validate the TDI relative to other established methods, including atomic force microscopy, nanoindentation, and bulk stress relaxation. PA gel moduli increased dose-dependently with crosslinker concentration ($p=0.012$). (c) To construct a stratified elastic modulus gel, a 0.2mm thick layer of “compliant” PA gel was poured over a pre-polymerized 1mm thick “stiff” PA gel. (d) The force vs.

displacement curve produced by the TDI revealed two distinct slopes on the loading curve for the stratified gels. Each slope of the composite gel matches the corresponding slopes for homogeneous 0.5% and 2% PA gel, demonstrating the capability to analyze stratified materials, such as cartilage. (e) A schematic of the indentation tests performed on cartilage, which were performed in hydrated conditions with phosphate buffered saline. (f) Using similar test conditions, the TDI easily distinguished between young cadaveric cartilage and aged degenerated cartilage measured in situ.

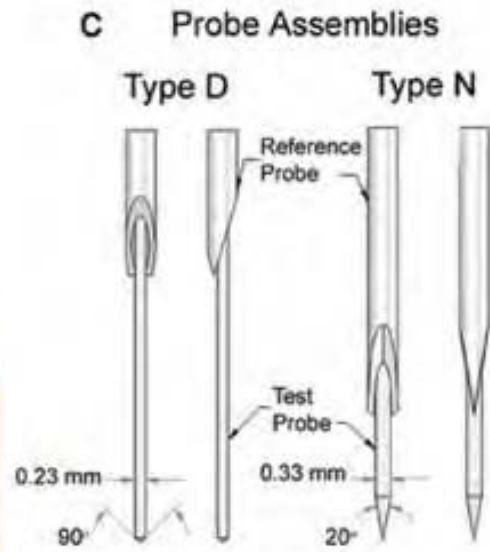
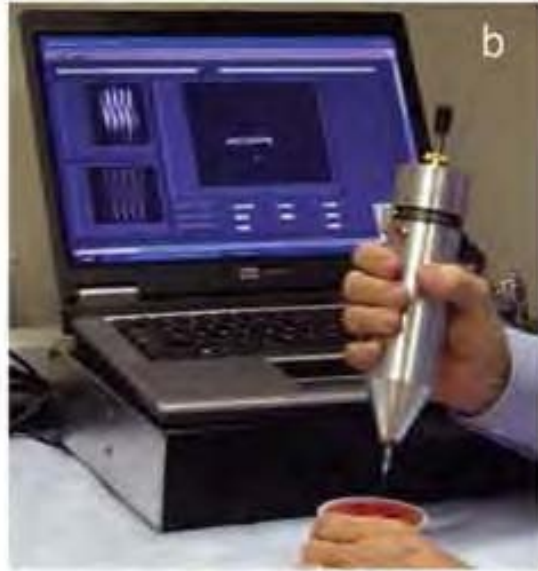
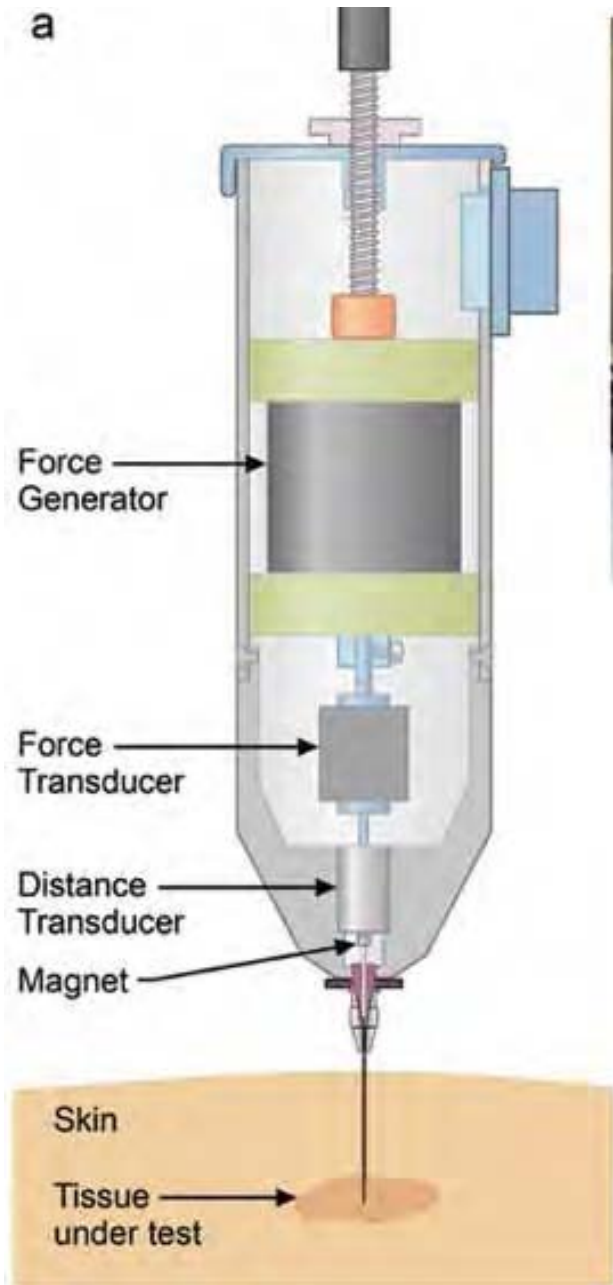
Fig. 5: Demonstration of the ability of the TDI to measure the Elastic Modulus and Hardness of human dentin to quantify the properties of the dentin left in a tooth cavity after each of multiple excavations and finally preparation. (a) The probe assembly for these measurements was designed to indent the hard tissue. The reference probe was a hypodermic needle that rested on the surface under test. The test probe was sharpened into a 90 degree cone with a 30 micron radius at the end. (Drawing by Haykaz Mkrtchyan) (b) The teeth after the various excavations and finally preparation. At each successive stage of excavation and preparation more dentin was removed from the cavity. (c,d) The Elastic Modulus and Hardness of the dentin remaining in the cavity was significantly ($p=.01$) less than that of healthy dentin. The error bars indicate standard deviation of the 10 measurements that were taken on each of the 5 teeth (a total of 50 measurements). Note that the Elastic Modulus of the healthy dentin is over 10 GPa, over 7 orders of magnitude greater than the normal mammary glands (Fig. 3), demonstrating the range of the TDI.

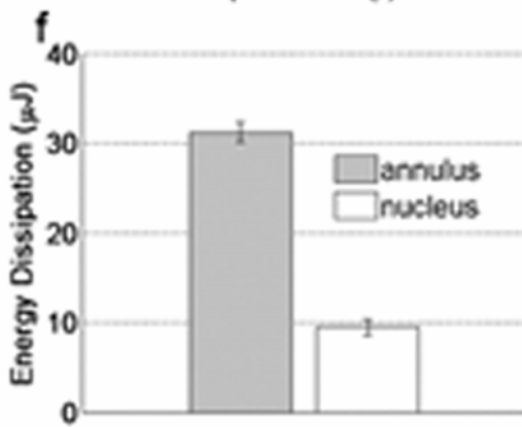
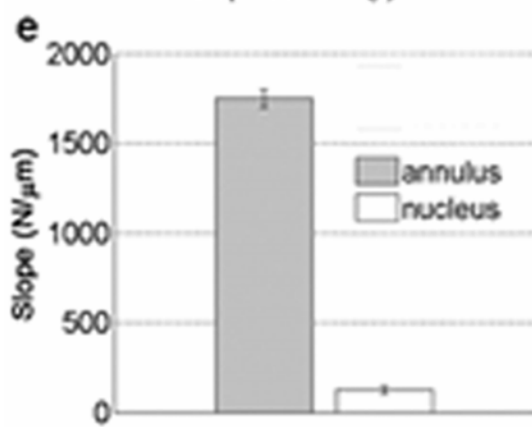
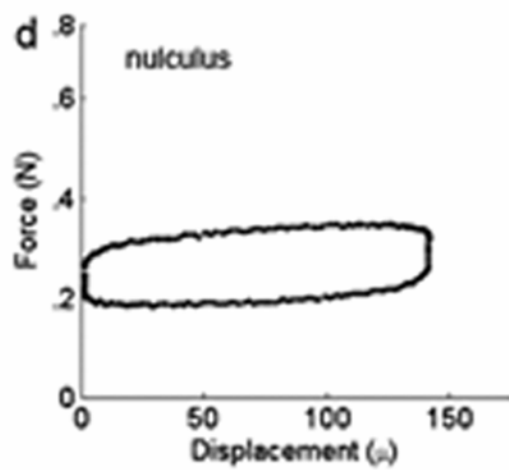
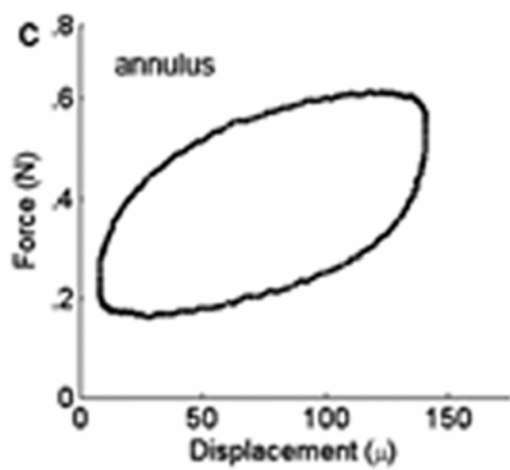
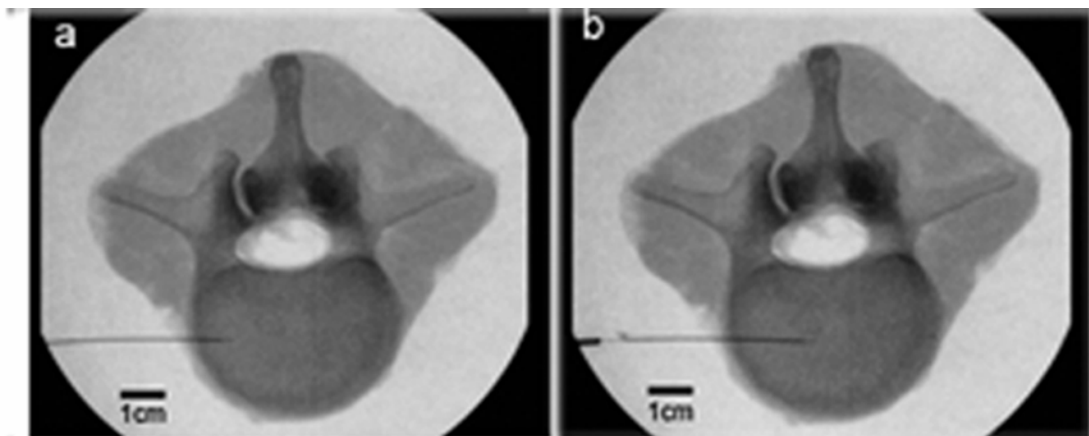
Fig. 6: Demonstration of the ability of the TDI to do measurements on a living patient. (a) The probe assembly of the TDI is lowered by a physician (A.D.P.) to penetrate the skin and soft tissue covering the tibia of the patient (D.B.) after the test site has been sterilized and locally anesthetized. (b) Close up of the physician's hand on the probe assembly as he lowers it to the bone surface. (c) Representative Force vs. Distance curves measured on the bone of the patient. This patient and the other patients tested to date experienced neither pain nor complications with the procedure. The most important parameter is the Indentation Distance Increase, IDI, defined in the image as the increase

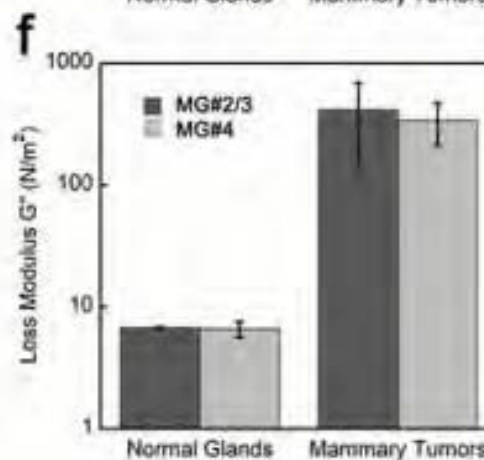
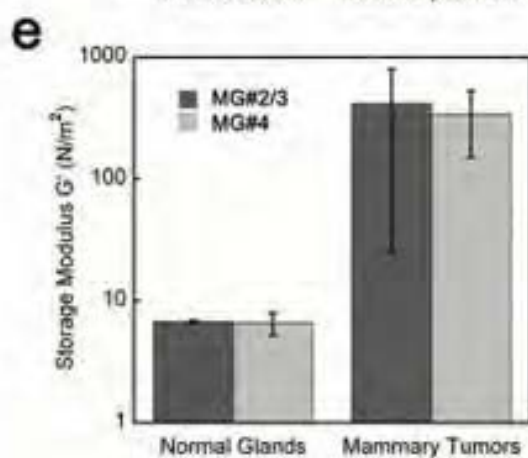
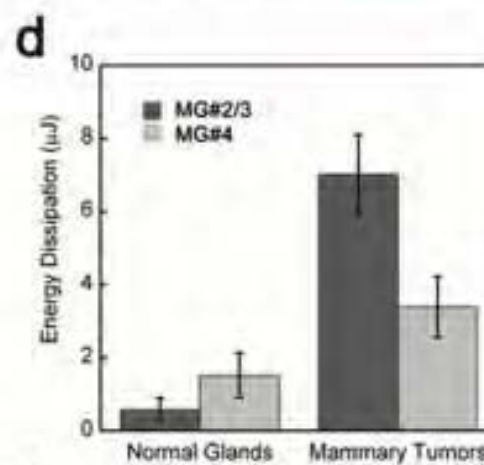
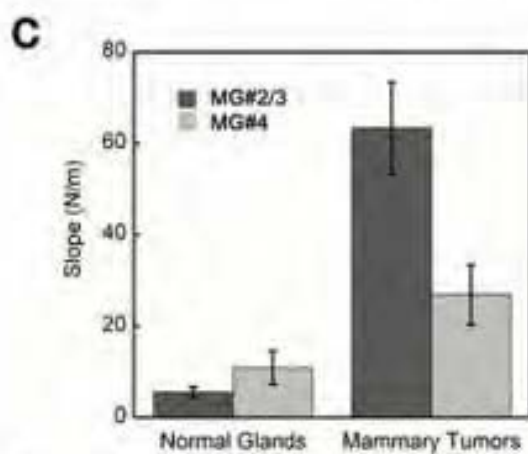
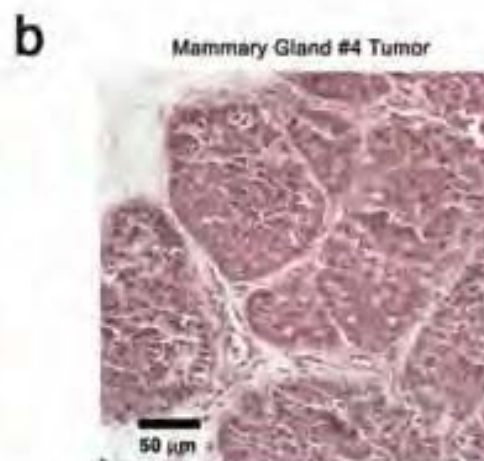
in indentation distance from the first cycle to the last. In model systems the IDI is greater for more easily fractured bone. Other parameters such as the creep at nearly constant force (the plateau on the top of the curves), the Elastic Modulus, the Energy Dissipation and the Hardness can also be determined from analysis of the Force vs. Distance curves.

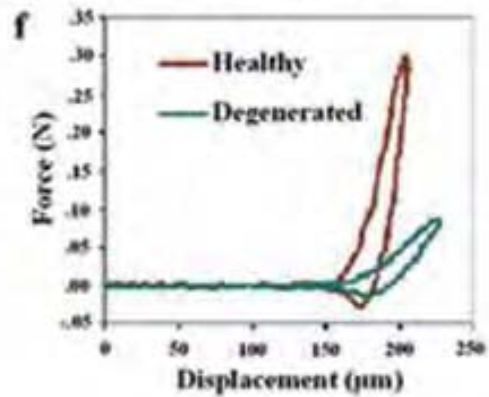
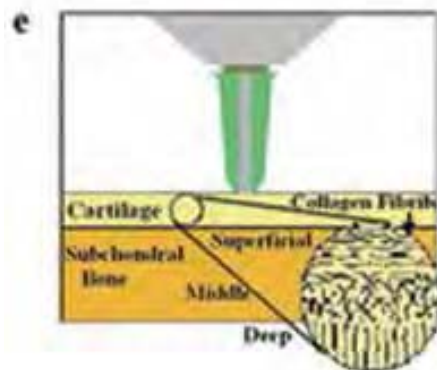
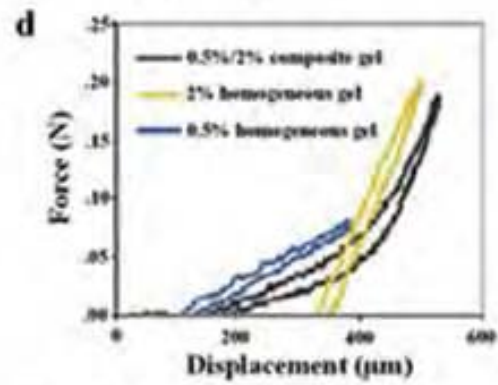
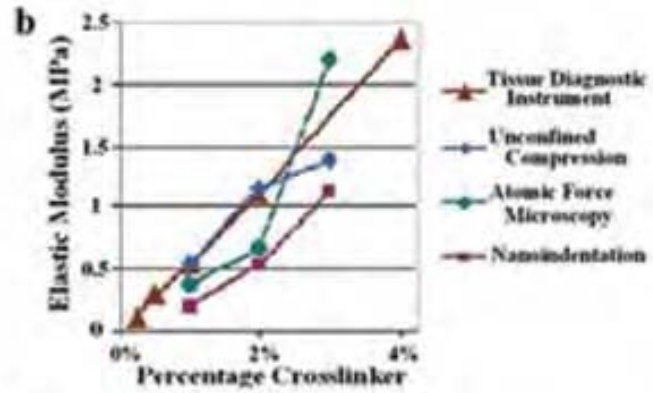
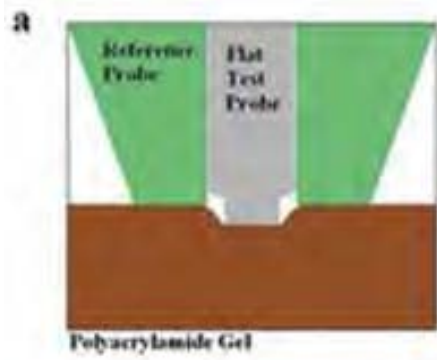
- ¹ P. K. Hansma, P. J. Turner, and G. E. Fantner, *Review of Scientific Instruments* **77**, 075105 (2006).
- ² P. Hansma, P. Turner, B. Drake, E. Yurtsev, A. Proctor, P. Mathews, J. Lelujian, C. Randall, J. Adams, R. Jungmann, F. Garza-de-Leon, G. Fantner, H. Mkrtchyan, M. Pontin, A. Weaver, M. B. Brown, N. Sahar, R. Rossello, and D. Kohn, *Rev Sci Instrum* **79**, 064303 (2008).
- ³ See EPAPS Document No. [*number will be inserted by AIP*] for details regarding the measurements and test methods of the Tissue Diagnostic Instrument on various biomaterials. For more information on EPAPS, see <http://www.aip.org/pubservs/epaps.html>.
- ⁴ C. W. A. Pfirrmann, A. Metzdorf, M. Zanetti, J. Hodler, and N. Boos, *Spine* **26**, 1873 (2001).
- ⁵ S. M. Klisch and J. C. Lotz, *Journal of Biomechanics* **32**, 1027 (1999).
- ⁶ N. R. M. Jordan M. Cloyd, Lihui Weng, Weiliam Chen, Robert and L. M. a. D. M. Elliott, *European Spine Journal*, Springer-Verlag online (2007).
- ⁷ J. L. Wang, Y. C. Tsai, and Y. H. Wang, *Spine* **32**, 1809 (2007).
- ⁸ G. D. Sarvazyan A, Maevsky E and Oranskaja G, *Proc. Int. Workshop on Interaction of Ultrasound with Biological Media*, 6981 (1994).
- ⁹ A. Samani, J. Zubovits, and D. Plewes, *Physics in Medicine and Biology* **52**, 1565 (2007).
- ¹⁰ A. Samani and D. Plewes, *Physics in Medicine and Biology* **52**, 1247 (2007).
- ¹¹ M. J. Paszek, N. Zahir, K. R. Johnson, J. N. Lakins, G. I. Rozenberg, A. Gefen, C. A. Reinhart-King, S. S. Margulies, M. Dembo, D. Boettiger, D. A. Hammer, and V. M. Weaver, *Cancer Cell* **8**, 241 (2005).
- ¹² N. F. Boyd, H. Guo, L. J. Martin, L. M. Sun, J. Stone, E. Fishell, R. A. Jong, G. Hislop, A. Chiarelli, S. Minkin, and M. J. Yaffe, *New England Journal of Medicine* **356**, 227 (2007).

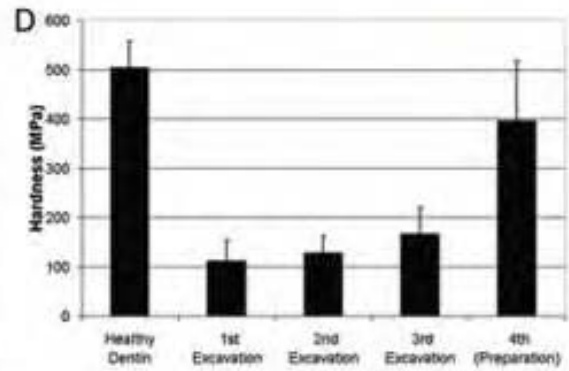
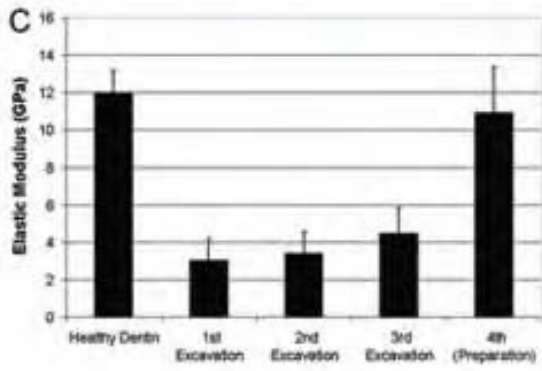
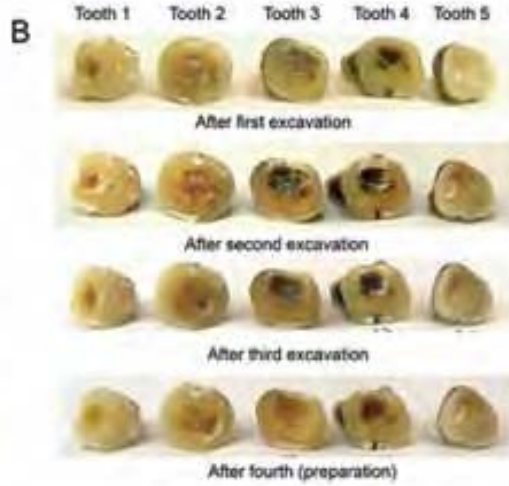
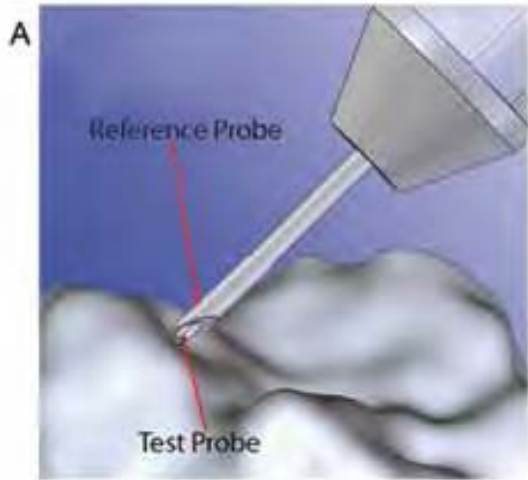
- 13 R. U. Kleemann, D. Krockner, A. Cedraro, J. Tuischer, and G. N. Duda, *Osteoarthritis and Cartilage* **13**, 958 (2005).
- 14 W. C. Oliver and G. M. Pharr, *Journal of Materials Research* **19**, 3 (2004).
- 15 J. H. Kinney, S. J. Marshall, and G. W. Marshall, *Critical Reviews in Oral Biology and Medicine* **14**, 13 (2003).
- 16 S. Habelitz, G. W. Marshall, M. Balooch, and S. J. Marshall, *Journal of Biomechanics* **35**, 995 (2002).
- 17 W. D. Nix and H. J. Gao, *Journal of the Mechanics and Physics of Solids* **46**, 411 (1998).
- 18 W. C. Oliver and G. M. Pharr, *Journal of Materials Research* **7**, 1564 (1992).
- 19 Y. Huang, F. Zhang, K. C. Hwang, W. D. Nix, G. M. Pharr, and G. Feng, *Journal of the Mechanics and Physics of Solids* **54**, 1668 (2006).
- 20 Z. A. Cole, E. M. Dennison, and C. Cooper, *Curr Rheumatol Rep* **10**, 92 (2008).
- 21 E. Durchschlag, E. P. Paschalis, R. Zoehrer, P. Roschger, P. Fratzl, R. Recker, R. Phipps, and K. Klaushofer, *J Bone Miner Res* **21**, 1581 (2006).
- 22 H. S. Gupta, P. Fratzl, M. Kerschnitzki, G. Benecke, W. Wagermaier, and H. O. K. Kirchner, *Journal of the Royal Society Interface* **4**, 277 (2007).
- 23 R. K. Nalla, J. J. Kruzic, J. H. Kinney, and R. O. Ritchie, *Bone* **35**, 1240 (2004).
- 24 M. Rief, F. Oesterhelt, B. Heymann, and H. E. Gaub, *Science* **275**, 1295 (1997).
- 25 J. Helenius, C. P. Heisenberg, H. E. Gaub, and D. J. Muller, *Journal of Cell Science* **121**, 1785 (2008).
- 26 L. G. Griffith and M. A. Swartz, *Nat Rev Mol Cell Biol* **7**, 211 (2006).
- 27 J. G. Jacot, S. Dianis, J. Schnall, and J. Y. Wong, *J Biomed Mater Res A* **79**, 485 (2006).

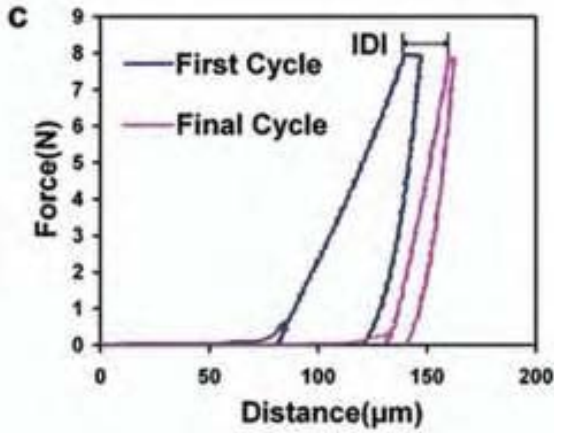












Supplementary material for the online version:

The Measurement of Viscoelasticity with the Tissue Diagnostic Instrument

The measurement of viscoelasticity of biological tissues is an active area of current research with an extensive theoretical foundation. (See, for example, a recent book by Y. C. Fung ¹). Here we present a very simple theoretical model to help in the understanding of TDI data (Fig. 7).

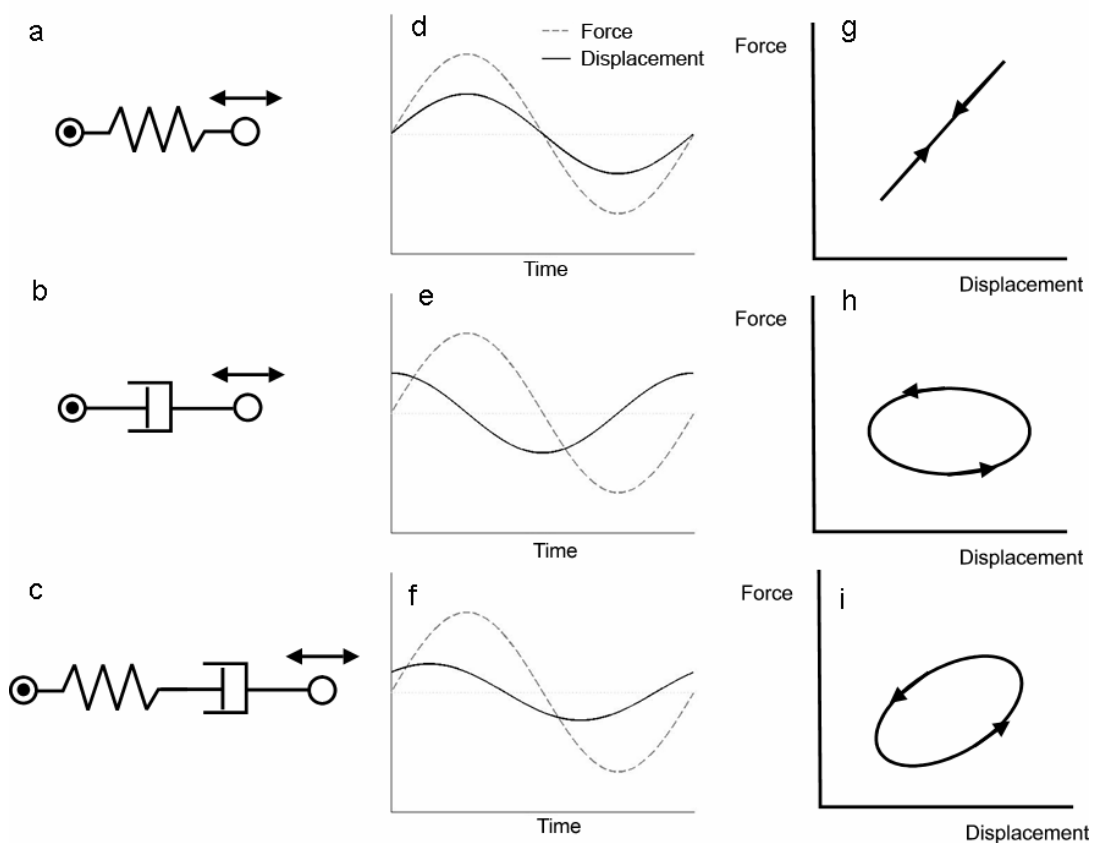


Fig. 7. A schematic view of the TDI driving (a) a simple spring, (b) a damper and (c) a simple spring plus damper in series with a sinusoidal displacement. For the simple spring, the Force measured by the TDI will be proportional to the displacement it is deflected, x , as shown in (d) and the Force vs. Displacement curve will be a straight line

with a slope equal to the spring constant of the spring and with no hysteresis (g). This is the elastic part of a viscoelastic response. For the damper, the Force measured by the TDI will be 90 degrees out of phase with the displacement since the force is proportional to the derivative of displacement, the velocity (e). The Force vs. Displacement curve will have a net slope equal to zero but non zero hysteresis (h). It has zero slope because the damping does not depend on the position of the damping element within the damper, but only on its velocity. The Force due to damping changes sign as the velocity changes sign. Thus the Force vs. Displacement curve is symmetric upon reflection in either the Force or the Displacement axes. The area inside the Force vs. Displacement curve will be the energy dissipated by the damper. This is the viscous part of the viscoelastic response. Thus the two parameters presented in this initial report, the Slope and the Energy Dissipation, are measures of the elastic and the viscous part of the viscoelastic response. For the simple spring plus damper (c) the Force will neither be perfectly in phase (as for the simple spring alone) or 90 degrees out phase (as for the damper alone) (f). The Force vs. Displacement curve will have a net slope and hysteresis (i).

There are more sophisticated mechanical models of viscoelastic tissue ¹, which can, in the future, be used to more precisely model the tissue and its interactions with the TDI probe, but they all share the same basics: the slope of a Force vs. Displacement curve is related to the elastic part of the viscoelastic response and the hysteresis is related to the viscous part of the viscoelastic response. These more sophisticated models become especially useful for describing frequency and time dependence of viscoelastic response. They can involve multiple springs and dampers in series and parallel combinations. Measurements at multiple frequencies and/or measurements of step responses can, in the future, be used to more fully specify the viscoelastic parameters of more sophisticated models.

It is important to note, however, that as Fung ¹ states: "The hysteresis curves of most biological soft tissues have a salient feature: the hysteresis loop is almost independent of the strain rate within several decades of rate variation. This insensitivity is incompatible with any viscoelastic model that consists of a finite number of springs and dashposts." This is in qualitative agreement with our preliminary observations of frequency

independent hysteresis with the TDI and is also reflected in the nearly vertical ends of the hysteresis curves, especially in very soft tissue like the breast tissue. That is, the dissipation depends on the sign of the velocity, but is relatively independent of the magnitude just as for simple models of friction.

Disc Study Methods

Human lumbar spine were harvested from donors and stored frozen at -20C. The lumbar segment featured in Fig. 2 was evaluated on an MRI degeneration grading scale (Pfirrmann scale ranges from 1-5) and given a grade of 3, indicating mild degenerative characteristics typical of aged discs. Prior to test the L12 motion segment was cut from the lumbar spine and thawed to room temperature. The medial-lateral axis of the disc was measured to be 55 mm. The reference probe from the TDI was then marked at insertion depths of 10% and 50% of that length corresponding to insertion depths for the annulus and nucleus respectively. At each of the two insertion depths 10 load cycles were recorded with the TDI. The friction was evaluated by taking one measurement in air before and after each insertion. The values from the air measurements were subtracted from the measurements in tissue. The transverse x-ray image was taken with a C-arm imaging system (Model Compact 7600, OEC Medical Systems, Salt Lake City, UT) (Fig. 2).

Mammary Gland Methods

The MMTV-PyMT mouse model (polyoma middle T antigen under the control of MMTV long terminal repeat promoter, Gay, 1993) was used in this work. MMTV-PyMT^{+/-} and their WT littermates FVB were housed and maintained in a barrier facility at UCSF until 13 week old when all the PyMT^{+/-} females developed mammary tumors. Mice were euthanized with 15psi CO₂ followed by cervical dislocation. All protocols were approved by the Institutional Animal Care and Use Committee at UCSF. After the mammary glands or associated tumors were located, the probe assembly was inserted

through the skin and held inside the tissue for 10 measurements on each of three insertions. The friction was evaluated by taking one measurement in air before and after each insertion. The values from the air measurements were subtracted from the measurements in tissue.

The shear storage modulus (G') and loss modulus (G'') of mammary gland tissues were obtained by using an AR2000ex rheometer (TA Instruments-Waters LLC., New Castle, DE). Briefly, 8mm-stainless steel plates were sanded to prevent the slippage between the samples and plates. The friction and inertia of instrument were then calibrated before and after the 8mm parallel plate geometry was attached (following the user-manual). Isolated mouse mammary glands were punched into 8mm sections and placed between the plates. The tissues were tested at zero normal force, a controlled 2% strain and an angular frequency of 10 rads/s (at which the parameters under tests have minimal frequency dependency).

Hematoxylin and eosin (H&E) staining of the same tissue samples was performed after the mechanical tests to evaluate the histological changes. Tissues were fixed in 4% paraformaldehyde overnight, dehydrated, paraffin embedded and then sectioned (5mm thickness). The sections were stained with hematoxylin for one minute and eosin for two minutes and evaluated under bright-field microscope with a 10x objective (Nikon, IX80). Images were captured with a CCD camera (Spot scientific).

The TDI was hand held. The probe assembly was inserted through the skin and held inside the tissue for 10 measurements on each of three insertions. The friction was evaluated by taking one measurement in air before and after each insertion, allowing its removal from the measurements in tissue

Validation with Polyacrylamide Gels

Polyacrylamide (PA) gels were tested at multiple scales by atomic force microscopy (AFM), nanoindentation (NI), and a standard mechanical load frame under

unconfined compression (UC); and these results were compared with those obtained from the TDI. The elastic moduli of PA gels can be modulated by varying the percentage of crosslinking agent from 0.25% to 4% w/v. To construct a stratified PA gel, pre-polymerized 1mm thick “stiff” PA gel was placed in a mold that allowed for the polymerization of a superior 0.2mm thick layer of “compliant” PA gel (Fig. 4c).

AFM was performed with a MFP-3D-BIO (Asylum Research, CA) using a 5 μ m borosilicate spherical tip on a cantilever. Five measurements at 4-5 different regions were taken for each gel. The Hertz equilibrium modulus was determined from the unloading force-displacement curve. NI was performed using a Hysitron TriboIndenter (Hysitron Inc., MN) with a 100 μ m conospherical diamond fluid tip under displacement control. Indentations were applied at a depth of 2-3 μ m and allowed to relax over 30s, and the Hertz equilibrium modulus was computed from the force-displacement curves. Gels were tested in unconfined compression using custom platens on a Bose ELF3200 load frame (Bose, MN, USA) under stress relaxation to 8% over a 300s relaxation time. The equilibrium moduli were computed from the force-displacement curves. TDI measurements were performed using the type V probe assembly at a frequency of 2Hz. For all tests, gels were fully immersed in a 0.01M HEPES solution at room temperature.

Cartilage Methods

Tibial plateaus with intact subchondral bone were harvested and fresh frozen from a human cadaver (19yo) and from human total knee arthroplasty with severe clinically confirmed osteoarthritis (63yo). Using the type V probe assembly, non-destructive indentation loads were applied *in situ* at 2Hz under a PBS bath (Fig 4e). Force-displacement curves were obtained from these measurements.

Dentin methods

Extracted human teeth (N=5) with extensive carious lesions into inner third of dentin were excavated using standardized procedures for selective caries removal. Material properties of healthy and irregularly shaped, affected dentin at the cavity floor were determined using a new handheld diagnostic instrument. The device, which measures the

hardness and elastic modulus of dentin by indenting the surface on the order of 50-100 μm , has a sharpened test probe which slides inside a hypodermic syringe that serves as a local reference. The instrument was hand held for convenience in positioning it over the interior surface of the cavity, perpendicular to the surface (as estimated by eye).

Bone Methods

The Osteoprobe™ II Bone Diagnostic Instrument was used in the Hospital del Mar in Barcelona on the tibias of living patients. First the patient's lower leg was positioned in padded "V" blocks on the base of the instrument such that the medial tibia surface was approximately level. Then the site for the tests was cleaned with alcohol and disinfected with 2% iodinated povidone solution. Next 1% mepivacain up to 10 ml was injected into the periosteum. As the anesthesia took effect (about 5 minutes) a sterilized probe assembly (like the one shown in figure 5 for dentin) was attached to the BDI and calibration curves were run on PMMA standard block. Then 5 tests were run by lowering the probe assembly through the skin and soft tissue over the tibia onto the tibia's surface, then scraping 5 times away from the direction of the opening of the bevel on the syringe and then stopping in the middle of the scraped region. Each scrape was 3 – 5 mm long at the same location for each of the 5 scrapes. Enough force was applied to scrape away the periosteum. A video of this procedure is available at the following website:

<http://hansmalab.physics.ucsb.edu/bdi.html>

Data Analysis Methods for Hard Tissue

The automatic data collection protocol involves loading pre-cycles followed by 2 primary loading cycles that were trapezoidal waves. Each trapezoidal wave consists of 1/3 of a cycle of linear force increase, followed by 1/3 of a cycle hold at maximum force, P_{max} , approximately 5 N, and then 1/3 of a cycle of linear force decrease. The total cycle time was 500 msec. The purpose of the hold at maximum force is to monitor creep effects and to minimize the effect of the remaining creep during the linear decrease. This type of hold at the maximum is used in instrumented indentation analysis, pioneered by Oliver

and Pharr¹³, for getting valid retraction slopes for determining the elastic modulus. The purpose of the pre-cycles is to establish a reference position for subsequent indentation displacement measurements. The pre-cycles are modified trapezoidal waves similar to the primary cycles mentioned above. Unlike the primary cycles, which are of constant amplitude, the pre-cycles have gradually increasing load amplitudes typically starting at 0.1 N and increasing on the order of 0.1 N after each cycle. The maximum force during the pre-cycles is monitored. When the maximum force reaches a preset threshold value, typically about 1 N, the reference position for indentation displacement measurements is set at the displacement where the preset threshold force was reached.

The reference position is used to compute E and H using a modified form of the established Oliver and Pharr method¹³. The original method (Fig. 8a) is predicated on two assumptions: that the position corresponding to zero load is known and that the material behaves in a time-independent elastic-plastic manner. In this case, the properties are calculated from the load/unload hysteresis loops according to the formulae:

$$H = \frac{P_{\max}}{\alpha \left(h_{\max} - \frac{\varepsilon P_{\max}}{S} \right)^2} \quad (1a)$$

and

$$E = \frac{1}{2} \sqrt{\frac{\pi}{\alpha}} \left(\frac{S}{h_{\max} - \frac{\varepsilon P_{\max}}{S}} \right) \quad (1b)$$

where S is the unloading stiffness (indicated on Fig. 8a), h_{\max} is the displacement at the load maximum, $\varepsilon = 0.75$, and, for a conical indenter with half angle θ , $\alpha = \pi \tan^2 \theta$.

The method has been modified to account for two additional effects that usually arise during subcutaneous testing of biological tissues. First, when the position of zero load is unknown *a priori*, the *apparent* hardness and modulus can be calculated according to

$$H_{app} = \frac{P_{max}}{\alpha \left(\bar{h}_{max} - \frac{\varepsilon P_{max}}{S} \right)^2} \quad (2a)$$

and

$$E_{app} = \frac{1}{2} \sqrt{\frac{\pi}{\alpha}} \left(\frac{S}{\bar{h}_{max} - \frac{\varepsilon P_{max}}{S}} \right) \quad (2b)$$

where \bar{h}_{max} is the displacement from the reference position to the load maximum, i.e.

$\bar{h}_{max} = h_{max} - h_{ref}$. It can be readily shown that the reference displacement, h_{ref} , is related to the reference load, P_{ref} , through the relation:

$$h_{ref} = \sqrt{\frac{P_{ref}}{\alpha H}} \left(1 + \frac{\varepsilon \sqrt{\pi \alpha} H}{2 E} \right) \quad (3)$$

For typical property values, $\frac{\varepsilon \sqrt{\pi \alpha} H}{2 E} \ll 1$ and thus to a good approximation:

$$h_{ref} \approx \sqrt{\frac{P_{ref}}{\alpha H}} \quad (4)$$

Combining Eq. (4) and (2) yields:

$$H = H_{app} \left(1 - \sqrt{\frac{P_{ref}}{P_{max}}} \right)^2 \quad (5a)$$

and

$$E = E_{app} \left(1 - \sqrt{\frac{P_{ref}}{P_{max}}} \right) \quad (5b)$$

Thus, with knowledge of the reference and peak loads, the apparent property values can be corrected to obtain the true values.

Secondly, because of the viscoplastic nature of most biological tissues, the displacement increases by a finite amount during the hold at peak load, as illustrated in Fig. 8b. The

apparent properties calculated via Eq. 2a and 2b are corrected through analysis of a hypothetical monotonic loading curve for which the displacement is proportional to the actual displacement at each load and passes through the point of maximum load and maximum displacement (after the hold portion of the indentation cycle). For the latter scenario, it can be shown that the true values of E and H are related to the apparent values through the formulae:

$$H = H_{app} \left(1 - \frac{1}{\left(1 + \Delta h / \bar{h}_{max}\right) \left(\sqrt{P_{max} / P_{ref}} - 1\right) + 1} \right)^2 \quad (8a)$$

$$E = E_{app} \left(1 - \frac{1}{\left(1 + \Delta h / \bar{h}_{max}\right) \left(\sqrt{P_{max} / P_{ref}} - 1\right) + 1} \right) \quad (8b)$$

In the limit where $\Delta h \rightarrow 0$, Eq. 8a and 8b reduce to Eq. 5a and 5b, as required.

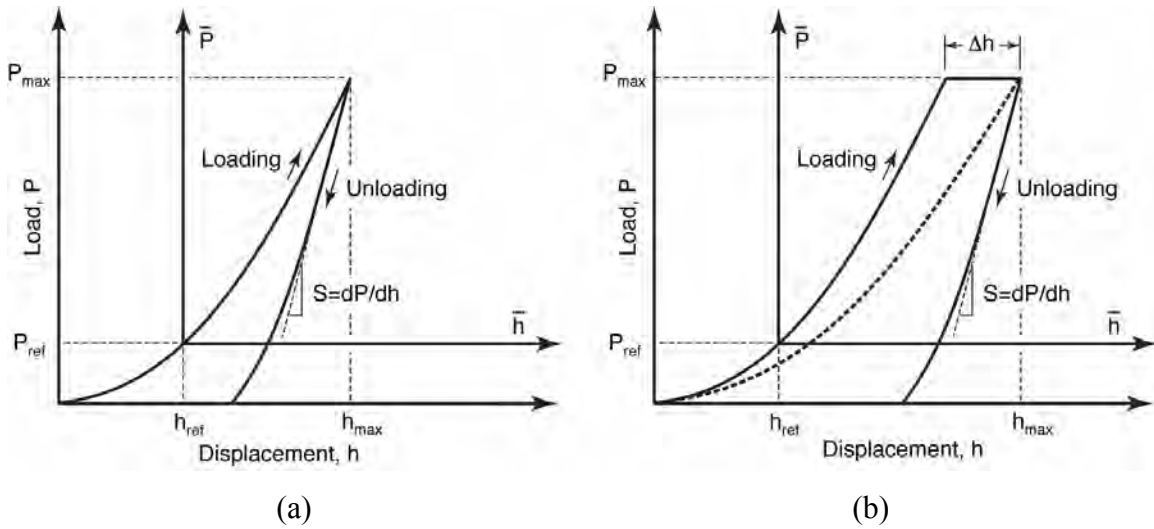


Fig. 8. Prototypical indentation curves. (a) Loading and unloading paths expressed in terms of the total load P and displacement h as well as the values measured from the reference point, denoted \bar{P} and \bar{h} , for an elastic-plastic material. (b) The corresponding loading/unloading response (with a finite hold period at peak load) for an elastic-viscoplastic material. Also shown is a hypothetical curve (dotted line) that would yield the same unloading response in an elastic-plastic material.

Gel

Calibration

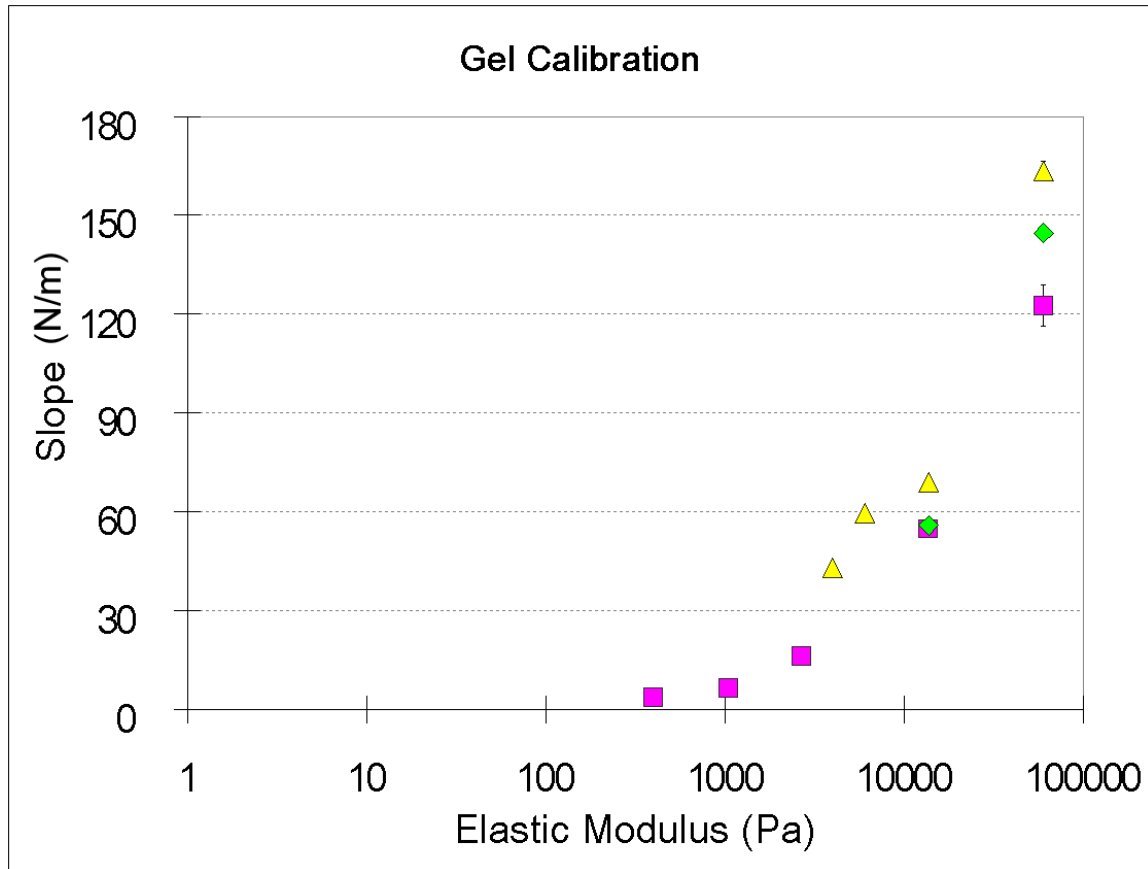


Fig. 7. The Slope as measured by the TDI with a Type D probe assembly (Fig. 1(c)) on polyacrylamide gels using the same amplitude and frequency (4 Hz) as for the mammary gland results reported in Fig. 3. The Elastic Modulus for these polyacrylamide gels was measured by a rheometer using the same protocol as for the mammary gland results reported in Fig. 3. Note that the Slope is an increasing function of the Elastic Modulus as would be expected from the simple model discussed above. The four different colored symbols in the graph refer to tests of four different sets of gels. The limit of measurement of Slope is set by instrumental noise and friction between the test probe and reference probe. For Type D probe assemblies this limit is about 5 N/m.

Adjusting the compliance of the TDI

The TDI prototype used here had an adjustable compliance. Fig. 1(a) shows a screw at the top of the prototype that is used for adjusting the compliance of the force generator. This screw presses against a block of rubber (shown in orange) that rests on the suspension of the force generator and can increase the effective spring constant of the suspension. In the limit that the screw is backed off the effective spring constant of the suspension (the compliance) is approximately 0.005 N/micron. It is used like that for hard tissues such as the dentin in this report. In this case the compliance of the suspension is much smaller than the effective spring constant of the hard tissue and the force generated by the force generator is nearly the same as the force applied to the hard tissue (the TDI is approximately force controlled). The details of operation in this mode are discussed above in the section on dentin methods.

Perhaps ironically, it is desirable to stiffen the suspension for soft tissues. The point is that for soft tissues the compliance of the suspension is no longer much smaller than the effective spring constant of the soft tissue. Since it would be very difficult to fabricate a softer suspension, we take the opposite approach and stiffen the suspension (by compressing the block of rubber against the top of the suspension (Fig. 1(a)) and make the suspension much stiffer than the tissue. In this case the TDI is approximately displacement controlled: the sinusoidal current to the force generator produces an approximately sinusoidal displacement curve in the tissue as discussed above (Fig. 5).

¹ Y. Fung, C., *Biomechanics: Mechanical Properties of Living Tissues* (Springer Science+Business Media, Inc., New York, 1993).

Matrix Cross-linking Forces Tumor Progression by Enhancing Integrin signaling

Kandice R. Levental¹, Hongmei Yu², Laura Kass², Johnathon N. Lakins², Janine T. Erler³, Mikala Egeblad⁴, Sheri F.T. Fong⁵, Katalin Csiszar⁵, Amato Giaccia³, Wolfgang Weninger⁶, Mitsuo Yamauchi⁷, Rebecca Wells⁸, David L. Gasser⁹, Valerie M. Weaver^{1,2,4,10,11}

1. Department of Bioengineering and Institute for Medicine and Engineering, University of Pennsylvania, Philadelphia, PA 19104
2. Center for Bioengineering and Tissue Regeneration, Department of Surgery, University of California at San Francisco, San Francisco, CA 94143
3. Department of Radiation Oncology, Stanford University School of Medicine, Stanford, CA 94305
4. Department of Anatomy, University of California at San Francisco, San Francisco, CA 94143
5. Cardiovascular Research Center, John A. Burns School of Medicine, University of Hawaii at Manoa, Honolulu, HI 96822
6. Immunology Program, Wistar Institute, Philadelphia, PA 19104
7. Dental Research Center, University of North Carolina, Chapel Hill, NC 27599
8. Department of Medicine, University of Pennsylvania, Philadelphia, PA 19104
9. Department of Genetics, University of Pennsylvania, Philadelphia, PA 19104
10. Department of Bioengineering and Therapeutic Sciences, Institute for Regenerative Medicine and UCSF Comprehensive Cancer Center, University of California at San Francisco, San Francisco, CA 94143

¹¹ Address all correspondence to:
Valerie M. Weaver Ph.D.
Associate Professor and Director
Center for Bioengineering and Tissue Regeneration
Department of Surgery
University of California, San Francisco
513 Parnassus Avenue
S1364, Box 0456
San Francisco, CA 94143-0456
Telephone: 415 476-3826
Email: weaverv@surgery.ucsf.edu

SUMMARY

Tumors are characterized by matrix remodeling and stiffening. The importance of matrix remodeling to tumorigenesis is appreciated; the relevance of stiffening to cancer is less clear. Here we report that breast tumor progression is accompanied by collagen cross-linking, matrix stiffening and increased focal adhesion signaling. We found that cross-linking collagen in culture and *in vivo* stiffened the matrix, promoted focal adhesions, enhanced growth factor stimulated PI3 Kinase activity, and induced invasion of an oncogene-transformed epithelium. Consistent with integrin-dependent mechano-transduction, we observed that forced integrin clustering also promoted focal adhesions and enhanced PI3 kinase activation to drive invasion of a premalignant mammary epithelium in three dimensional culture and *in vivo*. Moreover, reducing collagen cross-linking tempered tissue fibrosis, impeded cancer progression and lowered breast tumor incidence, and these phenotypes were accompanied by decreased focal adhesions and reduced PI3 Kinase signaling. These findings implicate matrix cross-linking in tissue stiffening and cancer fibrosis, and reveal a novel relationship between mechanical-force and focal adhesion-dependent PI3 Kinase signaling in cancer.

INTRODUCTION

Tumors are organs whose progress is orchestrated by a dialogue between the genetically abnormal cells within the tissue and the modified stroma (reviewed in (Bissell and Radisky, 2001; Ronnov-Jessen et al., 1996),(Grant et al., 2006; Nelson and Bissell, 2005; Radisky et al., 2001; Unger and Weaver, 2003)Butcher et al., 2009). The tumor stroma is characterized by changes in the levels, turnover and organization of extracellular matrix (ECM) which favours angiogenesis and promotes tumor invasion and metastasis (Beacham and Cukierman, 2005; Bhowmick and Moses, 2005; Burns-Cox et al., 2001; Kass et al., 2007; Santala et al., 1999). The tumor ECM is also significantly stiffer than normal (Netti et al., 2000; Paszek et al., 2005), and this trait has been exploited to detect cancer (Khaled et al., 2004; Krouskop et al., 1998; Sinkus et al., 2000). Matrix stiffness has been causally-implicated in cancer because it can enhance cell growth and survival and drive cell migration (Lo et al., 2000; Munevar et al., 2001; Pelham and Wang, 1997; Wang et al., 2000), and matrix rigidity can disrupt multi-cellular tissue morphogenesis by increasing cell tension (Paszek et al., 2005; Provenzano et al., 2008b; Wozniak et al., 2003). Reducing cellular tension represses the force-induced malignant behavior of mammary epithelial cells (MECs) in culture and normalizes the behavior of some breast cancer cells (Paszek et al., 2005). Why the matrix stiffens in tumors and whether cellular tension could drive malignancy and how is not clear.

Collagen is the most abundant ECM scaffolding protein in the interstitial stroma and contributes significantly to the tensile strength of the tissue (Kolacna et al., 2007). Collagen metabolism is deregulated in cancer, where increased expression of collagen genes, elevated deposition, altered organization, and enhanced collagen turnover by matrix metalloproteinases (MMPs) have been implicated in tumor progression and metastasis (Benyon and Arthur, 2001; Burrage et al., 2006; Egeblad and Werb, 2002; Elenbaas and Weinberg, 2001; Provenzano et al., 2006; Provenzano et al., 2008b), (Grant et al., 2006). Type I collagen synthesis and remodeling is required for tumor growth and angiogenesis, and for cell invasion and tumor metastasis (Burns-Cox et al., 2001; Ha et al., 2001; Ramaswamy et al., 2003; Ylissirnio et al., 2001). MMP-dependent collagen remodeling can create space for cells to migrate, produce specific substrate cleavage fragments with independent biological activity, regulate tissue architecture through effects on ECM and intercellular junctions, and activate, deactivate, or modify the activity of

signaling molecules (Egeblad et al., 2006; Egeblad and Werb, 2002; Fowlkes et al., 1995; Littlepage et al., 2005; Sternlicht and Werb, 2001; Whitelock et al., 1996). Despite the fact that high levels of MMPs correlate with poor prognosis in breast cancer patients (Hughes et al., 2007; Tetu et al., 2006; Zhang et al., 2008), and modulating MMP activity alters tumor phenotype, MMP inhibitors have failed clinically (Coussens et al., 2002). These findings underscore the inherent complexity of collagen homeostasis in cancer and suggest other parameters in addition to cleavage are involved.

Type I collagen has classically been considered a structural barrier against tumor invasion, yet in contradiction to this assumption, increased expression of types I and III collagens in tumors is associated with elevated risk of metastasis (Ramaswamy et al., 2003). Moreover, extensive mammographic density, which is associated with higher levels of collagen I and increased expression of the matrix cross-linker lumican, is strongly associated with breast cancer risk (Alowami et al., 2003; Boyd et al., 2007; Martin and Boyd, 2008; Vachon et al., 2007). Fibrillar collagens are synthesized as large precursor molecules and their processing requires a complex fibrillogenesis that involves multiple enzymes including the copper-dependent Lysyl oxidases and hydroxylases (Prockop and Kivirikko, 1995); (Kadler et al., 1996);(van der Slot et al., 2005). Lysyl Oxidase (LOX), which initiates the covalent cross-linking of the terminal hydroxyl groups of collagen to permit their fibril assembly and mechanical reinforcement (Eyre et al., 1984; Tanzer, 1973);(Katafuchi et al., 2007; Uzawa et al., 1998), is abundantly expressed in stromal fibroblasts and is elevated early in breast, lung, GI, and head and neck cancer patients (Erler and Weaver, 2008; Le et al., 2007). Fibrotic tissue contains high levels of LOX cross-linked collagen, and chronically-elevated LOX activity stiffens cardiovascular and liver tissues and compromises their function (Agache et al., 1980; Diridollou et al., 2001; Georges et al., 2007; Hansen and Jemec, 2002; Pfeiffer et al., 2005; Wells, 2005). Consistently, reducing LOX activity decreases tissue stiffness and prevents liver fibrosis (Georges et al., 2007). Moreover, increased expression of enzymes and proteoglycan cross-linkers that increase collagen stiffness accompany lung and skin fibrosis (Ebihara et al., 2000; Koslowski et al., 2001; Malmstrom et al., 2002; van der Slot et al., 2005), and fibrosis increases risk to malignancy (Krysa and Steger, 2007; Levrero, 2006; Maisonneuve et al., 2007; Zisman et al., 2005). Thus, elevated collagen

cross-linking could stiffen the matrix and drive malignancy by inducing tissue fibrosis. Nevertheless, the relationship between collagen cross-linking and cancer is unclear.

Integrins transduce mechanical and biochemical cues from the ECM by assembling cytoplasmic adhesion plaque complexes that initiate biochemical signaling and stimulate cytoskeletal remodeling to regulate cell growth, survival, motility/invasion and differentiation (Giancotti and Ruoslahti, 1999; Hynes, 2002; Miranti and Brugge, 2002). Integrin expression, activity and focal adhesions are increased by force and in cells interacting with a stiff matrix (Paszek et al., 2005; Sawada et al., 2006; Yeung et al., 2005). Moreover, human breast tumors, which are often fibrotic and stiff, and human breast cancer cells that exhibit high actomyosin tension, have elevated focal adhesions and enhanced integrin signaling (Beer et al., 2008; Bergamaschi et al., 2008; Cordes and Park, 2007; White and Muller, 2007). The matrix associated with experimentally-induced breast cancer is also stiff, and these tumors have increased integrins and focal adhesions and elevated integrin signaling (Beer et al., 2008; Bergamaschi et al., 2008; Cordes and Park, 2007; Guo and Giancotti, 2004; Mitra and Schlaepfer, 2006; White and Muller, 2007) Paszek, 2005 #9} (McDonald et al., 2008a; McDonald et al., 2008b; Park et al., 2008). This suggests that matrix stiffness could regulate malignancy by enhancing integrin-dependent mechano-transduction. Consistent with this paradigm, breast malignancy can be attenuated by genetically ablating integrin expression (White et al., 2004), and breast cancer cell behavior can be phenotypically-reverted to normal by either inhibiting integrin activity or reducing cell tension (Paszek et al., 2005; Weaver et al., 1997). Likewise, knocking down the expression or inhibiting the function of the focal adhesion plaque proteins (Lahlou et al., 2007; Provenzano et al., 2008a), focal adhesion kinase (FAK) and p^{130} Cas impedes breast tumor progression (Cabodi et al., 2006). Here we asked if collagen cross-linking could stiffen the breast stroma and induce fibrosis to promote oncogene-dependent breast tumorigenesis *in vivo*, and whether this involved integrins. We also explored whether inhibiting collagen cross-linking could prevent tissue fibrosis and reduce focal adhesions and integrin signaling to impede breast tumor progression.

RESULTS

Matrix stiffening and collagen cross-linking accompany breast tumor progression.

The HER-2 gene is a member of the epidermal growth factor receptor (EGFR) that is amplified in 20-25% of human breast cancers (Chibon et al., 2008; Nahta et al., 2006). The murine equivalent of HER-2 is the wild type Neu transgene which under the MMTV promoter (MMTV – Neu) has been used extensively to study the effect of elevated HER-2 signaling in the pathogenesis of breast cancer (Reviewed in (Kim and Muller, 1999)). Because the MMTV – Neu develops sporadic luminal breast tumors with a relatively long latency (6-10 months) it is useful to study the role of matrix remodeling in breast tumor progression. Therefore, to explore the relationship between tissue stiffness, fibrosis and cancer we assayed collagen levels, organization and breast tissue biophysical properties in MMTV - Neu mouse mammary glands at different stages of tumor progression. Using two independent methods to measure tissue mechanical properties of freshly excised breast tissue, unconfined compression and shear rheology, we detected an incremental stiffening of the mammary gland as it transitioned from histologically normal to pre malignant to invasive cancer (Fig 1A, B & C; top panel). We also determined that the stromal tissue adjacent to the invading epithelial lesions was substantially stiffer than normal. Prior to malignant transformation, total levels (Supp Fig 1) and amount of fibrillar collagen increased markedly (Fig 1C; quantified in D) coincident with tissue stiffening and consistent with fibrosis. Second harmonics generation (SHG) imaging revealed the progressive linearization of the collagen fibrils adjacent to the developing epithelial lesions (Fig 1E; quantified in F) with prominent linearized collagen tracts at the stromal-epithelial boundary of the invasive tumors (Fig 1E).

Consistent with the possibility that collagen linearization and reorganization reflected enhanced post translational modification we quantified an increase in the levels of iminium bifunctional cross-linked, dehydro-hydroxylysinoonorleucine (abbreviated here as HLNL) and ketoamine intermediate bifunctional cross-linked, dehydrodihydroxylysinoonorleucine (abbreviated here at DHLNL) collagen, reflecting elevated immature, reducible cross-linked collagen in the breast tumors (Fig 1G; (Yamauchi and Shiiba, 2008)). Indeed, we also detected

high levels of the key amine oxidase collagen cross-linker enzyme, lysyl oxidase LOX initially in the stroma surrounding the pre malignant Min foci, and thereafter within the epithelium and adjacent stroma of the cancerous lesions (Fig 1H). These data establish a relationship between increased collagen cross-linking, elevated LOX expression, matrix stiffness and tissue fibrosis in breast tumor progression. They suggest that collagen cross-linking could promote tissue stiffening and fibrosis.

LOX-mediated collagen cross-linking and tissue stiffening promote focal adhesions and tumor progression *in vivo*.

Because there was an increase in the level of reducible collagen cross-links and high LOX expression in the Her2/neu tumors (see Fig 1G & H), we next asked if LOX-mediated collagen cross-linking could stiffen the breast parenchyma to promote invasion of a premalignant human breast tissue. To test this possibility we used the Ha-ras transformed human MCF10AT MECs which upon injection into immunocompromised mice develop into non-invasive glandular premalignant glandular structures (Santner et al., 2001);(Hu et al., 2008). To test the effect of LOX-dependent collagen cross-linking, prior to MEC injection we conditioned paired inguinal mammary fat pads of three week old immuno-compromised NOD/SCID mice, surgically-cleared of their epithelium, with fibroblasts engineered to express activated LOX enzyme or with control fibroblasts (Fig 2A; Supp Fig 2 & 3). Two weeks following fibroblast injection shear rheology measurement of freshly excised epithelial-cleared mammary glands revealed that the LOX-treated tissues were substantially stiffer (Fig 2B) and contained considerably more fibrillar collagen, indicative of fibrosis (Fig 2C; quantified in D). The LOX-modified epithelial-cleared mammary glands also showed substantial collagen remodeling, as indicated by SHG imaging, which revealed abundant linearized collagen bundles in the LOX-conditioned mammary glands compared to control fibroblast-conditioned glands (Fig 2C bottom panel; quantified in E). Consistent with matrix stiffening, the fibroblasts residing within the LOX-treated glands stained positively for the focal adhesion marker FAK^{pY397} and the signaling molecule p¹³⁰Cas (Fig 2F).

Three weeks after the LOX-stiffened mammary glands were injected with pre malignant Ha-ras transformed MCF10AT mammary epithelial organoids, the tissue was significantly larger and stiffer than control (Figs. 2G, H & I; top panel). The mammary epithelial lesions in the LOX-

treated glands also lacked margins implying that they were invasive and they had more mature focal adhesions, as revealed by elevated FAK^{pY397} (Fig 2I middle and bottom panels) and ^{p130}Cas (data not shown) suggestive of enhanced mechanosignaling. Because LOX can also directly influence MEC behavior (Kagan and Li, 2003) in parallel at the same time that the animals were injected with the Ha-ras MCF10AT mammary organoids, we treated a cohort of animals with the irreversible pharmacological LOX inhibitor β -aminopropionitrile a natural, specific, and irreversible inhibitor of LOX activity (Hornstra et al., 2003),(Lucero and Kagan, 2006) (BAPN; (Georges et al., 2007)) by daily ingestion in the drinking water. Importantly, even in animals treated with BAPN, we noted that the LOX-preconditioned mammary glands injected with the Ha-ras premalignant MCF10AT mammary organoids were larger, stiffer and more vascular, and that the mammary epithelium in these glands lacked margins and had elevated FAK^{pY397}, indicating that the MECs had enhanced mechanosignaling and were invasive (Supp Fig 5, 6 & 7). Because we noted a similar epithelial phenotype in animals treated with or without BAPN at time of MCF10AT organoid injection, we concluded that LOX conditioning of the stroma and not direct actions of LOX on the mammary epithelium indirectly promoted breast tumor progression by inducing matrix stiffening and fibrosis. These findings show for the first time how matrix cross-linking and stiffening can induce focal adhesions and promote the growth and invasion of a pre malignant Ha-ras transformed mammary epithelium *in vivo*. The data also suggest that the cross-linking status and rigidity of an ECM could predispose an epithelium to malignancy.

Inhibiting LOX-dependent collagen cross-linking decreases fibrosis and reduces focal adhesions to inhibit breast tumor progression *in vivo*

LOX expression and collagen cross-linking were increased early in the MMTV - Neu model (Fig 1G & H), and we showed that LOX-dependent collagen cross-linking can stiffen a tissue and accompanies fibrosis (see Fig 2). Therefore, we next asked if reducing LOX-dependent collagen cross-linking could temper tissue fibrosis and decrease focal adhesions, and whether this would inhibit breast tumor progression. We inhibited LOX activity using either BAPN which is cell soluble and therefore can inhibit extracellular and intracellular LOX activity (Hornstra et al., 2003); (Lucero and Kagan, 2006) or a LOX-specific polyclonal function-blocking antibody which can only inhibit extracellular LOX activity (Erler et al., 2006). We then assayed for effects

on collagen cross-linking, tissue fibrosis, integrin adhesions and breast tumor development. Inhibition of LOX activity was initiated in five month old parous animals, when LOX levels were already increased in the stroma, but were low to non-detectable in the mammary epithelium (Fig 1H) and treatment was continued until the animals were 6 months of age, by daily ingestion of the pharmaceutical inhibitor BAPN in the drinking water or by twice weekly intraperitoneal injection of the LOX inhibitory antibody (Erler et al., 2006). Following treatment the animals were allowed to recover for one month, after which they were sacrificed and LOX activity, collagen expression, organization, and cross-linking, and tissue histology were assessed (e.g. animals were 7 months of age; Fig 3A). Palpable tumor development was monitored biweekly, time of detection noted, and tumor incidence was confirmed and quantified by histochemistry.

At time of sacrifice, the 7-7 1/2 month old non-treated MMTV - Neu mice had high levels of circulating active LOX (compared to non-transgene, control FVB mice; data not shown.) whereas animals treated for one month with either BAPN or LOX inhibitory antibody had reduced active LOX in their serum (Fig 3B). Animals with reduced LOX activity also had lower amounts of DHLNL and HLNL reversible, immature cross-linked collagen (Fig 3C). SHG revealed that the collagen fibrils adjacent to the epithelial lesions in the LOX-inhibited animals were less taut, indicated by an increase in the curvature ratio and decreased collagen linearity (Fig 3D; quantified in E). Consistent with the possibility that inhibiting collagen cross-linking prevented tissue fibrosis, LOX inhibition reduced total and fibrillar collagen, as revealed by reduced birefringence of picrosirius red-stained tissue (Fig 3E; compare parallel light and orthogonal images in untreated versus LOX-inhibited; quantified in F). Furthermore, animals with decreased cross-linked collagen had reduced focal adhesions, as indicated by negligible FAK^{pY397} (Fig 3G) and low ^{p130}Cas (data not shown).

Inhibiting LOX activity also increased tumor latency (Fig 4A) and decreased tumor incidence (Fig 4B), without reducing ErbB2 transgene activity (Fig 4C). Moreover, the palpable lesions formed in the LOX-inhibited animals were smaller (Fig 4D) and had reduced PCNA immunofluorescence staining suggesting they had decreased proliferation (Fig 4E). Furthermore, a higher proportion of the LOX inhibited mammary glands stained positively for cytokeratin 14 along the basal periphery of the ducts, implying many of these structures had retained their

myoepithelium (Fig 4H; quantified in I). Histo-pathological examination of H&E sections revealed that a larger proportion of the lesions formed in the LOX-inhibited animals were hyperplastic or premalignant (hyperplastic alveolar nodules, HAN, or mammary intraepithelial neoplasia, MIN) and the tumors that did develop were mostly low grade carcinomas as opposed to the higher grade carcinomas observed in the untreated MMTV - Neu mammary tumor model (Fig 4F; quantified in G; (Kim and Muller, 1999)). These results show how inhibiting stromal LOX activity can reduce the levels of immature collagen cross-linking and can temper tissue fibrosis. The work also suggests that decreasing collagen cross-linking reduces focal adhesions in the mammary epithelium and that this impedes tumor progression and reduces tumor incidence.

Collagen cross-linking and matrix stiffening promote focal adhesions and drive invasion of oncogenically-transformed pre malignant mammary tissues in a three dimensional collagen gel

To clarify the molecular mechanism whereby matrix cross-linking and tissue stiffness could influence tumor progression we explored the effect of non-specific, LOX-independent collagen cross-linking and matrix stiffening on tumor invasion. Ribose can rapidly glycate and cross-link collagen and stiffen the matrix. Therefore, we added the ribose to the media of pre assembled nonmalignant, polarized and growth-arrested MCF10A mammary acini embedded within a three dimensional compliant collagen I/reconstituted basement membrane gels (Col/rBM gel; (Johnson et al., 2007; Paszek et al., 2005)). This strategy permits an assessment of the direct effect of rapidly and non-specifically inducing collagen cross-linking and stiffening on epithelial invasion in a 3-dimensional (3D) ECM; in the absence of fibroblasts, immune cells and other stromal and systemic cellular and soluble factors (Fig 5A experimental schemata).

To determine whether MEC invasion required oncogenic signaling we also engineered the nonmalignant MCF10A MECs to express an activatable ErbB2 chimera (ErbB2.chim; also called HER-2; the human homologue of Neu that is frequently amplified in human breast cancers; (Kim and Muller, 1999) construct, consisting of the extracellular and transmembrane domains of low-affinity nerve growth factor receptor (p75NGFR), and the cytoplasmic kinase domain of ErbB2 linked to the synthetic ligand-binding domain from the FK506-binding protein (FKBP). In this

model addition of the synthetic bivalent FKBP ligand AP1510 leads to homodimerization of ErbB2, activation of the kinase domain and initiation of ErbB2 signaling (Muthuswamy et al., 1999; Muthuswamy et al., 2001). Activation of this chimeric ErbB2 drives proliferation and luminal filling but fails to induce invasion of preassembled mammary organoids within a compliant rBM (Fig 5E). To address the possibility that the tyrosine kinase signaling achieved with the chimeric ErbB2 was insufficiently high to drive epithelial invasion, and to recapitulate ErbB2 heterodimerization with epidermal growth factor receptor (EGFR), we also constructed MECs in which the full length exogenously over-expressed ErbB2 molecule could be induced and activated through addition of doxycycline (ErbB2.TetOn; Supp Fig 8 & 9). This construct permits homo- (ErbB2/ErbB2) and heterodimer (ErbB1/ErbB2) formation and recapitulates the ErbB2-dependent signaling observed in experimental and human breast tumors.

Consistent with previous findings (Friedland et al., 2007; Paszek et al., 2005; Weaver et al., 1997), three weeks following embedment within a compliant collagen/rBM gel, we noted that in the absence of the FKBP ligand AP1510, or doxycycline the MECs assembled growth-arrested and polarized acini with lumens, as illustrated by basally-oriented $\beta 4$ integrin and cell-cell localized beta catenin (Fig 5E). Glycation-mediated collagen cross-linking stiffened the matrix (Fig 5B), increased the size of the mammary colonies (Fig 5C), and perturbed their architecture substantially, as revealed by diffusely localized beta catenin and the appearance of cells within the lumens (Fig 5E). Consistent with matrix stiffening, MECs within the ribose cross-linked collagen gels had elevated levels of co-localized $\beta 1$ integrin and FAK^{PY397}, indicative of tension-induced focal adhesion assembly (Fig 5D; compare untreated to ribose stiffened). Nevertheless and critically, in the absence of ErbB2 activity, matrix stiffening did not drive the invasion of MECs into the collagen gel (Fig 5E; quantified in F).

Addition of either AP1510 (1 μ M) or doxycycline (0.2 μ g/mL) to the mammary acini within the compliant collagen I/rBM gels, induced and activated (ErbB2.TetOn) or activated ErbB2 (ErbB2.chim) (Supp Fig 9), promoted cell growth (data not shown; (Muthuswamy et al., 2001), drove luminal filling, and destabilized cell-cell junctions, as revealed by diffusely localized beta catenin (Fig 5E). Consistent with previous findings however, (Muthuswamy et al., 2001) sustained ErbB2 activation did not drive MEC invasion, as indicated by the retention of basally-

localized $\beta 4$ integrin (Fig 5E; quantified in 5F). Yet, when ErbB2 was activated in the mammary colonies in the cross-linked and stiffened collagen I/rBM gels, colony architecture disintegrated, as revealed by the virtual absence of detectable beta catenin and decreased and disorganized $\beta 4$ integrin staining, and invasion of cells into the collagen gels (Fig 5E & F). Interestingly, SHG imaging revealed that either ErbB2 activation or matrix stiffening was accompanied by the appearance of prominent collagen bundles around the noninvasive colonies, and that single MECs could be observed invading into the matrix on fibrils that extended perpendicularly into the cross-linked, stiffened gels after ErbB2 activation (Fig 5E; see also Supp Fig 10). These findings show how collagen cross-linking and matrix stiffening, per se, can cooperate with an oncogene such as ErbB2 to promote the invasive behavior of a pre assembled, growth-arrested mammary epithelium. The data implicate focal adhesions and collagen remodeling in this mechanically-induced phenotype.

Integrin clustering promotes focal adhesions to drive invasion of a Ha-ras premalignant mammary epithelium *in vitro* and *in vivo*

Because matrix cross-linking and stiffness and tumor invasion were consistently associated with elevated focal adhesions whereas reduced collagen cross-links and tumor inhibition was accompanied by decreased focal adhesions we next assessed the role of integrin and focal adhesions in tension-dependent breast tumor invasion. Immunofluorescence imaging revealed elevated p^{130} Cas and FAK pY397 staining that co-localized with $\beta 1$ integrin in the epithelium and stromal cells in the stiffened premalignant and invasive breast tissue of the MMTV - Neu mice (Fig 6A; see also magnified image in insert) and reduced FAK pY397 in the mammary epithelium of the LOX inhibited MMTV – Neu mice (Fig 3H).

To distinguish between increased integrin expression, elevated integrin activity and tension-dependent integrin oligermization, we expressed a series of integrin constructs in nonmalignant MCF10A and Ha-ras pre malignant MCF10AT MECs and assayed for invasive behavior in soft reconstituted basement membrane gels (rBM) and in subcutaneous xenografts (Fig 6B). Ectopic expression of the V737N integrin, which recapitulates tension-dependent integrin clustering (Paszek et al., 2005; other reference), promoted focal adhesions, as indicated by elevated FAK pY397 (Fig 6C; lower panels) and disrupted the integrity of nonmalignant mammary colonies

grown in rBM, as revealed by luminal filling and altered $\beta 4$ integrin localization (Fig 6C; top panels). In contrast, neither expression of a wild type (Fig 6C compare right to left panels) nor a constitutively active $\beta 1$ integrin (data not shown; (Paszek et al., 2005)) induced focal adhesions and disrupted tissue architecture. Importantly however, even the V737N $\beta 1$ integrin mutant failed to drive the invasive behavior of the nonmalignant MCF10A MECs in rBM (Fig 6C). Yet, the V737N integrin and not the wild type nor the constitutively active $\beta 1$ integrin induced the invasion of the Ha-ras premalignant MCF10AT mammary colonies in rBM (Fig 6D; quantified in Fig 6E). *In vivo*, the V737N integrin not only promoted focal adhesions, and increased lesion size, but also induced the invasive behavior of the Ha-ras pre malignant MCF10AT mammary organoids injected subcutaneously into nude mice, as revealed by the loss of margins surrounding the mammary epithelial lesions (see arrow in Fig 6F, G.). These findings implicate tension-dependent integrin clustering and focal adhesion assembly in breast tumor invasion. Importantly, because integrin clustering did not drive MEC invasion in the absence of Ha-ras, they also imply that integrin-dependent mechanotransduction must cooperate with oncogenic signaling to drive malignancy.

Collagen cross-linking and tissue stiffness promote integrin clustering and enhance PI3 kinase signaling to regulate invasion of a premalignant mammary epithelium *in vitro* and tumor progression *in vivo*.

Integrins activate PI3 Kinase and PI3 Kinase promotes tumor invasion in culture and tumor progression *in vivo* (Cabodi et al., 2006); (Chen and Guan, 1994; Delcommenne et al., 1998). Therefore, we next explored the relationship between focal adhesions and PI3 Kinase signaling in tension-dependent breast tumor invasion. We found Akt signaling, an established molecular target of PI3 Kinase, to be elevated in the premalignant and malignant, stiff mammary tissue (Fig 7A) and in the mammary colonies in the ribose-stiffened collagen gels (Fig 7B; compare levels of p-AKT/PI3K substrate activity in Colony in soft versus Ribose-cross-linked matrix). These observations are consistent with previous findings that elevated PI3K activity is associated with and necessary for breast tumor progression (Muller and Neville, 2001; Webster et al., 1998).

To determine if matrix stiffness could potentiate PI3 Kinase activity to promote breast tumor invasion, we assayed the effect of matrix rigidity on basal and ErbB-dependent PI3 Kinase

activity in nonmalignant MCF10A MECs plated on BM-functionalized polyacrylamide gels (BM PA gel) with calibrated elastic moduli of 400 (soft) and 5000-10,000 \geq (stiff) Pascals. These two rBM PA gel conditions represent the matrix stiffness we measured previously in healthy versus transformed breast tissue. Unlike natural collagen gels, these synthetic gels permit an assessment of the effect of matrix rigidity on MEC signaling independent of changes in ligand density, matrix pore size matrix topology (Johnson et al., 2007; Paszek et al., 2005). Although substrate stiffness did not increase the levels of Akt^{pS473} in un-stimulated MECs, the stiffer matrix did potentiate the magnitude and duration of ErbB1-activated Akt^{pS473} (Fig 7C) and did increase total levels of ErbB2-activated Akt^{pS473} (Fig 7D). MECs on soft rBM PA gels that expressed the β 1 integrin oligomerization V737N mutant (β 1.V737N), but not those ectopically-expressing wild-type β 1 integrin, also showed a significant increase in levels and duration of Akt^{pS473} activity following ErbB1 activation, thereby directly implicating integrin-dependent mechanotransduction in this signaling phenotype (Fig 7E; see also Fig 6B & C).

Pharmacological inhibition of PI3 Kinase activity with LY294002 also normalized the colony architecture of ErbB2-activated MECs embedded within Ribose cross-linked collagen gels, as revealed by reduced colony size, retention of beta catenin at cell-cell junctions and a repolarization of β 4 integrin (Fig 7F) and importantly, prevented the invasion of ErbB2-expressing MECs into the Ribose-stiffened collagen gels (Fig 7G). Consistently, LOX-inhibited MMTV – Neu mice, in which the level of cross-linked collagen was reduced, the amount of fibrosis tempered, detectable focal adhesions decreased and tumor incidence inhibited had lower PI3 Kinase signaling, shown by fainter staining for activated Akt/PI3 Kinase Substrate in the LOX-inhibited breast tissue sections (Fig 7H). These data are consistent with a role for integrin-dependent mechanotransduction in PI3 Kinase-mediated breast tumor invasion, and suggest that matrix stiffness induced by elevated collagen cross-linking could promote breast malignancy by enhancing integrin-growth factor receptor crosstalk (Bill et al., 2004; Miranti and Brugge, 2002). The results argue that while tissue stiffness itself might not drive malignancy matrix rigidity could change the context of oncogenic signaling to induce tumor formation.

Materials and Methods

Antibodies and Reagents: The following antibodies were used: monoclonal (mAb) β 4 integrin (mouse IgG₁, clone 3E1); β 1 integrin (rat IgG₁, clone AIIB2)(Chemicon); FAK (clone 77/FAK), YES (clone 1), β 1 integrin (clone 18), E-Cadherin (clone 610405)(BD Transduction Laboratories); laminin-5 (clone BM165; gift from M.P. Marinkovich); β actin (clone AC-15; Sigma); ErbB2 (clone 3B5; Calbiochem); polyclonal β catenin (Sigma); FAK^{pY397} (BioSource); Phospho-(Ser/Thr) Akt Substrates and Akt^{pS473}(Cell Signal); Akt (BD Pharmingen); p130Cas, ErbB2^{pY1248} (Abcam); cytokeratin 14 (Covance); LOX (S. Fong, University of Hawaii); LOX polyclonal activity inhibitory antibody (OpenBiosystems); and secondary AlexaFluor goat anti-mouse (488- and 555-conjugates), AlexaFluor goat anti-rabbit (488- and 555-conjugates), AlexaFluor goat anti-rat (488-conjugate), AlexaFluor phalloidin (488-conjugate, Invitrogen); Donkey anti-mouse (Cy2- and Cy3-conjugates) and Donkey anti-rabbit (Cy2- and Cy3-conjugates; Jackson ImmunoResearch); Sheep anti-mouse HRP-linked and Sheep anti-rabbit HRP-linked (Amersham). LY294002; (50 μ m in DMSO; Calbiochem) was used to inhibit PI3 Kinase.

Tissue culture and polyacrylamide gel manipulations: MCF10A MECs and NIH 3T3s were maintained in two and three dimensional culture as previously described (Johnson et al., 2007; Paszek et al., 2005). Collagen cross-linking was induced by addition of 15mM D-ribose to the cell culture medium upon each medium change. rBM-conjugated polyacrylamide gels with calibrated stiffness (400 and 5,000-10,000 Pascals) were prepared as previously described (Johnson et al., 2007).

Vector Constructs and ectopic gene expression: Full length human ErbB2 (gift from K. Ignatoski) was cloned into the pRet puro Tet IRES EGFP tetracycline-inducible vector. The β 1 integrin wild type, β 1 integrin glycan wedge constitutively active and β 1 integrin clustering mutant V737N constructs have been previously described (Paszek et al., 2005). Four myc-tags were added to the C-terminus of full length LOX (gift from K. Csiszar, University of Hawaii) and the gene was cloned into the multiple cloning site of the lentiviral vector pLV puro TetO₇mCMV tetracycline-inducible vector and expressed bicistronically with EGFP.

Retrovirus and lentivirus were produced in 293 and 293T cells, respectively. Target cells were infected with virus using 8 μ g/mL polybrene, and selected with G418 (β 1.WT, β 1.V737N, LOX), and puromycin (ErbB2). Further details are outlined in the Supplemental Materials.

Elastic modulus measurements: Unconfined compression analysis was performed on whole mammary glands using an electromechanical computerized indenter comprised of a linear stepper motor (minimal displacement of 0.0032mm), force transducer (load capacity 1.47N), and a linear variable displacement transducer. The tangent elastic modulus of the resulting stress-strain curves was calculated between 5-15% strain (Gefen et al., 2003; Paszek et al., 2005). Rheometrical analysis of mammary glands and polyacrylamide gels was performed using a controlled strain rheometer (Rheometric Scientific RFS-III, Piscataway, NJ) with 2% strain and a frequency of 10 rad/s. Mammary glands were tested with an 8 mm parallel plate geometry. Hydrated collagen cultures and polyacrylamide gels were measured with an 8 mm parallel serrated plate geometry.

Mice and Treatments: FVB-TgN MMTV - Neu (wild-type rat Neu gene expressed under the mouse mammary tumor virus LTR, referred to as MMTV-Neu in the text, obtained from Jackson Laboratory), NOD/SCID, and nude mice were maintained in specific pathogen-free conditions in accordance with the guidelines of the Laboratory of Animal Research at the University of Pennsylvania, Philadelphia, Pennsylvania and Institutional Animal Care and Use Committee at the University of California, San Francisco, California. Three week old NOD/SCID and nude mice were purchased from Jackson Laboratory (24 per study group two studies per treatment).

For lysyl oxidase (LOX) inhibition studies, uniparous WT or MMTV-Neu animals were treated with either BAPN (3mg/kg; Spectrum) in the drinking water (which was changed every other day; 4-8 per experimental group; four studies) or LOX inhibitory antibody (3mg/kg; OpenBiosystems, D8746; 3-4 per experimental group; one study) which was injected intraperitoneally twice a week. Treatment began when animals were 5 months of age and continued for one month. In these studies, all mice were sacrificed for further analysis at 7-7 1/2 months of age. All mice were monitored weekly for physical activity and weight changes. Control mice received fresh water every other day or Dulbeccos PBS injection. Tail vein blood

was collected before and after treatment and at sacrifice. Mice were monitored biweekly for mammary tumor development. Lesions were detected by palpation, and typically detected when the lesion size reached about 3mm in diameter. Final lesion volume was assessed using calipers and calculated by measurement of lesion length, width, and thickness. At sacrifice, mammary glands were excised and analyzed. Tissues were either assayed directly for rheology or imaging, snap frozen for protein and RNA or fixed in 4% paraformaldehyde, and 5 μ m paraffin sections were stained with Hematoxylin & Eosin for histopathological evaluation.

Tumor grading: Grading of the MMTV-neu tumors was performed blinded on haematoxylin and eosin (H&E) stained sections from untreated (n=14) or BAPN treated (n=13) #2-3 mammary glands. We define premalignant lesions as hyperplastic alveolar hyperplasia (HAN) or Mammary Intraepithelial Neoplasia (MIN)-like foci. Grade I lesions were well defined, homogenous carcinomas, Grade II contained areas with strong necrosis, stromal reaction and/or red blood cells outside of tumor blood vessels. Grade III also contained necrosis and nuclear pleiomorphy. A small set of anti-LOX treated mice (n=4) was compared with their controls (n=3), and showed the same tendency to less progressed lesions as observed in the BAPN treated animals.

Xenograft manipulations: NOD/SCID mice (n=24) were used for mammary fat pad transplantation techniques following the protocol outlined by Proia and Kuperwasser (Kuperwasser et al., 2004; Proia and Kuperwasser, 2005). Briefly, the rudimentary inguinal epithelium was removed from three week old anesthetized female mice, 5 x 10⁵ NIH 3T3 fibroblasts (2.5 x 10⁵ were treated with 4Gy irradiation 24 hours prior to injection) injected into the site, and the site was surgically repaired. To decrease variability, each mouse was injected with WT or LOX-expressing fibroblasts into the left and right mammary glands, respectively. Two weeks following fibroblast injection, 1x10⁶ DCIS.com MEC organoids (gift of B.A. Karmanos, National Cancer Institute); grown for 4 days in rBM to form mammary spheroids (16-20 cells per organoid) and dispase-treated to remove structures from ECM) were suspended in Dulbeccos modified PBS and injected into the fibroblast - conditioned epithelial cleared fat pads. All mice were sacrificed at 8 weeks of age (3 weeks following MEC injection and 5 weeks after fibroblast injection) and final lesion volume was assessed through length, width, and thickness by caliper measurement. Mammary glands were photographed *In Situ*, dissected and

tissues and segments of freshly excised tissue were either immediately imaged and subjected to shear rheology, or snap frozen for cross-linking and protein and RNA analysis or fixed and paraffin embedded for histochemistry.

Subcutaneous studies: Four day old, dispased, proliferating rBM organoids (16-20 cells per organoid) of Vector control, $\beta 1$ integrin wild type, $\beta 1$ integrin constitutively active glycan wedge and $\beta 1$ integrin cluster V737N mutant expressing MCF10AT DCIS.com MECs were injected subcutaneously into the rear flanks of BalbC Nu/Nu mice (6-8 animals per group; $5-10 \times 10^6$) and tumor formation was monitored for three weeks, as previously described (Weaver et al., 1997). At termination of the experiment animals were sacrificed and tumor tissue was treated as above.

Collagen cross-linking: Frozen mammary glands were pulverized in liquid nitrogen, washed with distilled water, and lyophilized. Each sample was then suspended in 0.15M *N*-trismethyl-2-aminoethane sulfonic acid, pH 7.4, reduced with standardized NaB_3H_4 , hydrolyzed with 6N HCl. Total collagen content was quantified in the hydrolysate by Hydroxyproline content measured by amino acid analysis and equal amount of Hyp was applied to an ion-exchange HPLC. The content of reducible cross-links and aldehydes as their reduced forms based on the specific activity of NaB_3H_4 was then determined by quantifying the fluorescent cross-links (pyridinoline and deoxypyridinoline) as an integration of the areas of the respective fluorescent peaks, standardized by the hydrolysate of an apparently pure pyridinoline containing peptides. The cross-links and cross-link precursor aldehydes were then calculated as a mole/mole of collagen basis based on the value of 300 residues of Hydroxyproline per collagen molecules (Yamauchi and Shiiba, 2008).

Quantification of picosirius red images: $5\mu\text{m}$ sections of paraffin-embedded mammary glands were stained with 0.1% Picosirius Red (Direct Red 80; Sigma Aldrich) and counterstained with Weigert's Hematoxylin. The sections were then serially imaged using an Olympus IX81 fluorescence microscope fitted with an analyzer (U-ANT; Olympus) and polarizer (U-POT; Olympus) oriented parallel and orthogonal to each other. Quantification of collagen was achieved by drawing $50\mu\text{m}$ by $50\mu\text{m}$ square regions at the stromal-epithelial border in the polarized (parallel) light images, transferring the regions to the cross-polarized

(orthogonal) light images, and calculating the area covered by a minimal threshold. A minimum of 4-6 areas were imaged per section and 4-6 sections per condition. The minimal threshold was set using normal mammary gland stroma as a control (Metamorph; Molecular Devices).

Two-photon second harmonics microscopy and image analysis: Second harmonics imaging was performed on a Prairie Technology Ultima System attached to an Olympus BX-51 fixed-stage microscope equipped with a 40× (NA 0.8) water immersion objective. The setup included external nondescanned dual-channel reflection/fluorescence detectors and a diode-pumped, wideband mode-locked Ti:Sapphire femtosecond laser (720–950nm, <140fs; 90MHz; Coherent Chameleon). The samples were exposed to polarized laser light at a wavelength of 920nm and emitted light was separated with a filter set (dichroic mirror, 495nm; band pass, 520/35nm; bandpass, 460/50nm). Z-stacks of a series of x-y planes of 284 by 284μm at a resolution of 0.55μm/pixel with a total thickness of at least 75μm (step size, 5μm) were captured using Prairie View acquisition software (Prairie Technologies) in at least 3 locations on each mammary gland or gel. Segmented line regions were drawn along the length of the fibers (A) and along the linear distance between the start and end of the fibers (B) of at least 15 fibrils each within two x-y planes from each stack (at least 40um apart) using ImageJ (Paszek et al., 2005). The curvature ratio (CR) of the collagen fibrils was calculated by dividing A by B. The CR of each condition was determined by averaging all of the fibrils from each image, and then averaging all the CRs per gland to give a final CR for each condition. N=4-8 samples per condition.

Immunofluorescence: 3D in vitro cultures were fixed in 2% paraformaldehyde, embedded in sucrose, frozen in Tissue-Tek OCT compound, and sectioned (20um)(Weaver et al., 2002). Paraffin-embedded tissue sections (5um) were subjected to antigen retrieval (0.01M, pH 6.0 citrate buffer) prior to immunostaining. All samples were incubated with the primary antibody following by either AlexaFluor 488/555- or Cy2/3-conjugated secondary antibodies. Nuclei were counterstained with diaminophenylindole (DAPI; Sigma). Slides were imaged using a Zeiss LSM510 confocal or a Nikon Eclipse E600 standard epifluorescent microscope equipped with a QICAM camera (Q Imaging, Surrey, British Columbia) and IPLab Imaging software (BD Biosciences Bioimaging, Rockville, MD).

Western analysis: Cells were lysed in RIPA or Laemmli buffer containing protease and phosphatase inhibitors (Johnson et al., 2007), and the protein concentration determined using a bicinchoninic acid (BCA; Pierce) assay. Equal protein was separated on SDS-PAGE gels, immunoblotted, and visualized using an ECL system (Amersham). The chemiluminescent intensity of bands was digitized using the Image Analyser LAS-1000 Plus system and the Image Reader LAS-1000 Pro version 1.0 software (Fuji, Tokyo, Japan).

LOX activity quantification: LOX activity was quantified as previously described (Erlor et al., 2006);(Fogelgren et al., 2005). LOX enzyme activity was measured in 5 μ L plasma samples using the Amplex Red fluorescence assay. The assay reaction mixture consisted of 50mM sodium borate (pH 8.5), 1.2M urea, 10 μ M Amplex Red, 1unit/ml horseradish peroxidase, and 10mM 1,5-diaminopentane (cadaverine) substrate. The samples were added to the reaction mix, in the presence or absence of 600 μ M BAPN, which was then incubated at 37°C. The fluorescent product was excited at 560nm, and the emission was read at 590nm using a fluorescence plate reader. LOX-specific fluorescence is reported as an increase over parallel BAPN-treated samples.

Discussion

We showed that collagen cross-linking and tissue stiffening accompany transition to malignancy in the breast and that collagen cross-linking stiffens the matrix to promote tissue fibrosis *in vivo* and induce invasion of a premalignant oncogene-transformed mammary epithelium (either ErbB2 or Ha-ras) *in vitro* and *in vivo*. We demonstrated that inhibiting collagen cross-linking diminished tissue fibrosis, impeded MMTV - Neu tumor progression and reduced tumor incidence. These findings identify collagen cross-linking as a critical regulator of desmoplasia and imply that the level and nature of matrix cross-links in a tissue could impact cancer risk and alter tumor behavior. The observations are consistent with established links between elevated levels of matrix cross-linking proteins and tissue stiffening in lung, pancreas and skin fibrosis and could explain the increased risk to malignancy associated with these conditions (Colpaert et al., 2003; Krysa and Steger, 2007; Sternlicht et al., 1999; Zisman et al., 2005). They might also explain why women with mammographically dense breasts, with elevated collagen and proteoglycans that likely stiffen the tissue have an increased relative risk of developing cancer (Alowami et al., 2003; Boyd et al., 2002; Boyd et al., 2007; Stone et al., 2006). Moreover, because aged tissues are stiffer than young tissue and the collagens in old tissue contain high levels of aberrant cross-links, the data offer a new paradigm for understanding why tumor incidence increases so dramatically in some aged tissues (Szauter et al., 2005).

Tissue fibrosis influences tumor progression by regulating the expression and activity of growth factors, chemokines and cytokines that induce inflammation and angiogenesis and stimulate cell proliferation and invasion (Bhowmick and Moses, 2005; Coussens et al., 1999; Coussens and Werb, 2002; Ilstiy and Hein, 2001). We showed that collagen cross-linking and matrix stiffness per se, two biophysical aspects of the fibrotic microenvironment induce the invasion of an oncogene transformed mammary epithelium, even in the absence of fibroblasts, immune cells and other cellular and soluble tissue and systemic factors. These findings imply that tissue fibrosis could also regulate cancer behavior through altered biophysical cues that increase mechanical force within a tissue. Consistently, extracellular force stimulates cellular tension to elevate integrin expression and activity and promote focal adhesions to potentiate growth factor signaling that then alters cell fate (Engler et al., 2006; Paszek et al., 2005; Wang et al., 2001). We noted that focal adhesions and integrin-dependent signaling were elevated in the

stiffened breast tumors and that a stiffened matrix induced focal adhesions and enhanced growth factor-stimulated PI3 Kinase activity to drive the invasion of a premalignant oncogene-transformed mammary epithelium, while inhibiting collagen cross-linking decreased focal adhesions and PI3 Kinase signaling and tempered tumor invasion and reduced tumor incidence. Forced clustering of $\beta 1$ integrin also increased focal adhesions and PI3 Kinase signaling and induced invasion of premalignant oncogenically-transformed MECs in a soft microenvironment, consistent with the notion that matrix stiffness increases actomyosin contractility to drive integrin clustering and enhance focal adhesion assembly, and growth factor-dependent signaling (Discher et al., 2005; Paszek et al., 2005; Wang et al., 2001). The observations support a critical role for ECM receptors and integrins in breast cancer, and suggest altered integrin adhesions and signaling and not merely an increase in integrin expression and/or activity is critical for tumor progression (Chen et al., 2006). Such a prediction could explain the frequently observed increase in activity of several focal adhesion plaque proteins including FAK and p130Cas in breast tumors, even when total integrin expression is so often decreased (Koukoulis et al., 1993; Zutter et al., 1998). Thus, the findings suggest that mechanical force promotes malignancy by altering the context of integrin and growth factor receptor signaling.

The data presented in this article illustrate how modulating the activity of one cross-linking enzyme, LOX, can either promote or attenuate tumor progression by regulating collagen cross-linking to alter tissue fibrosis and stiffness. The results are in accord with evidence that LOX and LOXL expression are elevated early in the epithelium of human breast tumors, and are increased in many clinically advanced cancers (Le et al., 2007) reviewed in (Erlar and Weaver, 2008). LOX is also induced by hypoxia-inducible factor (HIF-1) and up-regulated during experimental hypoxia; observations that are consistent with the fact that tumors are often hypoxic (Erlar et al., 2009; Erlar and Giaccia, 2006; Erlar and Weaver, 2008; Graeber et al., 1996; Postovit et al., 2008). Furthermore, cellular LOX and LOXL2 can promote breast cell migration and invasion (Kirschmann et al., 2002), and enhance tumor proliferation and survival and hypoxia-associated LOX can modulate tumor metastasis and condition the metastatic niche (Erlar et al., 2006; Erlar and Giaccia, 2006; Erlar and Weaver, 2008). Nevertheless, a major effect of LOX in tissues is to initiate the covalent cross-linking of collagens and elastins in the extracellular parenchyma and this in turn increases insoluble matrix deposition and tensile strength (Csiszar, 2001). Thus,

matrix stiffening is one of the primary consequence of LOX activity in the stroma (Szauter et al., 2005). We observed that LOX levels and collagen cross-linking were elevated early in MMTV - Neu (Fig 1) and human (data not shown) breast tumorigenesis, prior to its expression in the mammary epithelium (see Fig 1). Moreover, when we increased stromal LOX activity and induced collagen cross-linking and stiffness we promoted breast tumor progression (see Fig 2) consistent with the notion that stromal LOX can modulate malignant phenotype of the breast indirectly by altering the ECM. Consistently, by inhibiting LOX activity early, when levels were high in the stroma but nondetectable or low in the mammary epithelium we were able to attenuate tumor progression in the MMTV – Neu mouse (Figs 3 & 4). Indeed, we observed a similar reduction in tumor progression when we employed a LOX-specific inhibitory antibody that cannot inhibit intracellular LOX arguing that altering LOX-dependent collagen cross-linking indirectly regulated breast tumor progression by influencing tissue stiffness. Because focal adhesions and PI3 Kinase signaling were similarly modulated by altering LOX activity we contend that LOX modulated breast tumor phenotype by modulating focal adhesion assembly and growth factor receptor-dependent PI3 Kinase signaling. Consistent with this argument, we could show that ribose-mediated collagen cross-linking, which induces non-specific collagen glycation and cross-linking, similarly stiffened the matrix, enhanced focal adhesions and also permitted ErbB2-dependent MEC invasion suggesting an altered matrix and not specific effects of LOX modulated tumor behavior (Fig 3B, E & F). This idea is in accord with our recent work illustrating how LOX-mediated conditioning of the lung ECM stroma promotes breast tumor metastasis (Erler et al., 2009) and data indicating that fibrotic breast tumors have the poorest prognosis and higher rates of recurrence (Hasebe et al., 1997; Van den Eynden et al., 2007; Van den Eynden et al., 2008). Indeed, our findings underscore the notion that matrix cross-linking and stiffness per se is a key regulator of tumor phenotype. They imply that other matrix cross-linkers implicated in tissue fibrosis such as lysyl hydroxylase or the proteoglycans biglycan, fibromodulin, or versican or even non-specific metabolic glycation by products (AGEs) might also similarly alter tumor behavior.

Provocatively, LOX has been proposed as a tumor suppressor (Min et al., 2007; Payne et al., 2007), and elevated LOX activity in mammary epithelial cells can inhibit ECM adhesion and integrin signaling (Zhao et al., 2008) and some studies contend that matrix stiffening impedes

rather than enhances cell invasion into a 3D matrix (Zaman et al., 2007; Zaman et al., 2006). Consistently, fibrotic tissues and scars are also quite stiff and contain high levels of irreversible collagen cross-links, and many of these lesions never progress. We noted that neither matrix stiffness nor forced integrin clustering and focal adhesion assembly could induce invasion of a mammary epithelium unless oncogenic signaling was present (Fig 5E & 6D). This suggests that other factors including conditions or molecules that modulate integrin oligomerization and adhesions and/or matrix remodeling most likely cooperate with matrix stiffness to drive malignancy (Feral et al., 2005; Henderson et al., 2004; Katz et al., 2007; Wolf et al., 2007; Yang et al., 2008). Thus our results argue that matrix stiffness functions not as the primary driver of transformation but rather as a signaling rheostat that enables oncogenic signals to promote malignancy.

Cancer progression and metastasis are accompanied by ECM remodeling (Egeblad and Werb, 2002) and MMP-dependent matrix cleavage is considered a key step in tumor progression and metastasis (Duffy et al., 2000; Page-McCaw et al., 2007). Consistently, MMPs 3, 11, 12 and 13 are over expressed in the tumor stroma, and MMP-2 and 14 are up regulated in the transformed breast epithelium (Page-McCaw et al., 2007) (Dalberg et al., 2000; Jodele et al., 2006). Elevated expression of MMP-3 and 14 within the MECs of the breast of transgenic mice induce tissue desmoplasia and malignant transformation (Ha et al., 2001; Sternlicht et al., 1999). (Sternlicht and Werb, 2001) and genetic ablation of MMP expression or pharmaceutical inhibition of MMP activity reduces breast metastasis (Martin et al., 2008). These data argue convincingly that MMPs are critical for malignant transformation and invasion. Nevertheless, clinical trials with MMPs failed, suggesting the role of MMPs in cancer is more complicated than originally anticipated (Coussens et al., 2002). Consistently, MMPs collaborate with cross-linking enzymes such as LOX to facilitate collagen fibril assembly and maturation, and MMPs and LOX regulate the expression and activity of growth factors and cytokines including transforming growth factor beta (TGF β) (Atsawasuwan et al., 2008; Csiszar, 2001; Decitre et al., 1998; Szauter et al., 2005). Activated TGF β in turn regulates the expression of many matrix proteins and their cross-linkers including LOX and LOXL and several proteoglycans as well as an assortment of secreted chemokines and cytokines that evoke inflammation, induce fibrosis and promote migration and metastasis, and force can modulate TGF β activation and alter growth

factor signaling (Tschumperlin et al., 2004; Wells and Discher, 2008; Wipff et al., 2007) (Bierie and Moses, 2006; Kim et al., 2008; Oleggini et al., 2007; Stover et al., 2007). Indeed, MMPs may cooperate with matrix cross-linkers to create stiffened oriented collagen bundles on which cell migration would be enhanced (Provenzano et al., 2006; Sabeh et al., 2004). Thus cancer is best viewed as a dynamic, phenotypically-plastic and highly coordinated tissue remodeling process that is tightly regulated by both biochemical and biophysical cues. Accordingly, not only must we clarify the role of matrix cleavage in tumors but we should also understand how matrix remodeling is integrated within the context of matrix deposition, post translational modifications and topological rearrangements. To conclude then, the data in this article provide a compelling argument in favor of research aimed at understanding how mechanical force could synergize with the genetics of tumor cells and in collaboration with soluble and cellular components of the host microenvironment to regulate malignancy.

Acknowledgements

We thank K. Ignatoski for the full-length human ErbB2 construct, M.P. Marinkovich for the BM165 antibody, P. Mrass for two photon microscopy guidance and Jessica . A special thank you is extended to members of the Janmey laboratory and specifically to Ilya Levental for technical guidance. This work was supported by NIH grant R01-CA078731 to V.M.W, R01-CA057621 to Zena Werb to support M.E., and T32HL00795404 to K.R.L. and DOD grants DAMD17-01-1-0368, DAMD17-03-1-0396 and W81XWH-05-1-330 and DOE grant A107165 to V.M.W.

Figure Legends

Figure 1. Matrix stiffening, collagen cross-linking and tissue fibrosis accompany breast tumor progression. **A.** Bar graphs showing unconfined compression analysis, expressed as elastic modulus in Pascals (Pa), of freshly excised mammary glands from normal, pre-malignant (premal), tumor and tissue adjacent to tumors from FVB MMTV - Neu mice. **B.** Bar graphs showing shear rheology measurements of comparable tissues measured in A. The resulting G' values were translated to Elastic Modulus values “E” by assuming a Poisson’s ratio of 0.5 and are expressed as the elastic modulus Pa. **C.** Top row: Confocal immuno fluorescence images of tissue sections of normal, premalignant and tumor tissue from MMTV - Neu breast stained for the myoepithelial marker cytokeratin 14 (red) and counter stained with the chromatin dye DAPI (blue). Middle and bottom rows: Representative photomicrographs of sections of similar tissue to those shown above stained with Picrosirius Red and Hematoxylin, viewed under polarized light (middle row), and under cross-polarized light (bottom row). Bar $50\mu\text{m}$. **D.** Bar graphs showing fibrillar collagen quantification. For each image a $50\mu\text{m} \times 50\mu\text{m}$ area at the stromal-epithelial border was visualized under cross-polarized light, thresholding was set to minimize pixel intensity, and the intensity of the imaged area was measured. **E.** Representative SHG images of whole, unfixed mammary glands from normal, premalignant, tumor and tissue adjacent to tumors. Bar $50\mu\text{m}$. **F.** Bar graphs quantifying the degree of collagen linearity of conditions shown in E, as estimated by determining the Curvature Ratio (see Materials and Methods). **G.** Bar graphs showing level of DHLNL and HLNL reducible collagen cross links in normal mammary glands and in tumor tissue from MMTV - Neu mice. **H.** Confocal immuno fluorescence images of tissue sections of normal, premalignant, tumor and tissue adjacent to tumor stained for the collagen cross linker lysyl oxidase (green) and counter stained with the chromatin dye Propidium Iodide (red). Bar $20\mu\text{m}$. Microscopy images 40X. * $p \leq 0.05$ ** $p \leq 0.01$ *** $p \leq 0.001$. Values in A,B & D represent the Mean \pm SEM of analysis of multiple images and at least 4-6 glands per condition.

Figure 2. Collagen remodeling and tissue stiffening promote focal adhesions and tumor invasion *in vivo*. **A.** Schemata of experimental strategy. **B.** Bar graph of tissue rheology measurements of mammary glands conditioned for two weeks with fibroblasts expressing constitutively active lysyl oxidase (LOX; FB.LOX) or control fibroblasts (FB.WT). **C.** (Top and

middle panels) Representative photomicrographs of tissue sections described above in B stained with Picrosirius Red and Hematoxylin and viewed under polarized light (PS Red Parallel; top), and cross-polarized light (PS Red Orthogonal; middle). Bar 50 μ m. (Bottom panel) Representative SHG images of whole, unfixed tissues from LOX and control fibroblast-conditioned mammary glands, as described above. Bar 25 μ m. **D.** Bar graphs quantifying fibrillar collagen in cross-polarized light images shown in middle panel of C. For each image a 50 μ m x 50 μ m area at the stromal-epithelial border was visualized by cross-polarized light, thresholding was set to minimize pixel intensity, and the intensity of the imaged area was measured. **E.** Bar graphs quantifying collagen linearity in SHG images estimated by determining the Curvature Ratio (see Materials and Methods). **F.** Confocal immunofluorescence images of activated FAK (FAK^{P^{Y397}}; red) and p130Cas (p¹³⁰Cas; red) and nuclei counterstained with DAPI (DAPI; blue) of fibroblasts residing within LOX or control fibroblast-conditioned mammary glands. Bar 50 μ m. **G.** Bar graph of rheology of mammary tissue three weeks after injection with Ha-ras MCF10A MECs. **H.** Bar graph showing tumor burden for each cohort of mice at termination of experiment. **I.** Top panel: Photographs of LOX and control fibroblast-conditioned mammary glands three weeks after injection with premalignant Ha-ras MCF10A MECs. Middle panel: Representative Hematoxylin and Eosin stained tissue section from mammary gland shown in top panel of I. Bottom panel: Representative Confocal immunofluorescence images of tissues shown in top panel of I stained for β 1 integrin (red) and activated FAK (FAK^{P^{Y397}}; green) with nuclei counterstained with DAPI (blue). Bar 50 μ m. Mean \pm SEM. * $p \leq 0.05$. Values shown in D, E, G & H represent the Mean \pm SEM of multiple values obtained from several glands.

Figure 3. Inhibiting LOX-dependent collagen cross-linking tempers tissue fibrosis and reduces focal adhesions and PI3 Kinase activity. **A.** Schemata of experimental strategy. **B.** Bar graphs showing LOX activity in the serum of untreated (Control) compared to BAPN (+BAPN) or lysyl oxidase inhibitory antibody-treated (+LOX-Ab) MMTV - Neu mice. Values represent Mean \pm SEM of measurements from multiple animals. **C.** Bar graphs showing levels of DHLNL and HLNL reducible collagen cross links in the breast tissue of lysyl oxidase inhibited (LOX-Inhib) and untreated (Control) MMTV - Neu mice. **D.** Second harmonics generation images of whole, unfixed mammary glands from +BAPN treated animals treated as above. Bar 25 μ m. **E.** Bar graphs quantifying collagen linearity in breast tissues shown in D, as estimated

by determining the Curvature Ratio of multiple collagen fibrils (see Materials and Methods). Values represent Mean \pm SEM of multiple fibrils analyzed per gland with at least 4 glands per condition. **F.** Representative photomicrographs of tissue sections from nontreated (Control) and lysyl oxidase inhibited +BAPN treated (LOX-Inhib) MMTV - Neu mouse glands stained with Picrosirius Red and Hematoxylin and viewed under polarized light (top row) or cross-polarized light (bottom row). Bar 50 μ m. **G.** Bar graphs quantifying fibrillar collagen in glands from untreated (Control) and lysyl oxidase inhibited +BAPN treated (LOX-Inhib) animals shown in F. For each image a 50 μ m x 50 μ m area at the stromal-epithelial border was visualized under cross-polarized light, thresholding was set to minimize pixel intensity, and the intensity of the imaged area was measured. Values represent the Mean \pm SEM of multiple images (4-6) from several glands (4-8) per condition. **G.** Representative confocal immuno fluorescence images of tissue sections of mammary tissues excised from nontreated (Control) and lysyl oxidase inhibited +BAPN treated (LOX-Inhib) MMTV - Neu mice stained for activated focal adhesion kinase (FAK^{P^{Y397}}; red) with nuclei counter stained with the chromatin dye DAPI (blue). Bar 50 μ m.

Figure 4. Inhibiting LOX-dependent collagen augments tissue fibrosis to impede MMTV – Neu breast cancer progression and reduce tumor incidence. **A.** Bar graphs showing tumor latency as a function of animal age without (Control) or with LOX inhibition (LOX-Inhib). **B.** Bar graphs showing tumor incidence as a function of animal age without (Control) or with LOX inhibition (LOX-Inhib). **C.** Representative confocal immuno fluorescence images of activated ErbB2 transgene (ErbB2pY1248; red) in tissue sections from FVB (WT), MMTV - Neu untreated (MMTV-Neu) and typical LOX inhibited animals (MMTV-Neu +LOX-Inhib; example shown is typical LOX inhibitory antibody treated sample, similar results were observed with +BAPN treatment). Bar 50 μ m. **D.** Bar graphs illustrating reduced size of palpable tumors in untreated (Control) and LOX inhibited (LOX-Inhib) MMTV - Neu mice. Values represent Mean \pm SEM of multiple tumors per group. **E.** Representative confocal immuno fluorescence images of sections of tissue from LOX inhibited by treatment with inhibitory LOX antibody (LOX-Inhib) or untreated (Control) MMTV - Neu breasts stained for PCNA (red) with nuclei counter stained with the chromatin dye DAPI (blue). Bar 25 μ m. **G.** Grading of tumor lesions from mammary glands of Control (n=14) and BAPN (LOX-Inhib, n=13) treated animals showing significant reduction in high versus low grade tumors in LOX inhibited animals ($p \geq 0.05$).

Hyperplastic alveolar nodules (HAN) and mammary intraepithelial neoplasia (MIN) was defined as premalignant. MMTV - Neu animals, scored blinded. **H.** Representative confocal immunofluorescence images of breast tissue stained for cytokeratin 14 (CK 14; red) with nuclei counter stained with the chromatin dye DAPI (blue) in untreated (Control; left) and typical LOX inhibited (LOX-Inhib; right) animal mammary tissue section. Example shown is representative LOX inhibitory antibody treated animal tissue section. Note: Similar results were observed with BAPN treatment. Bar 50 μm . **I.** Bar graphs quantifying percent cytokeratin 14 positive glands detected in breast tissue sections from the untreated (Control) and LOX inhibited (LOX-Inhib) animals. Values in A, B, C, F & H represent Mean \pm SEM of measurements made in multiple tissue sections from the different experimental groups. *** $p \leq 0.001$.

Figure 5. Collagen cross-linking and matrix stiffening promote focal adhesions and drive invasion of oncogenic-transformed pre malignant mammary tissues within a three-dimensional collagen gel. **A.** Schemata of experimental design used to explore the role of collagen cross-linking on oncogene-dependent breast cell invasion using the 3D organotypic culture assay. **B.** Bar graphs showing elastic modulus of collagen gels determined by shear rheology. **C.** Bar graphs showing cross sectional area of traverse MEC colony sections. **D.** Confocal immuno fluorescence images of $\beta 1$ integrin (green) and activated FAK (FAK^{pY397}; red) with nuclei counterstained with DAPI (nuclei; blue) in acini in a soft (Untreated) and in a ribose-stiffened collagen/rBM gel (+Crosslinking). Bar 20 μm . **E.** (top row) Representative confocal immuno fluorescence images of β catenin (green) and $\beta 4$ integrin (red) with nuclei counterstained with DAPI (DAPI; blue) and (bottom row) two photon images of second harmonics generation of collagen and immunofluorescence of eGFP expressing MEC colonies engineered to express either the ErbB2/NGF chimera or a tetracycline-inducible wild type ErbB2, grown in soft collagen/rBM gels to assemble polarized, growth-arrested colonies (2 weeks). The matrix in half of the cultures was then cross-linked and stiffened by adding ribose to the media (2 weeks). Thereafter, ErbB2 dimerization and activity (+ErbB2) was induced in colonies in the soft and stiff matrices through exposure to either the dimerizer AP1510 (ErbB2.Chim) or doxycycline (ErbB2.tetOn). Colony integrity and invasion was monitored in all groups after an additional 10 days. Bar 20 μm . Images reveal collagen bundles surrounding the periphery of the colonies in which the ribose was cross-linked or the ErbB2 transgene was

activated (see yellow arrows) and show single MECs migrating onto collagen fibrils extending perpendicularly into the gels (see white arrow). **F.** Bar graphs quantifying MEC invasion in the various culture conditions. Values in B, C & F represent Mean values \pm SEM from multiple experiments and/or 50-100 colonies in 3 experiments. * $p \leq 0.05$, *** $p \leq 0.001$.

Figure 6. $\beta 1$ integrin clustering promotes focal adhesions to drive invasion of a Ha-ras pre malignant mammary epithelium in three dimensional culture and *in vivo* **A.** Confocal immuno fluorescence images of tissue sections of normal, premalignant and tumor tissue from MMTV-Her2/neu breast stained for p130Cas (p^{130} Cas red; top panels) or $\beta 1$ integrin ($\beta 1$ integrin; green) and activated FAK (FAK pY397 ; red; bottom panels) with nuclei counter stained with the chromatin dye DAPI (blue). Bar 20 μ m. [Is it really a 20 micron and not 50 micron scale bar? What are the insert supposed to show? What are arrows pointing to?] **B.** Cartoon showing integrin constructs used for the MEC organotypic and xenograft studies shown in C-G. Is mutant P737N the same as the mutant labeled “wedge” on subsequent panels? **C.** Representative confocal images of $\beta 4$ integrin ($\beta 4$ integrin; red; top) and activated FAK (FAK pY397 ; red; bottom) in nonmalignant MEC colonies expressing exogenous wild type $\beta 1$ integrin ($\beta 1$ (WT)) or the V737N auto-clustering $\beta 1$ integrin ($\beta 1$ (V737N)). **D.** Representative phase contrast images of pre malignant Ha-ras transformed MEC colonies grown in soft rBM for 6 days. Bar 50 μ m. **E.** Bar graphs showing percent invasive colonies induced through expression of the various $\beta 1$ integrin mutants shown in D. **F.** Bar graphs of lesion size formed by subcutaneously-injected pre malignant Ha-ras transformed MECs expressing the $\beta 1$ integrin V737N cluster mutant ($\beta 1$ (V737N)) compared to wild type $\beta 1$ integrin (WT). **G.** Top panels: Photomicrographs of Hematoxylin and Eosin stained sections of tumors formed by pre malignant Ha-ras transformed MECs expressing the $\beta 1$ integrin V737N cluster mutant ($\beta 1$ (V737N)) or wild type $\beta 1$ integrin (WT). Bottom panels: Representative confocal immuno fluorescence images of tissue section (as described for top panels in G) stained for activated FAK (FAK pY397 ; red) with nuclei counterstained with DAPI (blue). Bar 50 μ m. Values in E & F represent Mean \pm SEM of multiple measurements from at least 3 experiments. *** $p \leq 0.001$.

Figure 7. Tissue stiffness promotes integrin clustering and enhances growth factor-dependent PI3 Kinase activation

A. Confocal immuno fluorescence images of tissue sections of normal, premalignant and tumor tissue from MMTV - Neu breast stained for Activated Akt Substrate (red) with nuclei counter stained with the chromatin dye DAPI (blue). Bar 50 μ m. **B.** Representative confocal immuno fluorescence images of activated Akt substrate (Akt substrate; green) with nuclei counterstained with DAPI (DAPI; blue) in MEC colonies grown for 5 weeks in soft rBM/collagen gels (left; Control) or for 3 weeks in a soft gel and 2 weeks in a ribose cross-linked gel (right; Cross-linked). Bar 50 μ m. **C.** Representative immunoblots of ErbB1-stimulated phospho-Akt (Akt^{pS473}) normalized to total Akt in MECs plated on soft and stiff rBM-PA gels, and corresponding line graphs of immunoblot data quantified as relative phosphorylated Akt normalized to total Akt. **D.** Bar graphs quantifying levels of ErbB1-stimulated phospho-Akt (AKT^{pS473}) normalized to total AKT of ErbB2-expressing MECs plated on soft and stiff rBM-PA gels as deduced through immunoblot analysis. Values shown are relative to EGF-starved MECs. **E.** Line graphs of averaged immunoblot data quantified as relative phosphorylated Akt normalized to total Akt. of EGF-induced phospho-Akt (Akt^{pS473}) normalized to total Akt in MECs expressing the wild type β 1 integrin β 1(WT) or the autoclustering β 1 integrin V737N mutant β 1(V737N) plated on soft rBM-PA. **F.** Representative confocal immuno fluorescence images of β catenin (green) and β 4 integrin (red) with nuclei counterstained with DAPI (DAPI; blue) in MEC colonies engineered to express a tetracycline-inducible wild type ErbB2 construct. MECs were grown within a compliant collagen/rBM gel until they assembled polarized, growth-arrested colonies (2 weeks), were then exposed to media with ribose (+Cross-linking) to cross-link and stiffen the matrix (2 weeks) and ErbB2 dimerization and activation (+ErbB2) was induced through exposure to doxycycline and colony integrity and invasion was monitored 10 days later in cultures either treated with (+LY294002) or without the PI3 Kinase inhibitor LY294002. Bar 20 μ m. **G.** Bar graphs quantifying MEC invasion in the ErbB2 activated colonies in the ribose-stiffened gels in the presence and absence of PI3 Kinase activity. **H.** Representative confocal immuno fluorescence images of tissue sections of mammary tissues excised from nontreated (Control) and lysyl oxidase inhibited +BAPN treated (LOX-Inhib) MMTV - Neu mice stained for activated Akt substrate (Akt Substr; red) with nuclei counter stained with the

chromatin dye DAPI (blue). Bar 50 μm . Values in C, D and E represent Mean \pm SEM of multiple values obtained from at least 3 experiments and at least 50-100 colonies per experiment. *** $p \leq 0.001$.

Supplemental Figure Legends:

S1. Representative photomicrographs of Trichrome stained tissue sections of mouse mammary glands from non-malignant, pre malignant and tumor MMTV-Her2/neu mice. Bar 100 μm . **S2.** Cartoon depicting myc-tagged LOX construct used in studies. **S3.** Representative immunoblot showing c-myc-tagged LOX expression normalized to total Actin in NIH 3T3 cells following doxycycline treatment (0 to 1.0 $\mu\text{g}/\text{mL}$). **S4.** Photomicrographs of BAPN inhibited, LOX-conditioned tissues (FB.LOX) compared to control (FB.WT) 21 days following injection with premalignant Ha-ras transformed MECs **S5.** Bar graphs comparing tumor burden at termination of experiment in LOX versus control fibroblast conditioned mammary glands injected with Ha-ras MCF10AT premalignant cells with and without BAPN treatment. **S6.** Photomicrographs of Hematoxylin and eosin stained tissue sections of BAPN inhibited, LOX-conditioned tissues (FB.LOX) compared to control (FB.WT) 21 days after injection with premalignant Ha-ras transformed MECs. Bar is 100 μm . **S7.** Cartoon depicting ErbB2.TetOn expression construct used for experiments. **S8.** Representative immunoblot showing increased ErbB2-expression in nonmalignant MCF10A MECs following treatment with 0.2 $\mu\text{g}/\text{mL}$ doxycycline normalized to total cellular Yes. **S9.** Representative SHG images showing ErbB2 activated MECs invading into ribose-cross-linked gels onto fibers extending perpendicularly into the collagen matrix.

References

- Agache, P. G., Monneur, C., Leveque, J. L., and De Rigal, J. (1980). Mechanical properties and Young's modulus of human skin in vivo. *Arch Dermatol Res* 269, 221-232.
- Alowami, S., Troup, S., Al-Haddad, S., Kirkpatrick, I., and Watson, P. H. (2003). Mammographic density is related to stroma and stromal proteoglycan expression. *Breast Cancer Res* 5, R129-135.
- Atsawasuwan, P., Mochida, Y., Katafuchi, M., Kaku, M., Fong, K. S., Csiszar, K., and Yamauchi, M. (2008). Lysyl oxidase binds transforming growth factor-beta and regulates its signaling via amine oxidase activity. *J Biol Chem* 283, 34229-34240.
- Beacham, D. A., and Cukierman, E. (2005). Stromagenesis: the changing face of fibroblastic microenvironments during tumor progression. *Semin Cancer Biol* 15, 329-341.
- Beer, A. J., Niemeyer, M., Carlsen, J., Sarbia, M., Nahrig, J., Watzlowik, P., Wester, H. J., Harbeck, N., and Schwaiger, M. (2008). Patterns of alphavbeta3 expression in primary and metastatic human breast cancer as shown by 18F-Galacto-RGD PET. *J Nucl Med* 49, 255-259.
- Benyon, R. C., and Arthur, M. J. (2001). Extracellular matrix degradation and the role of hepatic stellate cells. *Semin Liver Dis* 21, 373-384.
- Bergamaschi, A., Tagliabue, E., Sorlie, T., Naume, B., Triulzi, T., Orlandi, R., Russnes, H. G., Nesland, J. M., Tammi, R., Auvinen, P., *et al.* (2008). Extracellular matrix signature identifies breast cancer subgroups with different clinical outcome. *J Pathol* 214, 357-367.
- Bhowmick, N. A., and Moses, H. L. (2005). Tumor-stroma interactions. *Current opinion in genetics & development* 15, 97-101.
- Bierie, B., and Moses, H. L. (2006). Tumour microenvironment: TGFbeta: the molecular Jekyll and Hyde of cancer. *Nat Rev Cancer* 6, 506-520.
- Bill, H. M., Knudsen, B., Moores, S. L., Muthuswamy, S. K., Rao, V. R., Brugge, J. S., and Miranti, C. K. (2004). Epidermal growth factor receptor-dependent regulation of integrin-mediated signaling and cell cycle entry in epithelial cells. *Mol Cell Biol* 24, 8586-8599.
- Bissell, M. J., and Radisky, D. (2001). Putting tumours in context. *Nat Rev Cancer* 1, 46-54.
- Boyd, N. F., Dite, G. S., Stone, J., Gunasekara, A., English, D. R., McCredie, M. R., Giles, G. G., Trichler, D., Chiarelli, A., Yaffe, M. J., and Hopper, J. L. (2002). Heritability of mammographic density, a risk factor for breast cancer. *N Engl J Med* 347, 886-894.
- Boyd, N. F., Guo, H., Martin, L. J., Sun, L., Stone, J., Fishell, E., Jong, R. A., Hislop, G., Chiarelli, A., Minkin, S., and Yaffe, M. J. (2007). Mammographic density and the risk and detection of breast cancer. *N Engl J Med* 356, 227-236.
- Burns-Cox, N., Avery, N. C., Gingell, J. C., and Bailey, A. J. (2001). Changes in collagen metabolism in prostate cancer: a host response that may alter progression. *J Urol* 166, 1698-1701.
- Burrage, P. S., Mix, K. S., and Brinckerhoff, C. E. (2006). Matrix metalloproteinases: role in arthritis. *Front Biosci* 11, 529-543.
- Cabodi, S., Tinnirello, A., Di Stefano, P., Bisaro, B., Ambrosino, E., Castellano, I., Sapino, A., Arisio, R., Cavallo, F., Forni, G., *et al.* (2006). p130Cas as a new regulator of mammary epithelial cell proliferation, survival, and HER2-neu oncogene-dependent breast tumorigenesis. *Cancer Res* 66, 4672-4680.
- Chen, H., Zou, Z., Sarratt, K. L., Zhou, D., Zhang, M., Sebzda, E., Hammer, D. A., and Kahn, M. L. (2006). In vivo beta1 integrin function requires phosphorylation-independent regulation by cytoplasmic tyrosines. *Genes & development* 20, 927-932.

Chen, H. C., and Guan, J. L. (1994). Stimulation of phosphatidylinositol 3'-kinase association with focal adhesion kinase by platelet-derived growth factor. *J Biol Chem* 269, 31229-31233.

Chibon, F., de Mascarel, I., Sierankowski, G., Brouste, V., Bonnefoi, H., Debled, M., Mauriac, L., and Macgrogan, G. (2008). Prediction of HER2 gene status in Her2 2+ invasive breast cancer: a study of 108 cases comparing ASCO/CAP and FDA recommendations. *Mod Pathol*.

Colpaert, C. G., Vermeulen, P. B., Fox, S. B., Harris, A. L., Dirix, L. Y., and Van Marck, E. A. (2003). The presence of a fibrotic focus in invasive breast carcinoma correlates with the expression of carbonic anhydrase IX and is a marker of hypoxia and poor prognosis. *Breast Cancer Res Treat* 81, 137-147.

Cordes, N., and Park, C. C. (2007). beta1 integrin as a molecular therapeutic target. *International journal of radiation biology* 83, 753-760.

Coussens, L. M., Fingleton, B., and Matrisian, L. M. (2002). Matrix metalloproteinase inhibitors and cancer: trials and tribulations. *Science* 295, 2387-2392.

Coussens, L. M., Raymond, W. W., Bergers, G., Laig-Webster, M., Behrendtsen, O., Werb, Z., Cughey, G. H., and Hanahan, D. (1999). Inflammatory mast cells up-regulate angiogenesis during squamous epithelial carcinogenesis. *Genes & development* 13, 1382-1397.

Coussens, L. M., and Werb, Z. (2002). Inflammation and cancer. *Nature* 420, 860-867.

Csiszar, K. (2001). Lysyl oxidases: a novel multifunctional amine oxidase family. *Progress in nucleic acid research and molecular biology* 70, 1-32.

Dalberg, K., Eriksson, E., Enberg, U., Kjellman, M., and Backdahl, M. (2000). Gelatinase A, membrane type 1 matrix metalloproteinase, and extracellular matrix metalloproteinase inducer mRNA expression: correlation with invasive growth of breast cancer. *World J Surg* 24, 334-340.

Decitre, M., Gleyzal, C., Raccurt, M., Peyrol, S., Aubert-Foucher, E., Csiszar, K., and Sommer, P. (1998). Lysyl oxidase-like protein localizes to sites of de novo fibrinogenesis in fibrosis and in the early stromal reaction of ductal breast carcinomas. *Lab Invest* 78, 143-151.

Delcommenne, M., Tan, C., Gray, V., Rue, L., Woodgett, J., and Dedhar, S. (1998). Phosphoinositide-3-OH kinase-dependent regulation of glycogen synthase kinase 3 and protein kinase B/AKT by the integrin-linked kinase. *Proc Natl Acad Sci U S A* 95, 11211-11216.

Diridollou, S., Vabre, V., Berson, M., Vaillant, L., Black, D., Lagarde, J. M., Gregoire, J. M., Gall, Y., and Patat, F. (2001). Skin ageing: changes of physical properties of human skin in vivo. *International journal of cosmetic science* 23, 353-362.

Discher, D. E., Janmey, P., and Wang, Y. L. (2005). Tissue cells feel and respond to the stiffness of their substrate. *Science* 310, 1139-1143.

Duffy, M. J., Maguire, T. M., Hill, A., McDermott, E., and O'Higgins, N. (2000). Metalloproteinases: role in breast carcinogenesis, invasion and metastasis. *Breast Cancer Res* 2, 252-257.

Ebihara, T., Venkatesan, N., Tanaka, R., and Ludwig, M. S. (2000). Changes in extracellular matrix and tissue viscoelasticity in bleomycin-induced lung fibrosis. Temporal aspects. *Am J Respir Crit Care Med* 162, 1569-1576.

Egeblad, M., Shen, H.-C. J., Behonick, D. J., Wilmes, L., Eichten, A., Korets, L., Kheradmand, F., Werb, Z., and Coussens, L. M. (2006). Type I collagen is a modifier of matrix metalloproteinase 2 function in skeletal development. Submitted.

Egeblad, M., and Werb, Z. (2002). New functions for the matrix metalloproteinases in cancer progression. *Nat Rev Cancer* 2, 161-174.

Elenbaas, B., and Weinberg, R. A. (2001). Heterotypic signaling between epithelial tumor cells and fibroblasts in carcinoma formation. *Exp Cell Res* 264, 169-184.

Engler, A. J., Sen, S., Sweeney, H. L., and Discher, D. E. (2006). Matrix elasticity directs stem cell lineage specification. *Cell* *126*, 677-689.

Erler, J. T., Bennewith, K. L., Cox, T. R., Lang, G., Bird, D., Koong, A., Le, Q. T., and Giaccia, A. J. (2009). Hypoxia-induced lysyl oxidase is a critical mediator of bone marrow cell recruitment to form the premetastatic niche. *Cancer Cell* *15*, 35-44.

Erler, J. T., Bennewith, K. L., Nicolau, M., Dornhofer, N., Kong, C., Le, Q. T., Chi, J. T., Jeffrey, S. S., and Giaccia, A. J. (2006). Lysyl oxidase is essential for hypoxia-induced metastasis. *Nature* *440*, 1222-1226.

Erler, J. T., and Giaccia, A. J. (2006). Lysyl oxidase mediates hypoxic control of metastasis. *Cancer Res* *66*, 10238-10241.

Erler, J. T., and Weaver, V. M. (2008). Three-dimensional context regulation of metastasis. *Clin Exp Metastasis*.

Eyre, D. R., Paz, M. A., and Gallop, P. M. (1984). Cross-linking in collagen and elastin. *Annu Rev Biochem* *53*, 717-748.

Feral, C. C., Nishiya, N., Fenczik, C. A., Stuhlmann, H., Slepak, M., and Ginsberg, M. H. (2005). CD98hc (SLC3A2) mediates integrin signaling. *Proc Natl Acad Sci U S A* *102*, 355-360.

Fogelgren, B., Polgar, N., Szauter, K. M., Ujfaludi, Z., Laczko, R., Fong, K. S., and Csiszar, K. (2005). Cellular fibronectin binds to lysyl oxidase with high affinity and is critical for its proteolytic activation. *J Biol Chem* *280*, 24690-24697.

Fowlkes, J. L., Thrailkill, K. M., Serra, D. M., Suzuki, K., and Nagase, H. (1995). Matrix metalloproteinases as insulin-like growth factor binding protein-degrading proteinases. *Prog Growth Factor Res* *6*, 255-263.

Friedland, J. C., Lakins, J. N., Kazanietz, M. G., Chernoff, J., Boettiger, D., and Weaver, V. M. (2007). $\alpha 6 \beta 4$ integrin activates Rac-dependent p21-activated kinase 1 to drive NF- κ B-dependent resistance to apoptosis in 3D mammary acini. *J Cell Sci* *120*, 3700-3712.

Gefen, A., Gefen, N., Zhu, Q., Raghupathi, R., and Margulies, S. S. (2003). Age-dependent changes in material properties of the brain and braincase of the rat. *J Neurotrauma* *20*, 1163-1177.

Georges, P. C., Hui, J. J., Gombos, Z., McCormick, M. E., Wang, A. Y., Uemura, M., Mick, R., Janmey, P. A., Furth, E. E., and Wells, R. G. (2007). Increased stiffness of the rat liver precedes matrix deposition: implications for fibrosis. *Am J Physiol Gastrointest Liver Physiol* *293*, G1147-1154.

Giancotti, F. G., and Ruoslahti, E. (1999). Integrin signaling. *Science* *285*, 1028-1032.

Graeber, T. G., Osmanian, C., Jacks, T., Housman, D. E., Koch, C. J., Lowe, S. W., and Giaccia, A. J. (1996). Hypoxia-mediated selection of cells with diminished apoptotic potential in solid tumours [see comments]. *Nature* *379*, 88-91.

Grant, M. R., Mostov, K. E., Tlsty, T. D., and Hunt, C. A. (2006). Simulating properties of in vitro epithelial cell morphogenesis. *PLoS Comput Biol* *2*, e129.

Guo, W., and Giancotti, F. G. (2004). Integrin signalling during tumour progression. *Nat Rev Mol Cell Biol* *5*, 816-826.

Ha, H. Y., Moon, H. B., Nam, M. S., Lee, J. W., Ryoo, Z. Y., Lee, T. H., Lee, K. K., So, B. J., Sato, H., Seiki, M., and Yu, D. Y. (2001). Overexpression of membrane-type matrix metalloproteinase-1 gene induces mammary gland abnormalities and adenocarcinoma in transgenic mice. *Cancer Res* *61*, 984-990.

Hansen, B., and Jemec, G. B. (2002). The mechanical properties of skin in osteogenesis imperfecta. *Arch Dermatol* *138*, 909-911.

Hasebe, T., Tsuda, H., Tsubono, Y., Imoto, S., and Mukai, K. (1997). Fibrotic focus in invasive ductal carcinoma of the breast: a histopathological prognostic parameter for tumor recurrence and tumor death within three years after the initial operation. *Jpn J Cancer Res* 88, 590-599.

Henderson, N. C., Collis, E. A., Mackinnon, A. C., Simpson, K. J., Haslett, C., Zent, R., Ginsberg, M., and Sethi, T. (2004). CD98hc (SLC3A2) interaction with beta 1 integrins is required for transformation. *J Biol Chem* 279, 54731-54741.

Hornstra, I. K., Birge, S., Starcher, B., Bailey, A. J., Mecham, R. P., and Shapiro, S. D. (2003). Lysyl oxidase is required for vascular and diaphragmatic development in mice. *J Biol Chem* 278, 14387-14393.

Hu, M., Yao, J., Carroll, D. K., Weremowicz, S., Chen, H., Carrasco, D., Richardson, A., Violette, S., Nikolskaya, T., Nikolsky, Y., *et al.* (2008). Regulation of in situ to invasive breast carcinoma transition. *Cancer Cell* 13, 394-406.

Hughes, S., Agbaje, O., Bowen, R. L., Holliday, D. L., Shaw, J. A., Duffy, S., and Jones, J. L. (2007). Matrix metalloproteinase single-nucleotide polymorphisms and haplotypes predict breast cancer progression. *Clin Cancer Res* 13, 6673-6680.

Hynes, R. O. (2002). Integrins: bidirectional, allosteric signaling machines. *Cell* 110, 673-687.

Jodele, S., Blavier, L., Yoon, J. M., and DeClerck, Y. A. (2006). Modifying the soil to affect the seed: role of stromal-derived matrix metalloproteinases in cancer progression. *Cancer Metastasis Rev* 25, 35-43.

Johnson, K. R., Leight, J. L., and Weaver, V. M. (2007). Demystifying the effects of a three-dimensional microenvironment in tissue morphogenesis. *Methods Cell Biol* 83, 547-583.

Kadler, K. E., Holmes, D. F., Trotter, J. A., and Chapman, J. A. (1996). Collagen fibril formation. *Biochem J* 316 (Pt 1), 1-11.

Kagan, H. M., and Li, W. (2003). Lysyl oxidase: properties, specificity, and biological roles inside and outside of the cell. *J Cell Biochem* 88, 660-672.

Kass, L., Erler, J. T., Dembo, M., and Weaver, V. M. (2007). Mammary epithelial cell: influence of extracellular matrix composition and organization during development and tumorigenesis. *The international journal of biochemistry & cell biology* 39, 1987-1994.

Katafuchi, M., Matsuura, T., Atsawasuwan, P., Sato, H., and Yamauchi, M. (2007). Biochemical characterization of collagen in alveolar mucosa and attached gingiva of pig. *Connect Tissue Res* 48, 85-92.

Katz, M., Amit, I., Citri, A., Shay, T., Carvalho, S., Lavi, S., Milanezi, F., Lyass, L., Amariglio, N., Jacob-Hirsch, J., *et al.* (2007). A reciprocal tensin-3-cten switch mediates EGF-driven mammary cell migration. *Nat Cell Biol* 9, 961-969.

Khaled, W., Reichling, S., Bruhns, O. T., Boese, H., Baumann, M., Monkman, G., Egersdoerfer, S., Klein, D., Tunayar, A., Freimuth, H., *et al.* (2004). Palpation imaging using a haptic system for virtual reality applications in medicine. *Stud Health Technol Inform* 98, 147-153.

Kim, D. J., Lee, D. C., Yang, S. J., Lee, J. J., Bae, E. M., Kim, D. M., Min, S. H., Kim, S. J., Kang, D. C., Sang, B. C., *et al.* (2008). Lysyl oxidase like 4, a novel target gene of TGF-beta1 signaling, can negatively regulate TGF-beta1-induced cell motility in PLC/PRF/5 hepatoma cells. *Biochem Biophys Res Commun* 373, 521-527.

Kim, H., and Muller, W. J. (1999). The role of the epidermal growth factor receptor family in mammary tumorigenesis and metastasis. *Exp Cell Res* 253, 78-87.

Kirschmann, D. A., Seftor, E. A., Fong, S. F., Nieva, D. R., Sullivan, C. M., Edwards, E. M., Sommer, P., Csiszar, K., and Hendrix, M. J. (2002). A molecular role for lysyl oxidase in breast cancer invasion. *Cancer Res* 62, 4478-4483.

Kolacna, L., Bakesova, J., Varga, F., Kostakova, E., Planka, L., Necas, A., Lukas, D., Amler, E., and Pelouch, V. (2007). Biochemical and biophysical aspects of collagen nanostructure in the extracellular matrix. *Physiological research / Academia Scientiarum Bohemoslovaca 56 Suppl 1*, S51-60.

Koslowski, R., Pfeil, U., Fehrenbach, H., Kasper, M., Skutelsky, E., and Wenzel, K. W. (2001). Changes in xylosyltransferase activity and in proteoglycan deposition in bleomycin-induced lung injury in rat. *Eur Respir J 18*, 347-356.

Koukoulis, G. K., Howedy, A. A., Korhonen, M., Virtanen, I., and Gould, V. E. (1993). Distribution of tenascin, cellular fibronectins and integrins in the normal, hyperplastic and neoplastic breast. *J Submicrosc Cytol Pathol 25*, 285-295.

Krouskop, T. A., Wheeler, T. M., Kallel, F., Garra, B. S., and Hall, T. (1998). Elastic moduli of breast and prostate tissues under compression. *Ultrason Imaging 20*, 260-274.

Krysa, J., and Steger, A. (2007). Pancreas and cystic fibrosis: the implications of increased survival in cystic fibrosis. *Pancreatology 7*, 447-450.

Kuperwasser, C., Chavarria, T., Wu, M., Magrane, G., Gray, J. W., Carey, L., Richardson, A., and Weinberg, R. A. (2004). Reconstruction of functionally normal and malignant human breast tissues in mice. *Proc Natl Acad Sci U S A 101*, 4966-4971.

Lahlou, H., Sanguin-Gendreau, V., Zuo, D., Cardiff, R. D., McLean, G. W., Frame, M. C., and Muller, W. J. (2007). Mammary epithelial-specific disruption of the focal adhesion kinase blocks mammary tumor progression. *Proc Natl Acad Sci U S A 104*, 20302-20307.

Le, Q. T., Kong, C., Lavori, P. W., O'Byrne, K., Erler, J. T., Huang, X., Chen, Y., Cao, H., Tibshirani, R., Denko, N., *et al.* (2007). Expression and prognostic significance of a panel of tissue hypoxia markers in head-and-neck squamous cell carcinomas. *Int J Radiat Oncol Biol Phys 69*, 167-175.

Levrero, M. (2006). Viral hepatitis and liver cancer: the case of hepatitis C. *Oncogene 25*, 3834-3847.

Littlepage, L. E., Egeblad, M., and Werb, Z. (2005). Coevolution of cancer and stromal cellular responses. *Cancer Cell 7*, 499-500.

Lo, C. M., Wang, H. B., Dembo, M., and Wang, Y. L. (2000). Cell movement is guided by the rigidity of the substrate. *Biophys J 79*, 144-152.

Lucero, H. A., and Kagan, H. M. (2006). Lysyl oxidase: an oxidative enzyme and effector of cell function. *Cell Mol Life Sci*.

Maisonneuve, P., Marshall, B. C., and Lowenfels, A. B. (2007). Risk of pancreatic cancer in patients with cystic fibrosis. *Gut 56*, 1327-1328.

Malmstrom, J., Larsen, K., Hansson, L., Lofdahl, C. G., Norregard-Jensen, O., Marko-Varga, G., and Westergren-Thorsson, G. (2002). Proteoglycan and proteome profiling of central human pulmonary fibrotic tissue utilizing miniaturized sample preparation: a feasibility study. *Proteomics 2*, 394-404.

Martin, L. J., and Boyd, N. F. (2008). Mammographic density. Potential mechanisms of breast cancer risk associated with mammographic density: hypotheses based on epidemiological evidence. *Breast Cancer Res 10*, 201.

Martin, M. D., Carter, K. J., Jean-Philippe, S. R., Chang, M., Mobashery, S., Thiolloy, S., Lynch, C. C., Matrisian, L. M., and Fingleton, B. (2008). Effect of ablation or inhibition of stromal matrix metalloproteinase-9 on lung metastasis in a breast cancer model is dependent on genetic background. *Cancer Res 68*, 6251-6259.

McDonald, P. C., Fielding, A. B., and Dedhar, S. (2008a). Integrin-linked kinase--essential roles in physiology and cancer biology. *J Cell Sci* *121*, 3121-3132.

McDonald, P. C., Oloumi, A., Mills, J., Dobreva, I., Maidan, M., Gray, V., Wederell, E. D., Bally, M. B., Foster, L. J., and Dedhar, S. (2008b). Rictor and integrin-linked kinase interact and regulate Akt phosphorylation and cancer cell survival. *Cancer Res* *68*, 1618-1624.

Min, C., Kirsch, K. H., Zhao, Y., Jeay, S., Palamakumbura, A. H., Trackman, P. C., and Sonenshein, G. E. (2007). The tumor suppressor activity of the lysyl oxidase propeptide reverses the invasive phenotype of Her-2/neu-driven breast cancer. *Cancer Res* *67*, 1105-1112.

Miranti, C. K., and Brugge, J. S. (2002). Sensing the environment: a historical perspective on integrin signal transduction. *Nat Cell Biol* *4*, E83-90.

Mitra, S. K., and Schlaepfer, D. D. (2006). Integrin-regulated FAK-Src signaling in normal and cancer cells. *Curr Opin Cell Biol* *18*, 516-523.

Muller, W. J., and Neville, M. C. (2001). Introduction: Signaling in mammary development and tumorigenesis. *J Mammary Gland Biol Neoplasia* *6*, 1-5.

Munewar, S., Wang, Y., and Dembo, M. (2001). Traction force microscopy of migrating normal and H-ras transformed 3T3 fibroblasts. *Biophys J* *80*, 1744-1757.

Muthuswamy, S. K., Gilman, M., and Brugge, J. S. (1999). Controlled dimerization of ErbB receptors provides evidence for differential signaling by homo- and heterodimers. *Mol Cell Biol* *19*, 6845-6857.

Muthuswamy, S. K., Li, D., Lelievre, S., Bissell, M. J., and Brugge, J. S. (2001). ErbB2, but not ErbB1, reinitiates proliferation and induces luminal repopulation in epithelial acini. *Nat Cell Biol* *3*, 785-792.

Nahta, R., Yu, D., Hung, M. C., Hortobagyi, G. N., and Esteva, F. J. (2006). Mechanisms of disease: understanding resistance to HER2-targeted therapy in human breast cancer. *Nat Clin Pract Oncol* *3*, 269-280.

Nelson, C. M., and Bissell, M. J. (2005). Modeling dynamic reciprocity: engineering three-dimensional culture models of breast architecture, function, and neoplastic transformation. *Semin Cancer Biol* *15*, 342-352.

Netti, P. A., Berk, D. A., Swartz, M. A., Grodzinsky, A. J., and Jain, R. K. (2000). Role of extracellular matrix assembly in interstitial transport in solid tumors. *Cancer Res* *60*, 2497-2503.

Oleggini, R., Gastaldo, N., and Di Donato, A. (2007). Regulation of elastin promoter by lysyl oxidase and growth factors: cross control of lysyl oxidase on TGF-beta1 effects. *Matrix Biol* *26*, 494-505.

Page-McCaw, A., Ewald, A. J., and Werb, Z. (2007). Matrix metalloproteinases and the regulation of tissue remodelling. *Nat Rev Mol Cell Biol* *8*, 221-233.

Park, C. C., Zhang, H. J., Yao, E. S., Park, C. J., and Bissell, M. J. (2008). Beta1 integrin inhibition dramatically enhances radiotherapy efficacy in human breast cancer xenografts. *Cancer Res* *68*, 4398-4405.

Paszek, M. J., Zahir, N., Johnson, K. R., Lakins, J. N., Rozenberg, G. I., Gefen, A., Reinhart-King, C. A., Margulies, S. S., Dembo, M., Boettiger, D., *et al.* (2005). Tensional homeostasis and the malignant phenotype. *Cancer Cell* *8*, 241-254.

Payne, S. L., Hendrix, M. J., and Kirschmann, D. A. (2007). Paradoxical roles for lysyl oxidases in cancer--a prospect. *J Cell Biochem* *101*, 1338-1354.

Pelham, R. J., Jr., and Wang, Y. (1997). Cell locomotion and focal adhesions are regulated by substrate flexibility. *Proc Natl Acad Sci U S A* *94*, 13661-13665.

Pfeiffer, B. J., Franklin, C. L., Hsieh, F. H., Bank, R. A., and Phillips, C. L. (2005). Alpha 2(I) collagen deficient oim mice have altered biomechanical integrity, collagen content, and collagen crosslinking of their thoracic aorta. *Matrix Biol* 24, 451-458.

Postovit, L. M., Abbott, D. E., Payne, S. L., Wheaton, W. W., Margaryan, N. V., Sullivan, R., Jansen, M. K., Csiszar, K., Hendrix, M. J., and Kirschmann, D. A. (2008). Hypoxia/reoxygenation: a dynamic regulator of lysyl oxidase-facilitated breast cancer migration. *J Cell Biochem* 103, 1369-1378.

Prockop, D. J., and Kivirikko, K. I. (1995). Collagens: molecular biology, diseases, and potentials for therapy. *Annu Rev Biochem* 64, 403-434.

Proia, D. A., and Kuperwasser, C. (2005). Stroma: tumor agonist or antagonist. *Cell Cycle* 4, 1022-1025.

Provenzano, P. P., Eliceiri, K. W., Campbell, J. M., Inman, D. R., White, J. G., and Keely, P. J. (2006). Collagen reorganization at the tumor-stromal interface facilitates local invasion. *BMC Med* 4, 38.

Provenzano, P. P., Inman, D. R., Eliceiri, K. W., Beggs, H. E., and Keely, P. J. (2008a). Mammary epithelial-specific disruption of focal adhesion kinase retards tumor formation and metastasis in a transgenic mouse model of human breast cancer. *Am J Pathol* 173, 1551-1565.

Provenzano, P. P., Inman, D. R., Eliceiri, K. W., Knittel, J. G., Yan, L., Rueden, C. T., White, J. G., and Keely, P. J. (2008b). Collagen density promotes mammary tumor initiation and progression. *BMC Med* 6, 11.

Radisky, D., Hagios, C., and Bissell, M. J. (2001). Tumors are unique organs defined by abnormal signaling and context. *Semin Cancer Biol* 11, 87-95.

Ramaswamy, S., Ross, K. N., Lander, E. S., and Golub, T. R. (2003). A molecular signature of metastasis in primary solid tumors. *Nat Genet* 33, 49-54.

Ronnov-Jessen, L., Petersen, O. W., and Bissell, M. J. (1996). Cellular changes involved in conversion of normal to malignant breast: importance of the stromal reaction. *Physiol Rev* 76, 69-125.

Sabeh, F., Ota, I., Holmbeck, K., Birkedal-Hansen, H., Soloway, P., Balbin, M., Lopez-Otin, C., Shapiro, S., Inada, M., Krane, S., *et al.* (2004). Tumor cell traffic through the extracellular matrix is controlled by the membrane-anchored collagenase MT1-MMP. *J Cell Biol* 167, 769-781.

Santala, M., Simojoki, M., Risteli, J., Risteli, L., and Kauppila, A. (1999). Type I and III collagen metabolites as predictors of clinical outcome in epithelial ovarian cancer. *Clin Cancer Res* 5, 4091-4096.

Santner, S. J., Dawson, P. J., Tait, L., Soule, H. D., Eliason, J., Mohamed, A. N., Wolman, S. R., Heppner, G. H., and Miller, F. R. (2001). Malignant MCF10CA1 cell lines derived from premalignant human breast epithelial MCF10AT cells. *Breast Cancer Res Treat* 65, 101-110.

Sawada, Y., Tamada, M., Dubin-Thaler, B. J., Cherniavskaya, O., Sakai, R., Tanaka, S., and Sheetz, M. P. (2006). Force sensing by mechanical extension of the Src family kinase substrate p130Cas. *Cell* 127, 1015-1026.

Sinkus, R., Lorenzen, J., Schrader, D., Lorenzen, M., Dargatz, M., and Holz, D. (2000). High-resolution tensor MR elastography for breast tumour detection. *Physics in medicine and biology* 45, 1649-1664.

Sternlicht, M. D., Lochter, A., Sympton, C. J., Huey, B., Rougier, J. P., Gray, J. W., Pinkel, D., Bissell, M. J., and Werb, Z. (1999). The stromal proteinase MMP3/stromelysin-1 promotes mammary carcinogenesis. *Cell* 98, 137-146.

Sternlicht, M. D., and Werb, Z. (2001). How matrix metalloproteinases regulate cell behavior. *Annu Rev Cell Dev Biol* 17, 463-516.

Stone, J., Dite, G. S., Gunasekara, A., English, D. R., McCredie, M. R., Giles, G. G., Cawson, J. N., Hegele, R. A., Chiarelli, A. M., Yaffe, M. J., *et al.* (2006). The heritability of mammographically dense and nondense breast tissue. *Cancer Epidemiol Biomarkers Prev* 15, 612-617.

Stover, D. G., Bierie, B., and Moses, H. L. (2007). A delicate balance: TGF-beta and the tumor microenvironment. *J Cell Biochem* 101, 851-861.

Szauter, K. M., Cao, T., Boyd, C. D., and Csiszar, K. (2005). Lysyl oxidase in development, aging and pathologies of the skin. *Pathol Biol (Paris)* 53, 448-456.

Tanzer, M. L. (1973). Cross-linking of collagen. *Science* 180, 561-566.

Tetu, B., Brisson, J., Wang, C. S., Lapointe, H., Beaudry, G., Blanchette, C., and Trudel, D. (2006). The influence of MMP-14, TIMP-2 and MMP-2 expression on breast cancer prognosis. *Breast Cancer Res* 8, R28.

Tlsty, T. D., and Hein, P. W. (2001). Know thy neighbor: stromal cells can contribute oncogenic signals. *Current opinion in genetics & development* 11, 54-59.

Tschumperlin, D. J., Dai, G., Maly, I. V., Kikuchi, T., Laiho, L. H., McVittie, A. K., Haley, K. J., Lilly, C. M., So, P. T., Lauffenburger, D. A., *et al.* (2004). Mechanotransduction through growth-factor shedding into the extracellular space. *Nature* 429, 83-86.

Unger, M., and Weaver, V. M. (2003). The tissue microenvironment as an epigenetic tumor modifier. *Methods Mol Biol* 223, 315-347.

Uzawa, K., Marshall, M. K., Katz, E. P., Tanzawa, H., Yeowell, H. N., and Yamauchi, M. (1998). Altered posttranslational modifications of collagen in keloid. *Biochem Biophys Res Commun* 249, 652-655.

Vachon, C. M., van Gils, C. H., Sellers, T. A., Ghosh, K., Pruthi, S., Brandt, K. R., and Pankratz, V. S. (2007). Mammographic density, breast cancer risk and risk prediction. *Breast Cancer Res* 9, 217.

Van den Eynden, G. G., Colpaert, C. G., Couvelard, A., Pezzella, F., Dirix, L. Y., Vermeulen, P. B., Van Marck, E. A., and Hasebe, T. (2007). A fibrotic focus is a prognostic factor and a surrogate marker for hypoxia and (lymph)angiogenesis in breast cancer: review of the literature and proposal on the criteria of evaluation. *Histopathology* 51, 440-451.

Van den Eynden, G. G., Smid, M., Van Laere, S. J., Colpaert, C. G., Van der Auwera, I., Bich, T. X., van Dam, P., den Bakker, M. A., Dirix, L. Y., Van Marck, E. A., *et al.* (2008). Gene expression profiles associated with the presence of a fibrotic focus and the growth pattern in lymph node-negative breast cancer. *Clin Cancer Res* 14, 2944-2952.

van der Slot, A. J., van Dura, E. A., de Wit, E. C., De Groot, J., Huizinga, T. W., Bank, R. A., and Zuurmond, A. M. (2005). Elevated formation of pyridinoline cross-links by profibrotic cytokines is associated with enhanced lysyl hydroxylase 2b levels. *Biochim Biophys Acta* 1741, 95-102.

Wang, H. B., Dembo, M., Hanks, S. K., and Wang, Y. (2001). Focal adhesion kinase is involved in mechanosensing during fibroblast migration. *Proc Natl Acad Sci U S A* 98, 11295-11300.

Wang, H. B., Dembo, M., and Wang, Y. L. (2000). Substrate flexibility regulates growth and apoptosis of normal but not transformed cells. *American Journal of Physiology-Cell Physiology* 279, C1345-C1350.

Weaver, V. M., Lelievre, S., Lakins, J. N., Chrenek, M. A., Jones, J. C., Giancotti, F., Werb, Z., and Bissell, M. J. (2002). beta4 integrin-dependent formation of polarized three-dimensional

architecture confers resistance to apoptosis in normal and malignant mammary epithelium. *Cancer Cell* 2, 205-216.

Weaver, V. M., Petersen, O. W., Wang, F., Larabell, C. A., Briand, P., Damsky, C., and Bissell, M. J. (1997). Reversion of the malignant phenotype of human breast cells in three-dimensional culture and in vivo by integrin blocking antibodies. *J Cell Biol* 137, 231-245.

Webster, M. A., Hutchinson, J. N., Rauh, M. J., Muthuswamy, S. K., Anton, M., Tortorice, C. G., Cardiff, R. D., Graham, F. L., Hassell, J. A., and Muller, W. J. (1998). Requirement for both Shc and phosphatidylinositol 3' kinase signaling pathways in polyomavirus middle T-mediated mammary tumorigenesis. *Mol Cell Biol* 18, 2344-2359.

Wells, R. G. (2005). The role of matrix stiffness in hepatic stellate cell activation and liver fibrosis. *J Clin Gastroenterol* 39, S158-161.

Wells, R. G., and Discher, D. E. (2008). Matrix elasticity, cytoskeletal tension, and TGF-beta: the insoluble and soluble meet. *Science signaling* 1, pe13.

White, D. E., Kurpios, N. A., Zuo, D., Hassell, J. A., Blaess, S., Mueller, U., and Muller, W. J. (2004). Targeted disruption of beta1-integrin in a transgenic mouse model of human breast cancer reveals an essential role in mammary tumor induction. *Cancer Cell* 6, 159-170.

White, D. E., and Muller, W. J. (2007). Multifaceted roles of integrins in breast cancer metastasis. *J Mammary Gland Biol Neoplasia* 12, 135-142.

Whitelock, J. M., Murdoch, A. D., Iozzo, R. V., and Underwood, P. A. (1996). The degradation of human endothelial cell-derived perlecan and release of bound basic fibroblast growth factor by stromelysin, collagenase, plasmin, and heparanases. *J Biol Chem* 271, 10079-10086.

Wipff, P. J., Rifkin, D. B., Meister, J. J., and Hinz, B. (2007). Myofibroblast contraction activates latent TGF-beta1 from the extracellular matrix. *J Cell Biol* 179, 1311-1323.

Wolf, K., Wu, Y. I., Liu, Y., Geiger, J., Tam, E., Overall, C., Stack, M. S., and Friedl, P. (2007). Multi-step pericellular proteolysis controls the transition from individual to collective cancer cell invasion. *Nat Cell Biol* 9, 893-904.

Wozniak, M. A., Desai, R., Solski, P. A., Der, C. J., and Keely, P. J. (2003). ROCK-generated contractility regulates breast epithelial cell differentiation in response to the physical properties of a three-dimensional collagen matrix. *J Cell Biol* 163, 583-595.

Yamauchi, M., and Shiiba, M. (2008). Lysine hydroxylation and cross-linking of collagen. *Methods Mol Biol* 446, 95-108.

Yang, X. H., Richardson, A. L., Torres-Arzayus, M. I., Zhou, P., Sharma, C., Kazarov, A. R., Andzelm, M. M., Strominger, J. L., Brown, M., and Hemler, M. E. (2008). CD151 accelerates breast cancer by regulating alpha 6 integrin function, signaling, and molecular organization. *Cancer Res* 68, 3204-3213.

Yeung, T., Georges, P. C., Flanagan, L. A., Marg, B., Ortiz, M., Funaki, M., Zahir, N., Ming, W., Weaver, V., and Janmey, P. A. (2005). Effects of substrate stiffness on cell morphology, cytoskeletal structure, and adhesion. *Cell Motil Cytoskeleton* 60, 24-34.

Ylisirnio, S., Hoyhtya, M., Makitaro, R., Paaakko, P., Risteli, J., Kinnula, V. L., Turpeenniemi-Hujanen, T., and Jukkola, A. (2001). Elevated serum levels of type I collagen degradation marker ICTP and tissue inhibitor of metalloproteinase (TIMP) 1 are associated with poor prognosis in lung cancer. *Clin Cancer Res* 7, 1633-1637.

Zaman, M. H., Matsudaira, P., and Lauffenburger, D. A. (2007). Understanding effects of matrix protease and matrix organization on directional persistence and translational speed in three-dimensional cell migration. *Ann Biomed Eng* 35, 91-100.

Zaman, M. H., Trapani, L. M., Sieminski, A. L., Mackellar, D., Gong, H., Kamm, R. D., Wells, A., Lauffenburger, D. A., and Matsudaira, P. (2006). Migration of tumor cells in 3D matrices is governed by matrix stiffness along with cell-matrix adhesion and proteolysis. *Proc Natl Acad Sci U S A* 103, 10889-10894.

Zhang, B., Cao, X., Liu, Y., Cao, W., Zhang, F., Zhang, S., Li, H., Ning, L., Fu, L., Niu, Y., *et al.* (2008). Tumor-derived matrix metalloproteinase-13 (MMP-13) correlates with poor prognoses of invasive breast cancer. *BMC cancer* 8, 83.

Zhao, Y., Min, C., Vora, S., Trackman, P. C., Sonenshein, G. E., and Kirsch, K. H. (2008). The lysyl oxidase pro-peptide attenuates fibronectin-mediated activation of FAK and p130CAS in breast cancer cells. *J Biol Chem.*

Zisman, D. A., Keane, M. P., Belperio, J. A., Strieter, R. M., and Lynch, J. P., 3rd (2005). Pulmonary fibrosis. *Methods in molecular medicine* 117, 3-44.

Zutter, M. M., Sun, H., and Santoro, S. A. (1998). Altered integrin expression and the malignant phenotype: the contribution of multiple integrated integrin receptors. *J Mammary Gland Biol Neoplasia* 3, 191-200.

Figure 1

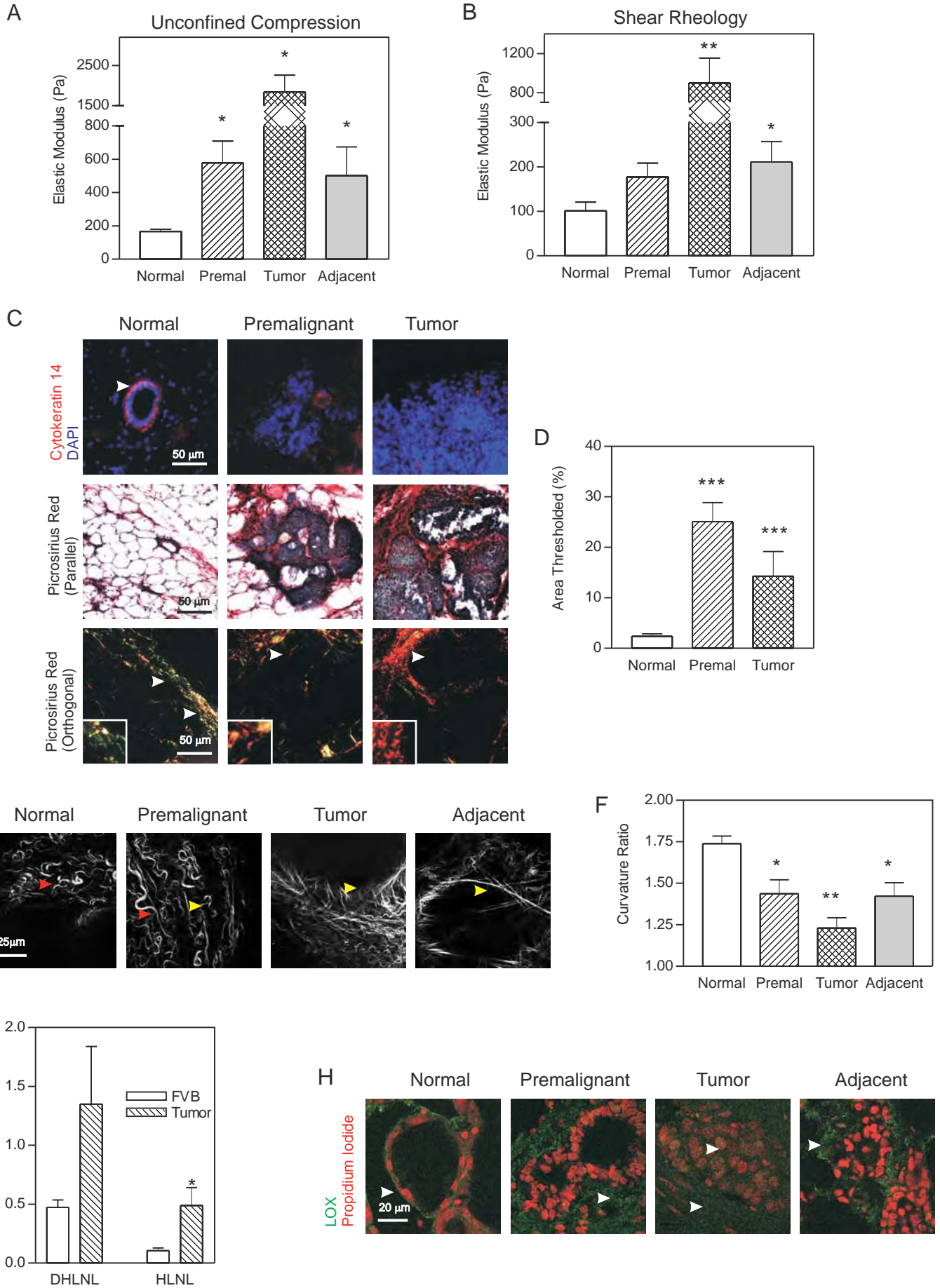


Figure 2

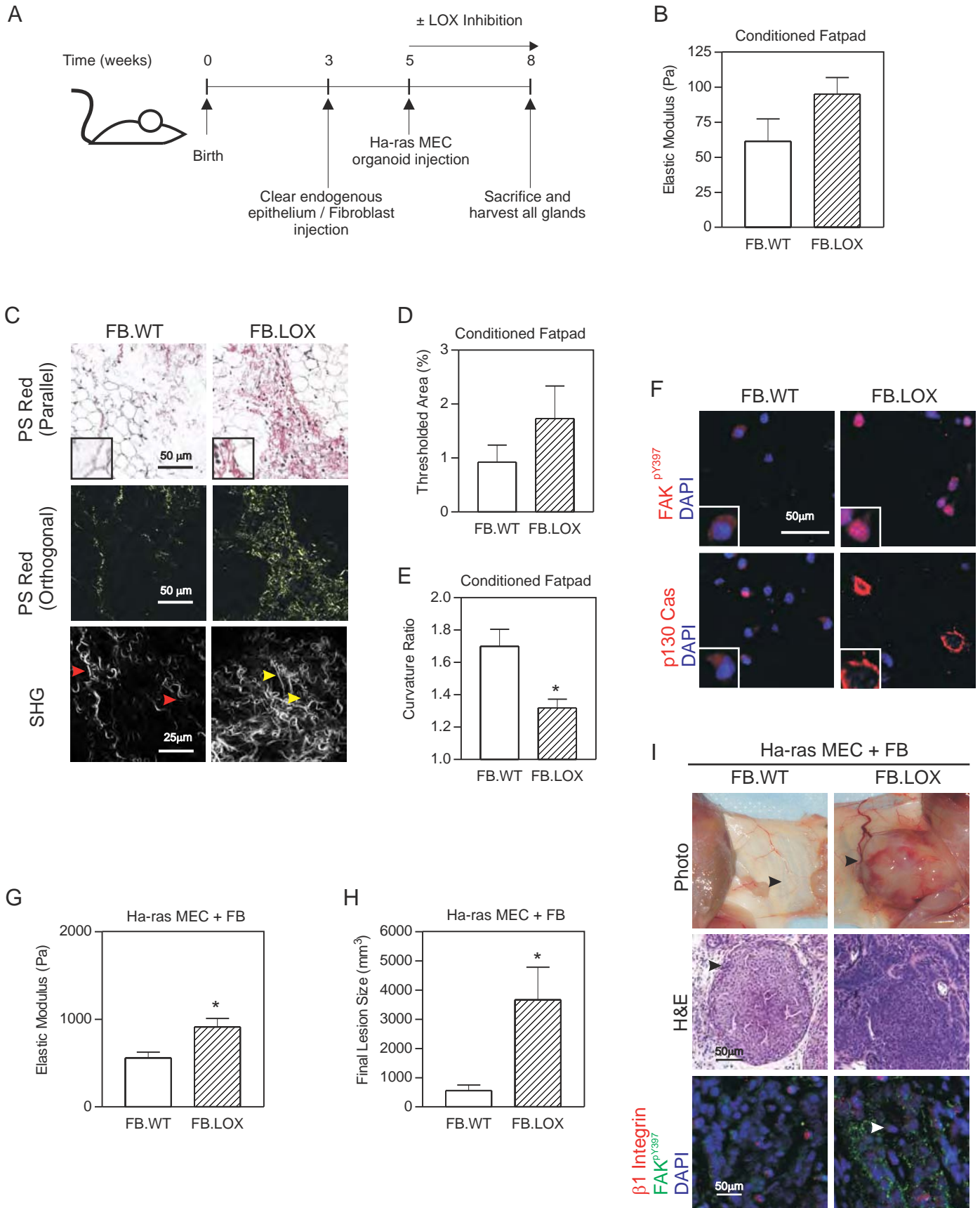


Figure 3

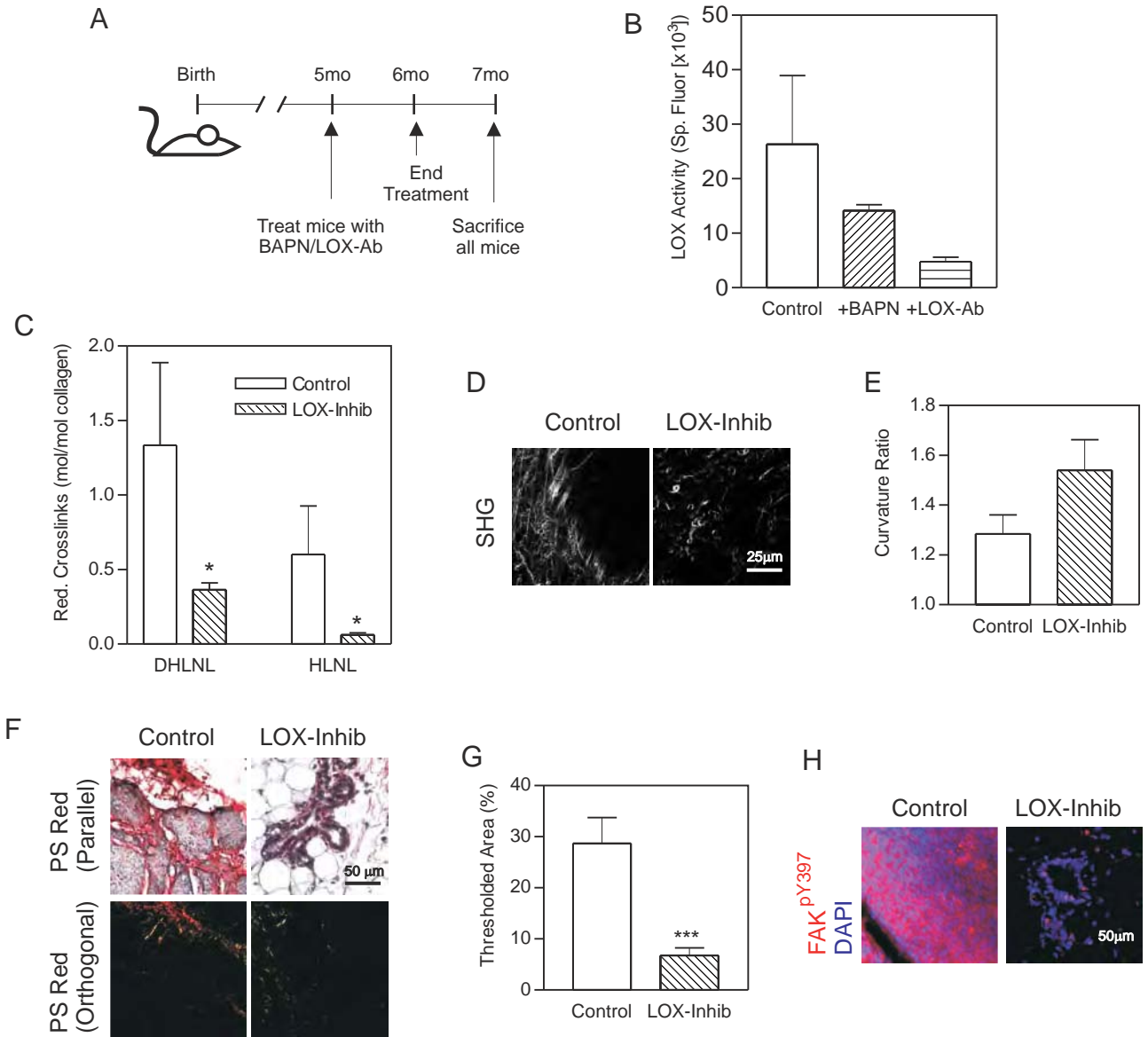


Figure 4

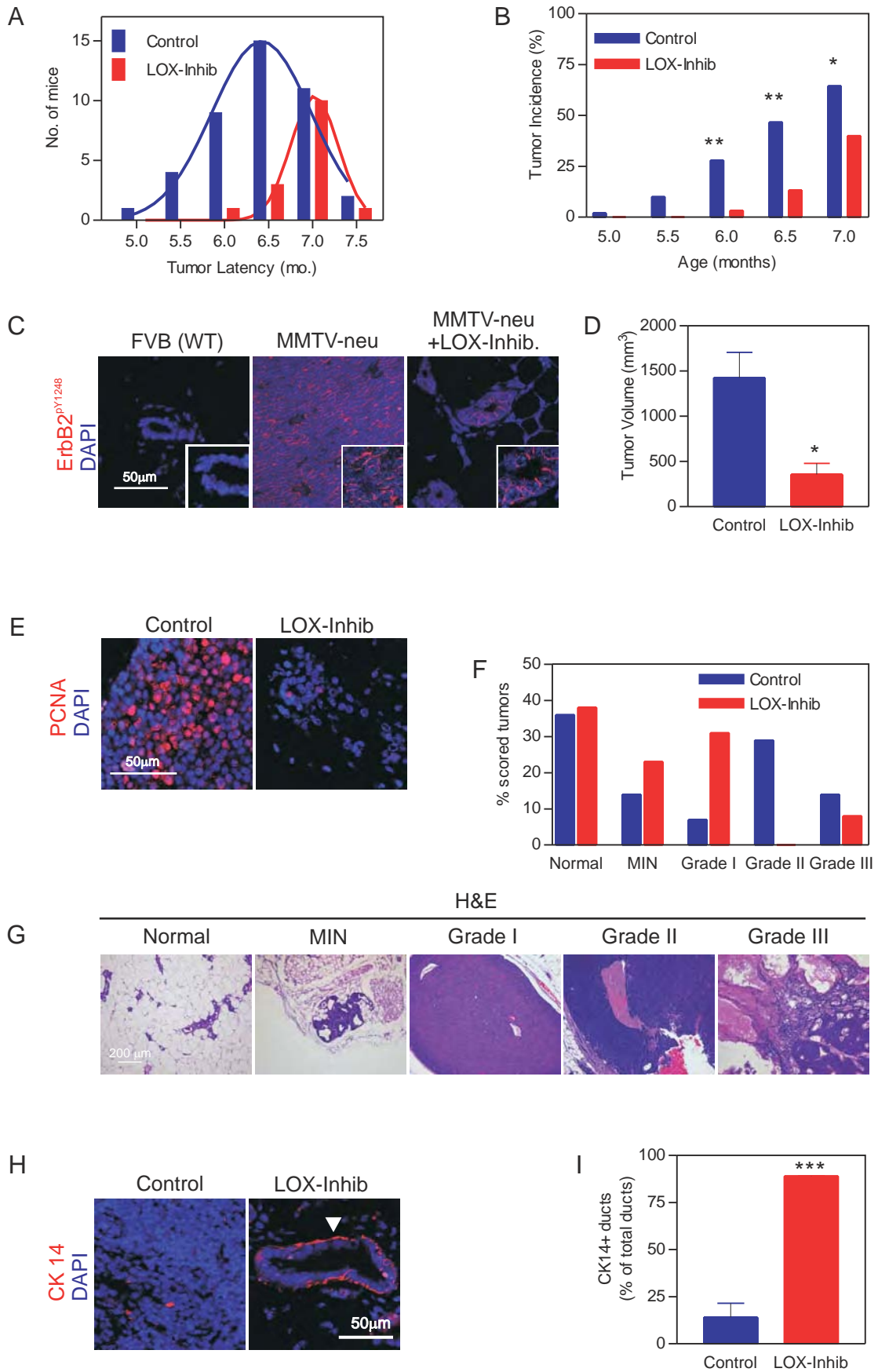


Figure 5

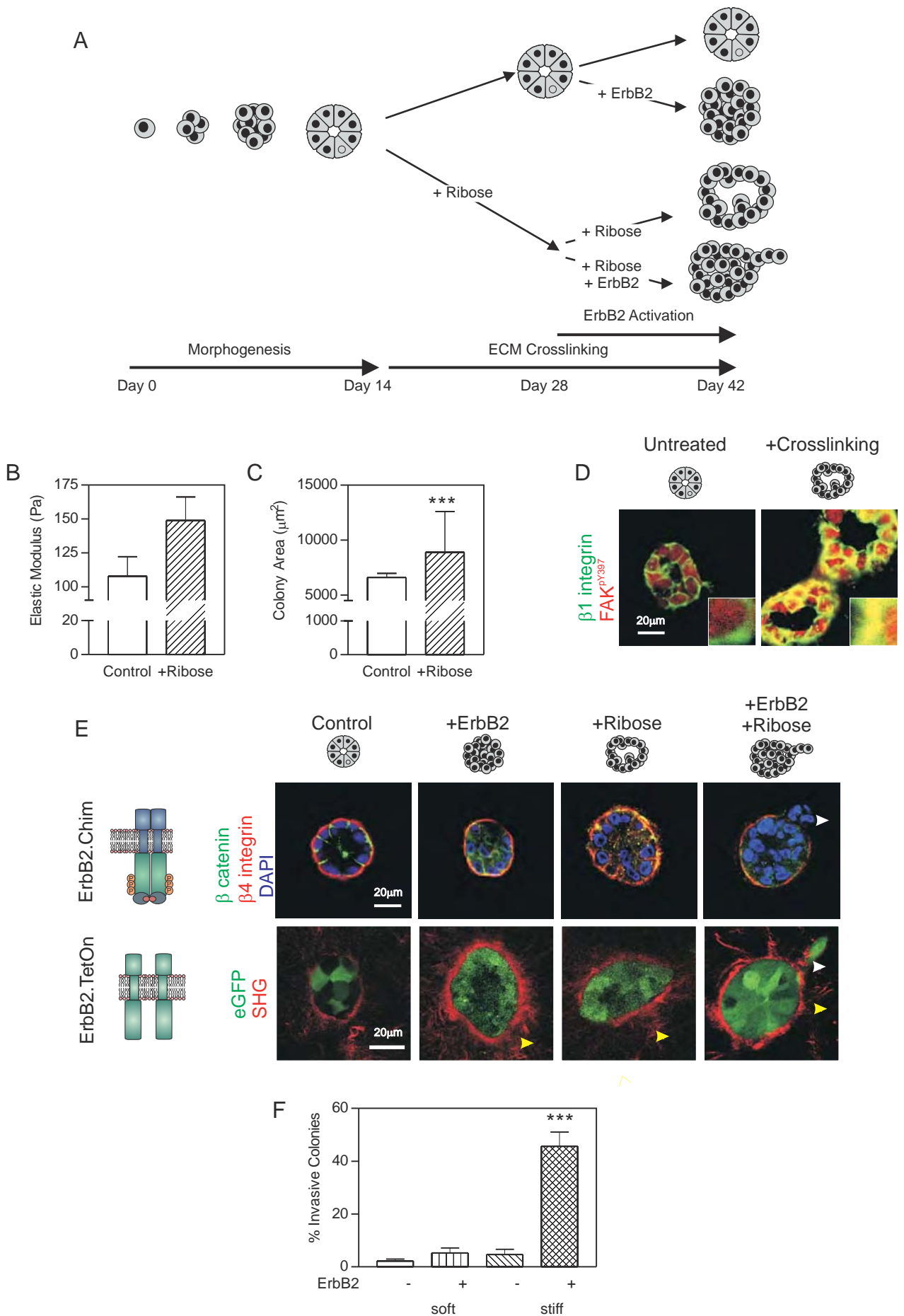


Figure 6

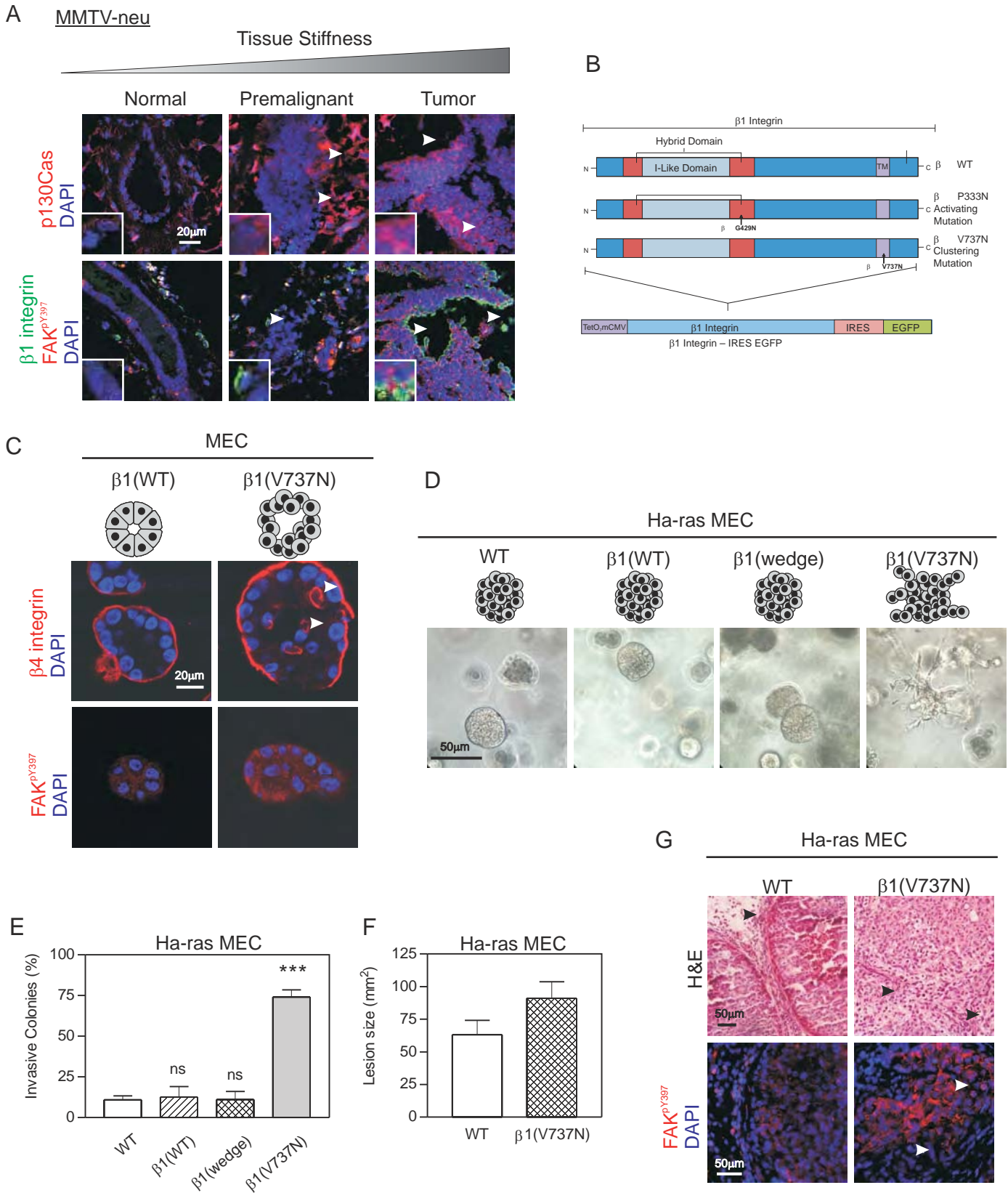
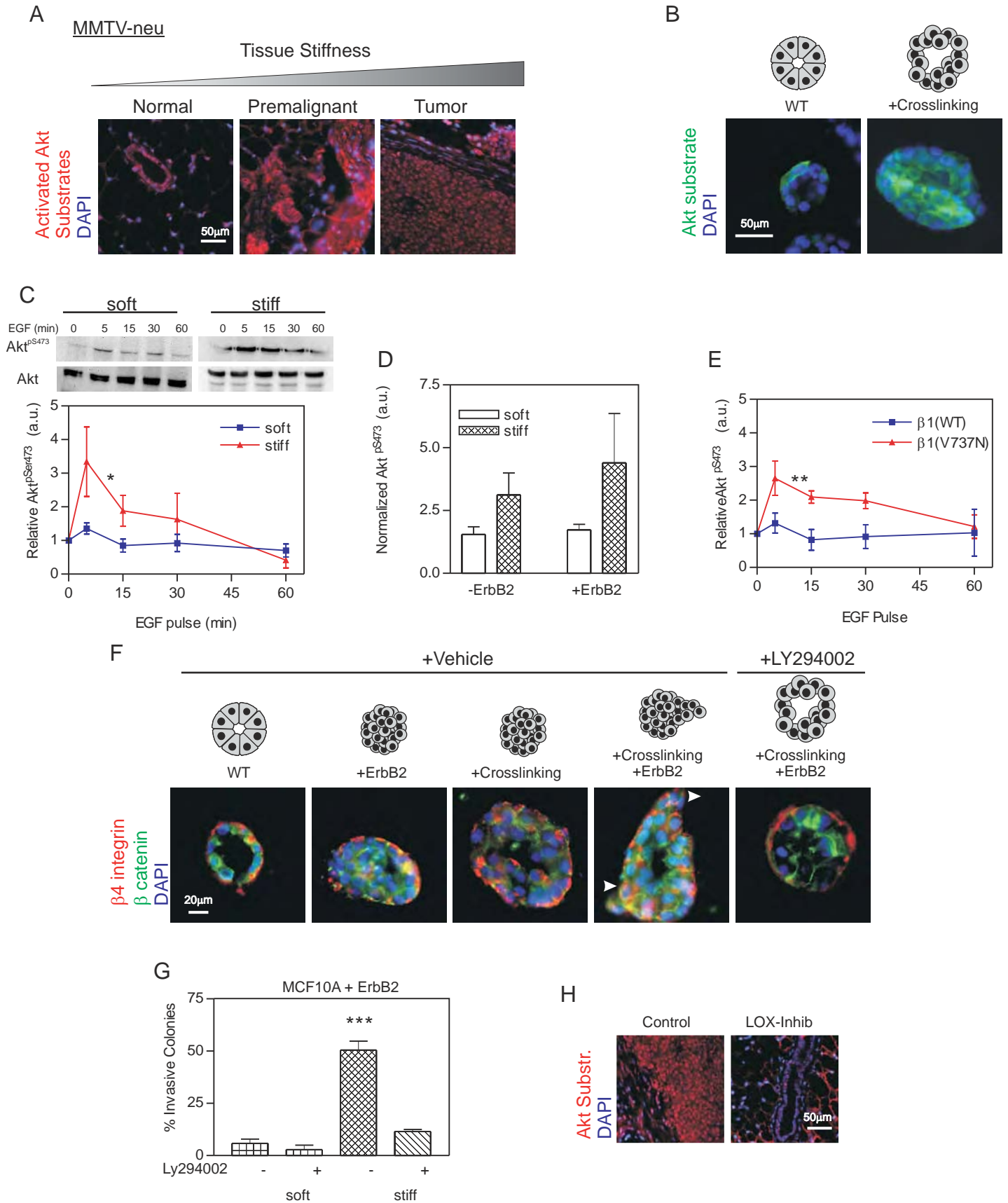


Figure 7



HoxA9 regulates BRCA1 expression to modulate mammary tissue growth and survival

Penney M. Gilbert^{1,2,3}, Janna K. Mouw^{4,5}, Meredith A. Unger⁶, Johnathon N. Lakins^{1,2,4,5}, Mawuse K. Gbegnon^{1,2}, Virginia B. Clemmer⁷, Miriam Benezra⁸, Michael D. Feldman², Nancy J. Boudreau⁴, Alana L. Welm⁹, Kelvin K.C. Tsai¹⁰, Barbara L. Weber⁶ and Valerie M. Weaver^{1,2,4,5,11,12,13}

¹Institute for Medicine and Engineering, University of Pennsylvania, Philadelphia, PA, 19104

²Departments of Pathology and Bioengineering, University of Pennsylvania, Philadelphia, PA, 19104

³Current: Department of Microbiology and Immunology/Baxter Laboratories, Stanford University, Palo Alto, CA 94305

⁴Department of Surgery, University of California San Francisco, San Francisco, CA 94143

⁵Center for Bioengineering and Tissue Regeneration, University of California San Francisco, San Francisco, CA 94143

⁶Abramson Family Cancer Research Institute, University of Pennsylvania, Philadelphia, PA 19104

⁷St. Francis Hospital, Wilmington, DE 19805

⁸Mount Sinai School of Medicine, NY, NY 10029

⁹Department of Oncological Sciences, Huntsman Cancer Institute, University of Utah, Salt Lake City, UT 84112

¹⁰Graduate Institute of Clinical Research, Taipei Medical University, Taiwan

¹¹Department of Anatomy, University of California San Francisco, San Francisco, CA 94143

¹²Department of Bioengineering and Pharmaceutical Sciences, University of California San Francisco, San Francisco, CA 94143

¹³Eli and Edythe Broad Center of Regeneration Medicine and Stem Cell Research, University of California San Francisco, San Francisco, CA 94143

Address correspondence to:

Valerie M. Weaver
University of California San Francisco
Center for Bioengineering and Tissue Regeneration
Department of Surgery
513 Parnassus Avenue, S1364C-0456
San Francisco, CA 94143
Email: Valerie.Weaver@ucsfmedctr.org
Telephone: (415) 476-3826
Fax: (415) 476-3985

Nonstandard abbreviations used:

HOX, homeobox; rBM, reconstituted basement membrane; ER, estrogen receptor; PR, progesterone receptor; MEC, mammary epithelial cell; DNA BM, DNA binding mutant

Abstract

Tumors often express altered levels of homeobox genes although the relevance of this finding is unclear. We found that HoxA9 is expressed in the breast epithelium, its protein and gene expression were significantly reduced in a cohort of ER/PR-negative breast tumors and cancer cell lines and that reduced HoxA9 significantly associates with large and high grade tumors, late stage disease, lymph node involvement, distant metastasis, and reduced patient survival. Knocking down HoxA9 enhanced the growth and survival and disrupted the morphogenesis of nonmalignant breast cells, and restoring HoxA9 expression repressed the growth and survival, and inhibited the malignant behavior of breast cancer cells coincident with increased BRCA1 expression. Consistently, HoxA9 consensus binding sequences were identified in the BRCA1 promoter and molecularly confirmed. Moreover, a wild-type BRCA1 but not a mutant BRCA1 phenocopied the tumor suppressor effect of HoxA9, while reducing BRCA1 levels and/or function promoted the growth and survival of nonmalignant breast cells. Because compromising BRCA1 function also prevented HoxA9 from inhibiting the malignant behavior of breast tumor cells, the data imply that HoxA9 could restrict breast cancer progression by modulating levels of BRCA1. The data suggest homeobox genes may regulate tissue homeostasis by regulating expression of critical tumor suppressors.

Introduction

Developmental regulators which specify embryogenesis and direct tissue morphogenesis are often functionally subverted in adult tissues to promote the growth and invasion of tumors (1, 2). In particular, the homeobox (HOX) gene family of developmental regulators are critical for the establishment of embryonic patterning during embryogenesis and for the maintenance of tissue homeostasis in the adult organism (3). HOX genes are transcription factors that regulate the expression of multiple genes that influence cell growth and viability and that mediate stromal-epithelial interactions to drive tissue-specific differentiation (2). Not surprisingly, HOX expression is frequently perturbed in tumors (3) where they can act as oncogenes by promoting cell growth and invasion (4, 5) or as tumor suppressors because they can alter cell survival and morphogenesis (6-9). HOX genes are especially important in the mammary gland which undergoes repeated rounds of developmental cycles in the adult organism (10, 11). In the breast, HOX genes have been implicated in the control of embryonic development, branching morphogenesis and hormonally-controlled differentiation (10, 12), and HOX genes are frequently lost or over-expressed in breast tumors (12). Nevertheless, the molecular mechanisms whereby HOX genes regulate mammary development and how they might be modified to drive breast tumor progression remain poorly defined.

Women with hereditary mutations in BRCA1 are predisposed to develop breast and ovarian cancers (13). BRCA1 can maintain genome integrity by functioning as an ubiquitin ligase (14, 15) and can modulate the cellular stress response by acting as a transcriptional regulator (16, 17). In addition, BRCA1 has a well established role in the regulation of mammary epithelial cell (MEC) proliferation and survival (18-20). Consistently, loss of BRCA1 expression and/or function is associated with increased breast tumor aggression, enhanced cancer metastasis, and a poor clinical prognosis (21). There is also a clinical association between familial BRCA1 tumors and an aggressive basal-like breast cancer phenotype (22). Interestingly, many sporadic breast cancers show decreased BRCA1 expression and display a 'BRCA1-like' phenotype despite the absence of genetic deletions, methylation or

haploinsufficiency (23, 24). The molecular mechanisms leading to reduced BRCA1 expression and/or function in this group of sporadic breast cancers remain unclear (25, 26). Studies designed to elucidate molecular regulators of BRCA1 have identified negative regulators which in some cases are over-expressed during breast tumorigenesis (27-29). Conversely, the identification of transcription factors which positively and directly regulate BRCA1 expression and whose expression might be concurrently lost during malignant transformation has proven elusive.

BRCA1 expression and MEC proliferation are functionally linked indicating BRCA1 likely regulates mammary gland development and homeostasis and inhibits tumorigenesis by restricting MEC growth (30-32). Intriguingly, BRCA1 also modulates mammary gland differentiation, and BRCA1 expression is repressed following basement membrane (rBM)-induced acinar morphogenesis in culture (20, 33, 34). BRCA1 expression additionally increases during embryonic mammary gland development and BRCA1 expression spikes prior to acquisition of acini polarity and pregnancy-associated lactation (28, 35, 36). These observations suggest that BRCA1 expression might also be functionally-linked to tissue differentiation. If true, BRCA1 may restrict cell proliferation and regulate genome integrity by cooperating with pathways that regulate tissue differentiation, including molecules which promote tissue homeostasis and the establishment of tissue architecture.

Through the use of a small number of paired "normal" and adjacent tumor tissues, we identified HoxA9 as a gene whose levels were reduced primarily in estrogen receptor (ER) and progesterone receptor (PR) negative breast tumors and whose re-expression could promote breast morphogenesis and restrict tumor behavior. HoxA9 is important in skeletal (37), urogenital tract (38), kidney (39), and mammary gland development (40), and HoxA9 expression can be regulated by microRNAs that have been implicated in tissue differentiation (41). Paradoxically, although HoxA9 has been characterized as a leukemic oncogene (4) and angiogenesis promoter (42), the functional data we present here demonstrate that HoxA9 restricts the proliferation and survival of mammary epithelial cells and inhibits the malignant phenotype of breast cancer cells in three dimensional rBM cultures and *in vivo*. Moreover,

bioinformatics analysis of multiple independent gene expression studies linked the loss of HoxA9 to aggressive breast disease so that low HoxA9 levels significantly predicts increased risk of metastasis and death or disease relapse in ER-negative breast tumors. Our findings also indicate that HoxA9 represses the malignant behavior of breast cells by directly modulating expression of the tumor suppressor gene BRCA1, thereby offering an alternate explanation for why BRCA1 expression is so frequently lost in sporadic human breast tumors even in the absence of genetic modifications. Indeed, HoxA9 is frequently silenced in human breast tumors by gene methylation (43), and we could link HoxA9 levels to BRCA1, and BRCA1 to MEC growth and survival and tissue morphogenesis. This suggests that HOX genes could regulate tissue development and restrict tumorigenesis by modulating the levels and/or activity of critical tumor suppressor genes functionally-linked to growth and survival; processes which are also critical to the establishment and maintenance of differentiated tissues.

Results

Breast malignancy is associated with reduced HoxA9 expression

Expression profiling is a useful tool to identify gene expression signatures associated with patient prognosis (44, 45), treatment responsiveness (46-48), and risk of tumor metastasis (44, 49-51). Expression profiling has also been used to identify tissue-specific tumor suppressor genes (52, 53). However, the application of this technique to identify tumor suppressors in the breast has been less successful, possibly because sporadic mammary tumors likely arise through input from multiple cooperating, yet poorly penetrating genetic, epigenetic and microenvironmental factors (54-56). To increase the probability of identifying a low abundance breast tumor suppressor gene using expression profiling, we selected five paired sets of tumor tissue with similar aggressive phenotypes. Our objective was to discover genes lost in the tumor tissues when compared to their patient-matched “normal” tissue. Because of the compelling link between developmental regulators and tumor aggression, we focused on identifying mis-expressed developmental regulators (1, 57-60). Moreover, given the paucity of information on basal-like tumors and their recognized aggressive nature in younger patients, we chose samples from individuals whose ages ranged from 44 to 54 years and whose tumors were at least 1.5 cm in diameter (Supplemental Table 1). We also choose tumors that were ER/PR negative, and were of uniformly high nuclear and histological grade.

Rosetta Resolver 2D agglomerative clustering of genes significantly differentially-expressed between the normal adjacent and invasive tumor tissue identified 40 transcripts whose expression was elevated in the tumors and 115 transcripts with reduced gene expression ($p \leq 0.01$; Figure 1a and Supplemental Table 2). Of the genes with reduced expression were two developmental HOX genes HoxA4 (mean 3.1 fold reduction) and HoxA9 (mean 4.4 fold reduction). Because findings from the *hoxa9-hoxb9-hoxd9* triple knock-out mouse suggest that HoxA9 regulates mammary gland differentiation (40), leukemia studies have implicated HoxA9 in oncogenesis (4), and HoxA9 was

shown to be silenced via methylation in a small cohort of human breast tumors (43), we selected HoxA9 for further study.

Quantitative real-time PCR (Q-RT-PCR) verified that HoxA9 mRNA levels were reduced in the majority of the normal to tumor matched clinical samples and demonstrated that HoxA9 levels were significantly reduced (~75%) in an expanded clinical cohort of invasive, predominantly ER/PR negative, primary ductal breast carcinomas (n=38) when compared to levels of transcript expressed in normal human breast (n=8; Figure 1b). *In situ* and immunohistochemical analysis confirmed that both HoxA9 mRNA and protein were expressed in the epithelium of the normal breast and that levels were greatly reduced in mammary tumors (Figures 1c, 1d). To explore possible relationships between HoxA9 levels and clinical features of breast cancer, we utilized the Oncomine Cancer Profiling Database (<http://www.oncomine.org>) to survey a large number of breast cancers from multiple independent studies. We found that low HoxA9 expression correlated with features of aggressive disease, such as large or high grade tumors, late stage disease, lymph node involvement, distant metastasis, and reduced survival (Supplemental Table 3). This approach also validated our original observation that HoxA9 levels were reduced in breast cancers when compared to normal breast tissue. We additionally observed this same result when we analyzed data from two additional independent clinical array studies (Supplemental Table 3).

To definitively establish an association between HoxA9 levels and clinical outcome of breast cancer patients, we thereafter analyzed gene expression data from two independent studies. First, we assessed the relationship between HoxA9 mRNA levels and relapse free survival in a cohort of 227 patients with available clinical follow-up information (61). We found that the patients whose tumors expressed the lowest HoxA9 levels (lowest quartile) experienced significantly reduced relapse free survival (p=0.025; Figure 1e). We then asked whether low HoxA9 levels were an early marker of eventual distant metastasis, using an independent dataset of 295 patients with early breast cancer, all of whom had no evidence of distant metastasis at the time of tumor collection (Supplemental Table 4) (45).

Consistently, the group of patients whose primary tumors expressed HoxA9 in lowest quartile developed significantly more distant metastasis as a first adverse event, when compared to all other patients in the study ($p=0.02$; Figure 1f). A multivariate Cox proportional-hazards analysis revealed that HoxA9 predicted death or disease relapse independent of standard clinico-pathological variables of breast cancers in ER-negative tumors (Table 1). In contrast, the correlation between HoxA9 expression levels and clinical outcomes was less prominent in ER-positive tumors (Supplemental Table 5). Together, these data strongly suggest that HoxA9 is down regulated during the development of particularly aggressive breast cancers that are predominantly ER negative, and that diminution of HoxA9 levels correlates with aggressive disease.

HoxA9 modulates the growth and survival of breast cancer cells

To explore the functional relevance of HoxA9 loss to breast cancer, we examined the effect of HoxA9 re-expression on tumor cell growth and survival. We observed that HoxA9 mRNA was abundant in the MCF10A nonmalignant human mammary epithelial cell (MEC) line (Figure 2a, Supplemental Figure S1) and that its expression was reduced in the non-invasive, estrogen receptor positive breast cancer cell lines T47-D and MCF-7 (Supplemental Figure S1), and was virtually non-detectable in the estrogen receptor negative, basal-like breast cancer cell lines MDA-MB-231 (MDA-231) and HMT-3522 T4-2 (T4-2) (Figure 2a, Supplemental Figure S1) (62). We therefore created multiple pooled clonal populations of MDA-231 and T4-2 breast cancer cells expressing either HA- or FLAG-tagged wild-type HoxA9. Transgene expression was confirmed at the mRNA and protein level (Figure 2b, Supplemental Figures S2, S2') and the expressed protein was found to localize in both the nucleus and cytoplasm of the infected breast cancer cell lines (Figures 2b' and 2b'') similar to its localization in primary breast tissue (Figure 1d). For easy visualization and manipulation the HoxA9 transgene was expressed bicistronically with enhanced Green-Fluorescent Protein (EGFP) under the control of a tetracycline-repressible promoter (Supplemental Figure S3).

Although HoxA9 re-expression had only a marginal effect on breast tumor cell growth when the cells were propagated on tissue culture plastic (Supplemental Figure S4), we noted that upon embedment within rBM, both MDA-231 and T4-2 breast cancer cells re-expressing HoxA9 grew much slower, as quantified by significantly reduced Ki-67 levels (Figure 2c) and both cell lines had a decreased colony size at day 10 (Figure 2d). In fact, re-expression of HoxA9 reverted the malignant phenotype of both of the tumor cell lines towards that of a smaller, more uniform and less invasive and more cohesive nonmalignant colony, similar to that reported previously when epidermal growth factor receptor signaling is inhibited in these cell lines (Figure 2e, Supplemental Figure S7) (63, 64). HoxA9 re-expression had a particularly pronounced effect on the morphology of the T4-2 rBM colonies such that the HoxA9 re-expressing tumor colonies re-assembled adherens junctions, as indicated by a re-localization of β -catenin to sites of cell-cell interaction, and acquired apical-basal polarity, as revealed by basal re-localization of $(\alpha 6)\beta 4$ integrin and deposition of an endogenous laminin-5 BM around the periphery of the acini (Figure 2e, Supplemental Figure S5). We also noted that HoxA9 re-expression exerted a substantial effect on cell viability, as revealed by the appearance of lumens within the acini (Figures 2e, 2f). Soft agar assays confirmed that HoxA9 re-expression, but not HoxA10, another member of the HoxA cluster (65), influenced tumor cell survival as shown by a significant inhibition of anchorage-independent growth and survival in both the HMT-3522 T4-2 and MDA-MB-231 tumor cells (Figures 2g, 2g', Supplemental Figures S6, S7).

To address the functional relevance of our cell culture observations to breast cancer *in vivo*, we conducted xenograft studies using BalbC nu/nu mice. T4-2 breast cancer cells re-expressing HoxA9 (to levels comparable to that detected in the non-malignant HMT-3522 S-1 MECs; data not shown) failed to grow and survive when injected into the rear flanks of the BalbC nu/nu mice. Thus, while vector control T4-2 MECs grew continuously and rapidly to form large, highly angiogenic tumors that were densely populated with actively dividing cancer cells (10/10 lesions), the lesions formed by the T4-2 MECs expressing HoxA9 either completely regressed within 56 days (8/10 lesions), or were highly cystic,

avascular and fibrotic (2/10 lesions) (Figures 2h, 2h'). Taken together, the data indicate that HoxA9 restricts tumorigenic behavior of breast cancer cells by inhibiting cell growth and survival and by promoting tissue morphogenesis.

HoxA9 regulates BRCA1 expression

Hox genes are transcriptional regulators that exert their effects on cell and tissue phenotype indirectly by modulating gene expression (66). To identify putative HoxA9 targets critical for breast tumor suppression, we defined the global transcriptional profile of MDA-231 breast cancer cells before and after tetracycline-dependent HoxA9 expression (Supplemental Table 6). Amongst the genes up regulated following HoxA9 re-expression, we observed that the level of the breast cancer susceptibility gene BRCA1 was dramatically increased and confirmed this by Q-RT-PCR (Figure 3a). Because BRCA1 is a tumor suppressor gene that regulates MEC growth and survival and can modulate rBM morphogenesis, we chose to explore the functional relationship between HoxA9 and BRCA1 regulation (20, 36, 67). Immunoblot analysis demonstrated that HoxA9 re-expression consistently elevated BRCA1 protein levels in MDA-231 and T4-2 breast cancer cells (Figures 3b). These results suggest that HoxA9 could repress breast tumor behavior by regulating expression of the tumor suppressor gene BRCA1 (68).

BRCA1 can be induced by multiple stimuli that might each be independently regulated by HoxA9 (28). While a number of negative regulators of BRCA1 transcription have been reported, identification of factors that directly up regulate BRCA1 expression has proven elusive (27, 69-71). Because HoxA9 is a transcription factor, we reasoned there was a strong probability HoxA9 was regulating BRCA1 levels by directly inducing BRCA1 gene expression. Computer-assisted analysis confirmed there were indeed several putative HOX consensus binding sites in the BRCA1 promoter. To definitively test whether HoxA9 could directly modulate BRCA1 expression, we conducted BRCA1 promoter chromatin immunoprecipitation (ChIP) studies using HA-tagged exogenously expressed HoxA9 as the bait. Whereas acetyl H3 histone easily and repeatedly co-precipitated the β -globin

promoter from both vector control and HoxA9 expressing cell lines, we could only amplify BRCA1 promoter product above background from the breast tumor cells re-expressing the exogenous HA-tagged HoxA9 (Figures 3c, 3c'). Reporter assays using regions of the BRCA1 5' promoter region containing HoxA9 consensus binding sites (72) confirmed basal luciferase activity could be significantly enhanced following co-transfection with increasing amounts of a wild-type HoxA9 and not a HoxA9 expression plasmid containing an N255T mutation (DNA BM) in the conserved DNA binding domain (Figures 3d, 3e). Furthermore, HoxA9-dependent BRCA1 reporter induction could be significantly enhanced by addition of the HOX gene cofactor PBX1 (Figure 3f) (73). In contrast, no increase in reporter activity could be induced by HoxA9 co-transfection with BRCA1 luciferase promoter constructs lacking residues -223 to +44, wherein reside putative HoxA9 consensus binding sites (Genbank U37574; Figure 3g). Interestingly, site directed mutagenesis of individual HoxA9 consensus binding sites did not significantly compromise BRCA1 promoter activity, suggesting cooperative release of tandem HOX consensus binding sites might be necessary to ablate HoxA9-dependent control of BRCA1 gene expression (Supplemental Figure S9). These observations are consistent with previous reports of promoter site cooperation and redundancy in other HOX regulated genes (74-76). These findings indicate that DNA binding of HoxA9 could directly regulate BRCA1 expression in breast cells.

HoxA9 regulates non-malignant MEC growth by modulating BRCA1 expression

To further implicate HoxA9 as a tumor suppressor, we identified two independent shRNA lentiviral clones which could substantially reduce HoxA9 mRNA (Supplemental Figure S10) and protein levels in nonmalignant MCF-10A MECs (Figure 4a). Consistent with the notion that HoxA9 inhibits breast tumor progression by regulating MEC growth and survival through BRCA1 modulation, nonmalignant MECs expressing a HoxA9 shRNA were unable to induce BRCA1 transcription in response to exogenous stress (Supplemental Figure S11). In addition, MCF-10A MECs with reduced HoxA9 levels failed to

growth-arrest in response to rBM and instead formed continuously growing, non-polarized colonies that lacked adherens junctions and detectable lumens (Figures 4b, 4c, 4d).

To determine if similar to HoxA9 loss, reducing BRCA1 in non-transformed MECs could promote their malignant behavior, we identified two shRNA clones to knock down BRCA1 levels in the nonmalignant MCF-10A MECs (Figure 4a'). Consistent with previous reports implicating BRCA1 in breast tissue differentiation (20, 31, 36, 67), reducing BRCA1 in the non-malignant MECs increased their proliferation (inferred by elevated colony size; Figures 4b', 4d'), enhanced their survival as revealed by luminal filling in the rBM colonies (Figures 4c', 4d') and disrupted their rBM-dependent tissue morphogenesis (evidenced by loss of cell-cell localized β -catenin; Figure 4d'). Likewise, compromising BRCA1 function in the nonmalignant MCF-10A MECs by expressing the BRCA1 Δ exon11b mutant (Supplemental Figure S12) promoted growth and survival and perturbed rBM-dependent tissue morphogenesis (Figures 4e, 4e', 4f). These observations illustrate the importance of HoxA9 and BRCA1 expression to MEC growth, survival and rBM-induced tissue morphogenesis.

HoxA9 regulates BRCA1 to repress the malignant behavior of mammary epithelial cells

We next manipulated the expression and function of BRCA1 and HoxA9 in breast cancer cells and non-malignant MECs to directly explore the relevance of HoxA9-dependent BRCA1 regulation. Consistent with a functional link between HoxA9 and BRCA1, we determined that increasing the levels of wild-type BRCA1 in the breast tumor cells reduced their rBM-dependent growth such that they assembled colonies that were similar in size and morphology to those formed by tumors re-expressing HoxA9 (compare in Figures 5a, 5b, 5d). In addition, rBM-dependent tumor colonies expressing elevated levels of wild type BRCA1 had cell-cell localized β -catenin (Figure 5a) and formed lumens (Figure 5d), suggesting that analogous to HoxA9, BRCA1 could also revert the malignant phenotype of breast cells towards the normal polarized, growth-arrested acini structure assembled by nonmalignant MECs in a rBM assay (Figures 4d and 4e). Similarly, ectopic expression of wild type BRCA1 reduced the

anchorage-independent growth and survival of breast cancer cells (Figure 5c). These data show how BRCA1 can phenocopy the tumor suppressor effects of HoxA9 and can repress the growth and survival of breast tumor cells in a rBM assay.

To more directly explore the functional relationship between HoxA9 and BRCA1 expression in MEC behavior, we compromised BRCA1 function in the T4-2 tumor cells re-expressing HoxA9 through co-expression of the Δ exon 11b BRCA1 mutant and then assayed for effects on rBM growth, survival and morphology. Disrupting BRCA1 function antagonized the ability of HoxA9 to repress the malignant behavior of the T4-2 tumor cells (Figure 5a'). Thus, tumor cells simultaneously expressing HoxA9 and the Δ exon 11b BRCA1 mutant failed to phenotypically revert when grown within rBM, and instead formed continuously growing, invasive and non-polarized colonies that lacked cell-cell localized β -catenin and a lumen (Figures 5a', 5b', 5d'). These studies demonstrated that the ability of HoxA9 to repress the malignant behavior of MECs was functionally-dependent upon BRCA1.

To address the *in vivo* relevance of a functional link between HoxA9 and BRCA1, we conducted xenograft studies using BalbC nu/nu mice injected with human breast cancer cells with and without HoxA9 and a functional BRCA1 and assessed tumor growth (as indicated by lesion size). Re-expression of HoxA9 in T4-2 breast cancer cells significantly reduced the rate of lesion growth compared to T4-2 vector controls (Figures 5e, 5e'). In contrast, the HoxA9 expressing T4-2 MECs in which BRCA1 function was simultaneously compromised, through co-expression of the Δ exon11b BRCA1 mutant, grew robustly and at a rate that was comparable to that observed by the vector control T4-2 MECs. T4-2 HoxA9 tumor cells in which BRCA1 function was compromised achieved lesions that on average were comparable in size and morphology to those formed by the wild-type tumors (28 days; Figures 5e, 5e'). These data demonstrate that HoxA9 not only restricts the growth and survival of human breast cancer cells by regulating BRCA1 expression in culture but also does so *in vivo*.

Clinical correlation between HoxA9 and BRCA1 expression

To address the clinical relevance of a functional link between HoxA9 and BRCA1, we examined mRNA levels of HoxA9 and BRCA1 in a panel of clinically diverse human breast cancer and normal tissue (n=50). We noted that the epithelium of the normal breast co-expresses appreciable levels of both HoxA9 and BRCA1 protein (Figure 6a). More importantly, Q-RT-PCR data showed that reduced levels of HoxA9 in human breast tumors correlated significantly with BRCA1 expression (Figure 6b). These clinical data are consistent with our experimental observations and imply that HoxA9 could modulate BRCA1 expression and/or function within the breast epithelium. (25, 28)

Discussion

To identify developmental regulators mis-expressed during malignant transformation of the breast, we used global expression profiling of micro-dissected breast tumors and their adjacent normal tissue. We identified the homeobox gene HoxA9, which has previously been implicated in mammary development (12, 40), as a gene whose levels were significantly down regulated in the majority of the breast tumors examined. We confirmed the microarray observations using Q-RT-PCR, *in situ* hybridization and immunohistochemistry, and showed that HoxA9 is highly expressed in the luminal epithelium of the normal breast and that its expression is frequently decreased in a high proportion of predominantly ER negative invasive human breast tumors and breast cancer cell lines (Figure 1b and Supplemental Figure S1). Bioinformatics analysis confirmed these findings and also indicated that HoxA9 loss significantly correlates with features of aggressive disease including large and high grade tumors, late stage disease, lymph node involvement, distant metastasis, and reduced patient survival (Figures 1e, 1f, Table 1 and Supplemental Tables 3-5). Using two ER/PR/ErbB2 negative “basal-like” breast cancer cell lines, we then showed that re-expressing HoxA9, but not another member of the HoxA cluster HoxA10, inhibited tumor cell growth and survival and promoted acini morphogenesis in culture and restricted tumorigenesis *in vivo* and, furthermore, that reducing levels of HoxA9 in nonmalignant MECs enhanced growth and survival and perturbed acini morphogenesis (Figures 2, 4). Although investigators have previously reported that HoxA9 is methylated and its expression reduced in breast, lung and ovarian cancers (43, 77, 78), to our knowledge this is the first study to assess the clinical relationship of HoxA9 loss to solid tumors, the first to analyze the relevance of HoxA9 to the malignant behavior of MECs in culture and *in vivo*, and the first to identify a molecular mechanism for these effects. In this respect, we found that HoxA9 restricts the malignant behavior of MECs by directly modulating BRCA1, implying that HoxA9 reduces risk to malignancy by controlling levels of an established mammary gland tumor suppressor gene. These findings are consistent with the notion that developmental regulators such as the HOX family of transcription factors influence adult tissue

homeostasis by regulating the expression and/or activity of key tumor suppressor genes that regulate cell growth and survival and morphogenesis (12).

Homeobox genes regulate embryonic development and tissue patterning and their expression is frequently perturbed and often aberrantly increased in tumors (2, 3, 12, 65, 79). Until recently, the prevailing dogma has been that inappropriate expression of homeobox genes promotes tumor progression. Consistently, the homeobox genes that are highly expressed during early embryogenesis and that promote cell proliferation and survival and that induce migration are those that are most often over expressed in transformed cells and tissues (6, 8, 80, 81). These are the homeobox genes that have been implicated in altered growth receptor signaling, deregulated cell cycle control and the elevated growth and apoptosis resistance of cancer cells, and that regulate tumor invasion and metastasis and promote angiogenesis (42, 80, 82-86). For instance, the homeobox gene *Six1* is highly expressed during early mammary gland development where it drives epithelial cell proliferation by modulating levels of the cell cycle gene *cyclin A1* (87). Although *Six1* levels are down regulated and barely detectable in the differentiated adult mammary gland, *Six1* is frequently over expressed in aggressive breast tumors where it promotes cell growth and survival, enhances genomic instability and promotes tumor metastasis (88, 89). Similarly, enforced expression of the early embryonic homeobox gene *Msx1*, which is also often elevated in tumors, promotes the proliferation of undifferentiated stem cells, blocks the terminal differentiation of myoblasts and down regulates expression of the myogenic differentiation factor *MyoD1* to induce their malignant transformation (90-93).

It is now appreciated that homeobox genes of the ANT-C/BX-C type that control rostral-caudal patterning during embryogenesis and that are abundantly expressed in differentiated tissues can repress malignancy and may function as “tumor modulators” (9, 79, 94-97). Data that support this concept exist, although, unfortunately, many findings linking homeobox gene loss with tumorigenesis are largely circumstantial (43, 77, 78, 90, 98). At present, few methodical studies exist clarifying molecular mechanisms whereby reduced homeobox levels could restrict tumor progression and/or metastasis (9,

97). In this article, we present evidence that one of the posteriorly-expressed homeobox genes HoxA9 is both necessary and sufficient for normal MEC growth and survival and acini morphogenesis, a finding that is consistent with a previous article implicating HoxA9 in mammary morphogenesis (Figures 2, 4) (40). Our findings clarify these earlier observations and indicate that HoxA9 inhibits cell growth and survival and promotes morphogenesis in normal and transformed MECs by directly regulating expression of the tumor suppressor gene BRCA1 (Figures 3, 5). Our observations are consistent with and extend prior studies showing that PITX1, which is frequently down regulated in prostate, bladder and colon cancers (6), could function as a tumor suppressor by inhibiting oncogenic Ras signaling, and data indicating that HoxA5, which is lost in greater than sixty percent of mammary tumors and breast cancer cell lines, may restrict breast cancer by regulating levels of the tumor suppressor p53 to alter inappropriate MEC survival (8, 81). Distinct from these reports, we could show that HoxA9 not only modulates BRCA1 levels but that it also directly binds to and regulates BRCA1 transcription, and that HoxA9-dependent BRCA1 induction is markedly enhanced during tissue remodeling and following exposure of breast cells to an exogenous stress, consistent with a role for BRCA1 in cell cycle regulation and the DNA damage response (99-101). Intriguingly, HoxC8 was shown to bind directly to and regulate the mammalian homologue of lethal giant larvae tumor suppressor gene, however to date no functional data exist to clarify the relevance of this relationship (7). In the present studies, we not only showed that HoxA9 directly regulates BRCA1 transcription but we demonstrated that HoxA9-dependent BRCA1 expression is critical for the growth and survival and morphogenesis activity of HoxA9 in culture and for its tumor suppressor-like activity *in vivo* (Figures 4 and 5), and we provided additional evidence that this relationship likely has clinical relevance (Figures 1 and 6). These findings emphasize the importance of examining the role of homeobox family members as critical regulators of normal tissue differentiation and homeostasis and illustrate the potential permissive role of HoxA9 loss in tumor progression and as a regulator of treatment responsiveness.

In contrast to our observation that HoxA9 restricts the growth and survival and malignant behavior of breast epithelial cells, paradoxically, it is well known that HoxA9 plays an essential role in normal myeloid lineage development because it promotes expansion of the stem cell pool and inhibits differentiation (102). Consistently, increased expression or activation of HoxA9 in myeloid stem cells is causally-linked to acute myeloid leukemia (103) and enforced expression of HoxA9 in myeloid cells, due to chromosome translocation or over-expression of its regulator MLL, drives transformation (4). Furthermore, elevated HoxA9 expression induces angiogenesis by regulating growth and migration and invasion of endothelial cells (42). Interestingly, neither myeloid cells nor human endothelial cells ectopically over-expressing HoxA9 up-regulate BRCA1 transcript levels, thereby offering one likely explanation for the strikingly different phenotypic consequences of HoxA9 expression between MECs versus lymphocytes and endothelial cells (104, 105). This observation is consistent with previous studies indicating that homeobox target genes are cell and tissue specific. The data also accord with results showing that the expression profile and gene targets of each HOX factor depends upon the complement of co-factors present in each cell and the extracellular microenvironment the cell resides within (106). Thus, while HoxA5 can induce p53 expression in MECs, sustained HoxA5 failed to modulate p53 in endothelial cells and instead induced Thrombospondin-2 (8, 107). Such findings serve to illustrate the urgency of conducting comparative functional studies of homeobox gene regulation in different tissues and stress the relevance of tissue context as a key regulator of cellular behavior. The work also underscores the importance of considering tissue-specific gene regulation in order to understand cancer pathogenesis as well as to identify tissue-specific treatments.

BRCA1 is either lost or mutated in many cases of familial breast cancer (28, 108, 109). Nevertheless, BRCA1 expression is also frequently reduced in sporadic breast cancers, and gene methylation and silencing can only account for a subset of these sporadic tumors (28, 108). This means that other parameters and factors that are altered during breast carcinogenesis likely exist to regulate tissue-specific levels of BRCA1 (25, 28). Indeed, the BRCA1 promoter is a highly complex bi-

directional transcriptional unit with multiple binding motifs, it is subject to dynamic interactions between its promoter and terminator regions, and its activity can be modulated by multiple generic and tissue-specific factors including 53BP1, E2F proteins and GABP- α/β and conditions including stress, hypoxia, growth factors and estrogens (110-113). However, despite these findings, very few factors have been shown to bind to and directly modulate BRCA1 expression and of these most have been negative regulators. Furthermore, there is a paucity of evidence to link these BRCA1 regulators to defined BRCA1-dependent phenotypes (114-118). Thus, metastasis-associated tumor antigen 1 (MTA1) has been implicated in the transcriptional repression of BRCA1 and in abnormal centrosome number and chromosomal instability (70), and E2F4 and the pocket proteins p130/p107 have been shown to bind the BRCA1 promoter and basally repress transcription thereby regulating cell growth (119). Distinct from these studies we demonstrate that HoxA9 directly and positively modulates BRCA1 transcription thereby restricting the abnormal growth and survival and stress response of breast cancer cells and nonmalignant MECs in culture and *in vivo*, and we provide evidence that this relationship likely has clinical relevance. The fact that expression profiling did not reveal reduced BRCA1 transcripts in the four primary tumors with reduced HoxA9 expression is not surprising. In general, expression levels of BRCA1 are below the detection sensitivity of Affymetrix arrays and thus transcript level changes would not normally be noted. Instead, BRCA1 expression is tightly linked to cell cycling and the presence of damaged DNA (120) and we observed robust induction of BRCA1 in response to HoxA9 most predominantly during tissue remodeling or following exposure to an exogenous stress (Supplemental Figure S11). Thus, because the HoxA9 promoter is frequently methylated and HoxA9 levels are often reduced in invasive breast tumors and we showed that HoxA9 is often lost in ER negative breast tumors, our data offer an attractive explanation for why BRCA1 expression could be so frequently lost in sporadic human breast tumors, even in the absence of genetic aberrations, promoter methylation or haploinsufficiency.

Intriguingly, not only did we find that HoxA9-dependent BRCA1 expression restricts tumor progression by inhibiting MEC growth and survival, but we also observed that elevated HoxA9 and BRCA1 levels restore cell-cell adhesions and normalize acini morphogenesis (Figures 2, 5). These findings are consistent with previous reports which showed that loss of BRCA1 compromises the ability of nonmalignant MCF10A MECs to undergo morphogenesis into polarized acinar structures in a 3D rBM assay (20, 33, 34), and are consistent with data indicating that BRCA1 is critical for lumen formation in primary murine MECs (36). Indeed, during mammary gland remodeling BRCA1 levels peak prior to tight junction assembly and tissue-specific differentiation and they decline to barely detectable levels during lactation (28, 35, 36). Consistently, recent studies in which BRCA1 was over expressed in the epithelium of the breast showed that there was a moderate increase in lobular alveolar differentiation in the mammary gland, consistent with accelerated development, and these mice also showed resistance to mutagen-induced mammary neoplasia. By contrast, age matched mice expressing a mutated BRCA1 morphologically resembled animals at mid pregnancy, consistent with increased proliferation and secondary branching, and these mice showed enhanced DMBA-induced transformation (121). These findings raise the intriguing possibility that some HOX genes, particularly those expressed late during development and those that are expressed in differentiated tissues such as HoxA9 might regulate growth and survival and invasion to modulate body plan patterning during development by regulating levels of tumor suppressors that control these processes.

Methods

Substrates, Antibodies and Pharmacological Reagents

The materials used were: Commercial EHS matrix (Matrigel™, Collaborative Research; Bedford, MA) for the reconstituted basement membrane (rBM) assays; Vitrogen (Vitrogen 100, Inamed Biomaterials; Fremont, CA; bovine skin collagen I), 3mg/mL, for coating culture dishes, and Cellagen AC-5, 0.5% (ICN Biomedical Inc.; Costa Mesa, CA) for morphogenesis assays. Primary antibodies used were: actin, clone AC-40 (Sigma-Aldrich; Saint Louis, MO), BRCA1, clone Ab-1 (Oncogene; Boston, MA), β -Catenin, clone 14 (BD Transduction; San Jose, CA), β 4 integrin, clone 3E1 (Invitrogen; Carlsbad, CA), FLAG, clone M2 (Sigma-Aldrich), HA.11, clone 16B12 (Covance Research Products; Berkeley, CA), HA, clone Y-11 (Santa Cruz Biotech; Santa Cruz, CA), acetyl H3 histone, rabbit polyclonal (Upstate; Lake Placid, NY), Ki-67 clone 35 (BD Transduction), HoxA9 (N-20), goat polyclonal (Santa Cruz), HoxA9, rabbit polyclonal (gift, T. Nakamura, Tokyo, Japan), HoxA10 rabbit polyclonal (Abcam; Cambridge, MA), and laminin 5 (gift, P.Marinkovich; Stanford, CA) (122). Secondary antibodies used were: Alexa Fluor 488 and 555-conjugated polyclonal anti-rabbit and anti-mouse IgGs (Molecular Probes; Eugene, OR); and HRP-conjugated polyclonal rabbit and anti-mouse IgGs (Amersham Pharmacia; Piscataway, NJ). Pharmaceutical reagents included: Tyrphostin AG 1478 (100 μ M; DMSO) (Calbiochem, La Jolla, CA); *p*-Nitrophenyl phosphate disodium salt hexahydrate (Fisher Scientific; Pittsburgh, PA); and D-Luciferin, potassium salt (Biotium; Hayward, CA).

cDNA, Lentiviral and Retroviral and shRNA Constructs and Vectors

Please refer to the supplemental methods section for a detailed description of constructs used.

Cell Culture

The HMT-3522 S-1 and T4-2 MECs were grown and manipulated in 2D and 3D and the T4-2s were phenotypically-reverted exactly as described (63, 123). MDA-MB-231, MCF-7, and MCF10A cells were cultured according to manufacturer's recommendations (ATCC) and grown in 3D as described

(124). BT-20, MDA-MB-468, MDA-MB-435, T47D, ZR751 and SK-BR-3 cells were cultured according to manufacturer's recommendations (ATCC).

Retroviral and Lentiviral Infections

Amphotropic retrovirus was produced (125) and retroviral supernatant was harvested and used directly to spin infect cells, followed by antibiotic-induced selection with puromycin (0.5 μ g/mL media) or neomycin (100 μ g/mL) 72 hours post infection (126). Lentiviral particles were produced, harvested, and used to infect target cells as previously described (127).

Soft Agar Assay

Anchorage independent growth was assessed using a soft agar assay (63). In brief, 25,000 cells in 1.5ml 0.35% agarose containing 1X growth media was overlaid 1.5ml 0.5% agarose containing 1X growth media, and colonies >30 μ m were scored positive after 14 days.

***In Vivo* Studies**

All experiments were performed in accordance with the guidelines of Laboratory Animal Research at the University of Pennsylvania. Four week old BalbC nu/nu mice were subcutaneously injected into the rear flanks (5x10⁶ cells/injection together with MatrigelTM), and palpable lesions were detected and measured and monitored bi-weekly for 56 days (Instant read-out digital calipers; Electron Microscopy Sciences, Ft. Washington, PA). At experiment termination mice were sacrificed, lesions were dissected, measured and macroscopically analyzed, fixed in 4% paraformaldehyde, paraffin embedded, and H&E sections were evaluated for histopathological evidence of tumor phenotype.

Immunofluorescence

Immunofluorescence analysis of cells grown in 2D, 3D, and paraffin-embedded tissues was performed as previously described (123, 124).

Proliferation

Cell proliferation was measured by calculating the percent Ki-67 labeled nuclei and quantified as previously described (128).

Immunoblotting

Equal amounts of cell protein lysate (Laemmli; BCA; Pierce; Rockford, IL) were separated on reducing SDS-PAGE gels, transferred to nitrocellulose or PVDF membrane and probed with primary antibody. Bands were visualized and quantified using a Fujifilm Gel Documentation system in conjunction with HRP-conjugated secondary antibodies and ECL-Plus (Amersham Pharmacia)

Chromatin Immunoprecipitation (ChIP)

ChIP assays were performed according to manufacturer's directions (Upstate). In brief, proteins were cross-linked to chromatin (formaldehyde; 1%), cells were lysed and the chromatin was sheared (sonication; Misonix Ultrasonic; Farmingdale, NY). HA-tagged HoxA9/DNA fragments were immunoprecipitated (overnight; 4°C) using polyclonal anti-HA (clone Y-11) or polyclonal anti-HoxA9 with polyclonal anti-acetyl H3 histone serving as a positive control. Protein/DNA complexes were captured (Protein A agarose beads), washed (6-10X), and eluted from beads and cross-links were reversed (NaCl and phenol/chloroform extraction); and DNA was ethanol precipitated and used directly for PCR reactions. To amplify a human BRCA1 promoter fragment from anti-HoxA9 ChIP experiments we used: forward 5' GAT GGG ACC TTG TGG AAG AA 3' and reverse 5'ACG ACC AAA CCA ACA CCA AT 3', and to amplify the human beta-globin gene (129) from anti-acetyl H3 histone ChIP experiments we used: forward 5'ATC TTC CTC CCA CAG CTC CT 3' and reverse 5' TTT GCA GCC TCA CCT TCT TT 3'

BRCA1 reporter assay

Luciferase BRCA1 gene reporter assays were conducted in 293 cells by transient transfection and normalizing transfection efficiency by quantifying SEAP expression using a MRX microplate reader® (Dynex Technologies; Chantilly, VA) 36 hours post transfection as previously described (130). 48 hours post transfection cells were lysed (25mM glycylglycine, 2mM EGTA pH 8.0, 1% Triton X-100, 1mM DTT pH 7.8), aliquots of lysate were diluted (1:5) in assay buffer (25mM glycylglycine, 2mM EGTA pH 8.0, 10mM MgSO₄, 2.2mM ATP, 0.275mM Acetyl CoA, 1mM DTT pH7.8), transferred to a

Microfluor® plate (Thomas Scientific; Swedesboro, NJ), mixed with equal quantity of luciferin buffer (25mM glycylglycine, 2mM EGTA pH8.0, 10mM MgSO₄, 1mM DTT, 0.55mM luciferin pH7.8) and light emission from the reaction was detected using a Microtiter® plate luminometer (Dynex Technologies) in conjunction with Revelation® software. Experiments were quantified as the fold-change over appropriate control conditions.

Morphometric Analysis

Colony size and morphology in 3D rBM was assessed at indicated times, essentially as previously described (123, 124).

Clonogenic Survival Assay

Radiation survival was assessed using a standard clonogenic assay. Briefly, cells in log phase were irradiated (0-6 Grays; Mark I, Model 68A, dose rate=1.05Gy/min, Cesium 137), incubated (24 hours; 37°C) and serially diluted and replated at low density for assessment of clonogenic survival. 14 days post irradiation (IR) cells were fixed (methanol; -20°C), stained (0.5% crystal violet) and colonies (≥ 50 cells) were quantified and percentage survival was calculated as the number of colonies formed after irradiation divided by the number of colonies formed in the absence of irradiation.

Expression Profiling

All experiments were performed in accordance with Institutional Review Board approval at the University of Pennsylvania. Dissected tissues from human breast tumor and adjacent "normal" tissue were rapidly homogenized using the Tissue TearerTM apparatus (BioSpec Products, Inc; Bartlesville, OK) and log phase cultured breast cells were harvested and total RNA from samples was isolated and labeled, and cRNA was prepared, fragmented and hybridized to U95A arrays, essentially as recommended by the manufacturer (GeneChipTM protocol, Affymetrix, Inc.; Santa Clara, CA). The microarrays were scanned and images were assessed for quality and normalization using GeneChip Analysis Suite 5.0 (Affymetrix, Inc.). Data from each microarray analysis was exported as a .DAT file into Rosetta ResolverTM 3.0 (Rosetta Inpharmatics, Inc.; Seattle, WA) and statistically analyzed using

2D agglomerative clustering. Using this approach, expression data were clustered for similarity across experiments and experiments were clustered for similarity across genes. Probe set clusters detecting transcript level differences between normal and malignant tissue with $p \leq 0.01$ as calculated by Rosetta Resolver™ in at least four of five tumor/normal pairs were included in the list of genes that was significantly up- or down-regulated, using normal adjacent as the background sample. Thus up-regulated genes correspond to transcripts that are more highly expressed in tumor compared to normal tissue, and vice versa.

Semi-Quantitative PCR (Semi-Q-PCR)

Purified total RNA (2.0µg) was reverse-transcribed using random primers (Amersham Biosciences), and resultant samples were serially diluted 1:10, 1:100 and 1:1000 for subsequent PCR reactions. An initial PCR was performed to amplify the 18S ribosomal RNA subunit, together with a standard curve to determine cDNA copy number for each sample. Primer sequences were as follows: *18S* rRNA-F 5' CGG CTA CCA CAT CCA AGG AA 3' and *18S* rRNA-R 5' GCT GGA ATT ACC GCG GCT 3'. Corrected cDNA concentrations were calculated and a second PCR reaction was performed in which equal amounts of cDNA were added to primers specific for *HoxA9*. Primer sequences used to amplify *HoxA9* cDNA were: 5' GCT TGT GGT TCT CCT CCA GT 3' and 5' CCA GGG TCT GGT GTT TTG TA 3'. These primers cross the exon 1-2 boundary and thus should not amplify contaminating genomic DNA. Primer sequences used to amplify *BRCA1* cDNA were: 5' GGA ACT AAC CAA ACG GAG CA 3' and 5' TAG GTT TCT GCT GTG CCT GA 3'. Primer sequences used to amplify *HoxA10* cDNA were: 5' TAT CCC ACA ACA ATG TCA TGC TC 3' and 5' GTC GCC TGG AGA TTC ATC AGG A 3'.

Quantitative Real-Time PCR (Q-RT-PCR)

Total RNA was reverse transcribed using random primers (Amersham Biosciences) and 18S rRNA primers were used to control for cDNA concentration in a separate PCR reaction for each sample (see above for sequences). Primers used to amplify *HoxA9* exon 2, using the LightCycler apparatus (Roche

Diagnostics; Indianapolis, IN) are listed above. LightCycler Fast Start DNA Master SYBR Green mix (Roche) was added to each PCR reaction along with cDNA and 1 pmol primer in a total volume of 10 μ L. Primers and conditions used to amplify the BRCA1 cDNA junction between exon 12 and 13 were previously described (131).

***In Situ* Hybridization**

Sense or antisense riboprobe against HoxA9 was generated as previously described (96). Digoxigenin-labeled probes were prepared using T7 or SP6 RNA polymerase (Roche). Paraffin-embedded human breast tissue was hybridized with 800ng/mL of probe as previously described(96). Six normal and four invasive ductal carcinoma human breast samples were examined.

Immunohistochemistry

Formalin fixed, paraffin-embedded human breast tissue sections were deparaffinized and rehydrated through three concentrations of alcohol and incubated in 3% H₂O₂ for 15 minutes to block endogenous peroxidase. Antigen retrieval was carried out in 0.1 M citrate buffer pH 6.0 at 95°C for 20 minutes followed by 20 minutes at room temperature. Nonspecific binding was blocked using PBS containing 1% BSA and 5% goat serum for 30 minutes before primary goat polyclonal HoxA9 antibodies (1:200) were added for 1 hour at room temperature. Biotinylated secondary antibody and ABC reagent were used as directed (Vector Laboratories, Burlingame, CA). Vector® VIP was used as the chromagen (Vector Laboratories). Sections were counterstained with Mayer's hematoxylin (Sigma). Please refer to the supplemental method section for information regarding multispectral image acquisition and analysis. Six normal and four invasive ductal carcinoma samples were examined.

Bioinformatics Analysis

The mRNA expression levels for HoxA9 were analyzed from several independent cancer studies using Oncomine™ (www.oncomine.org) (132). Details of standard normalization methods and statistical calculations are provided on the Oncomine™ website.

Gene expression and clinical outcome information were obtained from two independent publicly available data sets (45, 61, 133). Clinical outcomes from the Pawitan study (133) was obtained from data published in the Ivshina study (61). In all cases, data for HoxA9 was culled from normalized expression data for each breast tumor sample, and patients were divided into quartiles based on HoxA9 expression. Each data set was analyzed separately. For the data from the van de Vijver study, distant metastasis was analyzed as first event only. If a patient developed a local recurrence, axillary recurrence, contra-lateral breast cancer, or a second primary cancer (except for non-melanoma skin cancer), she was censored at that time. Any distant metastasis after the first event was not analyzed, based on the theoretical possibility that the secondary cancers could be a source for distant metastases. An ipsilateral supra-clavicular recurrence was considered as first clinical evidence for metastatic disease for this analysis. Therefore, patients with ipsilateral supra-clavicular recurrence were not censored. Patients were censored at last follow-up. Kaplan-Meier survival curves were generated using the software WINSTAT FOR EXCEL (R. Fitch Software, Staufen, Germany), and p values were calculated by log-rank analysis. Multivariate analyses with Cox's proportional-hazards regression were performed on the expression levels of HoxA9 and clinicopathological variables provided in the NKI data set with SPSS 10.0 (SPSS), with patients stratified according to their local lymph node (LN) and estrogen receptor (ER) status, the molecular subtypes of breast cancer (134) and further grouped into quartiles based on the relative (untransformed) expression levels of HoxA9 (45). P-values less than 0.05 were considered significant.

Statistical Analysis

We used InStat software (Graphpad) to conduct the statistical analysis of our data. Unless otherwise stated, two-tailed Student *t*-tests were used for simple significance testing, and two-tailed Pearson tests for correlation analysis. Means are presented as \pm SEM of 3-5 independent experiments and statistical significance was considered $P < 0.05$. Unless otherwise noted, $n=3$.

Acknowledgements

We thank P. Marinkovich for the BM165 mAB; H. Blau for the Hermes-HRS-puro-IRES-EGFP construct; C. Largman for the PRC-CMV-HoxA9 construct; F. Rauscher for the HA tagged wild-type and Δ exon11b BRCA1 constructs; L.A. Chodosh for the pGL2-BRCA1 luciferase construct; G. Gray-Lawrence and G.I. Rozenberg for confocal microscopy guidance. This work was supported by NIH grant R01-CA078731, DOD grants DAMD17-01-1-0368, DAMD17-03-1-0396 and W81XWH-05-1-330, DOE grant A107165, CIRM grant RS1-00449 (to V.M. Weaver), Komen grant DISS0402407 (to P.M. Gilbert) and DOD grant BC062562 (to J.K. Mouw).

References

1. Chen, H., and Sukumar, S. 2003. HOX genes: emerging stars in cancer. *Cancer Biol Ther* 2:524-525.
2. Grier, D.G., Thompson, A., Kwasniewska, A., McGonigle, G.J., Halliday, H.L., and Lappin, T.R. 2005. The pathophysiology of HOX genes and their role in cancer. *J Pathol* 205:154-171.
3. Samuel, S., and Naora, H. 2005. Homeobox gene expression in cancer: insights from developmental regulation and deregulation. *Eur J Cancer* 41:2428-2437.
4. Nakamura, T., Largaespada, D.A., Lee, M.P., Johnson, L.A., Ohyashiki, K., Toyama, K., Chen, S.J., Willman, C.L., Chen, I.M., Feinberg, A.P., et al. 1996. Fusion of the nucleoporin gene NUP98 to HOXA9 by the chromosome translocation t(7;11)(p15;p15) in human myeloid leukaemia. *Nat Genet* 12:154-158.
5. Ford, H.L., Kabingu, E.N., Bump, E.A., Mutter, G.L., and Pardee, A.B. 1998. Abrogation of the G2 cell cycle checkpoint associated with overexpression of HSIX1: a possible mechanism of breast carcinogenesis. *Proc Natl Acad Sci U S A* 95:12608-12613.
6. Kolfschoten, I.G., van Leeuwen, B., Berns, K., Mullenders, J., Beijersbergen, R.L., Bernards, R., Voorhoeve, P.M., and Agami, R. 2005. A genetic screen identifies PITX1 as a suppressor of RAS activity and tumorigenicity. *Cell* 121:849-858.
7. Tomotsune, D., Shoji, H., Wakamatsu, Y., Kondoh, H., and Takahashi, N. 1993. A mouse homologue of the Drosophila tumour-suppressor gene *l(2)gl* controlled by Hox-C8 in vivo. *Nature* 365:69-72.
8. Raman, V., Martensen, S.A., Reisman, D., Evron, E., Odenwald, W.F., Jaffee, E., Marks, J., and Sukumar, S. 2000. Compromised HOXA5 function can limit p53 expression in human breast tumours. *Nature* 405:974-978.

9. Carrio, M., Arderiu, G., Myers, C., and Boudreau, N.J. 2005. Homeobox D10 induces phenotypic reversion of breast tumor cells in a three-dimensional culture model. *Cancer Res* 65:7177-7185.
10. Lewis, M.T. 2000. Homeobox genes in mammary gland development and neoplasia. *Breast Cancer Res* 2:158-169.
11. Duverger, O., and Morasso, M.I. 2008. Role of homeobox genes in the patterning, specification, and differentiation of ectodermal appendages in mammals. *J Cell Physiol* 216:337-346.
12. Chen, H., and Sukumar, S. 2003. Role of homeobox genes in normal mammary gland development and breast tumorigenesis. *J Mammary Gland Biol Neoplasia* 8:159-175.
13. Friedman, L.S., Ostermeyer, E.A., Szabo, C.I., Dowd, P., Lynch, E.D., Rowell, S.E., and King, M.C. 1994. Confirmation of BRCA1 by analysis of germline mutations linked to breast and ovarian cancer in ten families. *Nat Genet* 8:399-404.
14. Starita, L.M., Horwitz, A.A., Keogh, M.C., Ishioka, C., Parvin, J.D., and Chiba, N. 2005. BRCA1/BARD1 ubiquitinate phosphorylated RNA polymerase II. *J Biol Chem* 280:24498-24505.
15. Lou, Z., Minter-Dykhouse, K., and Chen, J. 2005. BRCA1 participates in DNA decatenation. *Nat Struct Mol Biol* 12:589-593.
16. Fan, W., Jin, S., Tong, T., Zhao, H., Fan, F., Antinore, M.J., Rajasekaran, B., Wu, M., and Zhan, Q. 2002. BRCA1 regulates GADD45 through its interactions with the OCT-1 and CAAT motifs. *J Biol Chem* 277:8061-8067.
17. Aprelikova, O., Pace, A.J., Fang, B., Koller, B.H., and Liu, E.T. 2001. BRCA1 is a selective co-activator of 14-3-3 sigma gene transcription in mouse embryonic stem cells. *J Biol Chem* 276:25647-25650.
18. Rosen, E.M., Fan, S., Pestell, R.G., and Goldberg, I.D. 2003. BRCA1 gene in breast cancer. *J Cell Physiol* 196:19-41.

19. Burga, L.N., Tung, N.M., Troyan, S.L., Bostina, M., Konstantinopoulos, P.A., Fountzilas, H., Spentzos, D., Miron, A., Yassin, Y.A., Lee, B.T., et al. 2009. Altered proliferation and differentiation properties of primary mammary epithelial cells from BRCA1 mutation carriers. *Cancer Res* 69:1273-1278.
20. Furuta, S., Jiang, X., Gu, B., Cheng, E., Chen, P.L., and Lee, W.H. 2005. Depletion of BRCA1 impairs differentiation but enhances proliferation of mammary epithelial cells. *Proc Natl Acad Sci U S A* 102:9176-9181.
21. Honrado, E., Benitez, J., and Palacios, J. 2005. The molecular pathology of hereditary breast cancer: genetic testing and therapeutic implications. *Mod Pathol* 18:1305-1320.
22. Sorlie, T., Tibshirani, R., Parker, J., Hastie, T., Marron, J.S., Nobel, A., Deng, S., Johnsen, H., Pesich, R., Geisler, S., et al. 2003. Repeated observation of breast tumor subtypes in independent gene expression data sets. *Proc Natl Acad Sci U S A* 100:8418-8423.
23. Turner, N., Tutt, A., and Ashworth, A. 2004. Hallmarks of 'BRCAness' in sporadic cancers. *Nat Rev Cancer* 4:814-819.
24. Wei, M., Grushko, T.A., Dignam, J., Hagos, F., Nanda, R., Sveen, L., Xu, J., Fackenthal, J., Treiakova, M., Das, S., et al. 2005. BRCA1 promoter methylation in sporadic breast cancer is associated with reduced BRCA1 copy number and chromosome 17 aneusomy. *Cancer Res* 65:10692-10699.
25. Thompson, M.E., Jensen, R.A., Obermiller, P.S., Page, D.L., and Holt, J.T. 1995. Decreased expression of BRCA1 accelerates growth and is often present during sporadic breast cancer progression. *Nat Genet* 9:444-450.
26. Futreal, P.A., Liu, Q., Shattuck-Eidens, D., Cochran, C., Harshman, K., Tavtigian, S., Bennett, L.M., Haugen-Strano, A., Swensen, J., Miki, Y., et al. 1994. BRCA1 mutations in primary breast and ovarian carcinomas. *Science* 266:120-122.

27. Baldassarre, G., Battista, S., Belletti, B., Thakur, S., Pentimalli, F., Trapasso, F., Fedele, M., Pierantoni, G., Croce, C.M., and Fusco, A. 2003. Negative regulation of BRCA1 gene expression by HMGA1 proteins accounts for the reduced BRCA1 protein levels in sporadic breast carcinoma. *Mol Cell Biol* 23:2225-2238.
28. Mueller, C.R., and Roskelley, C.D. 2003. Regulation of BRCA1 expression and its relationship to sporadic breast cancer. *Breast Cancer Res* 5:45-52.
29. Antonova, L., and Mueller, C.R. 2008. Hydrocortisone down-regulates the tumor suppressor gene BRCA1 in mammary cells: a possible molecular link between stress and breast cancer. *Genes Chromosomes Cancer* 47:341-352.
30. Marquis, S.T., Rajan, J.V., Wynshaw-Boris, A., Xu, J., Yin, G.Y., Abel, K.J., Weber, B.L., and Chodosh, L.A. 1995. The developmental pattern of Brca1 expression implies a role in differentiation of the breast and other tissues. *Nat Genet* 11:17-26.
31. Xu, X., Wagner, K.U., Larson, D., Weaver, Z., Li, C., Ried, T., Hennighausen, L., Wynshaw-Boris, A., and Deng, C.X. 1999. Conditional mutation of Brca1 in mammary epithelial cells results in blunted ductal morphogenesis and tumour formation. *Nat Genet* 22:37-43.
32. Kubista, M., Rosner, M., Kubista, E., Bernaschek, G., and Hengstschlager, M. 2002. Brca1 regulates in vitro differentiation of mammary epithelial cells. *Oncogene* 21:4747-4756.
33. O'Connell, F.C., and Martin, F. 2000. Laminin-rich extracellular matrix association with mammary epithelial cells suppresses Brca1 expression. *Cell Death Differ* 7:360-367.
34. Miralem, T., and Avraham, H.K. 2003. Extracellular matrix enhances heregulin-dependent BRCA1 phosphorylation and suppresses BRCA1 expression through its C terminus. *Mol Cell Biol* 23:579-593.
35. Magdinier, F., Dalla Venezia, N., Lenoir, G.M., Frappart, L., and Dante, R. 1999. BRCA1 expression during prenatal development of the human mammary gland. *Oncogene* 18:4039-4043.

36. Murtagh, J., McArdle, E., Gilligan, E., Thornton, L., Furlong, F., and Martin, F. 2004. Organization of mammary epithelial cells into 3D acinar structures requires glucocorticoid and JNK signaling. *J Cell Biol* 166:133-143.
37. Chen, F., and Capecchi, M.R. 1997. Targeted mutations in *hoxa-9* and *hoxb-9* reveal synergistic interactions. *Dev Biol* 181:186-196.
38. Taylor, H.S., Vanden Heuvel, G.B., and Igarashi, P. 1997. A conserved Hox axis in the mouse and human female reproductive system: late establishment and persistent adult expression of the *Hoxa* cluster genes. *Biol Reprod* 57:1338-1345.
39. Dintilhac, A., Bihan, R., Guerrier, D., Deschamps, S., and Pellerin, I. 2004. A conserved non-homeodomain *Hoxa9* isoform interacting with CBP is co-expressed with the 'typical' *Hoxa9* protein during embryogenesis. *Gene Expr Patterns* 4:215-222.
40. Chen, F., and Capecchi, M.R. 1999. Paralogous mouse Hox genes, *Hoxa9*, *Hoxb9*, and *Hoxd9*, function together to control development of the mammary gland in response to pregnancy. *Proc Natl Acad Sci U S A* 96:541-546.
41. Shen, W.F., Hu, Y.L., Uttarwar, L., Passegue, E., and Largman, C. 2008. MicroRNA-126 regulates HOXA9 by binding to the homeobox. *Mol Cell Biol* 28:4609-4619.
42. Bruhl, T., Urbich, C., Aicher, D., Acker-Palmer, A., Zeiher, A.M., and Dimmeler, S. 2004. Homeobox A9 transcriptionally regulates the EphB4 receptor to modulate endothelial cell migration and tube formation. *Circ Res* 94:743-751.
43. Reynolds, P.A., Sigaroudinia, M., Zardo, G., Wilson, M.B., Benton, G.M., Miller, C.J., Hong, C., Fridlyand, J., Costello, J.F., and Tlsty, T.D. 2006. Tumor suppressor p16INK4A regulates polycomb-mediated DNA hypermethylation in human mammary epithelial cells. *J Biol Chem* 281:24790-24802.

44. van 't Veer, L.J., Dai, H., van de Vijver, M.J., He, Y.D., Hart, A.A., Mao, M., Peterse, H.L., van der Kooy, K., Marton, M.J., Witteveen, A.T., et al. 2002. Gene expression profiling predicts clinical outcome of breast cancer. *Nature* 415:530-536.
45. van de Vijver, M.J., He, Y.D., van't Veer, L.J., Dai, H., Hart, A.A., Voskuil, D.W., Schreiber, G.J., Peterse, J.L., Roberts, C., Marton, M.J., et al. 2002. A gene-expression signature as a predictor of survival in breast cancer. *N Engl J Med* 347:1999-2009.
46. Sotiriou, C., Powles, T.J., Dowsett, M., Jazaeri, A.A., Feldman, A.L., Assersohn, L., Gadisetti, C., Libutti, S.K., and Liu, E.T. 2002. Gene expression profiles derived from fine needle aspiration correlate with response to systemic chemotherapy in breast cancer. *Breast Cancer Res* 4:R3.
47. Perou, C.M., Sorlie, T., Eisen, M.B., van de Rijn, M., Jeffrey, S.S., Rees, C.A., Pollack, J.R., Ross, D.T., Johnsen, H., Akslen, L.A., et al. 2000. Molecular portraits of human breast tumours. *Nature* 406:747-752.
48. Petty, R.D., Kerr, K.M., Murray, G.I., Nicolson, M.C., Rooney, P.H., Bissett, D., and Collie-Duguid, E.S. 2006. Tumor Transcriptome Reveals the Predictive and Prognostic Impact of Lysosomal Protease Inhibitors in Non-Small-Cell Lung Cancer. *J Clin Oncol*.
49. Livasy, C.A., Karaca, G., Nanda, R., Tretiakova, M.S., Olopade, O.I., Moore, D.T., and Perou, C.M. 2006. Phenotypic evaluation of the basal-like subtype of invasive breast carcinoma. *Mod Pathol* 19:264-271.
50. Ramaswamy, S., Ross, K.N., Lander, E.S., and Golub, T.R. 2003. A molecular signature of metastasis in primary solid tumors. *Nat Genet* 33:49-54.
51. Weigelt, B., Glas, A.M., Wessels, L.F., Witteveen, A.T., Peterse, J.L., and van't Veer, L.J. 2003. Gene expression profiles of primary breast tumors maintained in distant metastases. *Proc Natl Acad Sci U S A* 100:15901-15905.

52. Fernandez-Ranvier, G.G., Weng, J., Yeh, R.F., Shibru, D., Khafnashar, E., Chung, K.W., Hwang, J., Duh, Q.Y., Clark, O.H., and Kebebew, E. 2008. Candidate diagnostic markers and tumor suppressor genes for adrenocortical carcinoma by expression profile of genes on chromosome 11q13. *World J Surg* 32:873-881.
53. Iqbal, J., Kucuk, C., Deleeuw, R.J., Srivastava, G., Tam, W., Geng, H., Klinkebiel, D., Christman, J.K., Patel, K., Cao, K., et al. 2009. Genomic analyses reveal global functional alterations that promote tumor growth and novel tumor suppressor genes in natural killer-cell malignancies. *Leukemia*.
54. Hedenfalk, I., Ringner, M., Ben-Dor, A., Yakhini, Z., Chen, Y., Chebil, G., Ach, R., Loman, N., Olsson, H., Meltzer, P., et al. 2003. Molecular classification of familial non-BRCA1/BRCA2 breast cancer. *Proc Natl Acad Sci U S A* 100:2532-2537.
55. Kurose, K., Hoshaw-Woodard, S., Adeyinka, A., Lemeshow, S., Watson, P.H., and Eng, C. 2001. Genetic model of multi-step breast carcinogenesis involving the epithelium and stroma: clues to tumour-microenvironment interactions. *Hum Mol Genet* 10:1907-1913.
56. Comings, D.E., Gade-Andavolu, R., Cone, L.A., Muhleman, D., and MacMurray, J.P. 2003. A multigene test for the risk of sporadic breast carcinoma. *Cancer* 97:2160-2170.
57. Matushansky, I., Maki, R.G., and Cordon-Cardo, C. 2008. A context dependent role for Wnt signaling in tumorigenesis and stem cells. *Cell Cycle* 7:720-724.
58. Vernon, A.E., and LaBonne, C. 2004. Tumor metastasis: a new twist on epithelial-mesenchymal transitions. *Curr Biol* 14:R719-721.
59. Mani, S.A., Yang, J., Brooks, M., Schwaninger, G., Zhou, A., Miura, N., Kutok, J.L., Hartwell, K., Richardson, A.L., and Weinberg, R.A. 2007. Mesenchyme Forkhead 1 (FOXC2) plays a key role in metastasis and is associated with aggressive basal-like breast cancers. *Proc Natl Acad Sci U S A* 104:10069-10074.

60. Mani, S.A., Guo, W., Liao, M.J., Eaton, E.N., Ayyanan, A., Zhou, A.Y., Brooks, M., Reinhard, F., Zhang, C.C., Shipitsin, M., et al. 2008. The epithelial-mesenchymal transition generates cells with properties of stem cells. *Cell* 133:704-715.
61. Ivshina, A.V., George, J., Senko, O., Mow, B., Putti, T.C., Smeds, J., Lindahl, T., Pawitan, Y., Hall, P., Nordgren, H., et al. 2006. Genetic reclassification of histologic grade delineates new clinical subtypes of breast cancer. *Cancer Res* 66:10292-10301.
62. Kenny, P.A., Lee, G.Y., Myers, C.A., Neve, R.M., Semeiks, J.R., Spellman, P.T., Lorenz, K., Lee, E.H., Barcellos-Hoff, M.H., Petersen, O.W., et al. 2007. The morphologies of breast cancer cell lines in three-dimensional assays correlate with their profiles of gene expression. *Mol Oncol* 1:84-96.
63. Wang, F., Weaver, V.M., Petersen, O.W., Larabell, C.A., Dedhar, S., Briand, P., Lupu, R., and Bissell, M.J. 1998. Reciprocal interactions between beta1-integrin and epidermal growth factor receptor in three-dimensional basement membrane breast cultures: a different perspective in epithelial biology. *Proc Natl Acad Sci U S A* 95:14821-14826.
64. Wang, F., Hansen, R.K., Radisky, D., Yoneda, T., Barcellos-Hoff, M.H., Petersen, O.W., Turley, E.A., and Bissell, M.J. 2002. Phenotypic reversion or death of cancer cells by altering signaling pathways in three-dimensional contexts. *J Natl Cancer Inst* 94:1494-1503.
65. Cillo, C., Cantile, M., Faiella, A., and Boncinelli, E. 2001. Homeobox genes in normal and malignant cells. *J Cell Physiol* 188:161-169.
66. Hombria, J.C., and Lovegrove, B. 2003. Beyond homeosis--HOX function in morphogenesis and organogenesis. *Differentiation* 71:461-476.
67. Rajan, J.V., Wang, M., Marquis, S.T., and Chodosh, L.A. 1996. Brca2 is coordinately regulated with Brca1 during proliferation and differentiation in mammary epithelial cells. *Proc Natl Acad Sci U S A* 93:13078-13083.

68. Xu, B., Kim, S., and Kastan, M.B. 2001. Involvement of Brca1 in S-phase and G(2)-phase checkpoints after ionizing irradiation. *Mol Cell Biol* 21:3445-3450.
69. Beger, C., Pierce, L.N., Kruger, M., Marcusson, E.G., Robbins, J.M., Welch, P., Welch, P.J., Welte, K., King, M.C., Barber, J.R., et al. 2001. Identification of Id4 as a regulator of BRCA1 expression by using a ribozyme-library-based inverse genomics approach. *Proc Natl Acad Sci U S A* 98:130-135.
70. Molli, P.R., Singh, R.R., Lee, S.W., and Kumar, R. 2008. MTA1-mediated transcriptional repression of BRCA1 tumor suppressor gene. *Oncogene* 27:1971-1980.
71. Thakur, S., Nakamura, T., Calin, G., Russo, A., Tamburrino, J.F., Shimizu, M., Baldassarre, G., Battista, S., Fusco, A., Wassell, R.P., et al. 2003. Regulation of BRCA1 transcription by specific single-stranded DNA binding factors. *Mol Cell Biol* 23:3774-3787.
72. Thakur, S., and Croce, C.M. 1999. Positive regulation of the BRCA1 promoter. *J Biol Chem* 274:8837-8843.
73. Moens, C.B., and Selleri, L. 2006. Hox cofactors in vertebrate development. *Dev Biol* 291:193-206.
74. Maconochie, M., Nonchev, S., Morrison, A., and Krumlauf, R. 1996. Paralogous Hox genes: function and regulation. *Annu Rev Genet* 30:529-556.
75. Chang, C.P., Brocchieri, L., Shen, W.F., Largman, C., and Cleary, M.L. 1996. Pbx modulation of Hox homeodomain amino-terminal arms establishes different DNA-binding specificities across the Hox locus. *Mol Cell Biol* 16:1734-1745.
76. Beachy, P.A., Varkey, J., Young, K.E., von Kessler, D.P., Sun, B.I., and Ekker, S.C. 1993. Cooperative binding of an Ultrabithorax homeodomain protein to nearby and distant DNA sites. *Mol Cell Biol* 13:6941-6956.

77. Choi, J.S., Zheng, L.T., Ha, E., Lim, Y.J., Kim, Y.H., Wang, Y.P., and Lim, Y. 2006. Comparative genomic hybridization array analysis and real-time PCR reveals genomic copy number alteration for lung adenocarcinomas. *Lung* 184:355-362.
78. Wu, Q., Lothe, R.A., Ahlquist, T., Silins, I., Trope, C.G., Micci, F., Nesland, J.M., Suo, Z., and Lind, G.E. 2007. DNA methylation profiling of ovarian carcinomas and their in vitro models identifies HOXA9, HOXB5, SCGB3A1, and CRABP1 as novel targets. *Mol Cancer* 6:45.
79. Abate-Shen, C. 2002. Deregulated homeobox gene expression in cancer: cause or consequence? *Nat Rev Cancer* 2:777-785.
80. Hartwell, K.A., Muir, B., Reinhardt, F., Carpenter, A.E., Sgroi, D.C., and Weinberg, R.A. 2006. The Spemann organizer gene, Goosecoid, promotes tumor metastasis. *Proc Natl Acad Sci U S A* 103:18969-18974.
81. Stasinopoulos, I.A., Mironchik, Y., Raman, A., Wildes, F., Winnard, P., Jr., and Raman, V. 2005. HOXA5-twist interaction alters p53 homeostasis in breast cancer cells. *J Biol Chem* 280:2294-2299.
82. Boudreau, N., Andrews, C., Srebrow, A., Ravanpay, A., and Cheresch, D.A. 1997. Induction of the angiogenic phenotype by Hox D3. *J Cell Biol* 139:257-264.
83. Kroon, E., Kros, J., Thorsteinsdottir, U., Baban, S., Buchberg, A.M., and Sauvageau, G. 1998. Hoxa9 transforms primary bone marrow cells through specific collaboration with Meis1a but not Pbx1b. *Embo J* 17:3714-3725.
84. Myers, C., Charboneau, A., and Boudreau, N. 2000. Homeobox B3 promotes capillary morphogenesis and angiogenesis. *J Cell Biol* 148:343-351.
85. Boudreau, N.J., and Varner, J.A. 2004. The homeobox transcription factor Hox D3 promotes integrin alpha5beta1 expression and function during angiogenesis. *J Biol Chem* 279:4862-4868.
86. Salsi, V., and Zappavigna, V. 2006. Hoxd13 and Hoxa13 directly control the expression of the EphA7 Ephrin tyrosine kinase receptor in developing limbs. *J Biol Chem* 281:1992-1999.

87. Coletta, R.D., Christensen, K., Reichenberger, K.J., Lamb, J., Micomonaco, D., Huang, L., Wolf, D.M., Muller-Tidow, C., Golub, T.R., Kawakami, K., et al. 2004. The Six1 homeoprotein stimulates tumorigenesis by reactivation of cyclin A1. *Proc Natl Acad Sci U S A* 101:6478-6483.
88. Coletta, R.D., Christensen, K.L., Micalizzi, D.S., Jedlicka, P., Varella-Garcia, M., and Ford, H.L. 2008. Six1 overexpression in mammary cells induces genomic instability and is sufficient for malignant transformation. *Cancer Res* 68:2204-2213.
89. Christensen, K.L., Patrick, A.N., McCoy, E.L., and Ford, H.L. 2008. The six family of homeobox genes in development and cancer. *Adv Cancer Res* 101:93-126.
90. Ruhin-Poncet, B., Ghouli-Mazgar, S., Hotton, D., Capron, F., Jaafoura, M.H., Goubin, G., and Berdal, A. 2009. Msx and dlx homeogene expression in epithelial odontogenic tumors. *J Histochem Cytochem* 57:69-78.
91. Lee, H., Habas, R., and Abate-Shen, C. 2004. MSX1 cooperates with histone H1b for inhibition of transcription and myogenesis. *Science* 304:1675-1678.
92. Song, K., Wang, Y., and Sassoon, D. 1992. Expression of Hox-7.1 in myoblasts inhibits terminal differentiation and induces cell transformation. *Nature* 360:477-481.
93. Rauch, T., Wang, Z., Zhang, X., Zhong, X., Wu, X., Lau, S.K., Kernstine, K.H., Riggs, A.D., and Pfeifer, G.P. 2007. Homeobox gene methylation in lung cancer studied by genome-wide analysis with a microarray-based methylated CpG island recovery assay. *Proc Natl Acad Sci U S A* 104:5527-5532.
94. Abate-Shen, C., Shen, M.M., and Gelmann, E. 2008. Integrating differentiation and cancer: the Nkx3.1 homeobox gene in prostate organogenesis and carcinogenesis. *Differentiation* 76:717-727.
95. Ma, L., Teruya-Feldstein, J., and Weinberg, R.A. 2007. Tumour invasion and metastasis initiated by microRNA-10b in breast cancer. *Nature* 449:682-688.

96. Myers, C., Charboneau, A., Cheung, I., Hanks, D., and Boudreau, N. 2002. Sustained expression of homeobox D10 inhibits angiogenesis. *Am J Pathol* 161:2099-2109.
97. Abate-Shen, C., Banach-Petrosky, W.A., Sun, X., Economides, K.D., Desai, N., Gregg, J.P., Borowsky, A.D., Cardiff, R.D., and Shen, M.M. 2003. Nkx3.1; Pten mutant mice develop invasive prostate adenocarcinoma and lymph node metastases. *Cancer Res* 63:3886-3890.
98. Chen, K.N., Gu, Z.D., Ke, Y., Li, J.Y., Shi, X.T., and Xu, G.W. 2005. Expression of 11 HOX genes is deregulated in esophageal squamous cell carcinoma. *Clin Cancer Res* 11:1044-1049.
99. Mullan, P.B., Quinn, J.E., and Harkin, D.P. 2006. The role of BRCA1 in transcriptional regulation and cell cycle control. *Oncogene* 25:5854-5863.
100. Yoshida, K., and Miki, Y. 2004. Role of BRCA1 and BRCA2 as regulators of DNA repair, transcription, and cell cycle in response to DNA damage. *Cancer Sci* 95:866-871.
101. Boulton, S.J. 2006. BRCA1-mediated ubiquitylation. *Cell Cycle* 5:1481-1486.
102. Thorsteinsdottir, U., Mamo, A., Kroon, E., Jerome, L., Bijl, J., Lawrence, H.J., Humphries, K., and Sauvageau, G. 2002. Overexpression of the myeloid leukemia-associated Hoxa9 gene in bone marrow cells induces stem cell expansion. *Blood* 99:121-129.
103. Look, A.T. 1997. Oncogenic transcription factors in the human acute leukemias. *Science* 278:1059-1064.
104. Dorsam, S.T., Ferrell, C.M., Dorsam, G.P., Derynck, M.K., Vijapurkar, U., Khodabakhsh, D., Pau, B., Bernstein, H., Haqq, C.M., Largman, C., et al. 2004. The transcriptome of the leukemogenic homeoprotein HOXA9 in human hematopoietic cells. *Blood* 103:1676-1684.
105. Ferrell, C.M., Dorsam, S.T., Ohta, H., Humphries, R.K., Derynck, M.K., Haqq, C., Largman, C., and Lawrence, H.J. 2005. Activation of stem-cell specific genes by HOXA9 and HOXA10 homeodomain proteins in CD34+ human cord blood cells. *Stem Cells* 23:644-655.
106. Boudreau, N., and Bissell, M.J. 1998. Extracellular matrix signaling: integration of form and function in normal and malignant cells. *Curr Opin Cell Biol* 10:640-646.

107. Rhoads, K., Arderiu, G., Charboneau, A., Hansen, S.L., Hoffman, W., and Boudreau, N. 2005. A role for Hox A5 in regulating angiogenesis and vascular patterning. *Lymphat Res Biol* 3:240-252.
108. Turner, N.C., Reis-Filho, J.S., Russell, A.M., Springall, R.J., Ryder, K., Steele, D., Savage, K., Gillett, C.E., Schmitt, F.C., Ashworth, A., et al. 2007. BRCA1 dysfunction in sporadic basal-like breast cancer. *Oncogene* 26:2126-2132.
109. Margolin, S., and Lindblom, A. 2006. Familial breast cancer, underlying genes, and clinical implications: a review. *Crit Rev Oncog* 12:75-113.
110. Tan-Wong, S.M., French, J.D., Proudfoot, N.J., and Brown, M.A. 2008. Dynamic interactions between the promoter and terminator regions of the mammalian BRCA1 gene. *Proc Natl Acad Sci U S A* 105:5160-5165.
111. Kang, H.J., Kim, H.J., Cho, C.H., Hu, Y., Li, R., and Bae, I. 2008. BRCA1 transcriptional activity is enhanced by interactions between its AD1 domain and AhR. *Cancer Chemother Pharmacol* 62:965-975.
112. MacDonald, G., Stramwasser, M., and Mueller, C.R. 2007. Characterization of a negative transcriptional element in the BRCA1 promoter. *Breast Cancer Res* 9:R49.
113. Suen, T.C., Tang, M.S., and Goss, P.E. 2005. Model of transcriptional regulation of the BRCA1-NBR2 bi-directional transcriptional unit. *Biochim Biophys Acta* 1728:126-134.
114. Maor, S., Papa, M.Z., Yarden, R.I., Friedman, E., Lerenthal, Y., Lee, S.W., Mayer, D., and Werner, H. 2007. Insulin-like growth factor-I controls BRCA1 gene expression through activation of transcription factor Sp1. *Horm Metab Res* 39:179-185.
115. Atlas, E., Stramwasser, M., and Mueller, C.R. 2001. A CREB site in the BRCA1 proximal promoter acts as a constitutive transcriptional element. *Oncogene* 20:7110-7114.
116. Atlas, E., Stramwasser, M., Whiskin, K., and Mueller, C.R. 2000. GA-binding protein alpha/beta is a critical regulator of the BRCA1 promoter. *Oncogene* 19:1933-1940.

117. Wang, A., Schneider-Broussard, R., Kumar, A.P., MacLeod, M.C., and Johnson, D.G. 2000. Regulation of BRCA1 expression by the Rb-E2F pathway. *J Biol Chem* 275:4532-4536.
118. Rauch, T., Zhong, X., Pfeifer, G.P., and Xu, X. 2005. 53BP1 is a positive regulator of the BRCA1 promoter. *Cell Cycle* 4:1078-1083.
119. Bindra, R.S., and Glazer, P.M. 2006. Basal repression of BRCA1 by multiple E2Fs and pocket proteins at adjacent E2F sites. *Cancer Biol Ther* 5:1400-1407.
120. Venkitaraman, A.R. 2002. Cancer susceptibility and the functions of BRCA1 and BRCA2. *Cell* 108:171-182.
121. Hoshino, A., Yee, C.J., Campbell, M., Woltjer, R.L., Townsend, R.L., van der Meer, R., Shyr, Y., Holt, J.T., Moses, H.L., and Jensen, R.A. 2007. Effects of BRCA1 transgene expression on murine mammary gland development and mutagen-induced mammary neoplasia. *Int J Biol Sci* 3:281-291.
122. Russell, A.J., Fincher, E.F., Millman, L., Smith, R., Vela, V., Waterman, E.A., Dey, C.N., Guide, S., Weaver, V.M., and Marinkovich, M.P. 2003. Alpha 6 beta 4 integrin regulates keratinocyte chemotaxis through differential GTPase activation and antagonism of alpha 3 beta 1 integrin. *J Cell Sci* 116:3543-3556.
123. Weaver, V.M., Petersen, O.W., Wang, F., Larabell, C.A., Briand, P., Damsky, C., and Bissell, M.J. 1997. Reversion of the malignant phenotype of human breast cells in three-dimensional culture and in vivo by integrin blocking antibodies. *J Cell Biol* 137:231-245.
124. Paszek, M.J., Zahir, N., Johnson, K.R., Lakins, J.N., Rozenberg, G.I., Gefen, A., Reinhart-King, C.A., Margulies, S.S., Dembo, M., Boettiger, D., et al. 2005. Tensional homeostasis and the malignant phenotype. *Submitted, Cancer Cell*.
125. Kinsella, T.M., and Nolan, G.P. 1996. Episomal vectors rapidly and stably produce high-titer recombinant retrovirus. *Hum Gene Ther* 7:1405-1413.

126. Zahir, N., Lakins, J.N., Russell, A., Ming, W., Chatterjee, C., Rozenberg, G.I., Marinkovich, M.P., and Weaver, V.M. 2003. Autocrine laminin-5 ligates alpha6beta4 integrin and activates RAC and NFkappaB to mediate anchorage-independent survival of mammary tumors. *J Cell Biol* 163:1397-1407.
127. Zufferey, R., Dull, T., Mandel, R.J., Bukovsky, A., Quiroz, D., Naldini, L., and Trono, D. 1998. Self-inactivating lentivirus vector for safe and efficient in vivo gene delivery. *J Virol* 72:9873-9880.
128. Weaver, V.M., Lelievre, S., Lakins, J.N., Chrenek, M.A., Jones, J.C., Giancotti, F., Werb, Z., and Bissell, M.J. 2002. beta4 integrin-dependent formation of polarized three-dimensional architecture confers resistance to apoptosis in normal and malignant mammary epithelium. *Cancer Cell* 2:205-216.
129. Nikiforov, M.A., Chandriani, S., Park, J., Kotenko, I., Matheos, D., Johnsson, A., McMahon, S.B., and Cole, M.D. 2002. TRRAP-dependent and TRRAP-independent transcriptional activation by Myc family oncoproteins. *Mol Cell Biol* 22:5054-5063.
130. Sogaard, T.M., Jakobsen, C.G., and Justesen, J. 1999. A sensitive assay of translational fidelity (readthrough and termination) in eukaryotic cells. *Biochemistry (Mosc)* 64:1408-1417.
131. Kroupis, C., Stathopoulou, A., Zygalki, E., Ferekidou, L., Talieri, M., and Lianidou, E.S. 2005. Development and applications of a real-time quantitative RT-PCR method (QRT-PCR) for BRCA1 mRNA. *Clin Biochem* 38:50-57.
132. Rhodes, D.R., Yu, J., Shanker, K., Deshpande, N., Varambally, R., Ghosh, D., Barrette, T., Pandey, A., and Chinnaiyan, A.M. 2004. ONCOMINE: a cancer microarray database and integrated data-mining platform. *Neoplasia* 6:1-6.
133. Pawitan, Y., Bjohle, J., Amler, L., Borg, A.L., Egyhazi, S., Hall, P., Han, X., Holmberg, L., Huang, F., Klaar, S., et al. 2005. Gene expression profiling spares early breast cancer patients

from adjuvant therapy: derived and validated in two population-based cohorts. *Breast Cancer Res* 7:R953-964.

134. Sorlie, T., Perou, C.M., Tibshirani, R., Aas, T., Geisler, S., Johnsen, H., Hastie, T., Eisen, M.B., van de Rijn, M., Jeffrey, S.S., et al. 2001. Gene expression patterns of breast carcinomas distinguish tumor subclasses with clinical implications. *Proc Natl Acad Sci U S A* 98:10869-10874.

Multivariate analysis for relapse-free and overall survival according to HOXA9 transcript expression and clinical characteristics in ER-negative breast cancer patients				
Variable	Death		Relapse	
	Hazard Ratio (95% CI)	P Value	Hazard Ratio (95% CI)	P Value
HOXA9	0.394 (0.181-0.857)	0.019	0.433 (0.187-1.002)	0.05
Age (per 10-yr increment)	0.59 (0.338-1.027)	0.062	0.552 (0.314-0.973)	0.04
Tumor size (per cm)	1.58 (1.037-2.409)	0.033	1.49 (0.958-2.319)	0.077
Tumor grade (poorly vs. well differentiated)	0.923 (0.365-2.331)	0.865	1.053 (0.382-2.902)	0.921
Positive LN status vs. negative status	0.64 (0.209-1.954)	0.433	0.566 (0.196-1.631)	0.291
Chemotherapy vs. no chemotherapy	1.596 (0.513-4.962)	0.419	1.53 (0.54-4.335)	0.423
Hormonal treatment vs. no treatment	0.423 (0.083-2.154)	0.3	0.436 (0.089-2.149)	0.308
Mastectomy vs. breast-conserving therapy	2.1 (0.926-4.759)	0.076	2.187 (0.925-5.171)	0.075

The analysis included the 69 ER-negative breast cancer patients in the Netherlands Cancer Institute dataset. HOXA9 transcript expression, age and tumor size were modeled as continuous variables. The molecular subtypes of breast cancer are not included in the model as none of the tumors is categorized as the luminal A subtype plus there is no event of death or relapse for tumors categorized as the normal-like or luminal B subtype. CI denotes confidence interval.

Table 1. Multivariate analysis for relapse-free and overall survival according to HOXA9 transcript expression and clinical characteristics in ER-negative breast cancer patients.

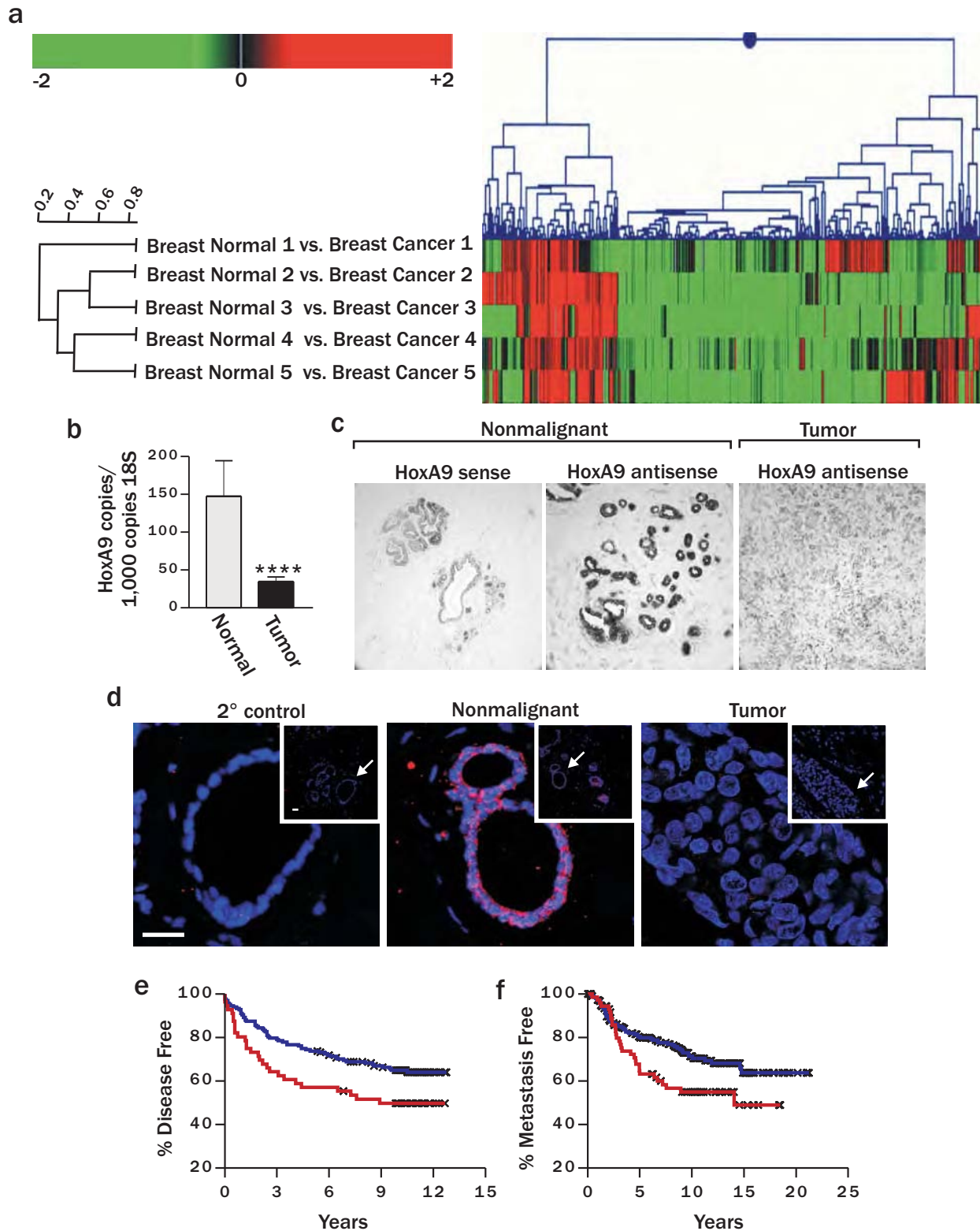


Figure 1. Breast malignancy is associated with reduced HoxA9 expression. **a.** Cluster diagram of Affymetrix microarray data using Rosetta Resolver to compare gene expression profiles of matched "normal" mammary tissue and adjacent primary breast cancers, revealing significantly lower HoxA9 transcript levels in 4 out of 5 expression sets analyzed ($p \leq 0.01$). **b.** Quantitative RT-PCR showing significantly reduced levels of HoxA9 mRNA in a panel of primary human mammary tumors ($n=38$) compared to "normal" breast tissue ($n=8$). P-value equals 0.00035 using the Man-Whitney test. **c.** *In situ* hybridization using a HoxA9 probe on nonmalignant or malignant mammary epithelial tissue ($n=6$), showing nuclear localization of HoxA9 mRNA transcript in the epithelial component and reduced levels in breast tumors ($n=4$). Bar equals 100 μ m. **d.** Immunofluorescent staining for HoxA9 demonstrates robust cytoplasmic and nuclear localized HoxA9 protein in the epithelium of nonmalignant human breast tissue, and reduced levels in breast tumors. Insets (20X) show a broader view of the breast tissue with arrows pointing to regions blown up in the main images. Bar equals 50 μ m. The 2° control shows that there is no nonspecific staining when the primary antibody is omitted. **e.** Breast cancer patients whose tumors expressed the lowest HoxA9 (lowest expression quartile; solid red line) experienced significantly reduced disease free survival compared to all other patients in the study (solid blue line). Censored samples are denoted with an 'X'. P-value equals 0.025. **f.** Patients with the lowest HoxA9 levels in their tumors (lowest expression quartile; solid red line) also had significantly increased metastasis as a first event when compared to all other patients (solid blue line). Censored samples are denoted with an 'X'. P-value equals 0.02.

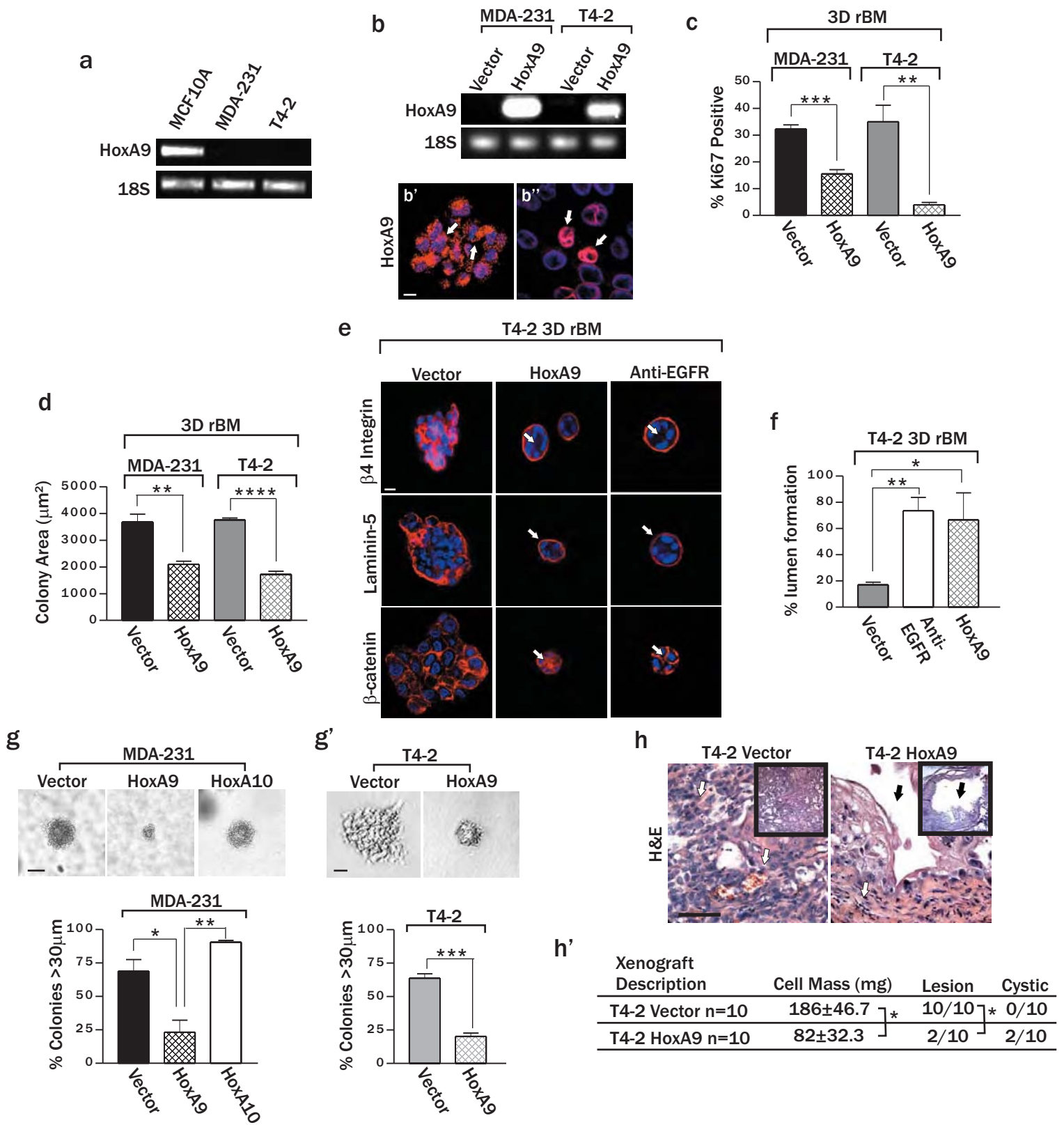


Figure 2. HoxA9 modulates the growth and survival of breast cancer cells. **a.** Semi-Q-PCR gel indicating HoxA9 mRNA levels expressed in human nonmalignant (MCF10A), metastatic (MDA-231), and transformed (T4-2) MECs. **b.** Semi-Q-PCR gel showing expressed transgenic HoxA9 mRNA levels attained in MDA-231 and T4-2 breast tumor cell lines. **b'** and **b''.** Confocal fluorescence microscopy images of DAPI stained nuclei (blue) and FLAG-tagged HoxA9 (red) showing nuclear and cytoplasmic staining of ectopically expressed HoxA9 in MDA-231 (**b'**) and T4-2 (**b''**) breast tumor cells. Bar equals 10 µm. **c.** Bar graph demonstrating reduced proliferation in breast tumor cells (MDA 231 and T4-2) following HoxA9 re-expression. Values were quantified as percentage of DAPI positive tumor cells grown within a reconstituted basement membrane (rBM) that were positive for Ki67. ***P-value equals 0.0003 and **P-value equals 0.0025. **d.** Bar graph quantifying cross-sectional area of MDA-231 and T4-2 breast tumor colonies in rBM expressing either the vector or HoxA9 transgene. **P-value equals 0.0068 and ****P-value equals 0.0001. **e.** Representative immunofluorescence confocal images of β4 integrin, Laminin-5 and β-catenin in T4-2 breast tumor colonies expressing the vector, the HoxA9 transgene or phenotypically-reverted (Anti-EGFR) tumor acini induced by inhibiting epidermal growth factor receptor (EGFR) activity using tyrothostin. Note the reduced colony size and appearance of lumens in the tumor colonies following re-expression of HoxA9 and in the phenotypically-reverted acini (white arrows). **f.** Bar graph quantifying lumens observed in rBM-generated T4-2 breast tumor colonies expressing the vector, the HoxA9 transgene or anti-EGFR “phenotypically-reverted” acini. *P-value equals 0.0188 and **P-value equals 0.0076. **g** and **g'.** Bar graph showing percentage of tumor colonies greater than 30 µm (bottom) and phase contrast images of tumor colonies embedded within soft agar (top), indicating that re-expression of HoxA9 significantly inhibits anchorage-independent growth and survival of MDA-231 (**g**) and T4-2 (**g'**) mammary tumor cells whereas another homeobox gene HoxA10 (**g**) has little effect. Bars equal 50µm (**g**) and 20µm (**g'**). ***P-value equals 0.0005, **P-value equals 0.018 and *P-value equals 0.0221. **h.** High (40X) and low magnification (10X; insert) phase contrast images of H&E stained tissue sections of positive control tumor (T4-2 vector) and HoxA9 re-expressing tumor (T4-2 HoxA9) xenografts. Note the high cell density and angiogenic phenotype of the vector control tumors, and the fibrous, acellular, non-vascularized lesion formed by HoxA9-expressing tumor cells. Scale bar equals 100µm. **h'.** Table describing the physical attributes of excised xenografts shown in **h**. Note the increase in cystic lesions formed by tumor cells re-expressing the HoxA9 transgene. P-values represent the mean ± SEM of multiple measurements of independent experiments of cells grown within a 3D rBM for 10-12 days or within soft agar for 14 days.

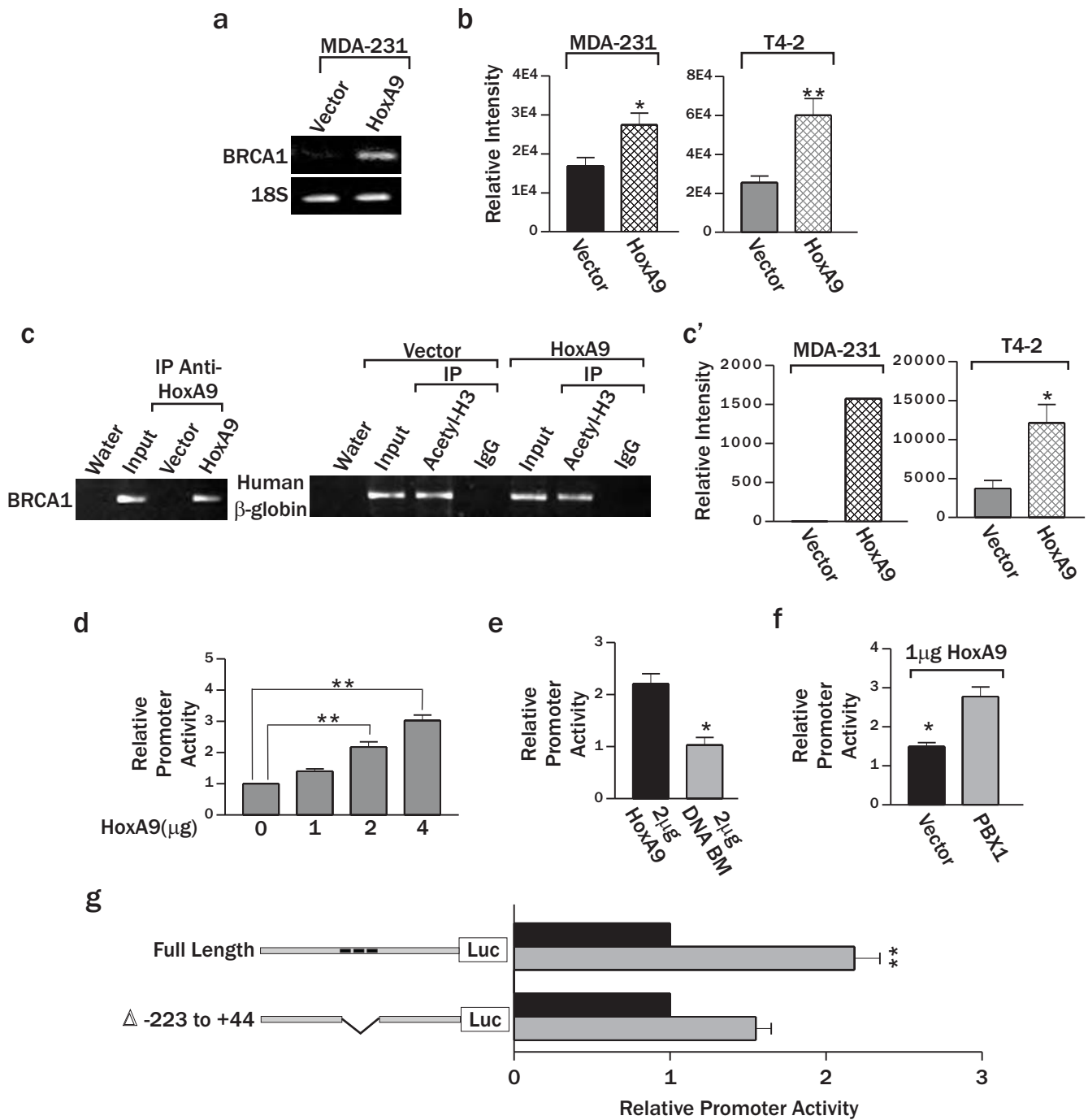


Figure 3. HoxA9 regulates BRCA1 expression. **a.** Semi-Q-PCR gel indicating increased BRCA1 expression with the re-expression of HoxA9 in MDA-231 cells. **b.** Bar graph quantifying immunoblot data from multiple experiments showing increased BRCA1 protein in MDA-231 or T4-2 breast tumor cells re-expressing HoxA9. *P-value equals 0.0457 and **P-value equals 0.0028. **c.** Representative gel of ChIP studies in breast cancer cells revealing co-precipitation of HoxA9 with the BRCA1 promoter and acetylated acetyl-H3-histone with the β -globin promoter. **c'.** Bar graphs quantifying ChIP experiments in MDA-231 (n=2) and T4-2 cells (P-value equals 0.0178, n=4). **d.** Luciferase reporter analysis showing a dose-dependent increase in BRCA1 promoter activity in response to addition of wild-type HoxA9. P-values equal 0.001. **e.** Luciferase reporter analysis displaying loss of BRCA1 promoter activity upon addition of HoxA9 containing an N255T (DNA BM) mutation in the conserved DNA binding domain. P-value equals 0.03. **f.** Luciferase reporter analysis indicating enhanced HoxA9-mediated BRCA1 promoter activity upon addition of PBX1 cofactor (2 μ g). P-value equals 0.0259. **g.** Luciferase reporter analysis showing a diminished responsiveness of a BRCA1 promoter construct containing a deletion in residues -223 to +44, which contains three putative Hox binding sites (gray bar). Data are normalized to matched vector control (black bars). Negative numbers refer to basepairs upstream of the BRCA1 transcription start site.

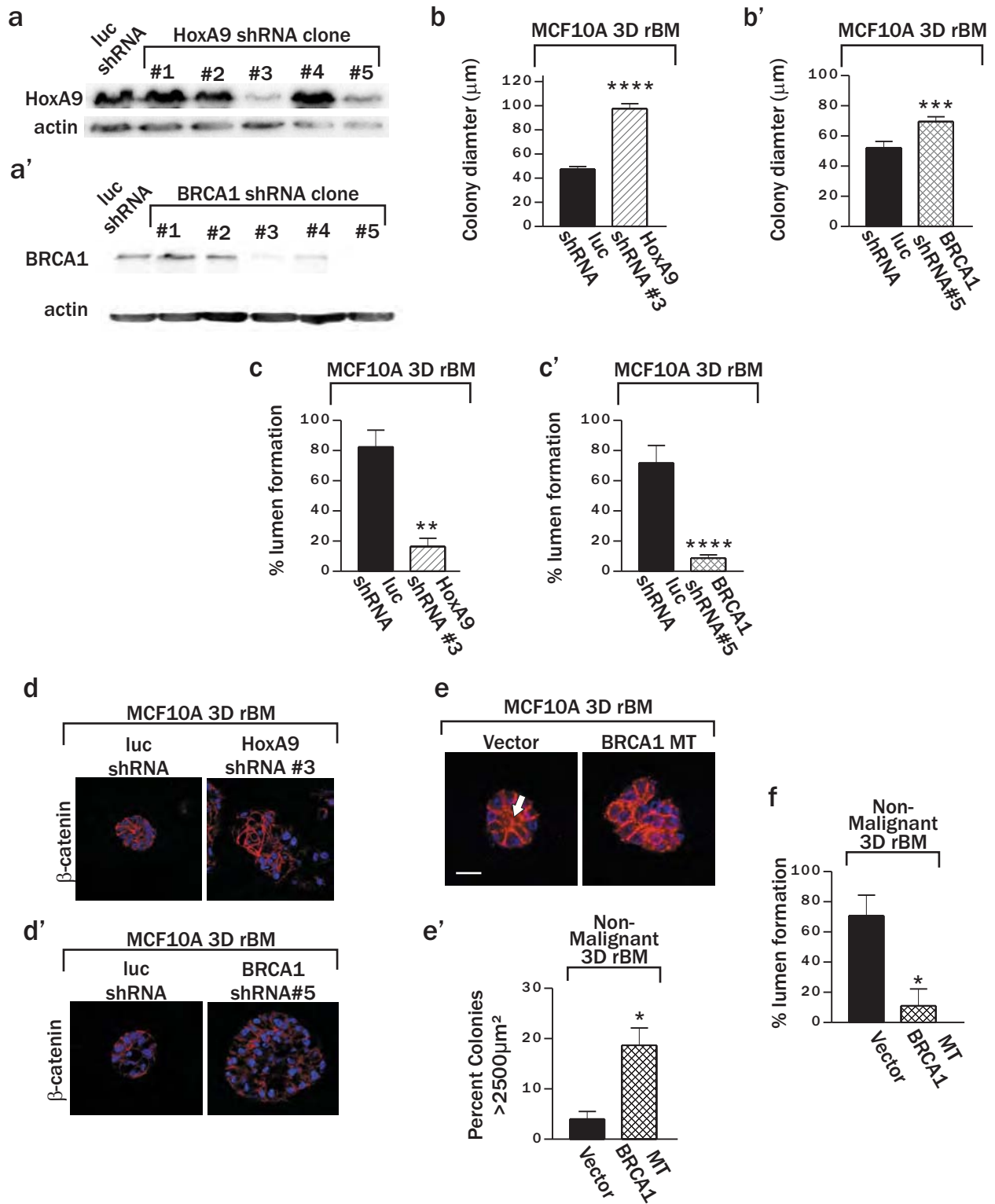


Figure 4. HoxA9 regulates non-malignant MEC growth by modulating BRCA1 expression. **a** and **a'**. Immunoblot showing representative image of shRNA-mediated knock down of HoxA9 (**a**, top), relative to beta actin protein (**a**, bottom), in 293 cells expressing a luciferase (luc) shRNA or the HoxA9 shRNA clone, and shRNA-mediated knock down of BRCA1 (**a'**, top), relative to beta actin protein (**a'**, bottom), in 293 cells expressing a luciferase (luc) shRNA or the BRCA1 shRNA clone. **b** and **b'**. Bar graph illustrating increased colony size of MCF-10A nonmalignant MECs cultured within a rBM and expressing either reduced HoxA9 levels (**b**, ****P-value equals 0.0001) or reduced BRCA1 levels (**b'**, ***P-value equals 0.0024). **c** and **c'**. Bar graph quantifying lumens observed in MCF-10A nonmalignant breast colonies expressing luc control shRNA as compared to those with shRNA-mediated HoxA9 knockdown (**c**, **P-value equals 0.0010) or with shRNA-mediated BRCA1 knockdown (**c'**, ****P-value equals 0.0003). **d**. Immunofluorescence confocal images of β -catenin in MCF-10A nonmalignant breast colonies expressing either luc control shRNA or shRNA-HoxA9 clone #3. **d'**. Immunofluorescence confocal images of β -catenin in nonmalignant breast colonies expressing either luc control shRNA or shRNA-BRCA1 clone #5. Note the increased colony size and absence of lumens in the colonies in the absence of either HoxA9 or BRCA1. Bar equals 50 μ m. **e**. Confocal immunofluorescence images of β -catenin (red) and DAPI stained nuclei (blue) in nonmalignant breast colonies expressing vector or mutant BRCA1 (BRCA1 MT). When BRCA1 function was compromised by co-expression of the BRCA1 MT, the nonmalignant mammary epithelial cells formed large colonies lacking lumens in rBM. Bar equals 10 μ m. **e'**. Bar graphs quantifying cross-sectional area of nonmalignant breast colonies in cells cultured within a rBM and co-expressing mutant BRCA1. Data indicate that BRCA1 regulates MEC growth. *P-value equals 0.05. **f**. Bar graph quantifying lumens observed in nonmalignant breast colonies expressing vector control as compared to those expressing a mutant BRCA1. *P-value equals 0.05. P-values represent the mean \pm SEM of multiple measurements of independent experiments of cells grown within a 3D rBM for 10-12 days.

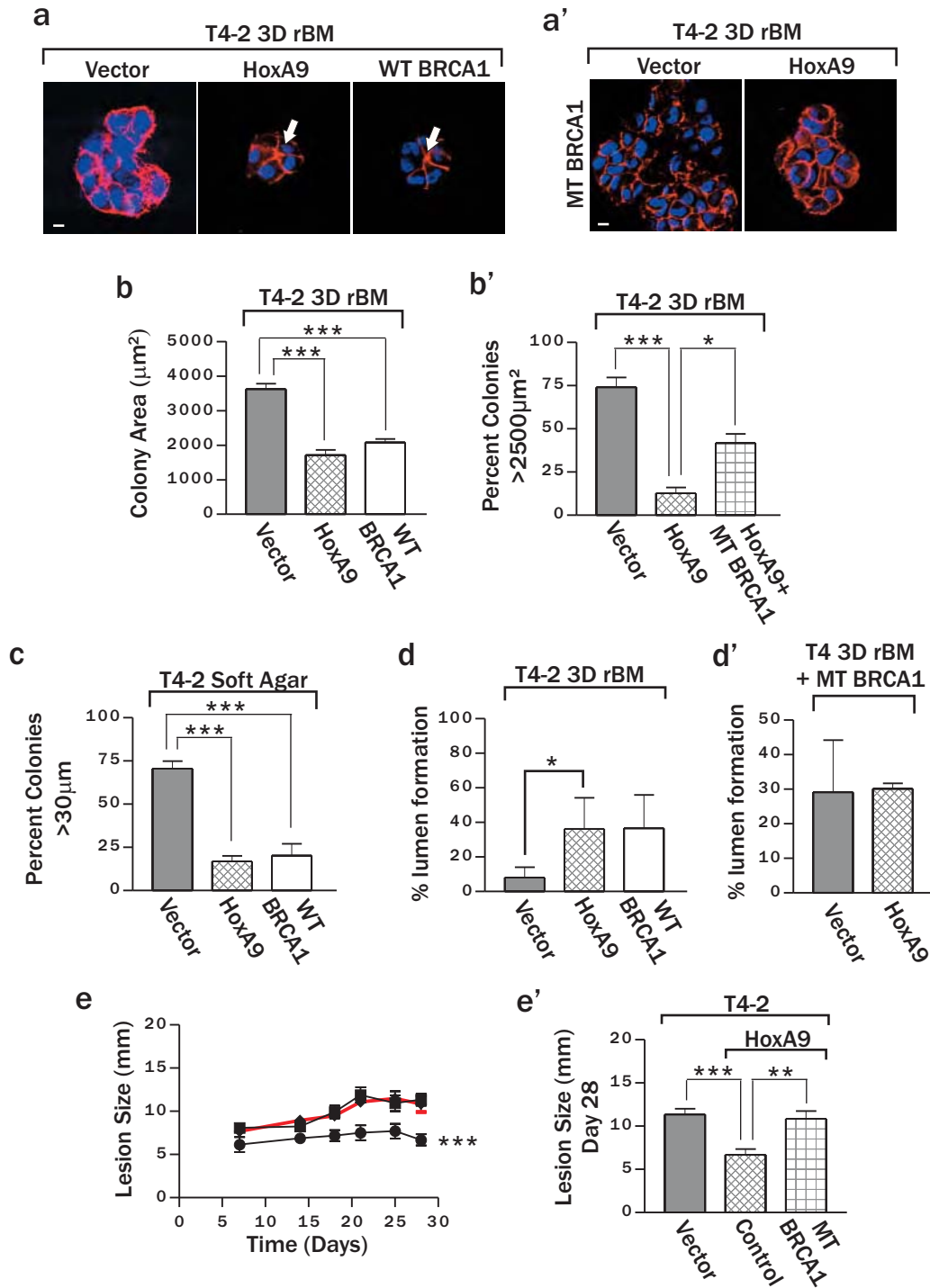


Figure 5. HoxA9 regulates BRCA1 to repress the malignant behavior of mammary epithelial cells. **a.** Representative confocal immunofluorescence images of β -catenin (red) and DAPI stained nuclei (blue) in breast tumor colonies re-expressing HoxA9 or wild-type BRCA1 cultured within a rBM. T4-2 tumor cells expressing either HoxA9 or BRCA1 formed smaller colonies and had lumens (white arrows). Bar equals $10\mu\text{m}$. **a'.** Confocal immunofluorescence images of β -catenin (red) and DAPI stained nuclei (blue) in T4-2 breast cancer colonies re-expressing HoxA9 alone or together with a mutant BRCA1 transgene showing that the growth inhibition effect of HoxA9 requires functional BRCA1. Scale bar equals $10\mu\text{m}$. **b.** Bar graph indicating decreased T4-2 colony size as measured by reduced cross-sectional area of breast tumor colonies re-expressing wild-type HoxA9 or BRCA1 transgene. ***P-value equals 0.001. **b'.** Bar graph quantifying cross-sectional area of T4-2 breast tumor colonies formed by breast tumor cells re-expressing the HoxA9 transgene together with empty vector or a mutant BRCA1 transgene. Data demonstrate that HoxA9-dependent growth regulation depends upon functional BRCA1. ***p value equals 0.001 and *P-value equals 0.05. **c.** Bar graph demonstrating that the re-expression of either HoxA9 or BRCA1 in T4-2 breast tumor cells significantly inhibits their anchorage-independent growth and survival. ***P-value equals 0.001. **d.** Bar graphs quantifying the percentage of T4-2 breast tumor colonies that formed lumens following the re-expression of HoxA9 or wild type BRCA1. *P-value equals 0.0263. **d'.** Bar graphs quantifying the percentage of rBM T4-2 breast tumor colonies with re-expressed HoxA9 that form lumens when BRCA1 function has been compromised through co-expression of a mutant BRCA1 transgene. P-values represent the mean \pm SEM of multiple measurements of independent experiments of cells grown within a 3D rBM for 10-12 days or in soft agar for several weeks. **e.** Line graph depicting time course of the progressive increase in xenograft size (5-30 days). Re-expression of HoxA9 in T4-2 tumor cells significantly reduced the rate of lesion expansion (black circles) compared to the T4-2 vector controls (black squares), which could be restored to that exhibited by wild-type T4-2 breast tumor cells if co-expressed with a mutant BRCA1 transgene (red line). ***P-value equals 0.001. **e'.** Bar graph illustrating lesion size (28 days) in each experimental group, indicating that lesion size decreased significantly in the T4-2 tumors re-expressing HoxA9, but not if BRCA1 function was inhibited through co-expression with a mutant BRCA1 transgene. ***P-value equals 0.001, **P-value equals 0.01. Values represent the mean \pm SEM of 6-10 tumor injections. 50

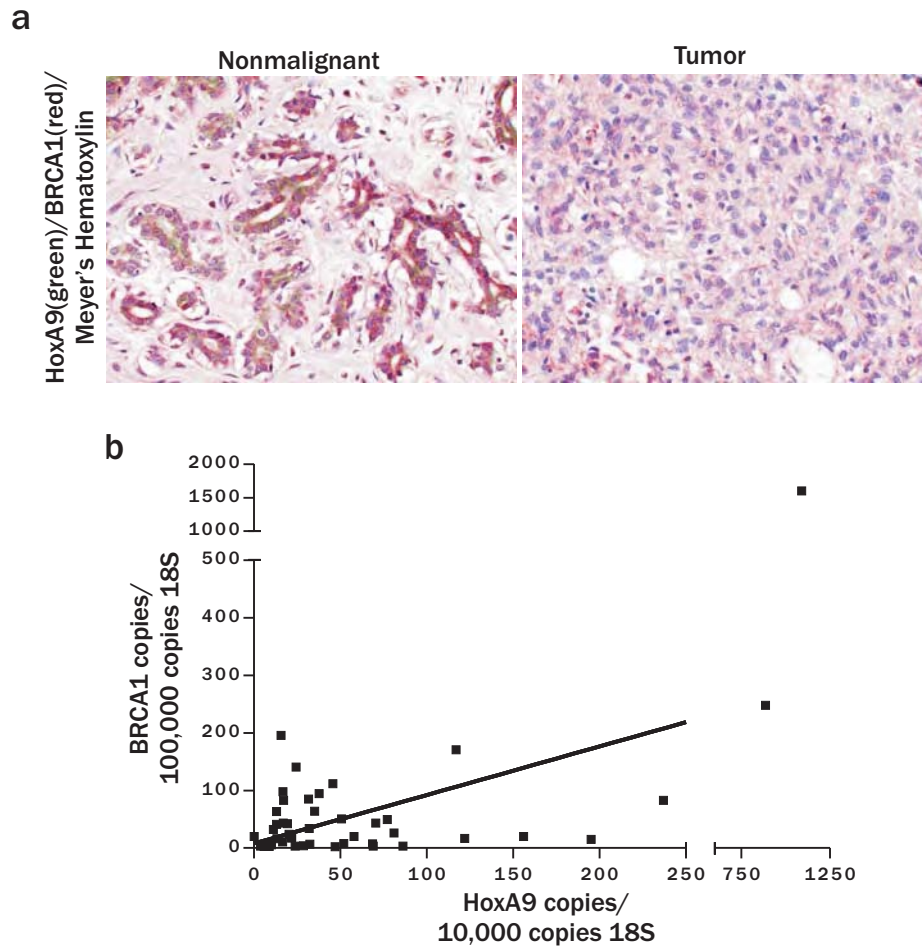
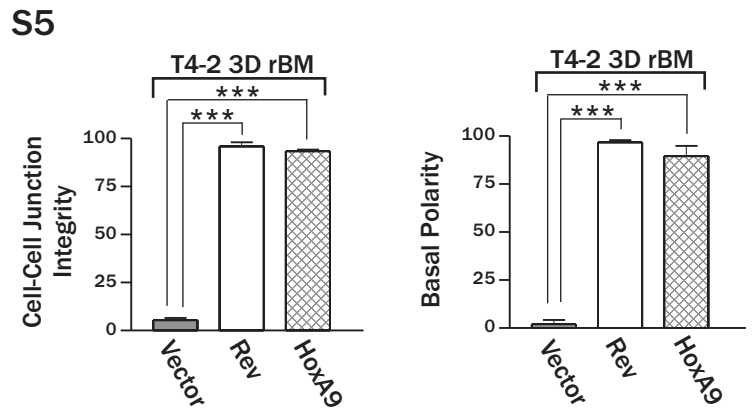
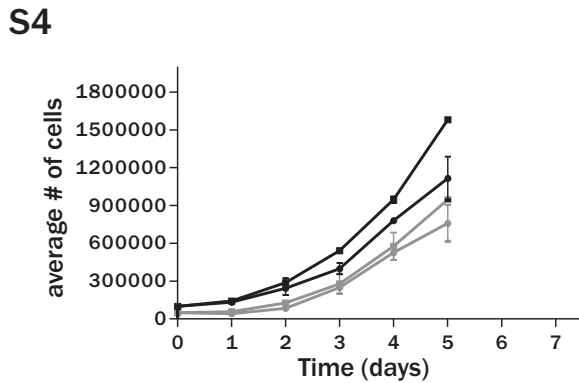
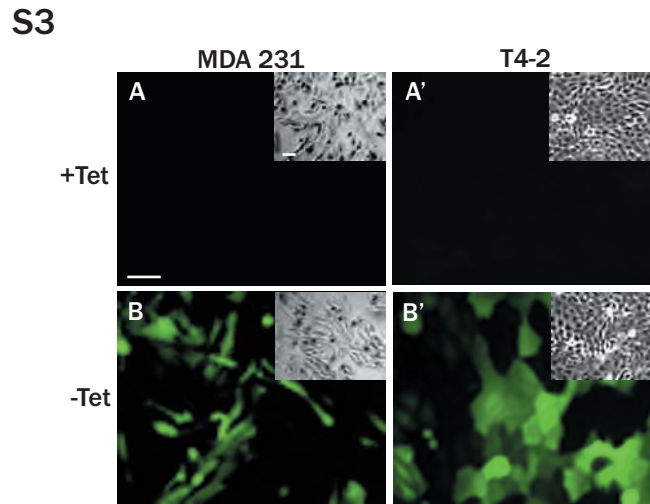
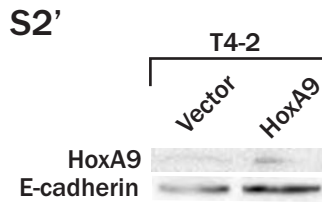
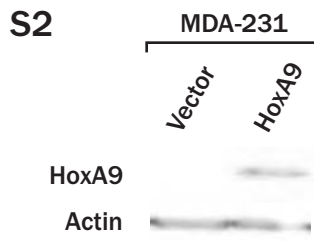
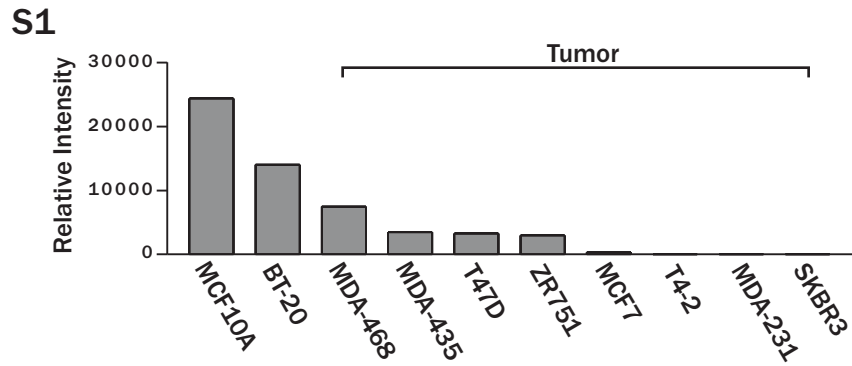


Figure 6. Clinical correlation between HoxA9 and BRCA1 expression. **a.** Immuno-histochemistry showing co-localized expression of HoxA9 and BRCA1 protein in the epithelium of normal human breast tissue (n=6). **b.** Line graph illustrating that there exists a significant correlation ($***p \leq 0.0001$; $R^2 = 0.5666$) between HoxA9 and BRCA1 mRNA levels expressed in a cohort of normal and tumorigenic human breast tissue specimens (n=50).



Supplemental Figure 1. Bar graph showing semi-Q-PCR analysis of HoxA9 mRNA levels expressed in nonmalignant and progressively transformed human breast cell lines.

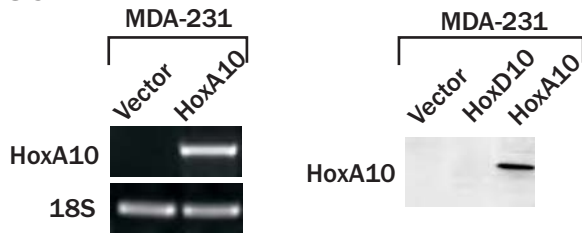
Supplemental Figure 2. Tetracycline regulated HoxA9 re-expression in breast tumor cell lines. Epi-fluorescence microscopy images of breast tumor cells (MDA-231, A & B; T4-2, A' & B') stably re-expressing retroviral HoxA9 bi-cistronically with EGFP, showing transgene expression in the absence (B & B') and its loss (A & A') upon tetracycline exposure (0.5 μ g/ml; 72 hours). Insert: Phase contrast microscopy images of A, A', B & B' indicating similar cell numbers were used under all experimental conditions. Bars equal 50 μ m.

Supplemental Figure 3 and 3'. Levels of HoxA9 protein upon re-expression in breast tumor cell lines. Immunoblot showing level of expressed transgenic HoxA9 protein attained in MDA-231 (left) and T4-2 (right) breast tumor cells compared to vector control cells.

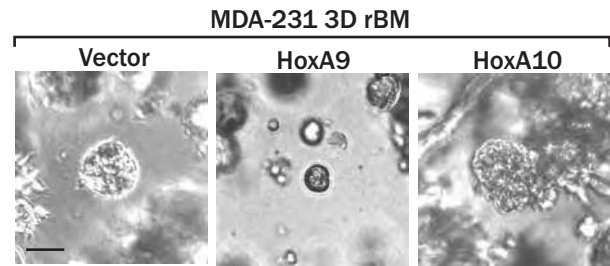
Supplemental Figure 4. HoxA9 expression does not influence proliferation on 2D tissue culture plastic. Growth curves of MDA-231 (black lines) and T4-2 (gray lines) breast tumor cells expressing a vector control (squares) or HoxA9 (circles) demonstrating that exogenous HoxA9 expression does not alter 2D proliferation (n=3).

Supplemental Figure 5. HoxA9 re-expression phenotypically reverts breast tumor cells. Bar graphs quantifying the tumor colony organization criteria shown in Figure 2e. ***p-value in all cases equals 0.001. Values represent the mean \pm SEM of multiple measurements of 3-5 independent experiments of cells grown within a 3D reconstituted basement membrane for 10-12 days.

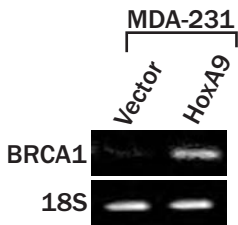
S6



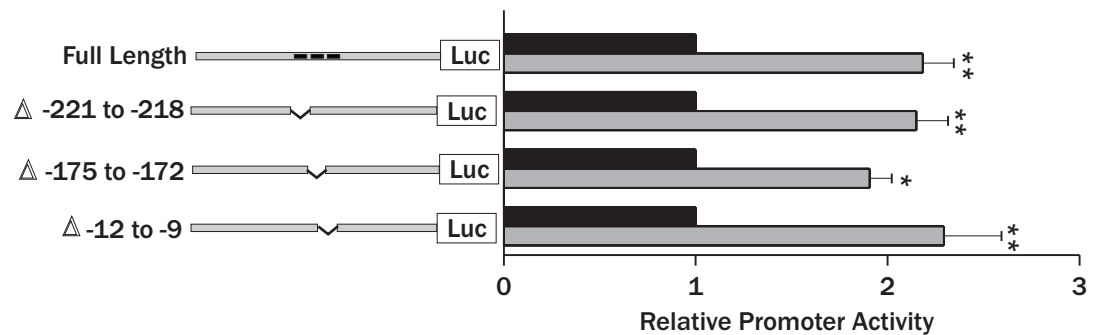
S7



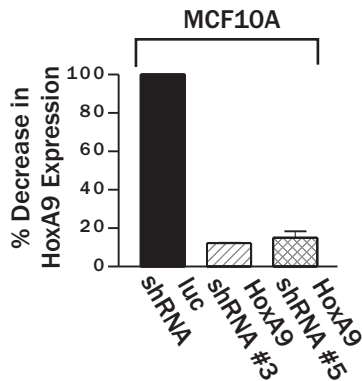
S8



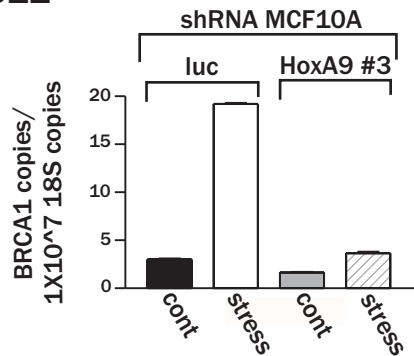
S9



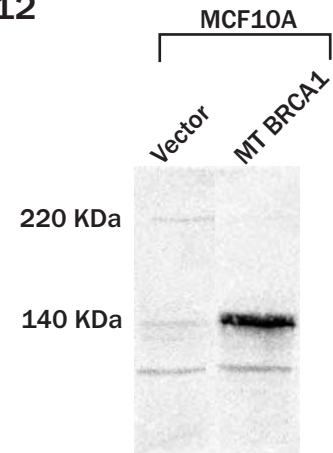
S10



S11



S12



Supplemental Figure 6. Exogenous HoxA10 expression in MDA-231 breast tumor cells. Semi-Q-PCR gel (left) and immunoblot (right) showing levels of HoxA10 RNA and protein achieved upon re-expression in MDA-231 breast tumor cells. Lack of chemiluminescent signal in HoxD10 lysates demonstrates the specificity of the HoxA10 antibody.

Supplemental Figure 7. HoxA10 expression in mammary epithelial tumor cells does not reduce rBM colony growth. Phase contrast images of MDA-231 mammary epithelial tumor cells expressing a vector control, HoxA9 or HoxA10 transgene showing that growth inhibition within a 3D rBM is HoxA9 specific. Bar equals 50 μ m.

Supplemental Figure 8. HoxA9 regulates BRCA1 expression. Image of semi-Q-PCR gel showing HoxA9-mediated induction of BRCA1 mRNA in breast tumor cells (left) and immunoblot image showing increased BRCA1 protein in breast tumor cells re-expressing HoxA9.

Supplemental Figure 9. Mutational analysis of putative HoxA9 binding sites. Luciferase reporter analysis showing continued responsiveness of BRCA1 promoter constructs to addition of wild-type HoxA9 when single putative HoxA9 binding sites are deleted (Δ -221 to -218, Δ -175 to -172, and Δ -12 to -9) that is comparable to the activation of the full length BRCA1 promoter construct (compare gray bars). Data are normalized to matched vector control (black bars). Negative numbers refer to basepairs upstream of the BRCA1 transcription start site (Xu et al., 1995).

Supplemental Figure 10. shRNA mediated HoxA9 knockdown. Q-RT-PCR analysis of HoxA9 RNA levels in nonmalignant MCF10A mammary epithelial cells expressing a vector control shRNA construct or a HoxA9 shRNA clone.

Supplemental Figure 11. Nonmalignant mammary epithelial cells lacking HoxA9 expression can not upregulate BRCA1 in response to stress. Q-RT-PCR analysis of BRCA1 levels in MCF10A cells expressing wild-type levels of HoxA9 or reduced HoxA9 levels resultant of shRNA knockdown before and after exposure to stress.

Supplemental Figure 12. The BRCA1 Δ exon11b mutant functions as a dominant negative mutant. Immunoblot demonstrating that exogenous expression of BRCA1 Δ exon11b (140KDa) in nonmalignant MCF10A cells completely abrogates levels of wild-type BRCA1 (220KDa) suggesting the BRCA1 mutant functions as a dominant negative.

Supplemental Table 1

Tumor ID	1	2	3	4	5
Diagnosis*	IDC	IDC	IDC	IDC	IDC
Max. Diameter (cm)	2.6	4.9	1.9	1.5	2.0
Nuclear Grade	HIGH	HIGH	HIGH	HIGH	HIGH
Histologic Grade	HIGH	HIGH	HIGH	HIGH	HIGH
Estrogen Receptor Status	NEG	ND	NEG	NEG	NEG

*IDC-Infiltrating Ductal Carcinoma

Supplemental Table 1. Tumor characteristics of matched normal-tumor pairs analyzed by global expression profiling.

Supplemental Table 2

Fold Change^a	Gene	Description
Transcripts upregulated in the tumor compared to the matched normal adjacent tissue in at least 4 out of 5 samples		
2.5	<i>PFN2</i>	Profilin 2
3.2	<i>TACSTD1</i>	Tumor-associated calcium signal transducer 1
3.2	<i>KRT7</i>	Keratin 7
3.5	<i>MTHFD2</i>	Mitochondrial methylene tetrahydrofolate dehydrogenase
3.7	<i>CCNB2</i>	Cyclin B2
6.1	<i>STAT1</i>	Signal transducer and activator of transcription 1
9.4	<i>COL11A1</i>	Collagen, type XI, alpha 1
11	<i>H2AFA</i>	H2A histone family, member A
12.9	<i>MUC1</i>	Mucin 1
48.6	<i>SI00BPP</i>	S-100 calcium binding protein B
Transcripts downregulated in the tumor compared to the matched normal adjacent tissue in at least 4 out of 5 samples		
-2.5	<i>TGFBR2</i>	Transforming growth factor beta receptor 2
-2.8	<i>GAS1</i>	Growth arrest specific 1
-3.1	<i>HOXA4</i>	<u>Homeobox A4</u>
-3.1	<i>ID1</i>	Inhibitor of DNA binding 1
-3.5	<i>SEMA3C</i>	Semaphorin 3C
-3.7	<i>MEOX2</i>	Mesenchyme homeobox 2
-4.2	<i>PECAM1</i>	Platelet/endothelial cell adhesion molecule 1
-4.4	<i>HOXA9</i>	<u>Homeobox A9</u>
-6.1	<i>JAM3</i>	Junctional adhesion molecule 3
-6.5	<i>RAPGEF</i>	Rap1 guanine-nucleotide-exchange factor
-7.6	<i>VWF</i>	von Willebrand factor
-7.7	<i>ABC1</i>	ATP-binding cassette 1
-8.4	<i>DUSP1</i>	Dual specificity phosphatase 1
-9	<i>Col17A1</i>	Collagen, type XVII
-10.5	<i>CXCL12</i>	Chemokine ligand 12 (<i>SDF1</i>)
-11	<i>MEOX1</i>	Mesenchyme homeobox 1
-11.8	<i>AQP1</i>	Aquaporin 1
-13.9	<i>FHL1</i>	Four and a half LIM domains 1
-14.5	<i>ITGA7</i>	Integrin alpha 7
-21.4	<i>CLDN5</i>	Claudin 5
-23.4	<i>FABP4</i>	Fatty acid binding protein 4
-26.9	<i>CNN1</i>	Calponin 1, basic, smooth muscle
-28.5	<i>ADH1C</i>	Alcohol dehydrogenase 1C
-34.7	<i>CCR5</i>	Chemokine receptor 5
-45.2	<i>c-fos</i>	Fos proto-oncogene

^a*p*-value ≤0.01

Supplemental Table 2. Select genes from a Rosetta-Resolver™ generated list of transcripts significantly altered in at least 4 out of 5 sets of matched tumor and normal adjacent tissue pairs.

Supplemental Table 3

Clinical parameters related to reduced HoxA9 mRNA levels in human breast cancers	n	P value	Reference
breast cancer vs. normal breast	47	0.0000014	Richardson, et al. Cancer Cell. 2006 Feb;9(2):121-32.
	10	0.002	Turashvili et al. BMC Cancer. 2007 Mar 27;7:55.
high grade breast cancers	278	0.000091	Bittner, et al. https://expo.intgen.org/expo/public/2005/01/15
	172	0.006	Soritrou et al. J Natl Cancer Inst. 2006 Feb 15;98(4):262-72.
	55	0.018	Ginestier et al. Clin Cancer Res. 2006 Aug 1;12(15):4533-44.
	249	0.018	Miller et al. Proc Natl Acad Sci U S A. 2005 Sep 20;102(38):13550-5.
	249	0.023	Ivshina et al. Cancer Res. 2006 Nov 1;66(21):10292-301.
	60	0.03	Ma et al. Cancer Cell. 2004 Jun;5(6):607-16.
high stage breasts cancers	244	0.00047	Bittner, et al. https://expo.intgen.org/expo/public/2005/01/15
tumors with complete response vs. residual disease	51	0.002	Hess et al. J Clin Oncol. 2006 Sep 10;24(26):4236-44.
tumors sensitive to docetaxel	24	0.003	Chang et al. Lancet. 2003 Aug 2;362(9381):362-9.
tumors with lymph node involvement (N3)	194	0.005	Bittner, et al. https://expo.intgen.org/expo/public/2005/01/15
large (T4) tumors	285	0.021	Bittner, et al. https://expo.intgen.org/expo/public/2005/01/15
tumors associated with distant metastasis	189	0.03	Desmedt et al. Clin Cancer Res. 2007 Jun 1;13(11):3207-14.
< 5 year survival	159	0.038	Pawitan et al. Breast Cancer Res. 2005;7(6):R953-64.

Supplemental Table 3. Clinical parameters related to reduced HoxA9 mRNA levels in human breast cancers.

Supplemental Table 4

Multivariate analysis for relapse-free and overall survival according to HOXA9 transcript expression and clinical characteristics in breast cancer patients				
Variable	Death		Relapse	
	Hazard Ratio (95% CI)	P Value	Hazard Ratio (95% CI)	P Value
HOXA9	0.892 (0.645-1.234)	0.49	1.083 (0.904-1.297)	0.39
Age (per 10-yr increment)	0.638 (0.43-0.946)	0.025	0.578 (0.407-0.822)	0.002
Tumor size (per cm)	1.245 (0.965-1.606)	0.092	1.238 (0.987-1.552)	0.065
<u>Tumor grade</u>				
<i>Grade 2 vs. grade 1</i>	4.063 (1.395-11.829)	0.01	2.387 (1.196-4.767)	0.014
<i>Grade 3 vs. grade 1</i>	5.31 (1.812-15.561)	0.002	3.018 (1.485-6.136)	0.002
Positive vs. negative LN status	1.465 (0.735-2.921)	0.278	1.534 (0.841-2.797)	0.163
Positive vs. negative ER status	0.73 (0.369-1.444)	0.366	1.076 (0.577-2.005)	0.818
Chemotherapy vs. no chemotherapy	0.592 (0.286-1.224)	0.157	0.544 (0.29-1.02)	0.058
Hormonal treatment vs. no treatment	0.751 (0.304-1.855)	0.535	0.663 (0.303-1.449)	0.303
Mastectomy vs. breast-conserving therapy	1.208 (0.747-1.954)	0.44	1.208 (0.794-1.837)	0.378
<u>Molecular subtype</u>				
<i>Normal-like & luminal B vs. luminal A</i>	1.541 (0.729-3.258)	0.258	1.372 (0.771-2.442)	0.281
<i>Basal & ERBB2+ vs. luminal A</i>	2.508 (1.057-5.949)	0.037	1.796 (0.9-3.587)	0.097

This Cox regression analysis included the 295 breast cancer patients in the Netherlands Cancer Institute (NCI) dataset. HOXA9 transcript expression, age and tumor size were modeled as continuous variables. CI denotes confidence interval.

Supplemental Table 4. Multivariate analysis for relapse-free and overall survival according to HOXA9 transcript expression and clinical characteristics in breast cancer patients.

Supplemental Table 5

Multivariate analysis for relapse-free and overall survival according to HOXA9 transcript expression and clinical characteristics in ER-positive breast cancer patients				
Variable	Death		Relapse	
	Hazard Ratio (95% CI)	P Value	Hazard Ratio (95% CI)	P Value
HOXA9	1.185 (0.91-1.541)	0.208	1.227 (1.045-1.439)	0.012
Age (per 10-yr increment)	0.615 (0.341-1.109)	0.106	0.527 (0.331-0.842)	0.007
Tumor size (per cm)	1.174 (0.832-1.658)	0.361	1.177 (0.896-1.546)	0.242
<u>Tumor grade</u>				
<i>Grade 2 vs. grade 1</i>	3.38 (1.123-10.172)	0.03	2.185 (1.075-4.445)	0.031
<i>Grade 3 vs. grade 1</i>	6.215 (2.063-18.718)	0.001	3.254 (1.559-6.792)	0.002
Positive vs. negative LN status	2.366 (0.995-5.628)	0.051	2.061 (1.011-4.201)	0.046
Chemotherapy vs. no chemotherapy	0.341 (0.137-0.844)	0.02	0.385 (0.185-0.802)	0.011
Hormonal treatment vs. no treatment	0.753 (0.239-2.373)	0.628	0.662 (0.265-1.656)	0.378
Mastectomy vs. breast-conserving therapy	1.283 (0.678-2.428)	0.444	1.377 (0.821-2.312)	0.225
<u>Molecular subtype</u>				
<i>Normal-like & luminal B vs. luminal A</i>	1.734 (0.804-3.74)	0.161	1.516 (0.843-2.726)	0.165
<i>Basal & ERBB2+ vs. luminal A</i>	2.309 (0.883-6.043)	0.088	1.608 (0.754-3.432)	0.219

This Cox regression analysis included the 226 ER-positive breast cancer patients in the Netherlands Cancer Institute (NCI) dataset. HOXA9 transcript expression, age and tumor size were modeled as continuous variables. CI denotes confidence interval.

Supplemental Table 5. Multivariate analysis for relapse-free and overall survival according to HOXA9 transcript expression and clinical characteristics in ER-positive breast cancer patients.

Supplemental Table 6

Signal Log Ratio	Fold Change ^a	Gene	Description
Transcripts decreased after <i>HoxA9</i> induction			
-4.2	-17.6	<i>NBR2</i>	Next to <u>BRCA1 gene 2</u>
-4.0	-16.0	<i>TOM1</i>	Target of Myb1
-3.7	-13.7	<i>CDK5R1</i>	Regulatory subunit of cyclin-dependent kinase 5
-3.7	-13.7	<i>DMXL1</i>	DmX-Like 1 regulatory protein
-3.5	-12.3	<i>RENT2</i>	Nuclear export protein
Transcripts increased after <i>HoxA9</i> induction			
1.0	+2.0	<i>HoxA9</i>	Homeobox domain protein A9
1.0	+2.0	<i>CDK9</i>	Cyclin-dependent protein kinase 9
1.3	+2.5	<i>MYB</i>	MYB oncogene
1.5	+2.8	<i>NDRG2</i>	N-myc downstream-regulated gene2
1.9	+3.7	<i>CSN1</i>	Alpha S1-casein
1.9	+3.7	<i>ACVR2</i>	Activin 2 (TGF-beta superfamily)
2.2	+4.6	<i>CDK8</i>	Cyclin-dependent protein kinase 8
2.4	+5.3	<i>MUC5B</i>	Mucin 5B
2.5	+5.7	<i>RAP2A</i>	RAS-related protein 2A
2.6	+6.0	<i>PCDH9</i>	Protocadherin 9
2.7	+7.3	<i>PRKCBP2</i>	Protein kinase C-binding protein RACK17
2.9	+8.4	<i>PTEN</i>	Dual specificity phosphatase
3.1	+9.6	<i>WNT10B</i>	Wingless-type MMTV integration site 10B
3.1	+9.6	<i>BMP1</i>	Bone morphogenetic protein 1
3.2	+10.2	<i>COL1A2</i>	Collagen alpha-2 type I
3.3	+10.9	<i>NEO1</i>	Member of NCAM cell adhesion family
3.3	+10.9	<i>MMP1</i>	Matrix metalloproteinase 1
4.1	+16.8	<i>MUC1</i>	Mucin 1
4.1	+16.8	<i>ERBB3</i>	Epidermal growth factor receptor 3 (HER3)
4.6	+21.1	<i>BRCA1</i>	BRCA1 Cancer-related gene 1

^aFold change is expressed as \log^2 of the signal log ratio calculated by Affymetrix Analysis Suite 5.0
 p -values ≤ 0.001

Supplemental Table 6. Selected gene expression differences following *HoxA9* induction in MDA-MB-231 cells.

Supplemental Experimental Procedures

CDNA Constructs and Vectors

Full length FLAG tagged murine HoxA9 (1) (99% homology to human) was PCR amplified from PRC-CMV-FLAG HoxA9 (gift, C.Largman, UCSF, San Francisco, CA.) using forward T7 and reverse *mur HoxA9-NotI* 5' GAT CGC GGC CGC TAA GCC CAA ATG GCA TCA 3' primers and subsequently subcloned into the *Sall-NotI* vector fragment of the Hermes HRS puro IRES eGFP retroviral plasmid (2) (gift, H.Blau, Stanford, CA). The *Sall-NotI* FLAG tagged HoxA9 fragment from Hermes HRS puro Hox9 IRES eGFP was replaced with an HA tagged murine HoxA9 PCR product amplified from pHRS-puro-Flag-HoxA9-ires-eGFP using forward primer *BamHI-Sall-HA-mur-HoxA9* 5' GCG GGA TCC GTC GAC CCA CCA TGG GCT ACC CCT ACG ACG TGC CCG ACT ACG CCA TGG CCA CCA CCG GGG CCC T 3' and reverse primer *mur HoxA9-NotI*. pcDNA3.1 HA HoxA9 was derived by cloning the HA tagged murine HoxA9 PCR product into the *BamHI-NotI* vector fragment of pcDNA3.1 (Invitrogen). Full length wild-type HA tagged BRCA1 (3) (gift, F.Rauscher, Wistar Institute, Philadelphia, PA) in the pcDNA3.1 vector was partially digested with *BamHI-KpnI* or *KpnI-NotI* to obtain the HA tagged 5' end or 3' end of BRCA1. Hermes HRS puro IRES eGFP was partially digested with *NotI-XbaI* to obtain the IRES-eGFP fragment. All three fragments were ligated into the Hermes HRS puro IRES eGFP *BamHI-NotI* vector fragment. pcDNA3.1 HA tagged BRCA1 Δ exon 11b (3) (gift, F.Rauscher, Wistar Institute, Philadelphia, PA) was digested with *BamHI-NotI* and cloned into the *BamHI-XbaI* vector fragment of Hermes HRS neo IRES eGFP together with the *NotI-XbaI* IRES-eGFP fragment (described above). The pGL2 BRCA1 luciferase plasmid (4) (gift, L.A. Chodosh, UPENN, Philadelphia, PA.) was used directly. The pGL2 BRCA1 luciferase mutants were generated by PCR amplification using *Pfu* turbo polymerase

(Stratagene; La Jolla, CA) and the following primer pairs: Δ -223 to +44 forward 5' GCG CGA TAT CTG CCT GCC CTC TAG CCT CTA CTC TTC 3' and Δ -223 to +44 reverse 5'GCG CGA TAT CCG GGG GAC AGG CTG TGG GGT TTC TCA 3', Δ -221 to -218 forward 5' GCG CGA TAT CGC AAA CTC AGG TAG AAT TCT TCC TC 3' and Δ -221 to -218 reverse 5' GCG CGA TAT CCT GCC CTC TAG CCT CTA CTC TTC CAG 3', Δ -175 to -172 forward 5' GCG CGA TAT CTC ATC CGG GGG CAG ACT GGG TGG CCA 3' and Δ -175 to -172 reverse 5'GCG CGA TAT CAA GAG ACG GAA GAG GAA GAA TTC TAC 3', Δ -12 to -9 forward 5' GCG CGA TAT CGA TAA ATT AAA ACT GCG ACT GCG CGG 3' and Δ -12 to -9 reverse 5'GCG CGA TAT CGC GCT TTT CCG TTG CCA CGG AAA CCA 3'. pcDNA3.1-SEAP was generated by cloning the *EcoRI-XbaI* SEAP fragment from pGRE-SEAP (Clontech, Mountain View, CA) into the *EcoRI-XbaI* vector fragment of pcDNA3.1-eGFP (Invitrogen). CMV-PBX1 was used directly (5). pcDNA3.1 HA-HoxA9 DNA binding mutant was generated by PCR amplification using *Pfu* turbo polymerase (Stratagene) and the following primer pair: 5'GGC AGG TCA AGA TCT GGT TCC AGA CCC GCA GGA TGA AAA TGA AGA AAA TCA 3' and 5'ATT TTC TTC ATT TTC ATC CTG CGG GTC TGG AAC CAG ATC TTG ACC TGC CTT TC 3'. HoxA10 cDNA (gift, J.Lawrence, San Francisco, CA) was excised from pBluescript and subcloned into the *EcoR1* restriction site of the pLXSN (Clontech) retroviral vector. Orientation was confirmed by Big DyeTM terminator analysis (PE Biosystems, Foster City, CA) at the UCSF Biomolecular Core facility. pLKO.1-puro-luciferase shRNA and BRCA1 shRNA lentiviral plasmids were used directly (Sigma-Aldrich, MISSIONTM TRC-Hs1.0)(6). The following MISSIONTM human BRCA1 shRNA clones were screened: TRCN0000039833 (#1), TRCN0000039834 (#2), TRCN0000039835 (#3), TRCN0000039836 (#4), TRCN0000039837 (#5). The following MISSIONTM murine HoxA9 shRNA clones were

screened: TRCN0000012508 (#1), TRCN0000012509 (#2), TRCN0000012510 (#3), TRCN0000012511 (#4), TRCN0000012512 (#5). The pMD2.G and pCMVΔR8.91 packaging plasmids were used directly (gift, D. Trono, Lausanne, Switzerland) (7). All plasmids were confirmed by restriction and sequence analysis.

Demethylation Reactivation Assay

Cells were plated at low density in 6-well plates in duplicate on day 0. On day 1, 5-aza 2'-deoxycytidine (Sigma-Aldrich) was added to final concentrations of 0, 1.0 and 10 μM in media containing 5% fetal bovine serum. On day three, the media was changed and fresh 5-aza 2'-deoxycytidine was added. On day 4, cells were harvested by trypsinization and washed. Total RNA was isolated using TRIzol™ (Life Technologies) followed by RNeasy™ (Qiagen) clean up. *HOXA9* transcript levels were determined following treatment using Q-RT-PCR as described.

Lentiviral Infection

Lentiviral particles were produced, harvested, and used to infect target cells as previously described (8).

Multispectral image analysis.

Immunohistochemistry slides were examined using a Leica DMRA2 microscope (Leica Microsystems Inc., Bannockburn, IL) equipped with plan apochromatic lenses. Fields containing tumor or normal tissues were imaged at 40X magnification through a liquid crystal filter using the Nuance Multispectral Imaging System (Cambridge Research and Instrumentation Inc., Woburn, MA). The spectromicroscopic system is linked to a CCD camera and a PC. The MSI system was used at full chip resolution, without data binning. Spectral data was acquired from 420-720 nm in 20 nm increments. Spectral unmixing was accomplished by using Nuance

software v1.42 using pure spectral libraries of individual chromagens (slides stained with only DAB, VIP, or hematoxylin). Images were then evaluated for the presence of BRCA1, HoxA9 or both in normal epithelium or tumor cells using unmixed images from the Nuance system.

Supplemental References

1. Shen, W.F., Rozenfeld, S., Kwong, A., Kom ves, L.G., Lawrence, H.J., and Largman, C. 1999. HOXA9 forms triple complexes with PBX2 and MEIS1 in myeloid cells. *Mol Cell Biol* 19:3051-3061.
2. Rossi, F.M., Guicherit, O.M., Spicher, A., Kringstein, A.M., Fatyol, K., Blakely, B.T., and Blau, H.M. 1998. Tetracycline-regulatable factors with distinct dimerization domains allow reversible growth inhibition by p16. *Nat Genet* 20:389-393.
3. Wilson, C.A., Payton, M.N., Elliott, G.S., Buaas, F.W., Cajulis, E.E., Grosshans, D., Ramos, L., Reese, D.M., Slamon, D.J., and Calzone, F.J. 1997. Differential subcellular localization, expression and biological toxicity of BRCA1 and the splice variant BRCA1-delta11b. *Oncogene* 14:1-16.
4. Thakur, S., and Croce, C.M. 1999. Positive regulation of the BRCA1 promoter. *J Biol Chem* 274:8837-8843.
5. Charboneau, A., East, L., Mulholland, N., Rohde, M., and Boudreau, N. 2005. Pbx1 is required for Hox D3-mediated angiogenesis. *Angiogenesis* 8:289-296.
6. Moffat, J., Grueneberg, D.A., Yang, X., Kim, S.Y., Kloepfer, A.M., Hinkle, G., Piqani, B., Eisenhaure, T.M., Luo, B., Grenier, J.K., et al. 2006. A lentiviral RNAi library for human and mouse genes applied to an arrayed viral high-content screen. *Cell* 124:1283-1298.
7. Yu, S.F., von Ruden, T., Kantoff, P.W., Garber, C., Seiberg, M., Ruther, U., Anderson, W.F., Wagner, E.F., and Gilboa, E. 1986. Self-inactivating retroviral vectors designed for transfer of whole genes into mammalian cells. *Proc Natl Acad Sci U S A* 83:3194-3198.

8. Zufferey, R., Dull, T., Mandel, R.J., Bukovsky, A., Quiroz, D., Naldini, L., and Trono, D. 1998. Self-inactivating lentivirus vector for safe and efficient in vivo gene delivery. *J Virol* 72:9873-9880.

ASCB 48th Annual Meeting 2008

Deconstructing the 3rd Dimension: How matrix dimensionality promotes survival.

C. Frantz¹, J. Friedland², J. Lakins¹, W. Liu², J. Chernoff³, M. Schwartz⁴, C. Chen², D. Boettiger², V.M. Weaver^{1,2}; ¹Department of Surgery and Center for Bioengineering and Tissue Regeneration, University of California, San Francisco, CA, ²Department of Bioengineering and Institute for Medicine and Engineering, University of Pennsylvania, Philadelphia, PA, ³Fox Chase Cancer Center, ⁴Department of Biochemistry, University of Virginia, Charlottesville, VA

Cancer metastasis depends upon the dissemination of isolated tumor cells into a three dimensional (3D) parenchyma and their subsequent survival in distal tissues. At present information about the molecular mechanisms regulating cell survival have largely been deduced by studying the behavior of cells on two dimensional (2D) matrices. To clarify how tumor cells might survive within a 3D microenvironment we assessed the effect of cell shape and matrix spreading and integrin-dependent adhesion on the survival of isolated mammary epithelial cells (MECs) in 2D versus 3D. Provocatively, we could show that MEC viability is sustained by laminin ligation of $\alpha6\beta4$ integrin and Rac-dependent Pak activity in round, non-spread MECs in 3D, but not in 2D. Conversely, we determined that laminin-dependent growth and survival of MECs depends upon $\beta1$ integrin ligation and ERK and PI3Kinase activity in spread MECs in 2D, but not in 3D. Such differential survival mechanisms could be attributed to enhanced GTP loading of Rac and Arf6 and reduced Rac-dependent ROS and MMP activation in 3D. Experiments revealed that elevated Arf6 GTPase activity promotes MEC survival by enhancing Rac-Pak signaling and reducing Rac-NADPH-ROS production. Because MECs interacting with laminin in 3D showed pronounced changes in cytoskeletal organization and cell size and shape, studies are in progress to test whether matrix presentation could modulate Arf6-dependent cell fate by influencing membrane curvature, protein trafficking or actin remodeling and if so how. (Supp: 7R01CA078731-07, W81XWH-05-1-330 and RS1-00449 to VMW).

ASCB 48th Annual Meeting 2008

Evidence of Durotaxis in Transformed Mammary Epithelial Cells.

J. Lopez, V. Weaver; UCSF, San Francisco, CA

The movement of cells in the direction of a stiffness gradient termed durotaxis has been demonstrated in recent years in fibroblasts and vascular endothelial cells. Here we present evidence that transformed mammary epithelial cells (MECs) respond to durotactic gradients. We explore this phenomenon in a 2D environment using gels of precisely calibrated stiffness as well as gels demonstrating a gradient of stiffness. MECs migrating along stiffer matrices display increased speed while also moving in the direction of stiffer substrates. We generated stiffness maps of mammary gland tumors derived from MMTV-PyV mT transgenic mice using atomic force microscopy. We found that the area surrounding the tumor vasculature and the invading front of the tumors are stiffer than the surrounding tissue. These areas may serve as a directional route by which transformed epithelial cells exit away from the primary site. (Support: DODWX81XWH-05-1-0330)

ASCB 48th Annual Meeting 2008

Analysis of MCF10A mammary epithelial cell acinar morphogenesis within a well-defined 3-dimensional system, the self assembling peptides

Miroshnikova, Y.A.¹, Frantz, C.², Leight J.L.³, Johnson, K.R.³, Jorgens, D.M.⁴, Auer, M.⁴, Spirio, L.⁵, Sieminski, A.L.¹, Weaver V.M.². ¹ Olin College Of Engineering, Needham, MA, ² University of California, San Francisco, San Francisco, CA, ³ University of Pennsylvania, Philadelphia, PA, ⁴ University of California, Berkeley, Berkeley, CA, ⁵ PuraMatrix/ 3DM Inc., Cambridge, MA

Epithelial tissue morphogenesis proceeds within the context of a three dimensional (3D) extracellular matrix (ECM). Accordingly, to clarify the molecular basis of tissue-specific differentiation and disease, a variety of 3D systems exploiting natural ECMs have been developed, such as reconstituted basement membrane (rBM) and purified collagen hydrogels. These natural hydrogels recapitulate epithelial tissue architecture and behaviors in vitro with reasonable fidelity. Nevertheless, natural matrices suffer from considerable preparation variability and remain poorly defined biochemically and biophysically. In addition, the methods to study and manipulate epithelial cell behavior in 3D, as well as the definition of 3D, vary appreciably between and even within laboratories. To understand epithelial cell biology requires defined biomaterials in which biochemical, topological and biophysical properties can be systematically varied. Towards this goal we used the nonmalignant MCF10A mammary epithelial cell (MEC) line and conducted a systematic analysis of acinar morphogenesis using the natural hydrogels collagen type I and rBM and three synthetic matrices: rBM-conjugated poly acrylamide gels, self assembling peptide gels (PuraMatrix) with and without rBM and hyaluronic acid gels with and without rBM. We assessed acini formation, cell growth and death and colony integrity and heterogeneity of MECs either fully embedded within these natural and synthetic gels compared to those receiving a matrix overlay or pseudo 3D matrix cue. All biomaterials supported acinar morphogenesis and yielded viable polarized, growth-arrested MEC structures with cell-cell adherens junctions and deposition of endogenous BM proteins, however, optimal growth control, survival and lumen formation, as well as colony integrity and homogeneity were observed when cells were completely embedded within the ECM and when ECM remodeling was permitted. Consequently, optimal acinar morphogenesis was observed using rBM, collagen I and PuraMatrix. Rigorous, morphometric and quantitative analysis as well as immunohistochemistry, and electron microscopy are in progress. (Supp: NIH 7R01CA078731-07, DOD W81XWH-05-1-330, CIRM RS1-00449, and DOE A107165 to VMW).

ASCB 48th Annual Meeting 2008

HoxA9 Regulates Stromal-Mammary Epithelial Interactions through Modulation of BRCA1 Expression.

J. Mouw^{3,4}, P. Gilbert^{1,2}, M. Unger⁵, J. Lakins^{1,3,4}, M. Gbegenon¹, M. Nuth¹, V. Clemmer⁶, T. Colligan⁵, M. Benezra⁷, J. Licht⁷, M. Feldman¹, N. Boudreau³, B. Weber^{5,8}, V. Weaver^{1,3,4}; ¹IME/Pathology and Lab Medicine, UPENN, Philadelphia, PA, ²Current: Department of Microbiology and Immunology/Baxter Laboratories, Stanford University, Stanford, CA, ³Department of Surgery and Anatomy, UCSF, San Francisco, CA, ⁴Center

for Bioengineering and Tissue Regeneration, UCSF, San Francisco, CA, ⁵Abramson Family Cancer Research Institute, UPENN, Philadelphia, PA, ⁶St. Francis Hospital, Wilmington, DE, ⁷Mount Sinai School of Medicine, New York, NY, ⁸Current: GlaxoSmithKline, Philadelphia, PA.

Stromal-epithelial interactions drive development and maintain tissue homeostasis through a network of soluble and insoluble factors that operate within a three-dimensional (3D) tissue. Genetic and epigenetic changes in mammary epithelial cells (MECs) cooperate with a modified tissue microenvironment to drive malignant transformation of the breast. Hox genes play a critical role in tissue development, and tumors often express altered levels of homeobox genes although the significance of this observation to tumor progression is unclear. Using global expression analysis of matched tumor/normal human breast tissues we found that expression of the homeobox gene HoxA9 was significantly lower in tumors. Q-RT-PCR, in situ, and immunohistochemical analysis revealed that HoxA9 was primarily expressed in the breast epithelium and significantly reduced in a cohort of primary breast tumors and aggressive breast cancer cell lines. Normalizing HoxA9 levels increased BRCA1 expression in breast tumor cells and repressed their growth and survival and reverted their malignant behavior in a three dimensional basement membrane assay and in vivo. Knocking down HoxA9 using shRNA reduced BRCA1 levels and enhanced the growth and survival and disrupted the acinar morphogenesis of nonmalignant mammary epithelial cells. HoxA9 consensus binding sequences were identified in the BRCA1 promoter and confirmed by ChIP and luciferase analysis and validated by mutational studies. Expression of a wild-type BRCA1 or a BRCA1 mutant phenocopied the HoxA9-dependent inhibition of the breast cancer cells, and shRNA knockdown of BRCA1 or co-expression of the BRCA1 mutant promoted growth and disrupted acinar morphogenesis of nonmalignant mammary epithelial cells. Because compromising BRCA1 function prevented HoxA9 from reverting the malignant behavior of breast tumor cells in culture and in vivo, we suggest that HoxA9 could regulate breast tumor progression by normalizing stromal-epithelial interactions through modulation of BRCA1 expression. Our results offer a plausible explanation for why sporadic breast cancers often have decreased BRCA1 expression even in the absence of genetic deletions, methylation or haplo insufficiency.

(Support: DODWX81XWH-05-1-0330)

ASCB 48th Annual Meeting 2008

An Integrated Response Mechanism That Encompasses Cell and Extracellular Matrix Mechanics Regulates Integrin Binding Cooperativity, Clustering, and Adhesion Function.

M. J. Paszek^{2,1}, D. Boettiger³, D. A. Hammer², V. Weaver^{1,2}; ¹Surgery, University of California - San Francisco, San Francisco, CA, ²Bioengineering, University of Pennsylvania, Philadelphia, PA, ³Microbiology, University of Pennsylvania, Philadelphia, PA

Integrins are part of a cellular-environment sensory machine that responds to chemical and physical extracellular matrix (ECM) cues by clustering into adhesion plaques with modified signaling functions. However, the "force sensors" and "molecular cross-linkers" that sense ECM cues to modulate integrin clustering have yet to be identified. We

developed an advanced spatial-temporal simulation that integrates the micro-mechanics of composite elastic materials at the cell-ECM interface with a simple chemical model of integrin activation and ligand interaction. Using this model we show that integrins possess innate properties that permit them to cluster in response to biochemical and biophysical cues received from the ECM. We predict that due to mechanical coupling, integrin-ligand interactions are highly cooperative with Hill coefficients that can approach or exceed those reported for ultra-sensitive signaling cascades. Through this cooperativity, integrin clustering appears to be driven solely by ligand binding interactions, yet remains highly responsive to ECM rigidity and ligand spacing. Use of live cells or “cell-free” plasma membranes interacting with deformable ECM substrates demonstrated that ligand binding is sufficient to trigger integrin clustering provided the ECM is sufficiently rigid. In addition, although we maintain that cytoskeletal forces are likely dispensable for integrin clustering and for interrogating ECM properties, our model nonetheless predicts that small contractile forces invariably augment integrin clustering by enhancing cell and ECM material deformations. Thus we could show that sub-pN forces applied to bound integrin receptors with a spinning disk device could stimulate integrin clustering before discernable recruitment of additional adhesion complex components. We also showed that expression of an auto clustering V737N integrin mutant could recapitulate integrin clustering on a compliant substrate. Provocatively, the model predicts that alterations in cellular and glycocalyx mechanics, as have been documented in metastatic tumor cells, would hypersensitize the integrin adhesion system to changes in ECM dynamics; a possibility we are now testing.

(DOD W81XWH-05-1-330 to VMW & DAH)

ASCB 48th Annual Meeting 2008

Loss of BRM Expression Contributes to a Tumor-Like Phenotype via Enhanced $\alpha 5 \beta 1$ Integrin Expression and Activity.

K. M. Stewart¹, N. Cohet², D. Reisman³, J. Lakins¹, G. I. Rozenberg⁴, A. N. Imbalzano², J. A. Nickerson², V. M. Weaver¹; ¹Surgery, University of San Francisco, San Francisco, CA, ²Cell Biology, University of Massachusetts Medical School, Worcester, MA, ³Internal Medicine, University of Michigan, Ann Arbor, MI, ⁴Genetics, University of North Carolina School of Medicine, Chapel Hill, NC.

$\alpha 5$ integrin and its ligands such as the fibronectin are critical for normal mammary epithelial cell (MEC)-extracellular matrix (ECM) interactions and are commonly perturbed in human breast tumors. In addition, elevated fibronectin levels are associated with breast tumors and the metastatic process. The mechanisms governing $\alpha 5 \beta 1$ expression, however, remain poorly defined. Recent evidence has demonstrated that loss of function of one of the catalytic subunits of the SWI/SNF chromatin remodeling complex, BRG-1, promotes an aggressive metastatic behavior in human fibroblasts via increased expression of $\alpha 5$ and αV integrins. Expressions of BRG-1 and the other SWI/SNF catalytic subunit, BRM, are often reduced or completely lost in tumors, including that of the lung, prostate and breast. Microarray data mining revealed that the mRNA levels of BRM are inversely related to breast tumor grade. We investigated the functional consequences of shRNA-mediated knockdown of BRM on non-transformed MEC behavior through the application of two- and three-dimensional reconstituted

basement membrane (2D and 3D rBM) culture assays. Data showed that loss of BRM expression enhanced adhesion and migratory behavior of MECs grown on 2D extracellular substrata. Additionally, loss of BRM expression perturbed normal tissue morphogenesis of MECs grown within 3D rBM, reflected by a significant increase in colony size, loss of lumen formation, and enhanced secretion and deposition of fibronectin. These data suggest that BRM may play a critical role in modulating MEC-ECM interactions to alter cell behavior in the pathogenesis of breast cancer via regulation of integrin expression. (Support: DODWX81XWH-05-1-0330)

ASCB 48th Annual Meeting 2008

Roles of Collagen Crosslinking and ECM Remodeling in Mammary Tumor

Malignant Transformation.

H. Yu¹, K. Levantal², L. Kass¹, J. Erler⁶, M. Yamauchi⁵, R. Wells⁴, D. Gasser³, V. Weaver^{1,2}; ¹Surgery, UCSF, San Francisco, CA, ²Institute for Medicine and Engineering, University of Pennsylvania, Philadelphia, PA, ³Genetics, University of Pennsylvania, Philadelphia, PA, ⁴Medicine, University of Pennsylvania, Philadelphia, PA, ⁵Dentistry, University of North Carolina at Chapel Hill, Chapel Hill, NC, ⁶Section of Cell and Molecular Biology, Institute of Cancer Research, London, United Kingdom.

In Vivo, cells are maintained in mechanical balanced microenvironments. Previously, we showed ECM stiffness alter cell proliferation, survival and polarity via integrin clustering, focal adhesion maturation, and cell-generated force. Increased tissue stiffness, changes of ECM (e.g. collagen) remodeling and ECM remodeling enzymes (such as MMPs, lysyl oxidase LOX) are strongly associated with breast cancer progression. We therefore hypothesis ECM remodeling affects tumor progression via increasing tissue stiffness. Since crosslinking of collagen I increase its mechanical strength, we tested if collagen crosslinking by Lysyl Oxidase (LOX) etc. affects tumor progression. We xenografted MCF10AT.DCIS into 3T3Lox^{+/+} pre-conditioned mammary fat-pad; we also inhibited the LOX activity in MMTV-Her2/Neu mice (with pharmacological inhibitor and function-blocking antibody). We found collagen I bundle and linearization around MMTVHer2/Neu tumors, and increased stiffness of the tumor were partially corrected by BAPN/mAb treatment; importantly, DCIS cells became invasive in the 3T3.Lox preconditioned fat pad; tumor incidence rate and progression rate of MMTV-Her2/neu mice were reduced by BAPN and LOX-mAb treatment. We found in the LOX inhibited her2/neu tumors, b1-integrin, P130cas, FAKpY397 and PI3Kinase activity decreased while PTEN levels increased. We tested and confirmed ECM stiffness can modulate PTEN level and PI3K activity in the culture system. Thus, collagen crosslinking and substrate stiffness can modulate oncogene effects through PTEN and integrin dependent pathways and thus affect breast cancer progression. (Support: DODWX81XWH-05-1-0330)

Annual BMES Society Meeting

Title: The integrated mechanics of the cell and ECM regulate integrin binding cooperativity and clustering

Authors: Matthew Paszek, David Boettiger, Valerie Weaver, and Dan Hammer

Abstract:

Interactions between integrin adhesion receptors and the extracellular matrix (ECM) regulate important cellular behaviors crucial for tissue development and maintenance. Integrin receptors mediate the cellular response to the ECM by clustering into adhesion plaques in a process that is astonishingly sensitive to both the chemical and physical properties of the ECM. The molecular mechanisms that drive chemo- and mechano-responsive integrin clustering are largely unknown, but most of the proposed strategies involve integrin crosslinking by intracellular scaffolding proteins. Integrin-ligand bond formation, however, is a mechanical interaction, and passive material deformations that are expected to occur in the cell and ECM during bond formation could also contribute to the integrin clustering response. To test this possibility, we developed a spatial-temporal simulation that integrates the chemistry of integrin bond formation with the mechanics of the cellular membrane and actin cortex, the cellular glycocalyx, and the ECM. Due to material deformations, we find that integrin bond formation is a highly cooperative process capable of driving receptor clustering on rigid ECM even in the absence of cytoskeletal crosslinkers. Binding cooperativity, however, is progressively lost on substrates of increasing compliance, and consequently integrin clustering is highly responsive to the mechanical stiffness of the ECM. Chemistry also plays an important role in integrin clustering. For a given set of mechanical parameters, integrin-ECM ligand bond affinity dictates whether or not clustering occurs. Furthermore, integrin clustering exhibits a mechanically-controlled threshold like response to ligand density, indicating a cellular mechanism to determine the physical spacing of ECM ligands. We thus propose a simple passive mechanism cells may use to “sense” important properties of the ECM that does not require complex cellular processes such as acto-myosin contractility. (DOD W81XWH-05-1-330 to VMW & DAH)

Annual BMES Meeting 2008

Collagen remodeling affects mammary tumor progression through PI3K mediated signaling.

Kandice Levantal¹, Hongmei Yu², Inkyung Kang², David Gasser³, Rebecca Wells⁴ and Valerie M. Weaver² 1. Institute for Medicine and Engineering, Univ Penn, Philadelphia, PA, 2. Dept of Surgery, UCSF, San Francisco, CA, 3. Dept of Genetics, Univ Penn, Philadelphia, PA, 4. Depts of Medicine, Univ Penn, Philadelphia, PA

Increased tissue stiffness is strongly associated with breast cancer progression. It is known ECM (e.g. collagen) remodeling and ECM remodeling enzymes (such as MMPs, lysyl oxidase LOX) changes during tumor progression, we hypothesis ECM remodeling can affect tissue stiffness, thus tumor progression. Since crosslinked collagen has increased mechanical strength, we test if collagen crosslinking affects tumor progression. We xenografted MCF10AT.DCIS into 3T3Lox^{+/+} pre-conditioned cleared mammary gland fat-pad; inhibited the LOX activity in MMTV-Her2/Neu mice with LOX pharmacological inhibitor (BAPN) or a functionally blocking monoclonal antibody against LOX. We found that DCIS cells became invasive in the 3T3.Lox^{+/+} preconditioned fat pad; BAPN and LOX-mAb treated MMTV-Her2/neu mice had lower tumor incidence rate and delayed tumor progression than the controls; with second harmonic imaging, we found collagen I bundled and linearized around the normal tumors but not around BAPN/mAb treated tumors. Since increased ECM stiffness enhances cell proliferation, survival by promoting integrin clustering, focal adhesion maturation through ERK, and cell-generated force (Paszek et al., Cancer Cell 2005). We assessed the immunohistology pattern of $\beta 1$ -integrin, P130cas and FAKpY397 in the tissue samples. We found these proteins involved in mechanical sensing decreased in the BAPN/Lox_mAb treated groups; we also found increased PI3Kinase activity, reduced PTEN expression and activity in these samples. Using 3D culture system, we confirmed that increasing ECM stiffness decreased PTEN and increased PI3K activity. Thus, PTEN and integrin activity is involved in collagen crosslinking and the subsequent increased mechanosensing, enhanced tumor progression.
(Supp: 7R01CA078731-07, W81XWH-05-1-330 and RS1-00449 to VMW).

Engineering strategies to recapitulate epithelial morphogenesis using natural and synthetic three dimensional matrices

Miroshnikova, Y.A.¹, Frantz, C.², Leight J.L.³, Johnson, K.R.³, Jorgens, D.M.⁴, Auer, M.⁴, Spirio, L.⁵, Sieminski, A.L.¹, Weaver V.M.^{2,3}

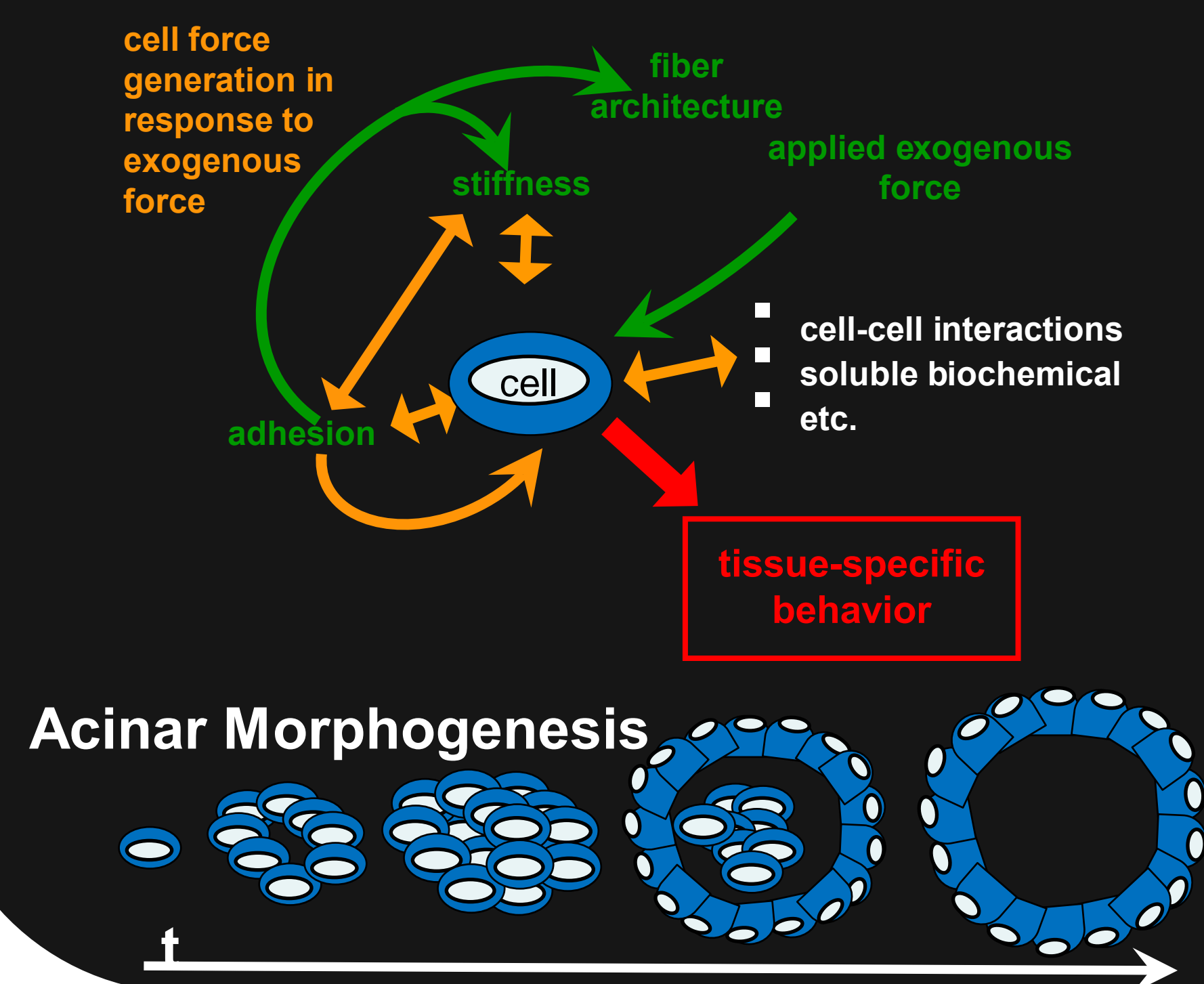
1,2: Olin College Of Engineering, Needham, MA, 2: Department of Surgery, Center for Bioengineering and Tissue Regeneration, University of California, San Francisco, San Francisco, CA, 3: Dept. of Bioengineering and Institute for Medicine and Engineering, University of Pennsylvania, Philadelphia, PA, 4: Lawrence Berkeley National Laboratory, UC Berkeley, Berkeley, CA, 5 PuraMatrix/ 3DM Inc., Cambridge, MA

Abstract

To understand epithelial cell biology requires defined biomaterials in which biochemical, topological and biophysical properties can be systematically varied. Towards this goal we used the nonmalignant MCF10A mammary epithelial cell (MEC) line and conducted a systematic analysis of acinar morphogenesis using the natural hydrogels collagen type I and rBM and three synthetic matrices: rBM-conjugated poly acrylamide gels, self assembling peptide gels (PuraMatrix) with and without rBM and hyaluronic acid gels with and without rBM. We assessed acini formation, cell growth and death and colony integrity and heterogeneity of MECs either fully embedded within these natural and synthetic gels compared to those receiving a matrix overlay or pseudo 3D matrix cue. All biomaterials supported acinar morphogenesis and yielded viable polarized, growth-arrested MEC structures with cell-cell adherens junctions and deposition of endogenous BM proteins, however, optimal growth control, survival and lumen formation, as well as colony integrity and homogeneity were observed when cells were completely embedded within the ECM and when ECM remodeling was permitted. Consequently, optimal acinar morphogenesis was observed using rBM, collagen I and PuraMatrix. Rigorous, morphometric and quantitative analysis as well as immunohistochemistry, and electron microscopy are in progress.

Background and Motivation

Our View of Differentiated Cell Behavior



Acinar Morphogenesis Assessment

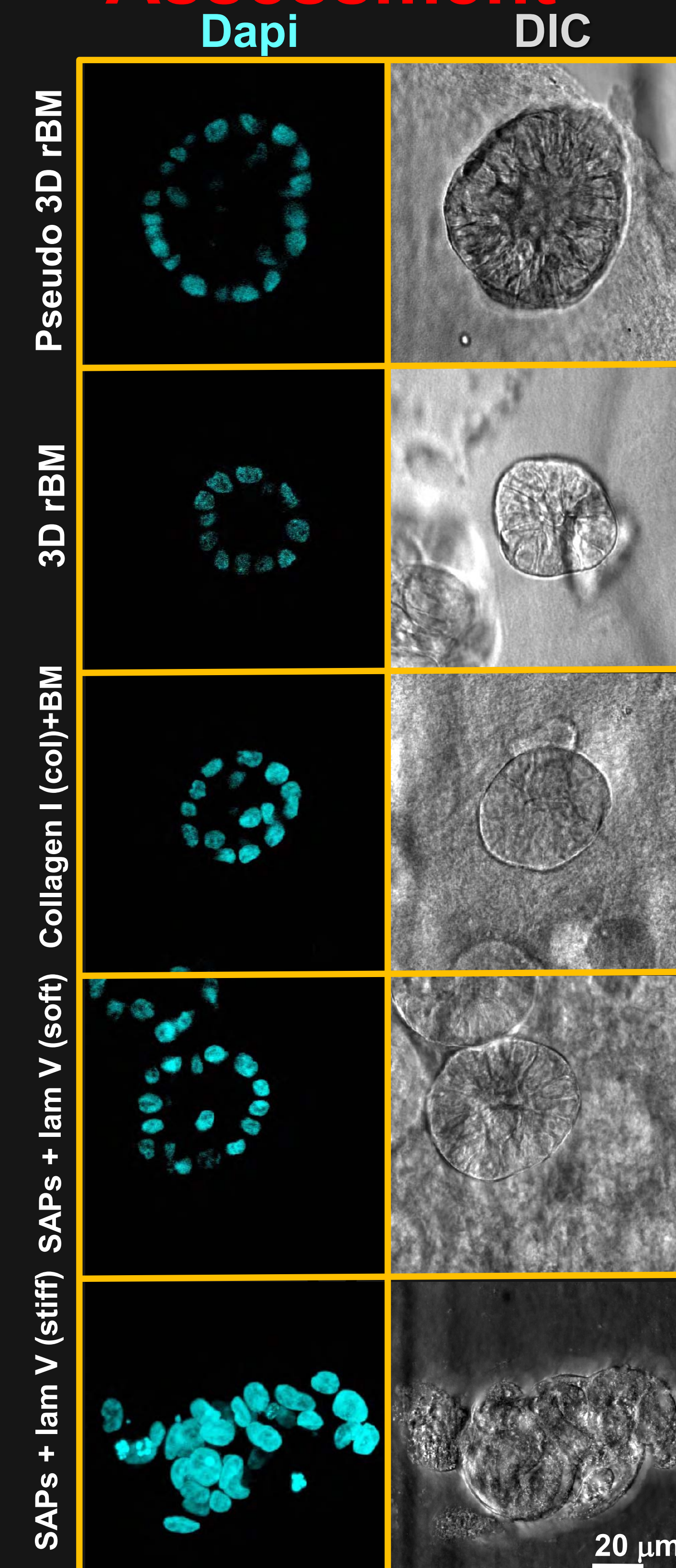
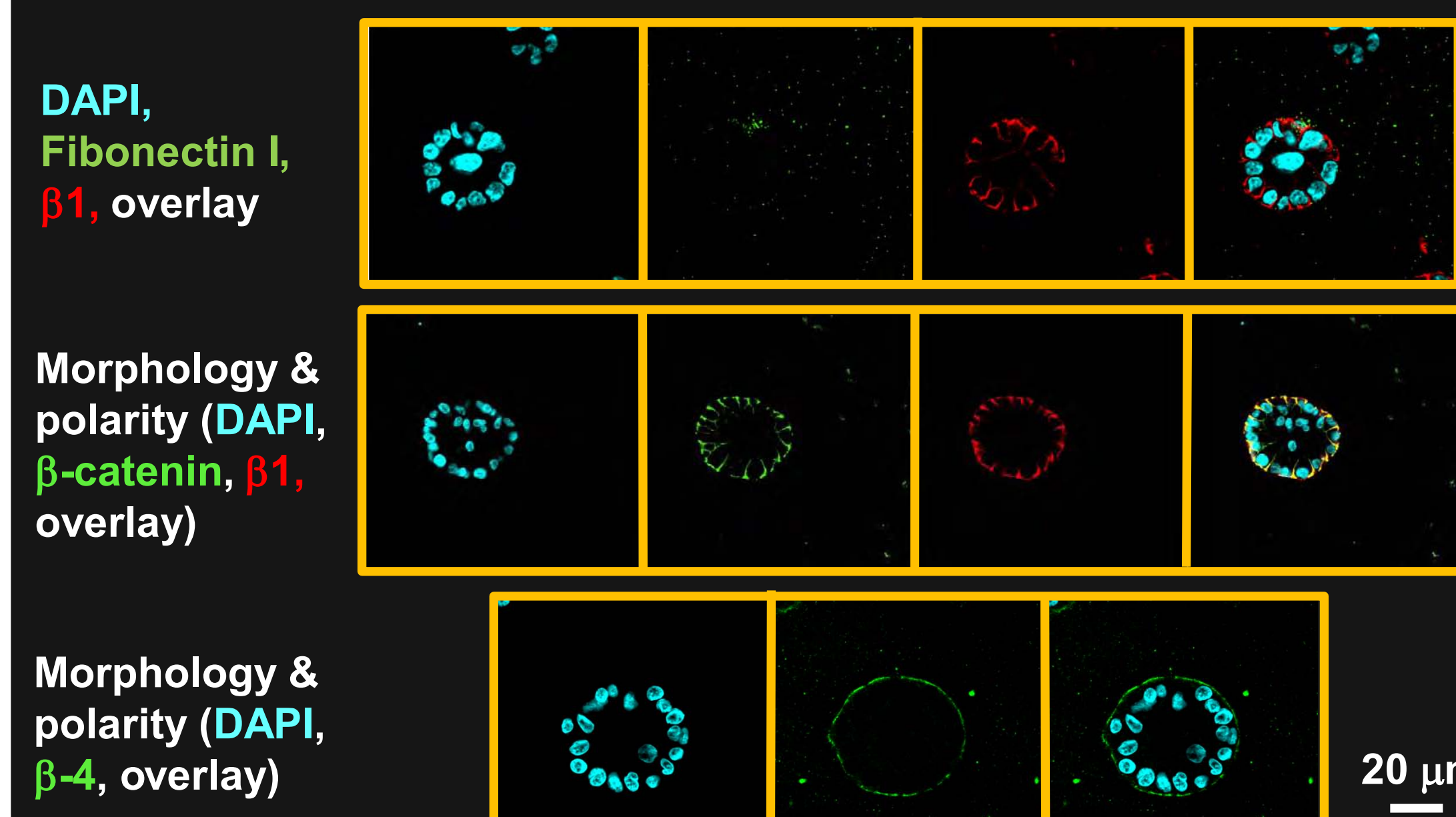


Figure 1. Acinar morphogenesis in natural and synthetic extracellular matrices (ECM). All biomaterials supported acinar morphogenesis and yielded growth-arrested MEC structures. Stiff laminin-supplemented SAPs did not support morphogenesis and yielded either disorganized structures as shown above or cell death at ~ day 3.

SAPs



Figures 2. Soft, laminin V - supplemented SAPs yield polarized acini with suppressed FN-1 expression.

Preliminary Quantification

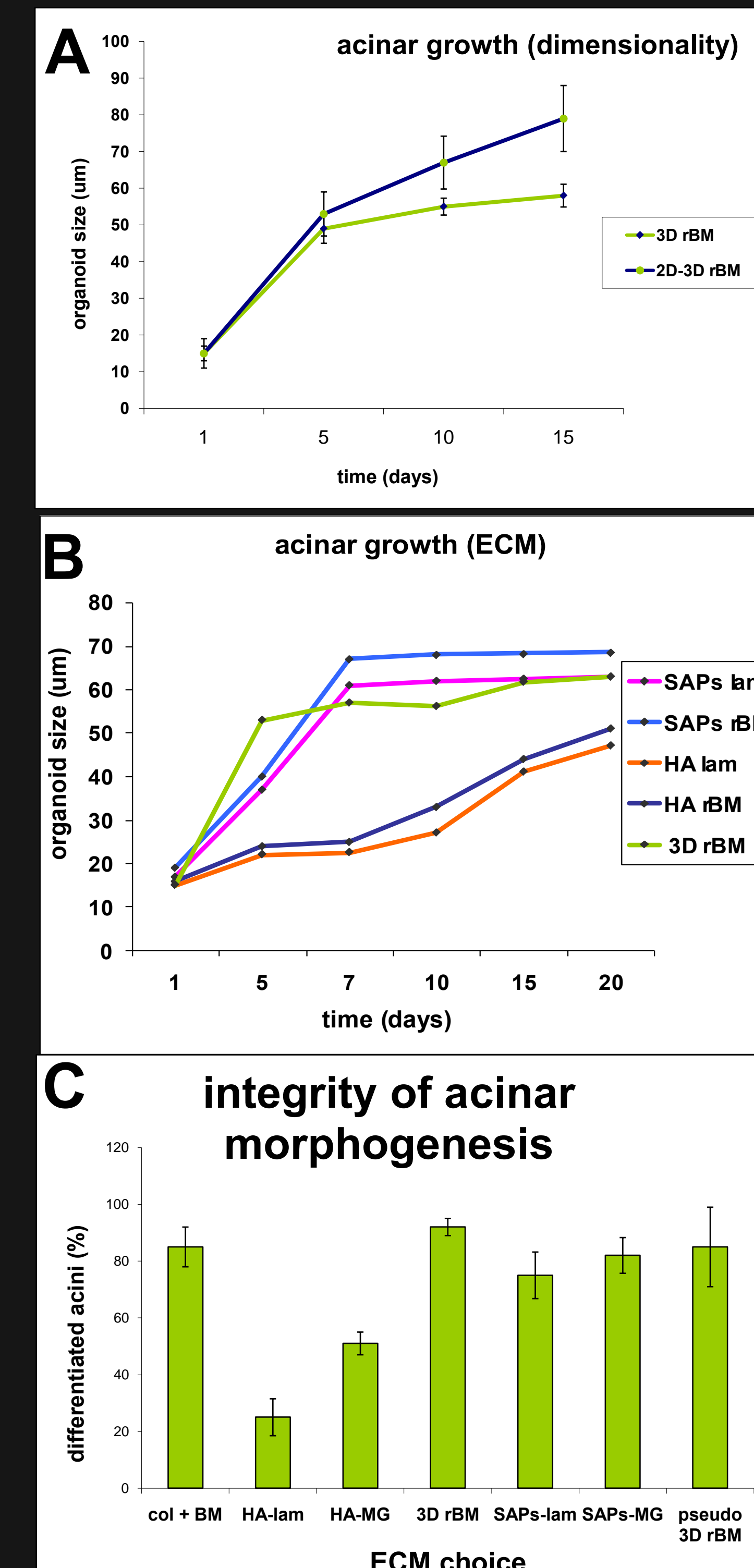


Figure 3. Quantification of 1) organoid size as a function of A) dimensionality and B) ECM choice and 2) colony integrity as a function of ECM choice.

Basement Membrane Assessment (TEM)

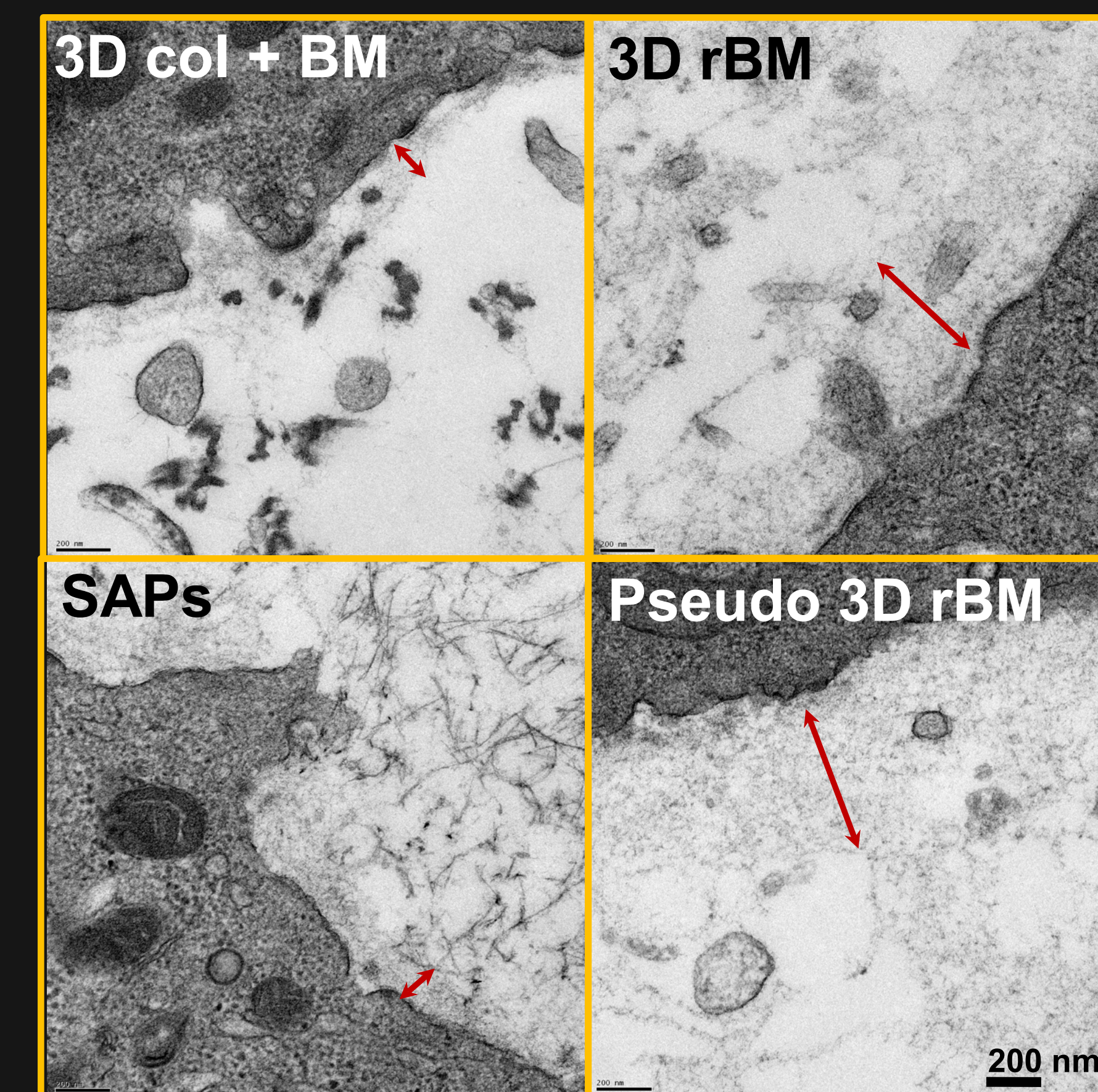
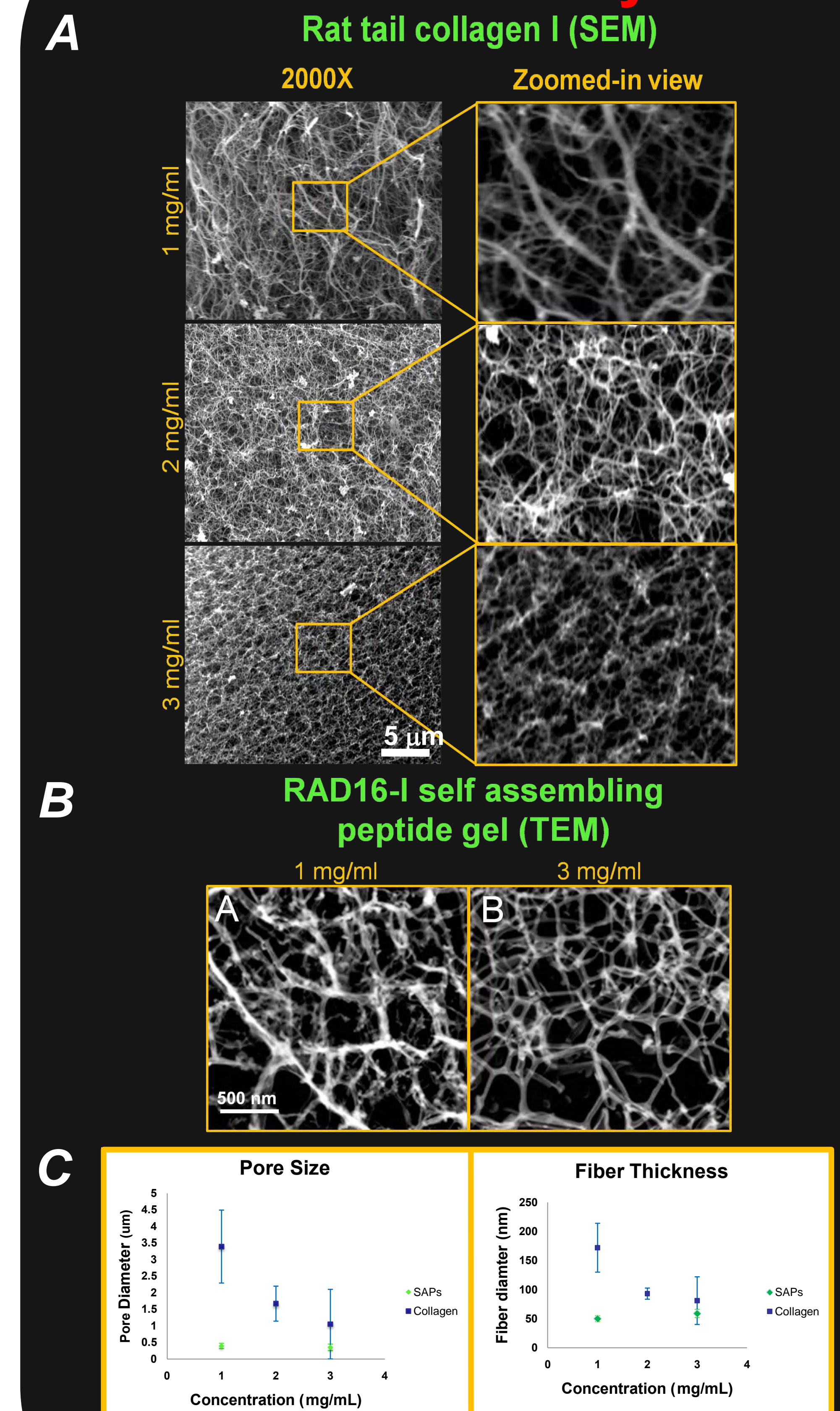


Figure 4. Preliminary TEM micrographs of acinar basement membrane (BM) morphology and membrane properties as a function of ECM choice

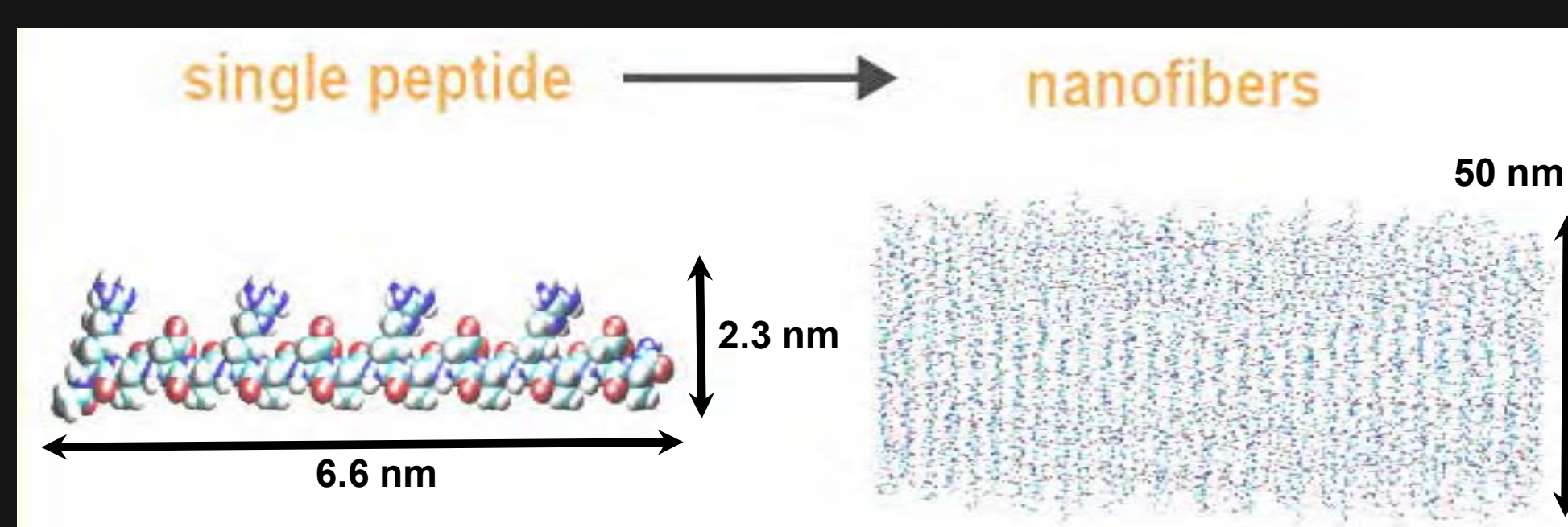
Pore Size Analysis



Figures 5. Pore and fiber diameter quantification (C) and the supporting SEM micrographs of collagen (A) and TEM micrographs of SAPs (B)

Self-Assembling Peptides (SAPs, RAD16-I)

Salt-induced molecular self-assembly into nano-fiber structures



Proposed advantages of SAPs

- 1) No batch to batch variability due to synthetic nature of SAPs
- 2) Control of ligand density with increasing ECM stiffness/concentration
- 3) Less variability in pore size /topology as a function of stiffness/concentration

Conclusions

- 1) Laminin-supplemented SAPs support acinar morphogenesis
- 2) Pore size of SAPs varies less than that of collagen → SAPs have a more consistent morphology as a function of stiffness

Future Direction

- 1) Further verify and develop SAP model of acinar morphogenesis via conjugation or supplementation of these synthetic systems with matrix metalloproteinases to better recapitulate *in vivo* matrix remodeling mechanisms
- 2) Finish basement membrane microarchitecture analysis

Acknowledgements

Greatly thank A.L. Sieminski for TEM images of SAPs and the view of differentiated cell behavior diagram